Diversity, specificity and evolutionary history of marine invertebrate symbioses and functions of the sulfur-oxidizing symbionts

Dissertation

zur Erlangung des Grades eines

Doktors der Naturwissenschaften

- Dr. rer. nat -

dem Fachbereich Biologie/ Chemie der

Universität Bremen

vorgelegt von

Judith Zimmermann

Bremen

Juni 2015

Die vorliegende Doktorarbeit wurde von Mai 2011 bis Juni 2015 in der Abteilung Symbiose am Max Planck Institut für marine Mikrobiologie in Bremen angefertigt.

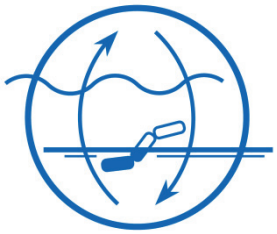

1. Gutachterin: Prof. Dr. Nicole Dubilier

2. Gutachter: Prof. Dr. Thomas Hoffmeister

Tag des Promotionskolloquiums: 9. Juli 2015

‘Enthusiasm is followed by disappointment and even depression, and then by renewed enthusiasm.‘

- Murray Gell-Mann -

Summary

The central role symbiosis has played in the ecology and evolution of eukaryotic organisms is now unquestioned. However, the evolutionary processes by which symbioses are established and maintained within host lineages are less clear. Several forms of symbiont integration are known: ectosymbiotic associations in which the symbionts are attached to the surface of the host, and endosymbiotic associations in which the symbionts live inside the host, either extra- or intracellularly. It is often assumed that the symbiotic lifestyle corresponds with the evolutionary stability of the association, i.e. ectosymbioses are the least intimate, and intracellular endosymbioses the most stable.

Many marine invertebrate hosts have established chemosynthetic symbioses with sulfur-oxidizing ecto- and endosymbiotic bacteria, which use reduced sulfur compounds as energy source for carbon fixation. Two key questions that have not been resolved for many chemosynthetic symbioses are: (1) How specific and evolutionarily stable are chemosynthetic symbioses? (2) What are the benefits for the symbiotic partners?

In the first part of this thesis I present three studies that investigated the diversity, specificity and evolutionary history of different sulfur-oxidizing symbioses: (I) Gutless vestimentiferan tubeworm endosymbioses were believed to harbor a single sulfur-oxidizing intracellular symbiont that provides nutrition to the host. Using phylogenetic analyses of host and symbiont marker genes and *in situ* hybridization with symbiont-specific probes I could show that *Lamellibrachia anaximandri* tubeworms from a Mediterranean hydrothermal vent harbor two distinct intracellular sulfur-oxidizing endosymbionts instead of one. Furthermore, I could show that water depth is the main factor that significantly influenced symbiont divergence in vestimentiferan tubeworms. (II) In the second study I investigated sulfur-oxidizing bacteria of the closely related *Candidatus* Thiosymbion clade that live in symbiosis with gutless phallodriline oligochaetes and stilbonematine nematodes – as extracellular endosymbionts in the first, and ectosymbionts on the latter. Both symbioses are highly abundant in sulfidic shallow water sediments but only few host species and symbionts had been characterized with molecular methods prior to this thesis. Unexpectedly, cophylogenetic analyses of gutless phallodriline species and their *Cand.* Thiosymbion endosymbionts revealed little correlation between host and symbiont genetic distances but a strong influence of geography. In contrast, cophylogeny analyses of stilbonematine species and their *Cand.* Thiosymbion ectosymbionts revealed a high degree of congruence and illustrated the high evolutionary stability of the ectosymbioses. On top of this, this study provided evidence for repeated host switches of *Cand.* Thiosymbion between the two host phyla, highlighting the evolutionary flexibility of this symbiont clade. (III) In a third study I investigated stilbonematine nematode species of the genus *Leptonemella* from the North Sea island Sylt. This study revealed an unexpected diversity of seven closely related and co-occurring *Leptonemella* species. The study showed that each species is consistently associated with its own species-specific symbiont type. In-depth 16S ribosomal RNA, intergenic spacer (ITS) analyses and metagenomic analyses of single worm symbiont populations revealed that each individual worm hosts a distinct and unique ectosymbiont strain, indicating microevolution at the level of individual worm hosts. With these three studies I show that evolutionary stability of a symbiotic association is not necessarily correlated with symbiotic lifestyle and emphasize the power of molecular analyses to uncover previously “hidden“ diversity.

In the second part of this thesis I present two studies on the function of the sulfur-oxidizing ectosymbionts of *Leptonemella* species from Sylt. (IV) Stilbonematine nematodes were long hypothesized to gain nutrition from their ectosymbionts via feeding on their symbiont coat, but convincing evidence was missing. With radiolabeled bicarbonate (HCO_3^-) incubations combined with scintillation counting and microautoradiography (MAR) I could show that the ectosymbionts are able to fix HCO_3^- into biomass and that over time, the host also becomes enriched in labeled carbon. *In situ* hybridizations with symbiont-specific probes further showed that ectosymbionts are present in the gut

lumen, supporting the hypothesis of the symbionts' nutritional role for their host. (V) Analysis of the draft genomes of *Leptonemella* ectosymbionts in the last part of this thesis uncovered previously unknown metabolic potentials of the *Cand.* Thiosymbion ectosymbionts. For example, I found that the ectosymbionts have the capability to live heterotrophically, which may be an adaptation to the organic-rich habitat or to the recycling of host waste compounds. I found several genomic features that are commonly found in biofilm-forming bacteria, and not usually present in sulfur-oxidizing symbionts, which corresponds well with the ectosymbiotic lifestyle of the symbionts. Examples include genes encoding antimicrobial peptides, pore-forming toxins, type IV pili, type II and type VI secretion systems that may be used for host attachment and defense from predators or pathogens. These last two studies indicate that *Leptonemella* ectosymbionts may not only provide nutrition, but may also function as protective barrier for their hosts.

Zusammenfassung

Die zentrale Rolle, die Symbiose für die Ökologie und Evolution von eukaryontischen Organismen gespielt hat, ist unumstritten. Die evolutionären Prozesse, durch welche Symbiosen entstanden sind und in Wirtslinien aufrecht erhalten werden, sind jedoch weniger klar. Mehrere Formen von Symbionten-Integration sind bekannt: Ektosymbiontische Assoziationen, bei denen die Symbionten auf der Oberfläche des Wirtes anhaften und endosymbiontische Assoziationen, in denen die Symbionten entweder extra- oder intrazellulär innerhalb des Wirtes leben. Es wird oft angenommen, dass die symbiontische Lebensweise mit der evolutionären Stabilität der Assoziation zusammenhängt, d.h. Ektosymbiosen sind die am wenigsten intimen, und intrazelluläre Endosymbiosen die evolutionär stabilsten Assoziationen.

Viele marine Evertebraten leben in einer chemosynthetischen Symbiose mit schwefeloxidierenden ekto- oder endosymbiontischen Bakterien, die reduzierte Schwefelverbindungen als Energiequelle für die Kohlenstofffixierung verwenden. Zwei Schlüsselfragen, die noch nicht für viele chemosynthetischen Symbiosen beantwortet wurden, sind: (1) Wie spezifisch und evolutionär stabil sind chemosynthetische Symbiosen? (2) Was ist der Nutzen für die symbiotischen Partner?

Im ersten Teil dieser Arbeit präsentiere ich drei Studien, die die Diversität, Spezifität und Evolutionsgeschichte verschiedener schwefeloxidierender Symbiosen untersuchen: (I) Es wurde bisher angenommen, dass darmlose Röhrenwurm-Endosymbiosen nur einen einzelnen schwefeloxidierenden intrazellulären Symbionten beherbergen, welcher den Wirt ernährt. Mit Hilfe phylogenetischer Analysen von Wirts- und Symbiontenmarkergenen und *in-situ*-Hybridisierungen mit symbiontenspezifischer Sonden konnte ich zeigen, dass der Röhrenwurm *Lamellibrachia anximandri* von Hydrothermalquellen im Mittelmeer zwei intrazelluläre schwefeloxidierende Endosymbionten statt nur einem beherbergt. Außerdem konnte ich zeigen, dass Wassertiefe und nicht der Wirt die genetische Diversität der Röhrenwurm Symbionten signifikant beeinflusst. (II) In der zweiten Studie untersuchte ich schwefeloxidierende Bakterien der nahverwandten *Candidatus* Thiosymbion, die in Symbiose mit darmlosen Oligochaeten und Nematoden der Unterfamilie Stilbonematinae leben - als extrazelluläre Endosymbionten in Ersteren und Ektosymbionten auf Letzteren. Beide Symbiosen kommen häufig in sulfidischen Flachwassersedimenten vor, aber nur wenige Wirtsarten und Symbionten wurden bisher molekular beschrieben. Wider Erwarten haben cophylogenetische Analysen von darmlosen Oligochaetenarten und deren *Cand.* Thiosymbion Endosymbionten eine geringe Korrelation genetischer Distanzen aufgezeigt. Stattdessen wurde ein starker Einfluss der Geografie auf die Symbiontenphylogenie gezeigt. Im Gegensatz dazu haben cophylogenetische Analysen verschiedener Stilbonematinen Arten und ihrer *Cand.* Thiosymbion Ektosymbionten ein hohes Maß an Kongruenz gezeigt und damit die ausgeprägte evolutionäre Stabilität der Ektosymbiosen veranschaulicht. Diese Studie hat außerdem gezeigt, dass wiederholte Wirtswechsel der *Cand.* Thiosymbion zwischen beiden Wirtsstämmen stattgefunden haben, was die sehr hohe Flexibilität dieser Symbiontengruppe unterlegt. (III) Eine Nachfolgestudie, in der ich Stilbonematinen der Gattung *Leptonemella* vor der Nordseeinsel Sylt untersucht habe, ergab eine unerwartete Vielfalt von sechs nah verwandten und nebeneinander vorkommenden *Leptonemella* Arten. Diese Studie zeigte, dass jede Spezies konsequent mit einem artspezifischen Symbiontentyp assoziiert ist. Detaillierte Analysen der 16S ribosomalen RNA, der intergenischen Region (IR) und der Metagenome einzelner Symbiontenpopulationen ergaben, dass jeder Wurm einen individuellen Ektosymbiontentyp beherbergt, was auf Mikroevolution auf der individuellen Ebene schließen lässt. Mit diesen drei Studien konnte ich zeigen, dass evolutionäre Stabilität einer Symbiose nicht unbedingt mit der symbiontischen Lebensweise zusammenhängen muss und dass molekulare Analysen sehr wirkungsvoll sein können, um „versteckte“ Diversität aufzudecken.

Im zweiten Teil dieser Arbeit präsentiere ich zwei Studien über die Funktion der schwefeloxidierenden Ektosymbionten der *Leptonemella* Arten auf Sylt. (IV) Es wurde lange angenommen, dass Stilbonematinen von ihren Ektosymbionten durch „Beweidung“ des Symbiontenmantels ernährt

werden. Schlüssige Beweise wurden hierfür aber bisher nicht erbracht. Mit einer Kombination von Inkubationen mit radioaktiv markiertem Hydrogencarbonat (HCO_3^-), Szintillationszählungen und Mikroautoradiographie (MAR) konnte ich zeigen, dass die Ektosymbionten HCO_3^- in Biomasse umwandeln können und dass mit zeitlicher Verzögerung die Radioaktivität im Wirt zunimmt. *In situ*-Hybridisierungen mit symbiontenspezifischer Sonden zeigten außerdem, dass Ektosymbionten im Darmlumen vorhanden sind, was die Hypothese der ernährenden Funktion der Symbionten für den Wirt unterstützt. (V) Die Analyse der Genome der *Leptonemella* Ektosymbionten im letzten Teil dieser Arbeit enthüllte bisher unbekannte Stoffwechselpotentiale der *Cand.* Thiosymbion Ektosymbionten. Zum Beispiel die Fähigkeit der Ektosymbionten, heterotroph zu leben, was eine Anpassung an den nährstoffreichen Lebensraum oder die Verwertung von Wirtsabfallprodukten sein könnte. Ich habe außerdem mehrere Gene entdeckt, die üblicherweise in biofilmbildenden Bakterien vorkommen aber nicht in schwefeloxidierenden Symbionten, was mit der extrazellulären Lebensweise der Ektosymbionten erklärt werden kann. Beispiele hierfür sind Gene, die für antibakterielle Peptide, Toxine, Typ-IV-Pili, Typ II- und Typ VI-Sekretionssysteme kodieren, welche für die Wirtsanhaftung und Verteidigung vor Fressfeinden oder Krankheitserregern eingesetzt werden könnten. Die letzten zwei Studien suggerieren, dass die *Leptonemella* Ektosymbionten nicht nur für die Ernährung, sondern auch als Schutzbarriere für ihren Wirt fungieren könnten.

Contents

List of abbreviations

APS	Adenosine-5'-phosphosulfate
Bp	Base pair
CARD	Catalyzed reporter deposition
CBB	Calvin-Benson-Bassham
COI	Cytochrome oxidase I
DAPI	4',6-diamidino-2-phenylindol
DNA	Deoxyribonucleic acid
et al.	and others
FISH	Fluorescence *in situ* hybridization
GSO	Glandular sensory organ
HPB	Hydroxypropionate bicycle
ITS	Internal transcriped spacer
PCR	Polymerase chain reaction
PHA	Polyhydroxyalkanoate
RNA	Ribonucleic acid
mRNA	messenger RNA
rRNA	ribosomal RNA
tRNA	transfer RNA
RuBisCO	Ribulose-1,5-bisphosphate carboxylase/ oxygenase
SEM	Scanning electron microscopy
SNP	Single nucleotide polymorphism
TEM	Transmission electron microscopy

Chapter I: Introduction

1.1 Symbiosis

1.1.1 Definition

Symbiosis describes the intimate and long-term association of different organisms. The term "symbiosis" (from the Greek "syn" = with and "bios" = life) was first coined by Albert Bernhard Frank (1839 – 1900) in 1877 who defined it as "two species live on or in one another" but the German mycologist Anton De Bary (1831 – 1888) is usually credited for its first use. De Bary defined symbiosis as "living together of unlike organisms" (de Bary 1879) and did not distinguish between beneficial or detrimental associations, while in the following years symbiosis was often equated with the concept of "mutualism" that describes a beneficial association for both partners (Table 1). The definition of symbiosis has sparked a long ongoing debate among scientists over 130 years but a review of the current literature has revealed that the more restrictive definition (i.e. symbiosis = mutualism) seems to have disappeared (reviewed by Martin & Schwab 2012).

In this thesis I will use the definition in its original sense that applies to any type of persistent biological interaction (mutualism, commensalism, parasitism) (Table 1) because it can often be challenging to judge the true nature of the association. In particular, it is difficult to estimate whether the symbiotic relationship is truly beneficial to both symbiotic partners (mutualistic), or whether only one partner gets a benefit from the association (commensalism). Especially in the case of intracellular bacterial endosymbionts that often show highly reduced genomes (Section 1.2), there is debate whether the host is the only partner that benefits and has simply "enslaved" its bacterial partner and appropriate experiments to measure symbionts' fitness are often lacking, (Frean & Abraham 2004; Garcia & Gerardo 2014). Furthermore, changing environmental or physiological conditions can sometimes lead to a change from a beneficial to a detrimental or parasitic partnership or vice versa (Redman *et al.* 2001; Tanaka *et al.* 2006; Kogel *et al.* 2006). I will refer to the symbiont as the smaller and the host as larger partner as defined by Starr (Starr 1975) and the definitions in Table 1 to refer to the symbiotic lifestyle and location.

Table 1: Symbiosis definitions that will be used in this thesis

Fitness effect on partners	
Mutualism	Symbiotic association where both partners benefit
Commensalism	Symbiotic association where one partner benefits and the other is unaffected
Parasitism	Symbiotic association where the parasite benefits and the host is negatively affected
Forms of mutualism	
Obligate	Essential for the survival of at least one of the partners
Facultative	Not essential for the survival of at least one of the partners
Symbiont location	
Ectosymbiosis	Symbiont lives on the surface of the host, whether externally or internally such as the lining of the digestive tract
Endosymbiosis	Symbiont lives inside the host and is separated from the environment by host tissue
extracellular	Symbiont is surrounded by host tissue
intracellular	Symbiont lives inside host cells

1.1 2 Relevance

It is widely accepted that symbiosis has played a key role in the evolution of life (Margulis & Fester 1991). The most fundamental events were the evolution of mitochondria and chloroplasts from prokaryotic ancestors that marked the beginning of eukaryotic life on Earth. Endosymbiosis theory predicts that mitochondria and chloroplasts evolved from an aerobic alphaproteobacterium and cyanobacterium that entered the primordial eukaryotic cell, respectively (reviewed by Kutschera & Niklas 2005). Until today, there is still considerable debate about the most recent common alphaproteobacterial and cyanobacterial ancestor of mitochondria and chloroplasts (Falcón *et al.* 2010; Criscuolo & Gribaldo 2011; Thrash *et al.* 2011; Rodríguez-Ezpeleta & Embley 2012; Dagan *et al.*, others 2013; Li *et al.* 2014). Both endosymbiosis events have paved the way for the development of the vast diversity of

multicellular organisms (animals, plants and fungi) on Earth today. The emergence of multicellular organisms provided new habitats for microbial organisms and it is widely believed that animals, plants and fungi were involved in symbiotic associations throughout evolutionary history (Moran 2006). For example, the majority of land plants live in symbiosis with mycorrhizal fungi, that help the plants to acquire nutrients for growth and it is widely accepted that colonization of land was only facilitate through this symbiosis (Smith & Read 2010). Similarly, coral reefs could only develop through the association of corals with symbiotic algae, called zooxanthellae, that are responsible for the hosts' nutrition (Muscatine 1990).

Symbiotic associations are ubiquitous and involve organisms from all three domains of life: Archaea, Bacteria and Eucarya (Moya *et al.* 2008; McFall-Ngai 2008). It is probable that all multicellular organisms interact with symbiotic partners in nature (Zilber-Rosenberg & Rosenberg 2008; Gordon *et al.* 2010; Singh *et al.* 2013). This has led to the holobiont theory, which describes that the holobiont (the host with all of its associated persistent microorganisms) acts as a unit of selection in evolution. In other words, the combined genetic diversity and metabolic capabilities of host and associated symbionts are responsible for the fitness of the holobiont under different environmental conditions (Zilber-Rosenberg & Rosenberg 2008; Gilbert *et al.* 2012).

1.1.3 Benefits of symbiosis

Through symbiotic associations, species can overcome their own physiological limitations by exploiting the capacities of others (Douglas 1994). Correspondingly, symbionts can confer diverse benefits to their host and these are usually based on certain biochemical functions that are exclusive to the symbionts (Moya *et al.* 2008). Table 2 provides an overview over the functions that a symbiotic association can provide to each partner.

Table 2: Benefits of associating with a symbiotic partner

General benefit		Specific benefit	Symbiotic system	References
For the host	Nutrient amendment	Provision of essential amino acids, vitamins or cofactors not contained in host diet	Sap- and blood-feeding insects and their intracellular symbiotic bacteria	reviewed by Zientz *et al.* (2004)
		Nitrogen-fixation to provide the host with poorly-accessible nitrogen compounds	*Rhizobia*-legume symbioses, Cyanobacteria in corals	reviewed by Kneip *et al.* (2007)
	Nutrient accessibility	Break-down of cellulose in plant material otherwise indigestable by the host	Ruminant animals (cattle, sheep) and rumen bacteria	reviewed by Mizrahi *et al.* (2013)
		Break-down of lignocellulose in wood otherwise indigestable by the host	Wood-eating termites, marine shipworms (bivalves) with endosymbiotic bacteria	(Brune & Ohkuma 2010; O'Connor *et al.* 2014)
	Nutritional function	Provision of entire nutrition by photosynthetically fixed carbon	Coral-unicellular algal symbioses	(Trench 1993; Yellowlees *et al.* 2008)
		Provision of entire nutrition by chemosynthetically fixed carbon	Deep-sea and shallow water invertebrates symbioses with chemosynthetic bacteria	(reviewed by Dubilier *et al.* 2008)
	Waste recycling	Recycling of carbon- and nitrogen-rich host waste products	Wood-eating termites, and gutless worm *Olavius algarvensis* with endosymbiotic bacteria	(Potrikus & Breznak 1981; Kleiner *et al.* 2012b)
	Defense	Production of bioactive compounds that act against predators or pathogens	Aphid resistance against parasitic wasps, and fungus-eating ants resistance against parasitic fungus due to symbiotic bacteria	(Currie *et al.* 1999; Oliver *et al.* 2003)
	Protection	Protections from heat	Sap-feeding insects endosymbiotic bacteria	(Russell & Moran 2006)
		Protection from sulfide-poisoning	Stilbonematine nematode ectosymbionts	(Hentschel *et al.* 1999)
	Predation	Usage of toxin-producing symbionts to kill prey	Entomopathogenic nematodes with endosymbiotic bacteria	reviewed by Forst and Clarke (2002)
For the symbionts	Protection	Protection from potential predators	Intracellular symbionts	(Garcia & Gerardo 2014)
	Nutrient amendment	Provision of metabolic products that cannot be produced	Endosymbiotic bacteria of sap-feeding insect	(Zientz *et al.* 2004)
	Nutrient accessibility	Mobile host that provides regular access to nutrients	Chemosynthetic symbionts of marine nematodes, gutless phallodrilines, ciliates	(Giere *et al.* 1991; Ott *et al.* 1991; Bright *et al.* 2014)
	Avoiding competition	Allocation of living space	Endosymbionts and ectosymbionts	(Polz *et al.* 2000)

1.2 Transmission mode and symbiont genome evolution

Transmission of symbionts plays a key role in symbiotic associations, because it guarantees their perpetuation through host generations. Two main modes of transmission have been described: vertical and horizontal transmission (reviewed by Bright & Bulgheresi 2010):

Vertical transmission describes the transfer of symbionts to the next generation via the female germ line. It ensures that the offspring is inoculated with exactly the same symbiont population harbored by the mother. Prior to reproduction, symbionts are often translocated from the symbiont-housing organ to the female gonad to ensure transmission to the next generation. The down-side of strict vertically transmitted symbionts is that they go through population bottlenecks and irreversibly accumulate harmful mutations (Moran 1996). This has been shown for many sap-feeding insects such as aphids that depend on essential amino acids or vitamins from their intracellular symbionts (reviewed by Moran *et al.* 2008). In aphids, for example, only the subpopulation of a single bacteriocyte[1]is transferred to the next generation, and the symbionts that "infect" the embryo are again divided into different bacteriocytes (Mira & Moran 2002). Genomes of such vertically transmitted endosymbiont are often very reduced, show a strong base composition bias towards A and T and lack DNA repair genes and genes for certain metabolic pathways (Moran *et al.* 2008; Toft & Andersson 2010; McCutcheon & Moran 2011). Due to this they are commonly not able to survive outside of their hosts.

Apart from strict vertical transmission "pseudo-vertical" transmission has been suggested for symbionts that do not have an intracellular lifestyle such as ectosymbionts of freshwater *Niphargus* amphipods (Bauermeister *et al.* 2012). *Niphargus* females have been hypothesized to transfer their symbionts to their progeny during breeding in their brood-pouch (Dattagupta *et al.* 2009). A similar way of transmission has been proposed for gutless phallodrilines (Annelida) where some of the extracellular symbionts are likely smeared onto the egg during oviposition (Giere 1981, Krieger, 2000, Section 1.6.3). In contrast to vertically transmitted intracellular symbionts, genomes of the extracellular symbionts are not reduced and also

[1] specialized host cell containing the symbiotic bacteria

encode a high number of transposases[2] and mobile elements (Woyke *et al.* 2006; Kleiner *et al.* 2012b, 2013). This has been postulated to be indicative for their current transition from a facultative to obligate symbiotic lifestyle (Woyke *et al.* 2006; Kleiner *et al.* 2012b, 2013).

Horizontal transmission describes the uptake of symbionts by non-symbiotic juveniles or eggs from the environment, or co-occurring hosts (Bright & Bulgheresi 2010). In contrast to strictly vertically transmitted symbionts, horizontally transmitted symbionts spend a certain period of their lifetime in the environment. Horizontal transmission has been described for the well-characterized shallow water squid-*Vibrio* symbiosis where the bacterium *V. fischeri* is selectively taken up from the environment by non-symbiotic juveniles every generation anew (Nyholm & McFall-Ngai 2004). The environmental pool of symbionts is replenished by adults that expel about 90% of their ectosymbionts from the light organ every morning (Lee & Ruby 1994). However, intracellular endosymbionts are also known to be horizontally transmitted, for example in deep-sea *Bathymodiolus* mussels or the hydrothermal vent tubeworms (for more details see Section 1.4.3) (Won *et al.* 2003; Nussbaumer *et al.* 2006; Fontanez & Cavanaugh 2014). The genomes of such facultative intracellular symbionts are commonly not as reduced as those of vertically transmitted intracellular symbionts (e.g. Robidart *et al.* 2008; reviewed by Toft & Andersson 2010). This can be explained by the presence of a free-living population that can freely recombine with closely related strains or take up novel genetic material by, e.g. horizontal gene transfer (HGT)[3] (Vrijenhoek 2010; Toft & Andersson 2010). Also in a genetically highly diverse free-living population, selection can act against deleterious mutations in alleles that have arisen by chance (Moran 1996).

Additionally to pure vertical or horizontal transmission, a mixed mode or leaky vertical transmission describes the combination of both transmission modes. Such mixed mode transmission is likely to be more common than strict vertical transmission (Bright & Bulgheresi 2010; Vrijenhoek 2010). For example, vertical transmission combined with intra- and interspecies symbiont transfer, so-called host switching, has been documented in numerous symbiotic associations, such as in sponge-microbe symbioses from the Caribbean but also in *Solemya* and *Vesicomya* clams (Stewart *et al.* 2008, 2009b; Schmitt *et al.* 2008;

[2] An enzyme that is responsible for the transposition of transposable elements (TE) (DNA sequence that can change its position within the genome) and this often leads to duplication of TEs.

[3] Transfer of genes between different organisms other than during reproduction

Decker *et al.* 2013). Interestingly, such a mixed mode transmission has been hypothesized to allow recombination or to partially escape the detrimental effects of genome reduction (Jiggins 2002; Stewart *et al.* 2009b).

1.2.1 Phylogenetic implications of transmission

Phylogenetic trees of strictly vertically transmitted symbionts and those of their hosts are often congruent (Fig. 1A). This is due to the intimate long-term association of both partners over successive host and symbiont speciation events. Due to the maternal transmission, host and symbiont genes are genetically coupled. This can lead to the speciation of host and symbionts at the same time and is also termed cospeciation or codiversification (de Vienne *et al.* 2013). Congruent host and symbiont phylogenies due to strict cospeciation have been reported for multiple intracellular symbionts in insects that are vertically transmitted (Fig. 1A) (reviewed by Moran *et al.* 2008). One prominent example are the *Buchnera*-aphid symbioses (Jousselin *et al.* 2009). However also vertically transmitted sulfur-oxidizing endosymbionts in deep-sea clams and catenulid flatworms underwent a history of cospeciation with their host (Peek *et al.* 1998; Gruber-Vodicka *et al.* 2011).

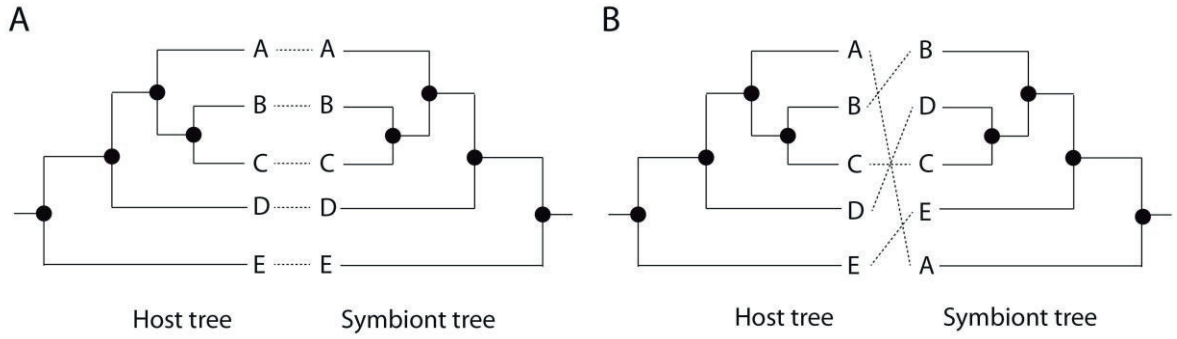

Fig. 1. Cophylogenies of host and symbiont trees. (A) Congruent phylogenies (B) incongruent phylogenies. The phylogenetic trees show evolutionary relationships between different host and symbiont taxa (A – E). The corresponding host and symbionts are connected by dashed lines. Each node represents a common ancestor or speciation event. Branch lengths correspond to genetic distance or divergence time.

In contrast, phylogenies of horizontally transmitted symbioses are often incongruent, due to the decoupling of host and symbiont genotypes and therefore the lack of co-speciation events between their partners (Fig. 1B). Incongruent host and symbiont phylogenies have for example been shown for deep-sea *Bathymodiolus* mussels or vestimentiferan tubeworms and their endosymbionts (McMullin *et al.* 2003; Vrijenhoek 2010). In the latter symbiont

diversification is not only influenced by the host, but also environmental factors and symbionts can even be shared among different host species. However, there are also rare examples where horizontal transmission can generate patterns of strict cospeciation. For example if splitting events involve geographic isolation or if the colonization of hosts is strictly regulated, such as shown for pigeons and their feather lice (Clayton *et al.* 2003; Vrijenhoek 2010).

1.2.2 Cospeciation versus coevolution

The term cospeciation is often confounded with coevolution, although the two are distinct concepts. Coevolution is the 'Process of reciprocal evolutionary change between interacting species, driven by natural selection' (Thompson 2005). The idea dates back until Charles Darwin (1809 – 1882) who described many specialized interactions between insects and the plants they fertilized (Darwin 1859, 1979). Some of the strongest available evidence for coevolution comes from phylogenetic codiversification between ecologically associated species. Cospeciation describes the process that leads to the parallle speciation of both interacting species, while coevolution explains the general process of reciprocal evolutionary change. For example ecologically associated species, such as hosts and their mutual symbionts can evolve new traits through interacting with each other. If these new traits are different enough to define a new species, cospeciation has occurred.

1.3 Chemosynthesis

1.3.1 Definition

Before 1977, scientists believed that all life on Earth was dependent on sunlight as the sole energy source. Photosynthesis was the only process known to convert inorganic carbon from the atmosphere into organic matter by using the energy of the sun. Sergei Winogradsky (1856 - 1953) suggested a novel life process in 1890 that some bacteria might solely live from inorganic matter (Ackert 2006). This alternative means of energy generation, from oxidation of inorganic molecules (e.g. hydrogen gas, hydrogen sulfide) or methane instead of from sunlight, to convert one-carbon molecules (usually carbon dioxide or methane) into biomass was later termed "chemosynthesis".

1.3.2 Substrates for chemosynthetic microorganisms

Growth of chemosynthetic microorganisms relies on energy-providing redox reactions between an electron donor and electron acceptor that lead to the production of adenosine triphosphate (ATP) and reducing equivalents (such as NADPH or reduced ferredoxin) used to fix carbon into biomass. Table 3 gives an overview of the substrates that chemosynthetic microorganisms can use for synthesizing metabolic compounds without the aid of light.

Table 3: Substrates for chemosynthetic microorganisms

<table>
<tr><td>Energy source</td><td>Breaking of chemical bonds</td><td>Chemo-</td><td colspan="2"></td><td rowspan="5">-troph</td></tr>
<tr><td rowspan="2">Electron donors</td><td>inorganic substances
(e.g. CO, H_2, H_2S, S^0, $S_2O_3^{2-}$, Fe(II), NH_3)</td><td rowspan="2"></td><td>litho-</td><td rowspan="2"></td></tr>
<tr><td>organic compounds
(e.g. CH_4, sugars, amino acids, fermentation products (acetate, propionate, etc.)</td><td>organo-</td></tr>
<tr><td rowspan="2">Carbon source</td><td>Inorganic carbon (CO_2 or $HCO3^-$)</td><td colspan="2" rowspan="2"></td><td>auto-</td></tr>
<tr><td>organic compounds
(e.g. CH_4, sugars, amino acids, fatty acids, fermentation products (acetate, propionate, etc.)</td><td>hetero-</td></tr>
</table>

Chemosynthetic microorganisms can either be chemolithoautorophs, chemolithoheterotrophs or chemoorganoheterotrophs. Examples for the first are sulfur-oxidizing bacteria that use reduced sulfur compounds as electron donor and CO_2 as carbon source. Chemolitho-heterotrophs such as *Thiobacillus* strain Q or some *Archaeoglobi* species that gain energy from sulfur oxidation but use organic compounds as sole carbon source (Gommers & Kuenen 1988; Brileya & Reysenbach 2014). Examples for chemoorganoheterotrophs are methanotrophic bacteria that use methane both as electron donor and carbon source. Mixotrophic organisms can gain carbon from both CO_2 and organic carbon compounds.

Electron acceptors that are widely used among chemosynthetic bacteria are molecular oxygen, nitrate (NO_3), fumarate, Fe(III), Mn(IV), sulfate (SO_4^{2-}) and carbon dioxide (CO_2).

1.3.3 Chemosynthetic symbioses

In 1977, scientists made a stunning discovery while searching for deep-sea hydrothermal vents on the bottom of the Pacific Ocean on the Galapagos Rift. Additionally to the hot and mineral-rich fluids that were gushing out of the seafloor, they discovered what Laubier called "oases of the depth" (1993). These contained large tubeworm colonies, mussel beds and other organisms living in high density at these vents (Lonsdale 1977). Researchers were puzzled about the richness of biomass because until then, the deep sea was regarded as a nutrient-poor, desert-like place due to the lack of sunlight for primary production. At first, it was believed that the animals were suspension feeders living on organic matter in the water column or directly grazing on dense populations of free-living chemosynthetic microorganisms (Lonsdale 1977; Corliss *et al.*, others 1979). However, studies on the giant hydrothermal vent tubeworm *Riftia pachyptila* revealed that it does not contain a mouth or gut, which precludes suspension feeding. Cavanaugh *et al.* (1981) instead showed that *R. pachyptila* harbors dense populations of sulfide-oxidizing bacteria that live endosymbiotically in the worm's body, and proposed that the bacteria may contribute to the worm's nutrition. Activity tests of enzymes involved in sulfide oxidation and inorganic carbon fixation finally confirmed that the tubeworms live in a nutritional symbiosis with chemosynthetic bacteria (Felbeck 1981). Soon after, many more sulfur-oxidizing bacteria were described to live on the body surfaces (ectosymbionts) or inside host tissues (endosymbionts) of diverse vent-associated fauna (Fig. 2) (Van Dover 2000; Cavanaugh *et al.* 2006). These hydrothermal vents were the first ecosystem known to be entirely dependent on organic carbon produced by chemosynthesis.

Since the discovery of symbiotic hydrothermal vent tubeworms, a vast diversity of animals that live in symbiosis with chemosynthetic bacteria have been described, including members of at least six animal phyla, Ciliophora and Archaea (reviewed by Cavanaugh *et al.* 2006; Dubilier *et al.* 2008; Muller *et al.* 2010) (Fig. 2). Although many electron donors can potentially be used by chemosynthetic microorganisms, most chemosynthetic symbioses that have been described to date rely on autotrophic sulfur-oxidizers that oxidize reduced sulfur compounds in order to fix CO_2 into biomass (reviewed by Dubilier *et al.* 2008; Kleiner *et al.* 2012a). The second most abundant chemical that fuels symbioses at chemosynthesis-based habitats is methane that is used by heterotrophic methane-oxidizing bacteria (methanotrophs). Methanotrophs use CH_4 both as energy and carbon source and are known

to live in symbiosis with at least four animal phyla (reviewed by Petersen & Dubilier 2009). Oxygen commonly serves as electron acceptor for sulfur- and methane-oxidizing symbionts, but several sulfur-oxidizing symbionts are also known to have the potential to use the reduction power of NO_3^- (Hentschel *et al.* 1999; Woyke *et al.* 2006; Kleiner *et al.* 2012b; Jan *et al.* 2014b; Dmytrenko *et al.* 2014). In the last four years, two further electron donors for chemosynthetic symbioses were identified: H_2 in sulfur-oxidizing symbionts of hydrothermal vent-associated *Bathymodiolus* mussels (Petersen *et al.* 2011) and carbon monoxide (CO) that can serve as alternative energy source for sulfur-oxidizing symbionts in the shallow water gutless worm *Olavius algarvensis* (Kleiner *et al.* 2012b).

1.3.4 Diversity of habitats and associated fauna

Since the discovery of a chemosynthesis-driven ecosystem in the deep sea, researchers have found many more habitats that harbor chemosynthetic symbioses, including deep-sea cold seeps, deep-sea whale and wood falls but also shallow water habitats (Fig. 2) (reviewed by Dubilier *et al.* 2008). Characteristics that are shared by all of them are the presence of reduced energy sources that can serve as electron donors for chemosynthetic bacteria and the presence of oxygen that is essential for all animals. Even though chemosynthesis-fueled communities do not rely on carbon compounds produced by phototrophs, they still ultimately rely on photosynthesis to meet their oxygen demands.

Hydrothermal vents are abundant along mid-ocean ridges where two tectonic plates diverge from one another, thereby creating new ocean floor but they can also be found at back-arc spreading centers and at seamounts (see Chapter II) (Van Dover 2000). Electron-donor-rich hydrothermal fluids are produced by seawater reacting with hot basalt rocks within fissures in the ocean floor and can have extreme fluctuations in chemical properties and in temperature (Edmond et al., 1982). The effusing anoxic vent fluids can reach temperatures up to 464°C (Perner *et al.* 2014) and are extremely enriched in metals and reduced gases, such as hydrogen sulfide, hydrogen and methane that represent energy sources for the vent communities (Van Dover 2000). Apart from hydrothermal vent tubeworms that make up large amounts of biomass at hydrothermal vents are *Bathymodiolus* mussels with sulfur- and/or methane-oxidizing symbionts, vesicomyid clams with sulfur-oxidizing symbionts, but also *Rimicaris* shrimps with sulfur-oxidizing ectosymbionts (Fig. 2) (Cavanaugh *et al.* 2006; Dubilier *et al.* 2008).

Like hydrothermal vents, cold seeps are also a result of plate tectonics. However, seeps occur where the oceanic crust meets the continental crust along active and passive continental margins (Sibuet & Olu-Le Roy 2003). Active margins occur at the leading edge of continents where subduction occurs, while passive margins are found along the remaining coastlines, where tectonic activity is minimal and thick sediment deposits build up. Unlike vents, cold seeps are usually sedimented areas, where fluid flow and temperatures are moderate. In contrast to the thermogenic origin of the reduced chemicals at vents, hydrogen sulfide and methane at seep sites often originate from biogenic sources as a result of archaeal methanogenesis and bacterial sulfate reduction (e.g. Joye *et al.* 2004). However, thermogenic production of reduced chemicals can also occur at seep sites when buried organic material is exposed to high temperatures and pressure (Carney 1994; Stewart *et al.* 2005). Typical cold seep fauna are *Bathymodiolus* mussles with sulfide- and/or methane-oxidizing endosymbionts and siboglinid tubeworms, such as *Siboglinum*, *Lamellibrachia or Escarpia* species that can harbor methane- or sulfur-oxidizing endosymbionts (e.g. Lösekann *et al.* 2008; Cordes *et al.* 2009) (Fig. 2).

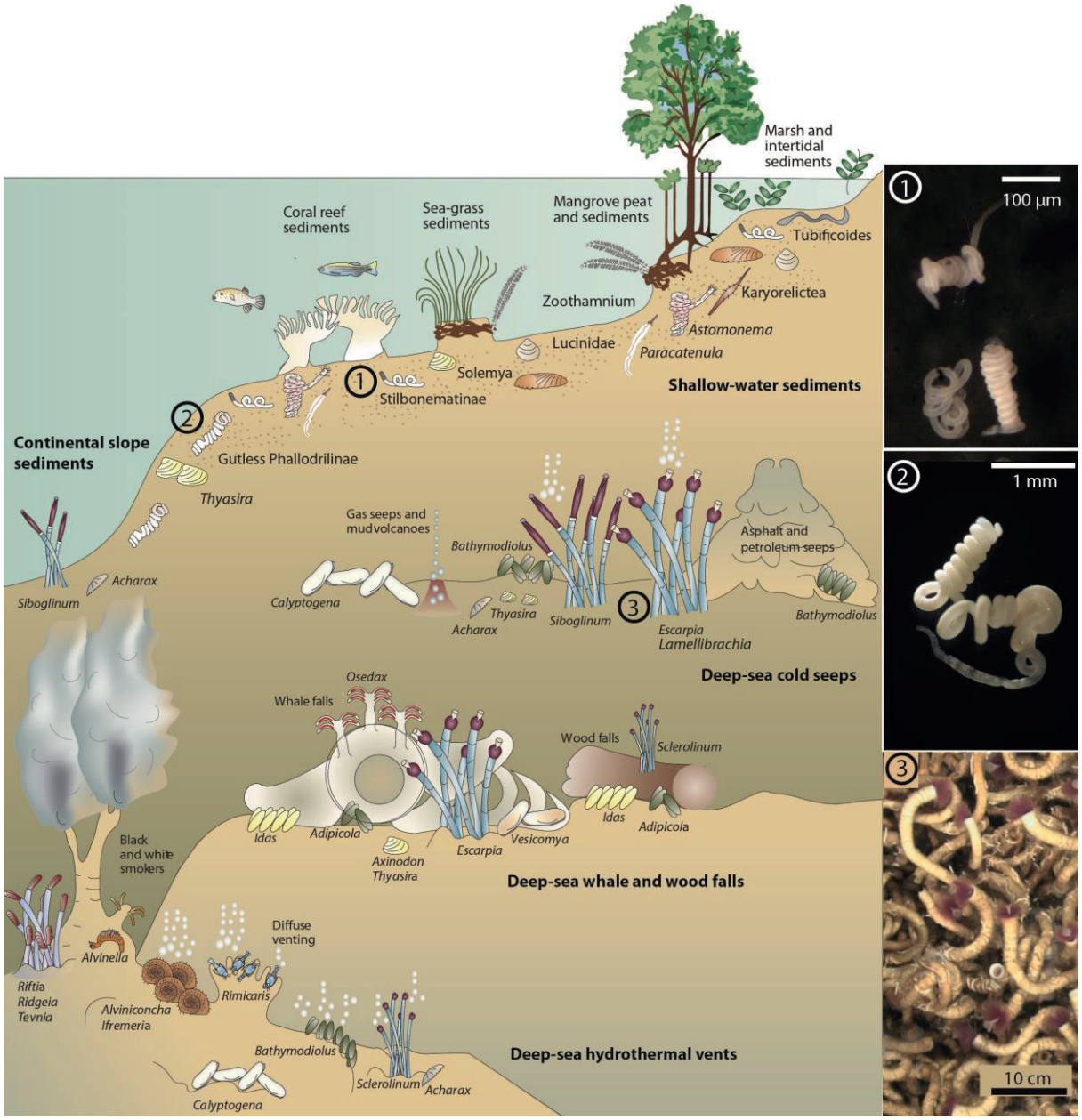

Fig. 2: Diversity of marine chemosynthetic habitats and their associated chemosynthetic symbioses. The organisms are not drawn to scale (modified from Dubilier *et al.* 2008). Picture bar on the right shows symbiotic systems that are discussed during this PhD thesis. (1) Stilbonematine nematodes with ectosymbiotic bacteria. (2) Gutless phallodriline annelids with extracellular endosymbionts (courtesy of C. Lott). (3) *Lamellibrachia* tubeworms with intracellular endosymbionts (courtesy of C. Lott and M. Weber).

Shallow water habitats are one of the most widely distributed habitats that support chemosynthetic symbioses (Fig. 2). Just as in whale- wood and some cold seep habitats, reduced energy sources originate from bacterial sulfate reduction and archaeal methanogenesis. Until now, sulfur-, hydrogen- and carbon monoxide-based symbioses have

been described from shallow water sediments (Ott *et al.* 2004; Dubilier *et al.* 2008). In contrast to hydrothermal vents and cold seeps that rely entirely on chemosynthesis-derived organic matter, shallow water ecosystems rely mainly on organic carbon produced by photosynthesis. Only a small part of the community is made up by chemosynthetic symbioses (Dubilier *et al.* 2008). Of those symbioses, gutless phallodriline annelids and stilbonematine nematodes represent one of the most abundant chemosynthetic symbioses in shallow water sediments (for more details see Sections 1.5 and 1.6).

1.3.5 Specificity of chemosynthetic symbioses

Specificity describes a clearly nonrandom pattern of a symbiont-host association where the ratio of observed combinations of hosts and symbionts is very small compared to the range of possible combinations (Dubos & Kessler 1963; Baker 2003). Strict specificity indicates that one host type is consistently associated with one symbiont type. However, depending on the perspective specificity can have different meanings. While strict host specificity describes the specificity of the host to a particular symbiont, strict symbiont specificity describes the specificity of symbionts to a particular host. Strictly host-specific associations are more common than strictly symbiont-specific associations but both have been reported.

Strict host and symbiont specificity has been shown for the symbiosis of the marine catenulid flatworm *Paracatenula* with its alphaproteobacterial endosymbiont where each species harbors a distinct symbiont type (Table 4) (Gruber-Vodicka *et al.* 2011). In contrast, the hydrothermal vent tubeworm *Riftia pachyptila* harbors one particular symbiont type but the symbionts can be more flexible and associate also with other host species, such as *Oasisia*, *Tevnia* and *Ridgeia* tubeworms (Table 4) (McMullin *et al.* 2003). The same holds true for deep-sea *Bathymodiolus* mussel endosymbiosis, e.g. *B. azoricus* and *B. puteoserpentis* share identical sulfur- and methane-oxidizing symbiont types (Duperron *et al.* 2006). One example for a low host- but strict symbiont-specifity is the *Oligobrachia haakonmosbiensis* (Frenulata) symbiosis where different individuals harbor one of two host species-specific methanotrophic symbiont types (Lösekann *et al.* 2008). Apart from these, various examples of rather flexible marine symbiotic associations exist. For example alvinellid polychaetes, *Rimicaris* shrimps or yeti crabs (*Kiwaidae*) harbour multiple ectosymbiotic bacteria on their surfaces that are not always host- nor symbiont-specific (Goffredi *et al.* 2008, 2014; Durand *et al.* 2010).

Table 4: Chemosynthetic symbioses with varying degrees of symbiosis specificity.

		Symbiont specificity (specificity of symbiont to a particular host)	
		high	**low**
Host specificity (specificity of host to a particular symbiont)	**high**	Catenulid flatworm (*Paracatenula*), deep-sea vesicomyid clams (Peek *et al.* 1998; Gruber-Vodicka *et al.* 2011)	Hydrothermal vent tubeworms (*Riftia, Tevnia*), deep-sea mussels (*Bathymodiolus*) (McMullin *et al.* 2003; Duperron *et al.* 2006)
	low	Siboglinid tubeworms (*Oligobrachia*) (Lösekann *et al.* 2008)	Deep-sea yeti crabs (*Kiwa* spp.) and cold seep tubeworms (*Lamellibrachia* and *Escarpia* spp.) (McMullin *et al.* 2003; Goffredi *et al.* 2008, 2014)

Extracellular or ectosymbiotic associations are generally assumed to be less intimate than endosymbiotic associations, because they are simply attached to the host surface (Smith 1979; Goffredi 2010). Thus, host-symbiont decoupling may be more likely. However, ectosymbionts of stilbonematine nematodes may be an exception to this, since a couple of studies have shown that each species is associated with a distinct ectosymbiont type (for more details see Section 1.5.4).

1.4 Vestimentiferan tubeworms and their intracellular endosymbionts

Vestimentiferan tubeworms (*Siboglinidae*, Annelida) are abundant members of hydrothermal vents and cold seep ecosystems worldwide. They build a monophyletic[4] group within the Siboglinidae and are commonly divided into two groups, based on ecology: the hydrothermal vent tubeworms *(Riftia, Oasisia, Tevnia* and *Ridgeia*) that exclusively colonize hydrothermal vent sites, and cold seep tubeworms (*Lamellibrachia, Escarpia, Paraescarpia* and

[4] A group of organisms that contain all the descendants of a particular common ancestor

Seepiophila) that preferentially colonize cold seep sites (Fig. 3) (reviewed by McMullin *et al.* 2003; Bright & Lallier 2010). All vestimentiferan tubeworms lack a mouth, anus and digestive tract and rely entirely on gammaproteobacterial sulfur-oxidizing bacteria, which they harbor in a special organ, called the trophosome. The trophosome fills out most of the tubeworm body and is densely packed with bacteria that are contained in bacteriocytes (Powell & Somero 1986; Hand 1987). While the host supplies its endosymbionts with hydrogen sulfide, oxygen, nitrate and inorganic carbon from the environment, the bacteria provide the host with autotrophically fixed carbon compounds (Fisher *et al.* 1989, 1990). Carbon transfer to the host can occur via two modes, direct transfer via leakage of small organic carbon compounds by the symbionts, or indirect transfer by digestion of the symbionts (Felbeck & Jarchow 1998; Bright, *et al.* 2000).

The bacterial symbionts are contained within the host body at high densities, and so do not have direct access to metabolic substrates from the environment. All tubeworms have to ensure a supply of substrates for their symboints, but the mode of substrate uptake and supply differs between tubeworm species. In hydrothermal vent tubeworms, such as *Riftia pachyptila,* all metabolites are taken up through the anterior blood-red gill plume from surrounding vent fluid and get transported via the vascular system to the trophosome (Childress & Fisher 1992). In cold seep tubeworms, such as *Lamellibrachia* cf. *luymesi,* sulfide is taken up via the root, a posterior thin-walled extension of the tube that is buried in the sediment, while inorganic carbon and oxygen are obtained via the plume (Julian *et al.* 1999; Freytag *et al.* 2001). Specialized extracellular hemoglobins in the blood of vestimentiferan tubeworms are able to bind both oxygen and sulfide, as a way to regulate sulfide toxicity (reviewed in Cavanaugh *et al.* 2006). Hydrothermal vents are richer in substrates than cold-seeps, but as geological features, the latter are much more persistent. This is reflected in the growth rates of tubeworms at vents vs. seeps: *R. pachyptila* is one the fastest-growing invertebrates on Earth, increasing its tube length by 85 cm per year (Girguis & Childress 2006). In contrast, *L. luymesi* only grows 0.77 cm per year and is thus the most long-lived (up to 250 years) non-colonial marine invertebrate known (Fig. 3) (Fisher *et al.* 1997; Bergquist *et al.* 2000).

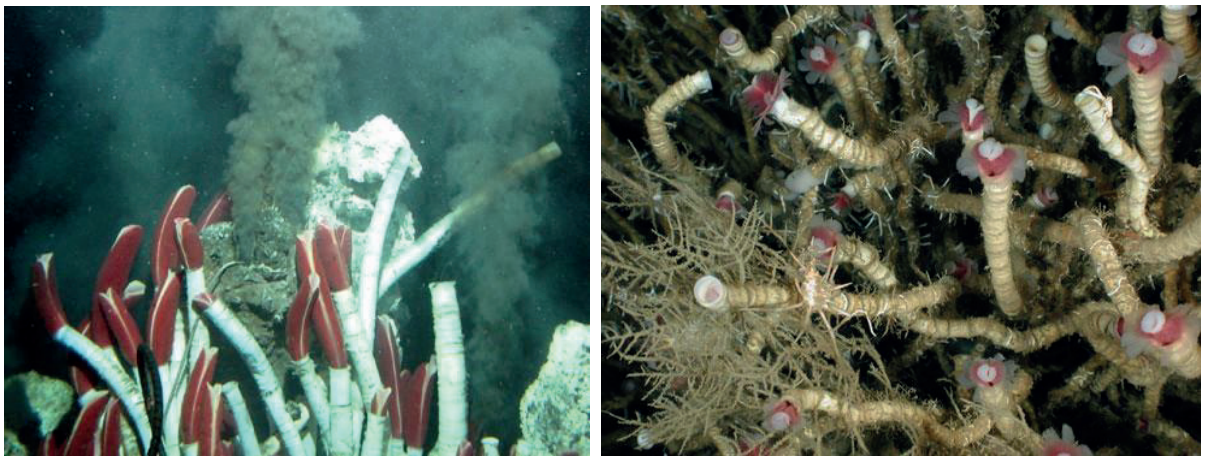

Fig. 3: The contrasting ecological settings of deep-Sea vestimentiferan tubeworms. (A) The well-studied and fast-growing *Riftia pachyptila* that lives on hard rock substrate close to black smokers at the East Pacific Rise. Sulfide and oxygen are taken up from the surrounding fluid by the red plume (picture from imcargade.com). (B) The long-lived *Lamellibrachia luymesi* that lives on sedimented cold seep sites in the Gulf of Mexico. Sulfide is acquired from the sediments through an extension of the trophosome, so-called "roots" (courtesy of MacDonald, Texas A&M).

1.4.1 Distribution

The hydrothermal vent tubeworms *Riftia, Ridgeia, Tevnia* and *Oasisia* have only been described from hot vents in the East-, Northeast and South Pacific, where they are often the dominant members of hydrothermal vent ecosystems (McMullin *et al.* 2003; Bright & Lallier 2010). The cold-seep genera *Lamellibrachia, Paraescarpia, Escarpia* and *Seepiophila* have a wider distribution and have been reported from the Gulf of Mexico, West- and East Pacific, the Atlantic Ocean, the North and the Mediterranean Sea (Bright & Lallier 2010). However, exceptions exist, since *Escarpia spicata* and several *Lamellibrachia* species have also been found to colonize moderate hydrothermal vent sites (e.g. Feldman *et al.* 1997; Kojima *et al.* 2002, 2006). In addition *E. spicata* has also been discovered at a whale fall (Feldman *et al.* 1997) and *Lamellibrachia sp.* in sunken shipwrecks (Dando *et al.* 1992; Hughes & Crawford 2008; Gambi *et al.* 2011). Prior to this PhD thesis, neither hydrothermal vent nor "cold seep tubeworms" have been described from hydrothermal vent sites apart from the Pacific Ocean. In my thesis I show that symbiotic tubeworms are not restricted to hydrothermal vent sites in the Pacific, but can also colonize hydrothermal vents in the Mediterranean Sea (Chapter I).

1.4.2 Diversity of symbionts

Most previous studies have reported the presence of a single gammaproteobacterial symbiont type in the trophosome of each vestimentiferan tubeworm species. This was based on clone libraries, direct sequencing of the 16S rRNA bacterial marker gene and metagenomic studies of the symbiont population from the hydrothermal vent tubeworm *R. pachyptila* and *Tevnia jerichonana* (reviewed by McMullin *et al.* 2003; Robidart *et al.* 2008; Gardebrecht *et al.* 2012). A few studies have questioned this paradigm and reported multiple co-occurring symbiont types including Bacteroidetes, Alpha-, Beta- and Gammaproteobacteria in the trophosome of some species (Naganuma *et al.* 1997, 2005; Elsaied *et al.* 2002; Kimura *et al.* 2003; Chao *et al.* 2007). However, in situ hybridization (ISH) results were inconclusive and thus evidence of whether the sequences originated from symbionts in the trophosome or were contaminants from the tube or environment is still missing (Bright & Lallier 2010). Prior to this PhD thesis there was one study that found two distinct but closely related gammaproteobacterial phylotypes in clone libraries of *L. anaximandri* from the Mediterranean Sea (Duperron *et al.* 2009). However it remained unclear whether these 16S rRNA sequences derived from two distinct symbionts or from one symbiont with multiple 16S rRNA operons. In this dissertation, I show conclusively that some tubeworms can contain multiple symbiont types, coexisting simultaneously in the same host individuals (Chapter II).

1.4.3 Transmission mode and specificity

Hydrothermal vent tubeworms are one of the few chemosynthetic symbioses, where the symbiont transmission mode has been resolved. Nussbaumer et al. (2006) showed with symbiont-specific fluorescence *in situ* hybridization (FISH) that once aposymbiotic larvae found a place to settle, free-living symbionts invade through the skin. After invasion, they migrate to the visceral mesoderm, and initiate the transformation of the digestive system into an endosymbiont-containing trophosome (Nussbaumer *et al.* 2006). The horizontal transmission of the symbionts was also confirmed by the detection of free-living symbionts that colonized bacterial-settlement devices deployed in vicinity to the tubeworms colonies (Harmer *et al.* 2008).

Even though horizontal transmission is commonly known to be more “risky”for the evolutionary stability of the symbiosis, all endosymbionts fall into a monophyletic clade within the Gammaproteobacteria, suggesting that all symbionts derived from a common ancestor (McMullin *et al.* 2003). Within this clade, four distinct sequence groups can be distinguished. Symbionts of the hydrothermal vent tubeworms all belong to one of the sequence groups, while symbionts of the cold seep tubeworms fall into one of the other three groups, respectively (McMullin *et al.* 2003). There seems to be no strict host-specificity for vestimentiferan tubeworms, since different individuals of the same host species do not always associate with the same symbiont type (McMullin *et al.* 2003; Bright & Lallier 2010). For example, the seep tubeworms *Lamellibrachia barhami* and *Escarpia laminata* can associate with endosymbionts from group 1 or 2 (Fig. 4). Furthermore both species can also share the exact same symbiont type, indicating that symbionts are also rather flexible (e.g. Feldman *et al.* 1997; Nelson & Fisher 2000). Similarly, hydrothermal vent tubeworms *Riftia, Oasisia* and *Tevnia* share the same symbiont type, indicating no strict symbiont specificity towards a certain host species (Fig. 4). Resulting from this, several scientists have speculated that apart from the host species, geographical location and water depth could influence symbiont phylogeny (Di Meo *et al.* 2000; McMullin *et al.* 2003). My thesis provides strong indications that one of the most important factors structuring endosymbiont diversity is water depth (Chapter II).

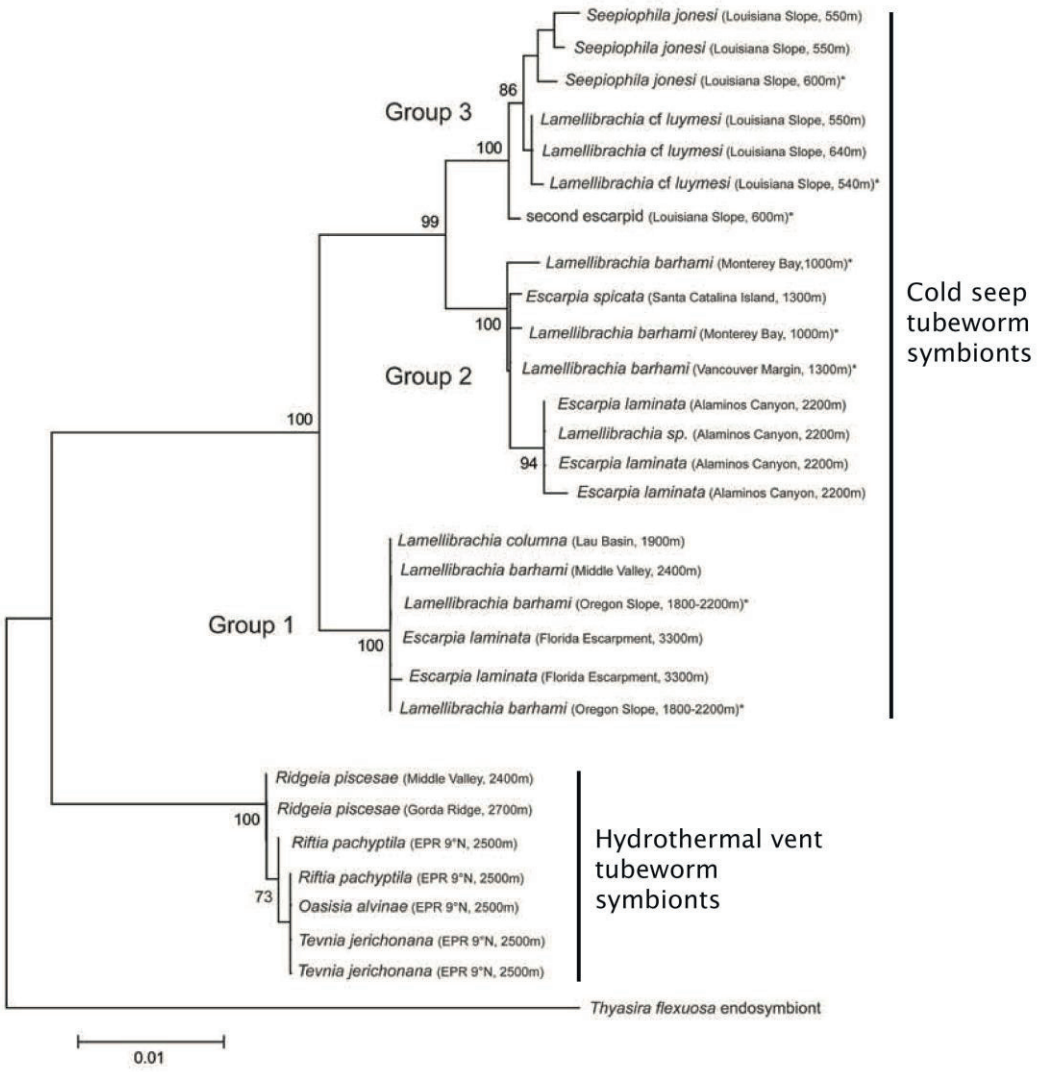

Fig. 4: Phylogenetic relationship of endosymbiotic bacteria from vestimentiferan tubeworms based on their 16S rRNA genes. Symbionts of cold seep tubeworms fall into three distinct sequence groups, while all symbionts of hydrothermal vent tubeworms, fall into one distinct symbiont group. The scale bar represents 1% estimated sequence divergence. EPR: East Pacific Rise (modified from McMullin *et al.* 2003).

1.5 Stilbonematine nematodes and their ectosymbiotic bacteria

Marine nematodes of the subfamily Stilbonematinae within the family *Desmodoridae* (*Chromadoria*: *Adenophorea*) are widely distributed in marine sulfidic sediments worldwide (Ott *et al.* 2004; Tchesunov 2013). Members of this group are characterized by three synapomorphic[5] characters: (1) Association with sulfur-oxidizing ectosymbiotic bacteria. (2) A

[5] relating to a character or trait which is found only (in a more or less modified form) in a particular group (clade) of organisms and is held to derive from a single character in their most recent common ancestor.

reduced and unarmed oral cavity and weak pharynx[6] (3) Special glandular sensory organs (GSOs) located below the nematodes' cuticle (reviewed by Ott *et al.* 2004):

(1) Sulfur-oxidizing ectosymbiotic bacteria

The morphologically diverse ectosymbiotic bacteria of stilbonematine nematodes are probably the most peculiar feature about these worms and cover their hosts' cuticle in fascinating ways (Fig. 5). For example, the cuticle of genera such as *Leptonemella* or *Stilbonema* is completely covered by coccoid bacteria, except for the head and the tail tip (Fig. 5C). In other species such as *Laxus oneistus, Robbea hypermnestra* or some *Catanema* sp., the bacteria are rod-shaped (Fig. 5D). Symbionts of *Eubostrichus* species are the most peculiar and largest in size. *E. dianae* is covered by filamentous bacteria that can reach up to 120 µm in size (Polz *et al.* 1992; Pende *et al.* 2014), while *E. fertilis and E. parasitiferus* are covered by crescent-shaped bacteria that confer a rope-like appearance to the worms (Fig. 5F). The morphology of the symbionts is however not always related to the host genus, because *Catanema* or *Robbea* sp. symbionts can either harbor symbionts that resemble corn kernels or rods (Fig. 5D - E). While the previously-mentioned symbiont shapes are the most common, other symbiont shapes have also been observed, such as rice-grain shaped symbionts on *Squanema* species (own observation).

Some of the symbionts have even developed unusual cell division mechanisms, arguably to not loose contact to the hosts' surface. For example, rod-shaped symbiont cells of *Catanema* sp. and *Laxus oneistus* from the Carribean Sea divide longitudinally rather than transversely to the long cell axis (Fig. 5D) (Polz *et al.* 1992; Leisch *et al.* 2012).

[6] The part of the alimentary canal immediately behind the mouth in invertebrates.

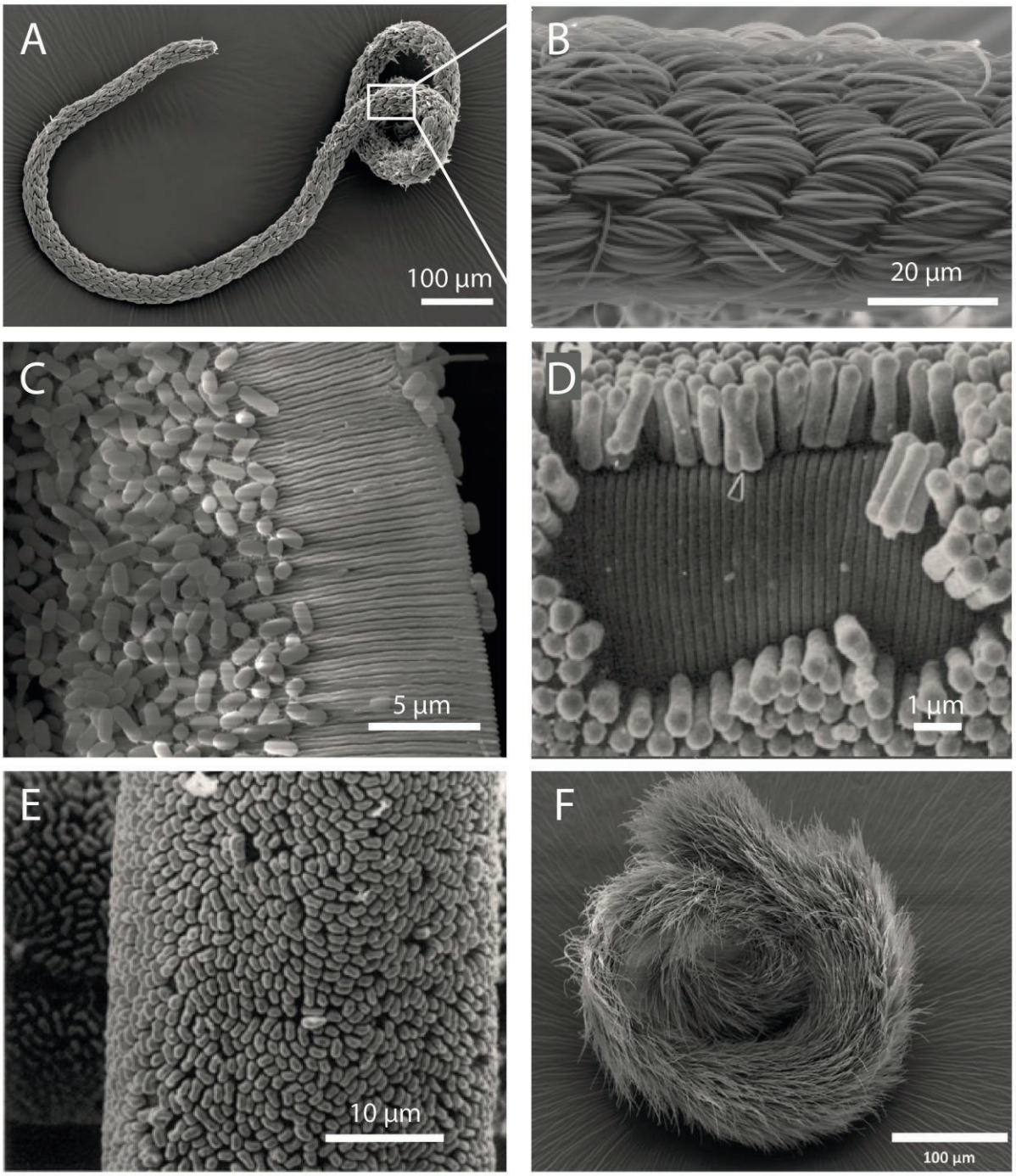

Fig. 5: Scanning electron microscopy images illustrating the morphological diversity of stilbonematine nematode ectosymbionts. A- B: *Eubostrichus fertilis* with crescent-shaped bacteria. C: *Leptonemella* sp. covered by multi-layered coat of coccoid symbionts. D: *Catanema sp.* covered by a monolayer of rod-shaped symbionts (arrow poins toward a cell dividing longitudinally) E: *Catanema* sp. with a monolayer of corn kernel-shaped symbionts. F: *Eubostrichus dianae* with long filamentous symbionts. A and F: modified from N. Leisch, S. Bulgheresi (CCRE Annual report 2012, 2013); B: modified from Pende *et al.,* (2014); C: courtesy of N. Leisch; D and E: modified from Polz *et al.*(1992).

On the other hand, the filamentous symbiont cells of *Eubostrichus* sp. divide transversely and it is nor clear whether the newly produced cells re-attach to the cuticle or are lost to the environment (Pende *et al.* 2014). It is also still unclear whether the host controls the longitudinal division of the symbionts (Pende *et al.* 2014). Some stilbonematine nematode species also show morphological adaptations towards their symbionts coat, which suggest coevolution between both partners. For example, some *Catanema, Robbea* and *Laxus* species have a symbiont-free head region and the symbiont coat begins at a sharp line behind the nematodes' anterior end. Astonishingly, the host diameter decreases at exactly this line to accommodate the thickness of the symbiont coat (Fig. 10A) (e.g. Polz *et al.* 1992; Ott *et al.* 1995). An even body thickness could be advantageous for a host living in the sand, because moving through sediment grains would result in less friction and thus prevent symbiont loss.

(2) Reduced/unarmed oral cavity

In contrast to non-symbiotic desmodorids, all members of the Stilbonematinae have a highly reduced oral cavity that is unarmed (no large teeth or jaws) and the main muscular pump behind the pharynx is mainly glandular (Hoschitz *et al.* 2001; Ott *et al.* 2004). Whether this is related to the symbiotic lifestyle is still unclear (Ott *et al.* 2004).

(3) Complex glandular sensory organs (GSOs)

GSOs in stilbonematine nematodes can be easily spotted in a light microscope due to their light-refractile storage granules and their omnipresence below the cuticle of their hosts (Bauer-Nebelsick *et al.* 1995). Their GSOs consist of a basiepidermal complex of three cells: a type A glandular cell, a monociliated type B glandular cell and a monociliated sensory cell and commonly terminate in a pore at the end of a hollow setae (Fig. 6) (Nebelsick *et al.* 1992; Bauer-Nebelsick *et al.* 1995). Other closely related non-symbiotic marine nematodes of the subfamilies Desmodorinae and Spiriniinae also have GSOs, but they are comparably simple and consist only of one type A glandular cell and one biciliated sensory cell (Bauer-Nebelsick *et al.* 1995). The number and size of the setae varies among the different stilbonematine nematode species. In *Catanema* species the setae end just above the symbiont coat and droplets have been observed on the tip of the setae (Fig. 9 in Nebelsick *et al.* 1992), indicating that they have a secretory function. These mucus secretions have been suggested to fulfill various functions: promoting symbiont recognition, adhesion, embedding

of the symbionts and exclusion of competitors (Nebelsick *et al.* 1992; Bauer-Nebelsick *et al.* 1995; Nussbaumer *et al.* 2004; Bulgheresi *et al.* 2006, 2011).

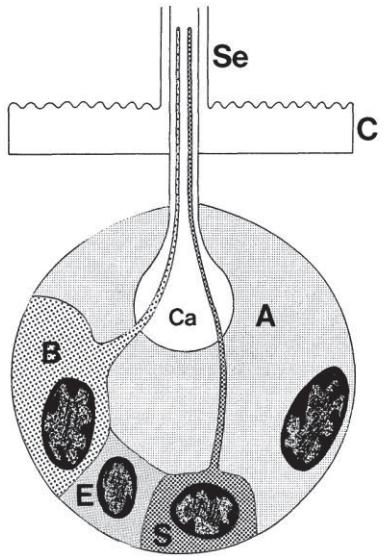

Fig. 6: Glandular sensory organ (GSO) of stilbonematine nematodes. GSOs are large gland cells that can be found below the nematodes' cuticle throughout the length of the nematodes. They consist of three cells: type A glandular cell (A) type B glandular cell (B) and a monociliated sensory cell (S), occasionally one undifferentiated epidermal cell (E) and a centrally positioned canal (Ca) that leads through the cuticle (C) and ends in a pore at the tip oft the hollow setae (SE). From Bauer-Nebelsick *et al.* (1995)

1.5.1 Host diversity and phylogeny

First descriptions of stilbonematine nematodes date back almost 150 years when Greeff (1869) described two *Eubostrichus* species from the Canary island and the North Sea. Since then, taxonomists have described a total of ten different genera, which include *Adelphos*, *Catanema*, *Centonema*, *Eubostrichus*, *Laxus*, *Leptonemella*, *Parabostrichus*, *Robbea*, *Stilbonema and Squanema* and more than 50 different species (Greeff 1869; Cobb 1894, 1920; Chitwood 1936; Gerlach 1956, 1963; Ott 1997; Tchesunov *et al.* 2012; Leduc 2013) (detailed list in Appendix). However, taxonomic nomenclature has proven especially difficult for stilbonematine nematode species, since unique identifying morphological characters of different genera have been controversial among taxonomists (Ott *et al.* 2004; Tchesunov 2013). Some nematode species have therefore gone through several re-namings and some genus-specific characters are still under debate. Closely related species are especially difficult to distinguish based on morphology.

Due to the general difficulty to distinguish nematodes based on morphological characters, molecular marker genes have been widely used and have gained acceptance among nematode taxonomists (Blaxter *et al.* 1998; Powers 2004). Apart from internal transcribed spacer regions of the ribosomal RNA operon and mitochondrial genes, the 18S rRNA gene

has widely been used to distinguish between closely related nematode species and to investigate their evolutionary history (Blaxter *et al.* 1998; Meldal *et al.* 2007).

Stilbonematines have been relatively neglected by molecular phylogenetics. Two studies have published 18S rRNA sequences from several stilbonematine nematode species and found that different species can be clearly resolved by the ribosomal gene (Kampfer *et al.* 1998; Bayer *et al.* 2009) (Fig. 7). Both studies supported monophyly of stilbonematine nematodes, suggesting that all Stilbonematinae evolved from a common ancestor. Kampfer *et al.* (1998) found that three different *Eubostrichus* species built a monophyletic group within the Stilbonematinae according to their 18S rRNA sequences. However, the study by Bayer *et al.* (2009) found that 18S rRNA sequences of three different *Robbea* species did not cluster together (Fig: 7). This discrepancy between morphological characters and molecular data has raised some doubt as to whether the 18S rRNA is a suitable marker to resolve different stilbonematine nematode genera and species or whether the descriptive morphological characters of *Robbea* need to be corrected. During the course of this dissertation, I have considerably increased the taxonomic sampling for stilbonematine molecular phylogenetics (Chapter III, IV and Appendix).

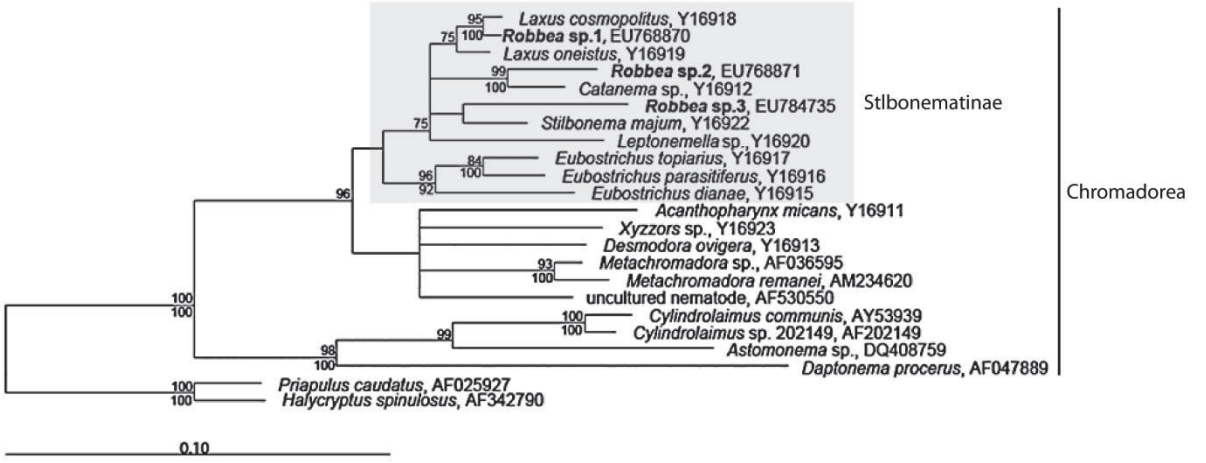

Fig: 7: Phylogenetic relationship among stilbonematine nematodes and other nematodes, based on their 18S rRNA genes. Consensus tree based on Maximum parsimony and Treepuzzle analyses. Treepuzzle support values (above tree branches) and parsimony bootstrap values (below tree branches) above 75 and 70% are shown. The scale bar represents 10% estimated sequence divergence (modified from Bayer *et al.* 2009).

1.5.2 Distribution

Highest abundances of stilbonematine nematodes can be found in tropical and subtropical continental shelf regions with calcareous sands such as the Caribbean (reviewed by Ott *et al.* 2004; Tchesunov 2013; Armenteros *et al.* 2014a). For example in the vicinity of the Caribbean island Carrie Bow Cay in Belize, numerous species of different genera often co-occur in just a small bucket of sand (own observation). Although not as abundant, stilbonematine nematodes have also been described from temperate beaches, such as the North Sea and even as far north as the White Sea in Russia (e.g. Greeff 1869; Gerlach 1950; Riemann *et al.* 2003; Tchesunov 2013) (Fig. 8). A few studies have also reported their existence in deep-sea sediments (Van Gaever *et al.* 2004; Leduc 2013), shallow hydrothermal vents (Kamenev *et al.* 1993; Thiermann *et al.* 1997) and methane seeps (Dando *et al.* 1994). Figure 8 summarizes published reports on the distribution of stilbonematines.

The genera *Eubostrichus* and *Leptonemella* are the most frequently reported and have been described from the Atlantic and Indian Oceans, and the Mediterranean, Red, Carribbean, and North Seas (Fig. 8A and D). Correspondingly, these genera are also the most speciose (14 and 11 spp. respectively) (Appendix). Members of *Eubostrichus* have also been reported from the Pacific coast of Mexico (Fig. 8D), but overall, sampling effort has been relatively small in the Pacific Ocean. The genera *Laxus, Stilbonema, Catanema* and *Robbea* have been less frequently reported with at least six, four, five and eight described species, respectively, however, their worldwide distribution is comparable to the most abundant species *Eubostrichus* and *Leptonemella* (Fig. 8). Overall, none of the six most abundant stilbonematine nematode genera is restricted to a certain geographical location (Fig. 8).

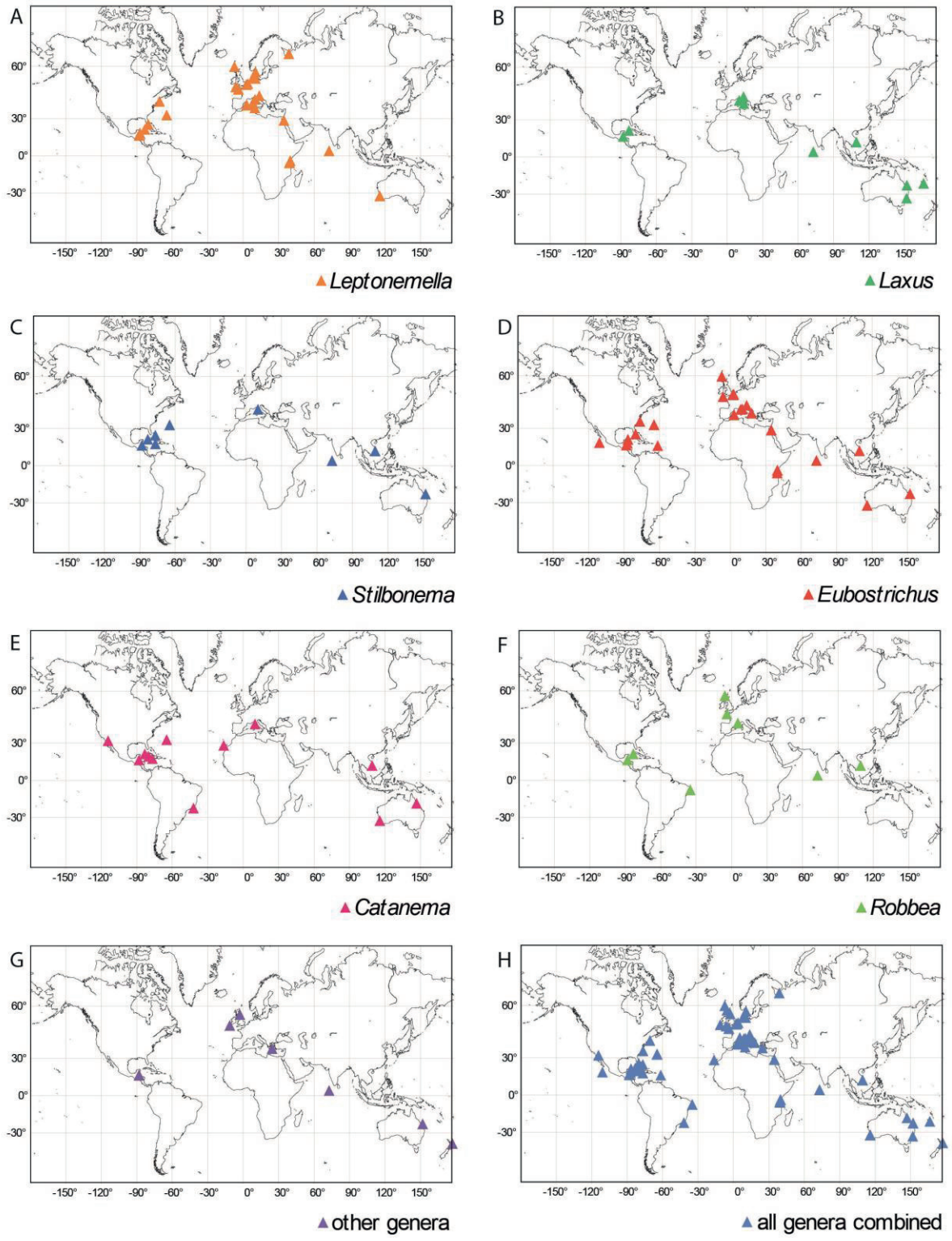

Fig. 8: Worldwide distribution of different genera of stilbonematine nematodes as reported in the literature until today. Other genera include *Parabostrichus, Squanema, Centonema*, and species of unknown or yet undescribed genera. A detailed list of record with respective citations can be found in the appendix. The map was generated using PanMap (Diepenbroek *et al.* 2002).

1.5.3 Symbiont metabolism

The symbiotic nature of the Stilbonematinae was not clear to early taxonomists. When species of the genus *Eubostrichus* were first described, the symbiont coat was interpreted as cuticular ornamentation (Greeff 1869), followed by their description as fungal spores (Chitwood 1936) and “blue-green algae” (cyanobacteria) (Wieser 1959). Twenty years later when Powell *et al*. (1979) investigated the toxic effect of ^{35}S-sulfide on meiofauna, including *E. dianae* he was surprised to find particularly high ^{35}S accumulation in the ectosymbionts. This incubation was the first indication that the symbionts are sulfur-oxidizers. The lack of photosynthetic pigments and cellular structures also led Ott *et al*. (1982) to suggest that the nematodes are covered by thiotrophic bacteria.

Subsequent biochemical studies and incubation experiments with Caribbean Stilbonematinae have confirmed these initial hypothesis (Schiemer *et al.* 1990; Polz *et al.* 1992; Hentschel *et al.* 1999). For example, physiological studies showed that oxygen respiration rates of symbiotic worms significantly increased when sulfide was present and the bright-white colour of the symbionts was taken as an indication for sulfur storage (Schiemer *et al.* 1990). Enzyme assays identified key enzymes of the sulfur metabolism, such as ATP sulfurylase and sulfite oxidase and high amounts of elemental sulfur were measured in bulk worm samples by high-performance liquid chromatography (HPLC) (Polz *et al.* 1992). Together with the fact that the symbioses thrive is sulfide-rich habitats, this provided strong evidence that the symbionts can gain energy from oxidizing reduced sulfur compounds with oxygen as electron acceptor. Later, incubations with *Laxus oneistus* and *Stilbonema* sp. under anoxic conditions showed that hydrogen sulfide and thiosulfate can also be oxidized by the symbionts with nitrate as alternative electron acceptor (Hentschel *et al.* 1999).

The autotrophic nature of the symbionts was confirmed by the presence of ribulose 1,5 bisphosphate carboxylase/oxygenase (RuBisCO), the key enzyme of the Calvin Benson Bassham (CBB) cycle (Polz *et al.* 1992), and by incubations with ^{14}C- labelled bicarbonate that led to label enrichment in the symbiosis (Schiemer *et al.* 1990). Furthermore, poly-β-hydroxybutyrate (PHB) and of poly-β-hydroxyvalerate (PHV) could also be measured in a pooled sample of *Catanema, Stilbonema* and *Robbea* species, demonstrating that the symbionts can store carbon in form of polyydroxyalkanoates (PHA) (Polz *et al.* 1992). Apart from the thioautotrophic nature of the ectosymbionts, nothing is known about further

metabolic capabilities. In Chapter IV of this thesis, I show that the energy and carbon metabolism of stilbonematine nematode ectosymbionts is more versatile than previously thought.

1.5.4 Symbiont diversity

Diverse stilbonematine nematode ectosymbionts have been described based on their peculiar morphologies (Fig.5, Ott *et al.* 2004). From morphology alone, the stilbonematine symbionts appear to be host-specific, because many of the bacterial morphotypes are correlated with specific host taxa. However, before molecular phylogenetic methods were widely available, it was not possible to show whether the morphological differences are correlated with molecular differences.

Polz *et al.* (1994) published the first bacterial 16S rRNA sequence from *Laxus oneistus* and found that the symbionts belong to the Gammaproteobacteria. FISH analyses with symbiont-specific oligonucleotide probes hybridized with all of the *L. oneistus* ectosymbiont and suggested that the coat must consist of only a single phylotype (Polz *et al.* 1994). In contrast a subsequent study detected multiple 16S rRNA sequences of the Alpha-, Gamma- and Deltaproteobacteria, Cytophaga and Caulobacter in clone libraries of *E. dianae*, but none of the Gammaproteobacteria was closely related to the symbionts of *L. oneistus* (Polz *et al.* 1999). This was resolved by a follow-up study that showed that only a single gammaproteobacterial symbiont type is attached to *E. dianae*, suggesting that the previously detected bacteria were either contaminations from the nematode gut or other sources (Pende *et al.* 2014). A number of other studies have also published 16S rRNA genes of stilbonematine nematode species, and all of them were distinct and closely related to the previously published *L. oneistus* symbiont (Vanura, 2008, Bayer *et al.* 2009; Bulgheresi *et al.* 2011) (Fig. 9).

Although each species seems to associate with a distinct and dominant symbiont type, most studies have only sequenced the symbionts of a single individual, leaving the question of host-species specificity largely unresolved. Vanura (2008) published slightly different 16S rRNA sequences from *Stilbonema* sp. from Belize, indicating that different individuals share highly similar symbionts (NCBI accession numbers FM9553329 - 31). However it was unclear whether the sequences derived from symbionts of the same *Stilbonema* host species

(Fig. 9). In this dissertation I considerably enlarged the taxonomic sampling of stilbonematine nematode ectosymbionts and could show that indeed every species is associated with its own symbiont type that is never shared among species (Chapter III and IV).

1.5.5 Thiosymbiont clade

Similar to the host 18S rRNA sequences, also all stilbonematine nematode symbiont sequences fell into a monophyletic clade, suggesting that all symbionts derive from a common ancestor (Fig. 9) (Bayer *et al.* 2009; Bulgheresi *et al.* 2011). While the symbiont sequences from *Stilbonema* species built one monophyletic cluster, *Robbea* symbiont sequences published by Bayer *et al.* (2009) were paraphyletic, similarly to their corresponding 18S rRNA genes (Fig. 7 and 9). This suggested that neither the three host species nor their symbionts shared a direct common ancestor and indicated that higher taxon sampling is necessary to resolve whether environmental factors would influence symbiont phylogeny more than their host (Fig. 9).

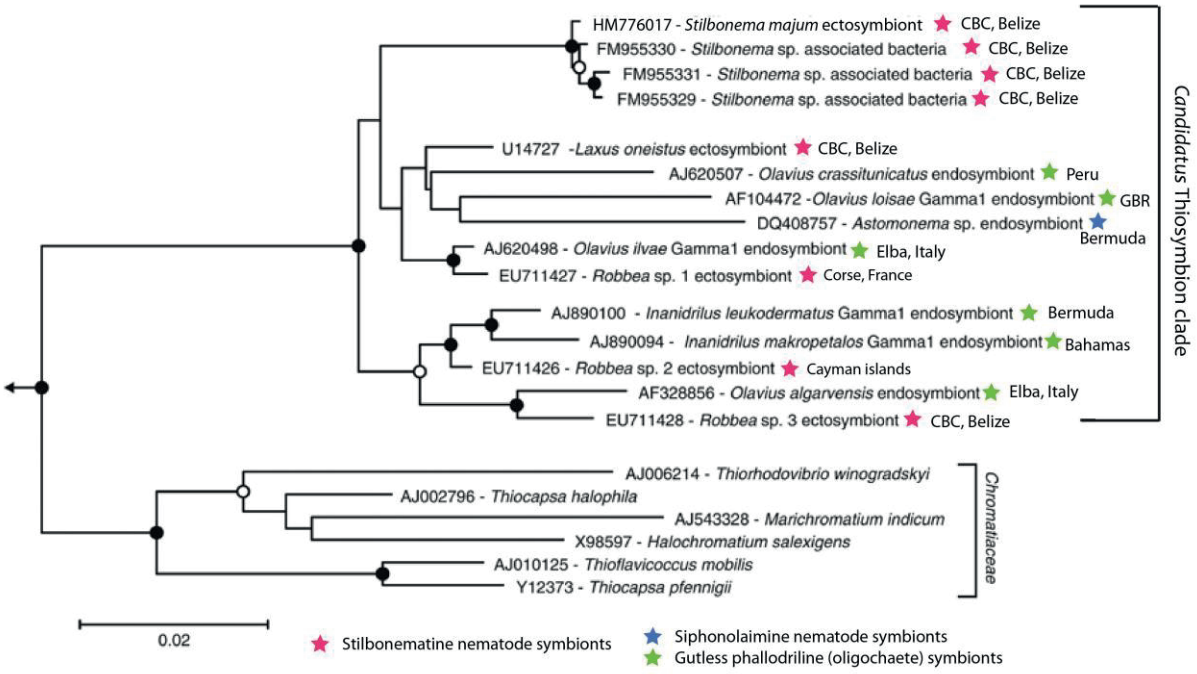

Fig. 9: Phylogenetic relationship of symbiotic bacteria from stilbonematine nematodes based on their 16S rRNA genes. Stilbonematine nematodes ectosymbionts fall into a highly supported cluster that also contains extracellular endosymbionts of gutless phallodriline annelids and endosymbionts of siphonolaimid nematodes. The scale bar represents 2% estimated sequence divergence. CBC: Carrie Bow Cay; GBR: Great Barrier Reef (modifed from Bulgheresi *et al.* 2011).

Interestingly, although the stilbonematine symbionts share a common origin, they do not exclusively associate with nematodes. The monophyletic clade also contains thiotrophic symbionts of other host animal groups, such as marine gutless phallodriline annelids (oligochaetes), which even belong to a different animal phylum, and siphonolaimid nematodes (*Astomonema* sp.), that belong to a different nematode family. Gruber-Vodicka *et al.* (in preparation) have named this clade *Candidatus* Thiosymbion, to reflect their common symbiotic and sulfur-oxidizing lifestyle. The *Cand.* Thiosymbion clade contains exclusively sequences of symbiotic bacteria, although one study has published partial 16S rRNA sequences from offshore waters that fall into the clade (Heindl *et al.* 2011). However, since only very short fragments of the 16S rRNA were amplified with nested PCR, is questionable whether these sequences derived from symbionts, closely-related free-living relatives or contaminants in the lab. The closest relatives that fall basal to the *Cand.* Thiosymbion clade are free-living sulfur-oxidizing bacteria of the family *Chromatiaceae* (Fig. 9).

Members of the *Cand.* Thiosymbion associate with host groups that have one thing in common: they all occur in shallow water sediments (Dubilier *et al.* 2008). However, the symbiotic lifestyle of all three closely related symbionts differs. Namely, symbionts of stilbonematine nematodes are attached to the host cuticle, whereas gutless phallodriline annelids contain their symbionts in the extracellular space between epidermal cells and the inner surface of the cuticle (Fig. 10A - F). Gutless phallodriline annelids harbor other endosymbionts in addition to *Cand.* Thiosymbion, but the only symbiont that is consistently found among all species is *Cand.* Thiosymbion (Fig. 10F, for more information see Section 1.6.3). *Astomonema* nematodes that belong to the mouthless siphonolaimine nematodes harbor *Cand.* Thiosymbion species in the gut lumen where they may be located intracellularly as in *A. jenneri,* or extracellularly as in *A. southwardum* and most likely also *A.* sp. from Bermuda (Fig. 10H - I) (Ott *et al.* 1982; Giere *et al.* 1995; Musat *et al.* 2007). In the phylogeny of the symbionts no clear clustering of symbionts according to host taxa is visible, and therefore host switching between these taxa may have occurred several times in the history of the *Cand.* Thiosymbion clade (Fig. 9).

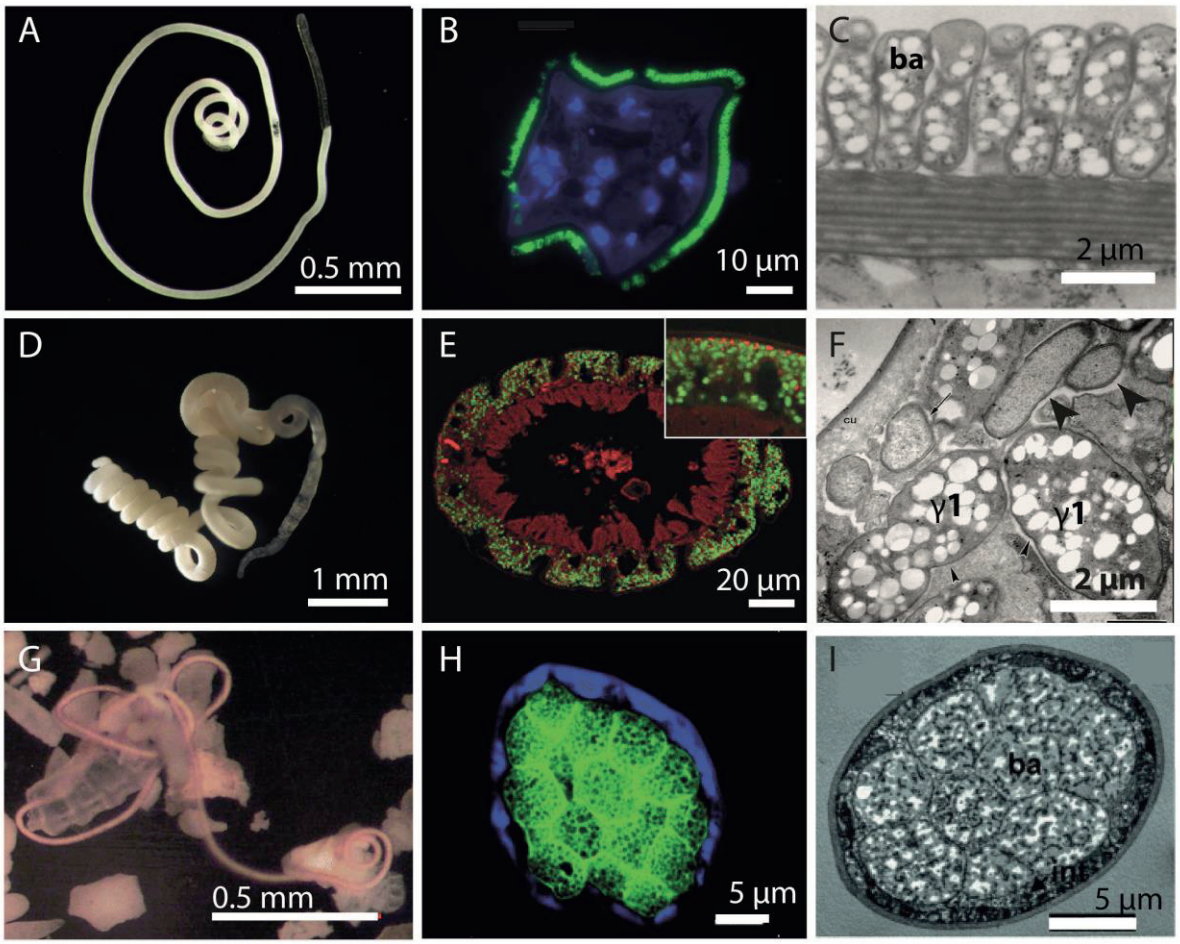

Fig. 10: Forms of symbiotic lifestyles of *Cand.* Thiosymbion with different marine invertebrate groups. A - C: Stilbonematine nematode *Laxus oneistus* with ectosymbiotic bacteria. D - F: Gutless phallodriline annelid *Olavius algarvensis* with extracellular endosymbiotic bacteria. G - I: Mouthless siphonolaimine nematode *Astomonema* sp. with endosymbiotic bacteria. A, D, G: Stereomicroscopy images of life animals. B, E, H: Fluorescence microscopy images of worm cross sections with symbiotic bacteria that were hybridized with gammaproteobacterial (B, E) (green) or general bacterial oligonucleotide probes (H) (green). *Olavius* cross sections were additionally hybridized with a deltapoteobacterial probe (red) (E). DNA was counterstained with DAPI (blue) (B, H). C, F, I: Transmission electron microscopy (TEM) images of worm cross sections showing the morphology of symbiontic bacteria (ba, γ1). The arrow heads point towards the smaller deltaproteobacterial cells in *O. algarvensis*. A: courtesy of N. Leisch; C: modified from Polz *et al*. (1992); D: courtesy of M. Kleiner; E: modifed from Ruehland *et al*. (2008); F: modifed from Dubilier *et al.* (2001); G - I: modified from Musat *et al.* (2007).

1.5.6 Symbiont transmission

The mode of symbiont transmission in stilbonematine nematodes has not been resolved yet. However, the current belief is that the ectosymbionts are transmitted horizontally, for the following reasons: (1) nematodes shed their cuticle together with their symbiont coat four times in their life cycle and the new cuticle needs to be re-colonized by symbionts (Nussbaumer *et al.* 2004), (2) unhatched early embryos of *Laxus oneistus* are symbiont-free, suggesting that symbionts are not transmitted maternally (S. Bulgheresi, unpublished in Bayer *et al.* 2009), (3) partial symbiont-specific 16S rRNA sequences have been found in offshore open water by PCR suggesting a free-living pelagic stage of the sulfur-oxidizing symbionts , but see above (Heindl *et al.* 2011).

The horizontal transmission mode has been supported by the detection of a highly symbiont-specific recognition mechanism in stilbonematine nematodes - host-secreted lectins (Ott *et al.* 2004; Nussbaumer *et al.* 2004). First indications that lectins are involved in symbiont recognition were given by Nussbaumer (2004) that showed that lectins binding specifically to D-glucose/D-mannose lead to symbiont detachment from the host. Bulgheresi *et al.* (2006) showed that mannose-specific lectins were only excreted by GSOs in the posterior region of *L. oneistus* but not the symbiont-free head region. A follow-up study demonstrated that symbionts of two co-occurring stilbonematine nematode species showed different affinities towards particular lectin isoforms (Bulgheresi *et al.* 2011). These studies demonstrated that lectins are a way to communicate between host and symbionts but whether horizontal or vertical transmission prevails, remains to be shown.

1.5.7 Benefits for both partners

Similarly to many other stable mutualistic associations, the mutual benefits for stilbonematine nematodes and their symbiotic partners have not been entirely resolved. For example, several indications exist that stilbonematine nematodes benefit by grazing on their own symbionts as food source. This has first been suggested by Wieser *et al.,* (1959) that observed similar microorganisms in the gut and on the cuticle of the nematodes. Subsequent TEM analyses of nematode cross sections by Jensen (1987), Ott & Novak (1989) and Ott et al. (1991) suggested the same (Fig. 11). Furthermore, $\delta^{13}C$ values of stilbonematine nematodes with and without symbionts were similarly low, suggesting that the nematodes live from their bacteria as sole food source (Ott *et al.* 1991). However, $\delta^{13}C$ values also

resembled those of free-living sulfur bacteria leaving the possibility open that their diet is based on sediment bacteria (Ott *et al.* 1991). Contrary to the feeding hypothesis, ingestion of bacteria has never been observed *in vivo* (e.g. Riemann *et al.* 2003; reviewed by Ott *et al.* 2004). Thus, conclusive evidence of whether stilbonematine nematodes feed on their own symbiotic bacteria or are general bacterivors that prey on free-living (sulfur) bacteria in the sediment is still missing. I shed light on this question in Chapter V of this thesis.

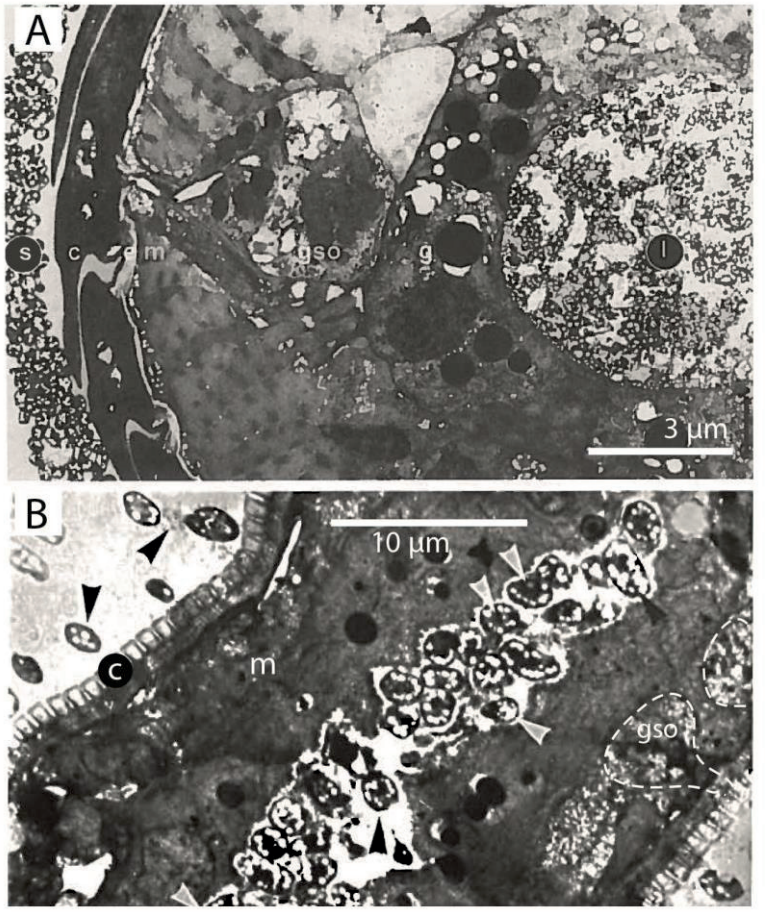

Fig. 11: Transmission electron microscopy image of stilbonematine nematode sections showing bacteria in the gut lumen. (A) *Stilbonema* sp. cross section. S: symbiont coat; c: cuticle; m: longitudinal muscles; gso: glandular sensory organ; g: gut epithelium; l: gut lumen. Picture taken from Ott *et al.* (2004). (B) *Leptonemella aphanothecae* longitudinal section. Black arrows point towards ectosymbionts; white arrows towards bacteria inside the gut lumen. GSOs are outlined in white. Picture modified from Jensen (1987).

A further benefit for the host may be the protection against sulfide poisoning by the symbiont coat (Ott *et al.* 1991; Hentschel *et al.* 1999). Hydrogen sulfide is known to reversibly bind and inhibit cytochrome c oxidase and oxygen transport proteins, and therefore interferes with the aerobic metabolism of animals. Evidence for a detoxification role by the ectosymbionts was given by Hentschel *et al*. (1999) that showed that stilbonematine nematodes have lower internal sulfide and thiosulfate concentrations than non-symbiotic nematodes from the same habitat. Furthermore, *Stilbonema majum* died rapidly in high sulfide concentrations (200 µM) after its symbionts were mechanically removed as compared to individuals with intact symbiont coat (Hentschel *et al.* 1999). Additionally, or alternatively, the nematodes may have

developed adaptations for tolerating certain levels of sulfide themselves. Detoxification of sulfide via methylation, oxidation or enzymatic binding have been described from many marine meiofauna organisms, including non-symbiotic nematodes that inhabit sulfide-rich habitats (Vismann 1991; Bagarinao 1992; Thiermann *et al.* 2000).

The benefit for the symbionts seems to be the mobility of their host (Ott *et al.* 2004). Highest abundances of stilbonematine nematodes can be commonly found in sediments that do not experience stable chemoclines. Instead, oxygen and sulfide gradients can often be separated by several cm (reviewed by Ott *et al.* 2004). Sulfur-oxidizing bacteria that depend on sulfur and oxygen for energy generation may thus gain benefit from the association with a mobile oxygen-dependent host that guarantees regular access to oxygen in upper and sulfide in lower sediment layers. Sulfur can be stored during availability of reduced sulfur compounds and oxidized in upper sediment layers where oxygen is available (Schiemer *et al.* 1990). However, nitrate can be used as alternative electron acceptor when oxygen is limited (Hentschel *et al.* 1999), which indicates that the symbiont metabolism does not entirely dependent on the mobility of their hosts. A further benefit for the symbionts may be a niche habitat where limited competition from other microorganisms is experienced (Polz *et al.* 2000).

1.6 Gutless phallodrilines and their extracellular endosymbionts

Gutless phallodrilines (Tubificidae, Annelida), also called gutless oligochaetes, are bright white and commonly found in tropical and subtropical marine shallow water sediments (Fig. 10D and 12 A) (Dubilier *et al.* 2006). The reduction of a mouth and gut in marine phallodrilines was first described in 1979, shortly after hydrothermal vents were discovered (Erséus 1979). Re-examination of the gutless phallodrilines revealed the presence of a thick layer of bacteria in the extracellular space between epidermal cells and cuticle (Fig. 10E and 12B) (Giere 1981). Shortly afterwards, enzyme essays and incubation experiments with ^{14}C-labeled bicarbonate confirmed the sulfur-oxidizing nature of the extracellular endosymbiotic bacteria (Felbeck *et al.* 1983). However, morphological, molecular and physiological studies over the last 35 years have revealed the true extent of a highly complex and metabolically versatile symbiotic community in gutless phallodrilines (see Section 1.6.4) (Dubilier *et al.*

2006). In addition to the lack of mouth and gut, excretory organs, such as nephridia, are apparently missing in these worms (Dubilier *et al.* 2006).

1.6.1 Host diversity and phylogeny

More than 80 species of gutless phallodrilines have been described from around the world since their description in 1979 and all of them have either been placed in the genus *Olavius* or *Inanidrilus* (Dubilier *et al.* 2006). Phylogenetic analyses of the mitochondrial cytochrome oxidase I (COI) gene and the nuclear 18S ribosomal ribonucleic acid (rRNA) gene, that are commonly used marker gene for invertebrates (Halanych & Janosik 2006; Bucklin *et al.* 2011), supported the monophyly of *Olavius* and *Inanidrilus* within the Phallodrilinae (Nylander *et al.* 1999; Erséus *et al.* 2000, 2002). While a common ancestor was supported for *Inanidrilus*, it was unclear whether *Olavius* is a sister group of *Inanidrilus* or is paraphyletic (Nylander *et al.* 1999). A further molecular study that included both the mitochondrial 16S rRNA gene and the nuclear 18S rRNA gene concluded that both genera are sister clades (Sjölin *et al.* 2005). However, the latter study only included sequences of six different species and thus a larger taxon sampling is needed to confirm this conclusion.

1.6.2 Distribution

The highest abundances of gutless phallodrilines have been reported from tropical and subtropical coral reef sediments (Dubilier *et al.* 2006). For example in the shallow water habitats around Bermuda, estimated densities of 80, 000 *I. leukodermatus* individuals per m^2 can be found in fairly organic matter-rich sulfidic sediments (Giere *et al.* 1982). However, high densities are also present in more temperate regions, such as the highly oligotrophic (nutrient-poor) silicate sediment off the coast of Elba, Italy (Giere & Erséus 2002; Dubilier *et al.* 2006). Here the worms dwell in coarse-grained sand close to seagrass meadows where only trace amounts of sulfide were measured (Dubilier *et al.* 2001, M. Kleiner, C. Wentrup, unpublished data). Apart from that, a number of species have also been described from other temperate to cold sandy sediments in the Northwest Atlantic and the continental margins off California and Peru (Davis 1985; Ftnogenova 1986; Erséus 1991). Members of the gutless phallodrilines are known to occur in the Pacific, Atlantic and Indian Ocean, the Caribbean, Red and Mediterranean Seas and several species can be found in more than one location (Bergin, 2009).

1.6.3 Symbiont diversity and transmission

All gutless phallodriline species that were investigated to date harbor a consortium of bacterial symbionts below their cuticle (Dubilier *et al.* 2006). Every species harbors one primary gammaproteobacterial symbiont from the *Cand.* Thiosymbion clade (previously called Y1-symbiont) that is also the largest and easily identifyable morphotype in cross sections (up to 7 µm). The *Cand.* Thiosymbion endosymbiont commonly contains large amounts of polyhydroxyalkanoate (PHA) vesicles and sulfur globules, as observed in transmission electron microscopy (TEM) cross sections that give the worms the bright white colour (Fig. 10D and F). Additionally, smaller bacteria commonly co-occur with the *Cand.* Thiosymbion (Fig. 10F) (Dubilier *et al.* 2006). Depending on the species they can belong to the *Alpha*-, *Gamma*- or *Deltaproteobacteria*, and in some species also symbionts affiliated with spirochetes have been found (e.g. Blazejak *et al.* 2005, 2006; Ruehland *et al.* 2008). Based on symbiont marker gene analyses, such as the 16S rRNA gene and FISH analyses, the number of symbionts can range from three phylotypes, e.g. in *O. loisae* and *I. makropetalus* (Dubilier *et al.* 1999; Blazejak *et al.* 2006) to six different phylotypes in *O. crassitunicatus* (Blazejak *et al.* 2005). The *Cand.* Thiosymbion has also been named the primary or obligate symbiont, because it is present in all so far investigated species, except for one (Bergin, 2009). The first 16S rRNA sequence was published from a *Cand.* Thiosymbion of *I leukodermatus* from Bermuda and since then all of the published sequences consistently fell into the *Cand.* Thiosymbion clade (Fig. 9) (Dubilier *et al.* 1995). While symbiont sequences of two *Inanidrilus* individuals built a monophyletic clade, symbionts of different *Olavius* species were paraphyletic (Fig. 9). Similarly to the stilbonematine nematode ectosymbionts, no clear clustering pattern of the endosymbionts due to host nor geographical location can be observed (Fig. 9).

The transmission mode of the symbionts has not been entirely resolved. Giere (1981) suggested that the symbionts are smeared onto the mucus-covered egg during oviposition and Krieger (2000) found evidence that bacteria are present between the egg and the mucus layer surrounding it. These observations together with the fact that the Y1-symbiont is present in almost all of the investigated species lead to the assumption that at least the Y1-symbiont is vertically transmitted (Dubilier *et al.* 2006). However, an indication that this process can be leaky is given by *I. exumae,* where instead of the Y1-symbiont, another symbiont has been discovered that does not belong to the *Cand.* Thiosymbion clade, the so-

called the Ɣ4-symbiont (Bergin, 2009). This discovery indicates that replacement of the primary symbiont is possible, not just with another Thiosymbion species, but by members of other bacterial clades.

1.6.4 Symbiont metabolism

The best-studied gutless phallodriline symbiosis in terms of symbiont metabolism is the *O. algarvensis* symbiosis off Elba, Italy. In 2001, a study that performed physiological and molecular analyses could show that the co-existing gamma- and deltaproteobacterial symbionts (*Cand.* Thiosymbion and δ1) in *O. algarvensis* do not compete with each other but are in fact involved in a syntrophic sulfur cycle (Dubilier *et al.* 2001). This was based on the fact that the δ1-symbionts are sulfate-reducers that produce sulfide, which can in turn serve as an energy source for the sulfur-oxidizing *Cand.* Thiosymbion. Two further gamma- and deltaproteobacterial symbionts (Ɣ3 and δ4) were detected in a later study and also a fifth spirochete symbiont was found in *O. algarvensis* (Dubilier *et al.* 2006; Ruehland *et al.* 2008). A metagenomic study by Woyke et al. (2006) showed that both gammaproteobacterial symbionts (*Cand.* Thiosymbion and Ɣ3) are sulfur oxidizers and both δ-symbionts sulfate reducers. An intriguing finding was that both symbionts also have the genetic machinery to recycle organic osmolytes and nitrogen-rich waste products of the host, which could explain why the host can survive without excretory organs (Woyke *et al.* 2006). Furthermore the study indicated that the δ-symbionts could use hydrogen as an energy source and the Ɣ3-symbiont nitrate as alternative electron acceptor to oxygen (Woyke *et al.* 2006). A follow-up study using metatranscriptomic and metaproteomic data disclosed even further metabolic capacities (Kleiner *et al.* 2012b). The presence of a partial 3-hydroxypropionate bicycle (3-HPB) in the *Cand.* Thiosymbion was suggested as novel pathway for the assimilation of carbon-rich host fermentation products (Fig. 12). A more energy-efficient version of CO_2 fixation via a modified version of the Calvin Benson Bassham (CBB) cycle was proposed in both gammaproteobacterial symbionts. The expression of hydrogenases in both δ-symbionts confirmed the initial hypothesis by Woyke (2006) that H_2 can be used for energy generation. Carbon monoxide dehydrogenases were expressed by the δ1-, δ4- and Ɣ3-symbionts, suggesting that yet another electron donor can fuel the symbiosis (Kleiner *et al.* 2012b) (Fig. 12). Together the physiological strategies of the symbionts and synthrophic relationship with their host might be the key to their success in the nutrient-poor habitats off Elba.

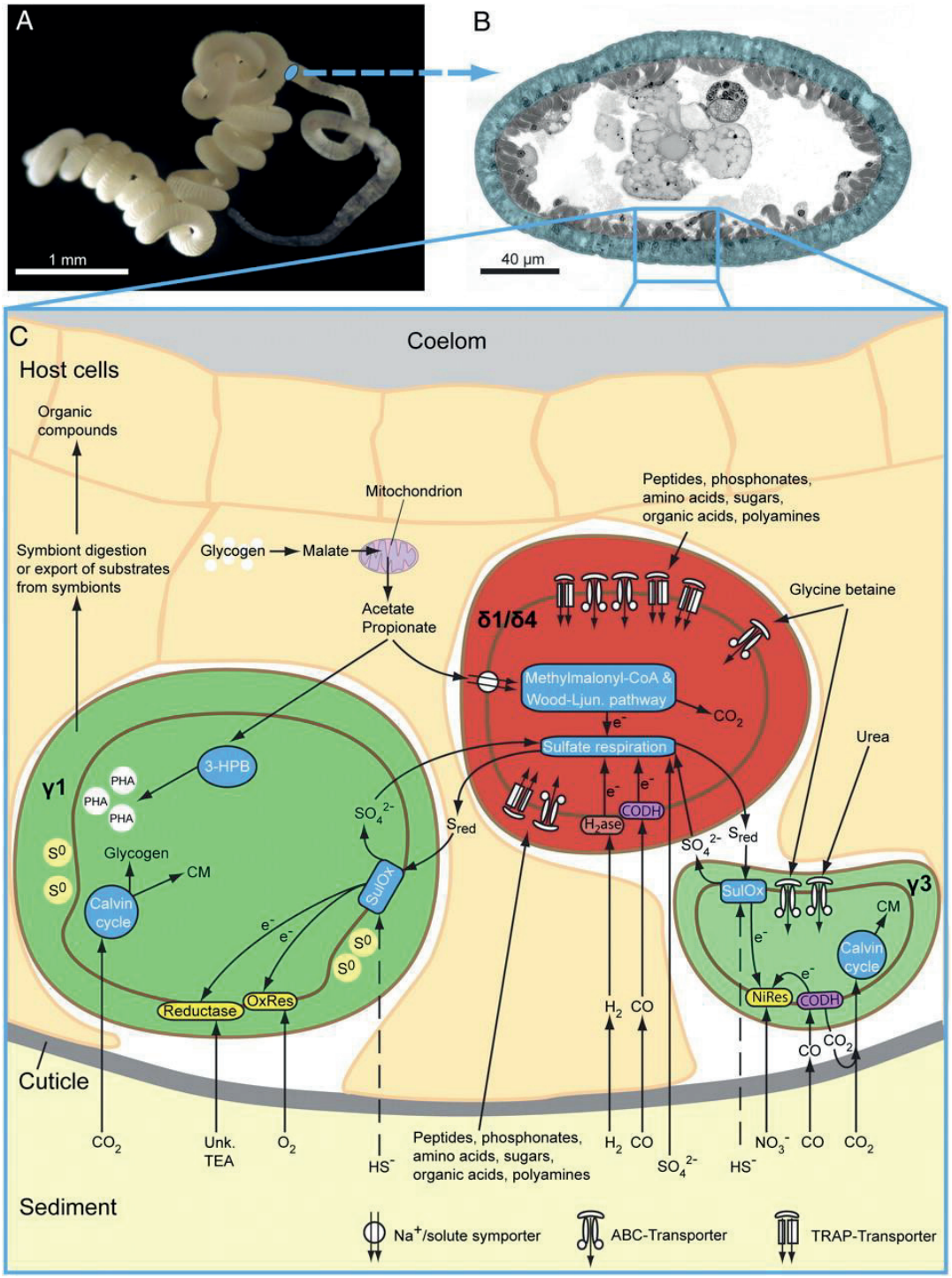

Fig. 12: Overview of symbiotic metabolism based on metaproteomic and metabolomic analyses. (A) Live *O. algarvensis* specimen. (B) Light micrograph of a cross section through *O. algarvensis*. The region containing the symbionts is highlighted in blue. (C) Metabolic reconstruction of symbiont and host pathways. The δ1- and δ4-symbionts are shown as a single cell, because most metabolic pathways were identified in the δ1-symbiont and only a small fraction of the same pathways were identified in the δ4-symbiont because of the low coverage of its metaproteome. 3-HPB, partial 3-hydroxypropionate bicycle; CM, cell material; CODH, carbon monoxide dehydrogenase (aerobic or anaerobic type); NiRes, nitrate respiration; OxRes, oxygen respiration; PHA, polyhydroxyalkanoate granule; S^0, elemental sulfur; S_{red}, reduced sulfur compounds; SulOx, sulfur oxidation; Unk. TEA, unknown terminal electron acceptor (from Kleiner et al. (2012b)).

1.7 Aims of this thesis

This thesis focusses on the diversity, specificity and evolutionary history of marine bacterial symbioses and the function of the sulfur-oxidizing bacteria by investigating a number of contrasting symbiotic systems, but with an emphasis on stilbonematine nematode ectosymbioses.

The broader aim was to understand whether the symbiotic lifestyle would influence the degree of specificity and evolutionary stability of a symbiotic relationship. To address these general themes, my work focused on the following specific questions:

Do deep-sea tubeworms from Marsili seamount harbor multiple endosymbionts and what influences their evolution?

Before I started this thesis, vestimentiferan tubeworms were generally believed to harbor a single sulfur-oxidizing endosymbiont type, except for a single study that suggested that some cold seep tubeworms in the Mediterranena Sea might associate with two sulfur-oxidizing symbionts. Furthermore, vestimentiferan tubeworms had never been found on a hydrothermal vent outside of the Pacific Ocean. This changed when tubeworm colonies were discovered on the Marsili seamount in the Mediterranean Sea. Christian Lott and Miriam Weber from the Hydra Station on Elba, Italy were the first to take samples from these colonies and through our collaboration I had the chance to investigate these unknown tubeworm symbioses. My work identified the symbionts of these as-yet-unknown tubeworms using comparative 16S rRNA analysis and FISH, and showed that more than one symbiont type could coexist in the same host individual. I also characterized their metabolic potential and host-symbiont specificity. The research concerning this aim has already been published and is included in the form of a self-contained manuscript (Chapter II).

Are ectosymbiotic associations of stilbonematine nematodes evolutionary more stable than endosymbiotic associations in gutless phallodriline annelids?

Stilbonematine nematode ectosymbioses are abundant in many marine shallow water environments worldwide but only few 18S rRNA sequences from stilbonematine nematodes had been published prior to this study. Furthermore, morphological classifications that conflicted with host phylogenies have questioned taxonomic species nomenclature. Similarly, few ectosymbiotic bacteria had been characterized molecularly and mostly from a pool of multiple individuals, leaving questions about specificity largely unresolved.

The main aims concerning this project were: (1) To re-evaluate the 18S rRNA gene as phylogenetic marker for stilbonematine nematode phylogeny in collaboration with the nematode taxonomist Prof. Jörg A. Ott (Chapter III and published manuscript in the Appendix). (2) Investigate the specificity and evolutionary history of stilbonematine nematode ectosymbioses from sampling locations around the world using the host 18S rRNA and symbiont 16S-ITS-23S rRNA as phylogenetic marker genes. This project was done in collaboration with Cécilia Wentrup (MPI Bremen) and Christer Erséus (Gothenborg, Sweden) who investigated the specificity and evolutionary history of gutless phallodriline annelid endosymbioses from sampling locations around the world. By combining our datasets we aimed to compare the evolutionary history and level of specificity of both systems with their symbionts (both fall into the Thiosymbion clade) using cophylogenetic analyses. We also aimed to resolve the ancestral state of Thiosymbion and to determine possible host switches between the symbiotic systems. The outcome of this project is shown in Chapter III.

How specific are closely related and co-occurring stilbonematine nematode ectosymbioses, also with emphasis on the individual level?

This project is a follow-up study on Chapter III. Multiple closely related stilbonematine nematode species of the genus *Leptonemella* were known to co-occur off the North Sea island Sylt but none of the hosts nor the symbionts had been characterized. Furthermore, symbiont diversity between different individuals of stilbonematine nematodes had not been investigated prior to this thesis. The aims of this project were: (1) Characterization of the host species and the whole extent of inter- and intraspecies symbiont diversity by using host 18S rRNA and symbiont 16S-ITS-23S rRNA as phylogenetic marker genes. (2) *In situ* confirmation of the specificity by species-specific symbiont FISH probes. (3) Investigation of

whether the clonality of the symbiont coat observable with symbiont marker genes also holds true when sequencing symbiont metagenomes and subsequent single nucleotide polymorphism analyses. The outcome of this project is shown in Chapter VI.

Do stilbonematine nematodes gain nutrition from their ectosymbionts?

For decades stilbonematine nematodes have been hypothesized to gain nutrition from their symbionts. This was based on two observations: (1) Light and electron microscopic images that showed bacteria in the gut lumen (2) A similar isotopic signature of host and chemosynthetic bacteria (Ott *et al.* 1991; Jensen 1995; Hoschitz *et al.* 2001). However, conclusive evidence that the bacteria in the gut are the same as the ectosymbionts was missing. Carbon transfer from symbionts to host would give additional proof that symbionts are used as food source. The aims of this project were: (1) Use of FISH with symbiont-specific probes to determine whether the bacteria in the gut of *Leptonemella* individuals from Sylt are the same as on the cuticle. (2) Incubation experiments of *Leptonemella* individuals with $^{14}C/^{13}C$-labeled bicarbonate to show autotrophic carbon fixation in the symbionts and label transfer to the host tissue using scintillation counting and microautoradiography. The results of this project are shown in Chapter V.

What is the metabolic potential of stilbonematine nematode ectosymbionts?

Incubations experiments have shown that stilbonematine nematode ectosymbionts are sulfur-oxidizing autotrophs. However, the exact metabolic pathways used and potentially novel functions, including host-symbiont interaction remained unanswered. Considering the availability of ectosymbiont draft genomes from Chapter IV I aimed to analyze the core metabolic functions and compare them to other chemosynthetic bacteria. I aimed to resolve the unique metabolic capabilities of the ectosymbionts compared to other symbiotic and free-living bacteria. The results of this project are shown in Chapter VI.

List of publications and chapters with author's contribution

1. **Dual symbiosis with co-occurring sulfur-oxidizing symbionts in vestimentiferan tubeworms from a Mediterranean hydrothermal vent.**

   Judith Zimmermann, Christian Lott, Miriam Weber, Alban Ramette, Monika Bright, Nicole Dubilier, and Jillian M. Petersen.

   Published in *Environmental Microbiology* (2014), 16(12): 3638–3656

2. **Codivergence and host switches between marine animal phyla with closely related ecto- and endosymbionts**

   Judith Zimmermann, Cécilia Wentrup, Miriam Sadowski, Anna Blazejak, Harald R. Gruber-Vodicka, Manuel Kleiner, Bodil Cronholm, Jörg A. Ott, Pierre de Wit, Christer Erséus, and Nicole Dubilier.

   Manuscript in preparation

3. **To each its own - diverse yet highly specific ectosymbionts on co-occuring nematodes from a temperate beach in the North Sea.**

   Judith Zimmermann, Harald R. Gruber-Vodicka, Rebecca Ansorge, Bruno Hüttel, Niculina Musat, Jörg A. Ott, Nicole Dubilier, and Jillian M. Petersen.

   Manuscript in preparation

4. **Investigating the nutritional role of ectosymbionts for their nematode host.**

   Judith Zimmermann, Rahel Yemanaberhan, Oliver Jäckle, Jörg A. Ott, Nicole Dubilier, and Jillian M. Petersen

   Preliminary results

5. **Genomic insights into marine nematode sulfur-oxidizing ectosymbionts**

   Judith Zimmermann, Jillian M. Petersen, Jasmine Berg, Nicole Dubilier, and Manuel Kleiner

   Manuscript in preparation

6. Phylogenetic confirmation of the genus *Robbea* (Nematoda: Desmodoridae, Stilbonematinae) with the description of three new species.

Jörg A. Ott, Harald R. Gruber-Vodicka, Nikolaus Leisch, and **Judith Zimmermann**

Published in *Systematics and Biodiversity* (2014), 12(4): 434-455

This manuscript has been published in the time frame of this PhD thesis and helped to resolve some of the aims formulated in this thesis.
The manuscript is included in the Appendix.

Chapter II

Dual symbiosis with co-occurring sulfur-oxidizing symbionts in vestimentiferan tubeworms from a Mediterranean hydrothermal vent

Authors: Judith Zimmermann[1], Christian Lott[2], Miriam Weber[2], Alban Ramette[2], Monika Bright[3], Nicole Dubilier[1], and Jillian M. Petersen[1]

[1]Department of Symbiosis, Max Planck Institute for Marine Microbiology, Celsiusstrasse, Bremen, Germany
[2]HGF MPG Group for Deep Sea Ecology and Technology, Max Planck Institute for Marine Microbiology, Celsiusstrasse, Bremen, Germany
[2]Elba Field station, Hydra Institute for Marine Sciences, Fetovaia, Campo nell' Elba (LI), Italy
[3]Department of Limnology and Oceanography, University of Vienna, Althanstrasse, Austria

Published in *Environmental Microbiology* (2014), 16(12): 3638–3656.

J.Z. developed the concept, perfomed the symbiont and host marker gene sequencing and phylogenetic analysis, designed the FISH and helper probes, tested those and performed the CARD-FISH experiments, image and bacterial abundance analyses, conceived and wrote the manuscript together with J.M.P.; C. L. and M. W. organized the research cruise, sampled the tubeworms and measured environmental parameters; A.R.: performed the statistical analysis; M.B. contributed with semithin sections and light microscopy analyses; N.D. helped to develop the concept and edited the manuscript; J.M.P developed the concept, conceived and helped to write the manuscript.

environmental microbiology

Environmental Microbiology (2014) **16**(12), 3638–3656 doi:10.1111/1462-2920.12427

Dual symbiosis with co-occurring sulfur-oxidizing symbionts in vestimentiferan tubeworms from a Mediterranean hydrothermal vent

Judith Zimmermann,[1] Christian Lott,[1,2] Miriam Weber,[1,2] Alban Ramette,[1] Monika Bright,[3] Nicole Dubilier[1] and Jillian M. Petersen[1]*

[1]*Max Planck Institute for Marine Microbiology, Celsiusstrasse, Bremen, Germany.*

[2]*Elba Field Station, HYDRA Institute for Marine Sciences, Fetovaia, Campo nell'Elba (LI), Italy.*

[3]*Department of Limnology and Oceanography, University of Vienna, Althanstrasse, Vienna, Austria.*

Summary

Vestimentiferan Tws colonize hydrothermal vents and cold seeps worldwide. They lack a digestive system and gain nutrition from endosymbiotic sulfur-oxidizing bacteria. It is currently assumed that vestimentiferan Tws harbour only a single endosymbiont type. A few studies found indications for additional symbionts, but conclusive evidence for a multiple symbiosis is still missing. We investigated Tws from Marsili Seamount, a hydrothermal vent in the Mediterranean Sea. Molecular and morphological analyses identified the Tws as *Lamellibrachia anaximandri*. 16S ribosomal RNA clone libraries revealed two distinct gammaproteobacterial phylotypes that were closely related to sequences from other *Lamellibrachia* symbionts. Catalysed reporter deposition fluorescence *in situ* hybridization with specific probes showed that these sequences are from two distinct symbionts. We also found two variants of key genes for sulfur oxidation and carbon fixation, suggesting that both symbiont types are autotrophic sulfur oxidizers. Our results therefore show that vestimentiferans can host multiple co-occurring symbiont types. Statistical analyses of vestimentiferan symbiont diversity revealed that host genus, habitat type, water depth and geographic region together accounted for 27% of genetic diversity, but only water depth had a significant effect on its own. Phylogenetic analyses showed a clear grouping of sequences according to depth, thus confirming the important role water depth played in shaping vestimentiferan symbiont diversity.

Received 26 September, 2013; revised 31 January, 2014; accepted 9 February, 2014. *For correspondence. E-mail jmpeters@mpi-bremen.de; Tel. +49 421 2028823; Fax +49 421 2028580.

Introduction

Vestimentiferan tubeworms (Tws) belong to the polychaete family *Siboglinidae* and are commonly found at reducing habitats such as hydrothermal vents and cold seeps. All vestimentiferans lack a digestive tract and rely on symbiotic bacteria for their nutrition (reviewed by Nelson and Fisher, 2000; Bright *et al.*, 2013). The symbionts are hosted intracellularly in an organ called the trophosome. All symbionts are considered to be chemoautotrophic sulfur oxidizers (reviewed by Stewart *et al.*, 2005), although the symbionts of the hydrothermal vent species *Riftia pachyptila* have the genomic potential to live heterotrophically and to use hydrogen as an additional energy source (Markert *et al.*, 2007; Robidart *et al.*, 2008; Gardebrecht *et al.*, 2011; Petersen *et al.*, 2011).

Vestimentiferan Tws are commonly divided into two main groups. The first group, which includes the genera *Riftia*, *Oasisia*, *Tevnia* and *Ridgeia*, has only been found at hydrothermal vents in the Pacific Ocean. The second group, which includes the genera *Lamellibrachia*, *Escarpia*, *Paraescarpia* and *Seepiophila*, is found mainly at cold seeps around the world. However, exceptions exist, as some 'cold seep' species such as *Escarpia spicata*, *Lamellibrachia barhami*, *Lamellibrachia satsuma* and *Lamellibrachia anaximandri* have been found at both vents and seeps (reviewed by Bright and Lallier, 2010; Thiel *et al.*, 2012). In addition, *E. spicata* has been described from a whale fall, and some *Lamellibrachia* Tws were found colonizing shipwrecks (Dando *et al.*, 1992; Feldman *et al.*, 1997; Hughes and Crawford, 2008; Gambi *et al.*, 2011). Nevertheless, the terms 'hydrothermal vent' and 'cold seep' vestimentiferans persist in the literature, possibly because both groups are considered to be highly specialized to either hydrothermal vent or cold seep habitats because of the contrasting mechanisms they have evolved for nutrient uptake. While vent-colonizing Tws such as *R. pachyptila* take up nutrients directly from the water through their anterior branchial plume, seep-colonizing Tws such as *Lamellibrachia luymesi* take up

sulfide through posterior body extensions called 'roots' that are buried in the sediment (Childress and Fisher, 1992; Julian *et al*., 1999; Freytag *et al*., 2001).

Most previous studies showed that each Tw individual harbours a single gammaproteobacterial sulfur-oxidizing symbiont type based on 16S ribosomal RNA (rRNA) analyses (reviewed by Bright and Lallier, 2010). Furthermore, the same symbiont phylotype can be shared by multiple species. For example, the symbionts of *Lamellibrachia columna*, *L. barhami* and *Escarpia laminata* all have identical 16S rRNA genes (Feldman *et al*., 1997; Nelson and Fisher, 2000; McMullin *et al*., 2003). On the other hand, Tws of one species can harbour a different symbiont phylotype depending on their location. For example, *E. laminata* from Alaminos Canyon in the Gulf of Mexico has a different symbiont phylotype to *E. laminata* from the Florida Escarpment (Nelson and Fisher, 2000). Previously identified patterns of host and symbiont distribution therefore attest to both the specificity (one host individual harbours only one symbiont) and the flexibility (hosts associate with a 'local' symbiont type) of these associations (McMullin *et al*., 2003).

A few studies have questioned this paradigm, reporting sequences other than the common gammaproteobacterial symbiont type. In clone libraries from the trophosome of *Ridgeia piscesae* in the East and *Lamellibrachia* sp. in the West Pacific, sequences belonging to the *Bacteroidetes*, *Alphaproteobacteria*, *Betaproteobacteria*, *Gammaproteobacteria* and *Epsilonproteobacteria* were found (Naganuma *et al*., 1997; 2005; Elsaied *et al*., 2002; Kimura *et al*., 2003; Chao *et al*., 2007). Two of these five studies did not use *in situ* hybridization (ISH) to confirm the observations from the clone libraries (Naganuma *et al*., 2005; Chao *et al*., 2007). Three of these studies did use ISH; however, there is doubt as to whether these sequences represent symbionts within the trophosome, or contaminants from the worm's tube or environment, because ISH results were inconclusive (Naganuma *et al*., 1997; Elsaied *et al*., 2002; Kimura *et al*., 2003; reviewed by Bright and Lallier, 2010).

In 2009, Duperron and colleagues found two distinct but closely related gammaproteobacterial 16S rRNA phylotypes in clone libraries of *L. anaximandri* from cold seeps in the eastern Mediterranean Sea. However, it was unclear whether these sequences were from two distinct symbionts or from one symbiont with multiple rRNA operons. In addition, Thiel and colleagues recently reported two different 16S rRNA phylotypes in clone libraries of *E. laminata* and *Lamellibrachia* sp. 2 from the Gulf of Mexico (Thiel *et al*., 2012). The presence of more than one symbiont type co-occurring in vestimentiferan Tws has therefore been hypothesized on a number of occasions, but has not yet been conclusively shown.

Recently, we discovered a vestimentiferan Tw population on the Marsili Seamount, an active hydrothermal venting region in the Western Mediterranean Sea North of Sicily (Fig. 1). We aimed to characterize the Tws and their symbionts using molecular methods to determine whether they are more closely related to Tws and their symbionts from surrounding hydrothermal vent and cold seep sites in the Mediterranean, or to hydrothermal vent vestimentiferans and their symbionts from the Pacific. Considering the preliminary indications for multiple co-occurring symbionts in vestimentiferan Tws, we also aimed to investigate whether the Marsili Seamount Tws harbour more than one endosymbiont.

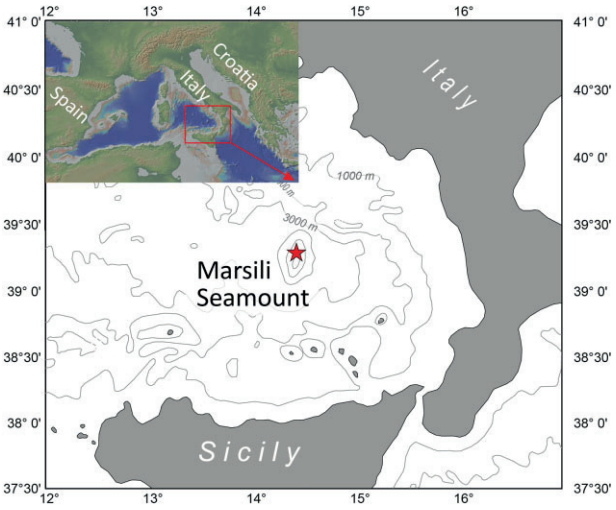

Fig. 1. Geographical setting of Marsili Seamount in the Southeast Tyrrhenian Sea. The sampling location of the tubeworms is indicated by the red star. The map was generated using PanMap (Diepenbroek *et al*., 2002) and the insert using GeoMapApp version 3.3.9, http://www.GeoMapApp.org (Ryan *et al*., 2009).

Results

Site description

Marsili is a diffuse hydrothermal vent site at a depth of 545–547 m on Marsili Seamount in the Western Mediterranean Sea (Fig. 1). The Tws grew on steep basalt cliffs and in crevasses. We observed single Tws, small groups and large bushes of several hundreds of Tws. At a few locations, the basal ends of the tubes were covered by a thin sediment layer. Marsili Seamount is known to be an active venting region (Uchupi and Ballard, 1989; Lupton *et al.*, 2011). However, we never measured temperatures higher than ambient seawater (13°C) and did not see shimmering water caused by density differences of hydrothermal fluids and seawater. Both *in situ* microsensor measurements and spectrophotometric S^{2-} measurements in discrete samples showed that close to the Tws, hydrogen sulfide concentrations were below the detection limit of 1 μM. This suggests that at the time of sampling, physicochemical conditions at Marsili Seamount more closely resembled those at cold seeps than those typically found at hydrothermal vents.

Marsili Seamount is colonized by L. anaximandri

To identify the vestimentiferan host species at Marsili Seamount, we sequenced partial cytochrome oxidase I genes (COI). In the nine Tws analysed, we found four COI haplotypes (H1–H4) with a nucleotide sequence identity (ntID) of > 99.7% (Fig. 2). Except for H3, where the nucleotide exchanges resulted in one amino acid substitution, nucleotide exchanges in the other haplotypes were

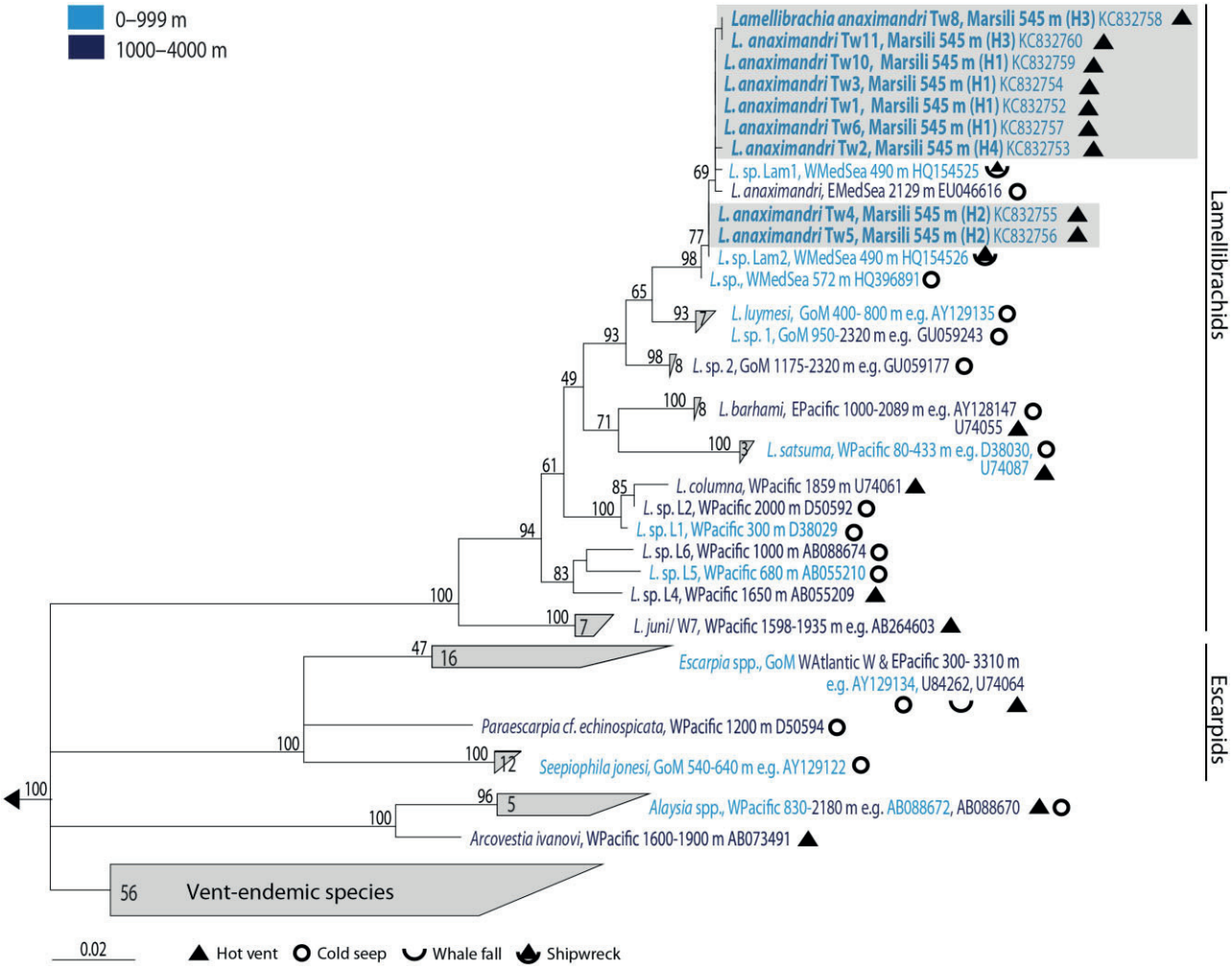

Fig. 2. Phylogeny of vestimentiferan tubeworms based on the COI gene. Sequences from this study are shown in bold and shaded in grey. Colours indicate the depth and black symbols the habitats where tubeworms were sampled. The tree is a consensus of NJ, ML and MP calculations. Numbers above the branching nodes represent ML bootstrap values above 60% (100 re-samplings). The scale bar represents 20% sequence divergence. Vent-endemic species include tubeworms of the genera *Riftia*, *Oasisia*, *Tevnia* and *Ridgeia*. *Osedax rubiplumus* (EU852486), *O. sagami* (FM998101) and *O. japonicus* (AB259569) were used as outgroup (indicated by the black arrow). H, COI haplotype; MedSea, Mediterranean Sea; GoM, Gulf of Mexico.

synonymous. Phylogenetic analyses showed that the COI sequences from Marsili Seamount Tws fell into a monophyletic cluster with all currently characterized Tws from Mediterranean Sea habitats including cold seeps, a hydrothermal vent and a shipwreck (Fig. 2) (Gambi *et al*., 2011; Hilário *et al*., 2011; Southward *et al*., 2011; Thiel *et al*., 2012). This Mediterranean cluster was supported by all three treeing methods [maximum likelihood (ML), maximum parsimony (MP) and neighbour joining (NJ)] and formed a sister group to *L. luymesi* and *Lamellibrachia* sp. 1 from cold seeps in the Gulf of Mexico (average COI ntID of 97.7%) (Fig. 2). Morphological analysis of two Marsili Tws confirmed their identity as *L. anaximandri* (E. Southward, pers. comm.).

Two distinct 16S rRNA sequences were found in L. anaximandri

Partial sequencing of 542 16S rRNA gene clones from eight Tws revealed two distinct gammaproteobacterial 16S rRNA phylotypes, which we call A and B. We found both phylotypes in clone libraries from five Tw individuals, and only a single phylotype, either A or B, in clone libraries from three individuals (Table 1, Supporting Information Table S1). Representative clones from each phylotype and each individual were chosen for full sequencing. The 16S rRNA phylotypes A and B differed consistently at 28 positions (98.1% ntID), including 22 nt differences between *Escherichia coli* positions 998–1043. Phylogenetic analyses showed that these two phylotypes did not fall into the previously described hydrothermal vent-endemic symbiont cluster, but instead clustered together with the symbionts of other *Lamellibrachia*, *Escarpia* and *Seepiophila* species (LES clusters) (Fig. 3).

The closest relatives to phylotype A were the symbionts of *L. anaximandri* from other Mediterranean habitats: the Palinuro vent field (100% ntID) and the Amon mud volcano (MV) (99.7% ntID) (Duperron *et al*., 2009; Southward *et al*., 2011; Thiel *et al*., 2012) (Fig. 3). The closest relative to phylotype B was not the second 16S rRNA phylotype found in clone libraries of *L. anaximandri* from the Amon MV in the Mediterranean. Instead, its closest relative was the symbiont of *L. satsuma* (99.8% ntID), which inhabits shallow hydrothermal vents in the West Pacific (Miura *et al*., 1997; Di Meo *et al*., 2000).

In situ *identification of the symbionts*

Catalysed reporter deposition fluorescence ISH (CARD-FISH) and light microscopy on transverse sections from five individuals showed that their trophosomes were packed with symbiotic bacteria and were arranged in lobules as in other vestimentiferan Tws (Fig. 4B, Supporting Information Fig. S1). Unlike *R. pachyptila* and *L. luymesi*, where bacteria in the centre of the lobule are rod shaped (Bright and Sorgo, 2003; Pflugfelder *et al*., 2009), the symbionts in *L. anaximandri* were coccoid (Fig. 4D–F). Bacteria in the centre of the lobules, in close proximity to the axial blood vessel, were the smallest (approximately 1 μm diameter), followed by medium-sized cocci in the middle region of the lobule (approximately 2–4 μm diameter) and larger to deformed cocci towards the lobule periphery and the degenerate region (approximately 5–7, sometimes up to 10 μm diameter) (Fig. 4F).

To determine whether the 16S rRNA phylotypes A and B correspond to two rRNA operons in the same symbiont genome or to two separate symbionts, we used specific CARD-FISH probes designed to target each phylotype. In the five Tws analysed by CARD-FISH, the specific probes always stained separate symbiont cells, which is consistent with the presence of two distinct symbiont types. Most

Table 1. Relative symbiont marker gene abundances in clone libraries from Marsili tubeworms (Tws).

	16S rRNA		*aprA*		*cbbM*	
	phylotype A (%)	phylotype B (%)	type A (%)	type B (%)	type A (%)	type B (%)
Tw 1	100	0	–	–	–	–
Tw 2	62.5	37.5	61	39	23	77
Tw 3	91	9	–	–	–	–
Tw 4	71	29	–	–	–	–
Tw 5	0	100, 100[a]	0	100	0	100
Tw 6	67.5	32.5	–	–	–	–
Tw 10	22	78	–	–	–	–
Tw 11	100	0	99[a]	1[a]	52[a]	48[a]

a. DNA from anterior, middle and posterior trunk region were pooled for the analyses.
The assignment of *aprA* and *cbbM* types A or B to the 16S phylotypes is explained in 'Symbiont metabolism' in *Results*. See Supporting Information Table S1 for more details, including the number of clones sequenced. Unless otherwise stated, all clone libraries are from the middle region of the tubeworm body.
aprA, partial gene sequence of adenosine-5'-phosphosulfate reductase; *cbbM*, partial gene sequence of the form II ribulose-1,5-bisphosphat-carboxylase/oxygenase.

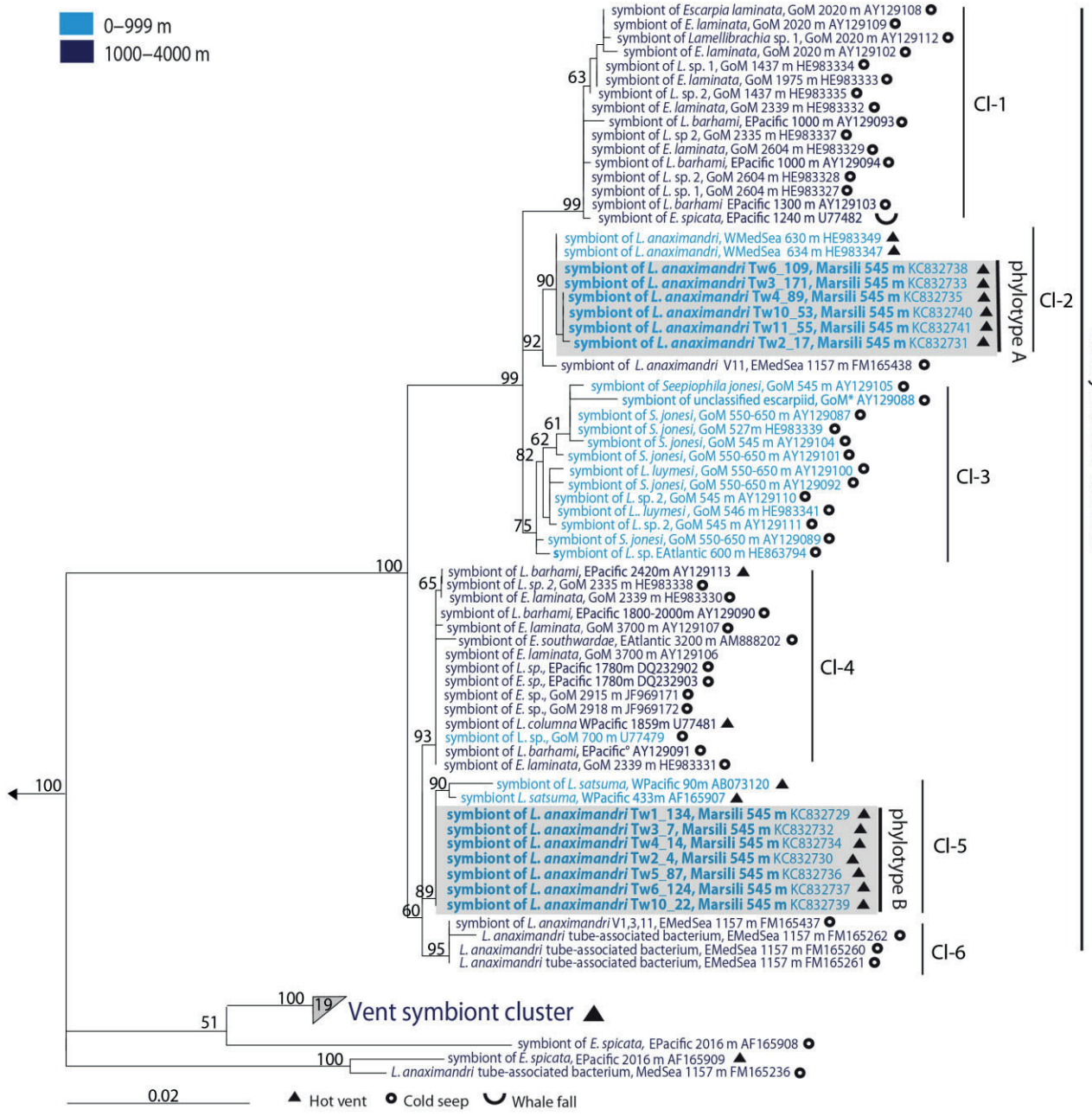

Fig. 3. Phylogeny of vestimentiferan symbionts based on the 16S rRNA gene. Sequences from this study are shown in bold and shaded in grey. Colours indicate the depth and symbols the habitats where tubeworms were sampled. The tree is a consensus of NJ, ML and MP calculations. Numbers above the branching nodes represent ML bootstrap values above 60% (100 re-samplings). The scale bar represents 20% sequence divergence. Symbionts (gamma3) of the marine oligochaetes *O. algarvensis* (AJ620496) and *O. ilvae* (AJ620499) were used as an outgroup (indicated by the black arrow). LES refers to *Lamellibrachia, Escarpia* and *Seepiophila* species. The vent group contains symbiont sequences of the genera *Riftia*, *Oasisia*, *Tevnia* and *Ridgeia*. MedSea, Mediterranean Sea; GoM, Gulf of Mexico; *collection depth above 650 m, °collection depth between 1000–1400 m.

lobules contained only one symbiont type, but some lobules contained both (Fig. 4C). All symbionts stained with the phylotype-specific probes also hybridized with the general bacterial probe EUB338 (I-III) (Amann *et al*., 1990b; Daims *et al*., 1999) and the *Gammaproteobacteria*-specific probe GAM42a (Manz *et al*., 1992). No signal was observed with the negative control probe NON338 (Glöckner *et al*., 1999) (data not shown).

In all cases except one, our CARD-FISH results mirrored our 16S rRNA clone libraries (Table 1, Fig. 5). For example, clone libraries from Tws 2, 3 and 4 contained both phylotypes, and we saw signals from both probes in

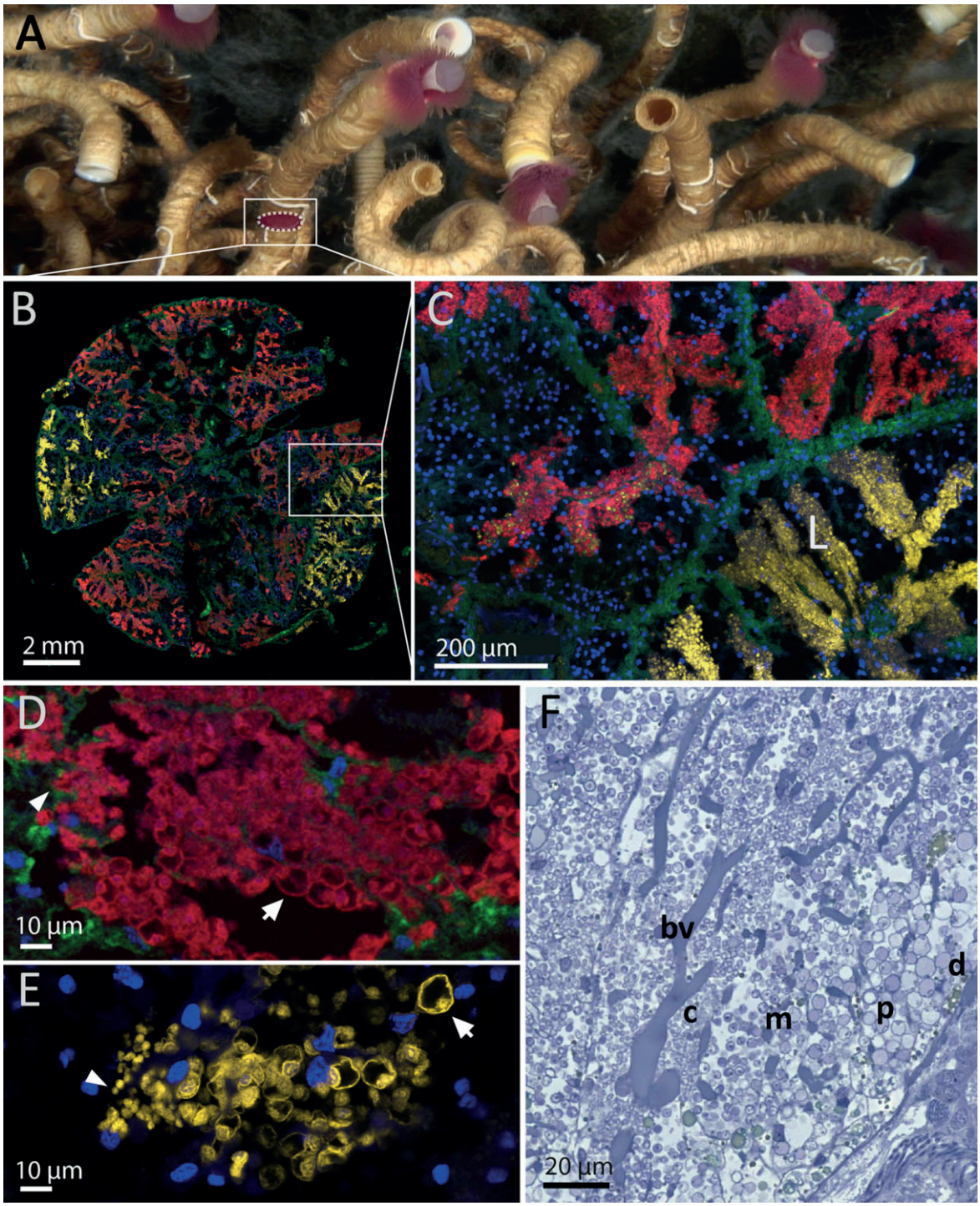

Fig. 4. *Lamellibrachia anaximandri* and its symbiotic bacteria.
A. *L. anaximandri* tubeworms on Marsili Seamount, with mats of white filamentous bacteria surrounding them.
B. CARD-FISH overview of a transverse section through the trophosome of tubeworm 4, containing symbiont type A (red) and B (yellow) that were stained with specific probes. Eukaryotic tissue was hybridized with the general EUK probe (green) and DNA was stained with DAPI (blue).
C. Enlargement of region in the white box in B showing lobules (L) with symbiont type A or B or both.
D–E. CARD-FISH sections showing the different cell sizes of symbiont types A and B. Arrowheads indicate cells of approximately 1 µm, arrows indicate cells of 7–10 µm.
F. Toluidine blue stained, semithin section of the trophosome showing half of a lobule with an axial blood vessel (bv) surrounded by small, medium and large coccoid cells in the central (c), median (m), peripheral (p) and degenerative (d) zone.

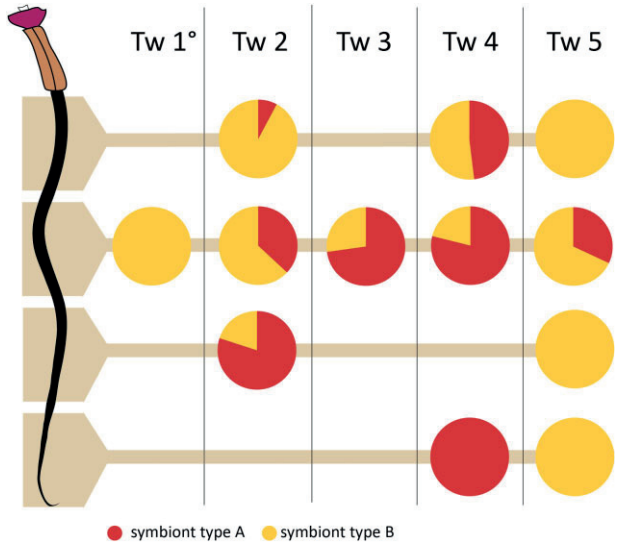

Fig. 5. Relative symbiont distribution in different Marsili seamount tubeworm (Tw) individuals. Pie charts represent the relative trophosome area occupied by the two symbiont types as determined from CARD-FISH images. For regions that had both symbiont types, average values were calculated via automated image analysis of five sections per body region. °The exact origin of the tubeworm piece along the trunk is unclear. For a detailed description, see 'Symbiont image analyses' in *Experimental procedures*.

these individuals (e.g. Fig. 4B and C). In Tw 1, which had only phylotype B based on clone libraries, all bacteria were stained by the probe targeting phylotype B, and no signals were seen with the probe for phylotype A (Supporting Information Fig. S1). The only exception was Tw 5, where 16S rRNA clone libraries only contained phylotype B, but CARD-FISH showed that this Tw had both symbiont types (Table 1, Fig. 5).

To investigate the relative abundance of the two symbionts in *L. anaximandri*, we did CARD-FISH on the middle trunk region of five individuals (Tws 1, 2, 3, 4 and 5). In regions where we found more than one symbiont type, we used image analysis to determine the relative area taken up by each type. In the middle region, the relative abundance of the two symbiont types varied between individuals (Fig. 5, Supporting Information Table S2). Symbiont type A was more abundant in Tws 3 and 4 (73.3% and 79.5%) and symbiont type B was more abundant in Tws 1, 2 and 5 (100%, 62.9% and 67.7%), mirroring the relative abundances of these phylotypes in four of five 16S rRNA clone libraries (Table 1). For three Tws (Tws 2, 4 and 5), FISH-fixed tissue was available from different parts of the body, and image analysis showed that symbiont abundances varied significantly along the anterior-posterior axis of Tw 2 and 4 (Mann–Whitney *U*-test ($P < 0.02$) (Fig. 5, Supporting Information Table S3). In these two Tws, the anterior end was dominated by symbiont type B. In the middle, the relative abundance of type B was lower than in the anterior end, and the posterior end was clearly dominated by symbiont type A (Fig. 5, Supporting Information Table S2). In Tw 5, we also observed symbiont heterogeneity along the Tw body. While only symbiont type B was found in the anterior and posterior parts, symbiont type A made up 32.3% of the total symbiont area in the middle.

Symbiont metabolism

To investigate the metabolic potential of the symbionts, we used PCR with primers specific for key genes of sulfur oxidation (*aprA*), autotrophic carbon fixation (*cbbM* and *cbbL*) and methane oxidation (*pmoA*) from three Tws. *AprA* encodes the alpha subunit of adenosine-5′-phosphosulfate (APS) reductase and is involved in the oxidation of sulfide to sulfate via the oxidative APS pathway. *CbbL* and *cbbM* encode the form I and II ribulose 1,5-bisphosphate carboxylase/oxygenase (RuBisCO), the key enzyme of the Calvin–Benson–Bassham (CBB) cycle of autotrophic CO_2 fixation. *PmoA* encodes the beta subunit of the particulate methane monooxygenase (pMMO) that catalyses the oxidation of methane to methanol in the methane oxidation pathway. Both *aprA* and *cbbM* were successfully amplified and sequenced from the three Tws, but *cbbL* and *pmoA* could not be amplified, suggesting that the symbionts do not have genes encoding the RuBisCO form I or pMMO.

Consistent with our 16S rRNA clone library results, we found two *aprA* sequence types (*aprA*-A and *aprA*-B) in our clone libraries (Table 1). Similarly, our *cbbM* clone libraries contained two distinct sequence types (*cbbM*-A and *cbbM*-B). *AprA*-A and *aprA*-B differed at seven nucleotide positions [98% ntID, 100% amino acid identity (aaID)] (Fig. 6A). Both fell into lineage II of the sulfur-oxidizing bacteria (SOB II) as defined by Meyer and Kuever (2007a), which supports the thiotrophic metabolism of the Marsili symbionts. *CbbM*-A and *cbbM*-B differed at 28 nucleotide positions (92.3% ntID, 99.2% aaID) (Fig. 6B). Both fell into a cluster containing sequences from vestimentiferan symbionts and free-living autotrophic bacteria (Fig. 6B). The lamellibrachid and escarpid symbiont *cbbM* sequences grouped in five clusters, and all of these five clusters mirrored their respective 16S rRNA gene clusters (Figs 3 and 6B).

In most cases, the two *aprA* and *cbbM* types found in our clone libraries reflected the presence of phylotypes A and B in 16S rRNA clone libraries. For example, Tw 2 had two 16S rRNA phylotypes, two *aprA* types and two *cbbM* types (Table 1). Likewise, in Tw 5, where only 16S rRNA phylotype B was detected, only *aprA*-B and *cbbM*-B were found. These results indicate that each symbiont phylotype is associated with one specific *aprA* and one specific *cbbM* sequence, and we assigned these

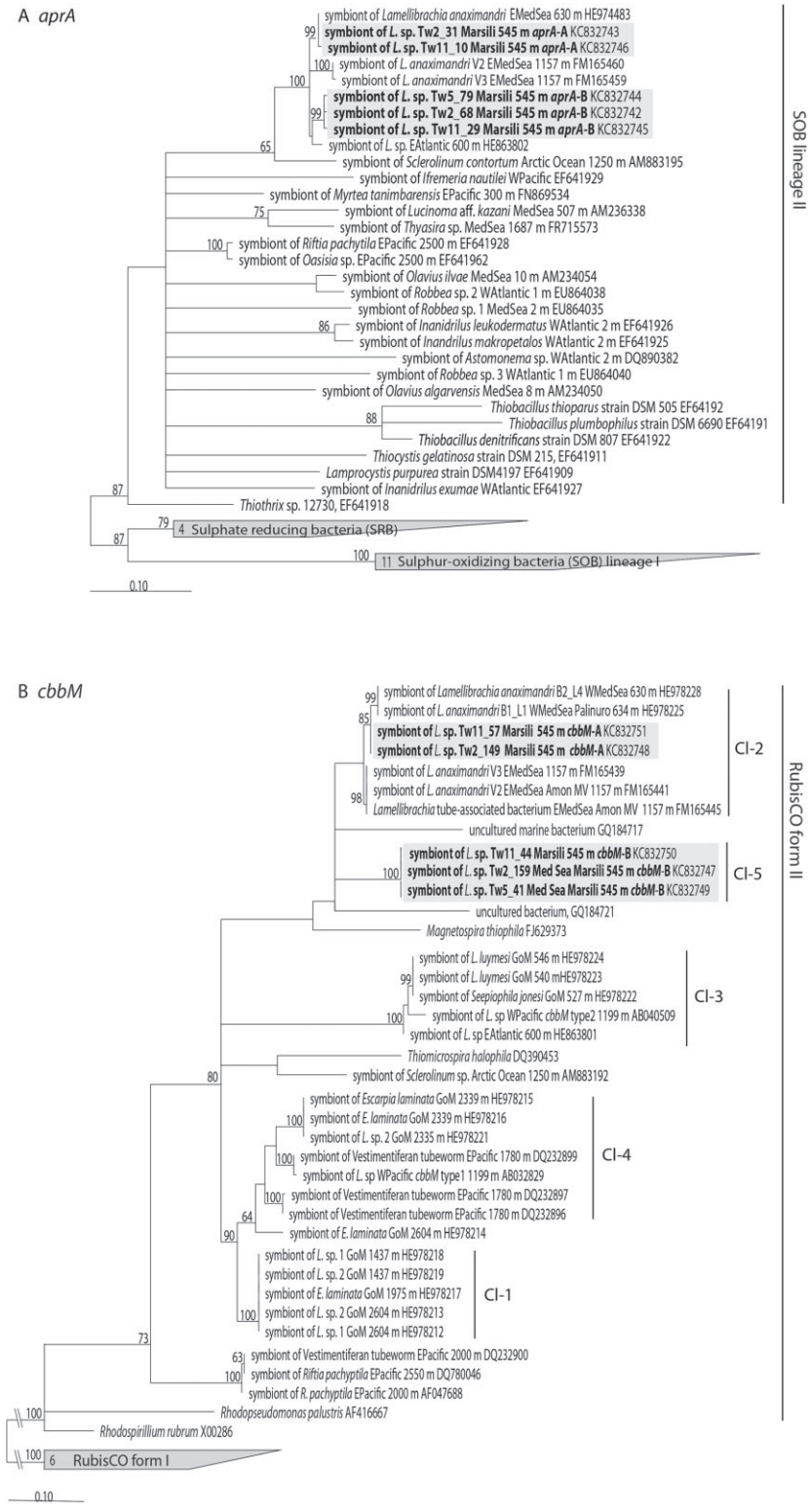

Fig. 6. Phylogenies of the metabolic marker genes for sulfur metabolism and autotrophic carbon fixation.
A. Phylogeny of the partial gene sequences of the alpha subunit of the adenosine-5'phosphosulfate reductase (*aprA*).
B. Phylogeny of the partial gene sequences of the form II RuBisCO (*cbbM*). Sequences from this study are shown in bold and shaded in grey. Clusters that combine *cbbM* symbiont sequences from lamellibrachids and escarpids are marked with numbers. Numbers above the branching nodes represent bootstrap values above 60% (100 re-samplings). These are consensus trees of NJ, ML and MP. The scale bars represent 10% sequence divergence. MedSea, Mediterranean Sea; GoM, Gulf of Mexico.

Table 2. db-RDA (1000 permutations) of different factors on vestimentiferan symbiont diversity.

	Factor[a]	Df[b]	F-ratio	Probability[c]	R^2 adjusted (%)
Analysis 1: LES	Reg + Hab + Depth + Host	10	3.334	0.002***	27.06
	Region●	5	2.059	0.059*	–
	Habitat●	2	1.090	0.341*	–
	Depth●	1	3.727	0.0479**	2.6
	Host type●	2	1.175	0.306*	–
Analysis 2: LES + VENT	Reg + Hab + Depth + Host	14	19.695	0.001***	81.1
	Region●	5	2.699	0.011**	0
	Habitat●	2	1.212	0.297*	–
	Depth●	1	4.282	0.016**	0
	Host type●	6	6.939	0.001***	3.4

a. The effects of each factor (indicated by ●) was assessed while accounting for the effects of all other factors via partial regression analyses. For more detailed information of included sequences and factors, see Supporting Information Table S4.
b. Degrees of freedom.
c. Probability levels and associated significance are indicated by ***$P < 0.001$; **$P < 0.05$; *$P > 0.05$ (not significant).
LES, symbionts of *Lamellibrachia*, *Escarpia* and *Seepiophila* species; VENT, symbionts of *Riftia* sp., *Ridgeia* sp., *Tevnia* sp. and *Oasisia* species.

sequences to the corresponding symbiont phylotype A and B in Table 1. In only one of the three individuals were the results of 16S rRNA and the *aprA* and *cbbM* clone libraries inconsistent. In Tw 11, we only found 16S rRNA phylotype A but both *aprA* and both *cbbM* sequence types (Table 1). However, the *cbbM* and *aprA* genes were amplified from DNA pooled from different parts of the trophosome, and the 16S gene was amplified from DNA from the middle part only. It is therefore likely that we underestimated the symbiont 16S diversity in this individual.

Phylogenetic and statistical analyses of factors influencing symbiont diversity

Phylogenetic analyses resolved seven highly supported vestimentiferan symbiont clusters: six clusters that contained LES symbiont sequences, and one cluster that only contained sequences from hydrothermal vent habitats (Figs 3 and 6B). Our analyses therefore confirmed the previously described 'hydrothermal vent' symbiont cluster, three 'cold seep' symbiont clusters (Cl-1, 3 and 4) and a Mediterranean symbiont cluster (Cl-2) that was recently identified by Thiel and colleagues (2012). Furthermore, we detected at least two additional symbiont clusters (Cl-5 and Cl-6) in our analyses, and these exclusively contained symbionts from *Lamellibrachia* species (Fig. 3).

We assessed the effects of the four factors hypothesized to shape vestimentiferan symbiont diversity: geographic region, habitat, host genus and water depth. We used host genus rather than species in our analyses because the species identification for many vestimentiferan Tws is still questionable, but identifications at the genus level are generally robust. Phylogenetic analyses showed that among the *Lamellibrachia*, *Escarpia* and *Seepiophila* symbionts, geographic region did not appear to play an important role, as four of our five LES clusters contained sequences from multiple regions (Fig. 3). Similarly, host specificity could not sufficiently explain our 16S rRNA phylogeny because half of the symbiont clusters contained sequences from multiple host genera (Fig. 3). The factors that best explained the clustering patterns seen in our symbiont phylogeny were habitat type (vent or seep) and water depth. Two clusters only contained sequences from hydrothermal vents, two clusters only contained sequences from cold seeps and two clusters contained sequences from more than one habitat type (Fig. 3). For depth, three clusters contained symbionts from regions shallower than 650 m (Cl-2, 3 and 5) and three clusters contained sequences from deeper regions below 1000 m (Cl-1, 4, 6), with one exception in Cl-4 (Fig. 3). A similar pattern was observed in the *cbbM* phylogeny, with three shallow water clusters (Cl-2, 3, 5) and two deep water clusters (Cl-1, 4), reflecting the clusters in the 16S rRNA phylogeny (Figs 3 and 6B).

To examine the relative influence of the variables geography, host, habitat and depth on vestimentiferan symbiont diversity, we used distance-based redundancy analysis (db-RDA) (Legendre and Anderson, 1999). Rather than investigating the relative effect of these factors on symbiont diversity based on phylogenetic clustering patterns, db-RDA quantifies the relative influence of these factors on the variability seen in a distance measure (here symbiont genetic distance). db-RDA partly confirmed the patterns we identified in our phylogenies. Water depth had a significant effect and accounted for 2.6% of the symbiont genetic diversity (Table 2). Nevertheless, when all factors were considered together, water depth, host genus, geographic region and habitat accounted for 27.1% of the symbiont genetic diversity. The remaining 72.9% could not be explained by any of the analysed factors (Table 2).

To test whether including the hydrothermal vent symbiont sequences would significantly change our results, we

repeated the db-RDA, this time including sequences from the LES clusters and the hydrothermal vent cluster. Consistent with our first analysis, water depth still had a significant effect (Table 2). However, host genus as well as geographic region also became significant. This likely reflects the fact that the vent symbiont cluster only contains sequences from vent-endemic Tws found in a single geographic region and in a restricted depth range (Fig. 3). In the following discussion, we therefore focus on the factor depth, as it was the only factor that had a significant effect in both the statistical and phylogenetic analyses.

Discussion

Dual symbiosis in Marsili Tws

Until now, vestimentiferan Tws were widely believed to harbour a single sulfur-oxidizing symbiont phylotype in their trophosome (reviewed by Bright and Lallier, 2010). Although a few molecular studies indicated the possibility of multiple symbionts in some vestimentiferan species, conclusive evidence was arguably still missing (Naganuma *et al*., 1997; 2005; Elsaied *et al*., 2002; Kimura *et al*., 2003; Chao *et al*., 2007; Duperron *et al*., 2009; Thiel *et al*., 2012). In all of our CARD-FISH analyses, specific probes matching the two phylotypes found in our 16S rRNA clone libraries bound separate symbiont cells, providing evidence that these phylotypes represent two distinct coexisting symbionts. Further support for this dual symbiosis was provided by our metabolic key gene analyses, as we identified patterns mirroring those of the 16S rRNA analysis. Multiple *cbbM* and *aprA* sequence types could be amplified from a worm with multiple 16S rRNA phylotypes, and only a single *cbbM* and *aprA* sequence type was found in a worm with only one 16S rRNA phylotype. Furthermore, our hypothesis that each symbiont phylotype is associated with one specific *aprA* and one specific *cbbM* sequence is supported by molecular studies of *L. anaximandri* from two additional sites in the Mediterranean Sea. In the Tws from Amon MV and the geographically very close Palinuro vent field, clone libraries of most individuals contained only one 16S rRNA, *cbbM* and *aprA* type, and all were closely related to the Marsili 16S rRNA phylotype A, *aprA*-A and *cbbM*-A (Duperron *et al*., 2009; Thiel *et al*., 2012) (Figs 3 and 6A and B). Interestingly, the single 16S rRNA type and *aprA* types that were found in the Palinuro vent Tws were both identical to the Marsili 16S rRNA phylotype A and *aprA-A*, indicating that the same symbiont type is hosted by Tws at these sites.

Are multiple symbioses widespread in vestimentiferan Tws, or is *L. anaximandri* unique? Most previous molecular studies of vestimentiferan symbionts used direct sequencing of polymerase chain reaction (PCR)-amplified 16S rRNA genes to characterize the symbionts (Black *et al*., 1997; e.g. Feldman *et al*., 1997; Nelson and Fisher, 2000; McMullin *et al*., 2003). Because direct sequencing would not always identify multiple closely related symbiont phylotypes, and because PCR-based approaches are known to be biased towards the most abundant phylotype, it is likely that vestimentiferan symbiont diversity has been underestimated. The limitations of the PCR-based approach were also evident in our results. CARD-FISH showed that symbiont type A in Tw 5 makes up around 30% of the symbiont population in the middle part (Fig. 5), but it was not found in our clone libraries, even though we used few PCR cycles and pooled 10 parallel PCR reactions before cloning to reduce bias (Polz and Cavanaugh, 1998). Alternatively, multiple symbiont types could be overlooked when analysing only a small piece of the Tw body because the symbionts can be patchily distributed throughout the worm (Fig. 5). We therefore hypothesize that multiple sulfur-oxidizing symbionts might also co-occur in other vestimentiferan species. In fact, Thiel and colleagues (2012) found two 16S rRNA phylotypes and also two ATP citrate lyase type II (*acl*) gene sequence types in clone libraries of *E. laminata* and *Lamellibrachia* sp. 2, both from the Gulf of Mexico, indicating that these species might also harbour two co-occuring symbiont types (Thiel *et al*., 2012). Multiple closely related sequences have also been found in *cbbM* gene clone libraries from *Lamellibrachia* and *Escarpia* Tws from the West Pacific and the Gulf of California (Elsaied *et al*., 2002; Vrijenhoek *et al*., 2007), but neither of these two studies found multiple 16S rRNA phylotypes. Vrijenhoek and colleagues (2007) used direct sequencing, which might not reveal multiple closely related phylotypes, and in the 50 clones sequenced by Elsaied and colleagues (2002), the 'typical' gammaproteobacterial sulfur-oxidizing symbiont sequence was not found, even though the two *cbbM* phylotypes found in their study are very closely related to other *Lamellibrachia* symbiont *cbbM* sequences (Fig. 6B). It is therefore likely that the latter studies also underestimated the 16S rRNA diversity. Using improved molecular methods in the future may help to uncover this hitherto hidden diversity (Dubilier *et al*., 2008).

Selective advantage of harbouring multiple symbionts

Multiple symbioses are widely considered unstable over evolutionary time because of competition among symbionts, which promotes the emergence of 'cheaters' (West *et al*., 2002; Hart *et al*., 2012). Nevertheless, numerous examples of stable dual or multiple symbioses are known (e.g. Takiya *et al*., 2006; Dubilier *et al*., 2008; Palmer *et al*., 2010). For example, *Bathymodiolus* mussels from hydrothermal vents and cold seeps have a dual symbiosis with two distinct *Gammaproteobacteria*:

one sulfur oxidizer and one methane oxidizer. Competition between symbionts is presumably avoided in such a dual symbiosis where the symbionts use different carbon and energy sources (Fisher *et al*., 1993; Duperron *et al*., 2006). Both *L. anaximandri* phylotypes were closely related to other known autotrophic sulfur oxidizers. Moreover, we could amplify two variants of key genes for autotrophic carbon fixation (*cbbM*) and sulfur oxidation (*aprA*) from our Tws. We therefore hypothesize that both symbionts are also chemoautotrophic sulfur oxidizers. The selective advantage to *L. anaximandri* of harbouring multiple closely related sulfur-oxidizing symbionts is not immediately clear from our study. However, even closely related microorganisms with apparently redundant metabolic capabilities can be adapted to subtly different environmental conditions (Gray *et al*., 2004; Jaspers and Overmann, 2004; Johnson *et al*., 2006; Šimek *et al*., 2010). If this is the case for the *L. anaximandri* symbionts, it could enable the symbiosis to cope with fluctuating substrate concentrations, which is one of the challenges to life at hydrothermal vents (Tunnicliffe, 1998; Zierenberg *et al*., 2000; Le Bris *et al*., 2006). This strategy has also been demonstrated in corals, where a high diversity of closely related *Symbiodinium* endosymbionts enhances their resilience to environmental stress (Jones *et al*., 2008). An alternative explanation for the existence of stable associations with multiple closely related symbionts is resource partitioning between the symbionts. A recent analysis of two sulfur-oxidizing symbionts that co-occur in the marine worm *Olavius algarvensis* showed that even though both are chemoautotrophic sulfur oxidizers, each has additional unique metabolic capabilities such as the use of carbon monoxide as an energy source or the ability to grow heterotrophically (Kleiner *et al*., 2012a). Thiel and colleagues (2012) recently suggested that the symbionts of *L. anaximandri* from the Palinuro vent field may be able to oxidize hydrogen in addition to sulfide. If one symbiont phylotype evolved the ability to use an additional source of energy such as hydrogen, possibly through horizontal gene transfer (Kleiner *et al*., 2012b) it may be more likely to stably coexist with closely related symbionts, as competition for resources such as sulfur would be reduced. In the future, whole genome sequencing and metabolic profiling of the co-occurring symbionts discovered in this study will help to show how extensively their nutritional needs overlap.

Which factors have influenced the evolution of vestimentiferan symbioses?

Based on 16S rRNA phylogeny, four factors have been hypothesized to influence vestimentiferan symbiont diversity: water depth, habitat type (vent versus seep), host selection and geography. Depending on the sequence data available and the phylogenetic methods used, previous studies came to contrasting conclusions about the relative influence of each factor. Nelson and Fisher (2000) and McMullin and colleagues (2003) identified depth and habitat type as the key factors. In contrast, Di Meo and colleagues (2000) and Thornhill and colleagues (2008) hypothesized that host selection, geography and habitat type were the most important factors. Because such patterns can be difficult to infer by subjective interpretation of phylogenetic trees, we did additional statistical analyses to quantify their relative influence. Our analyses showed that these four factors together could explain about one quarter of the LES symbiont diversity. However, our statistical analyses identified water depth as the only factor that on its own had a significant influence on symbiont diversity, whether the vent symbiont cluster was included or not. Reflecting this result, our phylogenetic analyses showed a clear grouping of symbionts according to sampling depth. Three of the six LES symbiont clusters contained sequences from only shallow waters to a depth of 650 m, and the other three clusters contained only sequences from Tws living below 1000 m depth, with only one exception (Cl-4; Fig. 3). Depth-based clustering was also clear in the *cbbM* phylogeny, but the *aprA* genes of vestimentiferan symbionts and their close relatives were too similar to resolve such patterns (Fig. 6A and B).

McMullin and colleagues (2003) suggested the existence of three LES symbiont groups: one confined to shallow water, one to intermediate water and one to deep water. The recent analyses by Thiel and colleagues (2012) point to the existence merely of shallow and deep water symbiont groups. Our analyses also suggest the existence of 'deep' and 'shallow' groups, separated by a barrier somewhere between 650 and 1000 m.

The factor water depth likely reflects a combination of many physical parameters such as pressure, density and temperature that change with depth and might be responsible for structuring marine microbial communities. Because pressure changes gradually with water depth, pressure alone cannot explain abrupt community changes between 650 and 1000 m water depth. One thousand metres marks the upper limit of the bathypelagic zone. Seawater below this depth is commonly characterized by relatively constant temperatures and salinities compared with the overlying epipelagic and mesopelagic layers because it is usually unaffected by seasonal temperature changes and mixing by wind. The beginning of the bathypelagic zone might therefore represent a physical barrier between surface waters and the deep sea. Accordingly, at around 1000 m, a change in community composition has also been shown for a number of free-living

planktonic microbial groups including picoeukaryotes, bacteria and crenarchaea (Karner *et al*., 2001; Kruse *et al*., 2009; Galand *et al*., 2010; Agogué *et al*., 2011). Similarly, 1000 m was also identified as a barrier for symbiotic bacteria of the marine siboglinid *Osedax* worms, which like the vestimentiferan symbionts are considered to be taken up from the environment by each new host generation and disperse in a free-living planktonic stage (Nussbaumer *et al*., 2006; Verna *et al*., 2010). For marine animals, 1000 m is also commonly identified as the boundary separating shallow and deep water species (reviewed by Carney, 2005; Cordes *et al*., 2007).

The clear separation of deep and shallow phylotypes we saw in our symbiont phylogenies was not exactly mirrored in the host COI phylogenies (Fig. 2). However, some vestimentiferan species cannot be distinguished by the COI gene because of its slow mutation rate (e.g. McMullin *et al*., 2003, Miglietta *et al*., 2010). Recent genetic divergence between Tw species is therefore not always detected in the COI gene. A separation of vestimentiferans according to depth has been proposed for many species (reviewed by McMullin *et al*., 2003), and recently, a depth restriction that was not apparent at the COI level was demonstrated for *Lamellibrachia* species in the Gulf of Mexico, using microsatellite markers (Cowart, 2013). Considering this, the depth range of *L. anaximandri* is exceptional among vestimentiferan host species: this species has been found at depths between 500 and 3000 m (Fig. 2, Southward *et al*., 2011). It is possible that the deep- and shallow-water Tws in the Mediterranean are actually two recently diverged species that the COI gene cannot resolve. However, morphological characters such as the number of gill lamellae and the weak development of collars on the tube also indicate that all individuals so far investigated in the Mediterranean likely belong to a single species, and morphological characters have so far been robust markers for distinguishing even recently diverged species (Cowart, 2013). A major genetic differentiation between deep and shallow *L. anaximandri* populations is therefore unlikely. Unlike most ocean basins, the Mediterranean Sea experiences stable temperatures of around 12°C below 250–400 m all year round (Lacombe *et al*., 1985). Intriguingly, temperature has been shown to affect larval metabolism and survival in laboratory experiments (Young *et al*., 1996; 2012). If the Tws colonizing deep and shallow sites in the Mediterranean do belong to one species, then the unique hydrographic conditions in the Mediterranean might allow larvae to cross depth barriers, thus explaining why this species has such an unusually broad depth range.

In contrast to free-living bacteria that are too small to control their dispersal through behaviour (McManus and Woodson, 2012), animal larvae might partially influence their own dispersal by altering their swimming behaviour or physical properties. Indeed, vestimentiferan larvae actively swim when reared in aquaria at ambient pressure (Young *et al*., 1996). If vestimentiferan host and symbiont dispersal is sometimes decoupled in this way, it would represent a significant evolutionary risk for the host, which relies on its symbionts for nutrition in the adult stage. This risk is presumably compensated by the flexibility to associate with locally adapted symbiont types, assuming that these are present in the environment. Further studies on the diversity and distribution of free-living symbionts will help to understand symbiont dispersal and the evolutionary risks associated with horizontal transmission.

Although we were able to explain more than a quarter of the symbiont genetic diversity with four factors, the majority remained unexplained. This implies that factors determining symbiont evolution are highly complex and that further parameters are involved, which we are still missing. One possible reason for the unexplained variability might be the ambiguity of the factor habitat. Most studies, including ours, defined habitat type as hydrothermal vent or cold seep. This, however, ignores differences in physicochemical conditions that can exist within these categories. The environmental conditions at hydrothermal vents can vary extensively, and only a few studies have characterized variables such as fluid composition or heavy metal and nutrient concentrations. Detailed measurements of vestimentiferan symbiont habitats, also including free-living symbiont populations, will help to understand the environment seen by the bacteria and the host and to reveal missing factors that determine vestimentiferan symbiont distribution.

Conclusions and outlook

In this study, we describe a dual symbiosis of closely related gammaproteobacterial symbionts in *L. anaximandri* from the Marsili Seamount. This species colonizes cold seeps, hydrothermal vents and shipwrecks – a habitat range so far unprecedented among vestimentiferans. In fact, the only Tw genera known to colonize different habitats are *Lamellibrachia*, *Escarpia* and *Alaysia*, and so far, indications for multiple symbioses come almost exclusively from *Lamellibrachia* and *Escarpia* (*Alaysia* symbionts have not yet been investigated). If multiple co-occurring symbionts are more frequent in these genera than in the vent-endemic lineages, then the ability to host multiple symbionts may be one of the key adaptations that allow these Tws to thrive in diverse habitats.

Our study raises a number of questions for future research. First, how widespread are multiple symbioses among vestimentiferans? Because most previous studies used either direct 16S rRNA sequencing or analysed very few clones, the true symbiont diversity in the multitude of vestimentiferan species described to date has probably

been underestimated. The second question is what is the selective advantage of harbouring two closely related sulfur-oxidizing symbionts? We showed that both *L. anaximandri* symbionts have the potential to oxidize sulfide and fix carbon dioxide via the CBB cycle. In the future, genome sequencing may uncover additional metabolic capabilities in one or both symbionts.

We found that symbiont abundances along the trophosome of individual Tws vary between and within Tws. Microhabitat variability is known to exist within a single Tw aggregation (Johnson *et al*., 1988a,b) and even within single Tws (de Burgh, 1986; Fisher *et al*., 1988). Activity measurements under different physiological conditions in combination with proteomics and metabolomics could be used to test our theory that the symbionts are adapted to subtly different niches. Further measurements are needed to investigate whether physiological gradients within the worms play a role in determining symbiont distribution along the trophosome. We expect that further insights into the symbiont metabolism and the environmental conditions experienced by the symbioses will help to understand how such closely related sulfur-oxidizing symbionts can stably coexist over evolutionary time.

Experimental procedures

Sampling site of the Tws

The specimens were collected at a depth of 545–547 m on top of Marsili Seamount (14°23,908′ E, 39°17,049′ N), 60 km north of Sicily in the Mediterranean Sea (Fig. 1). Collections were done with the remotely operated vehicle (ROV) 'Super Achille' (Comex) and the submersible 'Remora' (Comex) during a cruise with the French RV Minibex (H. Delauze, Comex) in July 2009. *In situ* chemical and temperature measurements were done with a handheld profiling unit (Glud *et al*., 2005) mounted to the ROV. Water samples were retrieved with glass syringes, and hydrogen sulfide was measured directly on board (Jeroschewski *et al*., 1996). Samples were also fixed in 5% ZnAc for later photometric total sulfide measurements according to Cline (1969). The hydrogen sulfide detection limit was 1 μM for both methods. Tubeworms for this study were taken from bushes found in basaltic crevasses and sectioned into pieces of about 1 cm length, directly after their retrieval. For DNA extraction, samples were either frozen at −20°C (Tw 1–6) or preserved in 70% ethanol (Tw 10–11). Pieces for FISH were fixed for 12 h in ice-cold 4% paraformaldehyde in 0.2 μm of filtered seawater. After fixation, pieces were washed three times in ice-cold 0.2 μm of filtered seawater and stored at 4°C in 70% ethanol. Pieces for light microscopy were fixed in ice-cold Trump's fixative (Science Services, München, Germany) overnight, washed three times in 0.2 M of cacodylate buffer and stored in buffer for up to 15 months.

DNA extraction

DNA was extracted from the middle body region of nine Tw individuals (Tw 1–6, 8, 10 and 11) and from a mixture of pieces from the anterior, middle and posterior part of Tw 5 and 11, according to Zhou and colleagues (1996). Because of an intense black colouring of the trophosome tissue, four additional 15 min washing steps with phenol : chloroform : isoamylalcohol (IAA) (25:24:1) at 65°C were included before the chloroform : IAA (24:1) washing steps. DNA extracts were purified with the Wizard® Clean-up System (Promega, USA), and DNA aliquots were stored at −20°C in 1× Tris-EDTA (TE) buffer [10 mM Tris/HCl; 1 M Ethylenediaminetetraacetic acid (EDTA); pH 8.0].

PCR amplification of symbiont genes

The bacterial 16S rRNA gene was amplified with the general eubacterial primer pair GM3/GM4 (Muyzer *et al*., 1993) using the Phusion® High Fidelity DNA polymerase (Finnzymes, Finland) with one exception. For Tw 2, 16S amplification was performed with the Takara *Ex Taq* DNA polymerase (Takara Bio, Shiga, Japan) because of unsuccessful amplification with the Phusion polymerase. For amplification of the symbiont metabolic marker genes *cbbL*, *cbbM*, *aprA* and *pmoA*, the primer pairs cbbL1c/cbblL2b (Blazejak *et al*., 2006), cbbM1F/cbbM2R (Elsaied and Naganuma, 2001), APS1F/APS4R (Meyer and Kuever, 2007b) and A189F/Mb661R (Costello and Lidstrom, 1999), and the Master Taq polymerase (5Prime, Hamburg, Germany) were used. The PCR cycling conditions were as follows: initial denaturation at 95°C for 5 min, followed by 24–28 cycles at 95°C for 1 min, annealing for 1.5 min [(temperature was adjusted for the different genes: 16S (44°C), *cbbL* (48°C), *cbbM* (62°C), *aprA* (56°C) and *pmoA* (55°C)], elongation at 72°C for 2 min and a final elongation step at 72°C for 10 min. To minimize PCR bias, cycle numbers were kept as low as possible, and 10 reactions per individual were pooled before loading the PCR mix on a 1% agarose gel. Bands of the correct size were excised and purified with PCR Purification Kit (Qiagen, Hilden, Germany).

Clone libraries of the 16S rRNA, aprA and cbbM genes

After A-tailing with Master Taq polymerase (5Prime), purified PCR products were either ligated into the pCR4-TOPO® vector (Invitrogen, Carlsbad, CA, USA), or, when ligation efficiency was insufficient, into the pGEM®-T Easy vector (Promega Corporation, Madison, WI, USA). Transformations of the ligation products were performed with the TOPO TA Cloning Kit (Invitrogen), and clone libraries of 190 clones per Tw and gene were constructed. To screen the recombinant white *E. coli* clones for the correct insert size, 0.5 μl of a 1:10 diluted liquid overnight culture were used as template in a 20 μl PCR reaction mixture, containing vector primers M13F/M13R (Yanisch-Perron *et al*., 1985). PCR products with correct insert sizes were purified by Sephadex® G-50 Superfine columns (GE Healthcare, Buckinghamshire, UK) and frozen at −20°C until sequencing was performed.

Sequencing

Sequencing was done using ABI BigDye and ABI PRISM 3100 genetic analyser (Applied Biosystems, Foster City, CA,

USA). Partial sequencing was performed using the primer 1408R (Lane, 1991) for the 16S rRNA gene and M13R (Yanisch-Perron *et al*., 1985) for the *aprA* and *cbbM* genes. Sequences were imported into BIOEDIT (Hall, 1997–2001) and aligned with CLUSTALW (Thompson *et al*., 1994). Sequence groups were identified visually by checking the alignment. The web-based search tool BLASTN (Altschul *et al*., 1997) was used for determining the phylogenetic affiliation for a few representatives from each group. Four to eight clones per sequence group and per Tw were selected for full sequencing. The *cbbM* and *aprA* genes were sequenced directly, and 16S rRNA gene sequencing was performed on plasmids isolated by the Montage Plasmid Miniprep96 kit (Millipore, Bedford, MA, USA). Full sequences were assembled using DNA BASER (HeracleSoftware, Germany) and chimera-checked by the BELLEROPHON (Huber *et al*., 2004) program.

Phylogenetic analysis of symbiont marker genes

Symbiont 16S rRNA sequences (approximately 1400 bp) and previously published symbiont-derived 16S rRNA sequences from other siboglinid Tws and invertebrates were imported into ARB (Ludwig *et al*., 2004). A final dataset of 92 sequences was aligned within the SILVA Ref_111 database (Pruesse *et al*., 2007), and alignments were manually adjusted. ML, MP and NJ phylogenies were calculated in ARB using a termini filter that included sequences of the same length only (1280 bp) and a 10% base frequency filter. A consensus tree was constructed using the ML tree as a backbone. Bootstrapping analysis was done with the PHYML package in ARB, with 100 re-samplings each.

The *aprA* and *cbbM* sequences (approximately 350 bp) from three of the Tw individuals (Tw 2, 5 and 11), as well as other previously published sequences for each of the genes were aligned with CLUSTALW (Thompson *et al*., 1994), imported into ARB and alignments were manually adjusted. Forty-six APS and 46 RuBisCO sequences were used for the ML, MP and NJ tree calculations as described above. Termini filters to remove primer sequences and include sequences of the same length only, using 359 bp (APS tree) and 313 bp (RuBisCO tree) respectively. Consensus tree construction and bootstrapping was done as described above. For the *aprA* tree, sequences of the SOB lineage I (SOB I) (described by Meyer and Kuever, 2007a) and sulfate-reducing bacteria (SRB) were used as outgroups [NCBI accession numbers EF641931, –34, –39, –44, –63, –58, –60; EU864037, –39 and FJ573249 (SOB I) and AF418117, –36; EF442925, –36 (SRB)]. For the *cbbM* tree, sequences of the RubisCO form I were used as outgroups (NCBI accession numbers AF447860, L42940, M26396, AY531637, AM228899 and AM234058).

Amplification and sequencing of the vestimentiferan COI gene

The partial COI gene was amplified with the primers 1490F/2198R (Folmer *et al*., 1994), using the same reaction mixture as for the metabolic marker genes (see above). The PCR program involved an initial denaturation step at 95°C for 5 min, followed by 36 cycles at 95°C for 1 min, 42°C for 1.5 min, 72°C for 2 min and a final elongation step at 72°C for 10 min. PCR products were used for full sequencing (see above).

Phylogenetic analysis of the COI gene

The COI sequences obtained from nine individuals in this study and previously published COI sequences from siboglinid Tws and other invertebrates were imported into ARB and aligned by CLUSTALW (Thompson *et al*., 1994). Alignments were manually adjusted. ML, MP and NJ phylogenies were calculated for 146 COI sequences, mainly derived from vestimentiferan Tws, and three members of the siboglinid *Osedax* spp. were used as an outgroup (EU852486, FM998101 and AB259569). Tree calculations were done using a termini filter to remove primer sequences and include sequences of the same length (641 bp). Consensus tree construction and bootstrapping analysis was done as described above.

Probe design and testing

Specific oligonucleotide probes (L.mars_symb1 and L.mars_symb2) targeting the 16S rRNA gene region of the symbionts were designed by visually identifying a suitable target site in the ARB alignment (Table 3). Because of the high similarity between 16S rRNA sequences of the symbionts of the Tw genera *Lamellibrachia* and *Escarpia*, both designed probes also perfectly matched the symbionts of some other vestimentiferan Tws. Because the binding site of these probes was defined as a region of very low *in situ* accessibility (Behrens *et al*., 2003), unlabelled helper oligonucleotides were designed to bind adjacent to the horseradish peroxidase (HRP)-labelled probes (Interactiva, Ulm, Germany) (Fuchs *et al*., 2000). A 10–60% formamide series

Table 3. Oligonucleotide probes designed for this study.

Probe	Target organisms	Probe sequence (5′ → 3′)	FA[a] (%)	Position[b]
L.mars_symb1	*L. anaximandri* symbiont type A	CTCTGCTGGATTCTGTCAAT	40	996–1015
L.mars_symb2	*L. anaximandri* symbiont type B	CTCTAACAAGTTCTGAGGAT	40	996–1015
L.mars1 + 2/helper1	*L. anaximandri* symbiont type A + B	GTCAAGGGTAGGTAAGGTTCTTCG	40	972–995
L.mars1/helper2	*L. anaximandri* symbiont type A	CAGGCCCGAAGGCACTCCTGCAT	40	1016–1038
L.mars2/helper2	*L. anaximandri* symbiont type B	AATTCCCGAAGGCACCAAGTTAT	40	1016–1038

a. Formamide concentration in the hybridization buffer.
b. Nucleotide position in the 16S rRNA of *E. coli.*
Additional probe details are available at probeBase (Loy *et al*., 2007).

was performed with both probes and distinct signals were observed between 30% and 40% formamide. We therefore used the probes at 40% formamide.

CARD-FISH

After dehydration in an ethanol series, Tw pieces were embedded in Steedman's wax (Steedman, 1957), sectioned (5–10 μm thick), dewaxed and rehydrated as described by Raggi and colleagues (2012). Sections were incubated in 0.2 M HCl for 12 min to inactivate endogenous peroxidases, followed by 10 min washing in Tris/HCl (20 mM, pH 8.0), and 30 min permeabilization in lysozyme (0.01 g ml^{-1} lysozyme, 0.05 M EDTA, 0.1 M Tris/HCl). After a further washing step, sections were circled with a Pap-pen (Kisker Biotech, Steinfurt, Germany). CARD-FISH was done as described by Pernthaler and colleagues (2002). EUB338 (I-III) (Amann *et al*., 1990a; Daims *et al*., 1999) and NON338 (Glöckner *et al*., 1999) were used as positive and negative controls respectively. For counterstaining of eukaryotic tissue, the probe EUK516 was used (Amann *et al*., 1990a). CARD was done with fluorochrome-labelled tyramides: Alexa 633 (L.mars_symb1), Alexa 546 (L.mars_symb2) and Alexa 488 (EUK516) (Molecular Probes, Leiden, the Netherlands). To inactivate the probe-bound HRPs between serial hybridizations, slides were incubated in 0.5% hydrogen peroxide in methanol for 30 min. Slides were washed in deionized water and 96% ethanol, and air-dried before counterstaining with 4,6-diamidino-2-phenylindole (DAPI) for 8 min and embedded for microscopy in a mixture of Citifluor (Citifluor Ltd, Leicester, UK) and Vectashield (Vector laboratories, Burlingame, CA, USA).

Confocal laser scanning microscopy. Samples were analysed using a confocal laser-scanning microscope (LSM 780, Carl Zeiss, Germany) with a 40× EC Plan-Neofluar/ 1.3 oil-immersion objective lens (Carl Zeiss). Pictures were acquired in a three or four track mode with excitation at 405 nm (DAPI), 561 nm (Alexa546), 633 nm (Alexa633) and 488 nm (Alexa488). Tile scans with at least 5% overlap and z-stacks of 6–10 planes, depending on the section thickness, were done for every Tw section. Tiles of every plane were combined using the 'stitch' function before further analysis with ZEN 2011 (Carl Zeiss) and IMARIS 7.4.0 (Bitplane, Zurich, Switzerland). Up to four planes were combined using maximum intensity projection for the overview and the symbiont detail pictures.

Symbiont image analyses. For the relative symbiont abundance analysis, overview images of five non-adjacent sections per Tw individual and body region were acquired as described above. All planes of each section were combined to a maximum intensity image. The ZEISS AXIO VISION SOFTWARE 4.8.2 was used to produce binary images for both symbiont channels using segmentation by automatic or, if necessary, interactive thresholding. Densitometric pixel counts for both regions of interest (symbiont type A and B) were obtained via the automatic measurement function and were used for relative symbiont abundance estimations. The non-parametric Mann–Whitney *U*-test, implemented in the software PAST (Hammer *et al*., 2001), was used to test for statistically significant differences of symbiont abundances within and among the Tws individuals.

Light microscopy. Tubeworm trophosome pieces were dehydrated, embedded in Agar low-viscosity resin (Agar scientific, Stansted, UK) and semithin sectioned following the procedure of Katz and colleagues (2011). Sections were stained with aqueous 1.5% toluidine blue and observed on a Zeiss Axio Imager A1 light microscope (Carl Zeiss, Germany) photographed using an Olympus Color View III CCD camera (Olympus, Tokyo, Japan).

Statistical analysis. db-RDA (Legendre and Anderson, 1999) consists of an RDA applied to the results of classical multidimensional scaling (i.e. principal coordinate analysis; see, e.g. Ramette, 2007 and Ramette and Tiedje, 2007 for more information). We used db-RDA to analyse the variation in symbiont genetic distance, represented by a Jukes-Cantor genetic distance matrix (response variable), as a function of depth, habitat type, geographic region and host genus. The categorical variables region, habitat and host genus were re-coded as sets of dummy variables, while the continuous variable 'depth' was left untransformed. Factors were checked for collinearity by running the function vif.cca() in R. This resulted in very low variance inflation factor values (out of 14 descriptors, all were < 20), confirming the lack of collinearity in our models. Variation partitioning was used to disentangle the effects of each factor on symbiont genetic distances while accounting for the variation in all other factors present in the models (Borcard *et al*., 1992). Significance of global and partial models was assessed by 1000 Monte Carlo permutations. Statistical analyses were implemented using the '*capscale*' function of the R library VEGAN (Oksanen *et al*., 2012) and custom R scripts.

Nucleotide sequence accession numbers. The sequences from this study were submitted to GenBank under accession numbers KC832729–KC832741 for the symbiont 16S rRNA gene, KC832742–KC832746 for the *aprA* gene, KC832747–KC832751 for the *cbbM* gene and KC832752–KC832760 for the host COI gene.

Acknowledgements

We would like to dedicate this publication to the memory of Henri Germain Delauze, founder of Comex and enthusiastic supporter of the expedition. We thank the staff of the RV Minibex for their great support in sampling the *Lamellibrachia* Tws, and Sigurd Tesche and Florian Guthknecht for their collaboration in the joint Marseille-Messina cruise. We are also very grateful to Eve Southward, who identified our Marsili specimens as *Lamellibrachia anaximandri*. We thank Carl Zeiss MicroImaging GmbH for providing the confocal laser scanning microscope LSM 780 and the technical assistance of Peter Attermeyer and Dario Furlani with image acquisition. Many thanks to Lisa Drews, Silke Wetzel, Sabine Kühn and Andreas Ellrott for excellent technical assistance. Finally, we would like to thank three anonymous reviewers whose suggestions helped us to improve our manuscript.

This work was supported by the Max Planck Society, the DFG Cluster of Excellence 'The Ocean in the Earth System' at MARUM, Bremen, and the Austrian Science Fund project # P20282-B17 (to M. B.).

References

Agogué, H., Lamy, D., Neal, P.R., Sogin, M.L., and Herndl, G.J. (2011) Water mass-specificity of bacterial communities in the North Atlantic revealed by massively parallel sequencing. *Mol Ecol* **20:** 258–274.

Altschul, S., Madden, T., Schaffer, A., Zhang, J., Zhang, Z., Miller, W., and Lipman, D.J. (1997) Gapped BLAST and PSI-BLAST: a new generation of protein database search programs. *Nucleic Acids Res* **25:** 3389–3402.

Amann, R.I., Binder, B.J., Olson, R.J., Chisholm, S.W., Devereux, R., and Stahl, D.A. (1990a) Combination of 16S rRNA-targeted oligonucleotide probes with flow cytometry for analyzing mixed microbial populations. *Appl Environ Microbiol* **56:** 1919–1925.

Amann, R.I., Krumholz, L., and Stahl, D.A. (1990b) Fluorescent-oligonucleotide probing of whole cells for determinative, phylogenetic and environmental studies in microbiology. *J Bacteriol* **172:** 762–770.

Behrens, S., Ruhland, C., Inacio, J., Huber, H., Fonseca, A., Spencer-Martins, I., *et al.* (2003) In situ accessibility of small-subunit rRNA of members of the domains bacteria, archaea, and eukarya to Cy3-labeled oligonucleotide probes. *Appl Environ Microbiol* **69:** 1748–1758.

Black, M.B., Halanych, K.M., Maas, P.A.Y., Hoeh, W.R., Hashimoto, J., Desbruyères, D., *et al.* (1997) Molecular systematics of vestimentiferan tubeworms from hydrothermal vents and cold-water seeps. *Mar Biol* **130:** 141–149.

Blazejak, A., Kuever, J., Erseus, C., Amann, R., and Dubilier, N. (2006) Phylogeny of 16S rRNA, ribulose 1,5-bisphosphate carboxylase/oxygenase, and adenosine 5′-phosphosulfate reductase genes from gamma- and alphaproteobacterial symbionts in gutless marine worms (Oligochaeta) from Bermuda and the Bahamas. *Appl Environ Microbiol* **72:** 5527–5536.

Borcard, D., Legendre, P., and Drapeau, P. (1992) Partialling out the spatial component of ecological variation. *Ecology* **73:** 1045–1055.

Bright, M., and Lallier, F.H. (2010) The biology of vestimentiferan tubeworms. *Oceanogr Mar Biol Ann Rev* **48:** 213–266.

Bright, M., and Sorgo, A. (2003) Ultrastructural reinvestigation of the trophosome in adult *Riftia pachyptila* (Vestimentifera). *Invert Biol* **122:** 347–368.

Bright, M., Kose, J., and Nussbaumer, A.D. (2013) Giant tubeworms. *Curr Biol* **23:** 224–225.

de Burgh, M.D. (1986) Evidence for a physiological gradient in the vestimentiferan trophosome: size-frequency analysis of bacterial populations and trophosome chemistry. *Can J Zool* **64:** 1095–1103.

Carney, R.S. (2005) Zonation of deep biota on continental margins. *Oceanogr Mar Biol Ann Rev* **43:** 211–278.

Chao, L.S.-L., Davis, R.E., and Moyer, C.L. (2007) Characterization of bacterial community structure in vestimentiferan tubeworm *Ridgeia piscesae* trophosomes. *Mar Ecol* **28:** 72–85.

Childress, J.J., and Fisher, C.R. (1992) The biology of hydrothermal vent animals: physiology, biochemistry, and autotrophic symbioses. *Oceanogr Mar Biol Ann Rev* **30:** 337–441.

Cline, J. (1969) Spectrophotometric determination of hydrogen sulfide in natural waters. *Limnol Oceanogr* **14:** 454–458.

Cordes, E.E., Carney, S.L., Hourdez, S., Carney, R.S., Brooks, J.M., and Fisher, C.R. (2007) Cold seeps of the deep Gulf of Mexico: community structure and biogeographic comparisons to Atlantic equatorial belt seep communities. *Deep Sea Res I Oceanogr Res Pap* **54:** 637–653.

Costello, A.M., and Lidstrom, M.E. (1999) Molecular characterization of functional and phylogenetic genes from natural populations of methanotrophs in lake sediments. *Appl Environ Microbiol* **65:** 5066–5074.

Cowart, D.A. (2013) Species distribution and population structure in cold seep vestimentiferan tubeworms of the genera *Escarpia* and *Lamellibrachia* (Polychaeta, Siboglinidae). PhD Thesis, The Pennsylvania State University, Eberly College of Science.

Daims, H., Brühl, A., Amann, R., Schleifer, K.H., and Wagner, M. (1999) The domain-specific probe EUB338 is insufficient for the detection of all bacteria: development and evaluation of a more comprehensive probe set. *Syst Appl Microbiol* **22:** 434–444.

Dando, P.R., Southward, A.J., and Southward, E.C. (1992) Shipwrecked tubeworms. *Nature* **356:** 667.

Di Meo, C.A., Wilbur, A.E., Holben, W.E., Feldman, R.A., Vrijenhoek, R.C., and Cary, S.C. (2000) Genetic variation among endosymbionts of widely distributed vestimentiferan tubeworms. *Appl Environ Microbiol* **66:** 651–658.

Diepenbroek, M., Grobe, H., Reinke, M., Schindler, U., Schlitzer, R., Sieger, R., and Wefer, G. (2002) PANGAEA – an information system for environmental sciences. *Comput Geosci* **28:** 1201–1210.

Dubilier, N., Bergin, C., and Lott, C. (2008) Symbiotic diversity in marine animals: the art of harnessing chemosynthesis. *Nat Rev Microbiol* **6:** 725–740.

Duperron, S., Bergin, C., Zielinski, F., Blazejak, A., Pernthaler, A., McKiness, Z.P., *et al.* (2006) A dual symbiosis shared by two mussel species, *Bathymodiolus azoricus* and *Bathymodiolus puteoserpentis* (Bivalvia: Mytilidae), from hydrothermal vents along the northern Mid-Atlantic Ridge. *Environ Microbiol* **8:** 1441–1447.

Duperron, S., De Beer, D., Zbinden, M., Boetius, A., Schipani, V., Kahil, N., and Gail, F. (2009) Molecular characterization of bacteria associated with the trophosome and the tube of *Lamellibrachia* sp., a siboglinid annelid from cold seeps in the eastern Mediterranean. *FEMS Microbiol Ecol* **69:** 395–409.

Elsaied, H., and Naganuma, T. (2001) Phylogenetic diversity of ribulose-1,5-bisphosphate carboxylase/oxygenase large-subunit genes from Deep Sea microorganisms. *Appl Environ Microbiol* **67:** 1751–1765.

Elsaied, H., Kimura, H., and Naganuma, T. (2002) Molecular characterization and endosymbiotic localization of the gene encoding D-ribulose 1,5-bisphosphate carboxylase-oxygenase (RuBisCO) form II in the deep-sea

vestimentiferan trophosome. *Microbiology* **148:** 1947–1957.
Feldman, R.A., Black, M.B., Cary, C.S., Lutz, R.A., and Vrijenhoek, R.C. (1997) Molecular phylogenetics of bacterial endosymbionts and their vestimentiferan hosts. *Mol Mar Biol Biotechnol* **6:** 268–277.
Fisher, C.R., Childress, J.J., Arp, A.J., Brooks, J.M., Distel, D., Favuzzi, J.A., *et al.* (1988) Physiology, morphology, and biochemical composition of *Riftia pachyptila* at Rose Garden in 1985. *Deep Sea Res A Oceanogr Res Pap* **35:** 1745–1758.
Fisher, C.R., Brooks, J.M., Vodenichar, J.S., Zande, J.M., and Childress, J.J. (1993) The co-occurrence of methanotrophic and chemoautotrophic sulfur-oxidizing bacterial symbionts in a deep-sea mussel. *Mar Ecol* **14:** 277–289.
Folmer, O., Black, M., Hoeh, W., Lutz, R., and Vrijenhoek, R. (1994) DNA primers for amplification of mitochondrial cytochrome c oxidase subunit I from diverse metazoan invertebrates. *Mol Mar Biol* **3:** 294–299.
Freytag, J.K., Girguis, P.R., Bergquist, D.C., Andras, J.P., Childress, J.J., and Fisher, C.R. (2001) A paradox resolved: sulfide acquisition by roots of seep tubeworms sustains net chemoautotrophy. *Proc Natl Acad Sci USA* **98:** 13408–13413.
Fuchs, B.M., Glockner, F.O., Wulf, J., and Amann, R. (2000) Unlabeled helper oligonucleotides increase the in situ accessibility to 16S rRNA of fluorescently labeled oligonucleotide probes. *Appl Environ Microbiol* **66:** 3603–3607.
Galand, P.E., Potvin, M., Casamayor, E.O., and Lovejoy, C. (2010) Hydrography shapes bacterial biogeography of the deep Arctic Ocean. *ISME J* **4:** 564–576.
Gambi, M.C., Schulze, A., and Amato, E. (2011) Record of *Lamellibrachia* sp. (Annelida: Siboglinidae: Vestimentifera) from a deep shipwreck in the western Mediterranean Sea (Italy). *Mar Biodivers Rec* **4:** e24.
Gardebrecht, A., Markert, S., Sievert, S.M., Felbeck, H., Thurmer, A., Albrecht, D., *et al.* (2011) Physiological homogeneity among the endosymbionts of *Riftia pachyptila* and *Tevnia jerichonana* revealed by proteogenomics. *ISME J* **6:** 766–776.
Glöckner, F.O., Fuchs, B.M., and Amann, R. (1999) Bacterioplankton compositions of lakes and oceans: a first comparison based on fluorescence in situ hybridization. *Appl Environ Microbiol* **65:** 3721–3726.
Glud, R.N., Wenzhöfer, F., Tengberg, A., Middelboe, M., Oguri, K., and Kitazato, H. (2005) Distribution of oxygen in surface sediments from central Sagami Bay, Japan: in situ measurements by microelectrodes and planar optodes. *Deep Sea Res I Oceanogr Res Pap* **52:** 1974–1987.
Gray, N.D., Comaskey, D., Miskin, I.P., Pickup, R.W., Suzuki, K., and Head, I.M. (2004) Adaptation of sympatric *Achromatium* spp. to different redox conditions as a mechanism for coexistence of functionally similar sulphur bacteria. *Environ Microbiol* **6:** 669–677.
Hall, T. (1999) BioEdit: a user-friendly biological sequence alignment editor and analysis program for Windows 95/98/NT. *Nucleic Acids Symp Ser* **41:** 95–98. [WWW document]. URL http://www.mbio.ncsu.edu/bioedit/bioedit.html.
Hammer, Ø., Harper, D.A.T., and Ryan, P.D. (2001) PAST: paleontological statistics software package for education and data analysis. *Palaeontol Electron* **4:** 1–9.
Hart, M.M., Forsythe, J., Oshowski, B., Bücking, H., Jansa, J., and Kiers, E.T. (2012) Hiding in a crowd – does diversity facilitate persistence of a low-quality fungal partner in the mycorrhizal symbiosis? *Symbiosis* **59:** 47–56.
Hilário, A., Comas, M.C., Azevedo, L., Pinheiro, L., Ivanov, M.K., and Cunha, M.R. (2011) First record of a Vestimentifera (Polychaeta: Siboglinidae) from chemosynthetic habitats in the western Mediterranean Sea – biogeographical implications and future exploration. *Deep Sea Res I Oceanogr Res Pap* **58:** 200–207.
Huber, T., Faulkner, G., and Hugenholtz, P. (2004) Bellerophon: a program to detect chimeric sequences in multiple sequence alignments. *Bioinformatics* **20:** 2317–2319.
Hughes, D.J., and Crawford, M. (2008) A new record of the vestimentiferan *Lamellibrachia* sp. (Polychaeta: Siboglinidae) from a deep shipwreck in the eastern Mediterranean. *Mar Biodivers Rec* **1:** e21.
Jaspers, E., and Overmann, J. (2004) Ecological significance of microdiversity: identical 16S rRNA gene sequences can be found in bacteria with highly divergent genomes and ecophysiologies. *Appl Environ Microbiol* **70:** 4831–4839.
Jeroschewski, P., Steuckart, C., and Kühl, M. (1996) An amperometric microsensor for the determination of H_2S in aquatic environments. *Anal Chem* **68:** 4351–4357.
Johnson, K.S., Childress, J.J., and Beehler, C.L. (1988a) Short-term temperature variability in the Rose Garden hydrothermal vent field: an unstable deep-sea environment. *Deep Sea Res A Oceanogr Res Pap* **35:** 1711–1721.
Johnson, K.S., Childress, J.J., Hessler, R.R., Sakamoto-Arnold, C.M., and Beehler, C.L. (1988b) Chemical and biological interactions in the Rose Garden hydrothermal vent field, Galapagos spreading center. *Deep Sea Res A Oceanogr Res Pap* **35:** 1723–1744.
Johnson, Z.I., Zinser, E.R., Coe, A., McNulty, N.P., Woodward, E.M.S., and Chisholm, S.W. (2006) Niche Partitioning among *Prochlorococcus* ecotypes along ocean-scale environmental gradients. *Science* **311:** 1737–1740.
Jones, A.M., Berkelmans, R., Oppen, M.J.H.V., Mieog, J.C., and Sinclair, W. (2008) A community change in the algal endosymbionts of a scleractinian coral following a natural bleaching event: field evidence of acclimatization. *Proc R Soc B Biol Sci* **275:** 1359–1365.
Julian, D., Gaill, F., Wood, E., Arp, A., and Fisher, C. (1999) Roots as a site of hydrogen sulfide uptake in the hydrocarbon seep vestimentiferan *Lamellibrachia* sp. *J Exp Biol* **202:** 2245–2257.
Karner, M.B., DeLong, E.F., and Karl, D.M. (2001) Archaeal dominance in the mesopelagic zone of the Pacific Ocean. *Nature* **409:** 507–510.
Katz, S., Klepal, W., and Bright, M. (2011) The *Osedax* trophosome: organization and ultrastructure. *Biol Bull* **220:** 128–139.
Kimura, H., Higashide, Y., and Naganuma, T. (2003) Endosymbiotic microflora of the vestimentiferan tubeworm

(*Lamellibrachia* sp.) from a bathyal cold seep. *Mar Biotechnol* **5:** 593–603.

Kleiner, M., Wentrup, C., Lott, C., Teeling, H., Wetzel, S., Young, J., *et al*. (2012a) Metaproteomics of a gutless marine worm and its symbiotic microbial community reveal unusual pathways for carbon and energy use. *Proc Natl Acad Sci USA* **109:** 7148–7149.

Kleiner, M., Petersen, J.M., and Dubilier, N. (2012b) Convergent and divergent evolution of metabolism in sulfur-oxidizing symbionts and the role of horizontal gene transfer. *Curr Opin Microbiol* **15:** 621–631.

Kruse, S., Bathmann, U., and Brey, T. (2009) Meso- and bathypelagic distribution and abundance of chaetognaths in the Atlantic sector of the Southern Ocean. *Polar Biol* **32:** 1359–1376.

Lacombe, H., Tchernia, P., and Gamberoni, L. (1985) Variable bottom water in the western Mediterranean basin. *Progr Oceanogr* **14:** 319–338.

Lane, D.J. (1991) 16S/23S rRNA sequencing. In *Nucleic Acids Techniques in Bacterial Systematics*. Stackebrandt, E., and Goodfellow, M. (eds). Chichester, UK: John Wiley & Sons, pp. 115–147.

Le Bris, N., Govenar, B., Le Gall, C., and Fisher, C.R. (2006) Variability of physico-chemical conditions in 9°50′N EPR diffuse flow vent habitats. *Mar Chem* **98:** 167–182.

Legendre, P., and Anderson, M.J. (1999) Distance-based redundancy analysis: testing multispecies responses in multifactorial ecological experiments. *Ecol Monogr* **69:** 1–24.

Loy, A., Maixner, F., Wagner, M., and Horn, M. (2007) ProbeBase – an online resource for rRNA-targeted oligonucleotide probes: new features 2007. *Nucleic Acids Res* **35:** D800–D804.

Ludwig, W., Strunk, O., Westram, R., Richter, L., Meier, H., Yadhukumar, *et al*. (2004) ARB: a software environment for sequence data. *Nucl Acids Res* **32:** 1363–1371.

Lupton, J., de Ronde, C., Sprovieri, M., Baker, E.T., Paolo Bruno, P., Italiano, F., *et al*. (2011) Active hydrothermal discharge on the submarine Aeolian Arc: new evidence from water column observations. *J Geophys Res* **116:** B02102.

McManus, M.A., and Woodson, C.B. (2012) Plankton distribution and ocean dispersal. *J Exp Biol* **215:** 1008–1016.

McMullin, E., Hourdez, S., Schaeffer, S.W., and Fisher, C.R. (2003) Phylogeny and biogeography of deep sea vestimentiferan tubeworms and their bacterial symbionts. *Symbiosis* **34:** 1–41.

Manz, W., Amann, R., Ludwig, W., Wagner, M., and Schleifer, K.-H. (1992) Phylogenetic oligodeoxynucleotide probes for the major subclasses of *Proteobacteria*: problems and solutions. *Syst Appl Microbiol* **15:** 593–600.

Markert, S., Arndt, C., Felbeck, H., Becher, D., Sievert, S.M., Hügler, M., *et al*. (2007) Physiological proteomics of the uncultured endosymbiont of *Riftia pachyptila*. *Science* **315:** 247–250.

Meyer, B., and Kuever, J. (2007a) Phylogeny of the alpha and beta subunits of the dissimilatory adenosine-5′-phosphosulfate (APS) reductase from sulfate-reducing prokaryotes – origin and evolution of the dissimilatory sulfate-reduction pathway. *Microbiol* **153:** 2026–2044.

Meyer, B., and Kuever, J. (2007b) Molecular analysis of the distribution and phylogeny of dissimilatory adenosine-5′-phosphosulfate reductase-encoding genes (aprBA) among sulfur-oxidizing prokaryotes. *Microbiol* **153:** 3478–3498.

Miglietta, M.P., Hourdez, S., Cowart, D.A., Schaeffer, S.W., and Fisher, C. (2010) Species boundaries of Gulf of Mexico vestimentiferans (Polychaeta, Siboglinidae) inferred from mitochondrial genes. *Deep Sea Res II Top Stud Oceanogr* **57:** 1916–1925.

Miura, T., Tsukahara, J., and Hashimoto, J. (1997) *Lamellibrachia satsuma*, a new species of vestimentiferan worms (Annelida: Pogonophora) from a shallow hydrothermal vent in Kagoshima Bay, Japan. *Proc Biol Soc Wash* **110:** 447–456.

Muyzer, G., de Waal, E.C., and Uitterlinden, A.G. (1993) Profiling of complex microbial populations by denaturing gradient gel electrophoresis analysis of polymerase chain reaction-amplified genes coding for 16S rRNA. *Appl Environ Microbiol* **59:** 695–700.

Naganuma, T., Kato, C., Hirayama, H., Moriyama, N., Hashimoto, J., and Horikoshi, K. (1997) Intracellular occurrence of e-proteobacterial 16S rDNA sequences in the vestimentiferan trophosome. *J Oceanogr* **53:** 193–197.

Naganuma, T., Elsaied, H., Hoshii, D., and Kimura, H. (2005) Bacterial endosymbioses of gutless tube-dwelling worms in nonhydrothermal vent habitats. *Mar Biotechnol* **7:** 416–428.

Nelson, K., and Fisher, C.R. (2000) Absence of cospeciation in deep-sea vestimentiferan tube worms and their bacterial endosymbionts. *Symbiosis* **28:** 1–15.

Nussbaumer, A.D., Fisher, C.R., and Bright, M. (2006) Horizontal endosymbiont transmission in hydrothermal vent tubeworms. *Nature* **441:** 345–348.

Oksanen, J., Blanchet, F.G., Kindt, R., Legendre, P., Minchin, P.R., O'Hara, R.B., *et al*. (2012). *Vegan: community ecology*. Package. R package version 2.0–4. URL http://CRAN.R-project.org/package=vegan.

Palmer, T.M., Doak, D.F., Stanton, M.L., Bronstein, J.L., Kiers, E.T., Young, T.P., *et al*. (2010) Synergy of multiple partners, including freeloaders, increases host fitness in a multispecies mutualism. *Proc Natl Acad Sci* **107:** 17234–17239.

Pernthaler, A., Pernthaler, J., and Amann, R. (2002) Fluorescence in situ hybridization and catalyzed reporter deposition for the identification of marine bacteria. *Appl Environ Microbiol* **68:** 3094–3101.

Petersen, J.M., Zielinski, F.U., Pape, T., Seifert, R., Moraru, C., Amann, R., *et al*. (2011) Hydrogen is an energy source for hydrothermal vent symbioses. *Nature* **476:** 176–180.

Pflugfelder, B., Cary, S., and Bright, M. (2009) Dynamics of cell proliferation and apoptosis reflect different life strategies in hydrothermal vent and cold seep vestimentiferan tubeworms. *Cell Tissue Res* **337:** 149–165.

Polz, M.F., and Cavanaugh, C.M. (1998) Bias in template-to-product ratios in multitemplate PCR. *Appl Environ Microbiol* **64:** 3724–3730.

Pruesse, E., Quast, C., Knittel, K., Fuchs, B.M., Ludwig, W., Peplies, J., and Gloeckner, F.O. (2007) SILVA: a comprehensive online resource for quality checked and aligned

ribosomal RNA sequence data compatible with ARB. *Nucl Acids Res* **35:** 7188–7196.
Raggi, L., Schubotz, F., Hinrichs, K.-U., Dubilier, N., and Petersen, J.M. (2012) Bacterial symbionts of *Bathymodiolus* mussels and *Escarpia* tubeworms from Chapopote, an asphalt seep in the southern Gulf of Mexico. *Environ Microbiol* **15:** 1969–1987.
Ramette, A. (2007) Multivariate analyses in microbial ecology. *FEMS Microbiol Ecol* **62:** 142–160.
Ramette, A., and Tiedje, J.M. (2007) Multiscale responses of microbial life to spatial distance and environmental heterogeneity in a patchy ecosystem. *Proc Natl Acad Sci* **104:** 2761–2766.
Robidart, J.C., Bench, S.R., Feldman, R.A., Novoradovsky, A., Podell, S.B., Gaasterland, T., *et al*. (2008) Metabolic versatility of the *Riftia pachyptila* endosymbiont revealed through metagenomics. *Environ Microbiol* **10:** 727–737.
Ryan, W.B.F., Carbotte, S.M., Coplan, J.O., O'Hara, S., Melkonian, A., Arko, R., *et al*. (2009) Global Multi-Resolution Topography synthesis. *Geochem Geophys Geosyst* **10:** Q03014.
Southward, E., Andersen, A.C., and Hourdez, S. (2011) *Lamellibrachia anaximandri* n. sp., a new vestimentiferan tubeworm from the Mediterranean (Annelida). *Zoosystema* **33:** 245–279.
Steedman, H.F. (1957) Polyester wax: a new ribboning embedding medium for histology. *Nature* **179:** 1345.
Stewart, F.J., Newton, I.L.G., and Cavanaugh, C.M. (2005) Chemosynthetic endosymbioses: adaptations to oxic-anoxic interfaces. *Trends Microbiol* **13:** 439–448.
Šimek, K., Kasalický, V., Horňák, K., Hahn, M.W., and Weinbauer, M.G. (2010) Assessing niche separation among coexisting *Limnohabitans* strains through Interactions with a competitor, viruses, and a bacterivore. *Appl Environ Microbiol* **76:** 1406–1416.
Takiya, D.M., Tran, P.L., Dietrich, C.H., and Moran, N.A. (2006) Co-cladogenesis spanning three phyla: leafhoppers (Insecta: Hemiptera: Cicadellidae) and their dual bacterial symbionts. *Mol Ecol* **15:** 4175–4191.
Thiel, V., Hügler, M., Blümel, M., Baumann, H.I., Gärtner, A., Schmaljohann, R., *et al*. (2012) Widespread occurrence of two carbon fixation pathways in tubeworm endosymbionts: lessons from hydrothermal vent associated tubeworms from the Mediterranean Sea. *Front Microbiol* **3:** 423.
Thompson, J.D., Higgins, D.G., and Gibson, T.J. (1994) CLUSTAL W: improving the sensitivity of progressive multiple sequence alignment through sequence weighting, position-specific gap penalties and weight matrix choice. *Nucleic Acids Res* **22:** 4673–4680.
Thornhill, D.J., Wiley, A.A., Campbell, A.L., Bartol, F.F., Teske, A., and Halanych, K.M. (2008) Endosymbionts of *Siboglinum fiordicum* and the phylogeny of bacterial endosymbionts in Siboglinidae (Annelida). *Biol Bull* **214:** 135–144.
Tunnicliffe, V. (1998) The biology of hydrothermal vents: ecology and evolution. *Oceanogr Mar Biol Ann Rev* **29:** 319–407.
Uchupi, E., and Ballard, R.D. (1989) Evidence of hydrothermal activity on Marsili Seamount, Tyrrhenian Basin. *Deep Sea Res A Oceanogr Res Pap* **36:** 1443–1448.
Verna, C., Ramette, A., Wiklund, H., Dahlgren, T.G., Glover, A.G., Gaill, F., and Dubilier, N. (2010) High symbiont diversity in the bone-eating worm *Osedax mucofloris* from shallow whale-falls in the North Atlantic. *Environ Microbiol* **12:** 2355–2370.
Vrijenhoek, R.C., Duhaime, M., and Jones, W.J. (2007) Subtype variation among bacterial endosymbionts of tubeworms (Annelida: Siboglinidae) from the Gulf of California. *Biol Bull* **212:** 180–184.
West, S.A., Kiers, E.T., Pen, I., and Denison, R.F. (2002) Sanctions and mutualism stability: when should less beneficial mutualists be tolerated? *J Evol Biol* **15:** 830–837.
Yanisch-Perron, C., Vieira, J., and Messing, J. (1985) Improved M13 phage cloning vectors and host strains: nucleotide sequences of the M13mp18 and pUC19 vectors. *Gene* **33:** 103–119.
Young, C.M., Vázquez, E., Metaxas, A., and Tyler, P.A. (1996) Embryology of vestimentiferan tube worms from deep-sea methane/sulphide seeps. *Nature* **381:** 514–516.
Young, C.M., He, R., Emlet, R.B., Li, Y., Qian, H., Arellano, S.M., *et al*. (2012) Dispersal of deep-sea larvae from the Intra-American seas: simulations of trajectories using ocean models. *Integr Comp Biol* **52:** 483–496.
Zhou, J., Bruns, M., and Tiedje, J. (1996) DNA recovery from soils of diverse composition. *Appl Environ Microbiol* **62:** 316–322.
Zierenberg, R.A., Adams, M.W.W., and Arp, A.J. (2000) Life in extreme environments: hydrothermal vents. *Proc Natl Acad Sci* **97:** 12961–12962.

Supporting information

Additional Supporting Information may be found in the online version of this article at the publisher's web-site:

Fig. S1. CARD-FISH section overview of Tw 1 containing only symbiont type B. The section was double-hybridized with a specific probe for symbiont type B (yellow) and type A (red). The overview shows only the trophosomal lobules of the tubeworm because the skin (cuticle, epidermis and somatic muscles) was lost during sectioning. Host nuclei are stained with DAPI (blue). The section was examined with an epifluorescence microscope (Zeiss, Axioplan 2, Germany) and edited with the software Axio Vision release 4.8.2.
Table S1. Summary of the clone library and CARD-FISH analyses performed in this study.
Table S2. Relative symbiont abundances (%) in trophosome sections of different tubeworms (Tws) in anterior (a), middle (m) or posterior (p) body parts. The values are based on automated area measurement of both symbiont types hybridized with specific CARD-FISH-oligonucleotide probes. For details, see 'Symbiont image analysis' in *Experimental procedures*.
Table S3. Mann–Whitney *U* pairwise comparison of symbiont distributions within and along Marsili tubeworms (Tws).The analyses were based on the relative abundance values in anterior (a), middle (m) and posterior (p) tubeworm regions calculated from the automated picture analyses as shown in Supporting Information Table S2.
Table S4. Overview of the vestimentiferan symbiont sequences and descriptors* that were used for the db-RDA.

Supplementary information

Judith Zimmermann, Christian Lott, Miriam Weber, Alban Ramette, Monika Bright, Nicole Dubilier, and Jillian M. Petersen.

SI Tables

Table S1: Summary of the clone library and CARD FISH analyses performed in this study.

Tube-worm no.	Trunk regions used*	16S rRNA type	No. of clones sequenced+	Genbank accession no.	Relative symbiont abundance (area %) determined by FISH°	*aprA* type	No. of clones sequenced~	Genbank accession no.	*cbbM* type	No. of clones sequenced~	Genbank accession no.	COI haplo-type	Tube-worm length [cm]	Genbank accession no.
1	a	—			0							H1	24	KC832752
		B	79 (8)	KC832729	100									
2	a	A			8							H4	53	KC832753
		B			92									
	m	A	50 (8)	KC832731	37	A	54 (8)	KC832743	A	17 (8)	KC832748			
		B	30 (8)	KC832730	63	B	34 (8)	KC832742	B	56 (8)	KC832747			
	p	A			80									
		B			20									
3	m	A	50 (8)	KC832733	73							H1	30	KC832754
		B	5 (5)	KC832732	27									
4	a	A			48							H2	35	KC832755
		B			52									
	m	A	60 (8)	KC832735	80									
		B	25 (8)	KC832734	20									
	p	A			100									
		B			0									

Tube-worm no.	Trunk regions used*	16S rRNA type	No. of clones sequenced+	Genbank accession no.	Relative symbiont abundance (area %) determined by FISH°	*aprA* type	No. of clones sequenced~	Genbank accession no.	*cbbM* type	No. of clones sequenced~	Genbank accession no.	COI haplo-type	Tube-worm length [cm]	Genbank accession no.
5	a	A			0							H2	60	KC832756
		B			100									
	m	A	0		32									
		B	67 (6)	KC832736	68	B	74 (8)	KC832744	B	70 (8)	KC832749			
	p	A			0									
		B			100									
	a+m+p	A	0											
		B	65											
6	m	A	52 (4)	KC832738								H1	25	KC832757
		B	25 (5)	KC832737										
10	m	A	9 (6)	KC832740								H1	—	KC832759
		B	32 (6)	KC832739										
11	m	A	58 (6)	KC832741								H3	>100	KC832760
		—												
	a+m+p					A	82 (8)	KC832746	A	47 (7)	KC832751			
						B	1 (1)	KC832745	B	34 (8)	KC832750			

*a: anterior, m: middle, p: posterior, 'a+m+p' means that anterior, middle and posterior parts were pooled for the analyses; +in parentheses, number of clones fully sequenced; ~in parentheses, number of clones sequenced in both directions; °average value of five analyzed sections

Table S2: Relative symbiont abundances (%) in trophosome sections of different tubeworms (Tws) in anterior (a), middle (m) or posterior (p) body parts. The values are based on automated area measurement of both symbiont types hybridized with specific CARD-FISH-oligonucleotide probes. For details see 'Symbiont image analysis' In Experimental procedures.

Symbiont type A	**Tw 2a**	**Tw 2m**	**Tw 2p**	**Tw 3m**	**Tw 4a**	**Tw 4m**	**Tw 5m**
section 1	2.2	31.8	75.8	77.0	47.46	97.2	42.2
section 2	8.0	20.9	64.4	85.7	41.92	76.7	38.2
section 3	3.5	38.1	92.7	66.4	51.91	58.5	34.4
section 4	5.3	46.1	71.2	64.0	58.34	85.5	12.3
section 5	20.4	48.7	93.9	73.4	59.56	79.5	34.4
Average	**7.9**	**37.1**	**79.6**	**73.3**	**51.8**	**79.5**	**32.3**
Stdev	6.6	10.1	11.8	7.8	7.4	12.6	10.4

Symbiont type B	**Tw 2a**	**Tw 2m**	**Tw 2p**	**Tw 3m**	**Tw 4a**	**Tw 4m**	**Tw 5m**
section 1	97.8	68.2	24.2	23.0	52.54	2.8	57.8
section 2	92.0	79.1	35.6	14.3	58.08	23.3	61.8
section 3	96.5	61.9	7.3	33.6	48.09	41.5	65.6
section 4	94.7	53.9	28.8	36.0	41.66	14.5	87.7
section 5	79.6	51.3	6.1	26.6	40.44	20.5	65.6
Average	**92.1**	**62.9**	**20.4**	**26.7**	**48.2**	**20.5**	**67.7**
Stdev	7.3	11.3	13.1	8.7	7.4	14.1	11.6

Table S3: Mann-Whitney *U* pairwise comparison of symbiont distributions within and along Marsili tubeworms (Tws).The analyses were based on the relative abundance values in anterior (a), middle (m) and posterior (p) tubeworm regions calculated from the automated picture analyses as shown in Table S2.

	Tw 1b	Tw 2a	Tw 2m	Tw 2p	Tw 3m	Tw4 a	Tw 4m	Tw4 p	Tw 5a	Tw 5m	Tw 5p
Tw 1b		0.0075	0.0075	0.0075	0.0075	0.0075	0.0075	0.0040	1.0000	0.0073	1.0000
Tw 2a			0.0122	0.0122	0.0122	0.0122	0.0122	0.0075	0.0075	0.0212	0.0075
Tw 2m				0.0122	0.0122	0.1437	0.0122	0.0075	0.0075	0.6752	0.0075
Tw 2p					0.5309	0.0122	0.8345	0.0075	0.0075	0.0119	0.0075
Tw 3m						0.0122	0.5309	0.0075	0.0075	0.0119	0.0075
Tw4 a							0.0122	0.0075	0.0075	0.0362	0.0075
Tw 4m								0.0075	0.0075	0.0119	0.0075
Tw4 p									0.0040	0.0073	0.0040
Tw 5a										0.0073	1.0000
Tw 5m											0.0073
Tw 5p											

Significant p-values <0.02 are highlighted.

Table S4: Overview of the vestimentiferan symbiont sequences and descriptors* that were used for the distance-based redundancy analysis (db-RDA).

Symbiont sequence	Geographical Region*	Water depth* [m]	Habitat*	Host*	Reference	Host group
HE9833339 endosymbiont of *Seepiophila jonesi*	GoM	527	Cold Seep	*Seepiophila*	Thiel *et al.*, 2012	LES
AY129087, endosymbiont of *Seepiophila jonesi*	GoM	550-650	Cold Seep	*Seepiophila*	McMullin *et al.*, 2003	LES
AY129105, endosymbiont of *Seepiophila jonesi*	GoM	545	Cold Seep	*Seepiophila*	Nelson and Fisher, 2000	LES
AY129104, endosymbiont of *Seepiophila jonesi*	GoM	545	Cold Seep	*Seepiophila*	Nelson and Fisher, 2000	LES
AY129101, endosymbiont of *Seepiophila jonesi*	GoM	550-650	Cold Seep	*Seepiophila*	McMullin *et al.*, 2003	LES
AY129100, endosymbiont of *Lamellibrachia* cf. *luymesi*	GoM	550-650	Cold Seep	*Lamellibrachia*	McMullin *et al.*, 2003	LES
AY129092, endosymbiont of *Seepiophila jonesi*	GoM	550-650	Cold Seep	*Seepiophila*	McMullin *et al.*, 2003	LES
HE983341 endosymbiont of *Lamellibrachia luymesi*	GoM	546	Cold Seep	*Lamellibrachia*	Thiel *et al.*, 2012	LES
AY129110, endosymbiont of *Lamellibrachia* sp. 2	GoM	545	Cold Seep	*Lamellibrachia*	Nelson and Fisher, 2000	LES
AY129111, endosymbiont of *Lamellibrachia* sp. 2	GoM	545	Cold Seep	*Lamellibrachia*	Nelson and Fisher, 2000	LES
HE983340 endosymbiont of *Lamellibrachia luymesi*	GoM	540	Cold Seep	*Lamellibrachia*	Thiel *et al.*, 2012	LES
AY129089, endosymbiont of *Seepiophila jonesi*	GoM	550-650	Cold Seep	*Seepiophila*	McMullin *et al.*, 2003	LES
HE863794 endosymbiont of *Lamellibrachia* Guinness	East Atlantic	600	Cold Seep	*Lamellibrachia*	Duperron *et al.*, 2012	LES
KC832740 *L. anaximandri* Tw10 endosymbiont phylotype A	Mediterranean	545	Hot Vent	*Lamellibrachia*	**this study**	LES
KC832731 *L. anaximandri* Tw2 endosymbiont phylotype A	Mediterranean	545	Hot Vent	*Lamellibrachia*	**this study**	LES
HE983349 endosymbiont of *L. anaximandri*, Palinuro	Mediterranean	630	Hot Vent	*Lamellibrachia*	Thiel *et al.*, 2012	LES
HE983347 endosymbiont of *L. anaximandri*, Palinuro	Mediterranean	634	Hot Vent	*Lamellibrachia*	Thiel *et al.*, 2012	LES
FM165438, *Lamellibrachia* sp. endosymbiont	Mediterranean	1157	Cold Seep	*Lamellibrachia*	Duperron *et al.*, 2009	LES
AY129109, endosymbiont of *Escarpia laminata*	GoM	2020	Cold Seep	*Escarpia*	Nelson and Fisher, 2000	LES
AY129102, endosymbiont of *Escarpia laminata*	GoM	2020	Cold Seep	*Escarpia*	Nelson and Fisher, 2000	LES
AY129108, endosymbiont of *Escarpia laminata*	GoM	2020	Cold Seep	*Escarpia*	Nelson and Fisher, 2000	LES
AY129112, endosymbiont of *Lamellibrachia* sp.	GoM	2020	Cold Seep	*Lamellibrachia*	Nelson and Fisher, 2000	LES
HE983336 endosymbiont of *Lamellibrachia* sp. 1	GoM	1437	Cold Seep	*Lamellibrachia*	Thiel *et al.*, 2012	LES
HE983333 endosymbiont of *Escarpia laminata*	GoM	1975	Cold Seep	*Escarpia*	Thiel *et al.*, 2012	LES
HE983334 endosymbiont of *Lamellibrachia* sp. 1	GoM	1437	Cold Seep	*Lamellibrachia*	Thiel *et al.*, 2012	LES
HE983332 endosymbiont of *Escarpia laminata*	GoM	2339	Cold Seep	*Escarpia*	Thiel *et al.*, 2012	LES
AY129093, endosymbiont of *Lamellibrachia barhami*	East Pacific	1000	Cold Seep	*Lamellibrachia*	McMullin *et al.*, 2003	LES
HE983337 endosymbiont of *Lamellibrachia* sp. 2	GoM	2335	Cold Seep	*Lamellibrachia*	Thiel *et al.*, 2012	LES

HE983329 endosymbiont of *Escarpia laminata*	GoM	2604	Cold Seep	*Escarpia*	Thiel *et al.*, 2012	LES
AY129094, endosymbiont of *Lamellibrachia barhami*	East Pacific	1000	Cold Seep	*Lamellibrachia*	McMullin *et al.*, 2003	LES
HE983328 endosymbiont of *Lamellibrachia* sp. 2	GoM	2604	Cold Seep	*Lamellibrachia*	Thiel 2012	LES
U77482, *Escarpia spicata* endosymbiont	East Pacific	1240	Whale fall	*Escarpia*	Feldman *et al.*, 1997	LES
AY129103, endosymbiont of *Lamellibrachia barhami*	East Pacific	1300	Cold Seep	*Lamellibrachia*	McMullin *et al.*, 2003	LES
HE983327 endosymbiont of *Lamellibrachia* sp. 1	GoM	2604	Cold Seep	*Lamellibrachia*	Thiel *et al.*, 2012	LES
HE983330 endosymbiont of *Escarpia laminata*	GoM	2339	Cold Seep	*Escarpia*	Thiel *et al.*, 2012	LES
AY129113, endosymbiont of *Lamellibrachia barhami*	East Pacific	2420	Hot Vent	*Lamellibrachia*	Nelson and Fisher, 2000	LES
AY129090, endosymbiont of *Lamellibrachia barhami*	East Pacific	1800-2200	Cold Seep	*Lamellibrachia*	McMullin *et al.*, 2003	LES
AM888202, uncultured gamma proteobacterium	East Atlantic	3200	Cold Seep	*Escarpia*	Cambon-Bonavita *et al.*, 2009	LES
AY129107, endosymbiont of *Escarpia laminata*	GoM	3700	Cold Seep	*Escarpia*	Nelson and Fisher, 2000	LES
U77479, *Lamellibrachia* sp. endosymbiont	GoM	700	Cold Seep	*Lamellibrachia*	Feldman *et al.*, 1997	LES
U77481, *Lamellibrachia columna* endosymbiont	West Pacific	1859	Hot Vent	*Lamellibrachia*	Feldman *et al.*, 1997	LES
JF969172 endosymbiont of *Escarpia* sp.	GoM	2915	Cold Seep	*Escarpia*	Raggi *et al.*, 2012	LES
JF969171 endosymbiont of *Escarpia* sp.	GoM	2918	Cold Seep	*Escarpia*	Raggi *et al.*, 2012	LES
DQ232903, endosymbiont of *Escarpia* sp.	East Pacific	1780	Cold Seep	*Escarpia*	Vriejenhoek *et al.*, 2007	LES
DQ232902, endosymbiont of *Lamellibrachia* sp.	East Pacific	1780	Cold Seep	*Lamellibrachia*	Vriejenhoek *et al.*, 2007	LES
AY129106, endosymbiont of *Escarpia laminata*	GoM	3700	Cold Seep	*Escarpia*	Nelson and Fisher, 2000	LES
HE983331 endosymbiont of *Escarpia laminata*	GoM	2339	Cold Seep	*Escarpia*	Thiel *et al.*, 2012	LES
AB073120, endosymbiont of *Lamellibrachia satsuma*	West Pacific	90	Hot Vent	*Lamellibrachia*	Yamamoto *et al.*, 2002	LES
AF165907, endosymbiont of *Lamellibrachia satsuma*	West Pacific	433	Hot Vent	*Lamellibrachia*	Di Meo *et al.*, 2000	LES
KC832730 *L. anaximandri* Tw2 endosymbiont phylotype B	Mediterranean	545	Hot Vent	*Lamellibrachia*	**this study**	LES
KC832739 *L. anaximandri* Tw10 endosymbiont phylotype B	Mediterranean	545	Hot Vent	*Lamellibrachia*	**this study**	LES
FM165437, *Lamellibrachia* sp. endosymbiont	Mediterranean	1157	Cold Seep	*Lamellibrachia*	Duperron *et al.*, 2009	LES
AY129117, endosymbiont of *Tevnia jerichonana*	East Pacific	2500	Hot Vent	*Tevnia*	Nelson and Fisher, 2000	VENT
AY129118, endosymbiont of *Tevnia jerichonana*	East Pacific	2500	Hot Vent	*Tevnia*	Nelson and Fisher, 2000	VENT
AY129115, endosymbiont of *Riftia pachyptila*	East Pacific	2500	Hot Vent	*Riftia*	Nelson and Fisher, 2000	VENT
AY129114, endosymbiont of *Oasisia alvinae*	East Pacific	2500	Hot Vent	*Oasisia*	Nelson and Fisher, 2000	VENT
U77478, endosymbiont of *Riftia pachyptila*	East Pacific	2637	Hot Vent	*Riftia*	Feldman *et al.*, 1997	VENT
DQ232901, endosymbiont of Vestimentiferan tubeworm	East Pacific	2000	Hot Vent	*Riftia*	Vriejenhoek *et al.*, 2007	VENT
AY129116, endosymbiont of *Riftia pachyptila*	East Pacific	2500	Hot Vent	*Riftia*	Nelson and Fisher, 2000	VENT
U77480, endosymbiont of *Ridgeia piscesae*	East Pacific	2847	Hot Vent	*Ridgeia*	Feldman *et al.* 1997	VENT
AY129119, endosymbiont of *Ridgeia piscesae*	East Pacific	2420	Hot Vent	*Ridgeia*	Nelson and Fisher, 2000	VENT
AY129120, endosymbiont of *Ridgeia piscesae*	East Pacific	2720	Hot Vent	*Ridgeia*	Nelson and Fisher, 2000	VENT

SI Figures

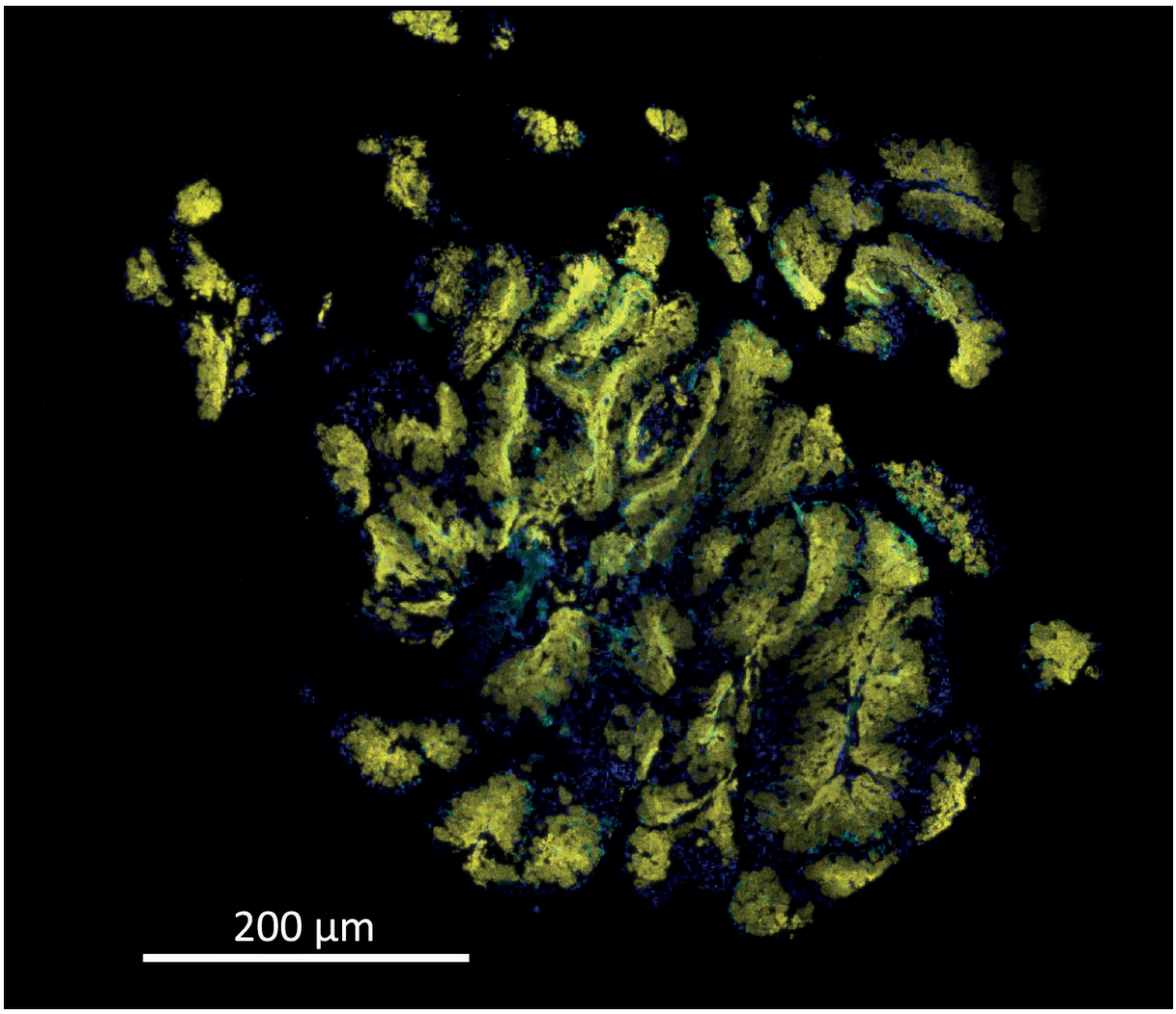

Fig. S1: CARD-FISH section overview of Tw 1 containing only symbiont type B. The section was double-hybridized with a specific probe for symbiont type B (yellow) and type A (red). The overview shows only the trophosomal lobules of the tubeworm, because the skin (cuticle, epidermis, somatic muscles) was lost during sectioning. Host nuclei are stained with DAPI (blue). The section was examined with an epifluorescence microscope (Zeiss, Axioplan 2, Germany) and edited with the software Axio Vision release 4.8.2

Chapter III

Codivergence and host switches between marine animal phyla with closely related ecto- and endosymbionts

Authors: Judith Zimmermann[1], Cécilia Wentrup[1], Miriam Sadowski[1], Anna Blazejak[1], Harald R. Gruber-Vodicka[1], Manuel Kleiner[1*], Jörg A. Ott[2], Bodil Cronholm[3], Pierre de Wit[4], Christer Erséus[5], and Nicole Dubilier[1]

[1]Department of Symbiosis, Max Planck Institute for Marine Microbiology, Celsiusstrasse, Bremen, Germany
[2]Department of Limnology and Oceanography, University of Vienna, Althanstrasse, Austria
[3]Department of Bioinformatics and Genetics, Swedish Museum of Natural History, Stockholm, Sweden
[4]Department of Marine Sciences, University of Gothenburg, Sven Lovén Centre for Marine Sciences Tjärnö, Hättebäcksvägen, Strömstad, Sweden
[5]Department of Biological and Environmental Sciences, University of Gothenburg, Sweden
*now affiliated with Department of Geoscience, Energy Bioengineering Group, University of Calgary, Canada

Manuscript in preparation

J.Z. and C.W contributed equally to this manuscript. J.Z and C.W conceived and designed the study, did parts of the sampling, constructed the molecular data and did the data analyses. J.Z. did the sequencing for the stilbonematine nematodes, performed the phylogenetic analyses, parts of the statistical analyses, conceived and wrote the manuscript; C.W. did the sequencing for the gutless clitellates and their symbionts, helped with the phylogenetic analyses, did parts of the statistical analyses and edited the manuscript; M.S., A.B. and B.C. contributed to the construction of the molecular data; H.G-V. helped to develop the concept and organized the sampling on Belize; M.K. organized the sampling of many gutless oligochaete species; P.D.W. contributed to the phylogenetic analyses; J.A.O. partly helped to develop the concept, identified and helped to sample Stilbonematine nematodes; C.E. partly helped to develop the concept, identified and helped to sample the gutless oligochaetes and contributed to the construction of the oligochaete host genes; N.D. helped to develop the concept, conceived and helped to write the manuscript. All authors edited the manuscript.

Abstract

The integration between symbiotic partners can range from ectosymbioses to extracellular and intracellular endosymbioses, and it is often assumed that this range reflects a continuum of specificity and stability from less intimate to evolutionarily highly stable associations. In this study, we examined the specificity and evolutionary history of symbioses in a group of closely related chemoautotrophic, sulfur-oxidizing bacteria, called *Candidatus* Thiosymbion, that have established ecto- and endosymbioses with two marine animal phyla, Nematoda and Annelida. Unexpectedly, in the 22 investigated stilbonematine nematode ectosymbioses we saw a high degree of congruence between host and symbiont phylogeny based on analyses of their ribosomal RNA (rRNA) genes. In contrast, in the 23 investigated gutless phallodriline annelid endosymbioses, we found no evidence for a relationship between symbiont and host genetic distances but a strong influence of biogeography, based on phylogenetic analyses of 16S rRNA symbiont genes and six host genes. Event-based cophylogenetic analyses identified 10 significant codivergence events between stilbonematine nematodes and their ectosymbionts but only one event between gutless phallodrilines and their endosymbionts. Phylogenetic analyses of 50 *Cand.* Thiosymbion 16S rRNA sequences revealed seven clades that contained both stilbonematine ectosymbionts and phallodriline endosymbionts. Two host switches from stilbonematines to gutless phallodrilines and one vice-versa were supported by cophylogeny reconstruction analyses. These results show that the evolutionary history of ecto- and endosymbiotic *Cand.* Thiosymbion bacteria and their hosts was closely coupled and that interphylum host and lifestyle switches are likely to have occurred multiple times.

Introduction

The central role symbiosis plays in the ecology and evolution of eukaryotic organisms is now unquestioned (Margulis & Fester 1991; McFall-Ngai *et al.* 2013). However, the evolutionary processes by which symbioses are established and maintained within host lineages are less clear. Several forms of symbiont integration are known. These range from ectosymbiotic associations in which the symbionts are attached to the outside of the host and endosymbiotic associations in which the symbionts live extracellularly or intracellularly inside the host.

It is often assumed that this range of lifestyles corresponds with the intimacy and evolutionary stability of the association, that is that ectosymbioses are the least intimate and intracellular endosymbioses the most specific. Correspondingly, it has been argued that there is a continuum in the evolution of obligate endosymbioses that begins with a free-living bacterial ancestor that goes through several steps of host adaptation: from extracellular to facultative intracellular and finally obligate and mutualistic intracellular symbiosis, accompanied by corresponding reductions in the symbionts' genome (Smith 1979; Moran *et al.* 2008; Moya *et al.* 2008; Toft & Andersson 2010). This continuum is often assumed to be influenced by the manner in which the symbionts are transmitted from one generation to the next (reviewed by Bright & Bulgheresi 2010; Ebert 2013).

Intracellular endosymbionts that are transmitted vertically from parent to offspring are generally regarded as the most intimate and stable associations (Bennett & Moran 2015). These types of associations are well known from insects, but also from marine hosts such as vesicomyid clams and catenulid flatworms, and are often reflected in congruent phylogenies of host and symbiont as a result of codiversification of the symbiotic partners over evolutionary time and genome reduction of the symbiont (Peek *et al.* 1998; Bright & Bulgheresi 2010; Gruber-Vodicka *et al.* 2011). However, evidence for cospeciation has also been found in ectosymbioses, although only rarely, for example in the associations between termite gut flagellates and their ectosymbiotic bacteria (Desai *et al.* 2010). Further evidence that symbiont lifestyle, transmission mode and evolutionary stability are not always related comes from obligate intracellular endosymbioses with lateral transmission, in which the host aquires its symbionts from the environment, either

from a free-living population or from co-occurring hosts. The association between the gutless hydrothermal vent tube worm *Riftia* that always aquires the same sulfur-oxidizing bacterial symbionts from the surrounding seawater is a good example of the latter (Cavanaugh *et al.* 1981; Nussbaumer *et al.* 2006).

An ideal group for investigating the relationship between evolutionary stability and symbiont integration is a monophyletic clade of marine sulfur-oxidizing Gammaproteobacteria within the Chromatiaceae, recently named *Candidatus* Thiosymbion (Gruber-Vodicka *et al.*, in prep.). Symbionts of this clade have adapted to different mutualistic symbiotic lifestyles with three marine animal groups from the phyla Annelida and Nematoda (Ott *et al.* 2004; Dubilier *et al.* 2006, 2008). *Cand*. Thiosymbion species live intracellularly in the mouthless siphonolaimid nematode *Astomonema jenneri* (Ott *et al.* 1982), extracellularly in the space just below the cuticle and above the epidermal cells of gutless phallodriline oligochaetes from the phylum Annelida (Clitellata, Naididae *sensu* Erséus *et al.* 2008) and as ectosymbionts attached to the cuticle of stilbonematine nematodes (family *Desmodoridae*) (Ott *et al.* 2004). While not much is known about the diversity and distribution of siphonolaimide nematodes, numerous species of gutless phallodrilines and stilbonematines have been described from around the world, particularly from tropical and subtropical shallow water habitats, where these hosts often co-occur (Erséus 1992; Tchesunov 2013, own observation).

Gutless Phallodrilinae lack a mouth and gut and have established stable associations with multiple chemosynthetic endosymbionts, which provide them with nutrition and recycle their waste compounds (Woyke *et al.* 2006; Kleiner *et al.* 2012b). The symbiotic consortium beneath the cuticle usually consists of one primary symbiont that belongs to the *Cand.* Thiosymbion and three to five secondary symbionts that belong to other bacterial groups (Dubilier *et al.* 1999, 2001; Blazejak *et al.* 2005, 2006; Ruehland *et al.* 2008). Over 100 species from the two known genera *Olavius* and *Inanidrilus* have been described morphologically (Erséus 1984, 2003). However, the specificity and evolutionary history of the gutless phallodriline endosymbioses are not well understood, as detailed molecular analyses of host and symbiont are lacking.

Stilbonematine nematodes are covered by a characteristic coat of sulfur-oxidizing ectosymbiotic bacteria that belong to the *Cand.* Thiosymbion and are assumed to serve as a source of nutrition

(Powell *et al.* 1979; Ott *et al.* 2004). The ectosymbionts occur in different shapes, including cocci, rods, crescent and filaments, and each species is associated with a particular morphotype (Ott *et al.* 1991; Polz *et al.* 1992). Many species from a total of ten genera have been described so far morphologically (reviewed by Tchesunov 2013). Similar to the gutless phallodrilines, only a few stilbonematine host species and ectosymbionts have been characterized with molecular methods and correspondingly, only little is known about the specificity and evolutionary history of these ectosymbioses (Polz *et al.* 1994; Kampfer *et al.* 1998; Bayer *et al.* 2009; Ott *et al.* 2014a; Pende *et al.* 2014).

In this study we sampled 23 species of gutless phallodriline oligochaetes and 22 stilbonematine nematodes from different locations around the world to investigate the evolutionary history of both host groups with their *Cand.* Thiosymbion endo- and ectosymbionts. To better understand factors influencing symbiont phylogeny, we used a combined approach of multi-locus phylogeny, codiversification analyses and statistics and examined the effects of host phylogeny and geography on symbiont specificity, stability and diversity.

Material and Methods

Meiofauna collection and preparation

Phallodriline oligochaetes and stilbonematine nematodes were collected from sites in the Atlantic and Pacific Oceans, the Mediterranean and the North Sea (Fig. 1, Table S1 - S2). Sediments containing the worms were collected using buckets or sediment cores, and the worms were extracted by decantation with a 64 µm mesh sieve for stilbonematines and a 250 µm mesh for phallodrilines. Live animals were sorted with a dissecting microscope and identified to the species level (for phallodrilines) or genus level (for stilbonematines) based on morphological characters. If a morphological identification of phallodrilines to the species level was not possible in the field, the specimens were cut in two: the anterior part was fixed in Bouin's fluid, stained and mounted on a microscope slide as described in (Erséus, 1994) for *a posteriori* host species identification while the posterior part was preserved in 95% ethanol for molecular analyses. All other specimens were washed in 0.2 µm filtered seawater

(stilbonematines) or unfiltered seawater (phallodrilines) and immediately fixed in 70 - 95% ethanol for molecular host and symbiont identification. Samples were stored at 4 °C or -20 °C until further processing.

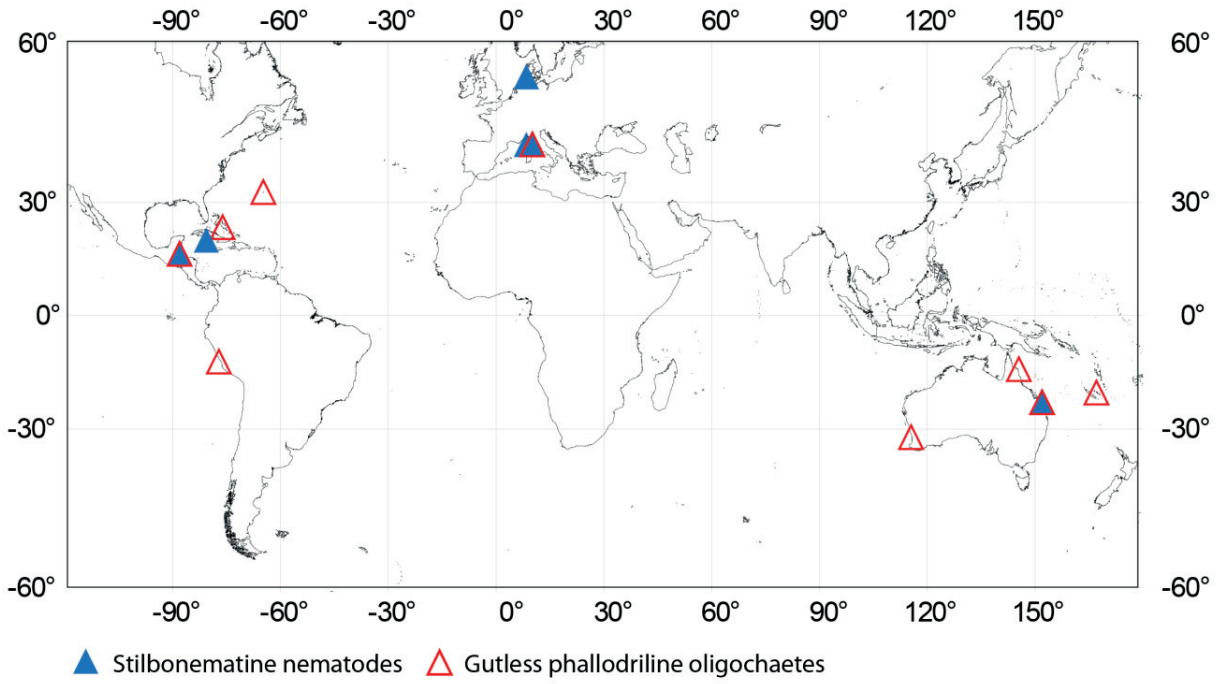

Fig. 1: Sampling sites of marine stilbonematine nematodes and gutless phallodriline oligochaetes. Specimens were sampled from shallow water habitats in the West Atlantic, Mediterranean Sea, North Sea, Australia and one deeper site on the continental margin off Peru in the East Pacific. For details see Table S1 and S2. The map was generated using PanMap (Diepenbroek *et al.* 2002).

DNA extraction, PCR and sequencing

For gutless Phallodrilinae, DNA was either extracted from whole or halved specimens using the DNAeasy Tissue Kit (Qiagen, Hilden, Germany) following the manufacturer's instructions. For the host, we sequenced six host genetic markers: mitochondrial (mt)12S rRNA, mt16S rRNA, 18S rRNA, 28S rRNA, the internal transcribed spacer (ITS) and mtCOI (cytochrome oxidase I). All polymerase chain reactions (PCR) and sequencing reactions were carried out as described previously (Sjölin *et al.* 2005; Blazejak *et al.* 2006; Table S3). Previous studies using clone library analyses of bacterial 16S rRNA PCR products showed that in all investigated individuals of a given gutless Phallodrilinae species, the 16S rRNA sequences of the *Cand.* Thiosymbion

symbionts were identical (> 99.95% nucleotide identity) (e.g. Blazejak *et al.* 2006; Ruehland *et al.* 2008). In this study, we therefore only amplified the 16S rRNA gene of *Cand.* Thiosymbion using a newly designed *Cand.* Thiosymbion-specific forward primer (G1_55_all) and a general bacterial reverse primer (GM4R, Muyzer *et al.* 1995) (Table S4). If available, we also amplified and sequenced host and symbiont genes from additional specimens of the same species. All host and symbiont PCR products were purified and sequenced bidirectionally with the primers listed in Table S3.

For stilbonematine nematodes two different DNA extraction methods were used. For nematodes from Sylt (North Sea) and Elba (Mediterranean), DNA was extracted and purified from single specimens as described previously (Schizas *et al.* 1997). Nematodes from Heron Island (Australian Great Barrier Reef) and Carrie Bow Cay (Belize) were treated with three 25 - 40 s ultrasonication pulses (Bandelin Sonoplus HD 70, Berlin, Germany) and vortexed between pulses to mechanically remove the symbionts from the worms. DNA from worm and symbiont fractions was extracted separately, the latter pelleted by centrifugation, with the DNAeasy Tissue Kit (Qiagen, Hilden, Germany) following the manufacturer's instructions. For the host we sequenced the 18S rRNA gene and for the symbionts the partial 16S rRNA-ITS-23S rRNA operon. The genes were amplified by PCR with Phusion® DNA polymerase (Finnzymes, Finland) and the primers listed in Table S3. Cycling conditions were as follows: initial denaturation at 96° C for 5 min, followed by 30 - 35 cycles of 96° C for 1 min, 55° C (18S rRNA)/ 48° C (16S-ITS-23S rRNA) for 1.5 min, 72° C for 2 min and final elongation at 72° C for 10 min. The purified host PCR products were sequenced bidirectionally with internal forward and reverse primer listed in Table S3. For DNA extracts from whole worms from Sylt and Elba, 16S-ITS-23S rRNA clone libraries were constructed and screened for positive inserts as described previously (Zimmermann *et al.* 2014). Up to 52 clones were partially sequenced with the universal primer 907RM (Table S2), and compared with sequences in GenBank by using BLASTn (Altschul *et al.* 1997). Similar to previous studies, some clone libraries from whole worm extracts yielded sequences of other marine bacteria, but previous studies showed that the ectosymbiont coat always consists of a particular gammaproteobacterial ectosymbiont type (Polz *et al.* 1994; Pende *et al.* 2014). Therefore, one to eight clones that contained sequences similar to previously sequenced ectosymbionts were selected per nematode specimen for full sequencing.

Since all clones yielded identical 16S-ITS-23S rRNA sequences per individual, PCR products of the pure symbiont extracts from Heron Island and Carrie Bow Cay were sequenced bidirectionally without cloning with internal forward and reverse primer listed in Table S3.

All sequencing reactions were performed with either an ABI PRISM 3100 genetic analyzer (Applied Biosystems, Foster City, CA, USA), or outsourced to Macrogen Inc., South Korea. Sequences were assembled using Sequencher v4.6 (GeneCodes Corporation, Ann Arbor, MI), manually curated and chimera-checked with the Bellerophon program (Huber *et al.* 2004). Host and symbiont genes were sequenced from multiple individuals per species, where available. For details see Table S1 and S2.

Phylogenetic analyses of host genes

For the Phallodrilinae phylogeny, the generated mt12S, mt16S, 18S, 28S rRNA, ITS and mtCOI sequences of gutless Phallodrilinae as well as five gut-bearing Phallodrilinae as outgroup taxa were used for phylogenetic reconstruction (not every gene was obtained for every species, see Table S3). For the nematode phylogeny, all generated 18S rRNA sequences and previously published sequences from other stilbonematine nematode species from which also the corresponding symbiont sequence was published, as well as four Draconematidae nematodes sequences as outgroup were downloaded from GenBank and used for the host phylogenetic reconstruction.

Sequences for each gene were aligned separately using MAFFT version 7 (Katoh & Standley 2013) with the Q-INS-I setting (Katoh & Toh 2008) that considers the predicted secondary structure of the RNA for the alignment for ribosomal genes and the L-INS-I setting (Katoh *et al.* 2005), that also considers gaps for Phallodrilinae ITS and COI sequences. Alignments were manually adjusted and 5' and 3' end-trimmed using Geneious software version 6 (Kearse *et al.* 2012). The optimal substitution model for each alignment was assessed using the Aikaike information criterion as implemented in jModeltest 2.1.4 (Guindon & Gascuel 2003; Darriba *et al.* 2012) and the following nucleotide substitution models were chosen for phylogenetic analyses: GTR+I+G for the nematode 18S rRNA and the Phallodrilinae ITS genes, GTR+G for the 12S and 16S rRNA genes and K80+I+G for the 18S and 28S rRNA genes. To account for codon

position in the COI gene, the alignment was partitioned into three parts, and the models assessed were GTR+G for the first, HKY+G for the second, and SYM+I+G for the third codon position.

Phylogenetic trees were reconstructed using Bayesian inference (MrBayes v. 3.2.1) (Ronquist & Huelsenbeck 2003) and Maximum likelihood- based methods (RaxML) (Stamatakis *et al.* 2008). Since specific nucleotide substitution models cannot be assigned separately to each gene partition using RaxML, the GTR+G+I substitution model was assigned to all partitions separately. For the Phallodrilinae phylogeny, the six aligned host genes were concatenated into one matrix using Geneious software version (Kearse *et al.* 2012), which was partitioned after locus and additionally codon position in the COI region of the alignment. The loci were unlinked from each other in all parameters except topology. Two separate MCMC analyses were run in MrBayes for each alignment, with 4 Markov chains each (one cold and three hot) for 20 million (Mio) generations and sampling every 1000 generations. Convergence was evaluated by plotting the generations versus logL and the resulting trees were summarized into a majority-rule consensus tree, after discarding the first 5000 sampled trees as the burn-in. Node stability was evaluated using posterior probabilities (pp, Bayesian inference) and bootstrap support (100 RaxML rapid bootstrap runs) with values above 0.80 considered significant. For comparison, phylogenetic trees were also calculated separately for each of the host genes (Fig. S1).

Phylogenetic analyses of symbiont genes

For the gutless Phallodrilinae endosymbiont phylogenetic reconstructions we only used symbiont sequences produced in this study, since previously published symbiont sequences were not always sequenced from single individuals. Sequences from pure cultures of free-living gammaproteobacterial sulfur-oxidizing bacteria (*Allochromatium vinosum* strain DSM180, *Marichromatium purpuratum* 984, *Thiorhodococcus drewsii* AZ1, *Thiocapsa marina* 5811, *Thiorhodovibrio* sp. 970) were downloaded from Genbank and used as an outgroup. The 16S rRNA dataset was aligned, manually adjusted and trimmed as described for the host phylogenies above. The optimal substitution model suggested by jModeltest (Guindon & Gascuel 2003; Darriba *et al.* 2012) was the GTR+I+G.

For the stilbonematine nematode ectosymbiont phylogeny, the generated partial 16S rRNA-ITS-23S rRNA sequences as well as other previously published 16S rRNA sequences derived from individuals from which also the 18S rRNA sequence was available were used for phylogenetic reconstruction. We used the same outgroup as for the gutless Phallodrilinae endosymbiont phylogeny. Both 16S rRNA and 23S rRNA genes (where available) were aligned separately using MAFFT Q-INS-I as described above. Because the ITS regions was difficult to align, ITS clusters were identified based on cluster analysis using CD-HIT (Li & Godzik 2006; Fu *et al.* 2012) applying a similarity threshold of 85%. Sequences that did not fall into a symbiont cluster or were single representatives of a host genus were excluded from the analysis. Five ITS clusters were identified in total (symbionts of "undescribed genus A*"* species, *Leptonemella* species, *Laxus* Heron Island species, *Stilbonema* Heron island species and *Eubostrichus* species) that were aligned separately using MAFFT G-INS-I (Katoh *et al.* 2005). The optimal substitution model was assessed for all alignments separately as described above, which were GTR+I+G for the 16S and 23S rRNA, and HKY, HKY+I or GTR+G for the different ITS aligments. The 16S rRNA, five ITS and 23S rRNA gene alignments were concatenated and all loci unlinked from each other in all parameters except topology. For comparison, phylogenetic tree calculations were also done with the 16S rRNA gene only (Fig. S2).

For reconstruction of the combined *Cand.* Thiosymbion phylogeny based on the 16S rRNA gene we included all sequences from this study and also previously published 16S rRNA sequences from single nematode (stilbonematines and *Astomonema* sp.) or gutless phallodriline oligochaetes. Two previously published sequences amplified from coral samples off Panama were also included into the tree but their origin cannot be clearly assigned to environmental or symbiotic (GU118064, -120 Sunagawa *et al.* 2010) (Fig. 4). Additionally to the outgroup sequences described above we included three more outgroup sequences of uncultured bacteria from the sediment (JF344100, -324, -607). The optimal substitution model suggested by jModeltest (Guindon & Gascuel 2003; Darriba *et al.* 2012) was the GTR+I+G.

All symbiont phylogenetic trees were reconstructed with MrBayes (Ronquist & Huelsenbeck 2003) and RaxML (Stamatakis *et al.* 2008) using the respective optimal substitution model but the same settings as described for the host trees. Since specific nucleotide substitution models

cannot be assigned separately to each gene partition using RaxML, the GTR+G+I substitution model was assigned to all partitions separately.

Codivergence analysis of host and symbiont trees

To investigate codivergence events between the ecto- or endosymbionts and their invertebrate hosts we used the program Jane (version 4, http://www.cs.hmc.edu/~hadas/jane/; Conow *et al.* 2010) that is an event-based method aiming to reconcile tree topologies of hosts and symbionts by taking coevolutionary events (codivergence, host-switch, duplication, loss, failure to diverge) into account and finding the best reconstruction by minimizing the global cost of those events. We assigned codivergence as most likely event (cost = 0), duplication, loss, and failure to diverge unlikely events (cost = 1) and host-switch as least probable event (cost = 2). The same costs schemes were used for both gutless phallodriline endosymbionts as well as stilbonematine ectosymbionts. Significant matching of host and bacterial phylogenies was assessed by computing randomized trees with random tip mapping that were analyzed with the same cost scheme to compare the average overall costs of our trees to randomized trees. We used the consensus trees of the hosts and their respective symbionts to run the analyses. To investigate coevolutionary events between all members of the *Cand.* Thiosymbion clade and both host groups we “artificially” connected the two host trees as sister groups. Before the analysis, we removed all symbiont sequences from the Thiosymbion tree, for which no corresponding host sequence was available, without changing the tree topology. Only events with a support higher than 80% were considered. Due to some unresolved branching patterns, indicated by multifurcations in our phylogenetic trees we could not use a global fit method such as ParaFit to asses host-symbiont congruence, because the programs does not support trees with multifurcations (Legendre *et al.* 2002).

Ancestral state reconstruction

Ancestral character state reconstructions were done with the combined ecto- and endosymbiont 16S rRNA phylogeny, using BayesTraits V2.0 (Pagel and Meade, 2014). Gutless phallodriline and *Astomonema* sp. sequences were assigned the character state ‘endosymbiont’, stilbonematine sequences the character state ‘ectosymbiont’. The environmental sequences that

we used as outgroup were assigned the character state ‘uncertain’. We used 5 Mio post burn-in trees and ran the analyses for 50 Mio generations, 500,000 burn-in generations and three runs each. Statistical support for the Bayesian ancestral state reconstruction was determined using posterior probabilities calculated with the ‘MRCA’ command in BayesTraits. To test for significance of the reconstructed ancestral state we used the log Bayes Factor test on the harmonic means calculated by the ‘fossil’ command.

Correlation analyses

Patristic distance matrices, estimated from Bayesian Inference phylogenies of gutless phallodrilines, stilbonematines and their respective symbionts were calculated with the program PATRISTIC (Fourment & Gibbs 2006). Jukes-Cantor distance matrices of single genes (16S rRNA of endo- and ectosymbionts and 18S rRNA of stilbonematines) and concatenated gene alignments (mt12S, mt16S, 18S, 28S rRNA, ITS and mtCOI of gutless phallodrilines) were calculated with the software package ARB (Ludwig *et al.* 2004). Gutless phallodiline hosts that had one of the marker sequences missing were excluded from the Jukes-Cantor genetic distance analyses. Geographical distances matrices were calculated based on sampling coordinates (Table S1 and S2) using the GeographicDistanceMatrixGenerator v1.2.3 (Ersts, 2014) while considering a sphere shape of the Earth. Mantel and partial Mantel tests to test the association of symbiont distances with host and geographical distances were performed with R (http://www.r-project.org/) using Pearson’s r-statistic and 999 Monte Carlo permutations implemented in the R package “*vegan”* (Oksanen *et al.*, 2012).

Results

Phylogenetic reconstruction of the gutless phallodriline endosymbiosis

Host phylogeny: Little congruence with geographic location

To compare the phylogeny of gutless phallodriline oligochaetes and their *Cand.* Thiosymbion endosymbionts, we sequenced host and symbiont marker genes from a total of 23 host species

collected from around the world (Fig. 1, Table S1). We sequenced six host genetic markers: mt12S rRNA, mt16S rRNA, 18S rRNA, 28S rRNA, ITS and mtCOI, because none of these alone could sufficiently resolve their phylogeny (Fig. S1, Table S6). A concatenated analysis of all six host genes supported the monophyly of the gutless Phallodrilinae and their clear separation from Phallodrilinae with a mouth and digestive tract (Fig. 2), as shown previously in phylogenetic analyses based on morphological and molecular characters (e.g. Erséus 1984, 1992; Ferraguti *et al.* 1999). Our analyses also confirmed the monophyly of the four *Inanidrilus* species we analysed in this study (*Inanidrilus* clade) (Nylander *et al.* 1999; Erséus *et al.* 2000, 2002). However, the 18 *Olavius* species investigated here did not form a monophyletic group, in contrast to earlier morphological and molecular analyses that indicated the monophyly of this genus (Sjölin *et al.* 2005) but similarly to what was suggested in an earlier molecular study that included four *Olavius* species (Nylander *et al.* 1999). We identified four highly supported *Olavius* clades (1, 2, 3, 4), with four *Olavius* species that did not fall into any of these four clades, and two *Olavius* species that were basal to all other gutless Phallodrilinae (Fig. 2). The polyphyly of the genus *Olavius* indicates that the taxonomy of gutless Phallodrilinae needs revision. Given the discrepancy between our molecular phylogeny and the current classification that names only two host genera, *Inanidrilus* and *Olavius*, in the gutless Phallodrilinae, we use the term “host clades” instead of host genera in this paper.

Our analyses revealed little congruence between the phylogeny of gutless Phallodrilinae and their geographic location (Fig. 2). Many closely related gutless Phallodrilinae species have a disjunct distribution, i.e., they are widely separated from each other geographically (Fig. 2). Only two clades, *Olavius* clades 1 and 4, consisted exclusively of species from the same geographic region, although *Olavius* clade 4 with only two species was most likely undersampled.

Symbiont phylogeny: High congruence with geographic location

To analyze the phylogeny of the *Cand.* Thiosymbion endosymbiotic bacteria of gutless Phallodrilinae, we sequenced the 16S rRNA gene from the same individuals used for host analyses (Table S3). Symbiont 16S rRNA gene sequences from different individuals of the same host species had highly similar to identical *Cand.* Thiosymbion phylotypes (> 99.93% nucleotide identity), a result also shown in earlier analyses (e.g. Blazejak *et al.* 2005; Ruehland *et al.* 2008)

(Table S1). Of the 22 host species investigated here, each was associated with a species-specific *Cand.* Thiosymbion phylotype that was never found in another host species (Fig. 2). The symbiont 16S rRNA sequences shared nucleotide identities that ranged from 94.7% (*O. imperfectus* A and *O. crassitunicatus*) to 99.9% (*O. algarvensis* and *O.* "pianosa 1"), except for the 16S rRNA sequence of the *O. geniculatus* symbiont, which had a 65 bp insertion not present in the other symbionts.

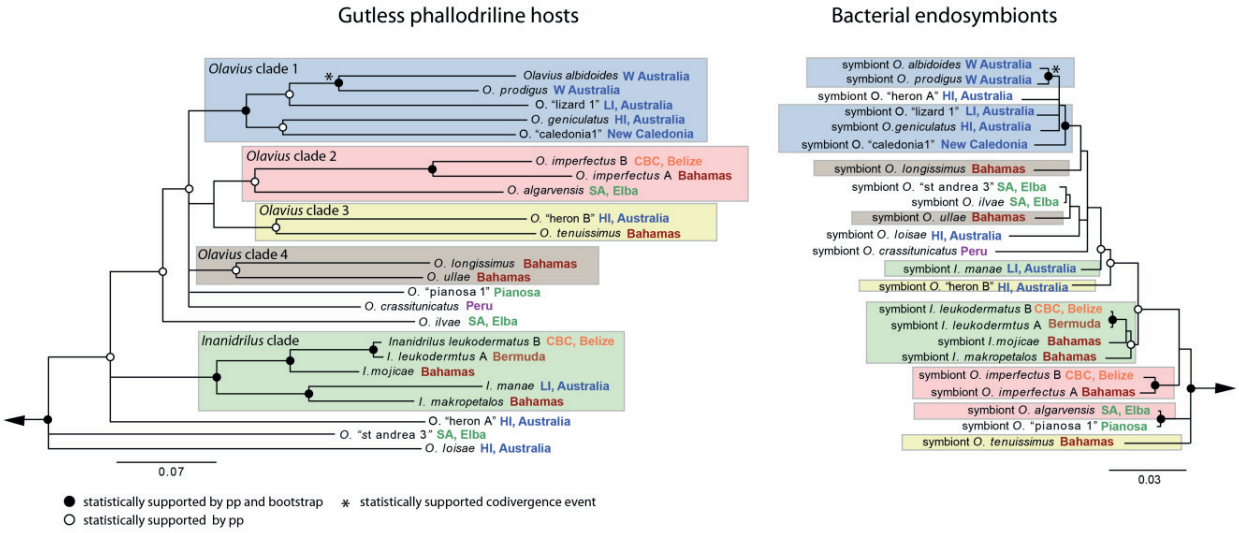

Fig. 2: Phylogeny of gutless phallodriline oligochaetes and their endosymbiotic *Candidatus* Thiosymbion bacteria. Consensus tree of Bayesian inference (mrBayes) and maximum likelihood (RaxML) analyses of six concatenated genetic markers for the host (mt12S, mt16S, 18S, 28S rRNA, mtCOI, ITS,) and the 16S rRNA gene for their *Cand*. Thiosymbion symbionts. For trees of each gene see Fig. S2. Colored boxes show monophyletic groups of gutless phallodriline hosts and their endosymbiotic bacteria, respectively, colored names the sampling locations. Stars indicate statistically supported codiversification events (> 80%, Jane v.4, Conow *et al.* 2010). Nodes that were statistically supported in both analyses (> 80% bootstrap value and 0.80 posterior probability (pp) value) are highlighted in black, nodes that were statistically supported only in Bayesian inference are highlighted in white. Provisional working names for undescribed species are in quotes. The scale bars represent 7% and 3% sequence divergence, respectively. The host tree was rooted with five gut-bearing Phallodrilinae *Albanidrilus wellsi*, *Pirodrilus minutes*, *Aktedrilus arcticus*, *Pectinodrilus rectisetsosus* and *Peosidrilus nr vicinus* (for details see Table S4). The symbiont tree was rooted with five free-living sulfur-oxidizing bacteria: *Allochromatium vinosum* strain DSM180, *Marichromatium purpuratum* 98, *Thiorhodococcus drewsii*, *Thiocapsa marina* 5811 and *Thiorhodovibrio* sp.

The phylogeny of the endosymbiotic *Cand.* Thiosymbion showed little congruence with host phylogeny (Fig. 2). For example, the symbionts of hosts from three of the four highly supported

Olavius clades did not cluster according to the phylogeny of their hosts but were rather interspersed throughout the tree. Furthermore, basal taxa in the host tree, such as *O.* "st andrea 3" and *O. loisae* have symbionts with a more derived position in the symbiont tree, and vice versa, basal taxa in the symbiont tree, such as the *O. algarvensis* and *O. "*pianosa 1" symbionts have hosts with a more derived position in the host tree (Fig. 2). Similarly, while all *Inandrilus* species formed a highly supported clade, not all of their symbionts clustered together. Congruent phylogenies were only observed in closely related hosts from similar geographic regions, such as within the *Olavius* clade 1, and *Inanidrilus* species from the West Atlantic (Belize, Bermuda and the Bahamas) (Fig. 2).

In contrast to the weak congruence between symbiont and host phylogeny, both treeing methods showed strong support for the clustering of endosymbionts according to their geographic location (Fig. 2). For example, the symbionts of *Inanidrilus* species from the West Atlantic formed a well supported clade and were not closely related to the Australian *I. manae* symbiont, while their *Inanidrilus* hosts were very closely related and formed a monophyletic clade (Fig. 2). Similarly, the symbiont of the Australian *Olavius* "heron island A" clustered with symbionts from other Australian hosts in the *Olavius* 1 clade, but their hosts did not (Fig. 2). In fact, the only four symbiont clusters with significant posterior probability values consisted of symbionts from similar geographic locations. These analyses suggest that the phylogeny of the *Cand*. Thiosymbion endosymbionts of gutless Phallodrilinae was more strongly affected by their biogeography than divergence of their hosts. This assumption was supported by the results of our Mantel test (Table 1) that showed higher support for a correlation between symbiont genetic distance and geographic distances (R^2 = 0.24, p = 0.006*) and weaker support for a correlation between symbiont and host genetic distances (R^2 = 0.26, p = 0.015*; Table 1).

Table 1: Mantel test of correlation between host and symbiont genetic distances and geographical distances, based on Pearson's product-moment correlation and 999 Monte Carlo permutations

Target group	Distance measure	Matrix A	Matrix B	R^2	Probability (p-value)°
Gutless phallodriline endosymbioses	Patristic distances	Host multigene distances	Symbiont 16S rRNA distances	0.26	0.015*
		Geographic distance matrix*	Symbiont 16S rRNA distances	0.24	0.006*
	Jukes Cantor distances	Host multigene distances	Symbiont 16S rRNA distances	-0.2	0.95
		Geographic distance matrix*	Symbiont 16S rRNA distances	0.3	0.001***
Stilbonematine ectosymbioses	Patristic distances	Host 18S rRNA distances	Symbiont 16S-ITS-partial 23S rRNA distances	0.28	0.027*
		Geographic distance matrix*	Symbiont 16S-ITS-partial 23S rRNA distances	0.15	0.04*
	Jukes Cantor distances	Host 18S rRNA distances	Symbiont 16S rRNA distances	0.22	0.056
		Geographic distance matrix*	Symbiont 16S rRNA distances	0.09	0.116

* based on geographic coordinates and calculated with the GeographicDistanceMatrixGenerator_v1.2.3 (Ersts, 2014).
° p-values and associated significance are indicated by *** p≤0.001; ** p<0.005, * p<0.05.

Phylogenetic reconstruction of the stilbonematine nematode ectosymbiosis

Host phylogeny: High congruence with generic classification

To compare the phylogeny of stilbonematine nematodes and their *Cand.* Thiosymbion ectosymbiotic bacteria, we sequenced host and symbiont marker genes from 18 host species collected from around the world, many of which co-occurred with the gutless Phallodrilinae analysed in this study (Fig. 1, Table S1). We sequenced the 18S rRNA gene from individual worms and found that it provided sufficient phylogenetic resolution to distinguish between closely related species (Fig. 3). The 18S rRNA gene phylogeny was consistent with the

morphological identification of host genera (Fig. 3). All stilbonematine nematode sequences formed a highly supported monophyletic group that was clearly distinct from the non-symbiotic desmodorid nematodes that we used as an outgroup (not shown) and which was shown in previous studies (Kampfer *et al.* 1998; Bayer *et al.* 2009; Ott *et al.* 2014a). All stilbonematine species from the same genus formed highly supported clades independent of their sampling location (Fig. 3). In addition to the six previously described stilbonematine nematode genera, we discovered two new host genera with 18S rRNA sequences that were distinct from all previously described genera. We preliminarily named these “undescribed genus A” (two new species from Australia and Belize) and “undescribed genus B“ (one species from Belize) (Fig. 3). While the relationships of species within the different genera were well resolved, the relationships between the different host genera were not well resolved (Fig. 3). The basal position of the *Eubostrichus* clade to all other nematode genera was the only node that was statistically supported in both maximum likelihood and Bayesian inference analyses (Fig. 3).

Symbiont phylogeny: High congruence with host generic classification

To characterize the *Cand.* Thiosymbion ectosymbiotic bacteria of each individual we sequenced the partial 16S rRNA-ITS-23S rRNA operon from the same individuals used for the host analyses in this study. Analyses of multiple clones from single individuals revealed highly similar to identical sequences (> 99.93% nucleotide identity), indicating that each individual is predominantly associated with a single ectosymbiont type, as shown in earlier studies (Polz *et al.* 1994; Bayer *et al.* 2009; Pende *et al.* 2014). Different individuals of a given stilbonematine species had symbionts with highly similar to identical 16S-ITS rRNA sequences (> 99.98% nucleotide identity). Each of the 18 stilbonematine species was associated with a species-specific 16S-ITS-23S rRNA phylotype that was never found on other host species. Nucleotide identities between 16S rRNA sequences ranged from 93.9% - 98.3% between symbionts of hosts from the same genus and from 98.3% - 99.95% between symbionts of hosts from different genera.

Symbiont sequences from hosts that belonged to the same genus formed highly supported clades independent of their geographical location in both maximum likelihood and Baysian inference analyses based on 16S-ITS-23S rRNA (Fig. 3). Phylogenetic analyses of the 16S

rRNA gene alone resulted in almost identical branching patterns, but with lower posterior probability and bootstrap values (Fig. S2). Within each host genus, symbiont and host branching patterns were always congruent (Fig. 3). The only exception was the genus *Laxus*, in which host and symbiont phylogenies were similar but not identical (Fig. 3). In contrast to the high congruence between symbiont and host phylogeny within each host genus, no congruence was observed between genera. For example, *Eubostrichus* species belonged to a basal branch of the host tree and were not closely related to *Laxus* host species, while *Eubostrichus* symbionts were more derived and most closely related to the symbionts of *Laxus* hosts (Fig. 3). Mantel test results confirmed the weak but significant correlation between symbiont and host genetic distances (R^2 = 0.28, p = 0.027*), but also indicated a weak correlation between symbiont genetic distances and their biogeography, although with slightly weaker support (R^2 = 0.15, p = 0.04*) (Table 1).

Phylogenetic reconstruction of the symbiont clade *Candidatus* Thiosymbion

Phylogenetic analyses of the 16S rRNA sequences from *Cand.* Thiosymbion bacteria from this study as well as those already published revealed that these formed a monophyletic group that also included the endosymbionts of marine nematodes from the genus *Astomonema* (Fig. 4). This confirms earlier studies with less species that showed the remarkably close relationships between these ecto- and endosymbionts despite the large phylogenetic distances between their three host groups (e.g. Musat *et al.* 2007; Bulgheresi *et al.* 2011; Heindl *et al.* 2011; Pende *et al.* 2014). The closest relatives of *Cand.* Thiosymbion are uncultured gammaproteobacteria from marine sediments and cultivated free-living anoxygenic phototrophic sulfur oxidizers of the family Chromatiaceae (Fig. 4).

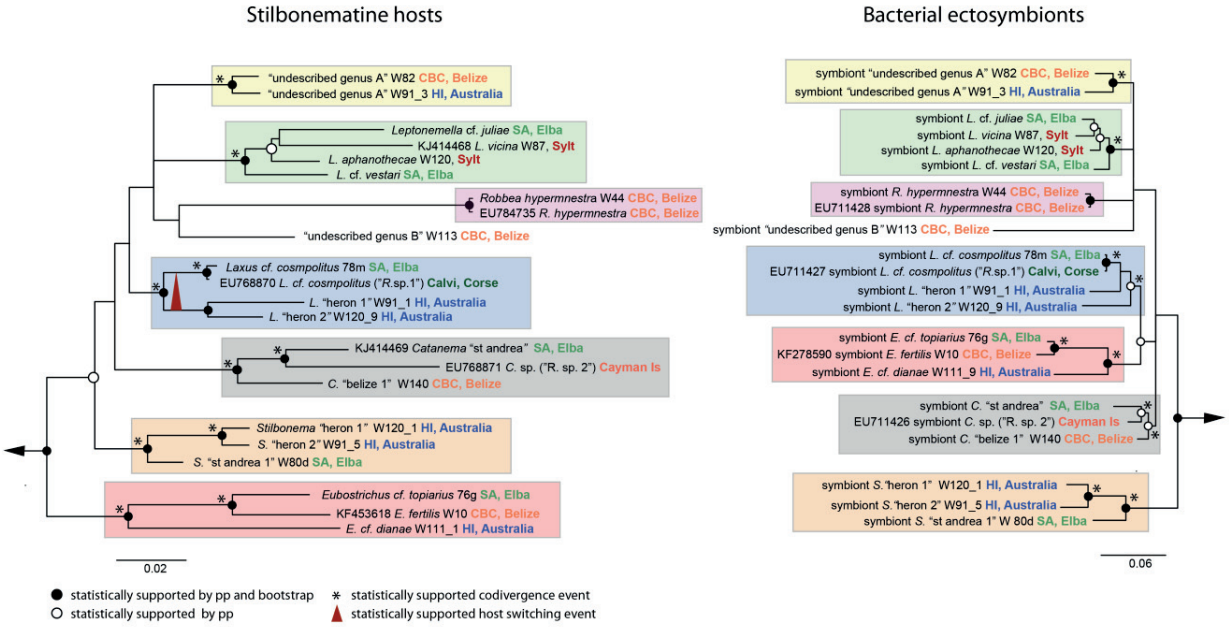

Fig. 3: Phylogeny of stilbonematine nematodes and their ectosymbiotic *Candidatus* Thiosymbion bacteria. Consensus tree of Bayesian inference (mrBayes) and maximum likelihood (RaxML) analyses of host 18S rRNA sequences and 16S-ITS-partial 23S rRNA sequences of their ectosymbiotic bacteria. Colored boxes show monophyletic groups of hosts and their symbionts, respectively, colored names the sampling locations. Sequences published prior to this study are discernible by their accession numbers. Stars indicate statistically supported codivergence events, red vertical arrows statistically supported host switching events (> 80%, Jane v.4, Conow *et al.* 2010). Nodes that were statistically supported in both analyses (> 80% bootstrap value and 0.80 posterior probability (pp) value) are highlighted in black, nodes that were statistically supported only in Bayesian inference are highlighted in white. Provisional working names for undescribed species are in quotes. The scale bars represent 2% and 6% sequence divergence, respectively. The host tree was rooted with four nematodes: *Prochaetosoma* sp. 2 and 3 (FJ182223 - 4), *Draconema japonicum* (FJ182217) and *Draconematidae* gen sp. (FJ182219). The symbiont tree was rooted with five free-living sulfur-oxidizing bacteria: *Allochromatium vinosum* strain DSM180, *Marichromatium purpuratum* 98, *Thiorhodococcus drewsii*, *Thiocapsa marina* 5811 and *Thiorhodovibrio* sp.

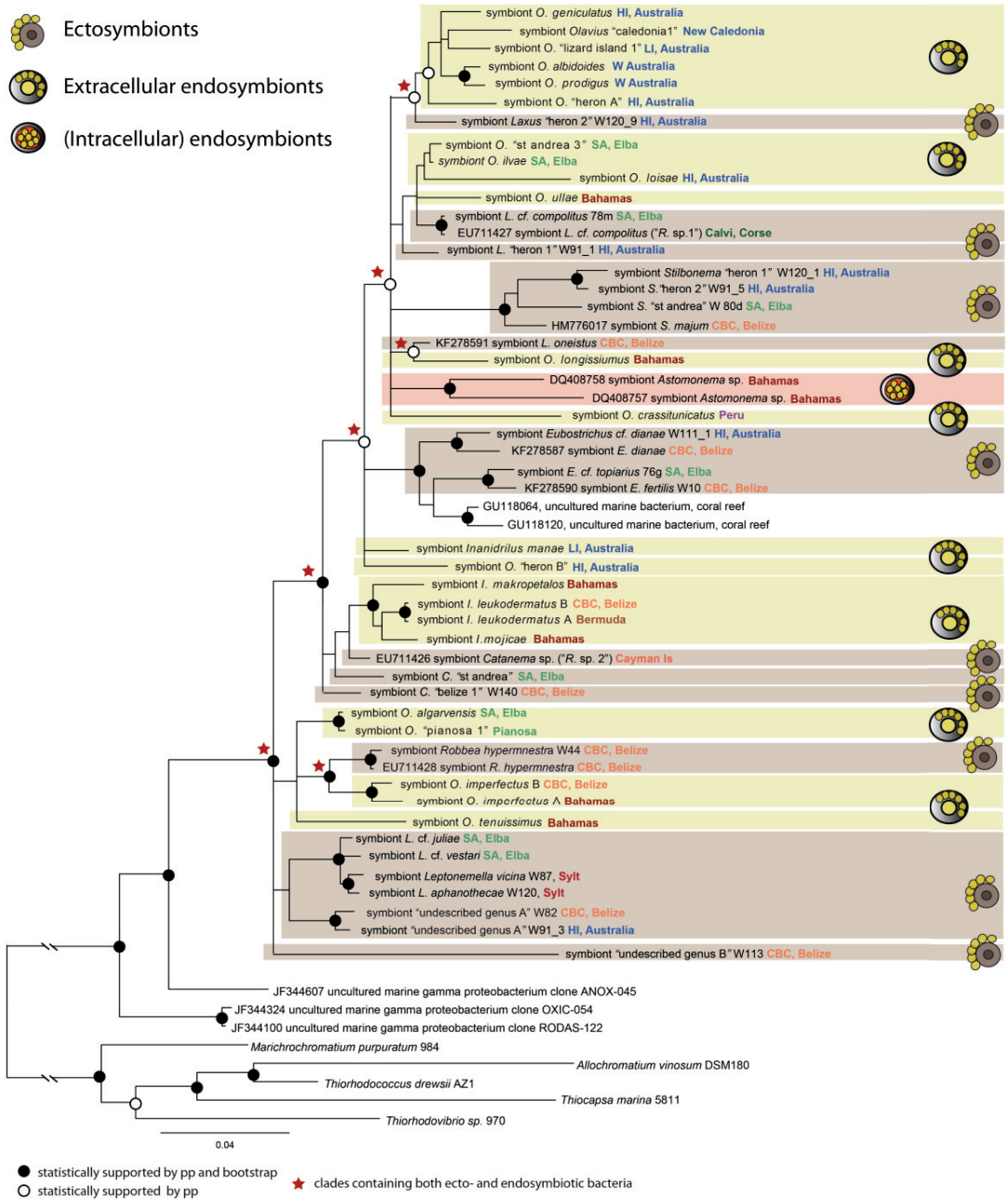

Fig. 4: *Candidatus* Thiosymbion phylogeny showing the evolutionary history of stilbonematine nematode ectosymbionts and gutless phallodriline endosymbionts. Consensus tree of Bayesian inference (mrBayes) and maximum likelihood (RaxML) analyses based on the 16S rRNA gene. Brown and yellow boxes highlight ectosymbiotic bacteria of stilbonematines and endosymbiotic bacteria of gutless phallodrilines, respectively. Colored names show the sampling location of the symbionts. Sequences published prior to this study are discernible by their accession numbers. Nodes that were statistically supported in both analyses (> 80% bootstrap and 0.80 posterior probability (pp) values) are highlighted in black, nodes that were statistically supported only in Bayesian inference in white. Red stars show well-supported clades that contain both ecto- and endosymbiotic bacteria. Provisional working names for undescribed species are in quotes. The scale bar represents 2% sequence divergence.

The *Cand.* Thiosymbiont clade consists of many well-supported subclades. Five of these subclades exclusively contain stilbonematine ectosymbionts (Fig. 4). One further clade contained stilbonematine symbionts of *Eubostrichus* but also two sequences from coral reef sediments, and it is highly likely that these were sequenced from stilbonematines present in the sediment sample (Fig. 4) (Sunagawa *et al.* 2010). Four of the subclades exclusively contain phallodriline endosymbionts and one contains the endosymbionts of *Astomonema* nematodes. A total of seven well-supported clades in the *Cand.* Thiosymbion phylogeny contained both ecto- and endosymbionts (red stars in Fig. 4). Intriguingly, four of the monophyletic subclades with closely related ecto- and endosymbionts always originated from hosts collected in the same geographic region (Fig. 4). For example, the ectosymbiont of the nematode *Laxus* "heron 2" from Australia formed a monophyletic group with the endosymbionts of Australian gutless Phallodrilinae (Fig. 4). Similarly, the ecto- and endosymbionts of *Catanema* spp. and *Inanidrilus* spp., *L. oneistus* and *O. longissimus* and *Robbea hypermnestra* and *O. imperfectus* fell into well-supported subclades, and all were sampled in the wider Caribbean region (i.e. Caribbean and Bermuda) (Fig. 4).

Ancestral state reconstruction

The ancestral state of the character traits endosymbiont and ectosymbiont was reconstructed based on the *Cand.* Thiosymbion consensus tree (Fig. 4). The analyses suggested that the ancestral state of the trait ectosymbiont had a slightly higher posterior probability (0.513) than the endosymbiont state (0.487). However, this result was not well supported by the log Bayes factor test (logBF = 0.3) where logBF > 6 is considered significant (Pagel and Meade, 2014).

Codivergence and host switching analyses

To explore the evolutionary relationships between *Cand.* Thiosymbion ecto- and endosymbionts and their hosts, we used the program Jane v.4 (Conow *et al.* 2010). For the gutless Phallodrilinae and their endosymbionts, only one codivergence event was highly supported, between the Australian hosts *O. albidoides* and *O. prodigus* and their endosymbionts (Table 2, Fig. 2). Randomized trees showed an average overall cost of 35 ± 2.6, which was only 1.4 times higher than the observed optimal cost, indicating no global codivergence between gutless

Phallodrilinae and their endosymbionts. In contrast, for stilbonematine nematodes and their ectosymbionts ten codivergence events were highly supported, as well as one host switch from the ancestor of Australian *Laxus* species to *Laxus* cf. *cosmopolitus* from the Mediterranean (Table 2, Fig. 3). Randomized trees showed an average overall cost of 33 ± 1.6, which was more than six times higher than the observed optimal cost, indicating global codivergence between stilbonematine nematodes and their ectosymbionts.

Table 2: Codivergence analyses

	Events (Cost)					**Global (Cost)**	
	Co-divergence (0)	**Dupli-cation (1)**	**Host switch (2)**	**Loss (1)**	**Failure to diverge (1)**	**Global cost for host and symbiont tree topology**	**Global cost for randomized host and symbiont tree topology**
Phallodrilinae and their endosymbionts	10 (of which 1 was supported with > 80%)	-	12 (none statistically supported)	1 (not statistically supported)	-	25	35
Stilbonematinae and their ectosymbionts	18 (of which 10 were supported with > 80%)	-	2 (of which 1 was supported with > 80%)*	1 (not statistically supported)	-	5	33
Both hosts and their symbionts	24 (of which 9 were supported with > 80%)	-	19 (of which 2 were supported with > 80% and 1 with > 66%)	1 (of which one was supported with > 80%)	-	43	75

* One of these events was predicted between host and symbionts of *Catanema* sp. and *C.* "st. andrea" but due to the fact that the ectosymbiont sequence of *Catanema* sp. ("Robbea sp. 2") was constructed from a pool of 200 individuals the symbiont sequence was likely not derived from the exact same individual as the host sequence, which is why one of the events has to be treated with caution.

We next compared the phylogeny of all *Candidatus* Thiosymbion ecto- and endosymbionts shown in Fig. 4 with a host tree that linked the gutless Phallodrilinae and the stilbonematine nematodes as sister groups (i.e. a host tree that combined the trees shown in Fig. 2 and 3). Jane analyses revealed nine highly supported codivergence events and three host switches, two of which were highly supported (Table 2, Fig. 5). Codivergence events were only supported for stilbonematine nematodes and their ectosymbionts. Of the three predicted host switches one was highly supported from an ancestor of *Catanema* nematodes to an ancestor of *Olavius* species from clade 1 and 4 (Fig. 5). The second host switch from a stilbonematine nematode to a gutless Phallodrilinae was predicted with lower support (from *Catanema* sp. (*R.* sp. 2) to the *Inanidrilus* clade (Fig. 5). The third host switch was highly supported and predicted to have occurred in the other direction than the first two, from the ancestor of the *Olavius* clade 1 from Australia to the nematode *Laxus* “heron 2” from Australia (Fig. 5). Furthermore, there was high support for the loss of symbionts in the ancestor of all *Laxus* host species (Table 2, Fig. 5).

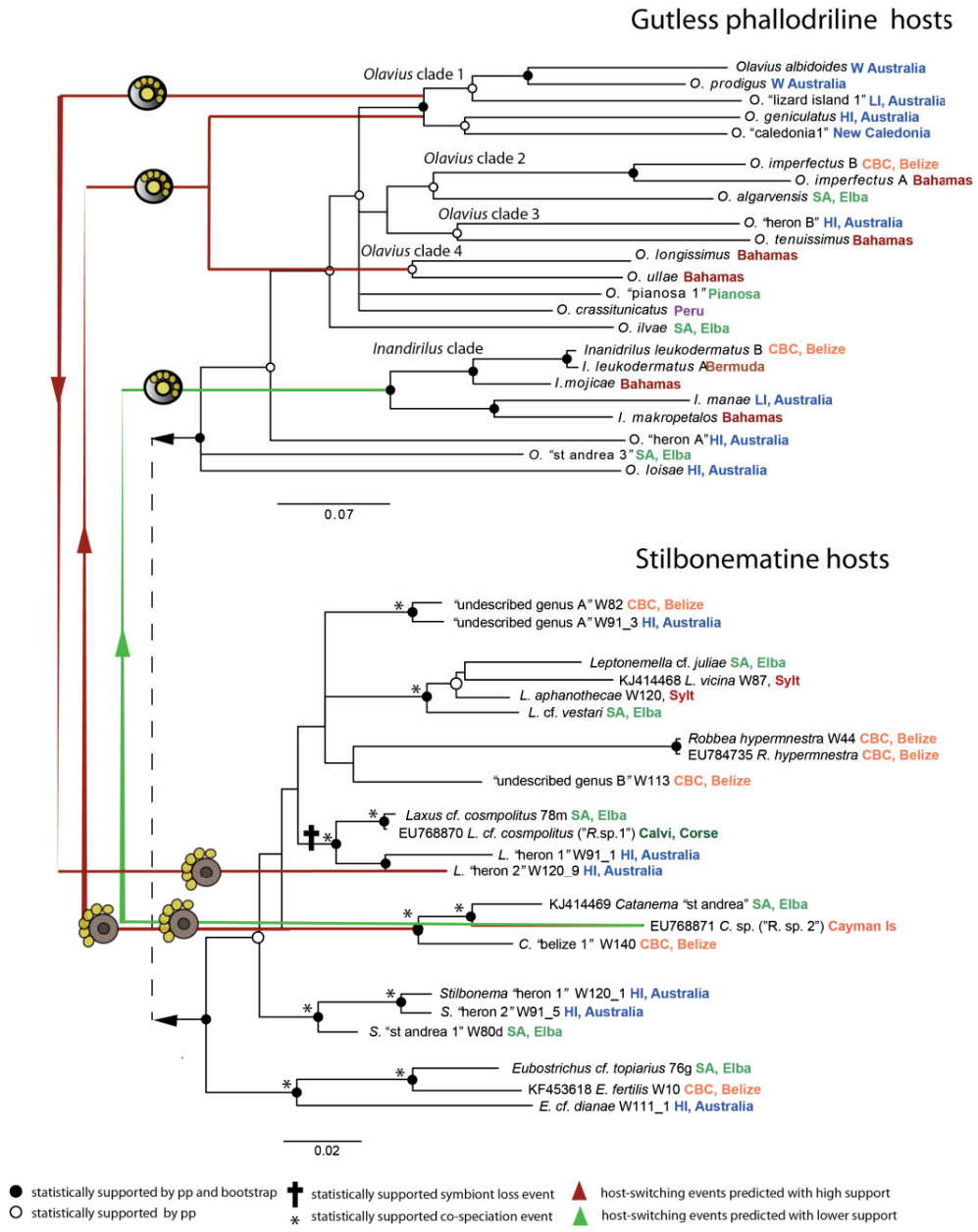

Fig. 5: Predicted host switching events between stilbonematine nematodes and gutless phallodriline annelids. The figure combines the phylogenetic consensus tree of Bayesian inference (mrBayes) and maximum likelihood (RaxML) analyses of gutless phallodrilines, based on mt12S, mt16S, 18S, 28S rRNA, mtCOI, ITS and stilbonematines, based on the 18S rRNA, respectively. Colored names show the sampling locations. Sequences published prior to this study are discernible by their accession numbers. The red and green vertical arrows show host switches that were well supported in Jane analyses (Table 1) (red > 80%, green = 66%) and stars show statistically supported codivergence events (> 80%, Jane v.4, Conow *et al.* 2010). Nodes that were statistically supported in both analyses (> 80% bootstrap and 0.80 posterior probability (pp) values) are highlighted in black, nodes that were statistically supported only in Bayesian inference in white. Provisional working names for undescribed species are in quotes. The scale bars represent 7% and 2% sequence divergence, respectively.

Discussion

The evolution of the gutless Phallodrilinae endosymbiosis was influenced by repeated symbiont replacements

Our analyses of the phylogeny of gutless phallodrilines and their *Cand.* Thiosymbion endosymbionts showed little congruence between host and symbiont branching patterns (Fig. 2). This weak congruence was confirmed by our codivergence analyses that predicted only a single codivergence event between two closely related species (Table 1, Fig. 2). In contrast, our analyses indicated that geography had a stronger influence on endosymbiont diversity, as shown by the many symbiont clades that contained symbionts from the same geographical region (Fig. 2). Mantel test results provided further support for a strong correlation between symbiont genetic distance and geographic distances (Table 1). These results indicate that gutless Phallodrilinae and their endosymbionts did not strictly cospeciate but that lateral acquisiton of symbionts from the environment or co-occurring hosts occurred repeatedly during their evolution. Lateral symbiont uptake could explain why very distantly related hosts that occur in the same geographic region have very closely related symbionts such as *O.* "st andrea 3*"* and *O. ilvae* from Elba, Italy or *O. "*heron A" and *O. geniculatus* from Heron Island, Australia (Fig. 2).

The lack of consistent codivergence between gutless phallodrilines and their obligate *Cand.* Thiosymbion endosymbionts is surprising given that these symbionts are assumed to be transmitted vertically via a smear infection from the parent to offspring during egg deposition (Giere & Langheld 1987, Krieger 2000). How could recurring events of symbiont replacement occur? Gutless phallodrilines lay single eggs together with sperm into a cocoon that they deposit into the sediments they inhabit (Giere & Langheld 1987, Krieger, 2000). The embryo develops within the cocoon before the juvenile worm eventually hatches. During this phase of exposure to the environment, symbionts from the environment or co-occurring hosts would have the opportunity to invade the cocoon, infect the developing embryo or juvenile, and displace the vertically transmitted symbiont. For successful displacement, the newly acquired symbiont must have a strong selective advantage over the original symbiont to be able to be sustained in the population. For example, the newly acquired symbiont could be better adapted to the host's environment or enable it to invade new habitats or niches.

Occasional events of lateral symbiont acquisition are well known from associations where the symbionts are predominantly transmitted vertically (reviewed by Bright & Bulgheresi 2010; Ebert 2013). For example, marine vesicomyid and solemyid clams that live in symbiosis with sulfur-oxidizing bacteria predominantly transmit their symbionts vertically, but molecular analyses indicate that lateral acquisition of symbionts has happened in the past (Stewart *et al.* 2008, 2009a; Decker *et al.* 2013). Other examples include the bryozoan *Bugula* species and their *Cand.* Endobugula symbionts (Lim-Fong *et al.* 2008) and leaf-cutter ants that cultivate specific symbiotic fungi strains for food (Bot *et al.* 2001; Green *et al.* 2002). In some hosts, such as insects, where vertically transmitted symbionts have undergone genome reduction, lateral acquisition of a novel symbiont enables the host to escape dependency on a degenerated, inefficient symbiont (Lefèvre *et al.* 2004; Conord *et al.* 2008; Koga *et al.* 2013). So far, only one genome of a *Cand.* Thiosymbion has been fully sequenced, from the gutless phallodriline *Olavius algarvensis* (Woyke *et al.* 2006). *Cand.* Thiosymbion algarvensis does not appear to have a reduced genome although unusually high amounts of transposases indicate that it may be in transition to an obligate, host-associated life style (Kleiner *et al.* 2013). However, we never found any evidence for the co-occurrence of more than one *Cand.* Thiosymbion species in any of the phallodriline hosts we examined. This suggests that co-occurrence of a primary vertically transmitted symbiont and a novel laterally acquired *Cand.* Thiosymbion is rare in these hosts, and that symbiont displacement occurs rapidly within a host population.

Evolutionary stability in stilbonematine nematode ectosymbioses

In contrast to gutless Phallodrilinae, closely related stilbonematine nematode hosts were consistently associated with closely related *Cand.* Thiosymbion ectosymbionts. This was visible in the clear congruence within most host and symbiont clades (Fig. 3). In contrast to the high congruence between symbiont and host phylogeny within each host genus, no congruence was observed between genera. This may be due to the poor phylogenetic resolution of both host and symbiont trees at the nodes connecting genera / clades. Mantel test results confirmed the significant relationship between symbiont and host genetic distances (Table 2), and Jane analyses confirmed the marked congruence between host and symbiont phylogeny with the identification of ten codivergence events (Table 2).

The evolutionary stability of the association between stilbonematine nematodes and their ectosymbiotic bacteria is remarkable given that the symbionts are attached to the surface or cuticle of their hosts and constantly exposed to the surrounding sediment. This exposure could cause detachment of the symbionts when the worms migrate through the sediment. Furthermore, as all marine nematodes, Stilbonematinae molt and shed their cuticle four times during their life cycle (Ott *et al.* 1995). This life style provides ample opportunities for free-living bacteria or symbionts from other hosts to invade and displace the host's symbionts, but our analyses indicate that only hosts from the genus *Laxus* and possibly *Catanema* were affected by such events (Fig. 4 and 5).

How can we explain the specificity and evolutionary stability of the stilbonematine ectosymbiosis? Clearly, highly specific mechanisms for recognition and maintenance must have evolved to sustain these symbioses throughout their evolutionary history. These could include morphological adaptations such as a reduced body diameter of the nematode host to accommodate the thickness of the symbiont coat (Polz *et al.* 1992), possibly to avoid friction and thus detachment of symbionts during movement through the sediments. Longitudinal division of the symbionts with an unusual shift in the fission plane may prevent the symbionts from losing contact with their host's surface during growth, as suggested for some rod-shaped bacterial symbionts (Polz *et al.* 1992; Leisch *et al.* 2012). Furthermore, special glandular sensory organs, which are only present in stilbonematine nematodes, contribute to specificity by secreting lectins on the hosts' cuticle that recognize specific sugar residues on the symbiont's cell membrane (Bauer-Nebelsick *et al.* 1995; Nussbaumer *et al.* 2004; Bulgheresi *et al.* 2006, 2011).

Transmission of the symbionts from one generation to the next and during the four molts of the host's life cycle are also critical for maintaining the symbiosis. It has been assumed that the symbionts are acquired laterally from free-living symbionts in the environment or co-occurring hosts based on i) the absence of symbionts on juvenile worms that had not yet hatched from their egg (Bulgheresi and Ott unpublished in Bayer *et al.* 2009), and ii) the amplification of partial 16S rRNA gene sequences with high similarity to symbiont sequences of stilbonematine nematodes from surface seawaters (Heindl *et al.* 2011). However, convincing evidence for codivergence in symbioses with lateral acquisition is rare (Bright & Bulgheresi 2010). It is therefore possible that vertical transmission between stilbonematine hosts and their symbionts

or a mixed mode of vertical and occasional lateral transmission occurs in these associations (Ebert 2013). The ectosymbionts could, for example, be transferred onto the egg or juvenile during passage through the female genital opening (vulva). Intriguingly, the glandular sensory organs that secrete lectins and are assumed to be involved in symbiont recognition, are especially numerous and large in the vulva region of many stilbonematine nematodes (e.g. Hopper & Cefalu 1973; Ott *et al.* 1991, 1995). A similar mode of transmission, in which symbionts are transmitted "pseudo-vertically" onto eggs or juveniles in the brood pouch has also been suggested for the ectosymbionts of *Niphargus* amphipods found in freshwater caves (Dattagupta *et al.* 2009).

Evidence for codivergence in ectosymbiotic associations has so far only been shown for devescovinid flagellates from termite guts and their *Bacteroidales* ectosymbionts (Desai *et al.* 2010). Our study provides an example for a highly specific marine ectosymbiosis where congruent host and symbiont phylogenies indicate a pronounced pattern of codivergence. Overall, it highlights that ectosymbiotic associations can be highly stable over long evolutionary time periods.

Repeated host switches between animal phyla

Our phylogenetic reconstruction of 50 *Cand.* Thiosymbion ecto- and endosymbionts from three unrelated host groups (Stilbonematinae, *Astomonema* and Phallodrilinae) belonging to two animal phyla (Nematoda and Annelida) from a wide range of environments around the world showed that these are monophyletic and share a single common ancestor, thus confirming earlier studies with much fewer species (e.g. Dubilier *et al.* 2008; Pende *et al.* 2014). Seven highly supported clades contained both stilbonematine ectosymbionts and phallodriline endosymbionts (Fig. 4). Two scenarios that are not mutually exclusive could explain the intermingled evolutionary history of the *Cand.* Thiosymbion ecto- and endosymbionts (we only discuss scenarios for the stilbonematine and phallodriline symbionts, because the *Astomonema* nematode symbiosis with only two published symbiont sequences is undersampled): i) closely related free-living bacteria from the environment repeatedly displaced symbionts associated with stilbonematine and / or gutless phallodriline hosts, or ii) the phallodriline endosymbionts evolved multiple times from stilbonematine ectosymbionts and / or vice-versa. The first scenario is less

likely for the stilbonematine ectosymbiosis because our phylogenetic and statistical analyses indicated that their evolution was genus-specific, and driven by codivergence and host genetic distance. For the gutless phallodriline endosymbiosis, this scenario is more likely given the lack of codivergence and strong influence of biogeography on their evolution. However, to date there is no strong evidence for free-living bacteria from the *Cand.* Thiosymbion clade despite intensive sequencing of marine environments (including those in which stilbonematines and phallodrilines occur) by others (e.g. Musat *et al.* 2006; Aravindraja *et al.* 2013) and ourselves (A. Kreutzmann, J. Wippler and N. Dubilier, unpublished results). In two studies 16S rRNA gene sequences were found that fall within the *Cand.* Thiosymbion clade but the origins of these sequences are ambiguous. In the first study on shallow-water coral-associated bacteria (Sunagawa *et al.* 2010), two sequences were found (GU118064 and GU118120) that form a monophyletic clade with the ectosymbionts of stilbonematines from the genus *Eubostrichus* (Fig. 4). These sequences may therefore have originated from symbionts of *Eubostrichus* individuals contained in the sampled coral fragments. The other sequences were found in surface seawaters and could only be amplified using nested PCR, a method that is particularly prone to contamination (Heindl *et al.* 2011).

The second scenario for explaining the intermingled evolutionary history of seven clusters that contain *Cand.* Thiosymbion ecto- and endosymbionts posits that stilbonematine ectosymbionts displaced phallodriline endosymbionts and / or phallodriline endosymbionts displaced stilbonematine ectosymbionts. Jane analyses predicted one event in which the ectosymbionts of the stilbonematine *Laxus* "heron 2" from Australia were displaced by phallodriline endosymbionts from the ancestors of *Olavius* hosts from Australia. Correspondingly, symbiont loss seems to have occurred in the last common ancestor of all *Laxus* hosts, which may have made hosts from this genus more prone for displacement and host switching (Fig. 3 and 5, Table 1). Vice versa, two host switches were reported from stilbonematine ectosymbionts to gutless phallodrilines, one that was highly supported and one with lower support (Fig. 5). Furthermore, ancestral state reconstruction provided weak support for an ectosymbiotic ancestor of the *Cand.* Thiosymbion clade.

How can we explain host switching in the *Cand.* Thiosymbion between the two animal phyla Nematoda and Annelida and the flexibility of these bacteria to live both as ecto- and

endosymbionts? Firstly, stilbonematine nematodes and gutless phallodrilines are almost always found in the same environments and usually at the same collection site. Their close co-occurrence provides numerous opportunities for exchange of symbionts through direct or indirect interactions. Secondly, the nutritional basis of the symbiosis is most likely similar in all *Cand.* Thiosymbion associations. These symbionts are all assumed to be autotrophic sulfur oxidizers that provide their hosts with nutrition, although evidence for chemolithoautotrophy is only available for some symbionts (Ott *et al.*, 2004; Blazejak *et al.*, 2006; Woyke *et al.*, 2006; Kleiner *et al.*, 2012), and the contribution of the symbionts to their host's nutrition remains to be clarified. Thirdly, the benefit the hosts provide to their symbionts is similar in both stilbonematines and phallodrilines. These worms migrate between the upper oxidized and the lower reduced layers of the sediment and can thus provide their symbionts with access to electron acceptors such as oxygen and nitrate in the surface layers and electron donors such as reduced sulfur compounds in the lower layers (Giere *et al.* 1991; Ott *et al.* 1991). Fourthly, major physiological adaptations might not have been needed for switches between an ectosymbiotic and an endosymbiotic lifestyle. Although the phallodriline associations are endosymbiotic, the bacteria are extracellular and only separated from the sediment environment by a very thin cuticle that is highly permeable for charged and uncharged molecules up to 70 kDa (Dubilier *et al.* 2006).

The *Cand.* Thiosymbion association is, to our knowledge, the only known marine symbiosis in which host switches may have occurred repeatedly between animal phyla. There is one other group of closely related marine symbionts that are associated with different animal phyla, sulfur-oxidizing bacteria that live as intracellular symbionts in deep-sea bathymodiolin mussels, in the tissues of a poecilosclerid sponge and as ectosymbionts on a marine terebellid polychaete (Nishijima *et al.* 2010; Petersen *et al.* 2012). However, the symbionts from these three host groups are not most closely related to each other, but rather to free-living sulfur-oxidizing bacteria in the environment, and there is no phylogenetic evidence for host switching between the symbionts of the mussels, sponge and polychaete (Petersen *et al.* 2012). In associations between terrestrial hosts and bacteria, host switching between animal phyla has been described more often, particularly in parasitic associations (e.g. Heath *et al.* 1999; Russell *et al.* 2003; Huigens *et al.* 2004). For example, intracellular *Wolbachia* bacteria that parasitize many arthropod species may have switched at least twice to another animal phylum, the nematodes,

(Casiraghi *et al.* 2005; Bordenstein *et al.* 2009), although multiple host switches between these phyla have recently been questioned (Comandatore *et al.* 2013). *Rickettsia* bacteria are also known to infect several animal and plant phyla, but most host switches are assumed to have occurred within the phylum Arthropoda (Weinert *et al.* 2009).

Conclusions and outlook

The intermingled evolutionary history within the *Cand.* Thiosymbion clade of ecto- and endosymbiotic bacteria that are able to associate with hosts from two animal phyla raises a number of questions: What determines the lifestyle of a symbiont, which factors lead to ecto- or endosymbiosis? Are there conserved recognition mechanisms in *Cand.* Thiosymbion bacteria that allow them to engage in symbiotic associations with hosts from three animal groups within two animal phyla? Which factors favor codivergence, which lead to host switching?

To answer these questions, comparative analyses of the symbionts genomes, transcriptomes, proteomes and metabolomes would help to identify the similarities and differences in their functional and metabolic interactions with phylogenetically distant hosts. In parallel, the collection and analysis of more hosts from a wider range of environments and locations would contribute to improving the reconstruction of the phylogenetic history of *Cand.* Thiosymbion and shedding light on the factors that contributed to their evolutionary flexibility and success.

Acknowledgements

We thank the staff of the HYDRA Institute on Elba, Italy, the Wadden Sea Station Sylt of the Alfred Wegener Institute in Bremerhaven, Germany, the Smithonian Institution and Carrie Bow Cay Marine Laboratory in Belize, and the Heron Island Research Station in Australia for providing laboratory facilities and technical assistance in the field. We gratefully acknowledge the collaboration with the Parco Nazionale Arcipelago Toscano for granting us access to the protected area of Pianosa, Italy (research permit no. 4440/2011) and the Bermuda Institute of Ocean Sciences in St. Geroge's, Bermuda for laboratory facilities and the Bermuda Aquarium in

Flatts Village for access to the sampling site and their facilities. Many thanks to Jillian M. Petersen and Lizbeth Sayavedra for valuable scientific discussions, Pierre Buttigieg for help with the statistical analyses and Silke Wetzel and Sabine Kuehn for excellent technical assistance. It is also a contribution from work performed by CE and ND at the Lizard Island Research Station (Great Barrier Reef, Australia), and the former Caribbean Marine Research Centre on Lee Stocking Island (Bahamas); CE is indebted to Philippe Bouchet, and the Total Foundation, for the invitation to participate in the LIFOU 2000 expedition to New Caledonia, to Fred E. Wells for hosting the International Marine Biological Workshop on The Marine Flora and Fauna of Rottnest Island, Western Australia, and to Anna Ansebo (University of Gothenburg) for invaluable assistance in the early phases of the molecular work on gutless Phallodrilinae. This work was supported by the Gordon and Betty Moore Foundation through Grant GBMF3811 to ND, the Max Planck Society and the Marie Sklodowska-Curie Initial Training Network 'Symbiomics'. CE was funded by the Swedish Research Council, and the Adlerbertska Foundation (Göteborg).

Data accessibility

All sequences were submitted to Genbank and are available under the following accession numbers: Gutless phallodriline oligochaete genes: 18S rRNA: KP943792 - KP943817, 28S rRNA: KP943818 - KP943844, mtCOI: KP943845 - KP943866, ITS: KP943867 - KP943884 mt12S rRNA: KP943885 - KP943908, mt16S rRNA: KP943909 - KP943931. Gutless phallodriline oligochaete endosymbiont 16S rRNA: KP943932 - KP943954. Stilbonematine nematode 18S rRNA genes: KP943955 - KP943970. Stilbonematine nematode ectosymbiont partial 16S rRNA-ITS-23S rRNA: KP943971 - KP943988.

References

Altschul S, Madden TL, Schäffer AA, *et al.* (1997) Gapped BLAST and PSI-BLAST: a new generation of protein database search programs. *Nucleic Acids Research*, **25**, 3389–3402.

Aravindraja C, Viszwapriya D, Karutha Pandian S (2013) Ultradeep 16S rRNA sequencing analysis of geographically similar but diverse unexplored marine samples reveal varied bacterial community composition. *PLoS ONE*, **8**, e76724.

Bauer-Nebelsick M, Blumer M, Urbancik W, Ott JA (1995) The glandular sensory organ of Desmodoridae (Nematoda)- ultrastructure and phylogenetic implications. *Invertebrate Biology*, **114**, 211–219.

Bayer C, Heindl NR, Rinke C *et al.* (2009) Molecular characterization of the symbionts associated with marine nematodes of the genus *Robbea*. *Environmental Microbiology Reports*, **1**, 136–144.

Bennett GM, Moran NA (2015) Heritable symbiosis: The advantages and perils of an evolutionary rabbit hole. *Proceedings of the National Academy of Sciences*, 201421388.

Blazejak A, Erséus C, Amann R, Dubilier N (2005) Coexistence of bacterial sulfide oxidizers, sulfate reducers, and spirochetes in a gutless worm (Oligochaeta) from the Peru margin. *Applied and Environmental Microbiology*, **71**, 1553–1561.

Blazejak A, Kuever J, Erséus C, Amann R, Dubilier N (2006) Phylogeny of 16S rRNA, ribulose 1,5-bisphosphate carboxylase/oxygenase, and adenosine 5'-phosphosulfate reductase genes from gamma- and alphaproteobacterial symbionts in gutless marine worms (Oligochaeta) from Bermuda and the Bahamas. *Applied and Environmental Microbiology*, **72**, 5527–5536.

Bordenstein SR, Paraskevopoulos C, Hotopp JCD *et al.* (2009) Parasitism and mutualism in *Wolbachia*: What the phylogenomic trees can and cannot say. *Molecular Biology and Evolution*, **26**, 231–241.

Bot ANM, Rehner SA, Boomsma JJ (2001) Partial incompatibility between ants and symbiotic fungi in two sympatric species of *Acromyrmex* leaf-cutting ants. *Evolution*, **55**, 1980–1991.

Bright M, Bulgheresi S (2010) A complex journey: transmission of microbial symbionts. *Nature Reviews Microbiology*, **8**, 218–230.

Bulgheresi S, Gruber-Vodicka HR, Heindl NR *et al.* (2011) Sequence variability of the pattern recognition receptor Mermaid mediates specificity of marine nematode symbioses. *The ISME Journal*, **5**, 986–998.

Bulgheresi S, Schabussova I, Chen T *et al.* (2006) A new C-type lectin similar to the human immunoreceptor DC-SIGN mediates symbiont acquisition by a marine nematode. *Applied and Environmental Microbiology*, **72**, 2950–2956.

Casiraghi M, Bordenstein SR, Baldo L *et al.* (2005) Phylogeny of *Wolbachia pipientis* based on gltA, groEL and ftsZ gene sequences: clustering of arthropod and nematode symbionts in the F supergroup, and evidence for further diversity in the *Wolbachia* tree. *Microbiology*, **151**, 4015–4022.

Cavanaugh CM, Gardiner S, Jones ML, Jannasch HW, Waterbury JB (1981) Prokaryotic cells in the hydrothermal vent tube worm *Riftia pachyptila* Jones: possible chemoautotrophic symbionts. *Science*, **213**, 340–342.

Comandatore F, Sassera D, Montagna M *et al.* (2013) Phylogenomics and analysis of shared genes suggest a single transition to mutualism in *Wolbachia* of nematodes. *Genome Biology and Evolution*, **5**, 1668–1674.

Conord C, Despres L, Vallier A *et al.* (2008) Long-term evolutionary stability of bacterial endosymbiosis in Curculionoidea: additional evidence of symbiont replacement in the Dryophthoridae family. *Molecular Biology and Evolution*, **25**, 859–868.

Conow C, Fielder D, Ovadia Y, Libeskind-Hadas R (2010) Jane: a new tool for the cophylogeny reconstruction problem. *Algorithms for Molecular Biology*, **5**, 16.

Darriba D, Taboada GL, Doallo R, Posada D (2012) jModelTest 2: more models, new heuristics and parallel computing. *Nature Methods*, **9**, 772–772.

Dattagupta S, Schaperdoth I, Montanari A *et al.* (2009) A novel symbiosis between chemoautotrophic bacteria and a freshwater cave amphipod. *The ISME Journal*, **3**, 935–943.

Decker C, Olu K, Arnaud-Haond S, Duperron S (2013a) Physical proximity may promote lateral acquisition of bacterial symbionts in vesicomyid clams. *PloS one*, **8**, e64830.

Desai MS, Strassert JFH, Meuser K *et al.* (2010) Strict cospeciation of devescovinid flagellates and Bacteroidales ectosymbionts in the gut of dry-wood termites (Kalotermitidae). *Environmental Microbiology*, **12**, 2120–2132.

Diepenbroek M, Grobe H, Reinke M *et al.* (2002) PANGAEA—an information system for environmental sciences. *Computers & Geosciences*, **28**, 1201–1210.

Dubilier N, Amann R, Erséus C *et al.* (1999) Phylogenetic diversity of bacterial endosymbionts in the gutless marine oligochaete *Olavius loisae* (Annelida). *Marine Ecology Progress Series*, **178**, 271–280.

Dubilier N, Bergin C, Lott C (2008) Symbiotic diversity in marine animals: the art of harnessing chemosynthesis. *Nature Reviews Microbiology*, **6**, 725–740.

Dubilier N, Blazejak A, Rühland C (2006) Symbioses between bacteria and gutless marine oligochaetes. In: *Molecular Basis of Symbiosis* Progress in Molecular and Subcellular Biology. (ed Overmann PDJ), pp. 251–275. Springer Berlin Heidelberg.

Dubilier N, Mulders C, Ferdelman T *et al.* (2001) Endosymbiotic sulphate-reducing and sulphide-oxidizing bacteria in an oligochaete worm. *Nature*, **411**, 298–302.

Ebert D (2013) The epidemiology and evolution of symbionts with mixed-mode transmission. *Annual Review of Ecology, Evolution, and Systematics*, **44**, 623–643.

Erséus C (1984) Taxonomy and phylogeny of the gutless Phallodrilinae (Oligochaeta, Tubificidae), with descriptions of one new genus and twenty-two new species. *Zoologica Scripta*, **13**, 239–272.

Erséus C (1992) A generic revision of the Phallodrilinae (Oligochaeta, Tubificidae). *Zoologica Scripta*, **21**, 5–48.

Erséus C (1994) The Oligochaeta. In Taxonomic atlas of the Santa Maria Basin and western Santa Barbara Channel. Vol. 4 - The Annelida Part 1. Oligochaeta and Polychaeta: Phyllodocida (Phyllodocidae to Paralacydoniidae) (eds. J.A. Blake & B. Hilbig): 5-38. Santa Barbara Museum of Natural History, Santa Barbara, California.

Erséus C (2003) The gutless Tubificidae (Annelida: Oligochaeta) of the Bahamas. *Meiofauna Marina*, **12**, 59–84.

Erséus C, Källersjö M, Ekman M, Hovmöller R (2002) 18S rDNA phylogeny of the Tubificidae (Clitellata) and its constituent taxa: Dismissal of the Naididae. *Molecular Phylogenetics and Evolution*, **22**, 414–422.

Erséus C, Prestegaard T, Källersjö M (2000) Phylogenetic analysis of Tubificidae (Annelida, Clitellata) based on 18S rDNA sequences. *Molecular Phylogenetics and Evolution*, **15**, 381–389.

Erséus C, Wetzel MJ, Gustavsson L (2008) ICZN rules–a farewell to Tubificidae (Annelida, Clitellata). *Zootaxa*, **1744**, 66–68.

Ersts PJ (2014) Geographic Distance Matrix Generator (version 1.2.3) American Museum of Natural History. Center for Biodiversity and Conservation Available from http://biodiversityinformatics amnh org/open_source/gdmg (Accessed on 16 June 2014).

Ferraguti M, Erséus C, Kaygorodova I, Martin P (1999) New sperm types in Naididae and Lumbriculidae (Annelida: Oligochaeta) and their possible phylogenetic implications. *Hydrobiologia*, **406**, 213–222.

Lim-Fong GE, Regali LA, Haygood MG (2008) Evolutionary relationships of "*Candidatus Endobugula*" bacterial symbionts and their bugula bryozoan hosts. *Applied and Environmental Microbiology*, **74**, 3605–3609.

Fourment M, Gibbs MJ (2006) PATRISTIC: a program for calculating patristic distances and graphically comparing the components of genetic change. *BMC Evolutionary Biology*, **6**, 1.

Fu L, Niu B, Zhu Z, Wu S, Li W (2012) CD-HIT: accelerated for clustering the next-generation sequencing data. *Bioinformatics*, **28**, 3150–3152.

Giere O, Conway NM, Gastrock G, Schmidt C (1991) "Regulation" of gutless annelid ecology by endosymbiotic bacteria. *Marine Ecology Progress Series. Oldendorf*, **68**, 287–299.

Giere O, Langheld C (1987) Structural organisation, transfer and biological fate of endosymbiotic bacteria in gutless oligochaetes. *Marine Biology*, **93**, 641–650.

Green AM, Mueller UG, Adams RMM (2002) Extensive exchange of fungal cultivars between sympatric species of fungus-growing ants. *Molecular Ecology*, **11**, 191–195.

Gruber-Vodicka HR, Dirks U, Leisch N *et al.* (2011) *Paracatenula*, an ancient symbiosis between thiotrophic Alphaproteobacteria and catenulid flatworms. *Proceedings of the National Academy of Sciences*, **108**, 12078–12083.

Gruber-Vodicka HR, Kleiner M, Wentrup C et al. (in preparation) '*Candidatus* Thiosymbion' spp., a genus of thiotrophic Gammaproteobacteria associated with diverse metazoan hosts.

Guindon S, Gascuel O (2003) A simple, fast, and accurate algorithm to estimate large phylogenies by maximum likelihood. *Systematic Biology*, **52**, 696–704.

Heath BD, Butcher RDJ, Whitfield WGF, Hubbard SF (1999) Horizontal transfer of *Wolbachia* between phylogenetically distant insect species by a naturally occurring mechanism. *Current Biology*, **9**, 313–316.

Heindl NR, Gruber-Vodicka HR, Bayer C *et al.* (2011) First detection of thiotrophic symbiont phylotypes in the pelagic marine environment. *FEMS Microbiology Ecology*, **77**, 223–227.

Hopper BE, Cefalu RC (1973) Free-living marine nematodes from Biscayne Bay, Florida V. Stilbonematinae: contributions to the taxonomy and morphology of the genus *Eubostrichus* Greeff and related genera. *Transactions of the American Microscopical Society*, **92**, 578–591.

Huber T, Faulkner G, Hugenholtz P (2004) Bellerophon: a program to detect chimeric sequences in multiple sequence alignments. *Bioinformatics*, **20**, 2317–2319.

Huigens ME, Almeida RP de, Boons P a. H, Luck RF, Stouthamer R (2004) Natural interspecific and intraspecific horizontal transfer of parthenogenesis–inducing *Wolbachia* in *Trichogramma* wasps. *Proceedings of the Royal Society of London. Series B: Biological Sciences*, **271**, 509–515.

Kampfer S, Sturmbauer C, Ott J (1998) Phylogenetic analysis of rDNA sequences from Adenophorean nematodes and implications for the Adenophorea-Secernentea controversy. *Invertebrate Biology*, **117**, 29–36.

Katoh K, Kuma K, Toh H, Miyata T (2005) MAFFT version 5: improvement in accuracy of multiple sequence alignment. *Nucleic Acids Research*, **33**, 511–518.

Katoh K, Standley DM (2013) MAFFT Multiple sequence alignment software version 7: improvements in performance and usability. *Molecular Biology and Evolution*, **30**, 772–780.

Katoh K, Toh H (2008) Recent developments in the MAFFT multiple sequence alignment program. *Briefings in Bioinformatics*, **9**, 286–298.

Kearse M, Moir R, Wilson A *et al.* (2012) Geneious Basic: An integrated and extendable desktop software platform for the organization and analysis of sequence data. *Bioinformatics*, **28**, 1647–1649.

Kleiner M, Wentrup C, Lott C, *et al.* (2012) Metaproteomics of a gutless marine worm and its symbiotic microbial community reveal unusual pathways for carbon and energy use. *Proceedings of the National Academy of Sciences,* **109**, 7148-7149.

Kleiner M, Young JC, Shah M, VerBerkmoes NC, Dubilier N (2013) Metaproteomics reveals abundant transposase expression in mutualistic endosymbionts. *mBio*, **4**, e00223–13.

Krieger J (2000) Funktion und Übertragung endosymbiotischer Bakterien bei bakteriensymbiontischen, darmlosen marinen Oligochaeten. (Function and transmission of endosymbiotic bacteria in gutless marine oligochaetes.). PhD Thesis (University of Hamburg, Germany).

Koga R, Bennett GM, Cryan JR, Moran NA (2013) Evolutionary replacement of obligate symbionts in an ancient and diverse insect lineage. *Environmental Microbiology*, **15**, 2073–2081.

Lefèvre C, Charles H, Vallier A *et al.* (2004) Endosymbiont phylogenesis in the Dryophthoridae weevils: evidence for bacterial replacement. *Molecular Biology and Evolution*, **21**, 965–973.

Legendre P, Desdevises Y, Bazin E (2002) A statistical test for host–parasite coevolution. *Systematic biology*, **51**, 217–234.

Leisch N, Verheul J, Heindl NR, *et al.* (2012) Growth in width and FtsZ ring longitudinal positioning in a gammaproteobacterial symbiont. *Current Biology*, **22**, R831–R832.

Li W, Godzik A (2006) Cd-hit: a fast program for clustering and comparing large sets of protein or nucleotide sequences. *Bioinformatics*, **22**, 1658–1659.

Ludwig W, Strunk O, Westram R *et al.* (2004) ARB: a software environment for sequence data. *Nucleic Acids Research*, **32**, 1363–1371.

Margulis L, Fester R (1991) *Symbiosis as a source of evolutionary innovation: speciation and morphogenesis*. MIT Press.

McFall-Ngai M, Hadfield MG, Bosch TCG *et al.* (2013) Animals in a bacterial world, a new imperative for the life sciences. *Proceedings of the National Academy of Sciences*, **110**, 3229–3236.

Moran NA, McCutcheon JP, Nakabachi A (2008) Genomics and evolution of heritable bacterial symbionts. *Annual Review of Genetics*, **42**, 165–190.

Moya A, Peretó J, Gil R, Latorre A (2008) Learning how to live together: genomic insights into prokaryote–animal symbioses. *Nature Reviews Genetics*, **9**, 218–229.

Musat N, Giere O, Gieseke A *et al.* (2007) Molecular and morphological characterization of the association between bacterial endosymbionts and the marine nematode *Astomonema* sp. from the Bahamas. *Environmental Microbiology*, **9**, 1345–1353.

Musat N, Werner U, Knittel K *et al.* (2006) Microbial community structure of sandy intertidal sediments in the North Sea, Sylt-Rømø Basin, Wadden Sea. *Systematic and Applied Microbiology*, **29**, 333–348.

Muyzer G, Teske A, Wirsen C, Jannasch H (1995) Phylogenetic relationships of *Thiomicrospira* species and their identification in deep-sea hydrothermal vent samples by denaturing gradient gel electrophoresis of 16S rDNA fragments. *Archives of Microbiology*, **164**, 165–172.

Nishijima M, Lindsay DJ, Hata J *et al.* (2010) Association of thioautotrophic bacteria with deep-sea sponges. *Marine Biotechnology*, **12**, 253–260.

Nussbaumer AD, Bright M, Baranyi C, Beisser CJ, Ott JA (2004) Attachment mechanism in a highly specific association between ectosymbiotic bacteria and marine nematodes. *Aquatic Microbial Ecology*, **34**, 239–246.

Nussbaumer AD, Fisher CR, Bright M (2006) Horizontal endosymbiont transmission in hydrothermal vent tubeworms. *Nature*, **441**, 345–348.

Nylander JAA, Erséus C, Källersjö M (1999) A test of monophyly of the gutless Phallodrilinae (Oligochaeta, Tubificidae) and the use of a 573-bp region of the mitochondrial cytochrome oxidase I gene in analysis of annelid phylogeny. *Zoologica Scripta*, **28**, 305–313.

Oksanen J, Blanchet FG, Kindt R et al. (2012) Vegan: community ecology. Package. R package version 2.0–4. URL http://CRAN.R-project.org/package=vegan.

Ott JA, Bauer-Nebelsick M, Novotny V (1995) The genus *Laxus* Cobb, 1894 (Stilbonematinae: Nematoda): Description of two new species with ectosymbiotic, chemoautotrophic bacteria. *Proceedings of the Biological Society of Washington*, **108**, 508–527.

Ott J, Bright M, Bulgheresi S (2004) Symbioses between marine nematodes and sulfur-oxidizing chemoautotrophic bacteria. *Symbiosis*, **36**, 103–126.

Ott JA, Gruber-Vodicka HR, Leisch N, Zimmermann J (2014) Phylogenetic confirmation of the genus *Robbea* (Nematoda: Desmodoridae, Stilbonematinae) with the description of three new species. *Systematics and Biodiversity*, **12**, 434–455.

Ott JA, Novak R, Schiemer F *et al.* (1991) Tackling the sulfide gradient: a novel strategy Involving marine nematodes and chemoautotrophic ectosymbionts. *Marine Ecology*, **12**, 261–279.

Ott J, Rieger G, Rieger R, Enderes F (1982) New mouthless interstitial worms from the sulfide system: Symbiosis with prokaryotes. *Marine Ecology*, **3**, 313–333.

Pagel M, Meade A (2014) BayesTraits v.2.0 Computer program and documentation available at http://www.evolution.rdg.ac.uk/BayesTraits.html.

Peek AS, Feldman RA, Lutz RA, Vrijenhoek RC (1998) Cospeciation of chemoautotrophic bacteria and deep sea clams. *Proceedings of the National Academy of Sciences*, **95**, 9962–9966.

Pende N, Leisch N, Gruber-Vodicka HR *et al.* (2014) Size-independent symmetric division in extraordinarily long cells. *Nature Communications*, **5**.

Petersen JM, Wentrup C, Verna C, Knittel K, Dubilier N (2012) Origins and evolutionary flexibility of chemosynthetic symbionts from deep-Sea animals. *The Biological Bulletin*, **223**, 123–137.

Polz MF, Distel DL, Zarda B, *et al.* (1994) Phylogenetic analysis of a highly specific association between ectosymbiotic, sulfur-oxidizing bacteria and a marine nematode. *Applied Environmental Microbiology*, **60**, 4461–4467.

Polz MF, Felbeck H, Novak R, Nebelsick M, Ott JA (1992) Chemoautotrophic, sulfur-oxidizing symbiotic bacteria on marine nematodes: morphological and biochemical characterization. *Microbial Ecology*, **24**, 313–329.

Powell EN, Crenshaw MA, Rieger RM (1979) Adaptations to sulfide in sulfide-system I. 35S-sulfide accumulation and the presence of a sulfide detoxification system. *Journal of Experimental Marine Biology and Ecology*, **37**, 57–76.

Ronquist F, Huelsenbeck JP (2003) MrBayes 3: Bayesian phylogenetic inference under mixed models. *Bioinformatics*, **19**, 1572–1574.

Ruehland C, Blazejak A, Lott C *et al.* (2008) Multiple bacterial symbionts in two species of co-occurring gutless oligochaete worms from Mediterranean sea grass sediments. *Environmental Microbiology*, **10**, 3404–3416.

Russell JA, Latorre A, Sabater-Muñoz B, Moya A, Moran NA (2003) Side-stepping secondary symbionts: widespread horizontal transfer across and beyond the Aphidoidea. *Molecular Ecology*, **12**, 1061–1075.

Schizas NV, Street GT, Coull BC, Chandler GT, Quattro JM (1997) An efficient DNA extraction method for small metazoans. *Molecular marine biology and biotechnology*, **6**, 381–383.

Sjölin E, Erséus C, Källersjö M (2005) Phylogeny of Tubificidae (Annelida, Clitellata) based on mitochondrial and nuclear sequence data. *Molecular Phylogenetics and Evolution*, **35**, 431–441.

Smith DC (1979) From extracellular to intracellular: The establishment of a symbiosis. *Proceedings of the Royal Society of London. Series B, Biological Sciences*, **204**, 115–130.

Stamatakis A, Hoover P, Rougemont J (2008) A rapid bootstrap algorithm for the RAxML web servers. *Systematic Biology*, **57**, 758–771.

Stewart FJ, Baik AHY, Cavanaugh CM (2009) Genetic subdivision of chemosynthetic endosymbionts of Solemya velum along the southern New England coast. *Applied and Environmental Microbiology*, **75**, 6005–6007.

Stewart FJ, Young CR, Cavanaugh CM (2008) Lateral symbiont acquisition in a maternally transmitted chemosynthetic clam endosymbiosis. *Molecular Biology and Evolution*, **25**, 673–687.

Sunagawa S, Woodley CM, Medina M (2010) Threatened corals provide underexplored microbial habitats. *PLoS One*, **5**, e9554.

Tchesunov AV (2013) Marine free-living nematodes of the subfamily Stilbonematinae (Nematoda, Desmodoridae): taxonomic review with descriptions of a few species from the Nha Trang Bay, Central Vietnam. *Meiofauna Marina*, **20**, 71–94.

Toft C, Andersson SGE (2010) Evolutionary microbial genomics: insights into bacterial host adaptation. *Nature Reviews Genetics*, **11**, 465–475.

Weinert LA, Werren JH, Aebi A, Stone GN, Jiggins FM (2009) Evolution and diversity of *Rickettsia* bacteria. *BMC Biology*, **7**, 6.

Woyke T, Teeling H, Ivanova NN *et al.* (2006) Symbiosis insights through metagenomic analysis of a microbial consortium. *Nature*, **443**, 950–955.

Zimmermann J, Lott C, Weber M *et al.* (2014) Dual symbiosis with co-occurring sulfur-oxidizing symbionts in vestimentiferan tubeworms from a Mediterranean hydrothermal vent. *Environmental Microbiology*.

Supporting Information

Judith Zimmermann, Cécilia Wentrup, Miriam Sadowski, Anna Blazejak, Harald Gruber-Vodicka, Manuel Kleiner, Jörg Ott, Bodil Cronholm, Pierre De Wit, Christer Erseus, and Nicole Dubilier

SI Tables

Table S1: Gutless phallodriline oligochaetes sampled for this study

Sample ID	Host species	Individuals analyzed	Sampling region	Ocean region	Location (Long/Lat)	Sampling date	Habitat (marine zone)	Habitat (sediment grain size)
CE1	*Olavius albidoides*	1	Rottnest Is, Western Australia	E Indian Ocean	-31.999, -115.490	Jan. 1991	subtidal	medium coarse
CE2 CE398	*I. prodigus**	2	Rottnest Is, Western Australia	E Indian Ocean	-32.015, -115.513	Jan. 1991	subtidal	coarse
244-1 244-2 244-3	*Inanidrilus leukodermatus* B	3	Carrie Bow Cay, Belize	W Atlantic, Caribbean Sea	16.80243, 88.08213	Apr. 2013	subtidal	medium coarse
CE901	*I. leukodermatus* A	1	Harrington Sound, Bermuda	W Atlantic	32.324, -64.738	2004	subtidal	fine
CE32	*O. loisae*	1	Heron Is, Australia	SW Pacific, Coral Sea	-23.443, -151.913	Apr. 1994	subtidal	medium coarse
CE81 CE360	*O. imperfectus* A*	2	Lee Stocking Is, Bahamas	W Atlantic, Gulf of Mexico	23.767, 76.100	Apr. 1999 Apr. 2002	subtidal	medium coarse
CE85	*O. ullae*	1	Norman's Cay, Bahamas	W Atlantic, Gulf of Mexico	23.767, 76.100	Apr. 1999	subtidal	coarse
CE94	*I. makropetalos*	1	Lee Stocking Is, Bahamas	W Atlantic, Gulf of Mexico	23.767, 76.100	Apr. 1999	subtidal	fine
CE151	*O. ilvae*	1	Elba, Italy	Mediterranean Sea	42.80816, -10.14202	Apr. 2000	deep water (6m)	medium coarse
CE152	*O. algarvensis*	1	Elba, Italy	Mediterranean Sea	42.80816, -10.14202	Apr. 2000	deep water (6m)	medium coarse

Sample ID	Host species	Individuals analyzed	Sampling region	Ocean region	Location (Long/Lat)	Sampling date	Habitat (marine zone)	Habitat (sediment grain size)
CE222	*O.* “caledonia 1”	1	Lifou, Loyality Is, New Caledonia	SW Pacific, Coral Sea	-20.917, -167.083	Nov. 2000	deep water (6m)	medium coarse
CE301 CE900 Blazejak et al. 2006	*O. crassitunicatus**	3	continental margin off Peru	NE Pacific	-12.73217, -77.13267	Jun. 2000	deep water (360m)	muddy
CE366 Olong1d	*O. longissimus**	2	Lee Stocking Is, Bahamas	W Atlantic, Gulf of Mexico	23.767, 76.097	Apr. 2002	subtidal	medium coarse
CE379 1 additional specimen	*I. mojicae*	2	Lee Stocking Is, Bahamas	W Atlantic, Gulf of Mexico	23.767, 76.100	Apr. 2002	subtidal	medium coarse
CE381 1 additional specimen	*O. tenuissimus*	2	Lee Stocking Is, Bahamas	W Atlantic, Gulf of Mexico	23.767, 76.100	Apr. 2002	subtidal	medium coarse
CE1053 2 additional specimens	*O. “*st andrea 3	3	Elba, Italy	Mediterranean Sea	42.80816, -10.14202	Jun. 2006	deep water (6m)	medium coarse
CE1317	*I. manae*	1	Lizard Is, Australia	SW Pacific, Coral Sea	-14.787, -145.452	Feb. 2006	subtidal	fine
CE1612	*O. "*lizard island 1*"*	1	Lizard Is, Australia	SW Pacific, Coral Sea	-14.693, -145.460	Feb. 2006	subtidal	medium coarse
CE11062 individual 14 individual 3	*O."*pianosa 1*"**	3	Pianosa, Italy	Mediterranean Sea	42.56667, -10.06667	May 2010	deep water (6m)	medium coarse
sample 98-1	*O. geniculatus*	1	Heron Is, Australia	SW Pacific, Coral Sea	-23.44572, -151.91335	Sep. 2012	subtidal	medium coarse
sample 180-1 1 additional specimen	*O. imperfectus* B	2	Carrie Bow Cay, Belize	W Atlantic, Caribbean Sea	16.80243, 88.08213	Apr. 2013	subtidal	medium coarse
sample 124-1	*O.* "heron A"	1	Heron Is, Australia	SW Pacific, Coral Sea	-23.43487, -151.94495	Sep. 2012	deep water (7m)	fine
sample 122-1	*O.* "heron B"	1	Heron Is, Australia	SW Pacific, Coral Sea	-23.43487, -151.94495	Sep. 2012	deep water (7m)	fine

Outgroup:

Sample ID	Host species	Individuals analyzed	Sampling region	Ocean region	Location (Long/Lat)	Sampling date	Habitat (marine zone)	Habitat (sediment grain size)
CE13	*Albanidrilus wellsi*	1	Rottnest Is, Western Australia	E Indian Ocean	-31.989, -115.535	Jan. 1991	subtidal	medium coarse
CE36	*Pirodrilus minutus*	1	Tjärnö Is, Swedish west coast	North Sea	58.8759, -11.1459	1997	intertidal	medium coarse
CE37	*Aktedrilus arcticus*	1	Tjärnö Is, Swedish west coast	North Sea	58.8759, -11.1459	1997	intertidal	medium coarse
CE153	*Pectinodrilus rectisetsosus*	1	Elba, Italy	Mediterranean Sea	42.8082, -10.1420	Apr. 2000	deep water	medium coarse
CE341	*Peosidrilus* nr *vicinus*	1	Lee Stocking Is, Bahamas	W Atlantic, Caribbean Sea	23.767, 76.100	Apr. 2002	subtidal	medium coarse

All PCR products obtained for the gutless phallodriline oligochaetes and the outgroup were sequenced without cloning in both directions.

Table S2: Stilbonematine nematodes sampled for this study

Sample ID	Host species	Individuals analyzed	Symbiont morphology	Sampling region	Ocean region	Location (Long/Lat)	Sampling date	Habitat (marine zone)	Habitat (sediment grain size)	Direct sequencing of 16S_ITS-23S rRNA	No of 16S-ITS-23S rRNA clones sequenced	Genbank accession no host	Genbank accession no ecto-symbiont
W91-3HI	"undescribed genus A"	2	coccoid	Heron Island, Australia	SW Pacific, Coral Sea	-23.44339 151.91307	Aug. 2012	intertidal	coarse	ds	-	KP943969	KP943985
W91-4HI										ds	-	√	√
W91-5HI	*Stilbonema* "heron 2"	1	coccoid	Heron Island, Australia	SW Pacific, Coral Sea	-23.44339 151.91307	Aug. 2012	intertidal	coarse	ds	-	KP943966	KP943982
W111-1HI	*Eubostrichus* cf. *dianae*	1	filaments	Heron Island, Australia	SW Pacific, Coral Sea	-23.43487 151.94495	Sep. 2012	subtidal	fine	-	15 (3)	KP943956	KP943975
W120-1HI	*Stilbonema* "heron 1"	2	coccoid	Heron Island, Australia	SW Pacific, Coral Sea	-23.43487 151.94495	Sep. 2012	subtidal	medium coarse	ds	-	KP943965	KP943983
W120-4HI										ds	-	√	√
W91-1HI	*Laxus* „heron 1"	2	rods	Heron Island, Australia	SW Pacific, Coral Sea	-23.44339 151.91307	Aug. 2012	intertidal	coarse	ds	-	KP943959	KP943987
W91-2HI										ds	-	-	√

W120-9HI	*Laxus* "heron 2"	1	rods	Heron Island, Australia	SW Pacific, Coral Sea	-23.43487 151.94495	Sep. 2012	subtidal	medium coarse	ds	-	KP943960	KP943988
WCat20SA	*Catanema* "standrea"	1	coccoid/ maize-kernel	Elba, Italy	Mediterranean Sea	42.80722 10.14111	May 2012	subtidal	medium coarse	-	22 (6)	KJ4144694 (Ott *et al.* 2014)	KP943973
W78mSA	*Laxus* cf. *cosmopolitus*	3	rods	Elba, Italy	Mediterranean Sea	42.80722 10.14111	May 2012	subtidal	medium coarse	-	5 (5)	KP943958	KP943986
W703A							June 2013			ds	-	√	√
W703B							June 2013			ds	-	√	√
W76gSA	*Eubostrichus* cf. *topiarius*	2	crescent	Elba, Italy	Mediterranean Sea	42.80722 10.14111	May 2012	subtidal	medium coarse	-	1 (1)	KP943957	KP943974
W734SA							June 2013			ds		√	√
W80dSA	*Stilbonema* "standrea 1"	1	coccoid	Elba, Italy	Mediterranean Sea	42.80722 10.14111	May 2012	subtidal	medium coarse	-	18 (6)	KP943967	KP943981
LEvestSA	*Leptonemella* cf. *vestari*	1	coccoid	Elba, Italy	Mediterranean Sea	42.80722 10.14111	May 2012	subtidal	medium coarse	-	46 (5)	KP943963	KP943976
LejuliSA	*Leptonemella* cf. *juliae*	1	coccoid	Elba, Italy	Mediterranean Sea	42.80722 10.14111	May 2012	subtidal	medium coarse	-	52 (8)	KP943962	KP943977
W87vic	*Leptonemella vicina*	3	coccoid	Sylt, Germany	North Sea	55.01467 8.43752	Jun. 2012	intertidal	fine	-	3 (3)	KJ4144684 (Ott *et al.* 2014)	KP943978
W36vic										-	3 (1)	√	√
W45vic										-	3 (3)	√	√
W120aph	*Leptonemella aphanothecae*	3	coccoid	Sylt, Germany	North Sea	55.01467 8.43752	Jun. 2012	intertidal	fine	ds	-	KP943961	KP943979
W6aph										-	5 (1)	√	√
W79aph										-	41 (1)	√	√
W140CBC	*Catanema* "belize 1"	2	coccoid/ maize-kernel	CBC, Belize	W Atlantic, Caribbean Sea	16.8693 - 88.1217	Apr. 2013	subtidal	very fine	-	17 (2)	KP943955	KP943972
W141CBC										-	5 (2)	√	√
W113CBC	"undescribed genus B"	1	rods	CBC, Belize	W Atlantic, Caribbean Sea	16.82861 - 88.10955	Apr. 2013	subtidal	very fine	-	12 (3)	KP943970	KP943971
W82CBC	"undescribed genus A"	2	coccoid	CBC Belize	W Atlantic, Caribbean Sea	16.82861 - 88.10955	Apr. 2013	subtidal	very fine	-	25 (2)	KP943968	KP943984
W94CBC										-	4 (2)	√	√
W44CBC	*Robbea hypermnestra*	1	rods	CBC, Belize	W Atlantic, Caribbean Sea	16.81311 - 88.08299	Apr. 2013	subtidal	coarse	-	12 (2)	KP943964	KP943980

ds: directly sequenced without cloning; [+] numbers indicate the number of partial sequences and the number in parentheses the number of fully sequenced clones.
√: sequences were amplified and >99.98% identical to published nucleotide sequence of the same host species, CBC: Carrie Bow Cay.

Table S3: Primers used in this study

Organism	Target gene	Primer	Primer sequence (5'-3')	Length of PCR product (bp)	Used for	Remarks	Reference
Stilbonematine nematodes	18S rRNA	18S_1F	GGTTGATYCTGCCAGT	~1800	PCR, Sequencing		modified after (Winnepenninckx *et al.* 1995)
		18S_2023R	GGTTCACCTACGRAAA				modified after (Pradillon *et al.* 2007)
		Nem01R	CAGACAAATCGCTCC			Internal sequencing primer 1272 bp downstream of 18S-1F	this study
Gutless Phallodrilinae	18S rRNA	TimA	AMCTGGTTGATCCTGCCAG	~1700	PCR, Sequencing	To increase yield of PCR-products, use 1µl of the PCR-product obtained with TimA and TimB as template for PCRs with the primer combinations Tima/1100R and TimB/660F or TimB/600F	
		TimB	TGATCCATCTGCAGGTTCACCT				
		660F	GATCTCGGGTCCAGGCT				
		600F	GGTGCCAGCMGCCGCGGT				
		1100R	GATCGTCTTCGAACCTCTG				
	mt16S rRNA	16S arL	CGCCTGTTTATCAAAAACAT	~ 480	PCR, Sequencing		(Palumbi 1991)
		16S brH	CCGGTCTGAACTCAGATCACGT				
		16S AnnF	GCGGTATCCTGACCGTRCWAAGGTA	~ 300	PCR, Sequencing		(Sjölin *et al.* 2005)
		16S AnnR	TCCTAAGCCAACATCGAGGTGCCAA				
	28S rRNA	28SC1	ACCCGCTGAATTTAAGCAT	~ 330	PCR, Sequencing		(Jamieson *et al.* 2002)
		28SC2	TGAACTCTCTCTTCAAAGTTCTTTTC				
	mt12S rRNA	12SE1	AAAACATGGATTAGATACCCRYCTAT	~ 400	PCR, Sequencing		(Jamieson *et al.* 2002)
		12SH	ACCTACTTTGTTACGACTTATCT				
	ITS	ITS-5	GGAAGTAAAAGTCGTAACAAGG	~ 900	PCR, Sequencing		(White *et al.*, others 1990)

		ITS-4	TCCTCCGCTTATTGATATGC				
		5.8muss F	CGCAGCCAGCTGCGTGAATTAATGT			To increase yield of PCR-products, use 1µl of the PCR-product obtained with ITS-5 and ITS-4 as template for PCRs with the primer combinations ITS5/5.8mussR and 5.8mussF/ITS4	(Källersjö *et al.* 2005)
		5.8mussR	GATGTCGATGTTCAATGTGTCCTGC		PCR, Sequencing		
	mtCOI	LCO1490__COI	GGTCAACAAATCATAAAGATATTGG	~700	PCR, Sequencing		(Folmer *et al.* 1994)
		HCO2198_COI	TAAACTTCAGGGTGACCAAAAAATC				
Stilbonematine nematode *Cand.* Thiosymbions	16S rRNA-ITS-partial 23S rRNA operon	GM3F	AGAGTTTGATCMTGGC	~2200	PCR, Sequencing	I	(Muyzer *et al.* 1995)
		L189R	TACTGAGATGYTTMARTTC				(Yu & Mohn 2001)
		907RM	CCGTCAATTCMTTTGAGTTT			Internal sequencing primer	Muyzer et al., 1997
		GM4F	TACCTTGTTACGACTT			Internal sequencing primer	(Muyzer *et al.* 1995)
		GM12F	GAGGAAGGTGMGGATGACG			Internal sequencing primer	(modified from MacGregor & Amann 2006)
		GM5F	CCTACGGGAGGCAGCAG			Internal sequencing primer	(Muyzer *et al.* 1993)
Gutless Phallodrilinae *Cand.* Thiosymbions	16S rRNA	GM4R	TACCTTGTTACGACTT	~ 1350	PCR, Sequencing		(Muyzer *et al.* 1995)
		G1_55_all	TTCGCGTTCGACTTGCAT				This study
		907RM	CCGTCAATTCMTTTGAGTTT			Internal sequencing primer	Muyzer et al., 1997
		907F	AAACTCAAAGGAATTGACGG			Internal sequencing primer	(Santegoeds *et al.* 1998)

Table S4: Amplified genes and Genbank accession numbers for gutless phallodriline oligochaetes and their symbionts

		Host genes and their accession numbers						Endosymbiont accession numbers
Sample ID	**Host Species**	**mt12S**	**mt16S**	**18S**	**28S**	**mtCOI**	**ITS**	**16S**
CE1	*Olavsus albidoides*	KP943895	KP943919	KP943805	KP943831	KP943857		KP943938
CE2	*O. prodigus**	KP943897				AF064038	KP943876	KP943939
CE398	*O. prodigus*		KP943926	KP943813	KP943840			
244-1	*Inanidrilus leukodermatus* B		KP943910	KP943795	KP943821	√ (1 nucleotide differences to 244-2)	KP943869	KP943947
244-2	*I. leukodermatus* B					KP943848		√
CE901	*I. leukodermatus* A	KP943907	KP943930	KP943816	KP943843	KP943865	KP943883	KP943948
CE32	*O. loisae*	KP943898	KP943921	KP943808	KP943834		KP943878	KP943951
CE81	*O. imperfectus* A*	KP943904	KP943927	KP943814	KP943841		KP943881	
CE360	*O. imperfectus* A					KP943860		KP943943
CE85	*O. ullae*	KP943905	KP943928	KP943815	KP943842	KP943864	KP943882	KP943934
CE94	*I. makropetalos*	KP943908	KP943931	KP943817	KP943844	KP943866	KP943884	KP943949
CE151	*O. ilvae*	KP943892	KP943916	KP943801	KP943827	KP943853	KP943873	KP943933
CE152	*O. algarvensis*	DQ459929	AY885596	KP943802	KP943828	KP943854	KP943874	KP943944
CE222	*O. "*caledonia 1*"*	KP943896	KP943920	KP943806	KP943832	KP943858	KP943875	KP943935
CE301	*O. crassitunicatus**			KP943807	KP943833		KP943877	KP943953
CE900	*O. crassitunicatus*	KP943906	KP943929					
CE366	*O. longissimus*	KP943900	KP943923	KP943810	KP943836	KP943861	KP943879	KP943940
O.long 1	*O. longissimus*							√
CE379	*I. mojicae*	KP943901	KP943924	KP943811	KP943837	KP943862	KP943880	KP943952
additional specimen 1	*I. mojicae*							√
CE381	*O. tenuissimus*	KP943903	KP943925	KP943812	KP943839	KP943863		KP943946
O. ten 2	*O. tenuissimus*							√
CE1053	*O. "*standrea 3*"**	KP943888	KP943912	KP943797	KP943823	KP943850	KP943871	
additional specimen 1	*O. "*standrea 3*"*					√		KP943932
additional specimen 2	*O. "*standrea 3*"*					√		√
CE1317	*I. manae*	KP943890	KP943914	KP943799	KP943825	KP943852		KP943954
CE1612	*O. "*lizard island 1*"*	KP943894	KP943918	KP943804	KP943830	KP943856	√	KP943937
CE11062	*O. "*pianosa 1"*	KP943889	KP943913			KP943851	KP943872	
individual 14	*O. "*pianosa 1"			KP943798	KP943824	√		KP943945
individual 3	*O. "*pianosa 1"					√		√
sample 98-1	*O. geniculatus*	KP943887	KP943911	KP943796	KP943822	KP943849	KP943870	KP943941
sample 180-1	*O. imperfectus* B			KP943794	KP943820	KP943847		KP943942
O. imp 8	*O. imperfectus* B							√

Sample ID	Host species	mt12S	mt16S	18S	28S	mtCOI	ITS	16S
sample 124-1	*O. "*heron A*"*	KP943886	KP943909	KP943793	KP943819	KP943846	KP943868	KP943936
sample 122-1	*O. "*heron B*"*	KP943885		KP943792	KP943818	KP943845	KP943867	KP943950

* It was sometimes not possible to get all genes from one individual. Based on taxonomic identification and if possible identical gene sequence, we ensured to amplify genes from individuals of the same species. √: sequences were amplified and >99.98% identical to published nucleotide sequence of the same host species.

Outgroup of gutless Phallodrilinae	Host species	mt12S	mt16S	18S	28S	mtCOI	ITS	16S
CE13	*Albanidrilus wellsi*	KP943891	KP943915	KP943800	KP943826			no amplification *of Cand.* Thiosymbion sequence
CE36	*Pirodrilus minutus*	DQ459880	DQ459958	DQ459986	GU902023	AF064043		no amplification *of Cand.* Thiosymbion sequence
CE37	*Aktedrilus arcticus*	KP943902	AY665591	AF209451	KP943838	AF064042		no amplification *of Cand.* Thiosymbion sequence
CE153	*Pectinodrilus rectisetsosus*	KP943893	KP943917	KP943803	KP943829	KP943855		no amplification *of Cand.* Thiosymbion sequence
CE341	*Peosidrilus nr vicinus*	KP943899	KP943922	KP943809	KP943835	KP943859		no amplification *of Cand.* Thiosymbion sequence

SI Figures

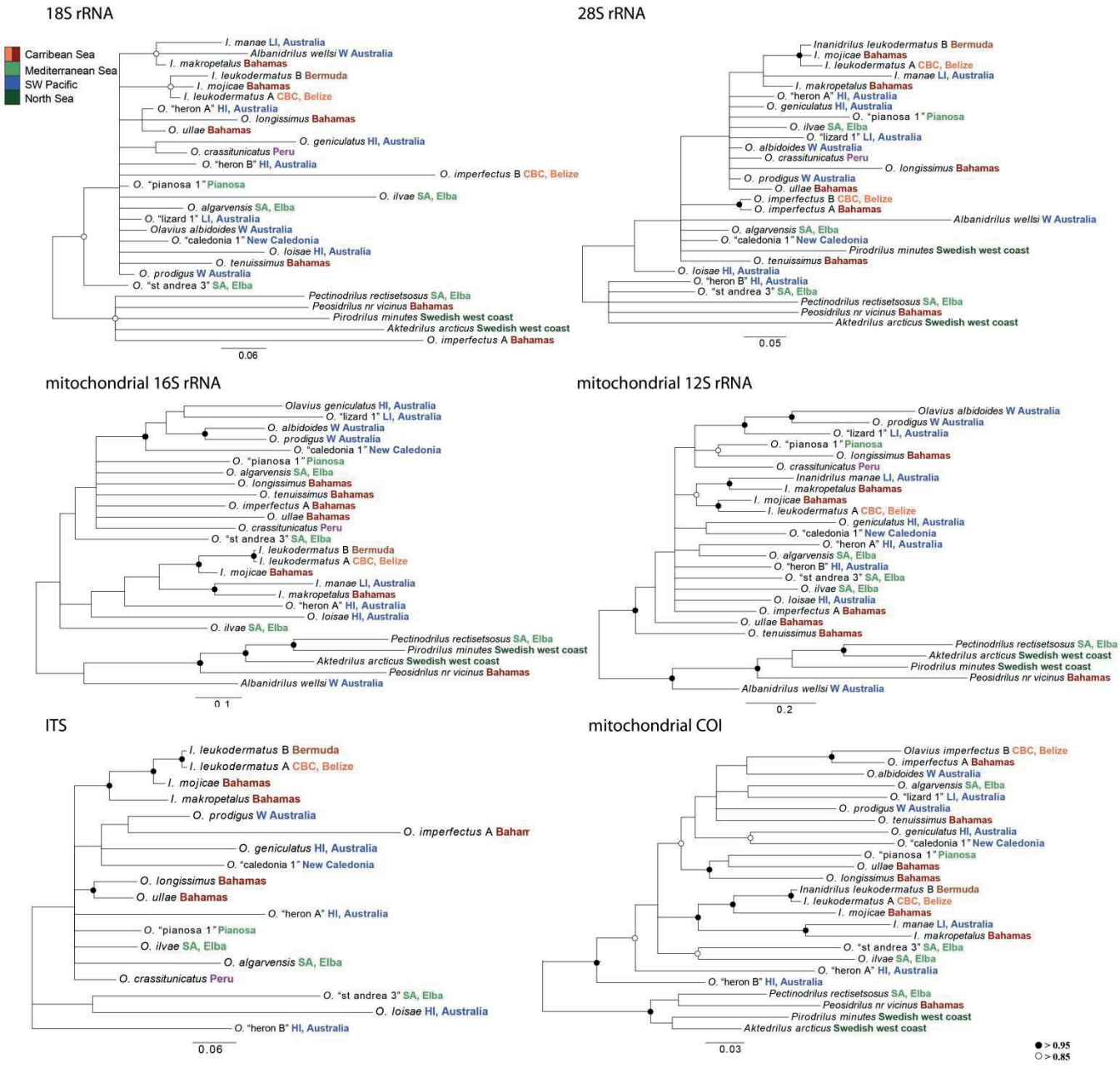

Fig. S1: Phallodriline oligochaete phylogenies, based on different host genetic markers. Consensus trees of Bayesian inference (mrBayes) and maximum likelihood (RaxML) analyses of six different host genetic markers. Colored names indicate the sampling locations. Nodes that were statistically supported in both analyses (> 80% bootstrap value and 0.80 posterior probability (pp) value) are highlighted in black, nodes that were statistically supported only in Bayesian inference are highlighted in white. Provisional working names for undescribed species are given in quotes. The scale bars represent sequence divergences: 18S rRNA and ITS: 6%; 28S rRNA: 5%; mt16S rRNA: 1%, mt12S rRNA: 2%; mtCOI: 3%.

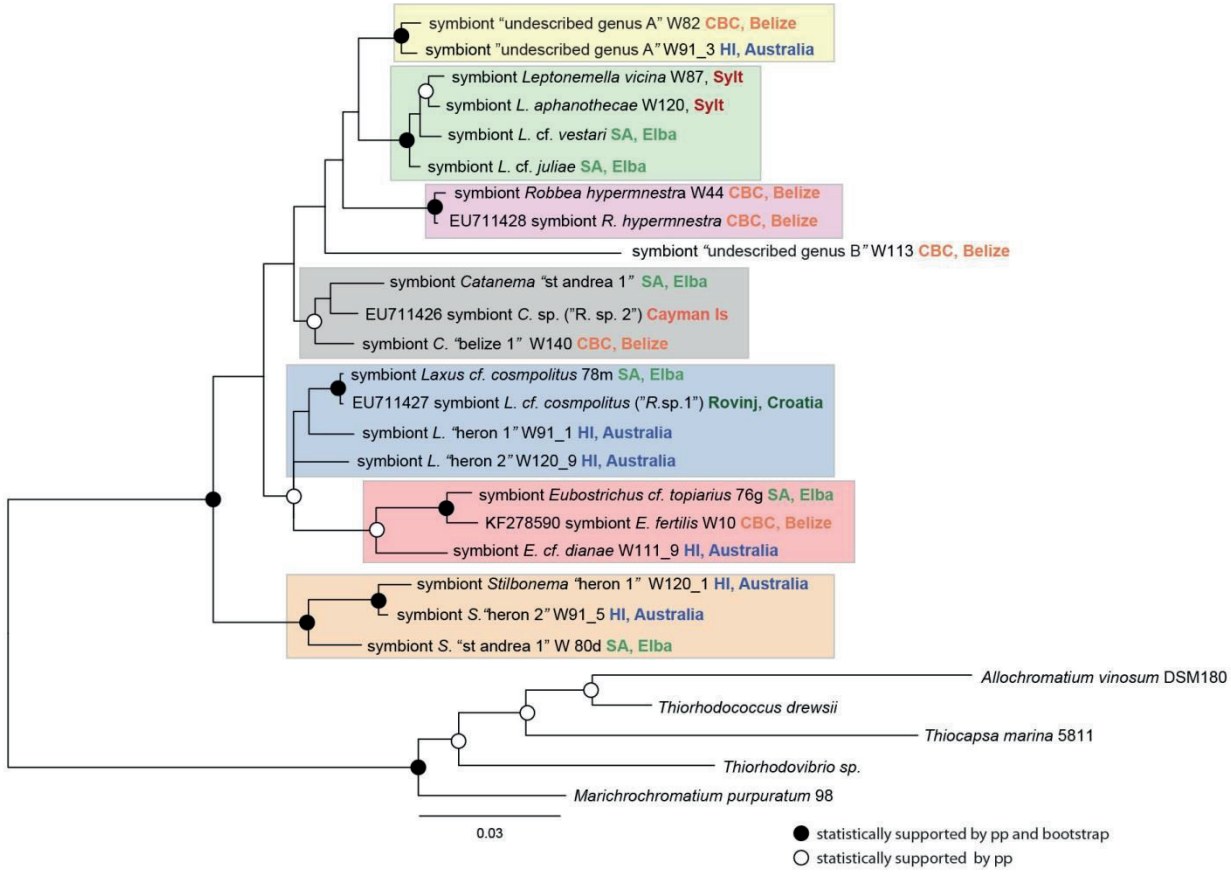

Fig. S2: Stilbonematine nematode ectosymbiont phylogeny, based on the 16S rRNA gene. Consensus tree of Bayesian inference (mrBayes) and maximum likelihood (RaxML) analyses. Colored boxes show monophyletic groups of host genera and their ectosymbiotic bacteria, respectively, colored names the sampling locations. Nodes that were statistically supported in both analyses (> 80% bootstrap value and 0.80 posterior probability (pp) value) are highlighted in black, nodes that were statistically supported only in Bayesian inference are highlighted in white. Provisional working names for undescribed species are given in quotes. The scale bar represents 3% sequence divergence.

References SI

Folmer O, Black M, Hoeh W, Lutz R, Vrijenhoek R (1994) DNA primers for amplification of mitochondrial cytochrome c oxidase subunit I from diverse metazoan invertebrates. *Molecular Marine Biology and Biotechnology*, **3**, 294–299.

Jamieson BG, Tillier S, Tillier A *et al.* (2002) Phylogeny of the Megascolecidae and Crassiclitellata (Annelida, Oligochaeta): combined versus partitioned analysis using nuclear (28S) and mitochondrial (12S, 16S) rDNA. *Zoosystema Paris*, **24**, 707–734.

Källersjö M, Von Proschwitz T, Lundberg S, Eldenäs P, Erséus C (2005) Evaluation of ITS rDNA as a complement to mitochondrial gene sequences for phylogenetic studies in freshwater mussels: an example using Unionidae from north-western Europe. *Zoologica Scripta*, **34**, 415–424.

MacGregor BJ, Amann R (2006) Single-stranded conformational polymorphism for separation of mixed rRNAS (rRNA-SSCP), a new method for profiling microbial communities. *Systematic and applied microbiology*, **29**, 661–670.

Muyzer G, Teske A, Wirsen C, Jannasch H (1995) Phylogenetic relationships of *Thiomicrospira* species and their identification in deep-sea hydrothermal vent samples by denaturing gradient gel electrophoresis of 16S rDNA fragments. *Archives of Microbiology*, **164**, 165–172.

Muyzer G, de Waal EC, Uitterlinden AG (1993) Profiling of complex microbial populations by denaturing gradient gel electrophoresis analysis of polymerase chain reaction-amplified genes coding for 16S rRNA. *Applied and Environmental Microbiology*, **59**, 695–700.

Muyzer G, Brinkhoff T, Nübel U, Santegoeds C, Schäfer H & Wawer C (1997) Denaturing gradient gel electrophoresis (DGGE) in microbial ecology. In: Akkermans ADL, van Elsas JD & de Bruijn FJ (Eds) Molecular Microbial Ecology Manual (3.4.4: pp. 1–27) Kluwer Academic Publishers, Dordrecht, The Netherlands.

Ott JA, Gruber-Vodicka HR, Leisch N, Zimmermann J (2014) Phylogenetic confirmation of the genus *Robbea* (Nematoda: Desmodoridae, Stilbonematinae) with the description of three new species. *Systematics and Biodiversity*, **12**, 434–455.

Palumbi, SR, Martin, A, Romano, S, McMillan, WO, Stice, L. & Grabowski, G (1991). The Simple Fool's Guide to PCR, Version 2.0. Privately published, Univ. Hawaii.

Pradillon F, Schmidt A, Peplies J, Dubilier N (2007) Species identification of marine invertebrate early stages by whole-larvae in situ hybridisation of 18S ribosomal RNA. *Marine Ecology Progress Series*, **333**, 103–116.

Santegoeds CM, Ferdelman TG, Muyzer G, de Beer D (1998) Structural and functional dynamics of sulfate-reducing populations in bacterial biofilms. *Applied and Environmental Microbiology*, **64**, 3731–3739.

Sjölin E, Erséus C, Källersjö M (2005) Phylogeny of Tubificidae (Annelida, Clitellata) based on mitochondrial and nuclear sequence data. *Molecular Phylogenetics and Evolution*, **35**, 431–441.

White TJ, Bruns T, Lee S, Taylor JW, others (1990) Amplification and direct sequencing of fungal ribosomal RNA genes for phylogenetics. *PCR protocols: a guide to methods and applications*, **18**, 315–322.

Winnepenninckx B, Backeljau T, Wachter RD (1995) Phylogeny of protostome worms derived from 18S rRNA sequences. *Molecular Biology and Evolution*, **12**, 641–649.

Yu Z, Mohn WW (2001) Bacterial diversity and community structure in an aerated lagoon revealed by ribosomal intergenic spacer analyses and 16S ribosomal DNA sequencing. *Applied and Environmental Microbiology*, **67**, 1565–1574.

Chapter IV

To each its own - diverse yet highly specific ectosymbionts on co-occurring nematodes from a temperate beach in the North Sea

Authors: Judith Zimmermann[1], Harald R. Gruber-Vodicka[1], Rebecca Ansorge[1], Bruno Hüttel[2], Niculina Musat[1*], Jörg A. Ott[3], Nicole Dubilier[1], and Jillian M. Petersen[1]

[1]Department of Symbiosis, Max Planck Institute for Marine Microbiology, Celsiusstrasse, Bremen, Germany
[2]Max Planck Genome Centre, Max Planck Insitute for Plant Breeding Research, Carl-von-Linne-Weg, Cologne, Germany
[3]Department of Limnology and Oceanography, University of Vienna, Althanstrasse, Austria
*now affiliated with Helmholtz Centre for Environmental Research - UFZ, Permoserstrasse, Leipzig, Germany

Manuscript in preparation

J.Z. developed the concept, performed the symbiont and host marker gene sequencing and phylogenetic analyses, designed and tested the FISH probes, performed the CARD-FISH experiments, performed the draft genome analyses and single nucleotide polymorphism analyses, conceived and wrote the manuscript; H.R.G. helped to develop the concept, performed the genome assemblies and prepared the reads for the SNP analyses; R.A. optimized the single nucleotide polymorphism analyses workflow and helped with the analyses; B.H. constructed the Illumina HiSeq libraries and performed the sequencing; N.M. started the project and contributed to the construction of the molecular data; J.A.O: contributed to the sampling and identification of the nematodes; N.D. helped to develop the concept; J.M.P: helped to developed the concept, conceived and edited the manuscript.

Abstract

The importance of symbiont diversity between individuals of the same host species is becoming widely recognized in the field of symbiosis but so far little is known for marine symbiotic associations. Stilbonematine nematodes are common in marine sulfidic sediments and live in symbiosis with sulfur-oxidizing Gammaproteobacteria of the *Candidatus* Thiosymbion clade, which form a dense layer on the nematode cuticle. The evolutionary stability and strict host specificity of stilbonematine ectosymbioses was recently shown, yet symbiont diversity within host species have not been investigated in detail. In this study we examined multiple individuals of several co-occurring species of the genus *Leptonemella* from a beach off the North Sea island Sylt. Three *Leptonemella* species had been previously described from this location based on their morphology. Our intensive sampling over 10 years combined with phylogenetic analyses based on the 18S rRNA gene revealed an unexpected diversity of seven co-occurring *Leptonemella* species. Bacterial 16S ribosomal RNA (rRNA) gene and ribosomal intergenic spacer region (ITS) analyses showed that each *Leptonemella* species was consistently associated with specific 16S-ITS symbiont types that were distinct from the symbionts of other species. Although the symbionts formed host-specific clusters, most of the worms hosted a unique 16S-ITS symbiont phylotype that differed up to 2.2% between worms from the same species. Intriguingly, five symbiont metagenomes from *L. aphanothecae* and *L. vicina* showed that each individual worm hosts a unique symbiont strain, corresponding to 97% intra- and 93% interspecies average nucleotide identities across the entire genome. Within the symbiont population of one worm, 16S-ITS and single-copy genes were identical, but single nucleotide polymorphism (SNP) densities ranged from 0.3 to 1 SNPs per kilobase genome, indicating that the population is not strictly clonal. The remarkable diversity, yet specificity of multiple co-occurring *Leptonemella* ectosymbioses suggests a combination of highly precise and co-evolved recognition mechanisms between both partners.

Introduction

Marine stilbonematine nematodes of the family *Desmodoridae* are diverse and abundant members of the meiofauna in marine sediments worldwide (Ott *et al.* 2004; Tchesunov 2013). All known stilbonematines associate with sulfur-oxidizing bacteria of the *Candidatus* Thiosymbion clade (Gruber-Vodicka *et al.,* in prep.) that cover the nematodes' cuticle in a dense layer (reviewed by Ott *et al.* 2004). The symbioses often occur in sediments without clear overlap of anoxic sulfidic and oxygenated surface layers (Ott *et al.* 2004). Thus, the major benefit for the chemoautotrophic bacteria was proposed to be the association with a motile host that provides regular access to the reductants and oxidants needed to fuel the symbionts' metabolism: oxygen in the surface layers and reduced sulfur compounds in the deeper sediment layers (Schiemer *et al.* 1990; Ott *et al.* 1991, 2004). The host is believed to gain nutrition from its symbionts, through 'grazing' on its own bacterial coat (Wieser 1959; Ott *et al.* 1991, 2004). However, bacteria in the gut region have not yet been clearly identified as symbionts, nor has nutritional transfer from the ectosymbiotic bacteria to the host been shown experimentally.

The abundance of stilbonematines is generally highest in subtropical and tropical continental shelf regions, but they have also been described from deep sea sediments, shallow methane seeps and hydrothermal vents and temperate ocean regions (e.g. Kamenev *et al.* 1993; Dando *et al.* 1994; Thiermann *et al.* 1997; Tchesunov *et al.* 2012; Leduc 2013). A total of ten different genera have been characterized, but unique identifying morphological characters are controversial among taxonomists. This has resulted in several synonymizations and re-namings of many species (Ott *et al.* 2004; Tchesunov 2013). However molecular tools, such as the small subunit of the ribosomal RNA (18S rRNA) have proven valuable for validation of the morphological identification and also to distinguish between closely related species (Ott *et al.* 2014, Zimmermann *et al.*, in review, Chapter III).

Stilbonematine nematode ectosymbioses are known to be host-specific. Early studies on stilbonematines showed that different species can have distinct symbiont morphologies including cocci, rods, crescent or filamentous shapes (Ott *et al.* 1991; Polz *et al.* 1992). Molecular studies that analyzed the 16S ribosomal RNA (rRNA) gene of the stilbonematine ectosymbionts in combination with symbiont-specific *in situ* hybridization analyses confimed that six host species were each associated with a distinct gammaproteobacterial

ectosymbiont type (Polz *et al.* 1994; Bayer *et al.* 2009; Pende *et al.* 2014). Our recent molecular study of a further 16 stilbonematine species and their symbionts from locations around the world provided further evidence for the species-specificity of stilbonematine ectosymbioses (Zimmermann *et al.*, in prep., Chapter III). Remarkably, we found that closely related host species of the same genus are consistently associated with closely related symbionts irrespective of their geographical location, except for symbionts of *Laxus* species, which were more closely related to endosymbionts of gutless phallodriline annelids (Zimmermann *et al.,* in prep., Chapter III). Due to the predominantly congruent host-symbiont phylogenies we hypothesized that the transmission mode of the ectosymbionts is predominantly vertical, i.e. from mother to offspring via an ectosymbiont smear infection (Zimmermann *et al.*, in prep., Chapter III).

Apart from the transmission of symbionts between parents and offspring, stilbonematine nematodes shed their cuticle four times in their life cycle and the new cuticle needs to be recolonized by symbionts after each moult (Ott *et al.* 2004). In addition, the ectosymbionts are consistently exposed to the microbial sediment community and many of these microbes are adapted to colonize surfaces such as sand grains. Thus, it is astonishing that stilbonematine nematode species apparently have only a single bacterial symbiont type colonizing their surface (Ott *et al.* 2004).

Previous studies used either direct sequencing of PCR products, or investigated only a few clones of a single marker gene such as the 16S rRNA gene or the ITS region. Some studies did not investigate individual worms but pooled multiple worms before sequencing (Polz *et al.* 1994; Bayer *et al.* 2009; Pende *et al.* 2014, Zimmermann *et al.*, in prep., Chapter III). These methods would only reveal the most dominant gammaproteobacterial symbiont type but would not necessarily show whether multiple closely related symbiont strains are present on one worm. Thus the true degree of ectosymbiont diversity on stilbonematine nematodes might be greater than previously assumed.

In this study we performed an in-depth characterization of the full diversity of closely related stilbonematine nematode ectosymbioses of the genus *Leptonemella* that co-occur on a single beach on the North Sea island of Sylt (Riemann *et al.* 2003). Our aims were the following: (1) Investigate species specificity by sequencing the host 18S rRNA gene and the symbiont partial 16S-ITS-23S rRNA sequences from multiple individuals of each co-occurring and closely related host species. (2) Resolve the full extent of ectosymbiont microdiversity by

a combination of extensive symbiont 16S-ITS-23S rRNA clone libraries and next generation sequencing of the symbiont population from five selected individuals. (3) Identify genes that show signatures of selection.

Material and Methods

Nematode collection and preparation

Sediment samples containing stilbonematine nematodes were collected on an intertidal flat ('Hausstrand' List, 55.015069 N, 8.437788 E) on the northern German island Sylt using sediment cores (Fig. 1). Cores were taken during low tide close to polychaete burrows where highest stilbonematine nematode densities were previously reported (Riemann *et al.* 2003). Worms were extracted from the sand by shaking and decanting through a 64 µm mesh sieve and the live animals were sorted using a dissecting microscope. If possible, species were identified morphologically with a differential interference contrast (DIC) microscope (Olympus BX53, Olympus, Hamburg, Germany), washed three times in 0.2 µm filtered seawater and immediately fixed in 70% ethanol for molecular analyses. Samples for fluorescence in situ hybridization (FISH) were either fixed in 1 - 2% paraformaldehyde in 0.2 µm filtered seawater at 4° C overnight and washed twice in cold 0.2 µm filtered seawater or fixed directly in 70% ethanol. All samples were stored at 4° C until further processing.

DNA extraction, amplification and Sanger sequencing

For some nematodes, DNA was extracted and purified from single individuals together with their ectosymbiont fractions as previously described (Schizas *et al.* 1997). Other individuals were treated with three 30 s pulses of ultrasonication at 20% activity (Bandelin Sonoplus HD 70, Berlin, Germany) and vortexed between each pulse to remove the symbionts from the worms. DNA was extracted separately from worm and pelleted symbiont fractions, either as described by Schizas *et al.* (1997) or with the Blood and Tissue Kit (Qiagen, Hilden, Germany), following manufacturer's instructions. Nematode 18S rRNA genes (~1800 base pairs (bp)) were amplified by polymerase chain reaction (PCR) with the 18S_1F/2023R primer pair (modified from Winnepenninckx *et al.* 1995; and Pradillon *et al.* 2007) as described by Zimmermann *et al*., (in prep., Chapter III). For some of the individuals where no PCR product could be obtained with the general primers, we used the modified eukaryotic

primer pair Nem01F (5'-GCCGAATTATGGTGA-3') and Nem01R (5´-CAGACAAATCGCTCC-3´) to amplify a shorter product of the 18S rRNA gene (~1200 bp). Cycling conditions were adapted for the Nem01F/Nem01R primer pair as follows: initial denaturation at 96° C for 5 min, followed by 30 - 35 cycles of 96° C for 1 min, annealing at 42° C for 1.5 min, elongation at 72° C for 2 min and final elongation at 72° C for 10 min. The purified PCR products (PCR Purification Kit; Qiagen, Hilden, Germany) were sequenced bidirectionally with the PCR primers.

To characterize the ectosymbiotic bacteria of selected hosts, bacterial 16S rRNA genes, intergenic transcribed spacer regions (ITS) and the partial 23S rRNA genes (~2200 bp) were amplified as described by Zimmermann *et al*., (in prep., Chapter III). A total of 21 clone libraries were constructed using PCR products amplified from *Leptonemella* DNA extracts that contained both host and symbiont DNA. Clone library construction and screening for positive inserts was performed as described previously (Zimmermann *et al.* 2014). A total of 50 - 100 clones with correct insert size were partially sequenced with the primer GM12F (5'-GAGGAAGGTGATGACG-3') (MacGregor & Amann 2006) and compared with sequences in GenBank by using BLASTn (Altschul *et al.* 1997). All 16S-ITS-23S rRNA sequences that were closely related to previously sequenced *Cand.* Thiosymbion bacteria were 100% identical per individual worm. Therefore, three to ten clones containing sequences related to *Cand.* Thiosymbion were selected per nematode specimen for full sequencing from plasmids isolated by the Montage™ Plasmid Miniprep96 kit (Millipore, Bedford, Massachusetts). Plasmids were Sanger-sequenced with the sequencing primers reported previously (Zimmermann *et al.,* Chapter III). The 16S-ITS-partial 23S rRNA PCR products from 13 symbiont fractions, removed from their hosts prior to DNA extraction were sequenced bidirectionally without cloning and always yielded clear chromatographs. To examine whether 16S-ITS phylotypes of lower abundance could be missed by direct sequencing, we constructed two 16S-ITS clone libraries from pure ectosymbiont fractions and partially sequenced a total of 126 and 183 clones, respectively. Every single clone contained the exact same sequence as obtained by direct sequencing of this symbiont extract (Table S1). All sequencing reactions were performed with an ABI PRISM 3100 genetic analyzer (Applied Biosystems, Foster City, CA, USA). Sequences were assembled using Sequencher v4.6 (GeneCodes Corporation, Ann Arbor, MI), manually curated and chimera-checked by the Bellerophon program (Huber *et al.* 2004).

Phylogenetic analyses of host and symbiont genes

For the nematode overview tree, the generated partial 18S rRNA and previously published 18S rRNA sequences from stilbonematine nematodes available in GenBank, as well as four Draconematinae sequences as outgroup were aligned using MAFFT Q-INS-I, which considers the predicted secondary structure of the RNA for the alignment (Katoh & Toh 2008). For the co-phylogeny analysis, only the generated 18S rRNA sequences from Sylt and previously published *Leptonemella* sequences from Elba, Italy as well as *Stilbonema* species from Heron Island, Australia as outgroup (sampling details see Zimmermann *et al.*, in in prep., Chapter III), were aligned as described above. Alignments were manually adjusted and 5' and 3' end-trimmed using Geneious software version 6 (Kearse et al., 2012). The optimal substitution model was assessed using the Akaike information (AIC) as implemented in jModeltest 2.1.4 (Guindon & Gascuel 2003; Darriba *et al.* 2012) and the GTR+I+G model was chosen. Phylogenetic trees were reconstructed using maximum likelihood- (RAxML) (Stamatakis 2006) and Bayesian inference-based (MrBayes) (Ronquist & Huelsenbeck 2003) methods. MrBayes was run for 20 Mio generations using four chains. Convergence was evaluated by plotting the generations versus logL and the burn-in was set to 5000 generations. Node stability was evaluated using posterior probabilities (pp, Bayesian inference) and bootstrap support (100 RAxML rapid bootstrap runs, maximum likelihood) (Stamatakis *et al.* 2008) with values above 0.80 considered significant.

For the ectosymbiont phylogeny, the 16S rRNA-ITS partial 23S rRNA sequences from this study and previously published *Leptonemella* ectosymbiont sequences from Elba, Italy were used for phylogenetic reconstruction. Symbiont sequences from *Stilbonema* species from Heron Island, Australia (sampling details see Zimmermann *et al.,* in in prep., Chapter III) were included as outgroup. 16S rRNA, ITS and partial 23S rRNA sequences were aligned separately from each other using MAFFT Q-INS-I for 16S rRNA and 23S rRNA or MAFFT G-INS-I for ITS (Katoh *et al.* 2005; Katoh & Toh 2008). Alignments were adjusted manually and ends were trimmed as described above. The optimal substitution models were assessed as described above and were GTR+I+G for the 16S and 23S rRNA, and HKY+G for the ITS alignment. Phylogenetic trees were constructed using MrBayes with partitioned 16S rRNA, ITS and 23S rRNA gene alignments using the suggested substitution models. The partitions were unlinked from each other in all parameters except topology and MrBayes was run for 20 Mio generations and settings as described above. For the phylogenetic analyses with

RAxML, the GTR+G substitution model was used for all three partitions and node support was evaluated using bootstrap support (100 RAxML rapid bootstrap runs, maximum likelihood) (Stamatakis *et al.* 2008). Phylogenetic analyses were repeated with only the symbiont 16S rRNA gene but otherwise the same settings. For comparison, phylogenetic tree calculations were also done with the 16S rRNA gene only (Fig. S1).

Statistical analyses

Patristic distance matrices, estimated from Bayesian Inference phylogenies of host and ectosymbionts were calculated with the program PATRISTIC (Fourment & Gibbs 2006). Jukes-Cantor distance matrices were calculated with the software package ARB (Ludwig *et al.* 2004). Mantel tests were calculated in R (http://www.r-project.org/) using Pearson's r-statistic and 999 Monte Carlo permutations implemented in the R package "*vegan"* (Oksanen *et al.*, 2012).

Probe design and testing

A general oligonucleotide probe targeting all Sylt *Leptonemella* ectosymbionts SE585 was designed using the probe design function in the ARB software package (Ludwig *et al.* 2004). The probe was checked against the SILVA Ref 111 database (Quast et al., 2012) (see Table 1 for all probe sequences). SE585 had a least two mismatches to all other publicly available full length 16S rRNA sequences, one mismatch to the ectosymbionts of the closely related *Leptonemella* species from Elba in the Mediterranean Sea and at least two mismatches to all other sequenced ectosymbionts of stilbonematine nematodes. To test the specificity of the general Sylt ectoymbiont-specific SE585 probe a 10% to 60% formamide series was performed on *Leptonemella* and *Laxus oneistus* sections. *L. oneistus* is a stilbonematine nematode from Belize in the Carribean Sea and served as a negative control because its symbionts have three mismatches to the probe target sequence. Signals were observed between 10 and 40% formamide on *Leptonemella* sections. No signals were observed on *L. oneistus* sections at any of the tested formamide concentrations. Because the ectosymbionts of *L. aphanothecae* and *L. vicina* differ at only 3 nucleotide positions along the entire 16S rRNA gene, oligonucleotide probes (Laph432, Lvic432) were designed by visually identifying a suitable one mismatch target site in the sequence alignment using BIOEDIT (Hall, 1997–2001) (Table 1). Due to the high similarity between 16S rRNA sequences of all Sylt

Leptonemella ectosymbionts both designed probes also perfectly matched the symbionts of other Sylt *Leptonemella* species and other stilbonematine nematodes. While Lvic432 perfectly matched the symbionts of *L*. sp. B, Laph432 perfectly matched the symbionts of *L*. sp. D, E and G. To prevent unspecific binding of the one mismatch probes to non-target symbionts, we designed unlabelled competitor probes (c_Laph432 and c_Lvic432) that we used in combination with the species-specific symbiont probes (Table 1). All probes, except for the competitors, were ordered with a horseradish peroxidase (HRP)-label for subsequent catalyzed-reporter deposition fluorescence *in situ* hybridization (CARD-FISH) from Interactiva (Ulm, Germany) (Table 1). A 10% to 60% formamide series was performed with both probes and distinct signals were observed between 10 and 40% formamide. For all following hybridizations we used the probes at the most stringent concentration of 40% formamide.

Table 1: Oligonucleotide probes designed for this study

Probe	Target organisms	Probe sequence (5' → 3')	FA° [%]	Position*
SE585	Sylt *Leptonemella* ectosymbionts	CATCTGACTTATCTAGCCGC	40	585 - 604
Lvic432	*L. vicina* and *L.* sp. B ectosymbionts	TCTTCCCGACTGAAAGTGCT	35 - 40	432 - 451
Laph432	*L. aphanothecae* and *L.* sp. C, D, E and G ectosymbionts	TCTTCCCAACTGAAAGTGCT T	35 - 40	432 - 451
c_Lvic432	*L. aphanothecae* and *L.* sp. C, D, E and G ectosymbionts	TCTTCCCAACTGAAAGTGCT	35 - 40	432 - 451
c_Laph432	*L. vicina* and *L.* sp. B ectosymbionts	TCTTCCCGACTGAAAGTGCT	35 - 40	432 - 451

° formamide concentration in the hybridization buffer; * position in the 16S rRNA of *Escherichia coli*

CARD-FISH

Leptonemella vicina and *L. aphanothecae* individuals that we identified based on morphology were pre-embedded in liquid BactoAgar 3% (w/v) containing 2% formaldehyde in flat silicon embedding moulds (Plano GmbH, Wetzlar, Germany) and dried for one hour. In case of uncertainty we used part of the worm for sequencing the 18S rRNA gene to confirm its identity before embedding the remaining worm half. Agar pieces containing the worms were gradually dehydrated in an ethanol series of 50 - 96% ethanol and embedded in Steedman's

Wax (Steedman 1957). Wax blocks were sectioned (6 - 8 µm thick), dewaxed and rehydrated as described by Raggi *et al.* (Raggi *et al.* 2012). CARD-FISH hybridizations on tissue sections were done as described by Zimmermann *et al.* (2014). Serial hybridizations were performed with the probes Lvic432, Laph432 and SE585 (Table 1). On some sections we performed serial hybridizations with the positive control probes Gam42a (Manz *et al.* 1992) and EUB338 (I-III) (Amann *et al.*, 1990; Daims *et al.,* 1999) and the negative control probe Non338 (Glöckner *et al.,* 1999). The following fluorochrome-labelled tyramides were used: Alexa 488 (SE585, Gam42a), Alexa 633 (Laph432, EUB338), Alexa 546 (Lvic432, Non338) (Molecular Probes, Leiden, Netherlands). For counterstaining of deoxyribonucleic acid (DNA), the sections were stained with DAPI (4,6-diamidino-2-phenylindole) for 8 min after the hybridizations. Sections were embedded in a (1:5.5) mixture of Citifluor (Citifluor Ltd, Leicester, UK) and Vectashield (Vector laboratories, Burlingame, CA, USA). The sections were analysed using a confocal laser-scanning microscope (Carl Zeiss, LSM 780, Germany) with a 63 x 1.4 oil-immersion objective lens or 100 x EC Plan-Neofluar/1.3 oil-immersion objective lens. Pictures were acquired in a four-track mode with excitation at 405 nm (DAPI), 561 nm (Alexa546), 633 nm (Alexa633) and 488 nm (Alexa488). Brightness and contrast were adjusted with the ZEN 2011 software (Carl Zeiss, Germany).

Illumina Hi Seq library construction sequencing

Ectosymbiont fractions for metagenome sequencing were removed from the worms as described above. DNA was extracted separately from ectosymbiont pellets of four *L. aphanothecae* and one *L. vicina* individual with the Blood and Tissue Kit (Qiagen, Hilden, Germany), following manufacturer's instructions. DNA was extracted from the host as well, to confirm the morphological species identification by 18S rRNA sequencing (as described above). Genomic DNA from the ectosymbiont fractions was fragmented (COVARIS S2; COVARIS, Brighton, U.K.) to get an average fragment size of 500 bp. DNA volume was reduced (MinElute PCR purification kit; Qiagen, Hilden, Germany) and an Illumina-compatible library was prepared as recommend (Ovation® Ultralow Library Systems kit; NuGEN, Leek, The Netherlands). Library fragments were further size selected with by agarose gel electrophoresis, the target size was recovered (MinElute Gel Extraction Kit, Qiagen, Hilden, Germany) and quality assessed by Agilent TapeStation (Agilent,

Waldbronn, Germany). Libraries were quantified by fluorometry, immobilized and processed onto a flow cell with a cBot (Illumina, San Diego, U.S.A) followed by sequencing-by-synthesis with TruSeq v3 chemistry on a HiSeq2500 (Illumina, San Diego, U.S.A). For each ectosymbiont fraction, 6- 8 Mio 100 bp paired-end reads were sequenced.

Metagenome, assembly, binning and analyses

Metagenomes were sequenced on an illumina HiSeq 2500 sequencer with 2x100bp paired end libraries of an insert size of approx. 450bp. Raw read data was screened using Phyloflash (https://github.com/HRGV/phyloFlash), which analyses SSU rRNA read diversity and distribution to detect contaminations other than the targeted nematode/ectosymbiont. One library was contaminated with reads from a transciptomic library as detected by a bimodal insertsize distribution with a peak at 126 and one at 427. The contaminating library had the significantly shorter insert size, and the contaminating reads were removed by deleting all reads that could be merged by bbmerge distributed in the bbtools software package (http://sourceforge.net/projects/bbmap/). We removed adapters and phiX control reads using bbduk from bbtools and trimmed the reads to a minimum phred quality of 2. Cleaned and trimmed reads longer than 36bp were assembled with Spades (Bankevich *et al.*, 2012) using kmers 21, 33, 55 and 77 and the metagenomic assemblies were binned using Metawatt (Strous *et al.*, 2012). Draft metawatt bins were completed by using the fastg information of path connectivity between scaffolds provided by the Spades assembler using the fastg_parsing module of genome-bin-tools (https://github.com/kbseah/genome-bin-tools). To test for the completeness and contamination of the symbiont genomes we used checkM (Parks et. al, 2014) which screens for 281 conserved and single-copy marker genes in a phylogenetic lineage (here: *Gammaproteobacteria*).

To investigate genome rearrangements and genome similarities we used Mauve (Darling *et al.* 2010) to construct genome alignments. We re-ordered the contigs of all assemblies using E104 as a reference and aligned the genomes after setting the minimum number of matching nucleotides in a collinear region to 5 Mb. We calculated Average Nucleotide Identities (ANI) of the bacterial genomes based on BLASTn (Altschul *et al.* 1997) (ANIb) using JSpecies (Richter & Rossello-Mora 2009). To visualize nucleotide sequence similarities among all draft genomes we used BLAST Ring Image generator v0.95 (BRIG) (Alikhan *et al.* 2011). Genomes were annotated using RAST (Aziz *et al.* 2008) and the function- and sequence-

based comparison tools in RAST were used to compare shared and unique genes among the genomes. To calculate average amino acid identities among *L. aphanothecae* draft genomes we only used genes with bidirectional BLAST hit.

Single nucleotide polymorphisms (SNP) analysis

To detect SNPs within ectosymbiont populations of each individual and to compare polymorphisms between the populations we used the following SNP detection pipeline: For each of the five draft genomes, illumina paired-end reads were quality-checked, trimmed with a quality cutoff of q - 2 and mapped on the assembly using BBmap (version 33, http://sourceforge.net/projects/bbmap/, Bushnell, 2014). Only reads with a minimum sequence similarity of 90% were considered and only the best hit of ambiguously mapping reads was considered. Samtools (Li *et al.* 2009) was used to convert the bbmap output into a sorted bam file and only reads with a minimum mapping quality of - Q 20 were included. The initial assemblies were improved using the Pilon assembly correction tool (Walker *et al.* 2014) and the mapping with BBmap was repeated as described above. Reads of each symbiont population were mapped onto their own draft genome and also onto each draft genome assembled from the other symbiont populations. From all new bam files PCR duplicated single and paired-end reads were removed using Samtools (*rmdup*) (Li *et al.* 2009). The read coverage of the bam files was normalized to an average of 48 x with Samtools (*depth*) which was the lowest observed average coverage to ensure the comparability of the SNP calling results between all datasets (Li *et al.* 2009). Whole genome SNPs were called from the bam files, using the Samtools (*mpileup*)/Bcftools (*view*) commands with base (*Q*) and mapping quality (q) of 20 and filtered with the vcfutilis script providing that only SNPs with minimum read depth (*d*) of five were retained (Li *et al.* 2009). To extract SNPs from genes shared among all five draft genomes (‘core genes’), the Blast Score Ratio (BSR) (Rasko et al., 2005) approach that uses protein similarity as a measure was used in a three-step procedure. Since we did not want to call false SNPs on repetitive regions, we filtered out all genes that had particularly high coverage deviating from the mean (outliers that are above 1.5 x interquartile range), which depending on the dataset was usually higher than 105 x coverage. SNP calling was performed with Samtools (Li *et al.* 2009) as decribed above. The Mann-Whitney U-test, implemented in Past (Hammer *et al.* 2009) was used to test for statistically significant differences of SNP abundances within and

among *Leptonemella* ectosymbiont metagenomes. The Integrative Genomics Viewer (Thorvaldsdóttir *et al.* 2012) was used to visualize SNPs within and between individuals. SnpEff was used to annotate and predict the effect of each SNP on the amino acid sequence per genome region (Cingolani *et al.* 2012).

Direction of selection analysis (DoS)

To calculate the adaptive divergence between *Leptonemella* ectosymbionts, we used the Ortholog Direction of Selection Engine (ODoSE) (http://www.odose.nl/, Dec 2014, Goecks *et al.* 2010; Vos *et al.* 2013) hosted in a Galaxy environment (Giardine *et al.* 2005). We compared the draft genomes of the four *L. aphanothecae* symbiont strains (E103, E104, E107, E112) and the *L. vicina* strain (E220), as an outgroup. Only orthologs shared by all strains were used for the analysis.

Results

Seven *Leptonemella* species co-occur at the "Hausstrand" on Sylt

To identify different co-occurring *Leptonemella* species we sequenced the partial 18S rRNA gene of a total of 198 individual worms that we collected on the 'Hausstrand' on Sylt over a period of 10 years (Table S1). Phylogenetic analyses showed that all 198 sequences formed a highly supported monophyletic clade with previously published *Leptonemella* species and supported their clear separation from other stilbonematine nematode genera (Fig. 1). We identified a total of seven distinct 18S rRNA types, represented by four highly supported 18S rRNA clusters and three single branches (Fig. 1). The two most abundant 18S rRNA sequences formed one cluster with the previously published sequences of *L. vicina* and *L. aphanothecae*, respectively, that were identified based on morphological characters in the previous study (Ott *et al.* 2014) (Fig. 2). We could not identify the only other morphologically described species from Sylt, *L. gorgo*, and therefore none of the other five 18S rRNA phylotypes could be assigned to this species (Fig. 1). Nucleotide identities (ntIDs) of 1460 bp of the 18S rRNA sequences ranged from 99.99 - 100% within species, and 99.96 – 99.99% between species (Fig. 1 and 2). Our analyses did not show clustering of the *Leptonemella* species due to their geographic location, as indicated by the two *Leptonemella* sequences from Elba in the Mediterranean Sea that were interspersed with those from Sylt (Fig. 1).

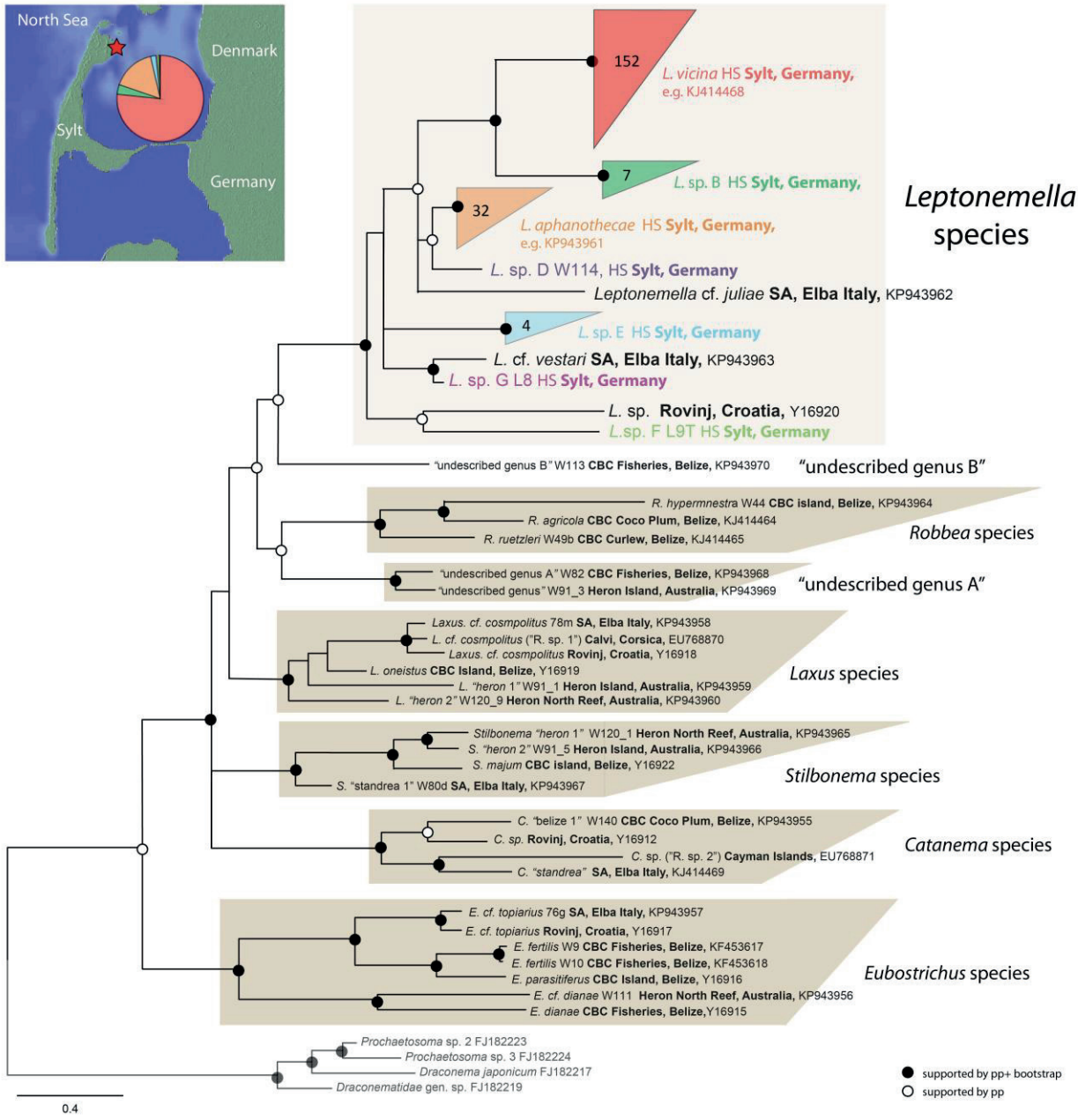

Fig. 1: Phylogeny of *Leptonemella* species with other stilbonematine nematodes. Consensus tree of Bayesian inference (mrBayes) and maximum likelihood (RaxML) analyses of stilbonematine 18S rRNA genes. *Leptonemella* sequences constructed in this study are highlighted in colors, corresponding to the seven co-occuring species. The sampling location is indicated by a red star in the map shown as an insert in the upper left. The pie chart shows the relative amount of sequences per species that was analyzed in this study. Brown boxes show monophyletic groups of stilbonematine species that belong to the same genus. Sequences published prior to this study are discernible by their accession numbers. Nodes that were statistically supported in both analyses (> 80% bootstrap value and 0.80 posterior probability (pp) value) are highlighted in black, nodes that were statistically supported only in Bayesian inference are highlighted in white. Provisional working names for undescribed species are in quotes. The scale bars represent 4% nucleotide sequence divergence. HS: Hausstrand, CBC: Carrie Bow Cay.

Each Leptonemella species is associated with specific ectosymbionts

To investigate the specificity of the *Leptonemella* ectosymbioses, we sequenced the bacterial 16S-ITS-partial 23S rRNA sequences of 39 individuals from six different *Leptonemella* species from which also the 18S rRNA gene was sequenced. We constructed symbiont 16S-ITS-23S rRNA clone libraries for 21 individuals, of which host DNA was extracted along with symbiont DNA, and for two individuals, from which we had pure symbiont extracts (Table S1). Partial ectosymbiont 16S-ITS sequences from each of the clone libraries always revealed highly similar to identical sequences (> 99.99% nucleotide identity), even when up to 183 clones were sequenced from a single individual (Table S1). Full and bidirectional sequencing of 1 - 10 selected clones always resulted in 100% identical 16S-ITS-23S rRNA sequences per individual, indicating that each *Leptonemella* individual is associated with a dominant 16S-ITS-23S rRNA phylotype. This was confirmed by direct sequencing of the full 16S-ITS-partial 23S rRNA sequence from pure ectosymbiont extracts of a further 13 individuals that always resulted in a very clear chromatogram.

Symbiont sequences from each of the six *Leptonemella* host species formed highly supported clades in both maximum likelihood and Bayesian inference analyses, based on the 16S-ITS-23S rRNA. Only the symbionts of one species, *L. sp.* B, formed two divergent, although highly host species-specific clades (Fig. 2). None of the seven species-specific 16S-ITS-23S rRNA phylotypes was found on any of the other co-occuring and closely related *Leptonemella* species (Fig. 2). While nucleotide sequence identities of 16S rRNA sequences ranged from 99.3 - 100% between symbionts from different species, ITS identities ranged from of 90 - 97.8%, resulting in a much higher phylogenetic resolution than the 16S rRNA alone (Fig. 2, Fig. S1).

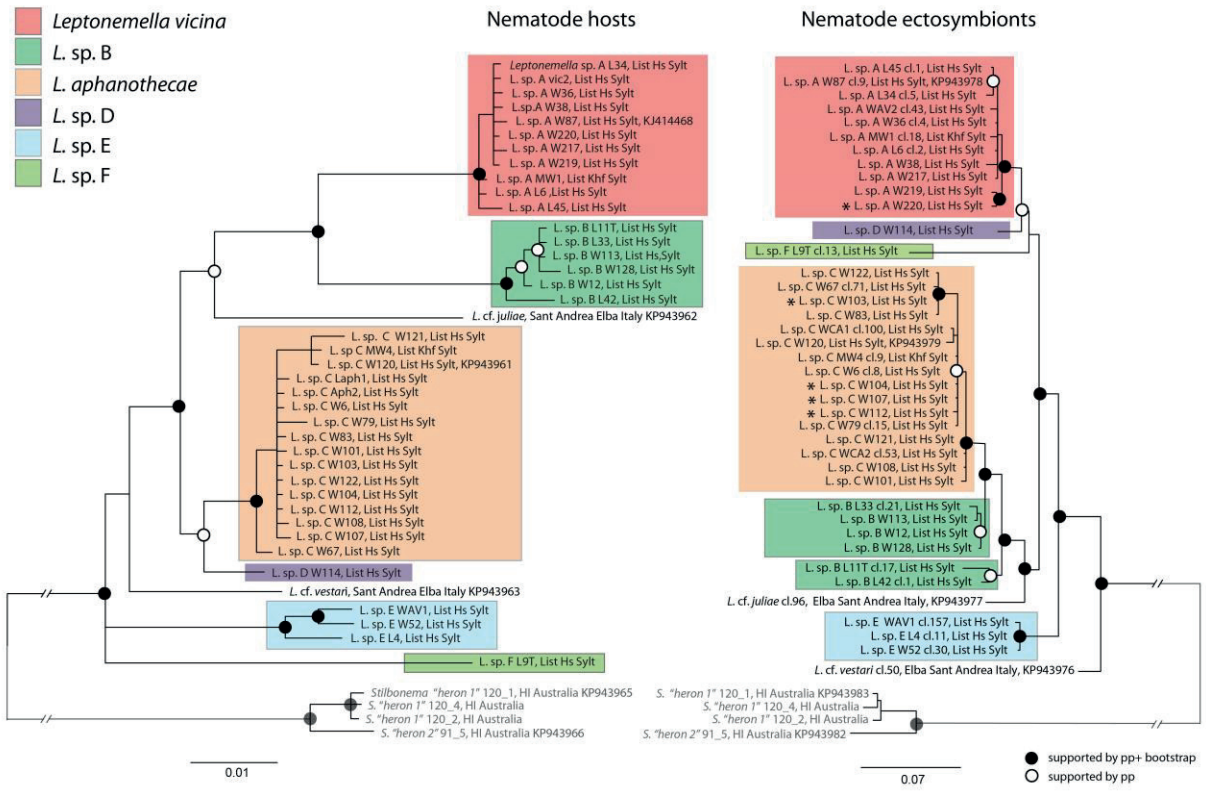

Fig. 2: Cophylogeny of Sylt *Leptonemella* nematodes with their ectosymbiotic bacteria. Consensus trees of Bayesian inference (mrBayes) and maximum likelihood (RaxML) analyses of host 18S rRNA sequences and 16S-ITS-partial 23S rRNA sequences of their ectosymbionts. Colored boxes show monophyletic groups of different *Leptonemella* host species and their ectosymbionts, respectively. Sequences published prior to this study are discernible by their accession numbers. Black stars show individuals that were used for symbiont metagenome sequencing. Nodes that were statistically supported in both methods (> 80% bootstrap value and 0.80 posterior probability (pp) value) are highlighted in black, nodes that were statistically supported only in Bayesian inference are highlighted in white. The scale bars represent 1% and 7% nucleotide sequence divergence, respectively. Hs: Hausstrand, Khf: Königshafen, HI: Heron Island.

Apart from the symbiont sequence differences between *Leptonemella* species, symbiont 16S-ITS-23S rRNA sequences from different individuals of the same *Leptonemella* species were sometimes slightly different, with up to 2.2 % nucleotide differences on the ITS level. This was particularly clear for *L. vicina* and *L. aphanothecae,* that were the most abundant species in our sample set (Fig. 2). *L. vicina* individuals were associated with at least three 16S-ITS types while *L. aphanothecae* individuals were associated with at least four 16S-ITS types. As explained above, the host 18S rRNA sequences were also not always identical within a species, but there was no clear association of particular host 18S rRNA sequences with particular 16S-ITS types at the individual level. Similarly, the Mantel test showed no significant correlation between intraspecific host and symbiont sequence distances using Jukes Cantor ($r < 0.2$, $P > 0.2$) or patristic distances ($r < 0.5$, $P > 0.4$) (Fig. 2).

The branching patterns of host and symbiont phylogenies were incongruent. For example, *L. vicina* and *L.* sp. B formed a monophyletic clade in the host tree, but their symbionts did not (Fig. 2). Similarly, *L.* cf. *juliae* from the Mediterranean Sea fell basal to *L. vicina* and *L.* sp. B from Sylt while its symbionts fell basal to *L. aphanothecae* and *L.* sp. B symbionts. A mantel statistic based on spearman's rank correlation showed that host and symbiont sequences were not significantly correlated when using Jukes-Cantor distances matrices ($r = 0.095$, $P = 0.176$).

Species-specific ectosymbionts confirmed *in situ*

To verify the species specificity of the symbionts *in situ*, we performed CARD-FISH on *Leptonemella* sections with specific 16S rRNA probes to target the symbionts of the most abundant species on Sylt. We analyzed two *L. aphanothecae* and four *L. vicina* individuals. Triple hybridizations were done on 5 - 10 sections per individual using the two species-specific symbiont probes (Lvic432; Laph432) with their respective competitor probes (Table 1). All ectosymbiotic bacteria on *L. vicina* hybridized with the Lvic432 probe while all bacteria on *L. aphanothecae* hybridized with the Laph432 probe, and never vice-versa (Fig. 3). All bacteria were stained by the general Sylt *Leptonemella* symbiont probe (LE585), which was used as positive control (Fig. 3). In addition, all bacteria hybridized with the Gammaproteobacteria-specific probe Gam42a but never with the negative control probe NON338 (Manz *et al.* 1992; Wallner *et al.* 1993) (Fig. S2).

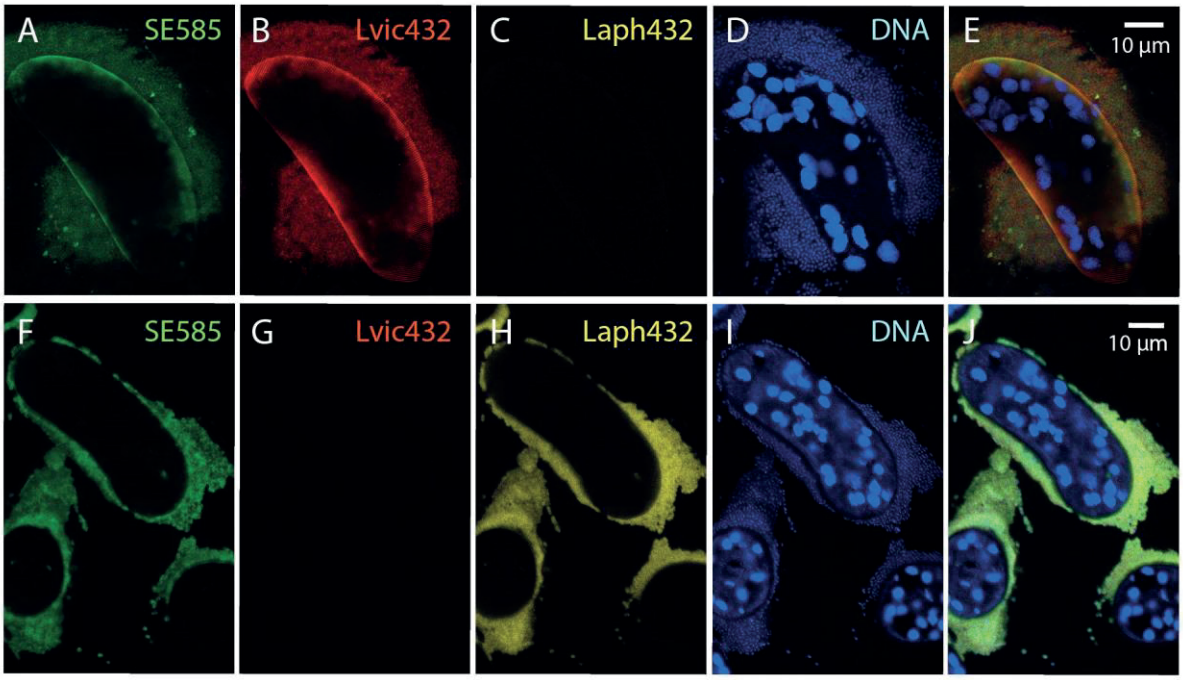

Fig. 3: Ectosymbionts of *Leptonemella vicina* (A - E) and *L. aphanothecae* (F - J) hybridized with species-specific symbiont probes. Laser scanning microscope pictures show longitudinal sections of both species that were hybridized with CARD-FISH probes targeting Sylt Leptonemella ectosymbionts (SE585) (A and F), *L. vicina* ectosymbionts (Lvic432) (B and G) and *L. aphanothecae* ectosymbionts (Laph432) (C and H). Sections D and I show counter-staining with DAPI and E and J shows an overlay of A - D and F - I, respectively.

Each worm individual is associated with a distinct symbiont strain

To investigate symbiont microdiversity and whether the individual differences in the symbiont ITS sequences reflected differences across the entire genome, we sequenced the metagenomes of ectosymbiont fractions from four *L. aphanothecae* individuals (E103, E104, E107 and E112) and one *L. vicina* individual (E220), as an outgroup, using paired-end Illumina sequencing. Small subunit rRNA reconstruction from the metagenome reads resulted in a single gammaproteobacterial rRNA per symbiont fraction that could be clearly assigned to the ectosymbionts (Table S2, Fig. S4). Similalry, the single copy marker genes *recA*, *dnaK*, *mreB*, *fumC*, *icd*, *gyrB*, *mdh* and *rpoD* were distinct between all symbionts (Fig. S5). Individual symbiont genome assemblies resulted in almost complete draft genomes, as indicated by one rRNA operon, 45 transfer RNAs (tRNAs), tRNA sequences for each of the 20 amino acids (aa) and the almost complete set of 281 conserved and single-copy marker genes (93 - 98%) (Table S2). Draft genomes were 4.7 to 5.1 mega base pairs (Mb), with a GC content of 58.4 – 58.9%. Four of the five draft genomes had a few duplicate marker genes (2 - 5), but the largest genome, E112 had 12 duplicate marker genes (Table S2). Although draft genomes were almost complete, they were contained on more than 1000

contigs (Fig. S3 and Table S2). This could either be due to genomic heterogeneity or repetitive elements that are longer than the library insert size (e.g. Treangen & Salzberg 2012). Due to the fragmentation, the correct contig order could not be resolved. However, whole genome alignments of re-ordered contigs indicated pronounced genome rearrangements between symbionts of *L. aphanothecae* compared to the *L. vicina* symbiont that could even be detected within these short contigs (Fig. 4).

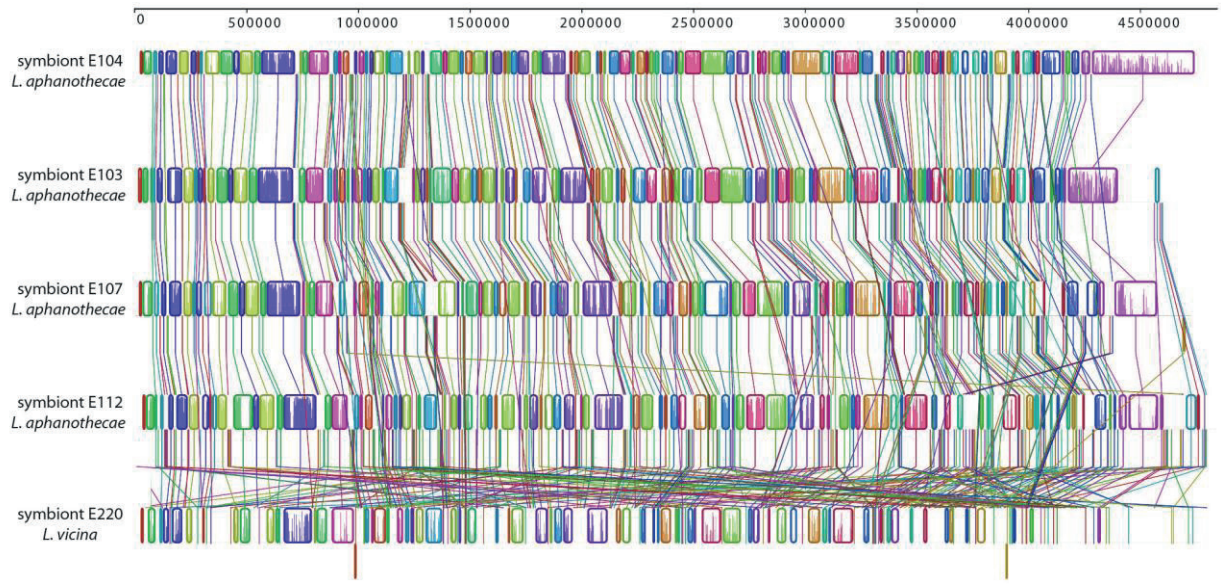

Fig. 4: Whole genome alignment of the *Leptonemella aphanothecae* and *L. vicina* ectosymbiont draft genomes. The draft genome of E104 was used as a reference and the contigs of all other assemblies were re-ordered according to the reference. Each colored block represents a linear collinear block (LCB), a conserved genome segment free of genome rearrangements between the aligned genomes. LCBs that are presumably homologous between the genomes are connected with lines. Regions outside blocks lack detectable homology among the input genomes. The height of the similarity profile inside each LCB corresponds to the average level of conservation in that genome region. Areas that are completely white probably contain sequence elements specific to a particular genome. The figure was created using Mauve (Darling et al. 2010).

Average nucleotide identities (ANI) between the four *L. aphanothecae* symbiont draft genomes were on average 97.4 ± 0.1%, which is above the commonly accepted prokaryotic species threshold of 95 - 96% ANI (Richter & Rossello-Mora 2009). Intra-species ANIs corresponded to amino acid sequence identities of 99.7 ± 0.1% (Fig. 5, Table S3). ANIs were similarly high between all sequenced *L. aphanothecae* strains and this was not necessarily correlated to differences on the 16S-ITS rRNA sequences. For example, 16S-ITS sequences of *L .aphanothecae* strains E104 and E107 were identical, while E103 showed 6 unique bp differences on the ITS level (Fig. S4). RAST sequence-based gene comparisons showed that each *L. aphanothecae* strain had 13.6 ± 1.6% unique genes, corresponding to 205 - 340

unique genes per genome, with 84 - 90% of these annotated as hypothetical genes (Table S4 and S5).

ANIs between the *L. aphanothecae* and the *L. vicina* symbiont E220 were 93.3 ± 0.3% and thus are different enough to be called species (Richter & Rossello-Mora 2009). Correspondingly, the *L. vicina* symbiont E220 draft genome contained 825 unique genes, corresponding to 25.16 ± 0.8% unique genes compared to the *L. aphanothecae* symbionts (Table S3, S4). Just as for the *L. aphanothecae* strains, most of the genes that were unique to *L. vicina* were hypothetical genes (74%) (Table S5). All genomes contained a high numer of mobile genetic elements (Table S2).

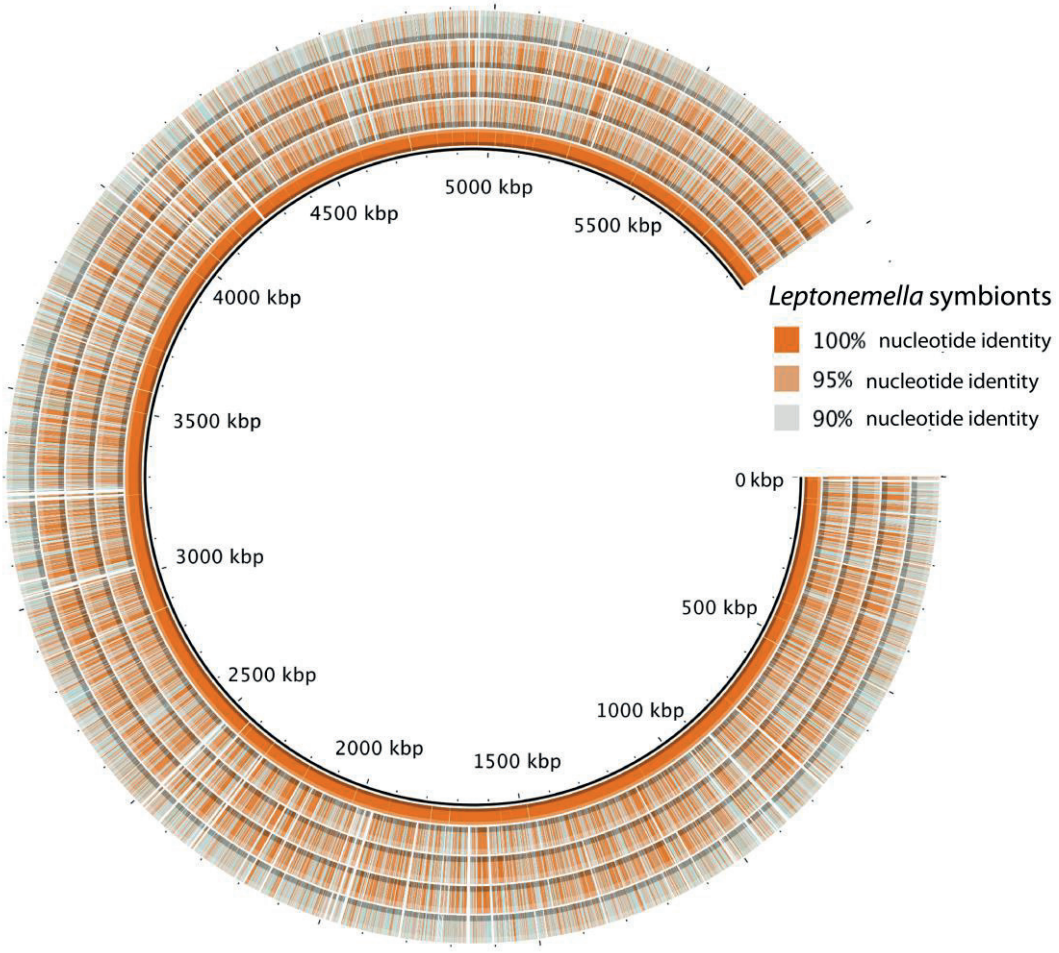

Fig. 5: Nucleotide sequence similarity comparison of *Leptonemella* ectosymbiont draft genomes based on BLASTn. The innermost ring shows the comparison of the reference draft genome of the *L. aphanothecae* symbiont E104 to itself (100%). The other rings, in order from innermost to outermost show comparisons to the other *L. aphanothecae* symbiont draft genomes: E103, E107, E112 and the draft genome of the *L. vicina* symbiont E220. The figure was created using the BLAST Ring Image Generator (BRIG) (Alikhan et al. 2011).

Adaptive selection analysis

To determine which genes could potentially be under selection, we calculated the Direction of Selection (DoS) statistics, using the four *L. aphanothecae* genomes as an ingroup and the *L. vicina* genome as an outgroup. DoS is an extension of the McDonald-Kreitman test that compares the ratio between non-synonymous and synonymous substitutions within a species, in our case *L. aphanothecae* strains E103, E104, E107, E112, to that between species (*L. vicina* strain E220), as a measure of selection pressure (McDonald *et al.* 1991; Eyre-Walker 2006; Stoletzki & Eyre-Walker 2011). We found that much more genes between the *Leptonemella* ectosymbionts were potentially under positive selection (positive DoS) than genes potentially under negative selection (negative DoS) (Table 2, and S6). Many of the genes with positive DoS were genes involved in energy-, sulfur- and carbon- metabolism, but also involved in host-symbiont recognition or attachment. Examples for the latter were genes, such as type IV pili that are often involved in biofilm formation or host attachment and rhamnose-containing glycans, that can be involved in cell-cell interaction, respectively (Hooper & Gordon 2001; Bahar *et al.* 2009).

Table 2: DoS results based on the comparison of *Leptonemella* symbiont draft genomes. Four *L. aphanothecae* symbiont draft genomes were used as ingroup and the *L. vicina* symbiont draft genome as outgroup.

DoS	House-keeping genes (maintaining basic cellular functions)	Energy/ sulfur/ carbon metabolism genes	Host recognition/ adhesion genes	Antimicrobial resistance genes	Defense gense	Other genes
Positive (> 0.2)	20	17	15	5	5	72
Negative (< - 0.2)	3	4	2	0	0	13

Genome-wide microdiversity in the symbiont population from single worms

To investigate whether multiple closely related symbiont strains can co-occur on one host individual, which would be masked by the consensus assembly, we performed polymorphism analyses with our optimized SNP pipeline by using the complete read sets from each of the *Leptonemella* ectosymbiont populations. No SNPs were found in the rRNA operons of any of the symbiont populations. Similarly, no SNPs were detected in single-copy and

housekeeping genes such as *recA*, *dnaK*, *mreB*, *fumC*, *icd*, *gyrB*, *mdh* and *rpoD.* Four of five symbiont populations SNP densities ranged from 0.07 - 0.23 SNPs/kb in core genes, and 0.37 – 0.76 SNPs/kb across the entire genome including intergenic regions (Fig. 6, Table S7). Only the symbiont population of *L. aphanothecae* strain E112 showed genome-wide SNPs densities that were 5 – 20 times higher compared to the other symbiont populations (Fig. 6, Table S7). SNPs were distributed throughout the genomes and we could not detect genes with a high number of SNPs that were shared among all of the *Leptonemella* strains (Fig. 6).

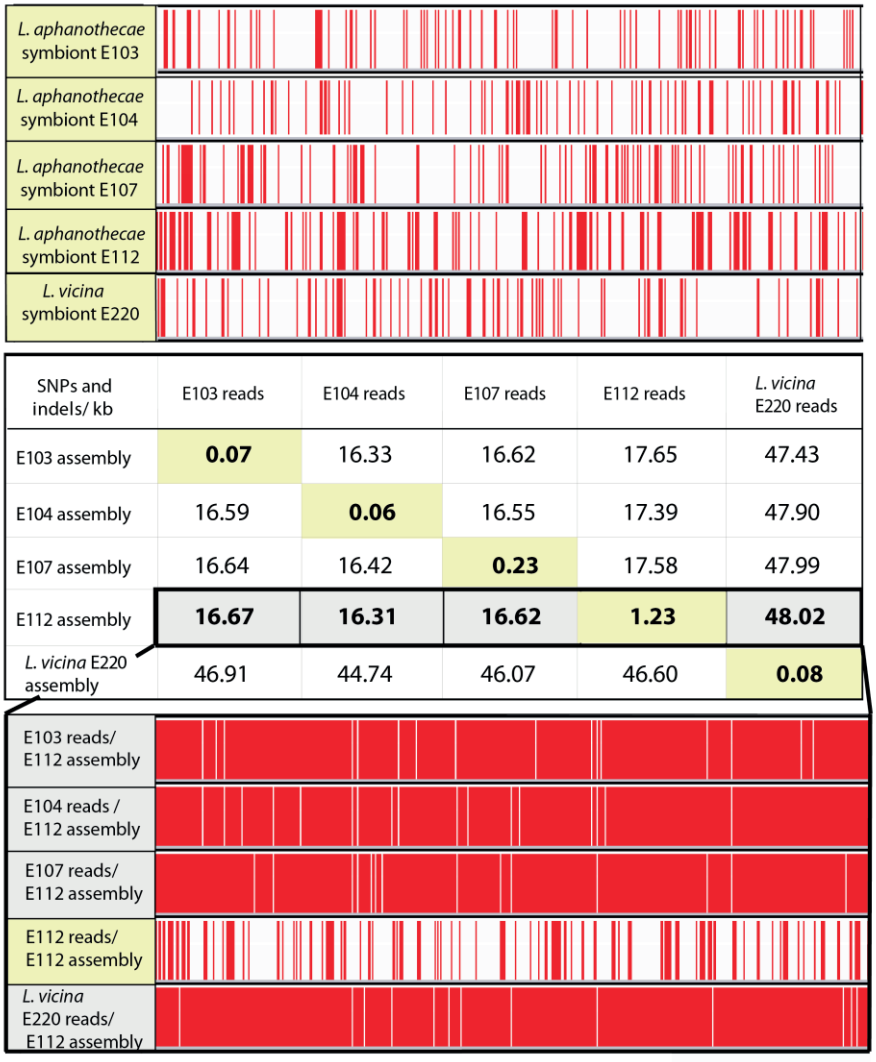

SNPs and indels/ kb	E103 reads	E104 reads	E107 reads	E112 reads	*L. vicina* E220 reads
E103 assembly	**0.07**	16.33	16.62	17.65	47.43
E104 assembly	16.59	**0.06**	16.55	17.39	47.90
E107 assembly	16.64	16.42	**0.23**	17.58	47.99
E112 assembly	**16.67**	**16.31**	**16.62**	**1.23**	**48.02**
L. vicina E220 assembly	46.91	44.74	46.07	46.60	**0.08**

Fig. 6: Pairwise single nucleotide substitutions (SNPs) and insertions/deletions (indels) in core genes within and between *Leptonemella* symbiont populations. Variants were called from shared genes when mapping reads of each *Leptonemella* symbiont population onto its own consensus assembly (upper and middle panel) or to the assemblies from other individuals (middle and lower panel). Each red bars represents one variant. The lower panel shows the amount of SNPs detected when mapping reads of each symbiont population onto the consensus assembly of E112. Variants were visualized with the Integrated Genome Viewer (IGV) (Thorvaldsdóttir et al. 2012).

To investigate how genetically different the *Leptonemella* symbiont populations are compared to each other we mapped the reads of each symbiont population onto the draft genomes of the other symbionts. SNP counts among the different *L. aphanothecae* symbiont populations were approximately 22 times higher than within-population heterogeneity when including the whole genome, corresponding to 12 - 14 SNPs/kb (Table S5). When only core genes were included SNP densities were similarly high, and ranged from 16 - 18 SNPs/kb, among the *L. aphanothecae* strains respectively (Fig. 6, Table S7). The Mann Whitney Test confirmed that SNP counts were significantly higher between than within individual fractions ($P < 0.002^{**}$), Table S8). For comparative reasons, we pooled all of the *L. aphanothecae* symbiont read sets and mapped them onto each of the draft genomes and got SNP numbers that were slightly higher, ranging from 18 - 21 SNPs/kb (not shown). We also mapped each of the four *L. aphanothecae* symbiont read sets onto the *L. vicina* E220 draft genome and vice versa, and SNP counts were significantly higher than within and among *L. aphanothecae* symbiont genomes (Mann Whitney Test ($P < 0.005^{**}$) (Fig. 6, Table S7 and S8).

Discussion

Leptonemella individuals with essentially clonal ectosymbiont populations

Our in-depth phylogenetic analyses of a total of 39 individual *Leptonemella* ectosymbioses from Sylt and metagenomic sequencing of four more symbiont populations showed that each *Leptonemella* individual is consistently associated with a single and dominant bacterial symbiont phylotype (Fig. 2 and 5). Clonal symbiont populations, have first been suggested by Polz et al. (1994) that noted the striking morphological uniformity of the *Laxus oneistus* symbionts and showed with *in situ* hybridizations that all ectosymbionts on one individual are stained by the symbiont-specific 16S rRNA probe. Multiple identical 16S rRNA clone sequences were also obtained from three *Robbea* and two *Eubostrichus* species, and similarly to the previous study, the 16S rRNA clonality was verified by symbiont-specific fluorescence *in situ* hybridization on the symbiont coat (Bayer *et al.* 2009; Pende *et al.* 2014). A recent study by Zimmermann *et al.* (in prep., Chapter III) added to the 16S rRNA clonality by showing with a number of clones that single individuals also harbor symbionts with identical ITS region, which provides higher resolution than the conserved 16S rRNA gene on

the strain level (e.g. Brown *et al.* 2005; Ngugi & Stingl 2012). However, the low sequencing depth in previous studies would have only revealed the most dominant bacterial phylotype and the usage of single marker genes does not reflect fine-scale genome diversity. In this study, we were able to confirm and add up to these previous results by investigating symbiont clonality with a total of three different molecular methods and two different sequencing technologies. Firstly, direct Sanger sequencing of the PCR product from ectosymbiont fractions always resulted in a very clear chromatogram. Secondly, multiple 16S-ITS-partial 23S rRNA clones that were Sanger-sequenced from each individual always resulted in the exact same gammaproteobacterial symbiont sequence, whether 2 or 180 clones were sequenced (Table S1). Thirdly, we sequenced up to 8 Mio paired-end Illumina reads of five selected *Leptonemella* symbiont populations, and we never found a single SNP-containing read in either metagenome that mapped to the small ribosomal rRNA operon (SSU rRNA) in the respective consensus assembly. The same held true when reads were mapped to eight commonly used single-copy marker genes. All three analyses clearly indicated that *Leptonemella* individuals do not harbour multiple closely related gammaproteobacterial symbiotic strains, at least none that can be distinguished by the commonly used strain genetic markers. This is similar to what has been found for some other marine chemosynthetic symbioses, such as the hydrothermal vent tubeworm or scaly-foot gastropods that both harbor a clonal and species-specific endosymbiont strain (Robidart *et al.* 2008; Nakagawa *et al.* 2014) (see also Discussion below). However, unlike endosymbionts that are enclosed in host tissue, ectosymbionts are constantly exposed to the environment and also to potential competitors. Still, *Leptonemella* ectosymbioses have apparently found very effective ways to keep their ectosymbiont coat “clean” from other bacteria than the ectosymbiont strain. This is consistent with evolutionary theory, which predicts that it should be most beneficial for hosts to sustain an essentially clonal symbiont population in order to prevent competition and virulence (Frank 2003).

Ectosymbionts are never shared between co-occurring *Leptonemella* species

Phylogenetic analyses of multiple individuals of the six co-occurring *Leptonemella* species and their ectosymbionts showed that the associations are species-specific without exception (Fig. 2). Symbionts of each *Leptonemella* species always fell into corresponding species-specific symbiont clades in the 16S-ITS-partial 23S rRNA phylogeny (Fig. 2). Mantel tests

results provided further support for a strong correlation between symbiont and host genetic distances. The species-specificity was also confirmed by specific CARD-FISH probes that either consistently hybridized with all symbionts of *L. aphanothecae* or *L. vicina,* but never both (Fig. 3). Further support that symbionts are distinct between *L. aphanothecae* and *L. vicina* was provided by the five assembled symbiont draft genomes that were highly divergent between both species, with ANIs of 93% (Fig. 4 and 5). Even when individuals of the *L. aphanothecae* and *L. vicina* were sampled from another location 1.5 kilometer away, symbiont 16S-ITS-partial-23S rRNA were identical to symbionts from the main sampling location ("Hausstrand"), supporting the strong influence of the host species on symbiont diversity (Fig. 2).

Previous studies on stilbonematine nematodes have also suggested that the associations are highly species-specific. For example Bayer *et al.* (2009) showed that each of three different stilbonematine species from different ocean regions were associated with different 16S rRNA symbiont types. A furthert study that examined two co-occurring *Eubostrichus* species in the Caribbean Sea found the same, as shown by distinct 16S rRNA sequences per species and specific FISH probes that stained all symbionts of the respective sepcies (Pende *et al.* 2014). Distinct 16S-ITS symbiont types were also reported by our recent large-scale study that analyzed 16 species from multiple stilbonematine nematode genera around the world (Zimmermann *et al*., in in prep., Chapter III). In addition to previous studies that investigated a maximum number of three individuals per species and a maximum of two co-occurring species, we were able to show that the species-specific patterns holds true, even when up to 16 individuals of a total of six co-occurring and very closely related species are investigated from the same beach. This indicates that recognition mechanisms, even between closely related species must be highly specific.

One of the mechanisms that could maintain species-specific ectosymbiotic associations was identified for the stilbonematine nematode *Laxus oneistus* that secretes lectins on the hosts' cuticle, which recognize specific sugar residues on the symbionts' cell membrane (Nussbaumer *et al.* 2004; Bulgheresi *et al.* 2006; Bulgheresi 2011). Lectins are secreted by glandular sensory organs (GSOs) only present in Stilbonematinae. *L. oneistus* lectins are only secreted by GSOs on the posterior region of the cuticle, and symbiotic bacteria are only found on this region of the worm (Nebelsick *et al.* 1992; Bauer-Nebelsick *et al.* 1995). The specific sugars involved in lectin interaction were identified as D-mannose and L-rhamnose

in *L. oneistus* (Nussbaumer *et al.* 2004). Interestingly a total of 12 genes involved in lipopolysaccharide synthesis, including two specifically involved in rhamnose glycane synthesis were listed to be under positive selection between the *Leptonemella* species in our DoS analysis (Table S6). Glycans are sugars bound to glycolipids or gylcoproteins on the outer surface of the cell and are also involved in host symbiont recognition in the Vibrio-squid and coral-dinoflagellate symbioses (McFall-Ngai *et al.* 1998; Hooper & Gordon 2001). The extraordinarily high level of amino acid (aa) substitutions in those genes indicates that selective pressure may especially drive those recognition proteins to adapt, possibly as a result of an arms race between closely related symbionts that might compete for living space on the host. Other genes potentially under positive selection were type IV pili and these are known to be involved in host attachment and colonization of e.g. symbiont-housing organs in squids or the earthworm symbioses (Table S6) (Mattick 2002; Stabb & Ruby 2003; Dulla *et al.* 2012). These results suggest that similar to *L. oneistus*, lectin-sugar interactions may also play a role in recognizing the specific symbionts of *Leptonemella*, and that type IV pili could also be involved in maintaining symbiont host-symbiont cohesion.

Incongruent phylogenies indicate host switching between *Leptonemella* species

Our cophylogeny analysis including *Leptonemella* species and their ectosymbionts from Sylt and the Mediterranean Sea did not show congruent patterns between host 18S rRNA and symbiont 16S-ITS trees (Fig. 2). This is in contrast to our previous study that suggested codiversification between *Leptonemella* symbionts and their host (Zimmermann *et al*., in in prep., Chapter III). However, the latter study only included four *Leptonemella* species into their analyses, while this study included individuals of eight different species. One illustrative example for the incongruent patterns are the 18S rRNA clade of *L.* sp. B that is closely related to *L. vicina,* but their symbionts are not (Fig. 2). *L.* sp. B was also the only exception in associating with either of two species-specific symbiont clades. This indicates that the evolutionary history of closely related and co-occuring *Leptonemella* species was not strictly coupled with the evolutionary history of their ectosymbionts but that either symbiont replacements or host switches between the species must have happened in the past. *L.* sp. B must have acquired a second symbiont in some point of evolution as indicated by two symbiont clades, specific to *L.* sp. B (Fig. 2). One explanation could be that the replacing symbiont had a strong selective advantage over the original symbiont, such as being much

better adapted to certain environmental conditions. However, whether the different symbionts of *L.* sp. B are restricted to a certain micro-niche on the Hausstrand on Sylt or whether their hosts also show differences not visible on the 18S rRNA level, which could give indications for a nascent speciation event is not clear from this analysis. Indications that symbiont replacement events may have also happened in other stilbonematine nematodes were given by our previous study that showed multiple origins of the *Laxus* symbionts (Zimmermann *et al.*, in prep., Chapter III). Even for intracellular symbionts that are strictly vertically transmitted, i.e. from mother to offspring, occassional symbiont replacement events have been suggested, and in fact are a rather common phenomenon for both ecto- and endosymbiotic associations (e.g. Lefèvre *et al.* 2004; reviewed by Bright & Bulgheresi 2010; Ebert 2013). However, if such events are likely to happen, why do we see a predominant codivergence pattern for closely related stilbonematine species within different genera around the world (Zimmermann *et al.*, in prep., Chapter III)? This can be explained by two factors: (1) chances for host switching events are higher for co-occurring stilbonematines, since physical proximity is needed for the event to occur, and (2) host switches are much more likely to occur between species of the same genus, as shown by our previous study that revealed consistent clustering of host and symbionts from different genera (Zimmermann *et al.,* in prep., Chapter III). Host and symbionts of more than two closely related stilbonematine species have never been investigated before and we thus hypothesize that incongruent phylogenies will be recurringly found when mutliple co-occurring and closely related species are examined from a single sampling location.

To each its own- distinct symbiont strain per individual

Population-level genetic diversity is a key driver of the ecology and evolution of free-living microbial communities but population-level diversity within marine symbioses is not well studied (Hughes *et al.* 2008; Parkinson & Baums 2014). Our results show that in addition to the remarkable species-specificity of the co-occurring *Leptonemella* species, the ectosymbionts on different individuals of the same species can be quite distinct. Different symbiont 16S-ITS-partial 23S rRNA phylotypes were found on all *Leptonemella* species for which more than three individuals were available (Fig. 2). These genetic differences at the host individual level were confirmed by our metagenome analyses of four ectosymbiont populations of *L. aphanothecae* individuals that resulted in distinct symbiont draft genomes

for each single worm with ANIs of 97.3 - 97.6% and which were also distinct on many single copy marker genes (Fig. 5 and S3, Table S3 and S4). Apart from individual-specificity in *Leptonemella* species, we also found evidence for individual-specific ectosymbionts on other stilbonematine nematode genera, e.g. *Stilbonema* "heron A" individuals from Australia showed clear symbiont sequence differences on the 16S-ITS level (Fig. 2) and we also have further evidence that symbionts are also different among *Eubostrichus* cf. *topiarius* individuals from Sant' Andrea in Elba, Italy (not shown). Considering the wide distribution, diversity and abundance of *Leptonemella* and other *Stilbonematinae* in sulfidic sediments worldwide, this suggests a tremendous pool of genetic diversity, with a vast potential for evolutionary novelty.

How is this individual-specificity comparable to other studies? Not many studies have investigated symbiont populations of single individuals of the same species across the entire symbiont genome. For example, one study compared genomes of four strains of the intracellular *Buchnera* Mp in the green peach aphid host *Myzus persicae,* and showed limited pairwise genetic differences of maximum 0.3 SNPs/kb along their highly conserved genomes, corresponding to ANIs > 99.9% (Jiang *et al.* 2013). *Buchnera* are vertically transmitted symbionts (from mother to offspring) that have highly reduced genomes, and due to their isolation from the environment they lack the possibility to recombine with other closely related strains, resulting in **population bottlenecks and therefore accumulation of harmful mutations over time (Moran 1996; Vrijenhoek 2010). Strain diversity in such vertically transmitted intracellular endosymbionts is therefore commonly very low. However, also symbionts that are horizontally acquired, can show very little genetic differences between individuals. For example, endo**symbiont draft genomes of the hydrothermal vent tubeworm *Riftia pachyptila* were based on reads sets from symbiont pools of two individual worms (Robidart *et al.* 2008). The authors did not find a single SNP on the SSU rRNA nor in single copy genes when pooling symbionts of two *Riftia* individuals, although polymorphism densities along the genome were reported as 2.9 SNPs/kb genome (Robidart *et al.* 2008). Genetic heterogeneity was also extremely low for potentially horizontally transmitted endosymbiont populations of different scaly-foot snail individuals (Nakagawa *et al.* 2014). In the latter study, 19 marker genes

including the SSU rRNA from a total of 32 individuals were compared and only in a single snail did the authors find indications for two SNPs or allele copies for two of the genes (Nakagawa *et al.* 2014). The authors argued that stringent symbiont selection by the host may prevent random genetic drift in the symbiont populations. In contrast, each of the *Leptonemella* symbionts had a dictinct SSU rRNA sequence and also most of the single copy genes were distinct between individuals (Fig. S4 and S4). Our results thus indicate that the *Leptonemella* ectosymbionts show a high intraspecies diversity compared to the endosymbionts of other characterized mutualistic symbioses.

Mechanisms that could explain the intraspecies diversity

How can we explain this relatively high genetic divergence between symbiont populations of *Leptonemella* individuals? To understand the differences between individuals, we first have to understand the processes that occur on a single individual. In contrast to endosymbionts, ectosymbionts are exposed to free-living environmental populations and therefore also new genetic material of free-living bacteria in the sediment. All of the *Leptonemella* ectosymbionts had large genomes of around 5 Mb, indicating that population bottlenecks apparently do not lead to genome reduction, such as known for intracellular and vertically transmitted endosymbionts, such as *Buchnera* (Moran 1996; Moran *et al.* 2009). Furthermore, SNP numbers ranged from 0.4 - 1 SNPs/kb genome per individual, indicating that even though distinct strains cannot be distinguished on the basis of commonly used marker genes, populations do show some signs of genetic heterogeneity.

Similar to other free-living bacteria, e.g. in microbial biofilms, acquisition of new genetic material from close-living relatives or other environmental bacteria would therefore be possible for ectosymbionts (Allen *et al.* 2007; Simmons *et al.* 2008). In addition, the *Leptonemella* genomes contained a high number of up to 180 transposable elements (TE) in their genomes (Table S2), which is similar to what has been observed in their closest relative, the extracellular endosymbiont of *O. algarvensis* (Woyke *et al.* 2006; Kleiner *et al.* 2013). TEs are selfish genetic elements that are involved in gene deletion, duplication and rearrangements and are known to drive evolutionary innovation, and can even lead to the evolution of new strains adapted to distinct ecological niches (Leavis *et al.* 2007; Werren 2011). Fast processes such as the spread of TE and phase inversions are commonly known to add to higher population level heterogeneity in otherwise clonal populations (Cerdeño-

Tárraga *et al.* 2005; Chain *et al.* 2006; Allen *et al.* 2007). Finally, horizontal uptake of genes from free-living bacterial populations may add to the genetic divergence of *Leptonemella* ectosymbionts. The high percentage of 12 - 14% unique genes in each of the ectosymbiont genomes indicate that such horizontal uptake could have happened, although the fact that we could not find these genes in the other assemblies could be an artefact of the fragmented assemblies (Table S4 and S5). Natural mutations combined with recombination and diversification through transposases that were involved in the microevolution of the ectosymbiont strains may explain the slightly diverse symbiont populations on a single worm.

Recent studies suggest that stilbonematine nematode ectosymbionts are predominantly vertically transmitted from mother to offspring, via a smear infection (Zimmermann *et al.,* in in prep., Chapter III). Alternatively, symbionts could be acquired horizontally, from the environment every generation anew, although arguably, evidence for free-living members of the *Cand.* Thiosymbion clade is still missing (Zimmermann *et al.,* in prep., Chapter III). Regardless of the initial symbiont transmission mode, stilbonematine nematodes shed their cuticle four times in one life cycle (Ott *et al.* 1995). Therefore, the same individual must go through a total of five rounds of symbiont re-colonization until they reach adulthood. Evidence exists that during the gradual shedding process of the old cuticle, the new cuticle is already colonized by symbionts (Ott *et al.* 2004). This indicates that the new cuticle is likely inoculated by symbionts from the old cuticle, which would also guarantee that the already adapted symbiont strain is retained. If only a few symbiont cells inoculate the new cuticle after each moult, then *Leptonemella* ectosymbiont populations would thus undergo five “bottlenecks” throughout their lifecycle. Mutations that have occurred in one lifestage may therefore be transferred onto the next etc., which will eventually lead to distinct symbiont lineages on *Leptonemella* individuals, caused by microevolution on each independent worm lineage.

A similar phenomenom of intraspecific symbiont divergence not visible on the 16S rRNA gene has recently been reported for bacterial species in honey bee gut microbiomes (Engel *et al.* 2014). The authors found that much of the symbiont diversification between individuals is caused by recurring recombination events between closely related strains that co-occur in the gut of a single individual, and proposed that such divergence will eventually lead to ecologically distinct lineages. A similar phenomen seems to be true for human gut

microbiota, where distinct persistent bacterial strains tend to be shared among relatives living together (Schloissnig *et al.* 2013; Faith *et al.* 2013).

Implications of the diversity for the symbiosis

Genetic diversity is a major driver of adaptation and therefore evolution (Fisher 1930). In a symbiotic relationship, symbiont and host, which together from the holobiont, are subject to shared selection pressures (Guerrero *et al.* 2013). Thus, for example, if one of the partners adapts to a new niche, the other partner is affected. In the case of *Leptonemella*, where ectosymbionts of one species are highly diverse, this may eventually lead to an accelerated speciation of the holobiont. Considering the very dynamic tidal- and seasonally-influenced permeable sand habitat near List, where nutrient fluxes, oxygen and sulfide concentrations are temporally and spatially highly variable (de Beer *et al.* 2005; Böer *et al.* 2009), *Leptonemella* ectosymbioses that have a semi-sessile lifestyle (Riemann *et al.* 2003) are thus exposed to different environmental conditions depending on their location over time. Therefore, the maintainance of heterogenous symbiont strains could be of advantage for a host, in a highly fluctuating environment, that most likely depends on its symbionts for nutrition.

Conclusions and Outlook

In this study we could show that bacterial 16S rRNA and ITS sequences are excellent markers to distinguish between closely related ectosymbiotic bacteria of closely related *Leptonemella* nematode species on Sylt. While could not resolve genetic differences between symbionts of all species by 16S rRNA gene phylogenies, we detected a distinct pattern of host species-specificity between all the seven co-occuring species when we included the more variable ITS region in our phylogenies. Unexpectedly, the ITS region also gave indications for symbiont diversity within host species, which we could confirm by metagenomic analyses of symbiont populations from five individual worms. Intriguingly, we found that even when 16S-ITS sequences were identical, draft genomes only show 97.3% ANI to any other sequenced ectosymbiont strains. Furthermore we found indications that this symbiont diversity does not seem to be restricted to the nematode species on Sylt, but seems to be common for stilbonematine ectosymbioses, that are widely distributed around

the world. Our study reveals a previously “hidden” ectosymbiont diversity among individual nematodes of a single species and suggests that a combination of vertical transmission and microevolution are responsible for this pattern.

Cosidering that bacteria with identical 16S rRNA genes show marked differences in their genomes, together with the fact that a recent study by Engel *et al.* (2014) found the same “hidden diversity” in honey bee gut microbes, implies the necessity to use whole genome sequencing for reliably assessing the “true” bacterial genetic diversity- not only for stilbonematine nematode ectosymbionts- but also for other symbiotic systems.

However, a few questions remain open:

(1) What are the mechanisms that maintain these highly specific but at the same time highly diverse symbioses?
(2) What are the metabolic differences between closely related symbiont strains within a species and between species?

Both of these questions could be approached with transcriptomic analyses. As discussed in the manuscript, potential recognition molecules such as sugar-containing glycans and lectins have been proposed to be involved in the specificity of stilbonematine nematode ectosymbioses. Comparative transcriptomics of multiple invidual hosts and symbionts of the co-occurring *Leptonemella* species could be applied to specifically investigate molecules that are potentially involved in host symbiont recognition.

To investigate metabolic differences between individual symbiont strains and speciess, differential gene expression analyses could be performed to understand to what extent closely related stilbonematine symbionts will differ in their metabolism.

(3) What is the mode of symbiont transmission and the life cycle of the hosts

The mode of symbiont transmission in stilbonematine nematodes, although recently suggested to be vertical, has not been conclusively resolved yet (Zimmermann *et al*., in prep., Chapter III). Similarly, no study has described the reproductive cycle of the hosts. To understand the ecology and evolution of stilbonematine nematodes and their ectosymbiotic bacteria, both of these aspects should be investigated in future studies. Different life cycle stages of the host, from eggs over each stage of juveniles and adult worms should be examined for the presence of symbionts.

Nucleotide sequence accession numbers

The 18S rRNA sequences and 16S-ITS partial 23S rRNA from this study will be submitted to GenBank before publication.

Acknowledgements

We thank the staff of the Wadden Sea station Sylt (Alfred Wegener Institute), especially Werner Armonies and Ragnhild Asmus for hospitality and providing access to laboratory facilities. Special thanks to Lizbeth Sayavedra for her valuable input and her expertise and help with Pearl and Linux. Thanks to Miriam Sadowski, Kay Simmack, Sabine Kuehn, Andreas Ellrott and Silke Wetzel for excellent technical assistance. This work was supported by the Max Planck Society.

Conflict of Interest Statement

The authors declare no conflict of interest.

References

Alikhan N-F, Petty NK, Zakour NLB, Beatson SA (2011) BLAST Ring Image Generator (BRIG): simple prokaryote genome comparisons. *BMC Genomics*, **12**, 402.

Allen EE, Tyson GW, Whitaker RJ *et al.* (2007) Genome dynamics in a natural archaeal population. *Proceedings of the National Academy of Sciences*, **104**, 1883–1888.

Altschul S, Madden TL, Schäffer AA, *et al.* (1997) Gapped BLAST and PSI-BLAST: a new generation of protein database search programs. *Nucleic Acids Research*, **25**, 3389–3402.

Amann RI, Krumholz L, Stahl DA (1990) Fluorescent-oligonucleotide probing of whole cells for determinative, phylogenetic, and environmental studies in microbiology. *Journal of Bacteriology*, **172**, 762–770.

Aziz RK, Bartels D, Best AA *et al.* (2008) The RAST server: rapid annotations using subsystems technology. *BMC Genomics*, **9**, 75.

Bahar O, Goffer T, Burdman S (2009) Type IV pili are required for virulence, twitching motility, and biofilm formation of *Acidovorax avenae* subsp. citrulli. *Molecular Plant-Microbe Interactions*, **22**, 909–920.

Bankevich A, Nurk S, Antipov D *et al.* (2012) SPAdes: a new genome assembly algorithm and its applications to single-cell sequencing. *Journal of Computational Biology: A Journal of Computational Molecular Cell Biology*, **19**, 455–477.

Bauer-Nebelsick M, Blumer M, Urbancik W, Ott JA (1995) The glandular sensory organ of Desmodoridae (Nematoda)- ultrastructure and phylogenetic implications. *Invertebrate Biology*, **114**, 211–219.

Bayer C, Heindl NR, Rinke C *et al.* (2009) Molecular characterization of the symbionts associated with marine nematodes of the genus *Robbea*. *Environmental Microbiology Reports*, **1**, 136–144.

De Beer D, Wenzhöfer F, Ferdelman TG *et al.* (2005) Transport and mineralization rates in north sea sandy intertidal sediments, Sylt-Rømø basin, Wadden sea. *Limnology and Oceanography*, **50**, 113–127.

Böer SI, Arnosti C, van Beusekom JEE, Boetius A (2009) Temporal variations in microbial activities and carbon turnover in subtidal sandy sediments. *Biogeosciences*, **6**, 1149–1165.

Bright M, Bulgheresi S (2010) A complex journey: transmission of microbial symbionts. *Nature Reviews Microbiology*, **8**, 218–230.

Brown MV, Schwalbach MS, Hewson I, Fuhrman JA (2005) Coupling 16S-ITS rDNA clone libraries and automated ribosomal intergenic spacer analysis to show marine microbial diversity: development and application to a time series. *Environmental Microbiology*, **7**, 1466–1479.

Bulgheresi S (2011) Calling the roll on *Laxus oneistus* immune defense molecules. *Symbiosis*, **55**, 127–135.

Bulgheresi S, Schabussova I, Chen T *et al.* (2006) A new C-type lectin similar to the human immunoreceptor DC-SIGN mediates symbiont acquisition by a marine nematode. *Applied and Environmental Microbiology*, **72**, 2950–2956.

Cerdeño-Tárraga AM, Patrick S, Crossman LC *et al.* (2005) Extensive DNA Inversions in the B. fragilis Genome Control Variable Gene Expression. *Science*, **307**, 1463–1465.

Chain PSG, Denef VJ, Konstantinidis KT *et al.* (2006) Burkholderia xenovorans LB400 harbors a multi-replicon, 9.73-Mbp genome shaped for versatility. *Proceedings of the National Academy of Sciences*, **103**, 15280–15287.

Cingolani P, Platts A, Wang LL *et al.* (2012) A program for annotating and predicting the effects of single nucleotide polymorphisms, SnpEff. *Fly*, **6**, 80–92.

Daims H, Brühl A, Amann R, Schleifer KH, Wagner M (1999) The domain-specific probe EUB338 is insufficient for the detection of all Bacteria: development and evaluation of a more comprehensive probe set. *Systematic and Applied Microbiology*, **22**, 434–444.

Dando PR, Jensen P, O'Hara SCM *et al.* (1994) The effects of methane seepage at an intertidal/shallow subtidal site on the shore of the Kattegat, Vendsyssel, Denmark. *Bulletin of the Geological Society of Denmark*, **41**, 65–79.

Darling AE, Mau B, Perna NT (2010) ProgressiveMauve: multiple genome alignment with gene gain, loss and rearrangement. *PLoS ONE*, **5**, e11147.

Darriba D, Taboada GL, Doallo R, Posada D (2012) jModelTest 2: more models, new heuristics and parallel computing. *Nature Methods*, **9**, 772–772.

Dulla GFJ, Go RA, Stahl DA, Davidson SK (2012) *Verminephrobacter eiseniae* type IV pili and flagella are required to colonize earthworm nephridia. *The ISME Journal*, **6**, 1166–1175.

Ebert D (2013) The epidemiology and evolution of symbionts with mixed-mode transmission. *Annual Review of Ecology, Evolution, and Systematics*, **44**, 623–643.

Engel P, Stepanauskas R, Moran NA (2014) Hidden diversity in honey bee gut symbionts detected by single-cell genomics. *PLoS Genet*, **10**, e1004596.

Eyre-Walker A (2006) The genomic rate of adaptive evolution. *Trends in Ecology & Evolution*, **21**, 569–575.

Faith JJ, Guruge JL, Charbonneau M *et al.* (2013) The long-term stability of the human gut microbiota. *Science*, **341**, 1237439.

Fisher RA (1930) *The Genetical Theory of Natural Selection: A Complete Variorum Edition*. OUP Oxford.

Fourment M, Gibbs MJ (2006) PATRISTIC: a program for calculating patristic distances and graphically comparing the components of genetic change. *BMC Evolutionary Biology*, **6**, 1.

Frank SA (2003) Repression of competition and the evolution of cooperation. *Evolution*, **57**, 693–705.

Giardine B, Riemer C, Hardison RC *et al.* (2005) Galaxy: a platform for interactive large-scale genome analysis. *Genome research*, **15**, 1451–1455.

Glöckner FO, Fuchs BM, Amann R (1999) Bacterioplankton compositions of lakes and oceans: a first comparison based on fluorescence in situ hybridization. *Applied and Environmental Microbiology*, **65**, 3721–3726.

Goecks J, Nekrutenko A, Taylor J, others (2010) Galaxy: a comprehensive approach for supporting accessible, reproducible, and transparent computational research in the life sciences. *Genome Biol*, **11**, R86.

Gruber-Vodicka HR, Kleiner M, Wentrup C et al. (in preparation) '*Candidatus* Thiosymbion' spp., a genus of thiotrophic Gammaproteobacteria associated with diverse metazoan hosts.

Guerrero R, Margulis L, Berlanga M (2013) Symbiogenesis: the holobiont as a unit of evolution. *International Microbiology: The Official Journal of the Spanish Society for Microbiology*, **16**, 133–143.

Guindon S, Gascuel O (2003) A simple, fast, and accurate algorithm to estimate large phylogenies by maximum likelihood. *Systematic Biology*, **52**, 696–704.

Hammer Ø, Harper DAT, Ryan PD (2009) PAST-PAlaeontological STatistics, ver. 1.89. *University of Oslo, Oslo*.

Hooper LV, Gordon JI (2001) Glycans as legislators of host–microbial interactions: spanning the spectrum from symbiosis to pathogenicity. *Glycobiology*, **11**, 1R–10R.

Huber T, Faulkner G, Hugenholtz P (2004) Bellerophon: a program to detect chimeric sequences in multiple sequence alignments. *Bioinformatics*, **20**, 2317–2319.

Hughes AR, Inouye BD, Johnson MTJ, Underwood N, Vellend M (2008) Ecological consequences of genetic diversity. *Ecology Letters*, **11**, 609–623.

Jiang Z, Jones DH, Khuri S *et al.* (2013) Comparative analysis of genome sequences from four strains of the *Buchnera aphidicola* Mp endosymbion of the green peach aphid, *Myzus persicae*. *BMC Genomics*, **14**, 917.

Kamenev GM, Fadeev VI, Selin NI, Tarasov VG, Malakhov VV (1993) Composition and distribution of macro- and meiobenthos around sublittoral hydrothermal vents in the Bay of Plenty, New Zealand. *New Zealand Journal of Marine and Freshwater Research*, **27**, 407–418.

Katoh K, Kuma K, Toh H, Miyata T (2005) MAFFT version 5: improvement in accuracy of multiple sequence alignment. *Nucleic Acids Research*, **33**, 511–518.

Katoh K, Toh H (2008) Recent developments in the MAFFT multiple sequence alignment program. *Briefings in Bioinformatics*, **9**, 286–298.

Kearse M, Moir R, Wilson A *et al.* (2012) Geneious Basic: An integrated and extendable desktop software platform for the organization and analysis of sequence data. *Bioinformatics*, **28**, 1647–1649.

Kleiner M, Young JC, Shah M, VerBerkmoes NC, Dubilier N (2013) Metaproteomics reveals abundant transposase expression in mutualistic endosymbionts. *mBio*, **4**, e00223–13.

Leavis HL, Willems RJL, van Wamel WJB *et al.* (2007) Insertion sequence–driven diversification creates a globally dispersed emerging multiresistant subspecies of *E. faecium*. *PLoS Pathog*, **3**, e7.

Leduc D (2013) One new genus and two new deep-sea nematode species (Desmodoridae, Stilbonematinae) from phosphorite nodule deposits on Chatham Rise, Southwest Pacific Ocean. *Marine Biodiversity*, **43**, 421–428.

Lefèvre C, Charles H, Vallier A *et al.* (2004) Endosymbiont phylogenesis in the Dryophthoridae weevils: evidence for bacterial replacement. *Molecular Biology and Evolution*, **21**, 965–973.

Li H, Handsaker B, Wysoker A *et al.* (2009) The Sequence Alignment/Map format and SAMtools. *Bioinformatics*, **25**, 2078–2079.

Ludwig W, Strunk O, Westram R *et al.* (2004) ARB: a software environment for sequence data. *Nucleic Acids Research*, **32**, 1363–1371.

MacGregor BJ, Amann R (2006) Single-stranded conformational polymorphism for separation of mixed rRNAS (rRNA-SSCP), a new method for profiling microbial communities. *Systematic and Applied Microbiology*, **29**, 661–670.

Manz W, Amann R, Ludwig W, Wagner M, Schleifer K-H (1992) Phylogenetic oligodeoxynucleotide probes for the major subclasses of proteobacteria : problems and solutions. *Systematic and Applied Microbiology*, **15**, 593–600.

Mattick JS (2002) Type Iv Pili and Twitching Motility. *Annual Review of Microbiology*, **56**, 289–314.

McDonald JH, Kreitman M, others (1991) Adaptive protein evolution at the Adh locus in Drosophila. *Nature*, **351**, 652–654.

McFall-Ngai M, Brennan C, Weis V, Lamarcq L (1998) Mannose adhesin—glycan interactions in the *Euprymna scolopes—Vibrio fischeri* symbiosis. In: *New Developments in Marine Biotechnology* (eds Gal YL, Halvorson HO), pp. 273–276. Springer US.

Moran NA (1996) Accelerated evolution and Muller's rachet in endosymbiotic bacteria. *Proceedings of the National Academy of Sciences*, **93**, 2873–2878.

Moran NA, McLaughlin HJ, Sorek R (2009) The dynamics and time scale of ongoing genomic erosion in symbiotic bacteria. *Science*, **323**, 379–382.

Muyzer G, Brinkhoff T, Nübel U, Santegoeds C, Schäfer H & Wawer C (1997) Denaturing gradient gel electrophoresis (DGGE) in microbial ecology. In: Akkermans ADL, van Elsas JD & de Bruijn FJ (Eds) Molecular Microbial Ecology Manual (3.4.4: pp. 1–27) Kluwer Academic Publishers, Dordrecht, The Netherlands.

Nakagawa S, Shimamura S, Takaki Y *et al.* (2014) Allying with armored snails: the complete genome of gammaproteobacterial endosymbiont. *The ISME journal*, **8**, 40–51.

Nebelsick M, Blumer M, Novak R, Ott J (1992) A new glandular sensory organ in *Catanema* sp. (Nematoda, Stilbonematinae). *Zoomorphology*, **112**, 17–26.

Ngugi DK, Stingl U (2012) Combined analyses of the ITS loci and the corresponding 16S rRNA genes reveal high micro- and macrodiversity of SAR11 populations in the Red Sea. *PLoS ONE*, **7**, e50274.

Nussbaumer AD, Bright M, Baranyi C, Beisser CJ, Ott JA (2004) Attachment mechanism in a highly specific association between ectosymbiotic bacteria and marine nematodes. *Aquatic Microbial Ecology*, **34**, 239–246.

Oksanen J, Blanchet FG, Kindt R et al. (2012) Vegan: community ecology. Package. R package version 2.0–4. URL http://CRAN.R-project.org/package=vegan.

Ott JA, Bauer-Nebelsick M, Novotny V (1995) The genus *Laxus* Cobb, 1894 (Stilbonematinae: Nematoda): Description of two new species with ectosymbiotic, chemoautotrophic bacteria. *Proceedings of the Biological Society of Washington*, **108**, 508–527.

Ott J, Bright M, Bulgheresi S (2004) Symbioses between marine nematodes and sulfur-oxidizing chemoautotrophic bacteria. *Symbiosis*, **36**, 103–126.

Ott JA, Gruber-Vodicka HR, Leisch N, Zimmermann J (2014) Phylogenetic confirmation of the genus *Robbea* (Nematoda: Desmodoridae, Stilbonematinae) with the description of three new species. *Systematics and Biodiversity*, **12**, 434–455.

Ott JA, Novak R, Schiemer F *et al.* (1991) Tackling the sulfide gradient: a novel strategy Involving marine nematodes and chemoautotrophic ectosymbionts. *Marine Ecology*, **12**, 261–279.

Overbeek R, Olson R, Pusch GD *et al.* (2013) The SEED and the Rapid Annotation of microbial genomes using Subsystems Technology (RAST). *Nucleic Acids Research*, **42**, D206-D214.

Parkinson JE, Baums IB (2014) The extended phenotypes of marine symbioses: ecological and evolutionary consequences of intraspecific genetic diversity in coral-algal associations. *Frontiers in Microbiology*, **5**.

Parks DH, Imelfort M, Skennerton CT, Hugenholtz P, Tyson GW. 2014. Assessing the quality of microbial genomes recovered from isolates, single cells, and metagenomes. In preparation.

Pende N, Leisch N, Gruber-Vodicka HR *et al.* (2014) Size-independent symmetric division in extraordinarily long cells. *Nature Communications*, **5**.

Polz MF, Distel DL, Zarda B, *et al.* (1994) Phylogenetic analysis of a highly specific association between ectosymbiotic, sulfur-oxidizing bacteria and a marine nematode. *Applied Environmental Microbiology*, **60**, 4461–4467.

Polz MF, Felbeck H, Novak R, Nebelsick M, Ott JA (1992) Chemoautotrophic, sulfur-oxidizing symbiotic bacteria on marine nematodes: morphological and biochemical characterization. *Microbial Ecology*, **24**, 313–329.

Pradillon F, Schmidt A, Peplies J, Dubilier N (2007) Species identification of marine invertebrate early stages by whole-larvae in situ hybridisation of 18S ribosomal RNA. *Marine Ecology Progress Series*, **333**, 103–116.

Raggi L, Schubotz F, Hinrichs K-U, Dubilier N, Petersen JM (2013) Bacterial symbionts of *Bathymodiolus* mussels and *Escarpia* tubeworms from Chapopote, an asphalt seep in the southern Gulf of Mexico. *Environmental Microbiology* 15(7): 1969-1987

Richter M, Rossello-Mora R (2009) Shifting the genomic gold standard for the prokaryotic species definition. *Proceedings of the National Academy of Sciences of the United States of America*, **106**, 19126–19131.

Riemann F, Thiermann F, Bock L (2003) *Leptonemella* species (Desmodoridae, Stilbonematinae), benthic marine nematodes with ectosymbiotic bacteria, from littoral sand of the North Sea island of Sylt: taxonomy and ecological aspects. *Helgoland Marine Research*, **57**, 118–131.

Robidart JC, Bench SR, Feldman RA *et al.* (2008) Metabolic versatility of the *Riftia pachyptila* endosymbiont revealed through metagenomics. *Environmental Microbiology*, **10**, 727–737.

Ronquist F, Huelsenbeck JP (2003) MrBayes 3: Bayesian phylogenetic inference under mixed models. *Bioinformatics*, **19**, 1572–1574.

Schiemer F, Novak R, Ott J (1990) Metabolic studies on thiobiotic free-living nematodes and their symbiotic microorganisms. *Marine Biology*, **106**, 129–137.

Schizas NV, Street GT, Coull BC, Chandler GT, Quattro JM (1997) An efficient DNA extraction method for small metazoans. *Molecular marine biology and biotechnology*, **6**, 381–383.

Schloissnig S, Arumugam M, Sunagawa S *et al.* (2013) Genomic variation landscape of the human gut microbiome. *Nature*, **493**, 45–50.

Simmons SL, DiBartolo G, Denef VJ *et al.* (2008) Population genomic analysis of strain variation in Leptospirillum group II bacteria involved in acid mine drainage formation. *PLoS Biol*, **6**, e177.

Stabb EV, Ruby EG (2003) Contribution of pilA to competitive colonization of the squid *Euprymna scolopes* by *Vibrio fischeri*. *Applied and Environmental Microbiology*, **69**, 820–826.

Stamatakis A (2006) RAxML-VI-HPC: maximum likelihood-based phylogenetic analyses with thousands of taxa and mixed models. *Bioinformatics*, **22**, 2688–2690.

Stamatakis A, Hoover P, Rougemont J (2008) A rapid bootstrap algorithm for the RAxML web servers. *Systematic Biology*, **57**, 758–771.

Steedman HF (1957) Polyester wax: a new ribboning embedding medium for histology. *Nature*, **179**, 1345.

Stoletzki N, Eyre-Walker A (2011) Estimation of the Neutrality Index. *Molecular Biology and Evolution*, **28**, 63–70.

Strous M, Kraft B, Bisdorf R, Tegetmeyer HE (2012) The Binning of Metagenomic Contigs for Microbial Physiology of Mixed Cultures. *Frontiers in Microbiology*, **3**.410

Tchesunov AV (2013) Marine free-living nematodes of the subfamily Stilbonematinae (Nematoda, Desmodoridae): taxonomic review with descriptions of a few species from the Nha Trang Bay, Central Vietnam. *Meiofauna Marina*, **20**, 71–94.

Tchesunov AV, Ingels J, Popova EV (2012) Marine free-living nematodes associated with symbiotic bacteria in deep-sea canyons of north-east Atlantic Ocean. *Journal of the Marine Biological Association of the United Kingdom*, **92**, 1257–1271.

Thiermann F, Akoumianaki I, Hughes JA, Giere O (1997) Benthic fauna of a shallow-water gaseohydrothermal vent area in the Aegean Sea (Milos, Greece). *Marine Biology*, **128**, 149–159.

Thorvaldsdóttir H, Robinson JT, Mesirov JP (2012) Integrative Genomics Viewer (IGV): high-performance genomics data visualization and exploration. *Briefings in Bioinformatics*, bbs017.

Treangen TJ, Salzberg SL (2012) Repetitive DNA and next-generation sequencing: computational challenges and solutions. *Nature Reviews Genetics*, **13**, 36–46.

Vos M, te Beek TAH, van Driel MA *et al.* (2013) ODoSE: A webserver for genome-wide calculation of adaptive divergence in prokaryotes. *PLoS ONE*, **8**, e62447.

Vrijenhoek RC (2010) Genetics and evolution of deep-sea chemosynthetic bacteria and their invertebrate hosts. In: *The Vent and Seep Biota* Topics in Geobiology. (ed Kiel S), pp. 15–49. Springer Netherlands.

Walker BJ, Abeel T, Shea T *et al.* (2014) Pilon: An integrated tool for comprehensive microbial variant detection and genome assembly improvement. *PLoS ONE*, **9**.

Wallner G, Amann R, Beisker W (1993) Optimizing fluorescent in situ hybridization with rRNA-targeted oligonucleotide probes for flow cytometric identification of microorganisms. *Cytometry*, **14**, 136–143.

Werren JH (2011) Selfish genetic elements, genetic conflict, and evolutionary innovation. *Proceedings of the National Academy of Sciences*, **108**, 10863–10870.

Wieser W (1959) Eine ungewöhnliche Assoziation zwischen Blaualgen und freilebenden marinen Nematoden. *Plant Systematics and Evolution*, **106**, 81–87.

Winnepenninckx B, Backeljau T, Wachter RD (1995) Phylogeny of protostome worms derived from 18S rRNA sequences. *Molecular Biology and Evolution*, **12**, 641–649.

Woyke T, Teeling H, Ivanova NN *et al.* (2006) Symbiosis insights through metagenomic analysis of a microbial consortium. *Nature*, **443**, 950–955.

Zimmermann J, Lott C, Weber M *et al.* (2014) Dual symbiosis with co-occurring sulfur-oxidizing symbionts in vestimentiferan tubeworms from a Mediterranean hydrothermal vent. *Environmental Microbiology*.

Supplementary material

Judith Zimmermann, Harald R. Gruber-Vodicka, Rebecca Ansorge, Niculina Musat, Bruno Hüttel, Jörg Ott, Nicole Dubilier, and Jillian M. Petersen

SI Tables

Table S1: Sample and sequencing details

Sampling ID	*Leptonemella* host species	directly sequenced from the 16S-ITS PCR product	partial ITS sequencing from clones	Full sequencing of 16S-ITS from clones	Symbiont meta-genome (Illumina PE)	Sampling Date
L6	*L. vicina* (sp. A)		x	4		Sept/Oct 2003
L34	*L. vicina* (sp. A)		x	9		2003-2007
L45	*L. vicina* (sp. A)		x	3		2003-2007
L.vic2	*L. vicina* (sp. A)		71	6		May 2011
Khf1*	*L. vicina* (sp. A)		2	2		Sept 2011
W36	*L. vicina* (sp. A)		3	1		Feb 2012
W38	*L. vicina* (sp. A)	1	183			Feb 2012
W87	*L. vicina* (sp. A)		3	1		June 2012
W219	*L. vicina* (sp. A)	1				June 2013
W220	*L. vicina* (sp. A)	1			1	June 2013
W217	*L. vicina* (sp. A)	1				June 2013
W33	*L.* sp. B		x	10		2003-2005
L11T	*L.* sp. B		x	10		2003-2005
L42	*L.* sp. B		x	4		2003-2007
W12	*L.* sp. B		29	1		May 2011
W128	*L.* sp. B	1				June 2013
W113	*L.* sp. B	1				June 2013
L.aph1	*L. aphanothecae* (sp. C)		70	9		May 2011
L.aph2	*L. aphanothecae* (sp. C)		51	9		May 2011
W6	*L. aphanothecae* (sp. C)		5	1		May 2011
Khf4*	*L. aphanothecae* (sp. C)		1	1		Sept 2011
W79	*L. aphanothecae* (sp. C)		41	1		Feb 2012
W67	*L. aphanothecae* (sp. C)		15	1		Feb 2012
W83	*L. aphanothecae* (sp. C)	1	126			Feb 2012
W101	*L. aphanothecae* (sp. C)	1				June 2013

Sampling ID	*Leptonemella* host species	directly sequenced from the 16S-ITS PCR product	partial ITS sequencing from clones	Full sequencing of 16S-ITS from clones	Symbiont meta-genome (Illumina PE)	Sampling Date
W108	*L. aphanothecae* (sp. C)	1				June 2013
W120	*L. aphanothecae* (sp. C)	1				June 2013
W121	*L. aphanothecae* (sp. C)	1				June 2013
W122	*L. aphanothecae* (sp. C)	1				June 2013
W103	*L. aphanothecae* (sp. C)				1	June 2013
W104	*L. aphanothecae* (sp. C)				1	June 2013
W107	*L. aphanothecae* (sp. C)				1	June 2013
W112	*L. aphanothecae* (sp. C)				1	June 2013
W114	*L.* sp. D	1				June 2013
L4	*L.* sp. E		x	10		Sept/Oct 2003
L.vic1	*L.* sp. E		73	12		May 2011
W52	*L.* sp. E		26	1		Feb 2012
L9T	*L.*sp. F		x	10		2003-2005

*were sampled from a different beach ~1.5 km north of the 'Hausstrand' called 'Am Königshafen'; x: between 5 – 50 clones were sequenced.

Table S2: Draft genome statistics

	L. aphanothecae ectosymbiont E103	*L. aphanothecae* ectosymbiont E104	*L. aphanothecae* ectosymbiont E107	*L. aphanothecae* ectosymbiont E112	*L. vicina* ectosymbiont E220
Total DNA used	1.17	1.26	1.08	1.12	2.60
Genome size [Mb]	4.73	4.84	4.83	5.10	4.97
GC content [%]	58.89	58.35	58.36	58.38	58.78
Average genome coverage (after removal of PCR duplicates)	292 (113)	208 (92)	146 (76)	245 (108)	200 (105)
N50	9127	13020	11283	13167	8261
L50	154	111	125	166	176
# contigs (> 0 bp)	1196	1496	1204	2079	2833
longest contig [kb]	47.382	53.252	69.922	67.019	49.102
Predicted genes [RAST]	3806	4021	3867	4200	4068
RNA genes	48	48	48 (51*)	48	48
5S rRNA genes	1	1	1	1	1
16S rRNA genes	1	1	1	1	1
23S rRNA genes	1	1	1	1	1
tRNA genes	45	45	45 (48*)	45	45
Conserved marker genes° 281 (duplicates)	275 (2)	274 (3)	274 (3)	262 (12)	271 (5)
Mobile elements$	82	78	92	106	194

*three tRNAs with anticodon GTT specific for threonine were annotated on contigs < 500 bp that contained no other annotation; °based on checkM v0.9.5 (Parks et al., 2014) using ubiquitous and single-copy genes present in Gammaproteobacteria; $including transposases, integrases and restriction modification systems.

Table S3: Average nucleotide identities (ANIs) of the *Leptonemella aphanothecae* ectosymbiont draft genomes. ANIs were calculated with Jspecies (Richter and Rossello-Mora, 2009) (based on BLASTn). Comparisons to the *L. vicina* symbiont genome are highlighted in grey.

Average nucleotide identity [%]	**E103**	**E104**	**E107**	**E112**	***L. vic* E220**
E103	—	97.52	97.31	97.52	92.78
E104	97.55	—	97.35	97.47	93.17
E107	97.37	97.38	—	97.29	92.72
E112	97.53	97.56	97.29	—	93.42
***L. vic* E220**	93.53	93.54	93.34	93.54	—

Table S4: Unique genes in *Leptonemella* ectosymbiont draft genomes. Sequence-based comparisons between *L. aphanothecae* and *L. vicina* symbiont (shaded in grey) genomes, based on RAST (http://rast.nmpdr.org/, Overbeek *et al.* 2013).

Unique genes [%] (>100 bp)	**E103**	**E104**	**E107**	**E112**	***L. vic* E220**
E103	—	11.38 (4.05)	12.82 (4.41)	12.14 (4.6)	24.36 (10.35)
E104	14.9 (5.45)	—	13.53 (5.02)	12.46 (4.77)	25.17 (10.52)
E107	14.58 (5.72)	12.46 (5.09)	—	12.59 (5.28)	24.8 (11.12)
E112	16.6 (6.55)	14 (5.57)	16.14 (6.24)	—	26.31 (11.4)
***L. vic* E220**	28.5 (12.17)	27.17 (11.63)	27.52 (11.26)	27.17 (11.46)	—

85 - 90% of the unique genes were hypothetical genes

Table S5: Unique genes in the *Leptonemella* ectosymbiont genomes. The list of genes is based on the sequence-based comparison in RAST (http://rast.nmpdr.org/, Overbeek *et al.* 2013). Only genes > 100 bp are listed.

***L. aphanothecae* symbiont population E103**			
Gene ID (RAST)	**Hypothetical Role**	**Subsystem**	**Length [bp]**
Gene_fig|6666666.84934.peg.1453	7,8-didemethyl-8-hydroxy-5-deazariboflavin synthase subunit 1 / 2	Coenzyme F420 synthesis	816
Gene_fig|6666666.84934.peg.1930	Arsenate reductase	Anaerobic respiratory reductases, Arsenic resistance, Transcription repair cluster	118
Gene_fig|6666666.84934.peg.2752	arylsulfatase regulator	- none -	469
Gene_fig|6666666.84934.peg.3163	Basic proline-rich protein precursor	- none -	530
Gene_fig|6666666.84934.peg.806	Bsr0071 protein	- none -	75
Gene_fig|6666666.84934.peg.1456	Coenzyme F420-0:L-glutamate ligase	Coenzyme F420 synthesis	259
Gene_fig|6666666.84934.peg.1817	dipeptidyl peptidase IV-related protein	- none -	352
Gene_fig|6666666.84934.peg.2235	GDP-mannose mannosyl hydrolase	Mannose Metabolism, Nudix proteins (nucleoside triphosphate hydrolases)	128
Gene_fig|6666666.84934.peg.2753	Glycerol uptake facilitator protein	Glycerol and Glycerol-3-phosphate Uptake and Utilization, Osmoregulation	324
Gene_fig|6666666.84934.peg.2950	HipB protein	- none -	80
Gene_fig|6666666.84934.peg.1455	Lactyl (2) diphospho-(5')guanosine:7,8-didemethyl-8-hydroxy-5-deazariboflavin 2-phospho-L-lactate transferase	Coenzyme F420 synthesis	328
Gene_fig|6666666.84934.peg.722	Msl3420 protein	- none -	110
Gene_fig|6666666.84934.peg.1124	NADH-ubiquinone oxidoreductase chain M	NADH ubiquinone oxidoreductase, Respiratory Complex I	58
Gene_fig|6666666.84934.peg.367	Phage protein	- none -	632
Gene_fig|6666666.84934.peg.2658	Phosphoenolpyruvate synthase / Pyruvate phosphate dikinase	- none -	363
Gene_fig|6666666.84934.peg.3038	probable ATP /GTP binding protein	- none -	439
Gene_fig|6666666.84934.peg.3039	probable membrane protein YPO2297	- none -	750
Gene_fig|6666666.84934.peg.3227	Putative glutamate dehydrogenase	- none -	411
Gene_fig|6666666.84934.peg.3739	Staphylococcal nuclease homologue	- none -	87
Gene_fig|6666666.84934.peg.1163	TIR	- none -	133
Gene_fig|6666666.84934.peg.1103	Transcriptional regulatory protein	- none -	472
	Hypothetical proteins	**184 x**	**23580**
***L. aphanothecae* symbiont population E104**			
Gene ID	**Function**	**Subsystem**	**Length [bp]**
Gene_fig|6666666.84933.peg.2360	amine oxidase-like protein family member	- none -	337
Gene_fig|6666666.84933.peg.211	ATP-dependent DNA helicase pcrA	DNA repair, bacterial UvrD & related helicases	642
Gene_fig|6666666.84933.peg.3854	cell wall surface anchor family protein	- none -	924
Gene_fig|6666666.84933.peg.1072	conserved hypothetical protein	- none -	422

L. aphanothecae symbiont population E104			
Gene ID	**Function**	**Subsystem**	**Length [bp]**
Gene_fig|6666666.84933.peg.2188	Cytochrome c552 precursor	Nitrate and nitrite ammonification, Soluble cytochromes and related electron carriers	398
Gene_fig|6666666.84933.peg.2485	DEAD-box helicase-related protein	- none -	2080
Gene_fig|6666666.84933.peg.1455	Diaminopimelate decarboxylase	Lysine Biosynthesis DAP Pathway, GJO scratch	435
Gene_fig|6666666.84933.peg.937	Ethidium bromide-methyl viologen resistance protein EmrE	- none -	109
Gene_fig|6666666.84933.peg.1162	Flagellar biosynthesis protein FlhA	- none -	208
Gene_fig|6666666.84933.peg.581	Flagellar protein FlgJ [peptidoglycan hydrolase]	- none -	125
Gene_fig|6666666.84933.peg.1763	Glycosyl hydrolase, BNR repeat	- none -	394
Gene_fig|6666666.84933.peg.1148	High-affinity branched-chain amino acid transport system permease protein LivH	- none -	255
Gene_fig|6666666.84933.peg.2200	Hypothetical SecA-related protein	- none -	586
Gene_fig|6666666.84933.peg.2362	L. lactis predicted coding region ORF00041	- none -	830
Gene_fig|6666666.84933.peg.3569	Plasmid maintenance system antidote protein	- none -	406
Gene_fig|6666666.84933.peg.1382	Predicted periplasmic protein	- none -	406
Gene_fig|6666666.84933.peg.3568	predicted protein	- none -	306
Gene_fig|6666666.84933.peg.140	Programmed cell death toxin YdcE	MazEF toxin-antitoxing (programmed cell death) system, Phd-Doc, YdcE-YdcD toxin-antitoxin systems	103
Gene_fig|6666666.84933.peg.3851	Protein kinase domain containing protein	- none -	1038
Gene_fig|6666666.84933.peg.3334	putative ISH4 transposase	- none -	161
Gene_fig|6666666.84933.peg.126	Putative phage-encoded peptidoglycan binding protein	- none -	301
Gene_fig|6666666.84933.peg.3850	putative transcriptional activator SRCAP homolog	- none -	1681
Gene_fig|6666666.84933.peg.1838	Transglycosylase associated protein	- none -	83
Gene_fig|6666666.84933.peg.3609	Type I restriction-modification system subunit S, DNA-methyltransferase subunit M	Restriction-Modification System, Type I	377
Gene_fig|6666666.84933.peg.147	Type III restriction-modification enzyme helicase subunit	- none -	873
Gene_fig|6666666.84933.peg.145	Type III restriction-modification system methylation subunit (2x)	Restriction-Modification System	1209
Gene_fig|6666666.84933.peg.175	vrrB protein (2x)	- none -	89
	Hypothetical proteins	**212 x**	**30925**

L. aphanothecae symbiont population E107			
Gene ID	**Function**	**Subsystem**	**Length [bp]**
Gene_fig|6666666.84932.peg.3632	1,4-alpha-glucan (glycogen) branching enzyme, GH-13-type	Glycogen metabolism, Glycogen metabolism cluster	40
Gene_fig|6666666.84932.peg.1796	ABC-type amino acid transport/signal transduction systems, periplasmic component/domain	- none -	475
Gene_fig|6666666.84932.peg.541	Alpha/beta hydrolase fold	- none -	113
Gene_fig|6666666.84932.peg.417	Chalcone synthase	- none -	396
Gene_fig|6666666.84932.peg.2665	Colicin	- none -	82
Gene_fig|6666666.84932.peg.1896	some similarity with a Photorhabdus luminescens protein	- none -	860
Gene_fig|6666666.84932.peg.3138	Cyanophycin synthase	Cyanophycin Metabolism	583
Gene_fig|6666666.84932.peg.3139	Deblocking aminopeptidase/ Cyanophycinase 2	Cyanophycin Metabolism, Protein degradation	370
Gene_fig|6666666.84932.peg.3449	DNA helicase, putative	- none -	854
Gene_fig|6666666.84932.peg.3450	DNA helicase, putative	- none -	687
Gene_fig|6666666.84932.peg.441	exopolysaccharide production protein Pss	- none -	491
Gene_fig|6666666.84932.peg.3179	Formate dehydrogenase -O, gamma subunit	Anaerobic respiratory reductases	338
Gene_fig|6666666.84932.peg.3130	Hypothetical protein VpsJ	- none -	530
Gene_fig|6666666.84932.peg.37	Glycosyl transferase, group 1	- none -	386
Gene_fig|6666666.84932.peg.2477	GTP pyrophosphokinase	- none -	567
Gene_fig|6666666.84932.peg.39	Heparinase II/III-like	CBSS-366602.3.peg.5141	557
Gene_fig|6666666.84932.peg.3311	Methionyl-tRNA synthetase	Scaffold proteins for [4Fe-4S] cluster assembly (MRP family), tRNA aminoacylation, Met	546
Gene_fig|6666666.84932.peg.1854	miscellaneous; unknown	- none -	65
Gene_fig|6666666.84932.peg.835	N6 adenine-specific DNA methyltransferase, N12 class	- none -	501
Gene_fig|6666666.84932.peg.3128	N-acetylmannosaminyltransferase	Teichoic and lipoteichoic acids biosynthesis	153
Gene_fig|6666666.84932.peg.3522	NADH-ubiquinone oxidoreductase chain M	NADH ubiquinone oxidoreductase, Respiratory Complex I	40
Gene_fig|6666666.84932.peg.558	NgrB	- none -	41
Gene_fig|6666666.84932.peg.3416	O-antigen flippase Wzx	KDO2-Lipid A biosynthesis	854
Gene_fig|6666666.84932.peg.38	oxidoreductase domain protein	- none -	39
Gene_fig|6666666.84932.peg.1884	Phage protein	- none -	82
Gene_fig|6666666.84932.peg.266	Probable polysaccharide synthesis protein	- none -	56
Gene_fig|6666666.84932.peg.242	SAM binding motif	- none -	379
Gene_fig|6666666.84932.peg.217	Serine/threonine protein kinase PrkC, regulator of stationary phase	Conserved gene cluster associated with Met-tRNA formyltransferase	75

***L. aphanothecae* symbiont population E107**			
Gene ID	**Function**	**Subsystem**	**Length [bp]**
Gene_fig|6666666.84932.peg.1125	Type II restriction enzyme Cfr9I (Endonuclease Cfr9I) (R.Cfr9I)	- none -	41
Gene_fig|6666666.84932.peg.1552	Type II restriction enzyme NspV (Endonuclease) (2x)	- none -	156
Gene_fig|6666666.84932.peg.141	UDP-N-acetylglucosamine 2-epimerase	CMP-N-acetylneuraminate Biosynthesis, Sialic Acid Metabolism	494
Gene_fig|6666666.84932.peg.3829	ABC transporter, ATP-binding protein	- none -	127
	Hypothetical proteins	**215 x**	**38184**
***L. aphanothecae* symbiont population E112**			
Gene ID	**Function**	**Subsystem**	**Length [bp]**
Gene_fig|6666666.84930.peg.2802	3,7-dideoxy-D-threo-hepto-2, 6-diulosonate synthase	Chorismate Synthesis, Synthesis of aromatic compounds (DAHP synthase to chorismate)	177
Gene_fig|6666666.84930.peg.160	Alpha-L-arabinofuranosidase	- none -	418
Gene_fig|6666666.84930.peg.2059	ATP synthase F0 sector subunit c	- none -	78
Gene_fig|6666666.84930.peg.3236	ATP-dependent DNA helicase	- none -	56
Gene_fig|6666666.84930.peg.2754	Basic proline-rich protein precursor	- none -	355
Gene_fig|6666666.84930.peg.3320	Butyryl-CoA dehydrogenase	- none -	591
Gene_fig|6666666.84930.peg.3900	Cholesterol oxidase	- none -	531
Gene_fig|6666666.84930.peg.2937	conserved domain protein	- none -	407
Gene_fig|6666666.84930.peg.905	Cytoplasmic axial filament protein CafA and Ribonuclease G	Bacterial Cell Division, RNA processing and degradation, bacterial	60
Gene_fig|6666666.84930.peg.480	D-alanyl-D-alanine dipeptidase	- none -	230
Gene_fig|6666666.84930.peg.2006	DEAD/DEAH box helicase domain protein	- none -	837
Gene_fig|6666666.84930.peg.3393	DNA primase	Macromolecular synthesis operon	453
Gene_fig|6666666.84930.peg.1670	DNA-binding protein	- none -	386
Gene_fig|6666666.84930.peg.901	encapsulation protein CapA	- none -	577
Gene_fig|6666666.84930.peg.2659	FAD-dependent oxidoreductase	- none -	626
Gene_fig|6666666.84930.peg.3851	Ferric iron ABC transporter, iron-binding protein	Iron acquisition in Streptococcus	335
Gene_fig|6666666.84930.peg.3850	Ferric iron ABC transporter, permease protein	Iron acquisition in Streptococcus	532
Gene_fig|6666666.84930.peg.4100	GCN5-related N-acetyltransferase; Histone acetyltransferase HPA2	CBSS-216591.1.peg.168	174
Gene_fig|6666666.84930.peg.2819	Glutamate synthase [NADPH] small chain	Ammonia assimilation, Glutamine, Glutamate, Aspartate and Asparagine Biosynthesis	41
Gene_fig|6666666.84930.peg.3906	Glycosyl transferase, family 2	- none -	266

L. aphanothecae symbiont population E112			
Gene ID	**Function**	**Subsystem**	**Length [bp]**
Gene_fig|6666666.84930.peg.1824	HigA protein (antitoxin to HigB)	Toxin-antitoxin replicon stabilization systems	375
Gene_fig|6666666.84930.peg.3503	Homolog of eukaryotic DNA ligase III	- none -	196
Gene_fig|6666666.84930.peg.1855	Inosamine-phosphate amidinotransferase 1/(Aminocyclitol amidinotransferase)	- none -	346
Gene_fig|6666666.84930.peg.3778	Metacaspase	- none -	1095
Gene_fig|6666666.84930.peg.3340	Mobile element protein (3)	- none -	704
Gene_fig|6666666.84930.peg.903	MORN repeat protein	- none -	634
Gene_fig|6666666.84930.peg.1138	Phage T7 exclusion protein	- none -	715
Gene_fig|6666666.84930.peg.2383	Phosphoenolpyruvate phosphomutase	- none -	523
Gene_fig|6666666.84930.peg.3321	Phosphopantetheine-binding	- none -	79
Gene_fig|6666666.84930.peg.3348	PilT protein, N-terminal	- none -	95
Gene_fig|6666666.84930.peg.1783	Prevent host death protein, Phd antitoxin	Phd-Doc, YdcE-YdcD toxin-antitoxin (programmed cell death) systems	91
Gene_fig|6666666.84930.peg.2156	probable vgr related protein	- none -	119
Gene_fig|6666666.84930.peg.996	Programmed cell death toxin MazF like	Phd-Doc, YdcE-YdcD toxin-antitoxin (programmed cell death) systems	150
Gene_fig|6666666.84930.peg.1853	Putative ATP:guanido phospho-transferase YacI	Proteolysis in bacteria, ATP-dependent	322
Gene_fig|6666666.84930.peg.4124	putative ATP-dependent protease	- none -	65
Gene_fig|6666666.84930.peg.1782	Putative bacterial haemoglobin	Bacterial hemoglobins	140
Gene_fig|6666666.84930.peg.437	putative prolin-rich exported protein (3x)	- none -	240
Gene_fig|6666666.84930.peg.481	putative protein Ymh	- none -	278
Gene_fig|6666666.84930.peg.2384	putative pyridoxal phosphate-dependent deaminase	- none -	363
Gene_fig|6666666.84930.peg.29	RNA polymerase ECF-subfamily sigma factor	- none -	46
Gene_fig|6666666.84930.peg.2789	RNA polymerase ECF-subfamily sigma factor	- none -	51
Gene_fig|6666666.84930.peg.2360	Sarcosine oxidase	- none -	405
Gene_fig|6666666.84930.peg.3196	Serine/threonine-protein kinase ULK1	- none -	827
Gene_fig|6666666.84930.peg.1852	Sulfate transporter	- none -	426
Gene_fig|6666666.84930.peg.2952	Transcription-repair coupling factor	Cell division-ribosomal stress proteins cluster, Transcription factors bacterial, Transcription repair cluster	78
Gene_fig|6666666.84930.peg.4125	Translation-disabling ACNase RloC	- none -	742
Gene_fig|6666666.84930.peg.2361	Tryptophan 2-monooxygenase	- none -	574
Gene_fig|6666666.84930.peg.992	Type I restriction-modification system, DNA-methyltransferase subunit M	Restriction-Modification System, Type I Restriction-Modification	49

L. aphanothecae symbiont population E112			
Gene ID	**Function**	**Subsystem**	**Length [bp]**
Gene_fig|6666666.84930.peg.3159	type I restriction-modification system, M subunit, putative	- none -	265
Gene_fig|6666666.84930.peg.3342	Very-short-patch mismatch repair endonuclease (G-T specific)	DNA repair, bacterial	128
	Hypothetical proteins	**286 x**	**59659**
L. vicina **symbiont population E220**			
Gene ID	**Function**	**Subsystem**	**Length [bp]**
Gene_fig|6666666.84935.peg.2089	[Genomic island nu Sa beta2]	- none -	1151
Gene_fig|6666666.84935.peg.992	5-oxo-L-prolinase, putative	- none -	310
Gene_fig|6666666.84935.peg.2568	ABC transporter ATP-binding protein	- none -	305
Gene_fig|6666666.84935.peg.492	ABC-type tungstate transport system, periplasmic binding protein (2x)	ABC transporter tungstate (TC 3.A.1.6.2)	417
Gene_fig|6666666.84935.peg.2236	Acetylornithine deacetylase/Succinyl-diaminopimelate desuccinylase and related deacylases	- none -	380
Gene_fig|6666666.84935.peg.3194	Adenosine deaminase	Purine conversions	310
Gene_fig|6666666.84935.peg.2828	Alanine dehydrogenase	Pyruvate Alanine Serine Interconversions	380
Gene_fig|6666666.84935.peg.1808	Alpha-1,4-N-acetylgalactosamine transferase PglJ	N-linked Glycosylation in Bacteria	95
Gene_fig|6666666.84935.peg.60	alternate gene name: yukI	- none -	349
Gene_fig|6666666.84935.peg.2300	antigen, putative	- none -	538
Gene_fig|6666666.84935.peg.2233	Argininosuccinate lyase	Arginine Biosynthesis -- gjo, Arginine Biosynthesis extended	103
Gene_fig|6666666.84935.peg.228	Arsenate reductase	Anaerobic respiratory reductases, Arsenic resistance, Transcription repair cluster	177
Gene_fig|6666666.84935.peg.2948	Arsenical pump-driving ATPase	Arsenic resistance	639
Gene_fig|6666666.84935.peg.754	Asparagine synthetase [glutamine-hydrolyzing]	Glutamine, Glutamate, Aspartate and Asparagine Biosynthesis	573
Gene_fig|6666666.84935.peg.986	ATPase required for both assembly of type IV secretion complex and secretion of T-DNA complex, VirB4	- none -	794
Gene_fig|6666666.84935.peg.3468	ATP-dependent protease La Type I	Proteasome bacterial, Proteolysis in bacteria, ATP-dependent	73
Gene_fig|6666666.84935.peg.1575	Basic proline-rich protein precursor	- none -	586
Gene_fig|6666666.84935.peg.3135	Carbohydrate kinase, PfkB	- none -	370
Gene_fig|6666666.84935.peg.197	Cell division protein FtsH	Bacterial Cell division, ribosomal stress proteins cluster, Folate biosynthesis	312

L. vicina symbiont population E220			
Gene ID	**Function**	**Subsystem**	**Length [bp]**
Gene_fig|6666666.84935.peg.3201	Citrate lyase beta chain	- none -	304
Gene_fig|6666666.84935.peg.3204	COG0503: Adenine/guanine phosphoribosyltransferases and related PRPP-binding proteins	- none -	398
Gene_fig|6666666.84935.peg.3532	COG1355, Predicted dioxygenase	- none -	193
Gene_fig|6666666.84935.peg.204	COG1396: Predicted transcriptional regulators	- none -	106
Gene_fig|6666666.84935.peg.1576	collagen, type 1, alpha 2	- none -	344
Gene_fig|6666666.84935.peg.952	Coupling protein VirD4, ATPase required for T-DNA transfer	- none -	596
Gene_fig|6666666.84935.peg.1838	CRISPR-associated protein Cas1	CRISPRs	326
Gene_fig|6666666.84935.peg.334	CRISPR-associated protein Cas2	CRISPRs	98
Gene_fig|6666666.84935.peg.333	CRISPR-associated RecB family exonuclease Cas4 / CRISPR-associated protein Cas1	CRISPRs	577
Gene_fig|6666666.84935.peg.254	Cupin 2, conserved barrel	- none -	166
Gene_fig|6666666.84935.peg.996	cysteinyl-tRNA synthetase	- none -	114
Gene_fig|6666666.84935.peg.1543	D-aminoacylase	- none -	553
Gene_fig|6666666.84935.peg.3805	Death on curing protein, Doc toxin	Phd-Doc, YdcE-YdcD toxin-antitoxin (programmed cell death) systems	126
Gene_fig|6666666.84935.peg.2158	DNA polymerase I	DNA Repair Base Excision	74
Gene_fig|6666666.84935.peg.4040	DNA primase, phage-associated	- none -	548
Gene_fig|6666666.84935.peg.1145	DNA repair protein RadC (9x)	Bacterial cell division cluster, DNA repair, bacterial	987
Gene_fig|6666666.84935.peg.1029	DNA-damage-inducible protein J	DNA repair, bacterial, Toxin-antitoxin replicon stabilization systems	66
Gene_fig|6666666.84935.peg.3168	D-tagatose 3-epimerase	- none -	251
Gene_fig|6666666.84935.peg.3063	Enoyl-CoA hydratase	Fatty acid metabolism cluster	225
Gene_fig|6666666.84935.peg.967	FOG: TPR repeat	- none -	311
Gene_fig|6666666.84935.peg.493	Formate dehydrogenase chain D	Formate hydrogenase	340
Gene_fig|6666666.84935.peg.2981	FunZ family protein,	- none -	547
Gene_fig|6666666.84935.peg.517	gas vesicle protein GVPa	- none -	75
Gene_fig|6666666.84935.peg.514	gas vesicle synthesis protein	- none -	267
Gene_fig|6666666.84935.peg.2104	GCN5-related N-acetyltransferase	- none -	702
Gene_fig|6666666.84935.peg.3293	Glutamate Aspartate periplasmic binding protein precursor GltI	- none -	342
Gene_fig|6666666.84935.peg.1540	Glutamate Aspartate transport system permease protein GltK	- none -	96
Gene_fig|6666666.84935.peg.3184	Glutathione-regulated potassium-efflux system protein KefB	Glutathione-regulated potassium-efflux system and associated functions	85

L. vicina symbiont population E220			
Gene ID	**Function**	**Subsystem**	**Length [bp]**
Gene_fig|6666666.84935.peg.3857	Glycosyltransferase (2x)	- none -	749
Gene_fig|6666666.84935.peg.1147	Glycosyltransferases involved in cell wall biogenesis	- none -	270
Gene_fig|6666666.84935.peg.3447	Helix-turn-helix motif	- none -	81
Gene_fig|6666666.84935.peg.1883	heterodisulfide reductase, subunit A/methylviologen reducing hydrogenase, subunit delta	Anaerobic respiratory reductases	43
Gene_fig|6666666.84935.peg.3738	HicA protein	- none -	85
Gene_fig|6666666.84935.peg.1117	HigB toxin protein	Toxin-antitoxin replicon stabilization systems	115
Gene_fig|6666666.84935.peg.750	High-affnity carbon uptake protein Hat/HatR (2x)	CO2 uptake, carboxysome	4356
Gene_fig|6666666.84935.peg.1802	HipA protein	Persister Cells	431
Gene_fig|6666666.84935.peg.2566	Histidine ammonia-lyase	- none -	562
Gene_fig|6666666.84935.peg.3699	hypothetical membrane protein	- none -	138
Gene_fig|6666666.84935.peg.199	hypothetical protein APECO1_2271	- none -	322
Gene_fig|6666666.84935.peg.198	hypothetical protein Francci3_0125	- none -	172
Gene_fig|6666666.84935.peg.3444	hypothetical protein-transmembrane prediction	- none -	422
Gene_fig|6666666.84935.peg.3512	Imidazoleglycerol-phosphate dehydratase	Histidine Biosynthesis	202
Gene_fig|6666666.84935.peg.971	IncP-type DNA relaxase TraI	- none -	729
Gene_fig|6666666.84935.peg.953	IncQ plasmid conjugative transfer DNA primase TraO (pTi TraA homolog)	- none -	216
Gene_fig|6666666.84935.peg.948	Inner membrane protein forms channel for type IV secretion of T-DNA complex, VirB8	- none -	226
Gene_fig|6666666.84935.peg.3430	Kinesin-related protein K4	- none -	677
Gene_fig|6666666.84935.peg.821	L-proline glycine betaine ABC transport system permease protein ProW	Choline and Betaine Uptake and Betaine Biosynthesis	295
Gene_fig|6666666.84935.peg.819	L-proline glycine betaine binding ABC transporter protein ProX (2x)	Choline and Betaine Uptake and Betaine Biosynthesis	328
Gene_fig|6666666.84935.peg.557	LSU ribosomal protein L34p	Cell Division Subsystem including YidCD, RNA modification cluster, Ribosome LSU bacterial	76
Gene_fig|6666666.84935.peg.1782	Mannosyltransferase WbkA	- none -	463
Gene_fig|6666666.84935.peg.2216	Methylmalonyl-CoA mutase	- none -	181
Gene_fig|6666666.84935.peg.689	Methyltransferase type 12	- none -	368
Gene_fig|6666666.84935.peg.2711	Mll7338 protein	- none -	133
Gene_fig|6666666.84935.peg.2020	Modification methylase EcoRV (Adenine-specific methyltransferase EcoRV)	- none -	304
Gene_fig|6666666.84935.peg.2991	Na+/Ca2+-exchanging protein	- none -	381
Gene_fig|6666666.84935.peg.770	N-Acetylneuraminate cytidylyltransferase	CMP-N-acetylneuraminate Biosynthesis, Sialic Acid	233

L. vicina symbiont population E220			
Gene ID	**Function**	**Subsystem**	**Length [bp]**
Gene_fig|6666666.84935.peg.3497	Neuropathy target esterase	- none -	117
Gene_fig|6666666.84935.peg.3203	orf; Unknown function	- none -	272
Gene_fig|6666666.84935.peg.2237	OrfE protein	- none -	435
Gene_fig|6666666.84935.peg.949	Outer membrane and periplasm component of type IV secretion of T-DNA complex, has secretin-like domain, VirB9	- none -	197
Gene_fig|6666666.84935.peg.1760	Phage T7 exclusion protein	- none -	465
Gene_fig|6666666.84935.peg.932	Phospholipase A1	- none -	393
Gene_fig|6666666.84935.peg.2337	Phosphoserine phosphatase	Glycine and Serine Utilization, Serine Biosynthesis, Serine Biosynthesis	219
Gene_fig|6666666.84935.peg.2758	Polysaccharide pyruvyl transferase	- none -	419
Gene_fig|6666666.84935.peg.205	Possible HipA protein	- none -	412
Gene_fig|6666666.84935.peg.972	Possible relaxosome component	- none -	120
Gene_fig|6666666.84935.peg.1356	Predicted membrane protein	- none -	536
Gene_fig|6666666.84935.peg.3725	Predicted pyrophosphatase	- none -	299
Gene_fig|6666666.84935.peg.3799	Prevent host death protein, Phd antitoxin #A	Phd-Doc, YdcE-YdcD toxin-antitoxin (programmed cell death) systems	75
Gene_fig|6666666.84935.peg.317	prevent-host-death family protein	- none -	73
Gene_fig|6666666.84935.peg.2574	Probable vanillate O-demethylase oxygenase subunit oxidoreductase protein	- none -	97
Gene_fig|6666666.84935.peg.1337	Prophage Lp2 protein 6	- none -	359
Gene_fig|6666666.84935.peg.666	Protein arginine N-methyltransferase 1	- none -	327
Gene_fig|6666666.84935.peg.3697	protein of unknown function DUF201	- none -	326
Gene_fig|6666666.84935.peg.555	Protein YidD	Cell Division Subsystem including YidCD, RNA modification cluster	78
Gene_fig|6666666.84935.peg.3202	putative ATP/GTP-binding protein protein	- none -	390
Gene_fig|6666666.84935.peg.1775	Putative DNA processing chain A	- none -	160
Gene_fig|6666666.84935.peg.2949	putative gas vesicle protein GvpG	- none -	81
Gene_fig|6666666.84935.peg.515	putative gas vesicle synthesis protein (4x)	- none -	722
Gene_fig|6666666.84935.peg.1369	Putative kinase protein	- none -	507
Gene_fig|6666666.84935.peg.3433	Putative phage protein	- none -	446
Gene_fig|6666666.84935.peg.631	Putative preQ0 transporter	Queuosine-Archaeosine Biosynthesis	229
Gene_fig|6666666.84935.peg.1606	putative restriction endonuclease	- none -	346
Gene_fig|6666666.84935.peg.2779	putative; ORF located using Glimmer/Genemark	- none -	378
Gene_fig|6666666.84935.peg.3837	Pyruvate-flavodoxin oxidoreductase	Pyruvate:ferredoxin oxidoreductase	79

L. vicina symbiont population E220			
Gene ID	**Function**	**Subsystem**	**Length [bp]**
Gene_fig|6666666.84935.peg.521	Radical SAM domain heme biosynthesis protein (2x)	- none -	948
Gene_fig|6666666.84935.peg.3189	Respiratory nitrate reductase alpha chain	Nitrate and nitrite ammonification	70
Gene_fig|6666666.84935.peg.67	Retron-type RNA-directed DNA polymerase (4x)	Group II intron-associated genes	212
Gene_fig|6666666.84935.peg.883	Sodium-dependent phosphate transporter	NhaA, NhaD and Sodium-dependent phosphate transporters, Phosphate metabolism	388
Gene_fig|6666666.84935.peg.3904	SrfB	- none -	1022
Gene_fig|6666666.84935.peg.14	Stability protein StdB (2x)	- none -	390
Gene_fig|6666666.84935.peg.3208	Tellurite resistance protein TerB	- none -	136
Gene_fig|6666666.84935.peg.3200	Tellurium resistance protein TerD (3x)	- none -	594
Gene_fig|6666666.84935.peg.2063	Toxin 1, PIN domain	- none -	152
Gene_fig|6666666.84935.peg.740	TPR repeat	- none -	399
Gene_fig|6666666.84935.peg.2893	TPR repeat:HAT (Half-A-TPR) repeat	- none -	244
Gene_fig|6666666.84935.peg.1412	transcriptional regulator, XRE family	- none -	73
Gene_fig|6666666.84935.peg.475	Transposase and inactivated derivatives (5x)	- none -	409
Gene_fig|6666666.84935.peg.2282	Type I restriction-modification system, restriction subunit R	Restriction-Modification System, Type I Restriction-Modification	102
Gene_fig|6666666.84935.peg.3507	Type I restriction-modification system, specificity subunit S	Restriction-Modification System, Type I Restriction-Modification	62
Gene_fig|6666666.84935.peg.3600	Xanthine and CO dehydrogenases maturation factor, XdhC/CoxF family	Molybdenum cofactor biosynthesis, Purine Utilization	39
Gene_fig|6666666.84935.peg.1810	YbbM seven transmembrane helix protein	Broadly distributed proteins not in subsystems	264
Gene_fig|6666666.84935.peg.1519	YcfA family protein	- none -	86
Gene_fig|6666666.84935.peg.963	zinc metalloproteinase Mpr protein	- none -	286
Gene_fig|6666666.84935.peg.1887	Zn-dependent proteases	- none -	126
	Mobile element proteins	56 x	16622
	Hypothetical proteins	**620 x**	**7003**

Table S6: Genes potentially under positive and negative selection between *L. aphanothecae* and *L. vicina* ectosymbionts as a result from the Direction of Selection (DoS) statistic as calculated by ODoSE (Vos *et al.* 2013)**.** DoS is positive when there is evidence of adaptive evolution, and is negative when deleterious mutations are selected against. Only orthologous genes that are shared among all strains were included in the analyses and only DoS values > 0.2 and < -0.2 are shown. Potential house-keeping and core genes are shaded in orange, genes involved in sulfur, carbon, nitrogen and phosphate metabolism and energy generation in green, cell membrane and putative host-symbiont interaction genes in blue, antibacterial resistance genes in red and genes potentially involved in defense are shaded yellow. Annotations are based on RAST (http://rast.nmpdr.org/, Overbeek *et al.* 2013).

Genes potentially under positive selection				
Function	**Subsystem**	**amount**	**potentially involved in**	**DoS**
Cell division trigger factor (EC 5.2.1.8)	Bacterial Cell Division		house-keeping	0,55
Ribosome hibernation protein YhbH	Ribosome activity modulation			0,50
transcriptional regulator, MerR family	- none -			0,47
Transcriptional regulator, ArsR family	CBSS-1085.1.peg.1363			0,46
tmRNA-binding protein SmpB	Heat shock dnaK gene cluster extended, Translation termination factors bacterial			0,45
Cell division protein	- none -			0,41
Transcriptional regulators of sugar metabolism	- none -			0,34
Ribosomal large subunit pseudouridine synthase B (EC 4.2.1.70)	CBSS-314276.3.peg.1499, RNA pseudouridine syntheses, Ribosome post-transcriptional modification and chromosomal segregation cluster			0,38
LSU ribosomal protein L20p	Mycobacterium virulence operon involved in protein synthesis (LSU ribosomal proteins), Ribosome LSU bacterial			0,36
Segregation and condensation protein B	CBSS-314276.3.peg.1499, Ribosome post-transcriptional modification and chromosomal segregation cluster			0,33
DNA polymerase III delta prime subunit (EC 2.7.7.7)	- none -			0,30
Translation elongation factor Tu	Mycobacterium virulence operon involved in protein synthesis (SSU ribosomal proteins), Translation elongation factors bacterial, Universal GTPases			0,28
Riboflavin kinase (EC 2.7.1.26) / FMN adenylyltransferase (EC 2.7.7.2)	Riboflavin, FMN and FAD metabolism in plants			0,27
Ribosomal-protein-S18p-alanine acetyltransferase (EC 2.3.1.-)	Bacterial RNA-metabolizing Zn-dependent hydrolases, Conserved gene cluster associated with Met-tRNA formyltransferase, Ribosome biogenesis bacterial, YrdC-YciO-Sua5 protein family			0,26

Function	Subsystem	amount	potentially involved in	DoS
Cell division topological specificity factor MinE	Bacterial Cell Division, Bacterial Cytoskeleton, Bacterial cell division cluster, Septum site-determining cluster Min			0,25
Chromosomal replication initiator protein DnaA	DNA replication cluster 1			0,25
Regulatory protein RecX	DNA repair system including RecA, MutS and a hypothetical protein, RecA and RecX			0,25
Tryptophanyl-tRNA synthetase (EC 6.1.1.2)	A cluster relating to Tryptophanyl-tRNA synthetase, tRNA aminoacylation, Trp			0,23
Cell division protein DivIC (FtsB), stabilizes FtsL against RasP cleavage	Bacterial Cell Division, Bacterial Cytoskeleton, Cell division-ribosomal stress proteins cluster, Stationary phase repair cluster			0,21
Transcriptional regulator	- none -			0,21
Fumarate reductase subunit C	Succinate dehydrogenase			0,40
Ribulose-phosphate 3-epimerase (EC 5.1.3.1)	Conserved gene cluster associated with Met-tRNA formyltransferase, Pentose phosphate pathway, Riboflavin synthesis cluster		energy/ carbon/ sulfur/ nitrogen metabolsim	0,35
PHA synthase subunit	- none -			0,33
Thiol:disulfide interchange protein DsbC	Periplasmic disulfide interchange			0,32
Cytochrome c4	Soluble cytochromes and functionally related electron carriers			0,31
4-hydroxybenzoate polyprenyltransferase (EC 2.5.1.39)	Ubiquinone Biosynthesis, Ubiquinone Biosynthesis - gjo			0,31
sodium/glucose cotransporter 2	- none -			0,28
Nitrogen regulatory protein P-II	Ammonia assimilation			0,26
Sucrose phosphate synthase	- none -			0,26
Glycogen debranching enzyme (EC 3.2.1.-)	Glycogen metabolism, Glycogen metabolism cluster			0,25
NAD kinase (EC 2.7.1.23)	NAD and NADP cofactor biosynthesis global			0,25
Succinate dehydrogenase iron-sulfur protein (EC 1.3.99.1)	5-FCL-like protein, Succinate dehydrogenase, TCA Cycle			0,24
Electron transport complex protein RnfG	Na(+)-translocating NADH-quinone oxidoreductase and rnf-like group of electron transport complexes			0,24
Sulfur carrier protein adenylyltransferase ThiF	Thiamin biosynthesis			0,22
ATP synthase epsilon chain (EC 3.6.3.14)	- none -			0,22
Pyruvate,phosphate dikinase (EC 2.7.9.1)	CBSS-349161.4.peg.2427, Glycolysis and Gluconeogenesis, Pyruvate metabolism I: anaplerotic reactions, PEP			0,21
Acetyl-coenzyme A synthetase (EC 6.2.1.1)	Pyruvate metabolism II: acetyl-CoA, acetogenesis from pyruvate			0,21
6-phosphofructokinase (EC 2.7.1.11)	Glycolysis and Gluconeogenesis			0,20
CDP-diacylglycerol--serine O-phosphatidyltransferase (EC 2.7.8.8)	Glycerolipid and Glycerophospholipid Metabolism in Bacteria			0,48

Function	Subsystem	amount	potentially involved in	DoS
LPS-assembly lipoprotein RlpB precursor (Rare lipoprotein B)	CBSS-208964.1.peg.3988, KDO2-Lipid A biosynthesis, Lipopolysaccharide assembly		Host recognition/ adhesion	0,44
Probable component of the lipoprotein assembly complex (forms a complex with YaeT, YfgL, and NlpB)	Lipopolysaccharide assembly			0,43
Flagellar motor rotation protein MotB	- none -			0,39
LptA, protein essential for LPS transport across the periplasm	KDO2-Lipid A biosynthesis, Lipopolysaccharide assembly, Lipopolysaccharide assembly cluster			0,36
PIN (PilT N terminus) domain	Type IV pilus			0,37
dTDP-4-dehydrorhamnose reductase (RmlD)	Rhamnose containing glycans, dTDP-rhamnose synthesis			0,29
O-antigen polymerase	- none -			0,28
Acyl-phosphate:glycerol-3-phosphate O-acyltransferase PlsY	Glycerolipid and Glycerophospholipid Metabolism in Bacteria			0,27
Type IV fimbrial assembly protein PilC	Type IV pilus	2		0,27
dTDP-4-dehydrorhamnose 3,5-epimerase (RmlC)	Capsular heptose biosynthesis, Rhamnose containing glycans, dTDP-rhamnose synthesis			0,26
Acyl-[acyl-carrier-protein]--UDP-N-acetylglucosamine O-acyltransferase (EC 2.3.1.129)	KDO2-Lipid A biosynthesis, Llipid A biosynthesis cluster			0,26
UDP-N-acetylmuramoylalanyl-D-glutamyl-2,6-diaminopimelate--D-alanyl-D-alanine ligase	Peptidoglycan Biosynthesis			0,22
Phospho-N-acetylmuramoyl-pentapeptide-transferase (EC 2.7.8.13)	Peptidoglycan Biosynthesis			0,21
Efflux transporter, RND family, MFP subunit, AcrA/E family	- none -		antimicrobial resistance	0,32
ABC-type multidrug transport system, permease component	- none -			0,25
ABC-type multidrug transport system, ATPase component	- none -			0,24
Conserved uncharacterized protein CreA	Tolerance to colicin E2	2		0,31
General secretion pathway protein D	- none -		Defense?	0,47
General secretion pathway protein N	- none -			0,40
General secretion pathway protein J	- none -			0,39
General secretion pathway protein K	- none -			0,25
Type I restriction-modification system methyltransferase subunit	- none -			0,21
16S rRNA m(2)G 1207 methyltransferase (EC 2.1.1.52)	- none -			0,46
1-deoxy-D-xylulose 5-phosphate synthase (EC 2.2.1.7)	Isoprenoid Biosynthesis, Nonmevalonate Branch of Isoprenoid Biosynthesis, Pyridoxin (Vitamin B6) Biosynthesis, Thiamin biosynthesis			0,28

Function	Subsystem	amount	potentially involved in	DoS
2,3,4,5-tetrahydropyridine-2,6-dicarboxylate N-succinyltransferase (EC 2.3.1.117)	Lysine Biosynthesis DAP Pathway,GJO scratch			0,29
Acetyl-coenzyme A carboxyl transferase alpha chain (EC 6.4.1.2)	Fatty Acid Biosynthesis FASII			0,32
Acetylglutamate kinase (EC 2.7.2.8)	Arginine Biosynthesis			0,21
acyltransferase 3	- none -			0,28
Adenylate kinase (EC 2.7.4.3)	Purine conversions			0,34
Aldehyde decarbonylase (EC 4.1.99.5)	- none -			0,30
Aspartate 1-decarboxylase (EC 4.1.1.11)	Coenzyme A Biosynthesis, Coenzyme A Biosynthesis cluster, Folate biosynthesis cluster			0,21
Aspartate aminotransferase (EC 2.6.1.1)	CBSS-216591.1.peg.168, Glutamine, Glutamate, Aspartate and Asparagine Biosynthesis, Threonine and Homoserine Biosynthesis			0,25
Aspartyl-tRNA(Asn) amidotransferase subunit A (EC 6.3.5.6) @ Glutamyl-tRNA(Gln) amidotransferase subunit A (EC 6.3.5.7)	tRNA aminoacylation, Asp and Asn, tRNA aminoacylation, Glu and Gln			0,25
Bme2 protein	- none -			0,20
cAMP-binding proteins - catabolite gene activator and regulatory subunit of cAMP-dependent protein kinases	cAMP signaling in bacteria			0,22
cytoplasmic chaperone TorD family protein	- none -			0,25
Dolichol-phosphate mannosyltransferase (EC 2.4.1.83) homolog	- none -			0,53
ErfK/YbiS/YcfS/YnhG family protein	- none -	3		0,23
exported protein	- none -			0,47
expressed protein	- none -			0,29
Ferritin-like protein 2	- none -			0,37
Fumarylacetoacetate hydrolase family protein	Gentisate degradation, Salicylate and gentisate catabolism			0,30
GMP synthase [glutamine-hydrolyzing] (EC 6.3.5.2)	Purine conversions	2		0,30
Homoserine O-succinyltransferase (EC 2.3.1.46)	- none -			0,40
HtrA protease/chaperone protein	Periplasmic Stress Response, Scaffold proteins for [4Fe-4S] cluster assembly (MRP family)			0,24
Hydrolase	- none -			0,22
hydrolase, haloacid dehalogenase-like family	- none -	6		0,21
hypothetical protein-transmembrane region and signal peptide prediction	- none -			0,24
Iron-sulfur cluster assembly scaffold protein IscU	Alanine biosynthesis	5		0,23
Kinesin light chain	- none -	3		0,27
Membrane metalloprotease	A cluster relating to Tryptophanyl-tRNA synthetase			0,21

Function	Subsystem	amount	potentially involved in	DoS
Membrane-bound lytic murein transglycosylase D precursor (EC 3.2.1.-)	CBSS-228410.1.peg.134, CBSS-342610.3.peg.1536, Murein Hydrolases			0,21
ParD protein (antitoxin to ParE)	Toxin-antitoxin replicon stabilization systems			0,32
Peptide deformylase (EC 3.5.1.88)	Bacterial RNA-metabolizing Zn-dependent hydrolases, Conserved gene cluster associated with Met-tRNA formyltransferase, Translation termination factors bacterial			0,46
Phosphopantothenoylcysteine decarboxylase (EC 4.1.1.36) / Phosphopantothenoylcysteine synthetase (EC 6.3.2.5)	Coenzyme A Biosynthesis, Coenzyme A Biosynthesis			0,25
Phosphoribosyl-ATP pyrophosphatase (EC 3.6.1.31)	Histidine Biosynthesis, Riboflavin synthesis cluster	5		0,22
Preprotein translocase subunit YajC (TC 3.A.5.1.1)	CBSS-211586.1.peg.2832			0,36
Prevent host death protein, Phd antitoxin	Phd-Doc, YdcE-YdcD toxin-antitoxin (programmed cell death) systems			0,54
Probable proline rich signal peptide protein	- none -			0,28
PTS system nitrogen-specific IIA component, PtsN	- none -			0,40
Putative 2-acylglycerophosphoethanolamine acyltransferase / acyl-acyl carrier protein synthetase (EC 6.2.1.20)	- none -			0,22
Putative transport protein	- none -			0,44
Shikimate 5-dehydrogenase I alpha (EC 1.1.1.25)	Chorismate Synthesis, Cluster containing Alanyl-tRNA synthetase, Common Pathway For Synthesis of Aromatic Compounds (DAHP synthase to chorismate)			0,30
Shikimate kinase I (EC 2.7.1.71)	Chorismate Synthesis, Common Pathway For Synthesis of Aromatic Compounds (DAHP synthase to chorismate)			0,25
Small GTP-binding protein domain	- none -	2		0,27
Sodium iodide symporter	- none -			0,21
tolB protein precursor, periplasmic protein involved in the tonb-independent uptake of group A colicins	Ton and Tol transport systems			0,22
Transporter	- none -	2		0,21
Trehalose-6-phosphate phosphatase (EC 3.1.3.12)	- none -			0,28
Two-component response regulator	- none -			0,29
VacJ-like lipoprotein precursor	- none -			0,21
Zinc ABC transporter, ATP-binding protein ZnuC	- none -			0,22
Zn-dependent protease with chaperone function PA4632	- none -			0,37

Genes potentially under negative selection

Function	Subsystem	amount	potentially involved in	DoS
LSU ribosomal protein L33p @ LSU ribosomal protein L33p, zinc-independent	Ribosome LSU bacterial, Ribosome LSU bacterial		house-keeping	-0,75
Peptidyl-tRNA hydrolase (EC 3.1.1.29)	Cell division-ribosomal stress proteins cluster, Sporulation-associated proteins with broader functions, Transcription repair cluster, Translation termination factors bacterial			-0,39
16S rRNA processing protein RimM	Ribosome biogenesis bacterial			-0,31
Type IV pilus biogenesis protein PilE	Type IV pilus		host attachment	-0,48
Uncharacterized protein YrbK clustered with lipopolysaccharide transporters	Lipopolysaccharide assembly, Lipopolysaccharide assembly cluster		membrane, glycosylation	-0,34
Lipopolysaccharide ABC transporter, ATP-binding protein LptB	KDO2-Lipid A biosynthesis, Lipopolysaccharide assembly, Lipopolysaccharide assembly cluster		"	-0,30
dTDP-glucose 4,6-dehydratase (RmlB) 1st	Rhamnose containing glycans, dTDP-rhamnose synthesis		rhamnose/ mannose	-0,29
2-octaprenyl-6-methoxyphenol hydroxylase (EC 1.14.13.-)	Ubiquinone Biosynthesis		energy	-0,44
Fumarate and nitrate reduction regulatory protein	- none -		"	-0,29
Death on curing protein, Doc toxin	Phd-Doc, YdcE-YdcD toxin-antitoxin (programmed cell death) systems			-0,47
18K peptidoglycan-associated outer membrane lipoprotein; Peptidoglycan-associated lipoprotein precursor; Outer membrane protein P6; OmpA/MotB precursor	Ton and Tol transport systems			-0,45
Cold shock protein CspD	Cold shock, CspA family of proteins			-0,51
Gene_fig004556: membrane metalloprotease	A cluster relating to Tryptophanyl-tRNA synthetase			-0,46
N-Acetylneuraminate cytidylyltransferase (EC 2.7.7.43)	CMP-N-acetylneuraminate Biosynthesis, Sialic Acid Metabolism			-0,47
Hypothetical nudix hydrolase YeaB	Nudix proteins (nucleoside triphosphate hydrolases)			-0,28
Methyltransferase type 11	- none -			-0,28
ortholog of Bordetella pertussis (BX470248) BP2475	- none -			-0,33
SAM-dependent methyltransferases	- none -			-0,53
ThiJ/PfpI family protein	- none -			-0,24
peroxidase, Bcp-type (EC 1.11.1.15)	CBSS-316057.3.peg.3521, Thioredoxin-disulfide reductase			-0,46
TsaE protein, required for threonylcarbamoyladenosine t(6)A37 formation in tRNA	Scaffold proteins for [4Fe-4S] cluster assembly (MRP family), YjeE, YrdC-YciO-Sua5 protein family			-0,50

Table S7: Genome-wide SNPs and SNPs/kb in the *L. aphanothecae* and *L. vicina* symbiont draft genomes

SNPs and indels	**E103 reads**	**E104 reads**	**E107 reads**	**E112 reads**	***L. vic* E220 reads**
E103 assembly	**1761**	60601	63090	65067	130231
E104 assembly	64160	**1802**	63285	65481	130121
E107 assembly	65192	66302	**3668**	61898	131977
E112 assembly	64994	61579	64132	**5315**	134700
***L. vic* E220 assembly**	130105	116534	122115	122873	**2326**

SNPs/kb [genome]	**E103 reads**	**E104 reads**	**E107 reads**	**E112 reads**	***L. vic* E220 reads**
E103 assembly	**0.37**	12.80	13.33	13.74	27.51
E104 assembly	13.25	**0.37**	13.07	13.52	26.87
E107 assembly	13.48	13.71	**0.76**	12.80	27.29
E112 assembly	12.73	12.06	12.56	**1.04**	26.39
***L. vic* E220 assembly**	26.18	23.45	24.57	24.72	**0.47**

Table S8: Mann-Whitney U pairwise comparison of single nucleotide polymorphisms (SNPs) within and among *Leptonemella* symbiont metagenomes. The analyses are based on the SNP data in Fig. 6 and Table S4. Probability levels and associated significance are indicated by ***P < 0.001, **P < 0.005.

whole genome SNPs/ shared gene SNPs	within *Leptonemella* symbiont metagenomes	among *L. aphanothecae* symbiont metagenomes	among *L. aphanothecae and* L. vicina symbiont metagenomes
within *Leptonemella* symbiont metagenomes	-	0.00185**/ 0.00186**	0.00426**/ 0.00431**
among *L. aphanothecae* symbiont metagenomes	-	-	0.00025***/ 0.00025***

SI Figures

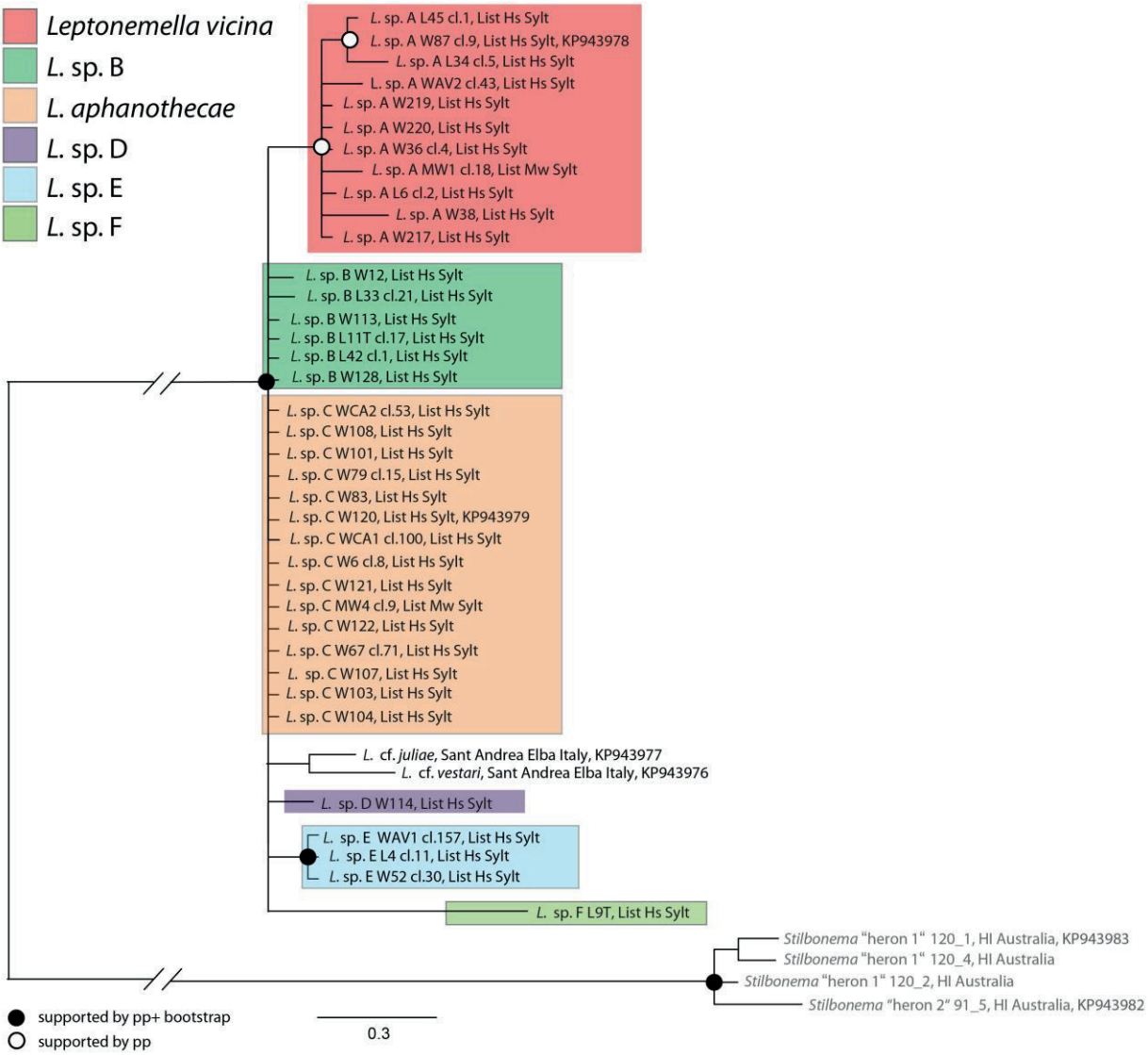

Fig. S1: Phylogenetic relationships of the *Leptonemella* symbionts based on the 16S rRNA gene. This is a consensus tree of bayesian inference (mrBayes) and maximum likelihood (RaxML) analyses. Nodes that were statistically supported with both methods (>80 % bootstrap value and 0.80 posterior probability (pp) value) are highlighted in black, nodes statistically supported only with pp (< 0.80) in white. The scale bar indicates 3 % nucleotide sequence divergence. Hs: Hausstrand; Khf: Königshafen; HI: Heron Island.

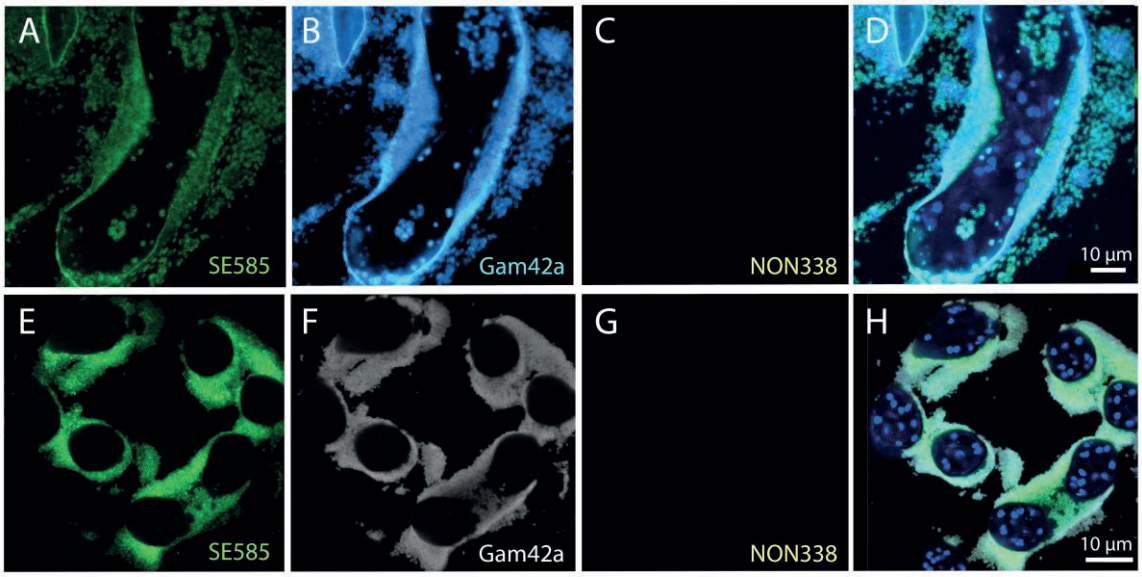

Fig. S2: Ectosymbionts of *Leptonemella vicina* (A- D) and *L. aphanothecae* (E- H) hybridized with CARD-FISH probes. Laser scanning microscope pictures show longitudinal sections of *L. vicina* (A- D) and *L. aphanothecae* (E- H) hybridized with the CARD-FISH probes targeting Sylt *Leptonemella* ectosymbionts (SE585) (A and E), the positive controls probe for Gammaproteobacteria (Gam42a) (B and F) and the negative control probe (NON338) (C and G). D and H: Overlay of A- D and E- F, respectively and DNA counterstain with DAPI (blue).

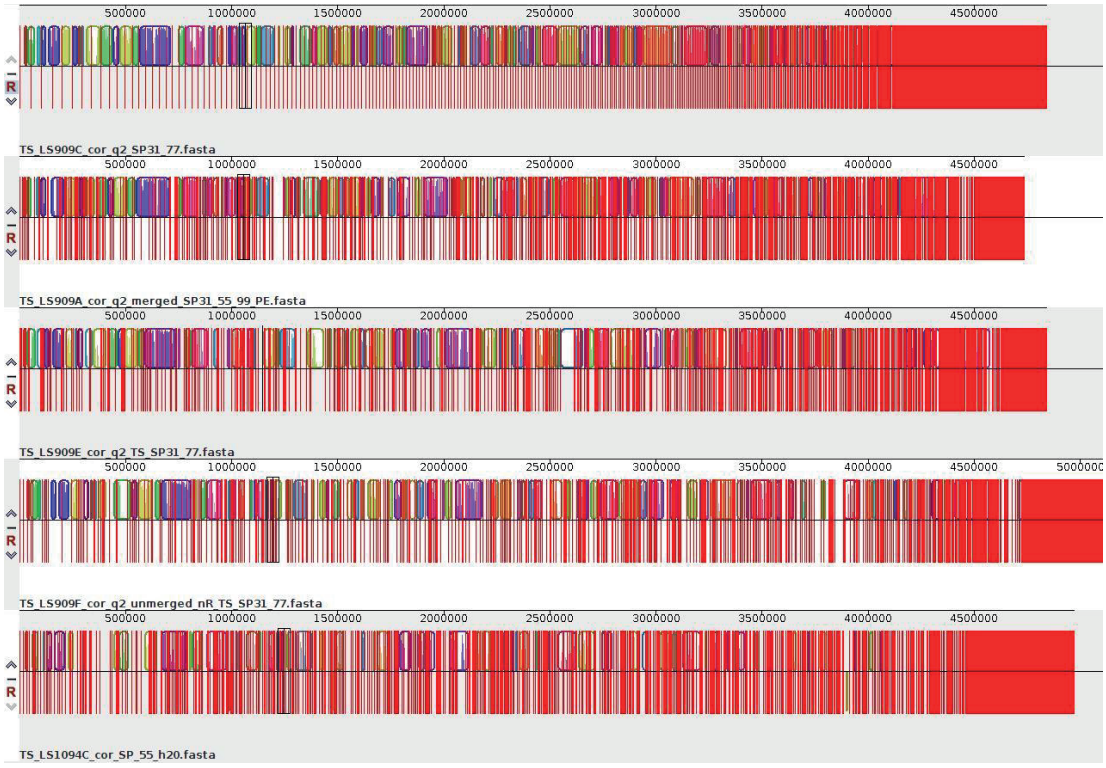

Fig. S3: Whole genome alignment of the *Leptonemella aphanothecae* and *L. vicina* ectosymbiont draft genomes showing the very fragmented assembly. From top to bottom: E104, E103, E107, E112 (*L. aphanothecae* strain genomes), E220 (*L. vicina* strain genome). The draft genome of E104 was used as a reference and the contigs of all other assemblies were re-ordered due to the reference. Red lines indicate the contig boundaries in each of the draft genomes. The figure was created using Mauve (Darling *et al.* 2010).

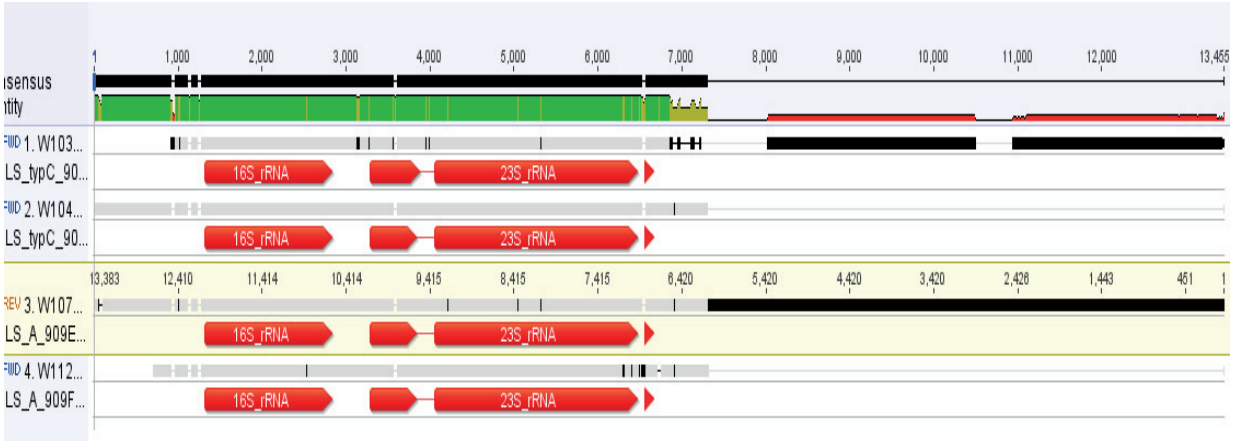

Fig. S4: Small ribosomal rRNA operon sequence differences between the *Leptonemella aphanothecae* strains E103, E104, E107 and E112. *L. aphanothecae* strain E104 was used as reference. The 16S rRNA and the 23S rRNA genes are highlighted in red. The gap inbetween 16S and 23S rRNA region contains the Internal transcribed spacer (ITS) region. Black lines within the sequences (grey bars) show single polymorphisms between the contigs. The aligment was extracted fom Geneious v.6 (http://www.geneious.com, Kearse *et al*. 2012).

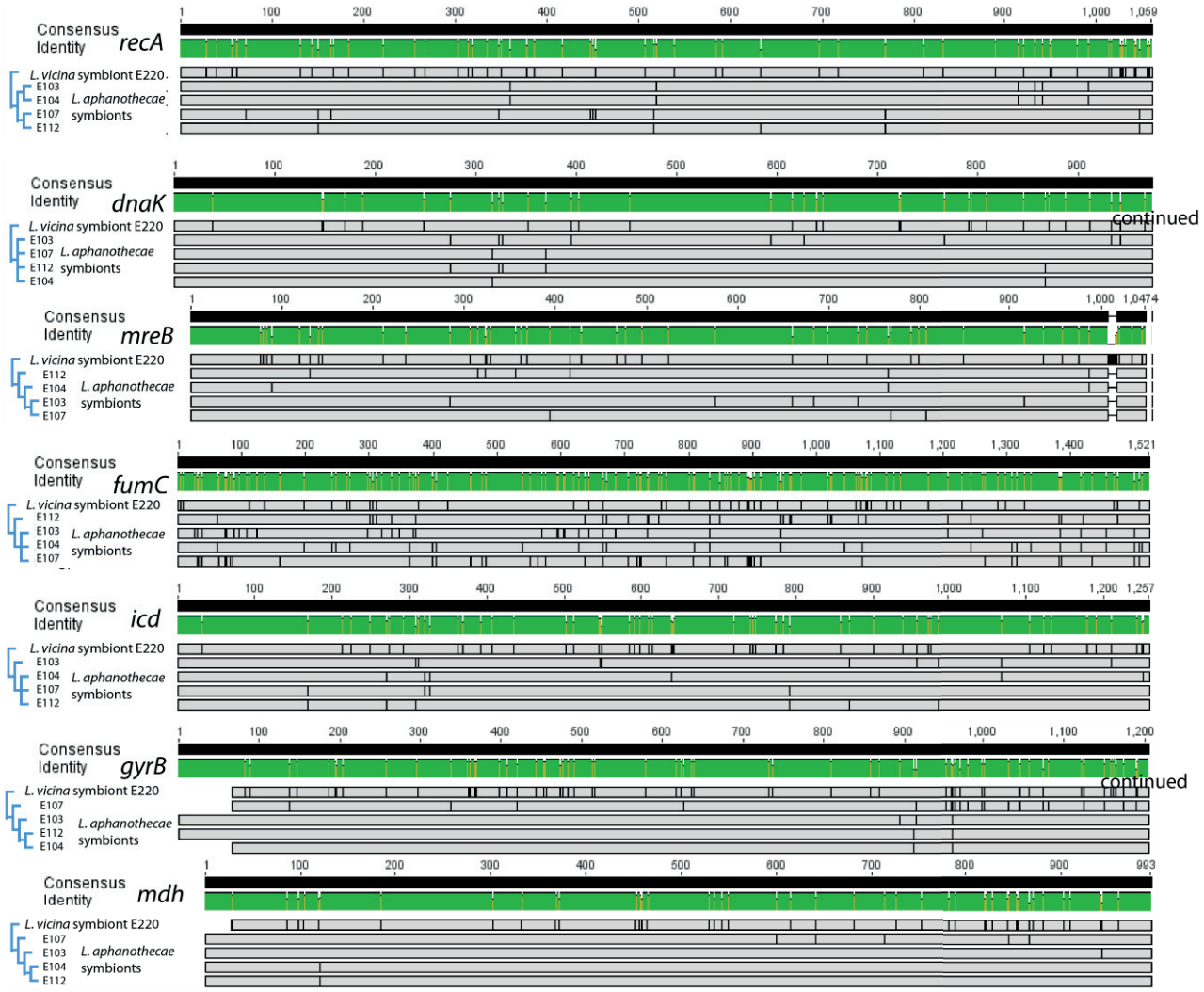

Fig. S5: Single copy marker gene sequence differences between the *Leptonemella aphanothecae* strains E103, E104, E107 and E112 and the symbiont of *L. vicina* (E220). Black lines within the sequences (grey bars) show single polymorphisms between the sequences. The aligments were extracted fom Geneious v.6 (http://www.geneious.com, Kearse *et al.* 2012)

SI References

Darling AE, Mau B, Perna NT (2010) progressiveMauve: Multiple Genome Alignment with Gene Gain, Loss and Rearrangement. *PLoS ONE*, **5**, e11147.

Kearse M, Moir R, Wilson A *et al.* (2012) Geneious Basic: An integrated and extendable desktop software platform for the organization and analysis of sequence data. *Bioinformatics*, **28**, 1647–1649.

Overbeek R, Olson R, Pusch GD *et al.* (2013) The SEED and the Rapid Annotation of microbial genomes using Subsystems Technology (RAST). *Nucleic Acids Research*, **42**, D206-D214.

Vos M, te Beek TAH, van Driel MA *et al.* (2013) ODoSE: A Webserver for genome-wide calculation of adaptive divergence in prokaryotes. *PLoS ONE*, **8**, e62447.

Chapter V

Investigating the nutritional role of ectosymbionts for their nematode host

Authors: Judith Zimmermann[1], Rahel Yemanaberhan[1], Oliver Jäckle[1], Jörg Ott[2], Nicole Dubilier[1], and Jillian M. Petersen[1]

[1]Department of Symbiosis. Max Planck Institute for Marine Microbiology, Celsiusstrasse, Bremen, Germany
[2]Department of Limnology and Oceanography, University of Vienna, Althanstrasse, Austria

Preliminary results

J.Z. developed the concept, designed and performed the incubation experiment, data analyses, and fluorescence in situ hybridizations, conceived and wrote the manuscript; R.Y. and O.J. performed the MAR analyses; O.J. conceived and edited the manuscript; J.O. helped to develop the concept, sample and identify the nematodes; N.D. helped to develop the concept; J.M.P. helped to perform the incubation experiments, helped to develop the concept and conceived the manuscript.

Abstract

Symbiotic associations in which the symbiotic partner provides nutritional benefits to the host are widespread. However, in the case of ectosymbiotic bacteria that live attached to the hosts' outer surface the nutritional role has rarely been investigated and is largely unknown. In this study we investigated stilbonematine nematodes of the genus *Leptonemella* that are widespread in marine sulfidic sediments and have long been hypothesized to feed on their sulfur-oxidizing symbionts that cover almost the complete nematode body. Incubation experiments with ^{13}C and ^{14}C-labeled inorganic carbon showed that symbionts first fix carbon autotrophically and that over time this labeled carbon is transferred to the host tissue. Catalyzed reporter deposition fluorescence *in situ* hybridization (CARD-FISH) on sections of *Leptonemella* individuals showed that bacteria attached to the hosts' surface and in the gut lumen are targeted by *Leptonemella* ectosymbiont-specific probes. Our study indicates that the sulfur-oxidizing ectosymbionts provide nutrition to their hosts and confirms the long-standing hypothesis of stilbonematine nematode grazing on their symbiont garden as food source.

Introduction

Symbiotic associations where eukaryotic hosts associate with symbiotic microorganisms are ubiquitous and many of the symbiotic partners are known to provide their host with certain metabolic products that the host cannot produce (Douglas 2010). While many insect symbionts amend their hosts' diet with, for example vitamins or amino acids (Moran *et al.* 2008), there are many cases of marine chemosynthetic symbionts that compensate for the entire nutrition of their invertebrate host (Cavanaugh *et al.* 2006). Some prominent examples are gutless deep-sea hydrothermal vent tubeworms or shallow water phallodriline annelids that depend on carbon compounds from chemosynthetic endosymbiotic bacteria that are harbored within specialized host cells or below the cuticle (Felbeck *et al.* 1983; Felbeck 1983; Childress *et al.* 1991; Bright, *et al.* 2000; Woyke *et al.* 2006; Kleiner *et al.* 2012b). For gutless animals such a nutritional dependency seems obvious, however there are also many cases of gut-bearing invertebrates that harbor specific ectosymbiotic bacteria on special body parts and some of these have also been suggested to benefit their host nutritionally (e.g. Goffredi *et al.* 2008; Ponsard *et al.* 2012). Transfer of nutrients is theoretically possible via two routes in gut-bearing systems: indirect transfer of nutrients that are leaked by intact ectosymbionts and absorbed through the epidermal cells or direct transfer through digestion of the symbiont cells. Indirect transfer has been concluded for the hydrothermal vent shrimp *Rimicaris exoculata* that is associated with ectosymbiotic bacteria located in the gill chamber, where isotope labeling experiments showed that host tissue got enriched after incubation with ^{14}C-labeled bicarbonate and acetate (Ponsard *et al.* 2012). However, since no pulse-chase incubation was performed it remains to be shown whether the label in the host tissue was due to anaplerotic carbon dioxide fixation by the host itself or by transfer from the bacteria. Anaplerotic reactions are common in all organisms, where carbon dioxide is fixed into three-carbon compounds to replenish intermediates of important metabolic pathways under specific conditions (e.g. Cataldi de Flombaum *et al.* 1977; Tang *et al.* 2009; Minet & Gaster 2010). Direct nutritional transfer via digestion has recently been suggested for epibionts attached to setae of *Shinkaia crosnieri* crabs (Watsuji *et al.* 2014), where feeding experiments with stained ectosymbionts revealed stained symbiont fragments in the gut. Additionally, symbiont phylotypes closely related to those on the setae were recovered from the gut, confirming that some of the symbionts may have a nutritional function (Watsuji *et al.* 2014). Except for preliminary pulse-chase experiments with ectosymbionts of the marine

ciliate *Zoothamnium* that indicated a combination of rapid transfer and subsequent symbiont digestion (Rinke, 2002), label tracking experiments over time are rarely applied for ectosymbiotic systems. Such experiments could differentiate between carbon that is transferred from symbionts to the host tissue and carbon dioxide fixation by anaplerotic reactions of the host itself.

An ideal symbiotic system to investigate carbon transfer from ectosymbionts to host tissue are the stilbonematine nematodes that are well-known for their intimate associations with sulfur-oxidizing bacteria that cover the hosts' cuticle in a species-specific matter (reviewed by Ott *et al.* 2004, Zimmermann *et al.*, in prep. ,Chapter III). Stilbonematine nematodes are highly abundant members of the meiofauna, especially in carbonate sands of tropical shallow waters (Tchesunov 2013), but they can also be found in lower abundances in deep sea sediments (Kamenev *et al.* 1993; Dando *et al.* 1994; Thiermann *et al.* 1997; Van Gaever *et al.* 2004; Leduc 2013) or temperate shelf regions (e.g. Riemann *et al.* 2003). The chemoautotrophic nature of the symbionts has been shown for some stilbonematine nematodes from the Caribbean (Powell *et al.* 1979; Schiemer *et al.* 1990; Polz *et al.* 1992). Separate incubation experiments with either labeled hydrogen sulfide or labeled bicarbonate under oxic conditions resulted in label-enriched symbionts and suggested that the symbionts are autotrophic sulfur-oxidizers (Powell *et al.* 1979; Schiemer *et al.* 1990). These results were subsequently confirmed by activity measurements of key enzymes of the Calvin cycle and the sulfur oxidation pathway (Polz *et al.* 1992). Measurements of elemental sulfur in ectosymbionts of two stilbonematine nematode species showed that the symbionts also store sulfur in their cytoplasm (Polz *et al.* 1992; Himmel *et al.* 2009). However, a nutritional benefit for the host by transfer of the fixed carbon from symbionts to host has not been shown for stilbonematine nematodes so far.

Stilbonematine nematodes have long been hypothesized to benefit from their symbionts nutritionally, by grazing on their own symbiont "garden" (Wieser 1959; Gerlach 1978). This was initially based on light microscopy analyses and subsequently on transmission electron microscopy (TEM) analyses that showed coccoid bacteria in the gut lumen of some stilbonematine nematode species (Ott *et al.* 1991). Additionally, the $\delta^{13}C$ isotopic signature of the nematodes suggested that the hosts carbon is mainly derived from chemolithotrophic bacteria that had the same $\delta^{13}C$ signature (Ott *et al.* 1991). However, final proof that

stilbonematine nematodes preferentially eat their own symbiotic bacteria instead of other chemolithotrophs from the sediment is still missing. The possibility that the host may also gain nutrition from leakage of organic carbon compounds by intact symbionts ("milking") in the gut or through the cuticle has also not been investigated so far. A schematic representation of the possible modes of carbon transfer in stilbonematine nematodes is given in Fig. 1.

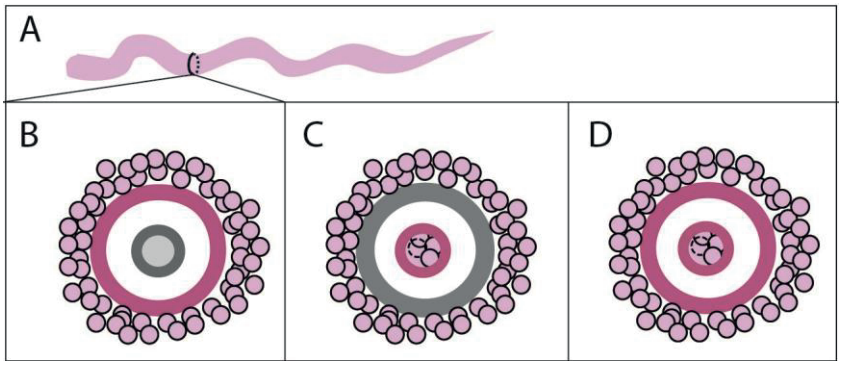

Fig.1: Schematic of possible modes of carbon transfer from ectosymbionts to the nematode host tissue. (A) Symbolic stilbonematine nematode (B) Nematode crosscut showing leakage of organic carbon compounds (pink) by intact cells through the cuticle. (C) Digestion of symbionts or milking of organic compounds by undigested cells (D) Combined leakage and digestion.

In this study we aimed to investigate whether ectosymbionts of stilbonematine nematodes contribute to the nutrition of their hosts. We sampled *Leptonemella* individuals from the temperate intertidal flat off the North Sea island of Sylt. Batches of worms were incubated with ^{13}C and ^{14}C-labeled bicarbonate in a pulse-chase and pulse-only incubation to trace label enrichment in symbionts and host over time. We used microautoradiography (MAR) on sections of some incubated *Leptonemella* individuals to visualize the localization of label uptake and mode of carbon transfer. Furthermore, general and symbiont-specific Catalyzed reporter deposition fluorescence *in situ* hybridization (CARD-FISH) probes were applied on sections of *Leptonemella* individuals, extracted from the sediment, to investigate whether we find the ectosymbionts in the gut lumen.

Material and Methods

Nematode collection and preparation

Sediment samples containing *Leptonemella* individuals were collected on an intertidal flat off List ('Hausstrand', 55.015069 N, 8.437788 E) on the North Sea island Sylt using sediment cores. Cores were taken during low tide close to polychaete burrows where highest *Leptonemella* densities were reported previously (Riemann *et al.* 2003). Samples for fluorescence *in situ* hybridization (FISH) were fixed in 1.5% paraformaldehyde (v/v) (PFA) in 0.2 µm filtered seawater at 4 °C overnight and washed twice in 4 °C 0.2 µm filtered seawater. Samples were stored in 50% ethanol (v/v) in filtered seawater at 4 °C until further processing. Stilbonematine nematode individuals intended for physiological experiments were pooled and transported in a small amount of the original washed sediment to the laboratory where they were stored for a maximum of three days at 4 °C before physiological experiments were performed. *Leptonemella* individuals were kept cool at 4 - 8 °C during the entire transport.

Preparation of the ^{13}C- and ^{14}C-labeled artificial seawater

Batches of oxic and microoxic 250 ml artificial seawater (ASW) containing ^{13}C and ^{14}C-labeled bicarbonate for the pulse-chase and the pulse-only incubation were prepared in 500 ml Schott flasks. Although we mainly used ^{14}C to trace label in our incubations we added ^{13}C-labeled bicarbonate as backup for potential stable isotopic analyses. All chemicals were purchased from Sigma-Aldrich (Munich, Germany) and the ASW was prepared as follows (final concentrations are given): 0.77 mM KBr, 8 mM KCl, 9.9 mM $CaCl_2*2H_2O$, 27 mM $MgCl_2*6H_2O$, 28 mM $MgSO_4*7H_2O$, 0.45 M NaCl were dissolved in 0.2 µm filtered Milli-Q water (Millipore, Darmstadt, Germany) and the pH was adjusted to 7.2 with NaOH before the medium bottle was autoclaved and cooled under N_2 gas atmosphere, introduced through a rubber plug, to keep the medium anoxic. The oxic ASW was cooled down with a slightly opened lid during mixing on a magnetic stirrer. The bottles were opened quickly to add 0.467 mM NH_4Cl, 0,147 mM KH_2PO_4, 0.024 µM $Na_2WO_4*2H_2O$, 0.023 µM $Na_2SeO_3*5H_2O$ and trace elements (for more information see Widdel and Bak, 1992). We added 2.3 mM ^{13}C-labeled $NaH^{13}CO_3^-$ into the ASW for the pulse medium and 2.3 mM $NaH^{12}CO_3^-$ in the ASW for the chase medium and flushed the headspace for 3 min with N_2 gas. To obtain microoxic conditions we substituted 40 ml of the headspace with pure oxygen gas and the ASW was

mixed on a magnetic stirrer in the gas-tight bottle overnight. We added 800 µl of a ^{14}C-labeled $NaH^{14}CO_3^-$ stock solution of 37 kBq (Perkin Elmer, Waltham, MA, USA) with a syringe to the $NaH^{13}CO_3^-$-containing pulse bottles and mixed the ASW thoroughly by shaking. For the microoxic pulse-only incubations this corresponded to a final concentration of 0.014 mM or 33 kBq/ ml ^{14}C and a final ^{13}C:^{14}C ratio of approximately 164:1 in the working solution. For the oxic pulse-chase incubations we did not measure the exact amount of radioactivity in the working solution but it was certainly comparable to the amount used for the pulse-only incubation. Gas-tight 5.9 ml Exetainers® (Labco Limited, High Wycombe, Buckinghamshire, England) were filled with the corresponding media without headspace and closed tightly. Oxygen microsensors (made in the Microsensor group of the Max Planck Institute for Marine Microbiology in Bremen, Germany) were used to measure the oxygen concentration in some of the prepared exetainers before the start of the incubations. In the microoxic pulse-only exetainers oxygen concentrations corresponded to around 140 µM oxygen (50% air saturation). In the oxic pulse-chase exetainers oxygen concentrations corresponded to around 280 µm oxygen (100% air saturation).

Pulse-chase and pulse-only incubations and scintillation counting

Incubation bags were prepared for easier handling of batches of nematodes. For each bag a 0.15 µm pore size polyamid mesh net (LABC, Labortechnik, Hennef, Germany) was fused with foil welding tongs (Model SZ, Kopp Verpackungssysteme, Stuttgart, Germany) from three sides to a standard size (Fig. 2). A glassbead mix (1:2 (v/v); 0.75 – 1 mm (ROTH): 0.4 – 0.6 mm (B. Braun Biotech International)) meant to mimic sediment grains was prepared and baked at 400 °C for 4 h to get rid of remaining organics. Incubation bags were filled with 3 cm^3 of the glass bead mix and autoclaved in a 96-well plate. Just before the incubations, unlabeled ASW was filled into the 96-well plate. Only bright white individuals, indicating sulfur storage in the bacteria (e.g. Polz *et al.* 1992; Hentschel *et al.* 1999) were picked from the sediment, washed in filtered seawater and transferred into the bags in ASW for preadaptation. Dead control individuals were fixed in 1.5% PFA (v/v) on ice for 3 hours prior to the incubation. For the pulse-chase incubation, 15 live *Leptonemella* individuals and 10 dead controls were incubated per time point (pulse: 2, 4, 6 h; chase: 5, 18 h) in one exetainer each. For the pulse-only incubation, 25 live *Leptonemella* individuals and 10 dead controls were incubated per time point (pulse: 1, 3, 5 h) in one exetainer each. The incubation bags

were closed with a Nylon thread and submerged into the exetainers containing the prepared labeled ASW. To guarantee homogenous conditions throughout the incubations exetainers were slowly shaken at approximately 100 rpm during the entire incubation. Incubations were performed in darkness at room temperature. We did not add an electron donor, but relied on the symbionts to use their stored sulfur compounds as energy source for carbon fixation. After each incubation timepoint, incubation bags were emptied out into petri dishes and the alive individuals were fixed in 1.5% PFA (v/v) overnight at 4 °C and washed twice in sterile filtered seawater. Pictures for subsequent length measurements of each individuals were taken using a stereomicroscope (Nikon SMZ, 745T; Nikon Corporation, Tokyo, Japan) with a mounted camera (Canon EOS 700D; Canon, Tokyo, Japan) before some individuals were stored in a mixture of ethanol and 2x phosphate-buffered saline (PBS) (1:1 v/v). While at least one quarter of the individuals was stored for subsequent microautoradiography (MAR) analyses the radioactivity of the remaining incubated individuals was measured via scintillation counting. To separate the ectosymbionts from the host tissue, single PFA-fixed nematodes in Eppendorf tubes (Eppendorf, Hamburg; Germany) were treated with three 30 s pulses of ultrasonication (Bandelin Sonoplus HD 70, 25% activitiy, Berlin, Germany) and vortexed in between. The content of the tube was emptied out into sterile petri dishes. Each worm was transferred onto a glass slide and microscopically inspected for remaining ectosymbionts. In case bacteria were still attached the ultrasonication step was repeated until no symbionts were left. Worms were washed in filtered seawater, pulled through 0.2 M HCl solution to remove left-over inorganic carbon and transferred into 5 ml scintillation vials containing the scintillation cocktail Ultima Gold™ (PerkinElmer, Waltham, MA, USA). The removed symbiont fractions were filtered onto 0.2 µm pore size polycarbonate filters (Sartorius, Göttingen, Germany), washed with 0.2 M HCl and transferred into scintillation vials too. To measure the specific activity in the incubation medium a 1:1 mixture (v/v) of the scintillation cocktails Carbo-Sorb and PermaFluor™ (PerkinElmer, Waltham, MA, USA) was used. All bulk measurements were done with the Scintillation Counter Tri-Carb 2900TR (PerkinElmer, Waltham, MA, USA). Dissociations per minute (DPM) of blanks containing pure scintillation cocktail (host) or scintillation cocktail with polycarbonate filter (symbionts) were subtracted from all measurements as background signal.

Data processing and carbon fixation rate calculation

Uptake of inorganic carbon per host and symbiont fractions (pmol C) and carbon uptake rates (µmol C g^{-1} wwt h^{-1}) were calculated based on the incorporated radioactivity of symbionts and host and the specific activity in the incubation medium. Uptake per host individual was normalized to mm worm length, estimated by image analysis done using ImageJ v1.45 (Rasband, National Institutes of Health, Bethesda, Maryland, USA, 1997-2014) using the picture taken directly after the incubations as a reference. To calculate average uptake rates per biomass, we based our calculations on previously reported average wet weight values of 10 - 30 µg per stibonematine nematode (Schiemer *et al.* 1990) Polz et al., 1992). Since *Leptonemella* individuals belong to one of the smallest stilbonematine nematode genera described so far, we assumed average wet weights of 10 µg.

Microautoradiography (MAR)

The incubated nematodes were embedded in medium grade LR-White low viscosity resin (London Resin Company, Reading, Berkshire, UK) in gelatin capsules (Plano, Wetzlar, Germany) as described before (Schimak *et al.* 2012). Capsules were placed in a 50 °C oven for four days to allow for complete polymerization of the LR-White resin. Blocks were trimmed with razor blades prior to sectioning and semi-thin sections (1 µm) were cut with an ultramicrotome (Leica EM UC7, Leica Microsystems, Germany) with a cutting speed of 1 mm per second. For microautoradiography the photographic emulsion type NTB (Carestream, USA) was used. The emulsion was first melted in a water bath at 46 °C for one hour and then diluted 1:1 (v/v) with 0.2% agarose. Slides with the tissue sections were immersed into the NTB/ agarose mix for 3 s, and subsequently held vertically for 10 s to ensure a uniform distribution of the emulsion. Slides were placed on ice-cold aluminum blocks for 5 min and transferred into lightproof boxes containing silica beads (Sigma-Aldrich Gmbh, Steinhein, Germany) serving as desiccants and stored at 4 °C. Exposure of the slides was stopped after three, five and seven days by immersing slides in GBX developer solution (Carestream Health, Rochester, NY, USA) for 2 min. Slides were washed with MilliQ for 50 s before being transferred into fixing solution (Eastman Kodak Company, Rochester, NY, USA) for 5 min. Slides were washed in MilliQ for 5 min and air dried. Tissue sections were stained with a 1% toluidine blue-borax solution for 4 min and excess stain was removed by washing in MilliQ.

Washed slides were dipped in 96% ethanol and air dried. Permount (Fisher Chemical Permount™ Mounting Medium, Schwerte Germany) was used for mounting. Slides were examined with a Nikon Eclipse 50i microscope (Nikon Corporation, Japan) under bright field settings. Images were taken with a mounted AxioCam MRc camera (Carl Zeiss, MicroImaging GmbH, Göttingen, Germany).

Catalyzed reported deposition fluorescence *in situ* hybridization (CARD-FISH)

PFA-fixed *Leptonemella* individuals were embedded in Agar and subsequently in Steedman's Wax (Steedman 1957), sectioned and dewaxed as described before (Zimmermann *et al.*, in prep.; Chapter IV). Serial CARD-FISH hybridizations on tissue sections were also performed as described before (Zimmermann *et al.*, in prep; Chapter IV). All horseradish peroxidase-labeled probes (Interactiva, Ulm, Germany) used in this study are listed in Table 1. For counterstaining of nuclear deoxyribonucleic acid (DNA) 4,6-diamidino-2-phenylindole dihydrochloride (DAPI) was directly added into the embedding medium, a (2:11 (v/v)) mixture of Citifluor (Citifluor Ltd, Leicester, UK) and Vectashield (Vector laboratories, Burlingame, CA, USA). Sections were analyzed with a Confocal Laser Scanning microscope (Zeiss CLSM 780, Carl Zeiss Microscopy GmbH, Jena, Germany) and contrast and brightness were adjusted with the Zen imaging software (Carl Zeiss Microscopy GmbH, Jena, Germany).

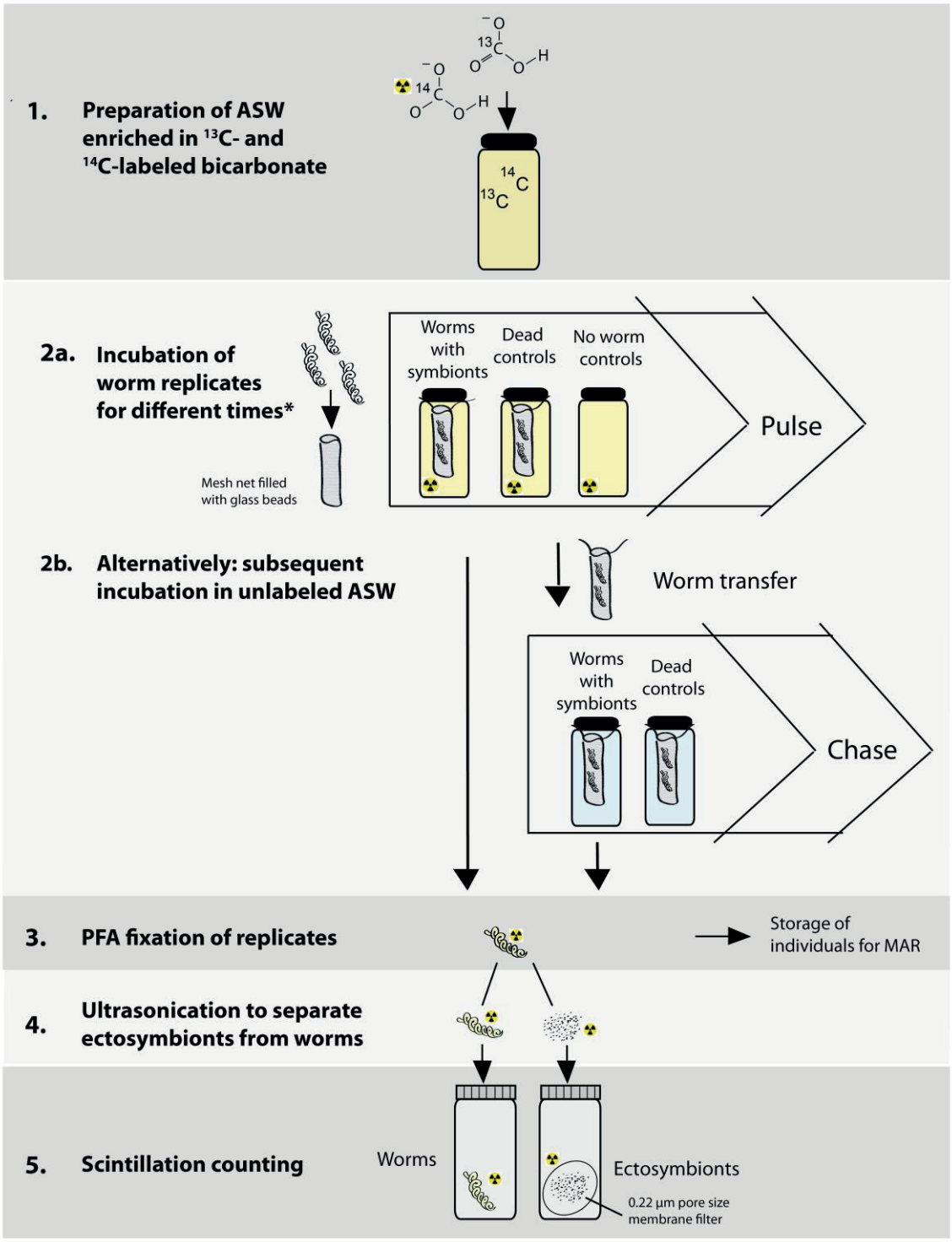

Fig. 2: Experimental setup of the $^{13}C/^{14}C$-labeled bicarbonate incubation to examine carbon fixation by symbionts and label transfer to the host. Freshly sampled *Leptonemella* individuals were transferred into incubation bags (0.15 µm mesh net) filled with glass beads meant to mimic sediment grains as holdfast for the nematodes. Nematodes were incubated in exetainers filled with artificial seawater (ASW) amended with ^{13}C and ^{14}C-labeled bicarbonate (pulse incubation). Alternatively, an incubation in unlabeled ASW followed (chase incubation). Incubations were terminated after different timepoints by fixation of the individuals in 1.5% (v/v) paraformaldehyde (PFA). Some individuals were stored for microautoradiography analyses (MAR). The remaining individuals were treated with ultrasonication to remove ectosymbionts from host and the radioactivity within both fractions was measured singly by scintillation counting.

Table 1: Probes used in this study

Probe	Target organisms	Probe sequence (5' → 3')	FA° [%]	Position*	Reference
Gam42a	Gammaproteobacteria	GCCTTCCCACATCGTTT	35	1027 - 1043*	(Manz *et al.* 1992)
NON338	Negative control	ACTCCTACGGGAGGCAGC	35	338 - 355	(Wallner *et al.* 1993)
SE585	Sylt *Leptonemella* ectosymbionts	CATCTGACTTATCTAGCC GC	40	585 - 604	Zimmermann *et al.* in prep.; Chapter IV
Probe	**Target organisms**	**Probe sequence (5' → 3')**	**FA° [%]**	**Position***	**Reference**
Lvic432	*L.. vicina* and *L.* sp. B ectosymbionts	TCTTCCCGACTGAAAGTG CT	35 - 40	432 - 451	Zimmermann *et al.* in prep.; Chapter IV
Laph432	*L. aphanothecae* and *L.* sp. C, D, E and G ectosymbionts	TCTTCCCAACTGAAAGTG CT T	35 - 40	432 - 451	Zimmermann *et al.* in prep.; Chapter IV
c_Lvic432	*L. aphanothecae* and *L.* sp. C, D, E and G ectosymbionts	TCTTCCCAACTGAAAGTG CT	35 -40	432 - 451	Zimmermann *et al.* in prep.; Chapter IV
c_Laph432	*L. vicina* and *L.* sp. B ectosymbionts	TCTTCCCGACTGAAAGTG CT	35 - 40	432 - 451	Zimmermann *et al.* in prep.; Chapter IV

°formamide concentration used in the hybridization buffer in % [v/v]; * position in the 23S rRNA of *E.coli*

Results

Autotrophic carbon fixation by the *Leptonemella* ectosymbionts and subsequent transfer of labeled compounds

We used two different approaches to investigate ectosymbiont carbon metabolism and transfer of organic carbon to the *Leptonemella* host. At first, we did an oxic pulse-chase incubation where *Leptonemella* ectosymbioses were incubated for 6 h in ^{13}C and ^{14}C-labeled bicarbonate and subsequently transferred into unlabeled artificial seawater for up to 18 h. We could only measure a slight decrease in oxygen in the end of the incubation, indicating that the worms were not limited in oxygen throughout the incubation. Label enrichment was observed within the first four hours, with maximum values of 178 dissociations per minute (DPM) per mm worm after 2 h, while label enrichment was very low at the 6 h timepoint, with maximum values of 80 DPM per symbiont fraction (Fig. 3A). Label in the symbionts was slightly higher during the chase period compared to the 4 h timepoint, with median value of 160 DPM per mm worm after 5 h chase and decreased to a median of around 80 DPM per symbiont fraction at the final timepoint of the incubation (Fig. 3A). The enrichment was

significantly higher compared to the dead controls, which did not show any label uptake (Mann-Whitney-U-Test; p =0.02*). The host tissue got slightly enriched during the pulse period with maximum values of 11 DPM per mm worm after 4 h and 4 DPM per mm worm after 6 h, which was significantly higher (p value was borderline to non-significant) compared to the dead controls (Mann-Whitney-U-Test; p =0.03*). Label enrichment was observed in the host tissue during the chase phase with highest values after 5 h, and median values of 18 DPM per mm worm. This value was nine times larger than the highest medians measured during the pulse time (Fig. 3B). After the peak at 5 h chase, label enrichment decreased to median values of 11 DPM per mm worm.

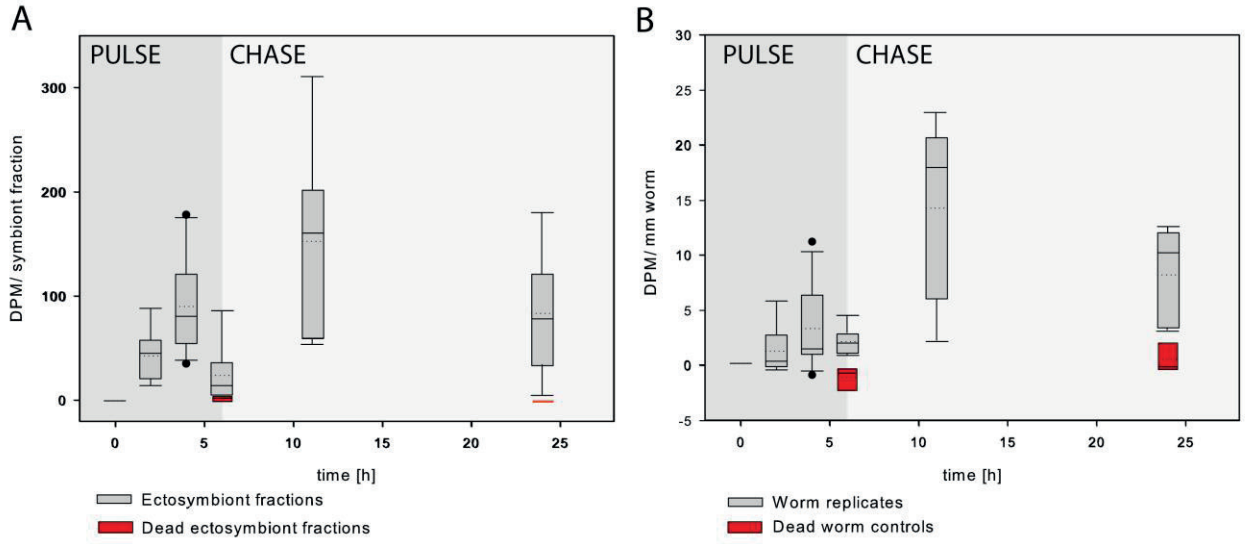

Fig. 3: ^{14}C-labeled enrichment in ectosymbiotic bacteria (A) and *Leptonemella* host (B) during oxic pulse-chase incubations in July 2012. *Leptonemella* individuals (host and symbionts) were incubated for 2, 4 and 6 h in artificial 87 - 92% air-saturated seawater spiked with ^{13}C/^{14}C-labeled bicarbonate (pulse) and subsequently transferred into unlabeled artificial seawater for up to 18 hours (chase). Worms and symbionts were separated by ultrasonication before their radioactivity was measured separately with the scintillation counter. Error bars indicate standard deviation from 5 - 11 replicates per timepoint, depending on loss rates during the incubation and washing steps. The dotted lines represent the mean.

At second, we did a pulse-only incubation under microoxic conditions for a maximum of 5 hours, where we included a 1 h and 3 h timepoint, instead of 2 h and 4 h in the oxic conditions. Similarly to the oxic incubation, oxygen levels remained equally high throughout the incubation indicating that the worms were not limited in oxygen at any point. The results of this incubation showed that carbon uptake of the ectosymbiont fractions was relatively continuous over time, with highest values of up to 805 DPM per symbiont fraction after 5 h

(Fig. 4A). The enrichment was significantly higher compared to the dead controls, which did not show any label uptake (Mann-Whitney-U-Test; p =0.0002***). Similarly, the host tissue got enriched over time with up to 46 and 42 DPM per mm worm after 3 and 5 h, respectively and this was significantly higher compared to the dead controls (Mann-Whitney-U-Test; p=0.0008*** and p =0.0002***) (Fig. 3B). While ectosymbiotic bacteria were already enriched after 1 h, uptake of carbon by the host was only measureable after 3 h (Fig. 4A and B). However, not all host individuals that were associated with highly enriched bacteria got enriched themselves (Fig. 4A and B). Additionally, the amount of carbon uptake varied considerably by a factor of ten between symbiont fractions and hosts per timepoint (Fig. 3 and 4). For example label enrichment per symbiont fraction ranged from 78 - 805 DPM and from 0.5 to 42 DPM per mm worm after the 5 h pulse period (Fig. 4B) and the same variability was observed for the pulse-chase incubation (Fig. 3).

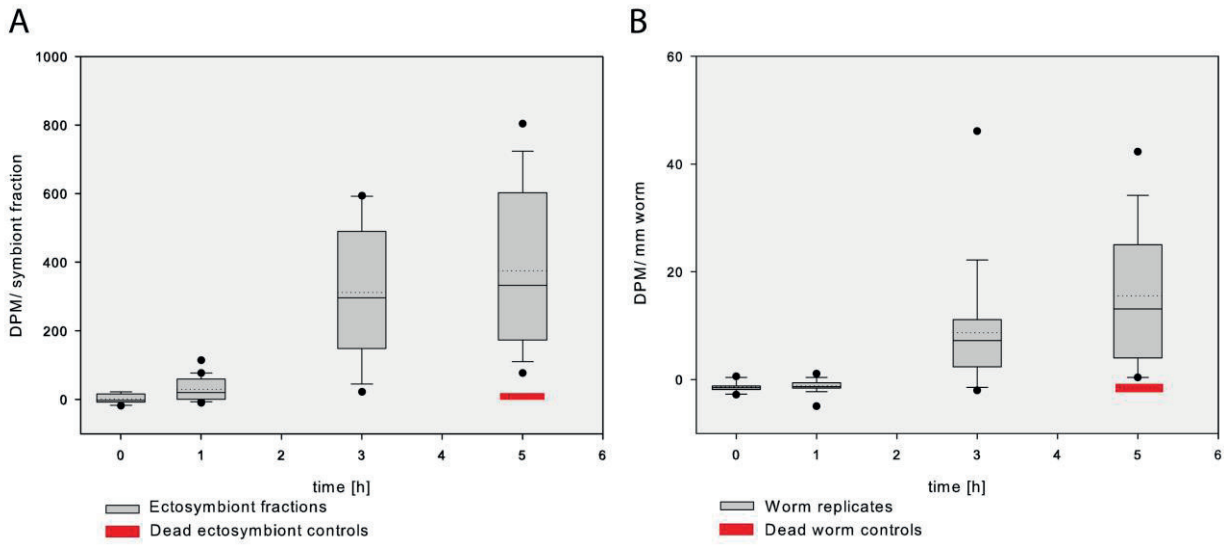

Fig. 4: ^{14}C-labeled bicarbonate uptake by ectosymbiotic bacteria (A) and *Leptonemella* host (B) during microoxic pulse-only incubations in September 2012. *Leptonemella* individuals (host and symbionts) were incubated up to 5 h in microoxic (50% air-saturated) artificial seawater spiked with ^{13}C/^{14}C-labeled bicarbonate. Worms and symbionts were separated by ultrasonication before their radioactivity was measured separately with the scintillation counter. Error bars indicate standard deviation from 12 - 18 replicates per timepoint, depending on loss rates during the incubation and washing steps. The dotted lines represent the mean.

For the pulse-only incubation, we measured the relative amount of ^{14}C in the ASW and therefore we could calculate the total carbon uptake per *Leptonemella* individual (host and symbionts). While total carbon uptake ranged from 16 to 159 pmol after 1 h, values ranged from 126 to 1021 pmol carbon per individual after 5 h (Fig. 5A). Although we observed a

continuous carbon uptake by *Leptonemella* individuals over time, the total carbon uptake data once more reflect the high variability between the individuals. When considering an average wet weight of 10 µg per individual, carbon uptake rates would range from 7 - 13 µmol C per g wwt and hour with highest uptake rates after 3 h (Fig. 5B). As mentioned before, we did not measure the exact initial ^{14}C concentration in the ASW of the almost oxic pulse-chase incubation. However, assuming that the amount of ^{14}C accounted for the aspired 0.7% of the total carbon in the media (see Material and Methods section) we would have maximum uptake of 397 pmol C per *Leptonemella* individual. Considering an average wet weight of 10 µg per individual and pulse time of 6 h, this would correspond to maximum carbon uptake rates of 6.6 µmol C per g wwt and h, which is a similar rate than calculated for the microoxic incubations.

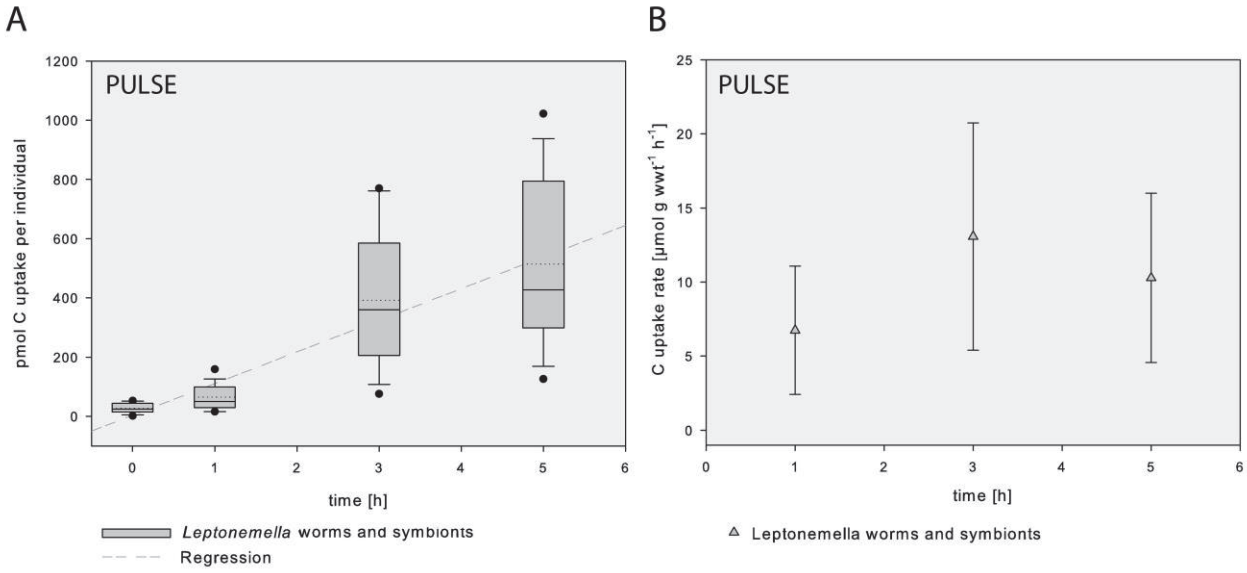

Fig. 5: Total carbon uptake (A) and average carbon uptake rates (B) by *Leptonemella* individuals during microoxic incubations in September 2012. (A) Carbon uptake quantities per individual were calculated from the combined radioactivity measured in the worms and symbiont fractions by scintillation counting (Fig. 4A and B). Error bars indicate standard deviation from 12 - 18 replicates per timepoint. The straight lines represent the medians, the dotted lines the means. (B) Average carbon uptake rates per timepoint were calculated from average carbon uptake quantities (shown in A) assuming an average wet weight of 10 µg per *Leptonemella* individual.

Visualization of carbon incorporation by *Leptonemella* individuals

To visualize the localization of ^{14}C uptake in the *Leptonemella* symbiosis over time, we applied MAR on sections from one incubated individual per time point (0 h, 1 h, 3 h and 5 h). While no MAR signals were observed after 5 or even 7 days exposure on sections of the 1 h

incubated individual (results not shown) sections of the 3 h and 5 h incubated individuals showed clear MAR signals after 5 days exposure time (Fig. 6A and B). Interestingly, symbionts attached to the 3 h incubated worm were not evenly enriched in MAR signals, indicated by high silver grain densities co-located with some ectosymbiont batches but not with others (Fig. 6A). Some silver grains were also observed in regions of host tissue, but these were considerably less than in symbiont regions (Fig. 6A). On the individual that was incubated for 5 h only few symbionts were left after the embedding procedure (Fig. 6B). One explanation for this is that most symbionts detached from the worm cuticle just before embedding, likely due to poor fixation. Here, high densities of silver grains were clearly co-located with these single symbionts (Fig. 6B, green arrow heads) but a high amount of silver grains was also observed within the host tissue (Fig. 6B). Sections of the control individual did not show any MAR signals (Fig. 6C).

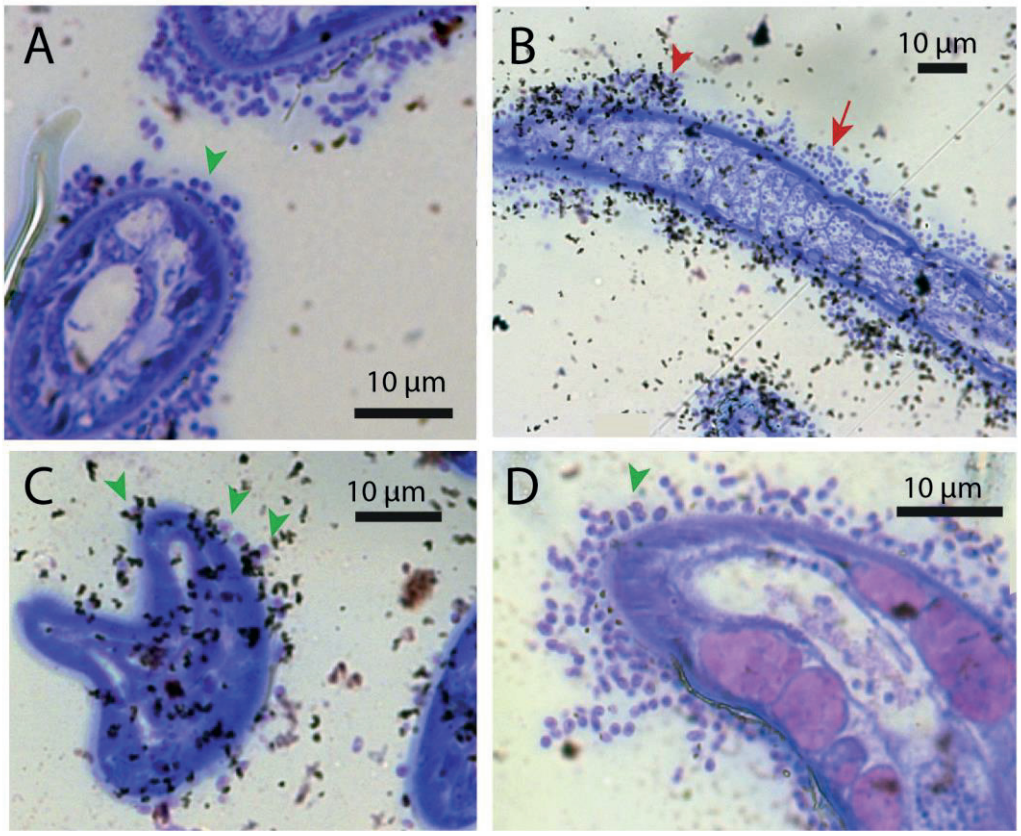

Fig. 6: Autoradiographs of sections from *Leptonemella* individuals incubated in September 2012 (Fig. 4 - 5). Individual that was incubated for 1 h (A), 3 h (B) and 5 h (C) in ^{14}C-labeled bicarbonate. (D) Control individual that was not incubated. The green arrow heads point towards single symbiont cells that remained on the worms after the embedding procedure. Silver grain precipitations (black dots) in B and C highlight locations of radiolabel in the tissue. The red arrow head and the red arrow point towards a batch of symbionts highly and barely enriched in ^{14}C, respectively. Sections were exposed to the MAR solution for 5 (B, C) to 7 days (A, D) and the tissue was counter-stained with toluidine blue.

Detection of *Leptonemella* ectosymbionts in the gut by CARD-FISH

To investigate the long-standing hypothesis of stilbonematine nematode grazing on their symbiont garden as food source, we investigated whether *Leptonemella* individuals contain their ectosymbionts in the gut. For this we screened sections of two *L. aphanothecae* and four *L. vicina* individuals that we identified based on morphology with ectosymbiont-specific CARD-FISH probes. In two of the *L. vicina* individuals we found bacteria not only attached to the outer surface but also in the gut. All bacteria were consistently stained with the general Gammaproteobacteria-specific probe and the previously designed SE585 probe (Zimmermann *et al*., in prep., Chapter IV) that targets specifically the Sylt *Leptonemella* ectosymbiotic bacteria (Fig. 7, A - C). To investigate whether the gut bacteria are species-specific, we additionally used the previously designed Lvic432 and Laph432 probes that target *L. aphanothecae* and *L. vicina* ectosymbionts, respectively (Zimmermann *et al*., in prep., Chapter IV). Because the probes only differ by one basepair we used the probes in combination with the previously designed competitor probes, to prevent false positives. Both the ectosymbiotic bacteria as well as the gut bacteria were stained by the probe targeting the *L. vicina*- but not the *L. aphanothecae*-specific ectosymbionts (Fig. 7, D - G).

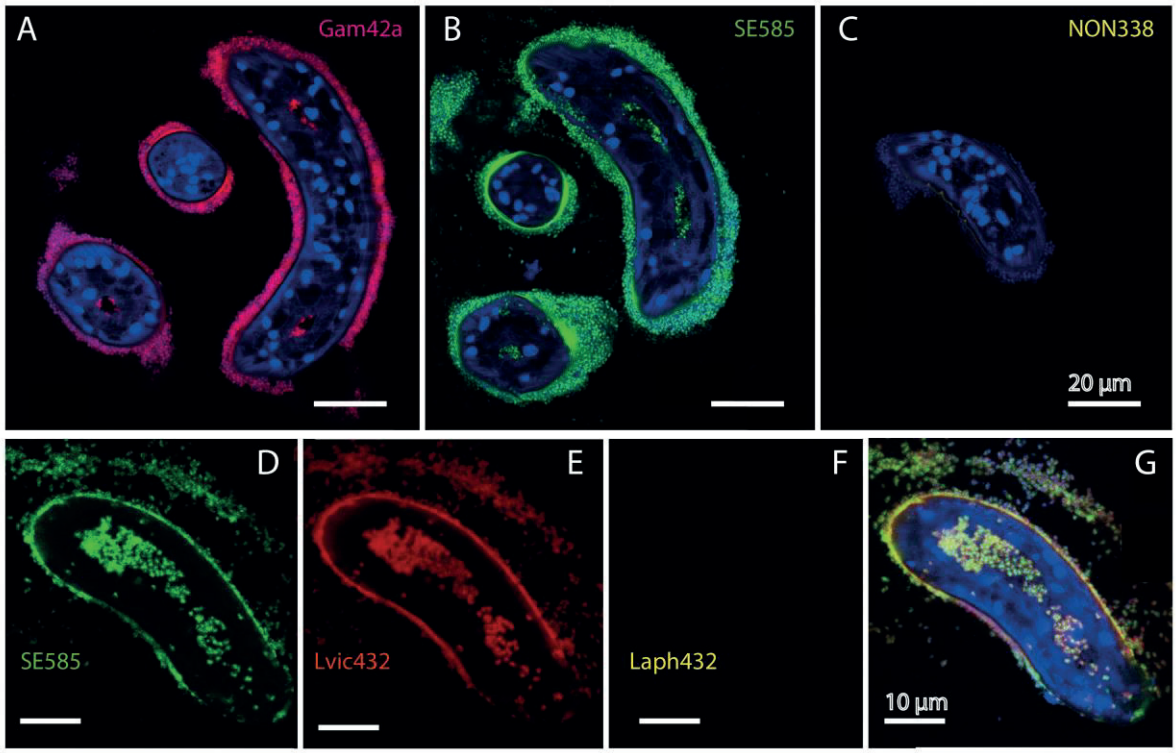

Fig. 7: Symbiont-specific CARD-FISH probes hybridized with ectosymbiotic bacteria as well as bacteria in the gut region of *Leptonemella vicina*. (A - C): Consecutive *L. vicina* cross-sections with bacteria in the gut region hybridized with the Gammaproteobacteria-specific probe Gam42a (A), the Sylt ectosymbiont-specific probe SE585 (B) but not with the negative control probe NON338 (C). All sections were counter-stained with DAPI (blue). (D - G): Triple hybridization of a *L. vicina* cross-section with the SE585 probe (D) the *L. vicina* ectosymbiont-specific probe (E) and the *L. aphanothecae* ectosymbiont-specific probe (F) yellow. (G): Overlay of D - F and DNA counterstain with DAPI (blue).

Discussion

Leptonemella species and its ectosymbionts – a nutritional symbiosis?

Our incubation experiments with labeled bicarbonate showed that the symbionts get enriched in label over time and that after a time period of 3 - 5 hours also the host gets enriched in label (Fig. 3, 4). Both our pulse-chase and pulse-only incubations showed similar trends, although the amount of label uptake varied strongly between individuals. There are two possibilities of label enrichment in *Leptonemella* hosts – either via transfer of labeled organic carbon that was fixed by the ectosymbionts autotrophically, or via anaplerotic CO_2 fixation by the host itself. Anaplerotic CO_2 fixation into a three-carbon compound such as phosphoenolpyruvate (PEP) or pyruvate to replenish tricarboxylic acid (TCA) cycle

intermediates is a common process in marine invertebrates, including nematodes (Hammen & Osborne 1959; Hammen & Wilbur 1959). The amount of carbon that is fixed via anaplerotic reactions has rarely been quantified. In the heterotrophic bacterium *R. denitrificans* anaplerotic carbon fixation accounts for only a fraction of the total carbon fixation (10 - 15%) (Tang *et al.* 2009). Similarly, for the vestimentiferan tubeworm endosymbiosis anaplerotic pathways have been suggested to account for lesser amounts of carbon fixation in host and symbionts compared to autotrophic carbon fixation by the symbionts (Stewart & Cavanaugh 2006). If carbon uptake via anaplerotic CO_2 fixation would be a major way of carbon uptake in *Leptonemella*, we would expect a linear label increase in the host with time during the pulse period and no increase in label during the chase time period. However, our incubations showed that the host tissue only got enriched after 2 - 3 hours of incubation in labeled bicarbonate while the symbiont fractions started after 1 h (Fig. 3 and 4). In addition, we saw a further increase of label in the host tissue during the chase phase in our pulse-chase incubation(Fig. 3 B). MAR analyses of worms, that were incubated for different time points also showed that symbiont and host enrichment did not occur simultaneously. Strong symbiont enrichment was visible in the worm that was incubated for 3 h but only few MAR signals were visible in the host tissue, while the host tissue was clearly enriched after 5 h of incubation (Fig. 6A). Our incubations thus suggest that anaplerotic carbon fixation was not responsible for the label enrichment in the host tissue, but that bicarbonate is primarily fixed by the symbionts and subsequently transferred to the host.

Two modes of carbon transfer are generally observed in symbiotic systems: (1) fast release or leakage of fixed carbon compounds, and (2) digestion of symbionts (e.g. Bosch & Grassé 1984; Fisher & Childress 1986; Distel *et al.* 1988; Herry *et al.* 1989; Felbeck & Jarchow 1998; Bright, *et al.* 2000). In contrast to endosymbionts that are located inside cells, *Leptonemella* ectosymbionts are attached to the surface and therefore leakage could either be possible by transferring small organic carbon molecules through the cuticle of the host or through absorption via the gut lumen. Leakage of small organic compounds can occur rapidly, such as shown in the vestimentiferan tubeworm *Riftia pachyptila* endosymbiosis where carbon enrichment in the symbiont-free host tissue was observed within 15 min (Bright, *et al.* 2000). On the other hand, slow transfer within hours or days was attributed to digestion of symbionts, such as in bathymodioline mussels, where significant carbon enrichment in symbiont-free tissue did not occur before 10 days of incubation time (Childress & Fisher

1992; Streams *et al.* 1997). Label enrichment in the *Leptonemella* host tissue started after 2 - 3 h in either incubation and not all host individuals that were associated with highly enriched bacteria got enriched themselves (Fig. 3 and 4). This indicates that immediate transfer due to leakage of organic compounds through the cuticle most likely does not play a big role in this symbiosis.

In MAR sections of individuals that were incubated in ^{14}C-enriched host tissue we did not see bacteria in the gut lumen (Fig. 6). However undigested *Leptonemella*-specific symbiont cells were found in the gut region of multiple *Leptonemella* individuals that were freshly extracted from the sediment by hybridizations with specific CARD-FISH probes (Fig. 7). The time-shifted host tissue enrichment in our incubations together with the fact that symbiont cells were present in the gut indicates that enrichment of the *Leptonemella* hosts was likely due to ingestion of their own symbionts. Previous studies have detected bacterial cells in the gut lumen of *Leptonemella aphanothecae* from the North Sea (Jensen 1987; Riemann *et al.* 2003) but their identity remained unknown. Our CARD-FISH analyses that identified the bacterial cells as symbionts provides evidence for the long-standing hypothesis that stilbonematine nematodes graze on their own symbionts (Wieser 1959; Ott *et al.* 1991). We did not detect bacteria other than symbionts in the *Leptonemella* gut region indicating that sediment bacteria, if at all, contribute little to the hosts' diet. Grazing of symbionts would also explain the large variability of host label enrichment between individuals, since food uptake relies on individual needs and is not continuous. Our analyses suggest that ectosymbionts represent a nutritional source to their host. The mechanism of carbon transfer, either via digestion or leakage of organic compound by the symbionts in the gut remains to be shown.

Possible explanations for physiological differences between *Leptonemella* individuals

We conducted our incubations without the presence of external energy sources, such as hydrogen sulfide or thiosulfate and found that the amount of carbon uptake differed by a factor of ten between individuals (Fig. 3 and 4). How can we explain such a high variability between individuals? It is known from other studies that pale gutless phallodriline annelids and stilbonematine nematode holobionts exhibit a lower carbon fixation rate than white, individuals, likely due to depleted sulfur stores that serve as energy source for carbon fixation (Giere *et al.* 1988; Schiemer *et al.* 1990). However, we only used bright white worms for our incubations to minimize the depletion effect of sulfur. Slightly variable carbon fixation rates

irrespective of the presence of external electron donors were also reported in previous incubations with other symbiotic organisms, such as the *Rimicaris* shrimp ectosymbiosis or Caribbean stilbonematine nematodes (Schiemer *et al.* 1990; Ponsard *et al.* 2012). A further factor that may have contributed to the large variability between individuals could be the variable amount of ectosymbionts present on different *Leptonemella* individuals. While some *Leptonemella* individuals are wrapped in a very thin and sometimes non-uniform layer of 2 - 5 cell layers, the symbiont layer of others can be uniform and around 20 cells thick (own observation). Additionally, MAR analysis on sections of the 3 h incubated *Leptonemella* individual showed that ectosymbionts of one worm can vary considerably in metabolic activity. While some symbiont batches were highly enriched in label, others did not show any MAR signal (Fig. 6A). Large difference in label enrichment between single cells of the same symbiont population were also observed in incubation experiments with the stilbonematine nematode *Laxus oneistus* and the marine flatworm *Paracatenula* (J. Zimmermann and O. Jäckle, unpublished results). Similarly, significant metabolic differences between single cells of the same population have also been observed for unicellular colonial and free-living cyanobacteria cells from surface waters (e.g. Foster *et al.* 2013).

Finally, we know from a recent molecular study that at least six different *Leptonemella* species can co-occur on Sylt and that each of them has slightly different symbionts that most likely differ in their metabolism (Zimmermann *et al.*, in prep., Chapter IV). It is impossible to distinguish the different species under the dissecting scope, but from microscopic analyses after the incubations we could identify individuals of at least two *Leptonemella* species. The amino acid (aa) sequence of the large subunit of the *ribulose* 1, 5-bisphosphate carboxylase (RuBisCO), the key enzyme of the Calvin-Benson-Bassham cycle for autotrophic carbon fixation between *L. aphanothecae* and *L. vicina* symbionts is 97% identical (Zimmermann *et al.*, in prep. Chapter IV). Differences in aa sequence can lead to changes in protein conformation and thus altered substrate affinity. Therefore it may be possible that carbon fixation efficiencies could also vary between symbionts of different species, which would also contribute to the differences in carbon fixation rate between *Leptonemella* individuals. Overall, the variable amounts of carbon fixed by each symbiont fraction and label transfer to the host is likely explained by a combination of the above discussed reasons.

Carbon fixation rates compared to closely related symbionts

In our microoxic pulse-only incubations we have calculated carbon fixation rates of 7 - 13 µmol C per g wwt and hour per *Leptonemella* holobiont (Fig. 5B) and the estimated rates for the pulse-chase incubation were comparable. This is around 1.5 - 2.5 times lower than calculated for Caribbean stilbonematine nematodes by Schiemer *et al.* (1990) under oxic conditions. How can we explain the relatively lower fixation rates for *Leptonemella* symbionts? One possibility is that the symbionts' physiology or enzyme affinities could differ between different nematode species, just as suggested for the closely related *Leptonemella* symbionts (see discussion above). Generally, it is known that metabolic rates increase with higher temperature (rule of van't Hoff-Cohen). Thus, *Leptonemella* symbionts that are adapted to colder temperatures may have slower metabolic rates compared to the tropical symbionts. Secondly, although no external electron donors were added in all incubations, we have used ASW for our incubations instead of filtered seawater, used by Schiemer and colleagues (1990). The ASW had a slightly lower pH than natural conditions and contained *HEPES* (4-(2-hydroxyethyl)-1-piperazineethanesulfonic acid) as chemical buffer. These additions may have had a negative effect on the *Leptonemella* symbiont carbon fixation rate compared to the Caribbean symbionts that were incubated under more natural conditions. An even lower carbon fixation rate as compared to the rates in this study was calculated for stilbonematine nematodes of the genus *Stilbonema* that fixed 1.8 µmol C per g wwt and hour (Hentschel *et al.* 1999). However, this rate was determined from anoxic incubations in which nitrate served as the terminal electron acceptor which is energetically less favorable compared to oxygen (Thauer *et al.* 1977) and thus very likely accounted for the lower rates. Generally, the carbon fixation rates but also the rate differences reported from different incubations with stilbonematine nematodes were comparable to other shallow water chemosynthetic symbioses. For example, carbon fixation rates in sulfur-oxidizing symbionts of shallow water marine clams varied from 0.8- 7 µmol C per g wwt and hour between two incubations (Felbeck *et al.* 1983; Fisher & Childress 1986). Similarly, carbon fixation rates between symbionts of gutless phallodriline annelids ranged from 0.6 - 29 µmol C per g wwt and hour, which corresponds to a factor of almost fifty between different incubations (Felbeck *et al.* 1983; Giere *et al.* 1988, Bergin, 2009). Standardized incubation conditions, such as medium additions, oxygen concentrations and incubation times in future incubations with chemoautotrophic symbionts would help to compare rate differences between different symbiotic systems or incubations more reliably. Furthermore, normalizations according to cell

number would help to resolve whether carbon fixation rate differences are due to variable symbiont numbers or physiologies.

Outlook

In this study we have shown that *Leptonemella* symbionts fix carbon autotrophically and that part of this carbon is transferred to the *Leptonemella* host tissue. However, a few questions remain to be answered:

(1) What is the exact mode of carbon transfer?

Two main modes of carbon transfer could theoretically contribute to the nutrition of the *Leptonemella* host. These are digestion of the symbionts or leakage of organic compounds by either undigested ectosymbionts in the gut lumen or intact ectosymbiotic cells through the cuticle. Using symbiont-specific CARD-FISH analyses we have shown that intact symbiont cells can be found in the gut and carbon tracer experiments combined with MAR analyses showed that the host tissue is getting enriched over time. However, the exact mode of carbon transfer could not be answered with the few individuals screened. Digested cells cannot be visualized by CARD-FISH analyses because the probes bind to ribosomal rRNA present in intact cells, but once the bacterial membrane disintegrates only few ribosomes will be left that could lead to a distinct signal in the gut. To investigate whether cells are digested transmission electron microscopy (TEM) analyses on *Leptonemella* cross sections is essential, because intact bacterial cells can be distinguished from bacteria in a stage of lysis. To examine the exact location of transfer, e.g. in the gut lumen or via the cuticle, both MAR or nanoscale secondary ion mass spectrometry (nanoSIMS) could be used. Since we included ^{14}C and ^{13}C-labeled bicarbonate in our incubations both imaging methods could be used in parallel. The advantage of MAR is that it is a high-throughput method while nanoSIMS is time-consuming but has extremely high spatial resolution. Thus MAR could be used to pre-screen highly enriched individuals and body regions of interest and nanoSIMS analyses could be done on selected consecutive sections afterwards. Correlative nanoSIMS or MAR and TEM analyses will show whether symbiont digestion or leakage of organic compounds is the main mode of carbon transfer in the *Leptonemella* ectosymbioses.

(2) Which metabolites are directly translocated from the symbionts to the host tissue?

Additionally to the mode of carbon transfer it would be interesting to analyze which exact metabolites are translocated from the symbionts to the host tissue. Therefore nematodes incubated with labeled bicarbonate and different time periods (minutes to hours) could be analyzed by gas chromatography-mass spectrometry (GC-MS) analyses to track label enrichment in symbiont and host fractions over time. GC-MS is a very sensitive and powerful method for metabolic profiling (Lisec *et al.* 2006) and has been successfully used to track ^{13}C-labeled bicarbonate in coral-dinoflagellate symbioses (Burriesci *et al.* 2012). In the latter study glucose that was already labeled after 2 min was found to be the major translocated carbon compound. Understanding which metabolites are being transferred from symbionts to host is of great interest for symbiosis research in common. Fortunately, *Leptonemella* host and symbiont fractions can be separated easily and so can the host and symbiont metabolomes. Using imaging techniques such as nanoSIMS and TEM together with quantitative metabolite data such as obtained with the GC-MS would help to understand both the mode of carbon transfer and the important compounds that help to sustain this symbiosis.

Acknowledgements

We thank the staff of the Wadden Sea station Sylt (Alfred Wegener Institute, Helmholtz Centre for Polar and Marine Reseach), especially Werner Armonies and Ragnhild Asmus for hospitality and providing access to laboratory facilities. Special thanks to Niculina Musat who started the project with me, Manuel Kleiner, Cecilia Wentrup, Tim Ferdelman and Lubos Polerecky for valuable scientific input regarding the incubation experiments. Special thanks to Kay Simmack and Miriam Sadowski for their help with extracting nematodes from sediment and measurements during and after the incubations. Many thanks also to Silke Wetzel, Daniela Franzke and Mirja Meiners for excellent technical assistance. This work was supported by the Max Planck Society.

References

Bahar O, Goffer T, Burdman S (2009) Type IV pili are required for virulence, twitching motility, and biofilm formation of *Acidovorax avenae* subsp. citrulli. *Molecular Plant-Microbe Interactions*, **22**, 909–920.

Bergin, C. (2009) Phylogenetic diversity and metabolic versatility of the bacterial endosymbionts in marine gutless oligochaete worms. Doctoral thesis. University of Bremen. Available at http://d-nb.info/1007323973.

Bosch C, Grassé P-P (1984) Cycle partiel des bactéries chimioautotrophes symbiotiques et leurs rapports avec les bactériocytes chez *Riftia pachyptila* Jones (Pogonophore Vestimentifère). II. L'évolution des bactéries symbiotiques et des bactériocytes. *Comptes rendus des séances de l'Académie des sciences. Série 3, Sciences de la vie* **299**, 413-419.

Bright, M, Keckeis H, Fisher CR (2000) An autoradiographic examination of carbon fixation, transfer and utilization in the *Riftia pachyptila* symbiosis. *Marine Biology*, **136**, 621–632.

Burriesci MS, Raab TK, Pringle JR (2012) Evidence that glucose is the major transferred metabolite in dinoflagellate–cnidarian symbiosis. *The Journal of Experimental Biology*, **215**, 3467–3477.

Cataldi de Flombaum MA, Cannata JJB, Cazzulo JJ, Segura EL (1977) CO_2-fixing enzymes in *Trypanosoma cruzi*. *Comparative Biochemistry and Physiology Part B: Comparative Biochemistry*, **58**, 67–69.

Cavanaugh C, McKiness Z, Newton I, Stewart F (2006) Marine chemosynthetic symbioses. In: *The Prokaryotes*, Springer New York, 475–507.

Childress JJ, Fisher CR (1992) The biology of hydrothermal vent animals: physiology, biochemistry, and autotrophic symbioses. *Oceanography and Marine Biology*, **30**, 337–441.

Childress JJ, Fisher CR, Favuzzi JA, Sanders NK (1991) Sulfide and carbon dioxide uptake by the hydrothermal vent clam, *Calyptogena magnifica*, and its chemoautotrophic symbionts. *Physiological Zoology*, **64**, 1444–1470.

Dando PR, Jensen P, O'Hara SCM *et al.* (1994) The effects of methane seepage at an intertidal/shallow subtidal site on the shore of the Kattegat, Vendsyssel, Denmark. *Bulletin of the Geological Society of Denmark*, **41**, 65–79.

Distel DL, Lane DJ, Olsen GJ *et al.* (1988) Sulfur-oxidizing bacterial endosymbionts: analysis of phylogeny and specificity by 16S rRNA sequences. *Journal of Bacteriology*, **170**, 2506–2510.

Douglas AE (2010) *The Symbiotic Habit*. Princeton University Press.

Felbeck H (1983) Sulfide oxidation and carbon fixation by the gutless clam *Solemya reidi*: an animal-bacteria symbiosis. *Journal of Comparative Physiology*, **152**, 3–11.

Felbeck H, Jarchow J (1998) Carbon release from purified chemoautotrophic bacterial symbionts of the hydrothermal vent tubeworm *Riftia pachyptila*. *Physiological and Biochemical Zoology*, **71**, 294–302.

Felbeck H, Liebezeit G, Dawson R, Giere O (1983) CO_2 fixation in tissues of marine oligochaetes (*Phallodrilus leukodermatus* and *P. planus*) containing symbiotic, chemoautotrophic bacteria. *Marine Biology*, **75**, 187–191.

Fisher CR, Childress JJ (1986) Translocation of fixed carbon from symbiotic bacteria to host tissues in the gutless bivalve *Solemya reidi*. *Marine Biology*, **93**, 59–68.

Foster RA, Sztejrenszus S, Kuypers MMM (2013) Measuring carbon and N_2 fixation in field populations of colonial and free-living unicellular cyanobacteria using nanometer-scale secondary ion mass spectrometry. *Journal of Phycology*, **49**, 502–516.

Van Gaever S, Vanreusel A, Hughes JA, Bett BJ, Kiriakoulakis K (2004) The macro-and micro-scale patchiness of meiobenthos associated with the Darwin Mounds (north-east Atlantic). *Journal of the Marine Biological Association of the UK*, **84**, 547–556.

Gerlach SA (1978) Food-chain relationships in subtidal silty sand marine sediments and the role of meiofauna in stimulating bacterial productivity. *Oecologia*, **33**, 55–69.

Giere O, Wirsen CO, Schmidt C, Jannasch HW (1988) Contrasting effects of sulfide and thiosulfate on symbiotic CO_2-assimilation of *Phallodrilus leukodermatus* (Annelida). *Marine Biology*, **97**, 413–419.

Goffredi SK, Jones WJ, Erhlich H, Springer A, Vrijenhoek RC (2008) Epibiotic bacteria associated with the recently discovered Yeti crab, *Kiwa hirsuta*. *Environmental Microbiology*, **10**, 2623–2634.

Hammen CS, Osborne PJ (1959) Carbon dioxide fixation in marine invertebrates: a survey of major phyla. *Science*, **130**, 1409–1410.

Hammen CS, Wilbur KM (1959) Carbon dioxide fixation in marine invertebrates I. The main pathway in the oyster. *Journal of Biological Chemistry*, **234**, 1268–1271.

Hentschel U, Berger EC, Bright M, Felbeck H, Ott JA (1999) Metabolism of nitrogen and sulfur in ectosymbiotic bacteria of marine nematodes (Nematoda, Stilbonematinae). *Marine Ecology Progress Series*, **183**, 149–158.

Herry A, Diouris M, Pennec ML (1989) Chemoautotrophic symbionts and translocation of fixed carbon from bacteria to host tissues in the littoral bivalve *Loripes lucinalis* (Lucinidae). *Marine Biology*, **101**, 305–312.

Himmel D, Maurin LC, Gros O, Mansot J-L (2009) Raman microspectrometry sulfur detection and characterization in the marine ectosymbiotic nematode *Eubostrichus dianae* (Desmodoridae, Stilbonematidae). *Biology of the Cell / Under the Auspices of the European Cell Biology Organization*, **101**, 43–54.

Jensen (1987) Feeding ecology of free-living aquatic nematodes. *Marine Ecology Progress Series*, **35**, 187–196.

Kamenev GM, Fadeev VI, Selin NI, Tarasov VG, Malakhov VV (1993) Composition and distribution of macro- and meiobenthos around sublittoral hydrothermal vents in the Bay of Plenty, New Zealand. *New Zealand Journal of Marine and Freshwater Research*, **27**, 407–418.

Kleiner M, Wentrup C, Lott C, *et al.* (2012) Metaproteomics of a gutless marine worm and its symbiotic microbial community reveal unusual pathways for carbon and energy use. *Proceedings of the National Academy of Sciences,* **109**, 7148-7149.

Leduc D (2013) One new genus and two new deep-sea nematode species (Desmodoridae, Stilbonematinae) from phosphorite nodule deposits on Chatham Rise, Southwest Pacific Ocean. *Marine Biodiversity*, **43**, 421–428.

Leisch N, Verheul J, Heindl NR, *et al.* (2012) Growth in width and FtsZ ring longitudinal positioning in a gammaproteobacterial symbiont. *Current Biology*, **22**, R831–R832.

Lisec J, Schauer N, Kopka J, Willmitzer L, Fernie AR (2006) Gas chromatography mass spectrometry-based metabolite profiling in plants. *Nature Protocols*, **1**, 387–396.

Manz W, Amann R, Ludwig W, Wagner M, Schleifer K-H (1992) Phylogenetic oligodeoxynucleotide probes for the major subclasses of proteobacteria : problems and solutions. *Systematic and Applied Microbiology*, **15**, 593–600.

Minet AD, Gaster M (2010) Pyruvate carboxylase is expressed in human skeletal muscle. *Biochemical and Biophysical Research Communications*, **402**, 196–197.

Moran NA, McCutcheon JP, Nakabachi A (2008) Genomics and evolution of heritable bacterial symbionts. *Annual Review of Genetics*, **42**, 165–190.

Ott J, Bright M, Bulgheresi S (2004) Symbioses between marine nematodes and sulfur-oxidizing chemoautotrophic bacteria. *Symbiosis*, **36**, 103–126.

Ott JA, Novak R, Schiemer F *et al.* (1991) Tackling the sulfide gradient: A novel strategy involving marine nematodes and chemoautotrophic ectosymbionts. *Marine Ecology*, **12**, 261–279.

Polz MF, Distel DL, Zarda B, *et al.* (1994) Phylogenetic analysis of a highly specific association between ectosymbiotic, sulfur-oxidizing bacteria and a marine nematode. *Applied Environmental Microbiology*, **60**, 4461–4467.

Polz MF, Felbeck H, Novak R, Nebelsick M, Ott JA (1992) Chemoautotrophic, sulfur-oxidizing symbiotic bacteria on marine nematodes: morphological and biochemical characterization. *Microbial Ecology*, **24**, 313–329.

Ponsard J, Cambon-Bonavita MA, Zbinden M et al. (2013) Inorganic carbon fixation by chemosynthetic ectosymbionts and nutritional transfers to the hydrothermal vent host-shrimp *Rimicaris exoculata*. *The ISME Journal*, **7**, 96–109.

Powell EN, Crenshaw MA, Rieger RM (1979) Adaptations to sulfide in sulfide-system I. ^{35}S-sulfide accumulation and the presence of a sulfide detoxification system. *Journal of Experimental Marine Biology and Ecology*, **37**, 57–76.

Riemann F, Thiermann F, Bock L (2003) *Leptonemella* species (Desmodoridae, Stilbonematinae), benthic marine nematodes with ectosymbiotic bacteria, from littoral sand of the North Sea island of Sylt: taxonomy and ecological aspects. *Helgoland Marine Research*, **57**, 118–131.

Rinke, C. (2002) Nutritional Processes in the Chemoautotrophic *Zoothamnium niveum* symbioses. Diploma thesis, University of Vienna, Austria. Available at: http://othes.univie.ac.at/32139.

Schiemer F, Novak R, Ott J (1990) Metabolic studies on thiobiotic free-living nematodes and their symbiotic microorganisms. *Marine Biology*, **106**, 129–137.

Schimak MP, Toenshoff ER, Bright M (2012) Simultaneous 16S and 18S rRNA fluorescence in situ hybridization (FISH) on LR White sections demonstrated in Vestimentifera (Siboglinidae) tubeworms. *Acta Histochemica*, **114**, 122–130.

Steedman HF (1957) Polyester wax: a new ribboning embedding medium for histology. *Nature*, **179**, 1345.

Stewart FJ, Cavanaugh CM (2006) Symbiosis of thioautotrophic bacteria with *Riftia pachyptila*. In: *Molecular Basis of Symbiosis* Progress in Molecular and Subcellular Biology, pp. 197–225. Springer, Berlin Heidelberg.

Streams ME, Fisher CR, Fiala-Médioni A (1997) Methanotrophic symbiont location and fate of carbon incorporated from methane in a hydrocarbon seep mussel. *Marine Biology*, **129**, 465–476.

Tang K-H, Feng X, Tang YJ, Blankenship RE (2009) Carbohydrate metabolism and carbon fixation in *Roseobacter denitrificans* OCh114. *PLoS ONE*, **4**. e7233.

Tchesunov AV (2013) Marine free-living nematodes of the subfamily Stilbonematinae (Nematoda, Desmodoridae): taxonomic review with descriptions of a few species from the Nha Trang Bay, Central Vietnam. *Meiofauna Marina* **20**, 71–94.

Thauer RK, Jungermann K, Decker K (1977) Energy conservation in chemotrophic anaerobic bacteria. *Bacteriological Reviews*, **41**, 100–180.

Thiermann F, Akoumianaki I, Hughes JA, Giere O (1997) Benthic fauna of a shallow-water gaseohydrothermal vent area in the Aegean Sea (Milos, Greece). *Marine Biology*, **128**, 149–159.

Wallner G, Amann R, Beisker W (1993) Optimizing fluorescent in situ hybridization with rRNA-targeted oligonucleotide probes for flow cytometric identification of microorganisms. *Cytometry*, **14**, 136–143.

Watsuji T, Yamamoto A, Motoki K *et al.* (2014) Molecular evidence of digestion and absorption of epibiotic bacterial community by deep-sea crab *Shinkaia crosnieri*. *The ISME Journal*. **9**, 821-831.

Wieser W (1959) Eine ungewöhnliche Assoziation zwischen Blaualgen und freilebenden marinen Nematoden. *Plant Systematics and Evolution*, **106**, 81–87.

Woyke T, Teeling H, Ivanova NN *et al.* (2006) Symbiosis insights through metagenomic analysis of a microbial consortium. *Nature*, **443**, 950–955.

Chapter VI

Genomic insights into marine nematode sulfur-oxidizing ectosymbionts

Authors: Judith Zimmermann[1], Jillian M. Petersen[1], Jasmine Berg[2], Nicole Dubilier[1], and Manuel Kleiner[1*]

[1]Department of Symbiosis, Max Planck Institute for Marine Microbiology, Celsiusstrasse, Bremen, Germany
[1]Department of Biogeochemistry, Max Planck Institute for Marine Microbiology, Celsiusstrasse, Bremen, Germany
*now affiliated with Department of Geoscience, Energy Bioengineering Group, University of Calgary, Canada

Manuscript in preparation

J.Z. developed the concept, did the genome data analyses, Nile Red analyses, conceived and wrote the manuscript; J.M.P. helped to develop the concept and conceived the manuscript; J.B. performed the Raman measurements; N.D. helped to develop the concept; M.K. helped with the genome analyses, conceived and edited the manuscript.

Abstract

Marine stilbonematine nematodes are well known for their symbiotic relationship with sulfur-oxidizing bacteria that cover the nematode cuticle and serve as a food source for their bacterivorous host. Our understanding of the metabolic capabilities of the ectosymbiotic bacteria is limited because they have not been successfully cultured to date, as is the case with most mutualistic endosymbionts. In this study we analyzed the recently published ectosymbiont genomes of two stilbonematine nematode species of the genus *Leptonemella* from an intertidal beach off the North Sea island Sylt. The symbionts have the hybrid rDsr-Sox sulfur-oxidation pathway and a modified Calvin-Benson-Bassham (CBB) cycle for autotrophic carbon fixation, which are both commonly found in sulfur-oxidizing symbionts. The genomes also contained the complete tricarboxylic acid (TCA) cycle, the glyoxylate bypass and a partial 3-hydroxypropionate bicycle, along with multiple transporters for sugars, organic and amino acids and peptides, suggesting that the symbionts can also live heterotrophically. This lifestyle could be of advantage for symbionts exposed to an organic-rich environment and potentially also host waste products. Many genes involved in sulfur, carbon and phosphate storage and for the usage of various electron acceptors suggest that the symbionts are well adapted to a highly fluctuating tidal-influenced environment. In contrast to other sulfur-oxidizing symbionts we found numerous genes that are commonly present in biofilm-forming bacteria. These included type II and type VI secretion systems, type IV pili, antimicrobial peptides, and pore-forming toxins, which are known to be involved in surface attachment and defense against predators, pathogens or competitors. These features are consistent with the extracellular lifestyle of *Leptonemella* ectosymbionts. Our study uncovered highly versatile metabolic capabilities of stilbonematine nematode ectosymbionts and may pave the way for their cultivation.

Introduction

Chemosynthetic symbioses between animals and sulfur-oxidizing bacteria were first discovered at hydrothermal vents in the deep sea (Lonsdale 1977; Cavanaugh *et al.* 1981; Felbeck 1981). Since then, chemosynthetic symbioses, which depend on energy from reduced chemical compounds, rather than sunlight, to fix carbon into biomass have been found in many other marine habitats (Dubilier *et al.* 2008). Shallow water coastal sediments are one of the most widespread and easily accessible habitats sustaining a wide array of chemosynthetic symbioses, most commonly those that use reduced sulfur (e.g. sulfide, thiosulfate) as an energy source. These chemosynthetic symbioses include hosts of diverse animal groups, including clams, ciliates, flatworms, annelids and nematodes (Fenchel & Finlay 1989; Ott *et al.* 2004; Dubilier *et al.* 2008; Gruber-Vodicka *et al.* 2011). One group of sulfur-oxidizing symbionts that dominate many shallow water sediments is the *Candidatus* Thiosymbion clade (Gruber-Vodicka *et al.*, in prep.). Members of *Cand.* Thiosymbion clade live in symbiosis with gutless phallodriline oligochaetes (Clitellata, *Tubificidae*) and stilbonematine nematodes (Nematoda, *Desmodoridae*). Both symbiotic systems often co-occur and there is evidence that host switches between both symbiotic systems have happened in the past (Zimmermann *et al*., in prep., Chapter III). Members of the *Cand*. Thiosymbion clade have different lifestyles, depending on which host animal they are associated with: as endosymbionts in the gutless phallodrilines and as ectosymbionts attached to the surface (cuticle) of stilbonematine nematodes (e.g. Polz *et al.* 1994; Dubilier *et al.* 1995, Zimmermann *et al.*, in prep., Chapter III). In contrast to stilbonematines that carry only *Cand.* Thiosymbion bacteria on their cuticle, gutless phallodrilines harbor multiple phylogenetically different endosymbionts, but only members of the *Cand.* Thiosymbion clade are consistently found in all gutless phallodriline species worldwide (Ott *et al.* 2004; Dubilier *et al.* 2006, Gruber-Vocika, et al., in prep.). For example, the gutless phallodriline *Olavius algarvensis* contains a total of five endosymbiont species in the extracellular space between epidermal cells and cuticle: two sulfur-oxidizing symbionts (*Cand.* Thiosymbion algarvensis and the γ3-symbiont), two sulfate-reducing symbionts (δ1- and δ3-symbiont) and a spirochaete with yet unknown function (Giere & Erséus 2002; Ruehland *et al.* 2008). While the metabolic capabilities of the *Cand* Thiosymbion algarvensis have been

investigated in detail using genomic and proteomic analyses (Woyke *et al.* 2006; Kleiner *et al.* 2012b), knowledge of the metabolic capabilities of their closest *Cand.* Thiosymbion relatives, the ectosymbionts of stilbonematine nematodes is limited.

Stilbonematine nematode ectosymbioses are widely present in sulfidic sediments worldwide but their abundances are highest in tropical and subtropical coralline sands (reviewed by Tchesunov 2013). The chemoautotrophic metabolism of the symbionts has been shown for a number of stilbonematine nematode species. For example, isotope labeling experiments with hydrogen sulfide and bicarbonate under oxic conditions resulted in symbiont label enrichment, suggesting that energy gained from sulfide oxidation is used to fix CO_2 into biomass (Powell *et al.* 1979; Schiemer *et al.* 1990, Zimmermann *et al*., in prep., Chapter V). The sulfur-oxidizing autotrophic nature was also supported by activity tests for key enzymes of the Calvin-Benson-Bassham (CBB) cycle and the sulfur oxidation pathway, and by the presence of elemental sulfur in some of the Caribbean species (Polz *et al.* 1992; Himmel *et al.* 2009). Due to the bright white color of the symbionts during anoxia it was hypothesized that symbionts build up sulfur stores while dwelling in sulfidic sediment layers and that they oxidize sulfur for energy generation during oxygen availability (Ott *et al.* 2004). However, physiological experiments with the well-characterized stilbonematine species *Laxus oneistus* and *Stilbonema* sp. showed that their symbionts can also use the energetically less-favorable nitrate as an alternative terminal electron acceptor (TEA) (Hentschel *et al.* 1999). This would allow the symbionts to metabolize sulfide in anoxic sediment layers where nitrate but no oxygen is available. The nematode host is believed to gain a nutritional benefit, by feeding on its ectosymbionts and this has recently been supported for *Leptonemella* species from Sylt (Wieser 1959; Gerlach 1978, Zimmermann *et al*., in prep., Chapter V). Bacteria in the gut were identified as ectosymbionts and incubation experiments with radiolabeled bicarbonate indicated that fixed carbon is transferred from symbionts to the host tissue (Zimmermann *et al.,* in prep., Chapter V). A further benefit for the host may be the protection from sulfide poisoning by the symbionts that form a thick layer on the cuticle (Hentschel *et al.* 1999). The benefit for the symbionts is assumed to be the association with a mobile host, which provides regular access to electron donors, such as sulfide in deeper sediment layers and oxygen in upper sediment layers (Ott *et al.* 2004).

Stilbonematine nematode ectosymbioses are highly specific, with each nematode species carrying its own distinct *Cand.* Thiosymbion species (Ott *et al.* 2004, Zimmermann *et al*., in prep., Chapter III, IV). Mucus secreted by the hosts' large glandular sensory organs (GSOs), which are located just below the cuticle, has been suggested to maintain the cohesion of the symbiont coat (Bauer-Nebelsick *et al.* 1995). Specific lectins (sugar-binding proteins) that are secreted by the GSOs are known to be involved in the recognition and binding of specific symbionts (Bulgheresi *et al.* 2006, 2011). In contrast to most other investigated sulfur-oxidizing symbionts that are enclosed by host tissue, these ectosymbionts are constantly exposed to the environment.

Draft genomes of ectosymbiont populations, of two closely related *Leptonemella* nematode species from an intertidal beach off Sylt in Germany were recently sequenced (Zimmermann *et al*., in prep., Chapter IV). Symbiont populations per individual were found to be essentially clonal and resulted in the first draft genomes available for the ectosymbionts of stilbonematine nematodes (Zimmermann *et al.,* in prep. Chapter IV). These draft genomes provide a great opportunity to gain insights into yet unknown metabolic capabilities of the ectosymbionts. In this study we analyzed core metabolic pathways of the *Leptonemella* ectosymbionts including carbon, sulfur, and nitrogen metabolism and used spectroscopic and microscopic methods to confirm the presence of storage compounds *in situ*. Furthermore we analyzed genes potentially involved in interactions with the host, and such that may aid an ectosymbiotic lifestyle, including biofilm formation, membrane transport, and defense. We also discuss our results with respect to other sulfur-oxidizing symbionts, including the *Cand.* Thiosymbion algarvensis, which are the closest sequenced relatives to the *Leptonemella* ectosymbionts.

Material and Methods

Nematode collection and preparation

Sediment samples containing *Leptonemella* species were collected on the intertidal flat off List ('Hausstrand', 55.015069 N, 8.437788 E) on the North Sea island Sylt using sediment cores. Cores were taken during low tide close to polychaete burrows where highest *Leptonemella*

densities were previously reported (Riemann *et al.* 2003). Individuals for storage compound analyses were fixed in 2% paraformaldehyde (PFA) (v/v) in 0.2 µm-fiiltered seawater at 4 °C over night and washed twice in cold 0.2 µm filtered seawater. Samples were finally stored in 50% ethanol (v/v) in filtered seawater at 4 °C until further processing. Some individuals were frozen at -20 °C for Raman measurements.

Metagenome analysis

We used recently assembled and published draft genomes of ectosymbionts from four *Leptonemella aphanothecae* (W103, 104, 107, 112) and one *L. vicina* (W220) individuals from the Hausstrand near List, Sylt (Zimmermann *et al*., in prep., Chapter IV) for our metagenome analysis. Open reading frames (ORFs) were predicted using RAST (Aziz *et al.* 2008; Overbeek *et al.* 2013). Functional annotations were manually verified using translated gene sequences of interest by queries against the National Centre for Biotechnology Information non-redundant database (NCBI-nr) using BLASTP (e-value cutoff 0.001, > 50% amino acid identity (aaID)) (Altschul *et al.* 1997; Camacho *et al.* 2009) and the Interpro database of protein families and domains (Hunter *et al.* 2009). For finding genes that were not annotated but likely present in the genomes we downloaded protein sequences from close relatives with verified function from NCBI and searched against our genomes using BLASTP (e-value cutoff 0.001, > 50% aaID) (Altschul *et al.* 1997; Camacho *et al.* 2009) using the built-in function in RAST (Aziz *et al.* 2008). The Metacyc database of metabolic pathways (Caspi *et al.* 2014) and the KEGG pathway database (Kanehisa *et al.* 2014) were used as references for building the metabolic model of the symbionts. Genomes for comparative genomics were downloaded from NCBI and analyzed in RAST (*Cand.* Thiosymbion (γ1) and γ3-symbiont genomes of *Olavius algarvensis:* DS021107:DS021197 and DS021198 - DS021219; *Escherichia coli* str. K-12 substr. MG1655: NC_000913; *Pseudomonas aeruginosa* PAO1: NC_002516; *Buchnera aphidicola* str. SG: NC_004061; Candidatus *Ruthia magnifica*: NC_008610; *Vibrio fischeri* MJ11: NC_011184-6; *Endoriftia persephone* str. Hot96_1, Hot96_2 AASF01000001:AASF01002170; *Solemya velum* symbiont NZ_JRAA00000000.1; *Allochromatium vinosum* DSM180 NC_013851.1).

Raman microscopy

Leptonemella individuals were mounted on a glass slide coated with 0.1% poly-L-lysine solution (Sigma-Aldrich) and analyzed with an NTEGRA Spectra (NT-MDT Eindhoven, Netherlands) confocal spectrometer coupled to an inverted Olympus IX71 microscope. The excitation light from a 532 nm solid-state laser was focused on the sample through an Olympus 100X/NA1.3 oil-immersion objective. The pinhole aperture was maintained at 55 µm corresponding to a spatial resolution of 250 - 300 µm and the laser power at the sample did not exceed 1 mW. Raman scattered light was dispersed with a 150 $l \cdot mm^{-1}$ grating and collected by an electron multiplying charge coupled device (EMCCD) camera (Andor Technology, Belfast, Northern Ireland) cooled to -70 °C. Raman spectra were recorded between 0 and ~4,500 cm^{-1} with a spectral resolution of 0.2 cm^{-1}. The software Nova_Px 3.1.0.0 (NT-MDT Eindhoven, Netherlands) was used for all spectral analyses. In order to visualize the location of specific compounds, relevant peak areas were first background corrected, and images were then overlaid and brightness/contrast adjusted in Adobe Photoshop CS2. Analytical grade elemental sulfur (purity > 99%) (Roth GmbH) was used as reference for sulfur measurements.

Microscopy and staining of lipophilic storage compounds

Leptonemella ectosymbiont storage compounds were investigated using whole individuals that were mounted on a 10-well glass slide (Gerhard Menzel GmbH, Braunschweig, Germany). Internal cell structures such as highly refractile sulfur globules were analyzed with a differential interference contrast (DIC) microscope (Olympus BX53, Olympus, Hamburg, Germany) with a mounted camera (Canon EOS 700D; Canon; Ota, Tokyo, Japan). For staining polyhydroxyalkanoates (PHAs) and other lipophilic substances, we stained *Leptonemella* individuals with Nile Red (2.5 µg/ml) for 10 min at RT. For counterstaining DNA, 4',6-diamidino-2-phenylindole dihydrochloride (DAPI) was directly added into the embedding medium, a (2:11 (v/v)) mixture of Citifluor (Citifluor Ltd, Leicester, UK) and Vectashield (Vector laboratories, Burlingame, CA, USA). Nile Red fluorescence was visualized with a confocal laser scanning microscope (CLSM 780, Carl Zeiss Microscopy GmbH, Jena, Germany) with excitation and emission wavelength of 561 nm and 570 - 620 nm, respectively.

Results and Discussion

Leptonemella ectosymbiont metabolism

Carbon metabolism

Carbon fixation is one of the key processes for chemosynthetic symbionts that supply their hosts with organic substrates for nutrition (Cavanaugh *et al.* 2006; Kleiner *et al.* 2012a). Autotrophic carbon fixation by stilbonematine nematode symbionts has previously been demonstrated by incubation experiments with isotope-labeled bicarbonate (Schiemer *et al.* 1990, Zimmermann *et al.,* Chapter V) and enzyme activity tests for RuBisCO (Polz *et al.* 1992).

Our *Leptonemella* ectosymbionts genome analysis confirmed the presence of all key genes necessary for autotrophic carbon fixation via the CBB cycle, including RuBisCO form IA that is more efficient in higher oxygen concentrations compared to RuBisCO form II (Badger *et al.* 2008). However, genes coding for a sedoheptulose-1,7 bisphosphatase and a fructose-1,6 bisphosphatase are missing (Table S1). This is similar to what is known for other gammaproteobacterial sulfur-oxidizing symbionts, such as the *Cand.* Thiosymbion and γ3-symbionts of the gutless phallodriline *O. algarvensis,* and symbionts of *Calyptogena* and *Solemya* clams and *Riftia* tubeworms (Newton *et al.* 2007; Markert *et al.* 2011; Kleiner *et al.* 2012b; a; Dmytrenko *et al.* 2014). Instead of the two missing enzymes a more energy-efficient version of the CBB cycle has been proposed for these symbionts that makes use of a pyrophosphate-dependent 6-phosphofructokinase (PPi-PFK) and neighboring proton-translocating pyrophosphatase (H^+-PPase) that commonly occur on the same operon (Kleiner *et al.* 2012b). These two genes were also co-localized in one operon in the *Leptonemella* ectosymbiont genomes. The presence of the modified CBB cycle in a variety of sulfur-oxidizing symbionts indicates that there may be selection pressure favoring the acquisition or usage of this pathway in chemosynthetic symbioses.

Based on the 16S rRNA gene, the *Cand.* Thiosymbion algarvensis is very closely related to *Leptonemella* ectosymbionts (97.8% nucleotide identity). Correspondingly, the large subunit of RuBisCO (*cbbL*) encoded in the ectosymbiont genomes was also most closely related to the

cbbL gene of the *Cand.* Thiosymbion algarvensis (84% nucleotide identity (ntID), 96% aaID). In addition, the amino acid sequences of the PPi-PFK and the H+-PPase were 95% and 78% identical between both *Cand.* Thiosymbion members. This suggests that this carbon fixation pathway may have already been present in the ancestral *Cand.* Thiosymbion.

Multiple CO_2 fixation pathways are not common in chemosynthetic symbionts. Only symbionts of *Riftia* and *Tevnia* tubeworms are known to use the reverse tricarboxylic acid cycle (rTCA) in addition to the modified CBB cycle (Markert *et al.* 2007; Robidart *et al.* 2008; Gardebrecht *et al.* 2011). Alternative autrotrophic carbon fixation pathways such as the rTCA and the reductive acetyl-CoA pathway were not present in the *Leptonemella* ectosymbionts.

Apart from the ability to use CO_2 as carbon source, we also detected many genes involved in pathways for assimilating organic substrates in the *Leptonemella* ectosymbiont genomes. We found the complete gene set for the energy-generating oxidative tricarboxylic acid (TCA) cycle and the isocitrate lyase and malate synthase necessary for the glyoxylate bypass (Fig. 1). The latter is a variation of the TCA cycle and used to refill intermediates in the TCA cycle for the synthesis of carbohydrates using two-carbon compounds, such as acetate (Kornberg & Madsen 1957; Walsh & Koshland 1984). The presence of both the TCA cycle and the glyoxylate bypass indicate that *Leptonemella* ectosymbionts can use organic carbon compounds not only as energy but also as a carbon source. Genes encoding uptake transporters for a large range of organic substrates, including amino acids, peptides, organic acids (e.g. acetate, succinate, malate or fumarate) and sugars, were found in the genomes (Fig. 1, Table S1). Organic acids could directly enter the TCA cycle while sugars could be broken down by glycolysis, for which all genes were present, except for the pyruvate kinase. The pyruvate kinase performs the last step of the glycolysis, the conversion from phosphoenolpyruvate (PEP) to pyruvate (Fig. 1, Table S1). In the *Leptonemella* ectosymbionts this reactions might instead be catalyzed by either pyruvate phosphate dikinase or the phosphotransferase system (PTS), that couples the conversion of PEP to sugar uptake (Table S1) (Postma & Lengeler 1985; Acosta *et al.* 2004; Raverdy *et al.* 2008). Additionally we found some chemotaxis genes in the genome that allow heterotrophs to respond to chemical stimuli in their environment (Seymour *et al.* 2010; Geng & Belas 2010). The presence of a variety of uptake transporters for organic substrates and pathways for breakdown

and assimilation of organics suggest that the symbionts may, at times, live as heterotrophs rather than only autotrophically.

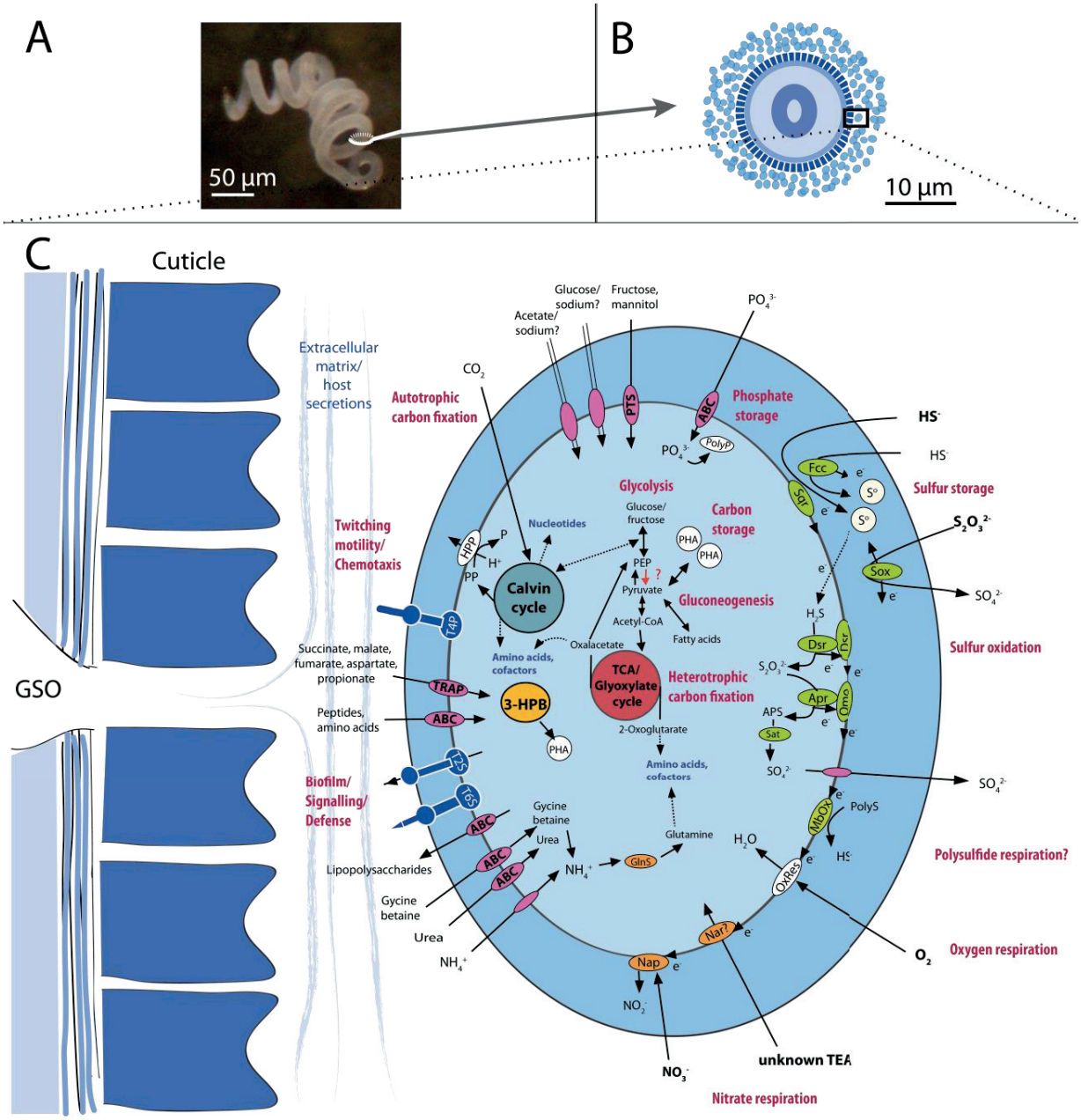

Fig. 1: Overview of *Leptonemella* ectosymbiont metabolism based on genomic analyses. (A) Live *Leptonemella* specimen. (B) Diagrammatic cross section through a *Leptonemella* individual with the cuticle and gut highlighted in dark blue and the ectosymbionts in light blue. (C) Metabolic reconstruction of the symbiont pathways from genome annotation. ABC: ATP-binding cassette transporter; Apr: *adenosine* 5-phosphosulfate reductase; APS: *adenosine* 5-phosphosulfate; Dsr: dissimilatory *sulfite* reductase; Fcc: flavocytochrome c; GlnS: glutamine synthetase; GSO: glandular sensory organ; 3-HPB: partial 3-hydroxypropionate bicycle; HPP: proton-translocating pyrophosphatase; MbOx: molybdopterin oxidoreductase; Nap: periplasmic respiratory nitrate reductase; Nar: membrane bound respiratory nitrate reductase; OxRes: oxygen respiration; PEP: phosphoenolpyruvate; PHA: polyhydroxyalkanoate inclusions; PP: inorganic pyrophosphate; PTS: phosphotranferase system; Qmo: quinone-interacting membrane-bound oxidoreductase; Sat: ATP sulfurylase; S^0: elemental sulfur; Sox: sulfur oxidation enzyme system; Sqr: sulfide-quinone oxidoreductase; TCA: tricarboxylic acid cycle; TEA: Terminal electron acceptor; TRAP: tripartite ATP-independent periplasmic transporter; T2S: type II secretion system, T4P: type IV pilus; T6S: type VI secretion system.

A mixotrophic lifestyle has been suggested for other sulfur-oxidizing endosymbionts, including the endosymbionts of *Riftia* tubeworms, *Solemya* clam and scaly-foot gastropods but also for the *Cand*. Thiosymbion algarvensis*,* (Robidart *et al.* 2008; Kleiner *et al.* 2012a; Nakagawa *et al.* 2014; Dmytrenko *et al.* 2014). However, in the latter not all genes necessary for the complete TCA cycle and only a few transporters for organic substrates were present (Table S2, Kleiner *et al.* 2012b; a). Instead, heterotrophic metabolism to recycle host fermentation products has been proposed to be possible via a partial 3-hydroxproprionate bicycle (3-HPB) that lacks the two enzymes malonyl-CoA reductase and propionyl-CoA synthase (Kleiner *et al.* 2012b). The 3-HPB is the main CO_2-fixation pathway in Chloroflexi bacteria, however without these two enzymes, the pathway cannot function as an autotrophic cycle but is believed to still be used for assimilating propionate and acetate. This partial 3-HPB was also present in the *Leptonemella* ectosymbiont genomes with exactly the same two enzymes missing, indicating that the symbionts have yet another possibilities to assimilate carbon heterotrophically (Table S1 and S2). The ability to use organic carbon compounds in addition to CO_2 would be of considerable advantage for an ectosymbiont that lives in Wadden Sea sediment where organic matter supply through photosynthetic primary productivity is high (e.g. Asmus 1982; Migné *et al.* 2004; Böer *et al.* 2009). Additionally, it could be an adaptation to the association with a nematode host that excretes energy-rich fermentation products (see Section “Host-symbiont interactions”).

Bacteria often store energy and carbon in form of lipophilic inclusions, such as PHA, when a carbon source is available in excess but other nutrients limit bacterial growth (Anderson & Dawes 1990; Lee 1996). The *Leptonemella* ectosymbiont genomes also contained genes involved in PHA synthesis and degradation (Table S1). The presence of lipophilic storage compounds, potentially PHA, was also confirmed by our Nile red staining approach that showed multiple inclusion bodies in the ectosymbionts (Fig. 2). This parallels previous studies on stilbonematine ectosymbionts where polyhydroxy butyric acid (PHB) and polyhydroxy valeric acid (PHV) were measured by gas chromatography in the Caribbean *Laxus* and *Stilbonema* species (Polz *et al.* 1992). Furthermore, the genomes contained genes involved in carbon starvation, carbon storage regulation. The presence of these genes together with PHA storage is likely an adaptation to the highly fluctuating environmental conditions on the intertidal flat off Sylt (Fig. 1, Fig. S1).

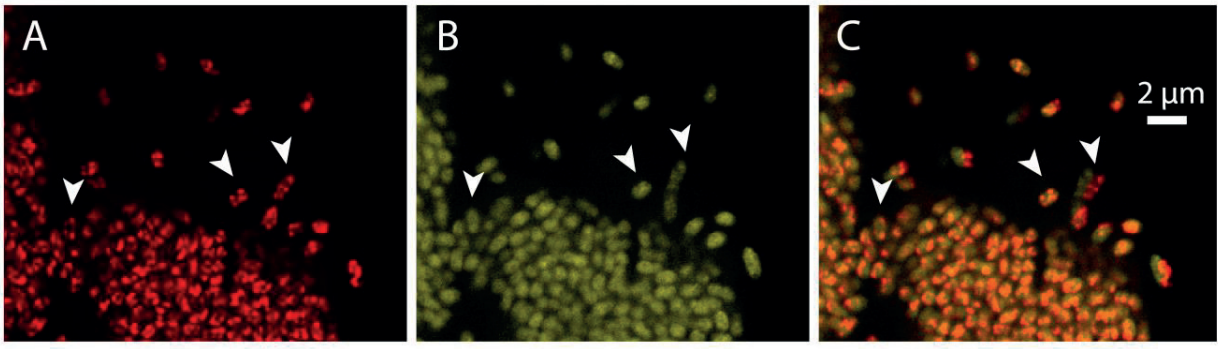

Fig. 2: Carbon storage in the *Leptonemella* ectosymbionts. (A) Laser scanning fluorescence micrograph of *Leptonemella* ectosymbionts stained with Nile Red, which stains lipophilic compounds, such as polyhydoxyalkanoates (PHAs). The arrow heads point towards single cells containing multiple distinct granules. (B) DNA counterstain with DAPI; (C) Overlay picture.

Sulfur metabolism

The *Leptonemella* ectosymbionts contained a large amount of genes involved in sulfur-oxidation pathways. These included genes involved in the periplasmic oxidation of reduced sulfur compounds (*fccAB*, *sqr, soxABXYZ*), the cytoplasmic sulfide and sulfite oxidation pathway and genes of the reverse-operating dissimilatory sulfate reduction pathway (*dsrABCEFHKMJOP*,

aprAB, qmoABC, sat) (Fig. 1, Table S1). This suggests that the ectosymbionts can oxidize both hydrogen sulfide, sulfite and thiosulfate. The presence of these pathways corresponds nicely with previous incubation experiments performed with other stilbonematine nematode ectosymbionts. For example, incubations with radiolabeled hydrogen sulfide led to radiolabeled symbionts of *Eubostrichus* nematodes and enzyme assays of *Stilbonema*, *Robbea* and *Catanema* pools from the Caribbean showed activity of ATP sulfurylase (Sat) and sulfite oxidase, which respectively oxidize APS or sulfite into sulfate (Powell *et al.* 1979; Polz *et al.* 1992). However, incubations of symbionts of *Stilbonema* sp. and *Laxus oneistus* with thiosulfate showed that only symbionts of *Stilbonema* sp. oxidized thiosulfate (Hentschel *et al.* 1999).

The *soxCD* genes, which are part of the complete sox system, were missing in all five ectosymbiont genomes. These genes are known to be required for complete oxidation of sulfide to sulfate in the periplasm (Friedrich *et al.* 2001; Dahl 2008). So far no sulfur-oxidizing symbiont was found to have the *soxCD* genes, and lack of both genes is commonly associated with storage of elemental sulfur as intermediate product (Dahl & Prange 2006; Harada *et al.* 2009; Dmytrenko *et al.* 2014). Sulfur storage in the *Leptonemella* ectosymbionts was indicated by multiple highly refractile vesicles using DIC microscopy (Fig. 3A, D) and confirmed by Raman spectroscopy on individual symbiont cells containing elemental sulfur in the form of cyclooctasulfur, S_8 (Fig. 3B - E). Similarly, elemental sulfur has also been measured in ectosymbionts of a few Caribbean stilbonematine nematode species before (Polz *et al.* 1992; Himmel *et al.* 2009).

Respiration

Oxygen is a commonly used TEA for sulfur-oxidizing symbionts, but many may also use nitrate as electron acceptor (Cavanaugh *et al.* 2006; Kleiner *et al.* 2012a). *Leptonemella* ectosymbionts can likely use oxygen and nitrate as TEAs as indicated by the presence of an aa3-type cytochrome c oxidase (*coxABC*), and the periplasmic respiratory nitrate reductase (*napABC*). The ability to respire oxygen verifies previous incubations of stilbonmatine nematodes, where oxygen respiration was coupled to the oxidation of reduced sulfur compounds (Schiemer *et al.* 1990; Ott *et al.* 1991). Similarly, nitrate respiration has been verified for the Caribbean

stilbonematine nematode *Laxus oneistus,* that showed oxidation of reduced sulfur compounds under anaerobic conditions (Hentschel *et al.* 1999). Additionally, the genome encoded a further enzyme of the molybdopterin superfamily that was highly similar to the unknown TEA that was present in the genome of *Cand.* Thiosymbion algarvensis (94% aa identity) and could either reduce nitrate, perchlorate or DMSO (Figure 1, Table S2, Kleiner *et al.* 2012b). Furthermore, we found another gene cluster containing a molybdopterin oxidoreductase (MbOx) in vicinity to a 4Fe-4S ferredoxin protein and a membrane-bound polysulfide reductase (Fig. 1, Table S1). Once more, the closest related MbOx sequence to the *Leptonemella* ectosymbionts was also found in *Cand.* Thiosymbion algarvensis with a sequence identity of (84% aaID) (Kleiner *et al.* 2012b). However, the same gene cluster has also been described from other sulfur-oxidizing symbionts, such as the endosymbionts of *Riftia* tubeworms, and the gamma- and epsilonproteobacterial ectosymbionts of *Rimicaris* shrimps (Robidart *et al.* 2008; Jan *et al.* 2014a). All of the above mentioned symbionts are known to store elemental sulfur, and thus polysulfides which are common intermediates of incomplete sulfide oxidation (Prange *et al.* 2004; Frigaard & Dahl 2008), could theoretically serve as additional TEA for a yet unknown electron donor in these symbionts. The presence of polysulfides in the ectosymbionts was also verified by Raman spectroscopy (not shown).

Oxygen concentrations on the intertidal flat on Sylt are strongly influenced by the tidal cycle and bioturbation by lugworms and thus symbionts are exposed to fluctuating levels of oxygen (Table S1) (Polerecky *et al.* 2006; Werner *et al.* 2006). Furthermore, *Leptonemella* species have a semi-sessile lifestyle and thrive for longer times in the anoxic sediment layers (Riemann *et al.* 2003). Thus, the capability to use one of the other alternative electron acceptors for sulfur oxidation during limited oxygen availability would be of advantage for the ectosymbionts.

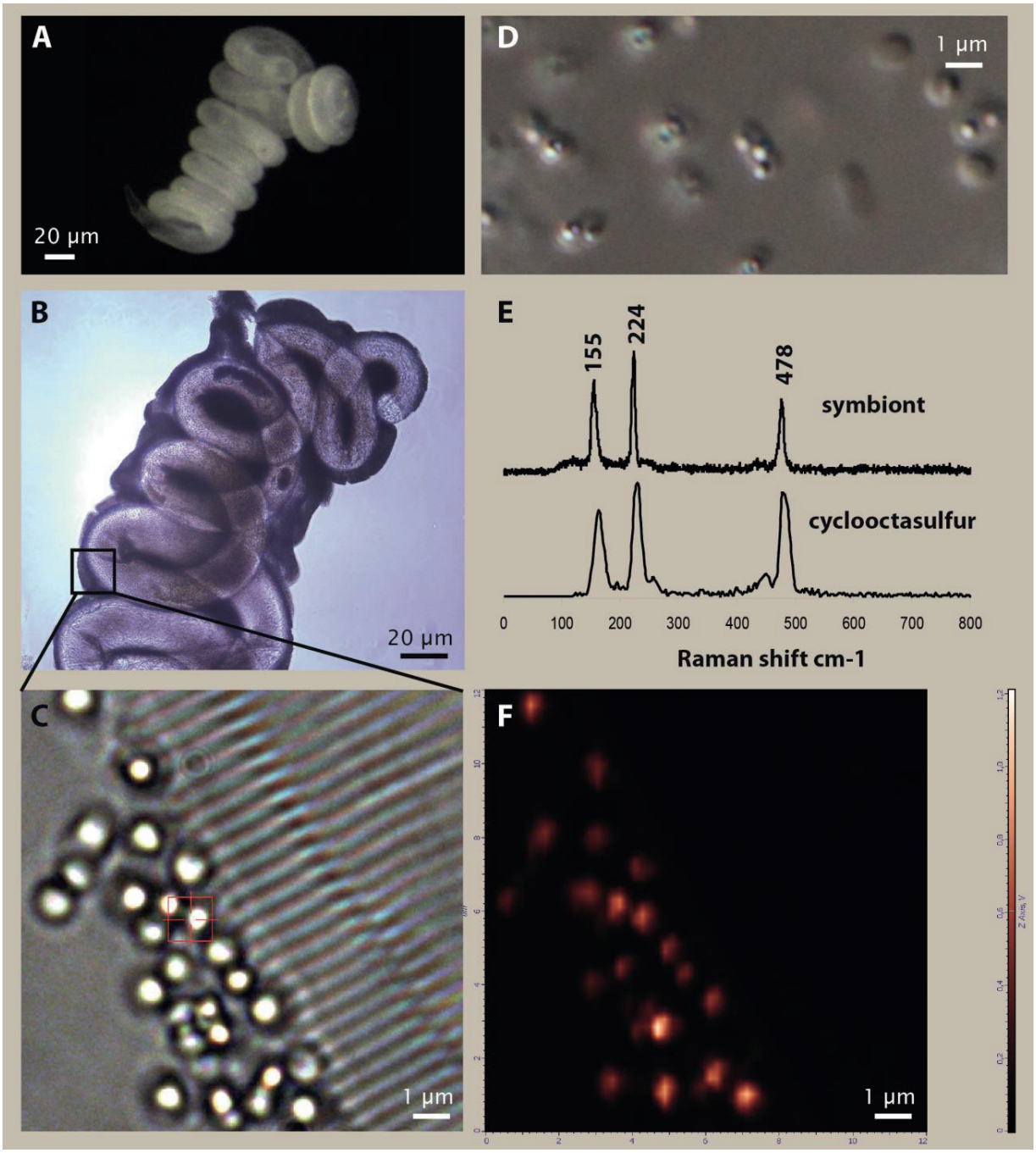

Fig. 3: Raman microscopy showing elemental sulfur inclusions in the *Leptonemella* ectosymbionts. (A) *Leptonemella* covered with a dense white bacterial coat under incident light and (B) phase-contrast illumination. (C) Bright-field microscopy of ectosymbionts attached to the cuticle with light-refractile inclusions. (E) Mapping of the elemental cyclooctasulfur Raman spectrum onto symbionts (orange) shown in (C). (E) Raman spectrum of symbionts measured on cells shown in (C) and reference spectrum (D) Differential interference contrast (DIC) microscopy showing a higher resolution and up to three light-refractile potential sulfur inclusions per symbiont cell.

Nitrogen metabolism

Ammonia and nitrate are known to be abundant in pore waters from the intertidal beach on Sylt, where we sampled the *Leptonemella* individuals, with concentrations reaching up to 80 µM and 40 µM, respectively (de Beer *et al.* 2005). Correspondingly, multiple nitrogen sensor proteins, and transporters for ammonium, nitrate and nitrite were found in the ectosymbiont genomes. Glutamine synthase, which plays an essential role for ammonium assimilation in bacteria, was also present in the *Leptonemella* ectosymbiont genomes (e.g. Almassy *et al.* 1986; Luque‐Almagro *et al.* 2011) (Fig. 1, Table S1). We did not find genes involved in assimilatory nitrate reduction and thus, ammonium may represent the main form of nitrogen assimilated by the symbionts, just as hypothesized for other shallow water sulfur-oxidizing symbionts, including *Cand.* Thiosymbion algarvensis (Kleiner *et al.* 2012b; a; Dmytrenko *et al.* 2014). In addition, the ectosymbionts contained transporters for urea and glycine betaine, that are both rich in nitrogen and may serve as additional nitrogen source for the symbionts (Fig. 1) (see Section "Host-symbiont interaction"). In contrast to *Cand.* Thiosymbion algarvensis*,* that thrives in the nutrient-poor waters of Elba, *Leptonemella* ectosymbionts additionally contained a respiratory nitrate reductase (*napABC*), as mentioned above. Hydrothermal vent tubeworm symbionts also contain both of these nitrate reductases and are exposed to similarly high nitrate concentrations as *Leptonemella* (Hentschel & Felbeck 1993; Bourbonnais *et al.* 2012)**.** The presence of genes for ammonium assimilation and nitrate reduction may thus be an adaptation of the ectosymbiont to a nitrate-rich ecological niche. Similarly, it has been suggested for endosymbionts of hydrothermal vent tubeworms and shallow water clams that environmental conditions dictate symbiont nitrogen metabolism (Liao *et al.* 2014; Dmytrenko *et al.* 2014).

Phosphorus metabolism

Phosphate is limiting in pore waters from the intertidal sand flat on Sylt, with maximum values of 2 µM phosphate in the upper sediment layers in summer (de Beer *et al.* 2005). This could possibly explain the presence of high-affinity phosphate transporters, phosphate sensors and starvation response genes in the genome of the *Leptonemella* ectosymbionts (Fig. 1, Table S1). Genes involved in the synthesis and degradation of inorganic polyphosphates, including a

polyphosphate kinase and exopolyphosphatase were also present in the symbiont genomes, just as known for the *Cand*. Thiosymbion algarvensis (Tabe S1) (Kleiner, 2012). Polyphosphate-chains are known to be synthesized at the expense of energy during favorable growth conditions and can be used to regain energy- although not part of the main energy-generating metabolism (Kornberg 1995; Achbergerová & Nahálka 2011). In *Beggiatoa* cultures polyphosphate decomposition was shown to be coupled to high sulfide concentrations and anoxia while oxic conditions resulted in polyphosphate accumulation (Brock & Schulz-Vogt 2011), indicating that phosphate storage can be a "byproduct" of excessive energy generation during sulfide oxidation. It is possible that energy stored in form of polyphosphate can also be used for the ectosymbiont metabolism when, sulfide or phosphorus availability is limited.

Host-symbiont interactions

Host metabolite recycling

As discussed above, *Leptonemella* ectosymbionts can possibly use organic carbon compounds as a carbon source, in addition to autotrophic fixation of CO_2. Organic acids such as succinate, propionate, malate, fumarate or acetate are common waste or fermentation end products of marine invertebrates (Grieshaber *et al.* 1994; Van Hellemond *et al.* 2003). Thus, a mixotrophic lifestyle would be of particular advantage for microbes associated with an invertebrate host because these carbon-rich host waste products could be recycled. Organic acids could be directly imported by the symbionts' tripartite ATP-independent periplasmic (TRAP) transporters and enter the TCA cycle for energy generation or the glyoxylate cycle and partial 3-HPB for carbon assimilation, as suggested for the *Cand.* Thiosymbion and Y3-symbionts of the gutless *O. algarvensis* (Fig. 1, Table S2) (Kleiner *et al.* 2012b). Furthermore, host-derived amino acids or peptides could be used for protein synthesis by the symbionts. We also found transporters for ammonium, urea and glycine betaine and enzymes for the breakdown of these nitrogenous compounds in the ectosymbiont genomes (Fig. 1, Table 1 and S2). Both urea and glycine betaine are common osmolytes of invertebrates (Yancey 2005) and could serve as additional nitrogen and carbon source in the ectosymbionts, just as known for other bacteria (Lisa *et al.* 1983; Smith *et al.* 1988) and suggested for the *O. algarvensis* Y3- and the *Solemy*a clam

endosymbiont (Woyke *et al.* 2006; Kleiner *et al.* 2012b; Dmytrenko *et al.* 2014). The *O. algarvensis* symbionts live in the extracellular space between the worms' epidermal tissue and cuticle and the clam symbionts are located intracellularly in the gills and thus nutrient exchange between host and symbionts is facilitated. *Leptonemella* ectosymbionts are attached externally to the thick cuticle of their hosts and one may argue that the hosts' waste products will not be directly available to the ectosymbionts but rather excreted by the host. However, just as known from gutless phallodriline annelids that lack an excretory system in form of nephridia (Giere 1981; Dubilier *et al.* 2006), secretory-excretory pores have not been observed with secondary electron microscopy (SEM) analyses and transmission electron microscopy (TEM) sections of stilbonematine nematodes (e.g. Hopper & Cefalu 1973; Berger *et al.* 1996; Kampfer *et al.* 1998; Ott *et al.* 2014a). An identifying character of stilbonematine nematodes are the large glandular sensory organs (GSOs) that are located just below the cuticle along the entire nematode body (Bauer-Nebelsick *et al.* 1995). One of the known functions of these GSOs is the secretion of lectins (sugar-binding proteins) that are involved in host-symbiont specificity by interacting with specific sugars on the symbiont cell membrane (Bulgheresi *et al.* 2006, 2011). Arguably, these GSOs could also be involved in the excretion of carbon- and nitrogen-rich host waste products that may be recycled by the ectosymbionts and we know from previous analyses that symbionts are ingested and serve as nutrient source for the host (Zimmermann *et al.,* in prep., Chapter V). This would conserve nitrogen, carbon and energy in the symbiosis, providing a benefit for both host and symbionts.

Surface attachment

Leptonemella individuals are almost completely covered by a multilayer coat of ectosymbionts that is on average 10 cells thick (Fig. 1B and 2B). The symbionts are embedded in a relatively stable mucus layer (Ott *et al.* 2004, own observation). This mucus has been suggested to be secreted by the numerous GSOs, and to sustain the ectosymbiont coat, together with host-derived lectins (Nebelsick *et al.* 1992; Bauer-Nebelsick *et al.* 1995; Bulgheresi *et al.* 2011). The symbiont genomes encoded genes for the type IV pilus, type II and type VI protein secretion systems (T2SS, T6SS) although comparable features are not commonly found in chemosynthetic or obligate endosymbionts (Fig. 1, Table 2). However, they are present in

genomes of free-living chemoautotrophs or symbionts, such as *Allochromatium vinosum* or biofilm-forming bacteria such as *Pseudomonas aeruginosa* or *Vibrio fischeri* (Table 2). The type IV pilus, for example, is a well-known structure primarily used for adherence to solid surfaces, host cells or other bacteria, and additionally involved in bacterial movement (Mattick 2002; Georgiadou *et al.*, others 2014). Similarly, in *Leptonemella* symbionts, type IV pili could be used to adhere to the host or neighboring cells and thus promote stabilization of the symbiont coat. The T2SS is generally known for the secretion of lytic enzymes (see discussion below) but has also been shown to be involved in biofilm formation. For example in *P. aeruginosa* T2SS can act as adhesive structure, similar to type IV pili (Durand *et al.* 2003), and in *Vibrio cholerae* TSS2 secretes biofilm matrix proteins (Johnson *et al.* 2014). Another important aspect in biofilm formation is the secretion of extracellular polymeric substances (EPS) that can consist of polysaccharides, proteins, nucleic acids and lipids, which provide mechanic stability of the cells and mediate their adhesion to surfaces (Flemming & Wingender 2010). EPS production is often synchronized by cell signaling or quorum sensing (Shrout *et al.* 2011). We found a number of transporters in the genomes that could potentially contribute to EPS production, for example ABC transporters for lipopolysaccharides, phospholipids, lipid A as well as oligopeptides and exporters for (capsular) polysaccharides (Fig. 1). Overall, the genomic repertoire of the *Leptonemella* ectosymbionts indicates that in addition to host-derived factors, such as lectins and mucus secretions from the GSOs the ectosymbionts are also actively involved in adherence to the hosts' cuticle. In contrast to the free-living or facultative symbionts, Leptonemella ectosymbionts contained a low number of chemotaxis genes in their genomes and also no flagella, which could indicate that they do not have a free-living life stage.

Defense

Unlike endosymbiotic bacteria, ectosymbionts are not protected by host tissue but are in direct contact to the environment and thus also potential predators. As mentioned above, the *Leptonemella* ectosymbionts encoded the T2SS that is present in many *Proteobacteria* and often associated with pathogenicity due to secretion of hydrolytic enzymes and toxins (Table 2) (Sandkvist 2001; Cianciotto 2005). In fact, a feature in *Leptonemella* ectosymbionts that has not

Table 2: Selected genome features of *Leptonemella* ectosymbionts compared to other symbiotic and free-living Ɣ-proteobacteria

Organism	*L. aphanothecae* symbionts				*L. vicina* symbiont E220	*Cand.* Thiosymbion algarvensis	*Calyptogena magnifica* symbiont	*Buchnera aphidicola*	*Solemya velum symbiont*	*Cand.* Endoriftia persephone	*Vibrio fischeri* MJ11	*Pseudomonas aeruginosa* PAO1	*E.coli* K-12 MG1655	*Allochromatium vinosum* DSM 180
	E103	**E104**	**E107**	**E112**										
Lifestyle	Ectosymbionts					Extracellular endosymbiont	Intracellular endosymbiont		Intracellular endosymbiont	Facultative endosymbiont	Symbiont with free-living stage	Free-living and host-associated		Free-living
Exposed to environment	yes	yes	yes	yes	yes	no°	no	no	no[$]	yes[#]	yes*	yes	yes	yes
Genome size [mb]	4.73	4.84	4.83	5.10	4.97	5.31	1.16	0.64	2.7	3.20	4.50	6.26	4.64	3.53
GC content [%]	58.9	58.4	58.4	58.4	58.8	57.5	34.0	25.3	51	57.9	38.2	66.6	50.8	64.6
Annotated genes	3806	4021	3867	4200	4068	1249	1079	621	2716	5404	4131	5697	4498	3116
Mobile elements[$]	82	78	92	106	194	185	–	–	75	23	5	24	90	25
Regulation & cell signaling	84	91	77	92	83	11	5	2	28	29	101	85	145	41
Cell wall and capsule	82	63	113	100	82	12	16	37	103	54	112	151	177	130
RND multidrug efflux systems	7	6	5	5	3	1	–	–	5	2	5	8	4	5
Hemolysins/ MARTX	2	2	1	2	2	–	–	–	–	–	–	3	1	–
YD-repeat toxins	4	3	3	7	2	–	–	–	–	–	–	2	–	–
Bacteriocins	9	9	9	7	7	1	–	–	7	1	8	13	12	8
Type I secretion system	–	–	–	–	–	–	–	–	–	–	1	1	–	–
Type II secretion system	1	1	1	1	1	–	–	–	1	1	1	1	1	1?
Type IV pilus	1	1	1	1	1	–	–	–	1	1	1	1	1	1
Flagellum	–	–	–	–	–	–	–	–	–	1	1	1	1	1
Type VI secretion system	1	1	1	1	1	–	–	–	–	–	2	3	–	–
Chemotaxis genes	5	5	6	7	5	–	–	–	1	49	48	44	9	61

°symbionts live below the cuticle that is permeable for molecules of up to 70 kDa (Dubilier *et al.* 2006); #symbionts are horizontally transmitted and able to survive in the environment (Nussbaumer *et al.* 2006); *90% of the symbionts are expelled every morning from the light organ into the environment (Lee & Ruby 1994); $including transposases, integrases and restriction modification systems

been described from any of the other closely related sulfur-oxidizing endosymbiont is the T6SS (Table 2). T6SS is a bacteriophage-like cell-puncturing device present in many pathogenic Gram-negative bacteria and known to inject effector proteins into target cells but is also involved in antagonistic and non-antagonistic bacterial interactions (Records 2011; Coulthurst 2013; Russell *et al.* 2014). T6SS in the ectosymbionts could thus be involved in maintaining a "clean" symbiont coat and support the high specificity of the ectosymbiotic assocations. Each of the *Leptonemella* symbionts also encoded multiple copies of large hemolysin (pore-forming) toxins, YD repeat toxins and bacteriocins, respectively (Table 2). Hemolysin toxins are known to be either involved in defense against pathogens or cell-cell interactions during biofilm formation (reviewed by Satchell 2011). YD repeat toxins are often involved in defense against predators or parasites (Gerardo & Parker 2014). Interestingly, host-parasitic suctoria (Ciliophora) can sometimes be attached to the cuticle of stilbonematine nematodes, but we have never observed them on individuals with an intact symbiont coat (Fig. S1). Consequently, the ectosymbiotic bacteria may not only defend themselves against predators or competitors, which is a common phenomenon of bacteria in biofilms (e.g. Matz *et al.* 2008) but likely also function as a protective barrier for their host against harmful bacterial pathogens, and eukaryotic parasites.

Conclusions

Our analyses of the first ectosymbiont genomes of stilbonematine nematodes have uncovered a large array of metabolic capabilities in the *Leptonemella* ectosymbionts. These include potential adaptations to a symbiotic lifestyle, such as recycling of host waste products by the partial 3-HPB cycle or by transporters for urea and glycine betaine and improved energy-efficiency during carbon fixation by a variant CBB cycle. Prior to this study stilbonematine nematode ectosymbionts were only known to fix carbon autotrophically (reviewed by Ott *et al.* 2004). However the complete TCA cycle including the glyoxylate bypass and partial 3-HPB indicated that organic substrates could be used for both energy generation and heterotrophic carbon assimilation. Thus, *Leptonemella* ectosymbionts are unlikely to be obligate autotrophs but are probably mixotrophs. Furthermore, we found genes for ammonium assimilation, oxygen and nitrate respiration and genes involved in sensing, storage and assimilation of carbon, sulfur and phosphorus. Overall, the large array of

metabolic capabilities would be of considerable advantage for an ectosymbiont that is attached to a motile host and exposed to highly fluctuating environmental conditions. Stilbonematine nematodes are highly diverse and abundant in numerous sulfidic and tidal-influenced environments worldwide and therefore the metabolic flexibility of their symbionts may have been one of the key factors that allowed these ectosymbioses to become highly successful.

One of the central questions for stilbonematine nematodes is which mechanisms provide the high specificity and stability of the ectosymbiont populations. In addition to host-secreted factors such as lectins, that are known to recognize specific symbiont cells (Bulgheresi *et al.* 2011), our genome analyses uncovered many bacterial genes that could be involved in symbiont cooperation and cohesiveness. These included genes involved in surface attachment, biofilm formation, cell-cell communication and defense strategies. While type IV pili are likely involved in attachment to solid surfaces and neighboring cells, anti-bacterial or anti-predatory substances excreted by the T2SS and T6SS might not only help the host to be protected from predators, but also help the ectosymbionts themselves to inhibit competing bacteria. In combination with lectins, these mechanisms may be critical for the maintenance of the highly specific stilbonematines ectosymbiont coat that is constantly exposed to foreign microbes and pathogens.

Acknowledgements

We thank the staff of the Wadden Sea station Sylt (Alfred Wegener Institute, Helmholtz Centre for Polar and Marine Research), especially Werner Armonies and Ragnhild Asmus for hospitality and providing access to laboratory facilities. Many thanks to Miriam Sadowski for excellent technical assistance. Special thanks to Lizbeth Sayavedra, Brandon Kwee Boon Seah, and Paul Antony Chakkiath for assistance with bioinformatics and valuable scientific input. This work was supported by the Max Planck Society.

References

Achbergerová L, Nahálka J (2011) Polyphosphate - an ancient energy source and active metabolic regulator. *Microbial Cell Factories*, **10**, 63.

Acosta H, Dubourdieu M, Quiñones W *et al.* (2004) Pyruvate phosphate dikinase and pyrophosphate metabolism in the glycosome of *Trypanosoma cruzi* epimastigotes. *Comparative Biochemistry and Physiology Part B: Biochemistry and Molecular Biology*, **138**, 347–356.

Almassy RJ, Janson CA, Hamlin R, Xuong N-H, Eisenberg D (1986) Novel subunit—subunit interactions in the structure of glutamine synthetase. *Nature*, **323**, 304–309.

Altschul S, Madden TL, Schäffer AA, *et al.* (1997) Gapped BLAST and PSI-BLAST: a new generation of protein database search programs. *Nucleic Acids Research*, **25**, 3389–3402.

Anderson AJ, Dawes EA (1990) Occurrence, metabolism, metabolic role, and industrial uses of bacterial polyhydroxyalkanoates. *Microbiological Reviews*, **54**, 450–472.

Asmus R (1982) Field measurements on seasonal variation of the activity of primary producers on a sandy tidal flat in the northern Wadden sea. *Netherlands Journal of Sea Research*, **16**, 389–402.

Aziz RK, Bartels D, Best AA *et al.* (2008) The RAST server: rapid annotations using subsystems technology. *BMC Genomics*, **9**, 75.

Badger MR, Bek EJ (2008) Multiple Rubisco forms in proteobacteria: their functional significance in relation to CO_2 acquisition by the CBB cycle. Journal of Experimental Botany, 59, 1525–1541.

Bauer-Nebelsick M, Blumer M, Urbancik W, Ott JA (1995) The glandular sensory organ of Desmodoridae (Nematoda)- ultrastructure and phylogenetic implications. *Invertebrate Biology*, **114**, 211–219.

De Beer D, Wenzhöfer F, Ferdelman TG *et al.* (2005) Transport and mineralization rates in north sea sandy intertidal sediments, Sylt-Rømø basin, Wadden sea. *Limnology and Oceanography*, **50**, 113–127.

Berger E, Urbancik W, Ott JA (1996) *Eubostrichus topiarius* sp. n., a new free-living, marine species of Stilbonematinae (Nematoda: Desmodoridae) from a shallow subtidal sand bottom. *Nematologica*, **42**, 521–536.

Böer SI, Arnosti C, van Beusekom JEE, Boetius A (2009) Temporal variations in microbial activities and carbon turnover in subtidal sandy sediments. *Biogeosciences*, **6**, 1149–1165.

Bourbonnais A, Lehmann MF, Butterfield DA, Juniper SK (2012) Subseafloor nitrogen transformations in diffuse hydrothermal vent fluids of the Juan de Fuca Ridge evidenced by the isotopic composition of nitrate and ammonium. *Geochemistry, Geophysics, Geosystems*, **13**, Q02T01.

Brock J, Schulz-Vogt HN (2011) Sulfide induces phosphate release from polyphosphate in cultures of a marine *Beggiatoa* strain. *The ISME journal*, **5**, 497–506.

Bulgheresi S, Gruber-Vodicka HR, Heindl NR *et al.* (2011) Sequence variability of the pattern recognition receptor Mermaid mediates specificity of marine nematode symbioses. *The ISME Journal*, **5**, 986–998.

Bulgheresi S, Schabussova I, Chen T *et al.* (2006) A new C-type lectin similar to the human immunoreceptor DC-SIGN mediates symbiont acquisition by a marine nematode. *Applied and Environmental Microbiology*, **72**, 2950–2956.

Camacho C, Coulouris G, Avagyan V *et al.* (2009) BLAST+: architecture and applications. *BMC Bioinformatics*, **10**, 421.

Caspi R, Altman T, Billington R *et al.* (2014) The MetaCyc database of metabolic pathways and enzymes and the BioCyc collection of pathway/genome databases. *Nucleic Acids Research*, **42**, D459–D471.

Cavanaugh CM, Gardiner S, Jones ML, Jannasch HW, Waterbury JB (1981) Prokaryotic cells in the hydrothermal vent tube worm *Riftia pachyptila* Jones: possible chemoautotrophic symbionts. *Science*, **213**, 340–342.

Cavanaugh C, McKiness Z, Newton I, Stewart F (2006) Marine chemosynthetic symbioses. In: *The Prokaryotes*, pp. 475–507.

Cianciotto NP (2005) Type II secretion: a protein secretion system for all seasons. *Trends in Microbiology*, **13**, 581–588.

Coulthurst SJ (2013) The Type VI secretion system–a widespread and versatile cell targeting system. *Research in microbiology*, **164**, 640–654.

Dahl C (2008) Inorganic sulfur compounds as electron donors in purple sulfur bacteria. In: *Sulfur metabolism in phototrophic organisms*, pp. 289–317. Springer.

Dahl C, Prange A (2006) Bacterial sulfur globules: occurrence, structure and metabolism. In: *Inclusions in prokaryotes,* pp. 21–51. Springer Berlin Heidelberg.

Dmytrenko O, Russell SL, Loo WT *et al.* (2014) The genome of the intracellular bacterium of the coastal bivalve, Solemya velum: a blueprint for thriving in and out of symbiosis. *BMC Genomics*, **15**, 924.

Dubilier N, Bergin C, Lott C (2008) Symbiotic diversity in marine animals: the art of harnessing chemosynthesis. *Nature Reviews Microbiology*, **6**, 725–740.

Dubilier N, Blazejak A, Rühland C (2006) Symbioses between bacteria and gutless marine oligochaetes. In: *Molecular Basis of Symbiosis* Progress in Molecular and Subcellular Biology. (ed Overmann PDJ), pp. 251–275. Springer Berlin Heidelberg.

Dubilier N, Giere O, Distel DL, Cavanaugh CM (1995) Characterization of chemoautotrophic bacterial symbionts in a gutless marine worm Oligochaeta, Ia) by phylogenetic 16S rRNA sequence analysis and in situ hybridization. *Applied and Environmental Microbiology*, **61**, 2346–2350.

Durand É, Bernadac A, Ball G *et al.* (2003) Type II protein secretion in *Pseudomonas aeruginosa*: the pseudopilus is a multifibrillar and adhesive structure. *Journal of Bacteriology*, **185**, 2749–2758.

Felbeck H (1981) Chemoautotrophic potential of the hydrothermal vent tube worm, *Riftia pachyptila* Jones (Vestimentifera). *Science*, **213**, 336–338.

Fenchel T, Finlay BJ (1989) *Kentrophoros*: a mouthless ciliate with a symbiotic kitchen garden. *Ophelia*, **30**, 75–93.

Flemming H-C, Wingender J (2010) The biofilm matrix. *Nature Reviews Microbiology*, **8**, 623–633.

Friedrich CG, Rother D, Bardischewsky F, Quentmeier A, Fischer J (2001) Oxidation of reduced inorganic sulfur compounds by bacteria: emergence of a common mechanism? *Applied and Environmental Microbiology*, **67**, 2873–2882.

Frigaard N-U, Dahl C (2008) Sulfur metabolism in phototrophic sulfur bacteria. *Advances in Microbial Physiology*, **54**, 103–200.

Gardebrecht A, Markert S, Sievert SM *et al.* (2011) Physiological homogeneity among the endosymbionts of *Riftia pachyptila* and *Tevnia jerichonana* revealed by proteogenomics. *The ISME Journal*, **6**, 766–776.

Geng H, Belas R (2010) Molecular mechanisms underlying roseobacter–phytoplankton symbioses. *Current Opinion in Biotechnology*, **21**, 332–338.

Georgiadou M, Pelicic V, Barocchi MA, Telford JL, others (2014) Type IV pili: functions and biogenesis. *Bacterial Pili: Structure, Synthesis and Role in Disease*, **27**, 71.

Gerardo NM, Parker BJ (2014) Mechanisms of symbiont-conferred protection against natural enemies: an ecological and evolutionary framework. *Current Opinion in Insect Science*, **4**, 8–14.

Gerlach SA (1978) Food-chain relationships in subtidal silty sand marine sediments and the role of meiofauna in stimulating bacterial productivity. *Oecologia*, **33**, 55–69.

Giere O (1981) The gutless marine oligochaete *Phallodrilus leukodermatus*. Structural studies on an aberrant tubificid associated with bacteria. *Marine Ecology Progress Series*, **5**, 353–357.

Giere O, Erséus C (2002) Taxonomy and new bacterial symbioses of gutless marine Tubificidae (Annelida, Oligochaeta) from the Island of Elba (Italy). *Organisms Diversity & Evolution*, **2**, 289–297.

Grieshaber MK, Hardewig I, Kreutzer U, Pörtner H-O (1994) Physiological and metabolic responses to hypoxia in invertebrates. In: *Reviews of Physiology, Biochemistry and Pharmacology,* **125**, 43–147.

Gruber-Vodicka HR, Dirks U, Leisch N *et al.* (2011) *Paracatenula*, an ancient symbiosis between thiotrophic Alphaproteobacteria and catenulid flatworms. *Proceedings of the National Academy of Sciences*, **108**, 12078–12083.

Gruber-Vodicka HR, Kleiner M, Wentrup C et al. (in preparation) '*Candidatus* Thiosymbion' spp., a genus of thiotrophic Gammaproteobacteria associated with diverse metazoan hosts.

Harada M, Yoshida T, Kuwahara H et al. (2009) Expression of genes for sulfur oxidation in the intracellular chemoautotrophic symbiont of the deep-sea bivalve *Calyptogena okutanii*. Extremophiles, 13, 895–903

Van Hellemond JJ, Van Der Klei A, van Weelden SH, Tielens AG (2003) Biochemical and evolutionary aspects of anaerobically functioning mitochondria. *Philosophical Transactions of the Royal Society B: Biological Sciences*, **358**, 205–215.

Hentschel U, Berger EC, Bright M, Felbeck H, Ott JA (1999) Metabolism of nitrogen and sulfur in ectosymbiotic bacteria of marine nematodes(Nematoda, Stilbonematinae). *Marine Ecology Progress Series*, **183**, 149–158.

Hentschel U, Felbeck H (1993) Nitrate respiration in the hydrothermal vent tubeworm *Riftia pachyptila*. *Nature*, **366**, 338–340.

Himmel D, Maurin LC, Gros O, Mansot J-L (2009) Raman microspectrometry sulfur detection and characterization in the marine ectosymbiotic nematode *Eubostrichus dianae* (Desmodoridae, Stilbonematidae). *Biology of the Cell / Under the Auspices of the European Cell Biology Organization*, **101**, 43–54.

Hopper BE, Cefalu RC (1973) Free-living marine nematodes from Biscayne Bay, Florida V. Stilbonematinae: contributions to the taxonomy and morphology of the genus *Eubostrichus* Greeff and related genera. *Transactions of the American Microscopical Society*, **92**, 578–591.

Hunter S, Apweiler R, Attwood TK *et al.* (2009) InterPro: the integrative protein signature database. *Nucleic Acids Research*, **37**, D211–D215.

Jan C, Petersen JM, Werner J *et al.* (2014) The gill chamber epibiosis of deep-sea shrimp *Rimicaris exoculata*: an in-depth metagenomic investigation and discovery of Zetaproteobacteria. *Environmental Microbiology*, **16**, 2723–2738.

Johnson TL, Fong JC, Rule C *et al.* (2014) The Type II secretion system delivers matrix proteins for biofilm formation by *Vibrio cholerae*. *Journal of Bacteriology*, **196**, 4245–4252.

Kampfer S, Sturmbauer C, Ott J (1998) Phylogenetic analysis of rDNA sequences from Adenophorean nematodes and implications for the Adenophorea-Secernentea controversy. *Invertebrate Biology*, **117**, 29–36.

Kanehisa M, Goto S, Sato Y *et al.* (2014) Data, information, knowledge and principle: back to metabolism in KEGG. *Nucleic Acids Research*, **42**, D199–D205.

Kleiner M, Petersen JM, Dubilier N (2012a) Convergent and divergent evolution of metabolism in sulfur-oxidizing symbionts and the role of horizontal gene transfer. *Current Opinion in Microbiology*, **15**, 621–631.

Kleiner M, Wentrup C, Lott C, *et al.* (2012) Metaproteomics of a gutless marine worm and its symbiotic microbial community reveal unusual pathways for carbon and energy use. *Proceedings of the National Academy of Sciences,* **109**, 7148-7149.

Kleiner, Manuel (2012). Metabolism and evolutionary ecology of chemosynthetic symbionts from marine invertebrates. Phd thesis. University of Bremen, Germany.

Kornberg A (1995) Inorganic polyphosphate: toward making a forgotten polymer unforgettable. *Journal of Bacteriology*, **177**, 491–496.

Kornberg HL, Madsen NB (1957) Synthesis of C4-dicarboxylic acids from acetate by a "glyoxylate bypass" of the tricarboxylic acid cycle. *Biochimica et Biophysica Acta*, **24**, 651–653.

Lee SY (1996) Bacterial polyhydroxyalkanoates. *Biotechnology and Bioengineering*, **49**, 1–14.

Lee K-H, Ruby EG (1994) Effect of the squid host on the abundance and distribution of symbiotic *Vibrio fischeri* in nature. *Applied and Environmental Microbiology*, **60**, 1565–1571.

Liao L, Wankel SD, Wu M, Cavanaugh CM, Girguis PR (2014) Characterizing the plasticity of nitrogen metabolism by the host and symbionts of the hydrothermal vent chemoautotrophic symbioses Ridgeia piscesae. *Molecular Ecology*, **23**, 1544–1557.

Lisa TA, Garrido MN, Domenech CE (1983) Induction of acid phosphatase and cholinesterase activities in *Ps. aeruginosa* and their in-vitro control by choline, acetylcholine and betaine. *Molecular and Cellular Biochemistry*, **50**, 149–155.

Lonsdale P (1977) Clustering of suspension-feeding macrobenthos near abyssal hydrothermal vents at oceanic spreading centers. *Deep Sea Research*, **24**, 857–863.

Luque-Almagro VM, Gates AJ, Moreno-Vivián C *et al.* (2011) Bacterial nitrate assimilation: gene distribution and regulation. *Biochemical Society Transactions*, **39**, 1838–1843.

Markert S, Arndt C, Felbeck H *et al.* (2007) Physiological proteomics of the uncultured endosymbiont of *Riftia pachyptila*. *Science*, **315**, 247–250.

Markert S, Gardebrecht A, Felbeck H *et al.* (2011) Status quo in physiological proteomics of the uncultured *Riftia pachyptila* endosymbiont. *Proteomics*, **11**, 3106–3117.

Mattick JS (2002) Type Iv Pili and Twitching Motility. *Annual Review of Microbiology*, **56**, 289–314.

Matz C, Webb JS, Schupp PJ *et al.* (2008) Marine biofilm bacteria evade eukaryotic predation by targeted chemical defense. *PLoS ONE*, **3**, e2744.

Migné A, Spilmont N, Davoult D (2004) In situ measurements of benthic primary production during emersion: seasonal variations and annual production in the Bay of Somme (eastern English Channel, France). *Continental Shelf Research*, **24**, 1437–1449.

Nakagawa S, Shimamura S, Takaki Y *et al.* (2014) Allying with armored snails: the complete genome of gammaproteobacterial endosymbiont. *The ISME journal*, **8**, 40–51.

Nebelsick M, Blumer M, Novak R, Ott J (1992) A new glandular sensory organ in *Catanema* sp. (Nematoda, Stilbonematinae). *Zoomorphology*, **112**, 17–26.

Newton ILG, Woyke T, Auchtung TA *et al.* (2007) The *Calyptogena magnifica* chemoautotrophic symbiont genome. *Science*, **315**, 998–1000.

Nunoura T, Sako Y, Wakagi T, Uchida A (2003) Regulation of the aerobic respiratory chain in the facultatively aerobic and hyperthermophilic archaeon *Pyrobaculum oguniense*. *Microbiology*, **149**, 673–688.

Nussbaumer AD, Fisher CR, Bright M (2006) Horizontal endosymbiont transmission in hydrothermal vent tubeworms. *Nature*, **441**, 345–348.

Ott J, Bright M, Bulgheresi S (2004) Symbioses between marine nematodes and sulfur-oxidizing chemoautotrophic bacteria. *Symbiosis*, **36**, 103–126.

Ott JA, Gruber-Vodicka HR, Leisch N, Zimmermann J (2014) Phylogenetic confirmation of the genus *Robbea* (Nematoda: Desmodoridae, Stilbonematinae) with the description of three new species. *Systematics and Biodiversity*, **12**, 434–455.

Ott JA, Novak R, Schiemer F *et al.* (1991) Tackling the sulfide gradient: a novel strategy Involving marine nematodes and chemoautotrophic ectosymbionts. *Marine Ecology*, **12**, 261–279.

Overbeek R, Olson R, Pusch GD *et al.* (2013) The SEED and the Rapid Annotation of microbial genomes using Subsystems Technology (RAST). *Nucleic Acids Research*, **42**, D206-D214.

Polerecky L, Volkenborn N, Stief P (2006) High temporal resolution oxygen imaging in bioirrigated sediments. *Environ. Sci. Technol.*, **40**, 5763–5769.

Polz MF, Distel DL, Zarda B, *et al.* (1994) Phylogenetic analysis of a highly specific association between ectosymbiotic, sulfur-oxidizing bacteria and a marine nematode. *Applied Environmental Microbiology*, **60**, 4461–4467.

Polz MF, Felbeck H, Novak R, Nebelsick M, Ott JA (1992) Chemoautotrophic, sulfur-oxidizing symbiotic bacteria on marine nematodes: morphological and biochemical characterization. *Microbial Ecology*, **24**, 313–329.

Postma PW, Lengeler JW (1985) Phosphoenolpyruvate:carbohydrate phosphotransferase system of bacteria. *Microbiological Reviews*, **49**, 232–269.

Powell EN, Crenshaw MA, Rieger RM (1979) Adaptations to sulfide in sulfide-system I. 35S-sulfide accumulation and the presence of a sulfide detoxification system. *Journal of Experimental Marine Biology and Ecology*, **37**, 57–76.

Prange A, Engelhardt H, Trüper HG, Dahl C (2004) The role of the sulfur globule proteins of *Allochromatium vinosum*: mutagenesis of the sulfur globule protein genes and expression studies by real-time RT-PCR. *Archives of Microbiology*, **182**, 165–174.

Raverdy S, Foster JM, Roopenian E, Carlow CK (2008) The *Wolbachia* endosymbiont of *Brugia malayi* has an active pyruvate phosphate dikinase. *Molecular and biochemical parasitology*, **160**, 163–166.

Records AR (2011) The type VI secretion system: a multipurpose delivery system with a phage-like machinery. *Molecular Plant-Microbe Interactions*, **24**, 751–757.

Riemann F, Thiermann F, Bock L (2003) *Leptonemella* species (Desmodoridae, Stilbonematinae), benthic marine nematodes with ectosymbiotic bacteria, from littoral sand of the North Sea island of Sylt: taxonomy and ecological aspects. *Helgoland Marine Research*, **57**, 118–131.

Robidart JC, Bench SR, Feldman RA *et al.* (2008) Metabolic versatility of the *Riftia pachyptila* endosymbiont revealed through metagenomics. *Environmental Microbiology*, **10**, 727–737.

Ruehland C, Blazejak A, Lott C *et al.* (2008) Multiple bacterial symbionts in two species of co-occurring gutless oligochaete worms from Mediterranean sea grass sediments. *Environmental Microbiology*, **10**, 3404–3416.

Russell AB, Peterson SB, Mougous JD (2014) Type VI secretion system effectors: poisons with a purpose. *Nature Reviews Microbiology*, **12**, 137–148.

Sandkvist M (2001) Type II Secretion and Pathogenesis. *Infection and Immunity*, **69**, 3523–3535.

Satchell KJF (2011) Structure and function of MARTX toxins and other large repetitive RTX proteins. *Annual Review of Microbiology*, **65**, 71–90.

Schiemer F, Novak R, Ott J (1990) Metabolic studies on thiobiotic free-living nematodes and their symbiotic microorganisms. *Marine Biology*, **106**, 129–137.

Seymour JR, Ahmed T, Durham WM, Stocker R (2010) Chemotactic response of marine bacteria to the extracellular products of *Synechococcus* and *Prochlorococcus*. *Aquatic Microbial Ecology*, **59**, 161.

Shrout JD, Tolker-Nielsen T, Givskov M, Parsek MR (2011) The contribution of cell-cell signaling and motility to bacterial biofilm formation. *MRS Bulletin / Materials Research Society*, **36**, 367–373.

Smith LT, Pocard JA, Bernard T, Le Rudulier D (1988) Osmotic control of glycine betaine biosynthesis and degradation in Rhizobium meliloti. *Journal of Bacteriology*, **170**, 3142–3149.

Tchesunov AV (2013) Marine free-living nematodes of the subfamily Stilbonematinae (Nematoda, Desmodoridae): taxonomic review with descriptions of a few species from the Nha Trang Bay, Central Vietnam, **20**, 71–94.

Walsh K, Koshland DE (1984) Determination of flux through the branch point of two metabolic cycles. The tricarboxylic acid cycle and the glyoxylate shunt. *The Journal of Biological Chemistry*, **259**, 9646–9654.

Werner U, Billerbeck M, Polerecky L *et al.* (2006) Spatial and temporal patterns of mineralization rates and oxygen distribution in a permeable intertidal sand flat (Sylt, Germany). *Limnology and Oceanography*, **51**, 2549–2563.

Wieser W (1959) Eine ungewöhnliche Assoziation zwischen Blaualgen und freilebenden marinen Nematoden. *Plant Systematics and Evolution*, **106**, 81–87.

Woyke T, Teeling H, Ivanova NN *et al.* (2006) Symbiosis insights through metagenomic analysis of a microbial consortium. *Nature*, **443**, 950–955.

Yancey PH (2005) Organic osmolytes as compatible, metabolic and counteracting cytoprotectants in high osmolarity and other stresses. *Journal of Experimental Biology*, **208**, 2819–2830

Supplementary material

Judith Zimmermann, Jillian M. Petersen, Jasmine Berg, Nicole Dubilier, and Manuel Kleiner

SI Tables

Table S1: Selected genes in the *Leptonemella aphanothecae* and *vicina* ectosymbiont genomes sorted by category. Genes that were not present in the assembly are highlighted in red. Annotations are according to RAST

Sulfur metabolism
Periplasmic sulfide and thiosulfate oxidation
soxAX Oxidation of reduced sulfur compounds
soxB
soxYZ
soxCD
sqr (sulfide quinone (oxido)reductase)
Sulfide dehydrogenase [flavocytochrome C] (*fccAB*)
Cytoplasmic sulfide oxidation
Dissimilatory sulfite reductase, alpha subunit (*dsrAB*)
Dissimilatory sulfite reductase, gamma subunit (*dsrC*)
tRNA 5-methylaminomethyl-2-thiouridine synthase (*dsrEFH*)
Sulfite reduction-associated transmembrane electron transport complex (*dsrMKJOP*)
dsrS
dsrR
dsrL, N
Sulfite oxidation
Adenylylsulfate reductase alpha-subunit *(aprAB*)
qmoA
qmoB
qmoC
Sulfate adenylyltransferase, dissimilatory-type (sat)
aprM
other sulfur-related genes
Thiosulfate sulfurtransferase, rhodanese
Cobyrinic acid A,C-diamide synthase
Protein similar to glutamate synthase [NADPH] small chain, clustered with sulfite reductase
Anaerobic polysulfide reductase?
Molybdopterin oxidoreductase
4Fe-4S ferredoxin iron sulfur binding protein
Polysulfide reductase *NrfD*
Energy metabolism
ATP synthases
ATP synthase subunit a and b
ATP synthase alpha, beta, gamma, delta, epsilon chain
NADH dehydrogenases
NADH:ubiquinone oxidoreductase chain ABCDEFHIJKLMN
Electron transport complex
RnfABCDEG (2x) (not on the same operons)
Quinone reductases
Succinate dehydrogenase subunit A
Succinate dehydrogenase subunit B

Succinate dehydrogenase subunit C
Terminal cytochrome oxidases
aa3-type cytochrome C oxidase *coxABC*, subunit A
aa3-type cytochrome C oxidase *coxABC*, subunit B
aa3-type cytochrome C oxidase *coxABC*, subunit C
aa3-type cytochrome C oxidase assembly protein
Ubiquinol-cytochrome C reductase iron-sulfur subunit
Ubiquinol-cytochrome C reductase, cytochrome B subunit
Ubiquinol-cytochrome C oxidoreductase, cytochrome C1 subunit
Cytochrome c oxidase (B(O/a)3-type) chain I
Transporters
Urea ABC transporter *UrtrABCDE*
Urease alpha beta gamma subunit and urease accessory protein *UreDEFG*
Oligopeptide ABC transporter (periplasmic)
Zinc ABC transporter (periplasmic)
Glycine betaine transporter
TRAP transporter
RND multidrug efflux transporter
Phospholipid-lipopolysaccharide ABC transporter
Lipopolysaccharide ABC transporter,
Phosphate ABC transporter,
Maltose/maltodextrin ABC transporter ModA (peripl.)
Predicted cobalt transporter cbtA
Molybdenum ABC transporter (peripl)
Sulfate transporter, CysZ type
Sulfate permease
Phosphotransferase system (PTS)
Phosphoenolpyruvate-protein phosphotransferase of PTS
PTS EIIA type-2 component, *PtsN*
ATPase P-loop containing
Serine kinase of the HPr protein, regulates carbohydrate metabolism
Carbon metabolism
Calvin-Benson-Bassham cycle (CBB)- energy-efficient form
RubisCO large subunit from IA
RubisCO small subunit
3-phosphoglycerate kinase
NADPH-dependent glyceraldehyde-3-phosphate dehydrogenase
Triosephosphateisomerase
Fructose-bisphosphate aldolase
Fructose-1,6 bisphosphatase
Transketolase
Sedoheptulose-1,7-bisphosphatase
Ribose-5-phosphate isomerase
Ribulose-phosphate 3-epimerase
Phosphoribulokinase
6-Phosphofructokinase (PPi-dependent)
H+ translocating pyrophosphatase
Tricarboxylic acid cycle (TCA)
Citrate synthase
Aconitate hydratase
2-oxoglutarate dehydrogenase E1 component
Isocitrate lyase
Isocitrate dehydrogenase
Succinyl-CoA ligase
Succinate dehydrogenase/ fumarate reductase
Fumarate hydratase class I
Malate dehydrogenase
other carbon-related genes
Carbon storage regulator (*csrA*)

Outer membrane lipoprotein- expressed under carbon starvation
3-hydroxypropionate bicycle (3-HPB) (partial)
Acetyl-CoA carboxylase
Malonyl-CoA reductase
Propionyl-CoA synthase
Propionyl-CoA carboxylase
Methylmalonyl-CoA epimerase
Methylmalonyl-CoA mutase
Succinyl-CoA:(S)-malate-CoA transferase
Succinate dehydrogenase
Fumarate hydratase
MMC lyase
Mesaconyl-C1-CoA hydratase
Mesaconyl-C1-CoA transferase
Mesaconyl-C4-CoA hydratase
Glycolyse/ Gluconeogenesis
Malate dehydrogenase
Phosphoenolpyruvate carboxykinase
Phosphoenolpyruvate synthetase
Enolase
2,3-bisphosphoglycerate-independent phosphoglycerate mutase
Phosphoglycerate kinase
NAD-dependent glyceraldehyde-3-phosphate dehydrogenase
Triosephosphate isomerase
Fructose-bisphosphate aldolase class II
Frucose-1,6-bisphosphatase (see CBB)
Phosphoglucose isomerase
Glucose-6-phosphate isomerase
Pyruvat kinase
Pyruvate phosphate dikinase
Glyoxylate cycle
Isocitrate lyase
Malate synthase
Malate dehydrogenase
Citrate synthase
Citrate hydro-lyase/ aconitase
Glyocgen biosynthesis
Phosphoglucomutase
Glucose-1-phosphate adenylyltransferase
Glycogen synthase
1,4-alpha glucan enzyme
Glycogen degradation
Glycogen phosphorylase
4-alpha-glucanotransferase
Beta glucosidase
Phosphoglucomutase
rTCA
Isocitrate dehydrogenase
Isocitrate lyase
Aconitate hydratase
ATP-citrate synthase/ lyase
Pyruvate ferredoxin oxidoreductase
Phosphoenolpyruvate synthetase
Phosphoenolpyruvate carboxylase
Malate dehydrogenase
Fumarate hydratase class I
Fumarate reductase
Succinyl-CoA synthetase
2-oxoglutarate ferredoxin oxidoreductase

Reductive Acetyl-CoA pathway
Taurine catabolism
PHA synthesis
Acetyl-coenzyme A carboxyl transferase alpha and beta chain
Propionyl-CoA carboxylase beta chain
3-oxoacyl-[acyl-carrier protein] reductase (*phaB*)
3-ketoacyl-CoA thiolase (*phaB*)
Malonyl-Coa_decarboxylase
Acetoacetyl-CoA synthase (*phaA*)
Polyhydroxyalkanoic acid synthase (*phaC*)
PHA synthase subunit
Poly(3-hydroxyalkanoate) depolymerase
3-hydroxyacyl-CoA dehydrogenase
Phosphate metabolism
Polyphosphate kinase
Exopolyphosphatase
Phosphate regulon sensor protein PhoR
Phosphate regulon transcriptional regulatory protein PhoB
Phosphate transport system regulatory protein PhoU
Phosphate transport system permease protein PstA
Phosphate transport ATP-binding protein PstB
Phosphate transport system permease protein PstC
Phosphate ABC transporter, periplasmic phosphate-binding protein PstS
Phosphate starvation-inducible protein PhoH, predicted ATPase
Nitrogen metabolism
Unknown terminal electron acceptor
Respiratory nitrate reductase alpha chain and beta chain (*narGH*) – related sequence
Respiratory nitrate reductase subunit, conjectural (gamma?) (*narI*) - related sequence
Cytoplasmic assimilatory
assimilatory nitrate reductase *NasA*
assimilatory nitrite reductase *NasD*
Periplasmic dissimilatory
periplasmic nitrate reductase NapA
periplasmic nitrate reductase NapB
napC (3x)
napD
napF
Polyferredoxin (periplasmic nitrate reductase) NapH
Ferredoxin-type protein (periplasmic nitrate reductase) NapG
Cytochrome c-type protein NapC
Nitrate/nitrite transporter
Nitric oxide reductase activation protein (2x)
Nitric oxide reductase NorBC
nitrous oxide reductase
Nitrogen regulation protein NtrBXY
Nitrogen regulation protein NR(I) and P-II
Nitrogen regulatory protein P-II
Nitrite reductase [NAD(P)H] small subunit
Nitrite reductase accessory protein NirV
Nitrate/nitrite sensor protein
Cell Division
Cell division protein FtsABIKLWQZ
Cell division protein MraZ
Cell division protein ZipA
Cell division topological specificity factor MinE
Z-ring-associated protein ZapA
Rod shape-determining protein MreABCD
Septum formation and site-determining protein Ma fand MinD
Chromosome (plasmid) partitioning protein ParA

Septum site-determining protein MinC
Biofilm production/ quorum sensing
Chemotaxis regulator - transmits chemoreceptor signals to flagelllar motor
Chemotaxis protein methyltransferase/ signal transduction histidine kinase (CheY-like superfamily) (1)
Methyl-accepting chemotaxis sensory transducer (1)
Methyl-accepting chemotaxis protein (2)
MeTrc, Methyltransferase, chemotaxis proteins (2)
Biopolymer transport protein ExbD/TolR
maltose, maltodextrin ung glycogen metabolismus (Produktion von EPS?)
Type IV pilus PilABCEFMNOPQRVWXZ
Type VI secretion Imcf ImpABCEFGHIJKM VgrG protein
Type II secretion AEDGHIJKLMN (General secretion pathway proteins)
Polysaccharide export protein
Capsule synthesis protein, CapA
Defense
Hemolysin/ MARTX
YD-repeat toxin
Multidrug efflux pump (RND) membrane fusion protein
Multidrug efflux pump (RND), exporter
Multidrug efflux pump (RND), efflux transporter, MFP subunit AcrA (2)
ABC-type multidrug transport system
Acriflavin resistance protein AcrB TolC (up to 5)
Arsenical resistance protein
Type I secretion outer membrane protein, TolC
Type II, III, V restriction endonucleases

Table S2: Comparison of selected metabolic pathways and transporters in *Leptonemella* ectosymbionts compared to the sulfur-oxidizing endosymbionts of *Olavius algarvensis.*

Category	Metabolic pathway or specific gene	***Leptonemella aphanothecae, L. vicina* (Nematoda, Stilbonematinae)**	***Olavius algarvensis* (Annelida, Phallodrilinae)**	
		ectosymbiont	***Candidatus* Thiosymbion algarvensis**	**Y'3-endosymbiont**
Carbon metabolism	modified CBB cycle	present	present	present
	TCA/ glyoxylate cycle	present	?*	present
	partial 3-HPB cycle	present	present	–
	PHA storage	present	present	present
Sulfur metabolism	SOX system	present	present	present
	Reverse Dsr pathway	present	present	present
	Sulfur storage	present	present	–
Nitrogen metabolism	Glutamine synthetase	present	present	present
Electron acceptors	Cyctochrome C oxidase (O_2)	present	present	–
	Respiratory nitrate reductase (NarGHI)	?	?	present
	Respiratory nitrate reductase (NapABC)	present	–	–
	MbOx (Polysulfide reductase?)	present	present	–
	CO dehydrogenase	–	–	present
Selected transporters	Dicarboxylate transporters (TRAP)	present	present	present
	Sugar transporters	present	present	–
	ABC transporter for urea	present	–	present
	ABC transporter for glycine betaine	present	–	present
	ABC transporters for amino acid	present	–	present
	ABC transporters for (oligo)peptides	present	–	present

* not all enzymes required for the TCA cycle were present in the metaproteome (Kleiner *et al.* 2012b; a); CBB: Calvin-Benson-Bassham cycle; 3-HPB: 3-hydroxypropionate bicycle TCA: tricarboxylic acid cycle; SOX: sulfur oxidation; Dsr: dissimilatory sulfate reduction; MbOx: molybdopterin oxidoreductase; CO: Carbon monoxide; ABC: ATP-binding cassette transporter

.

SI Figure

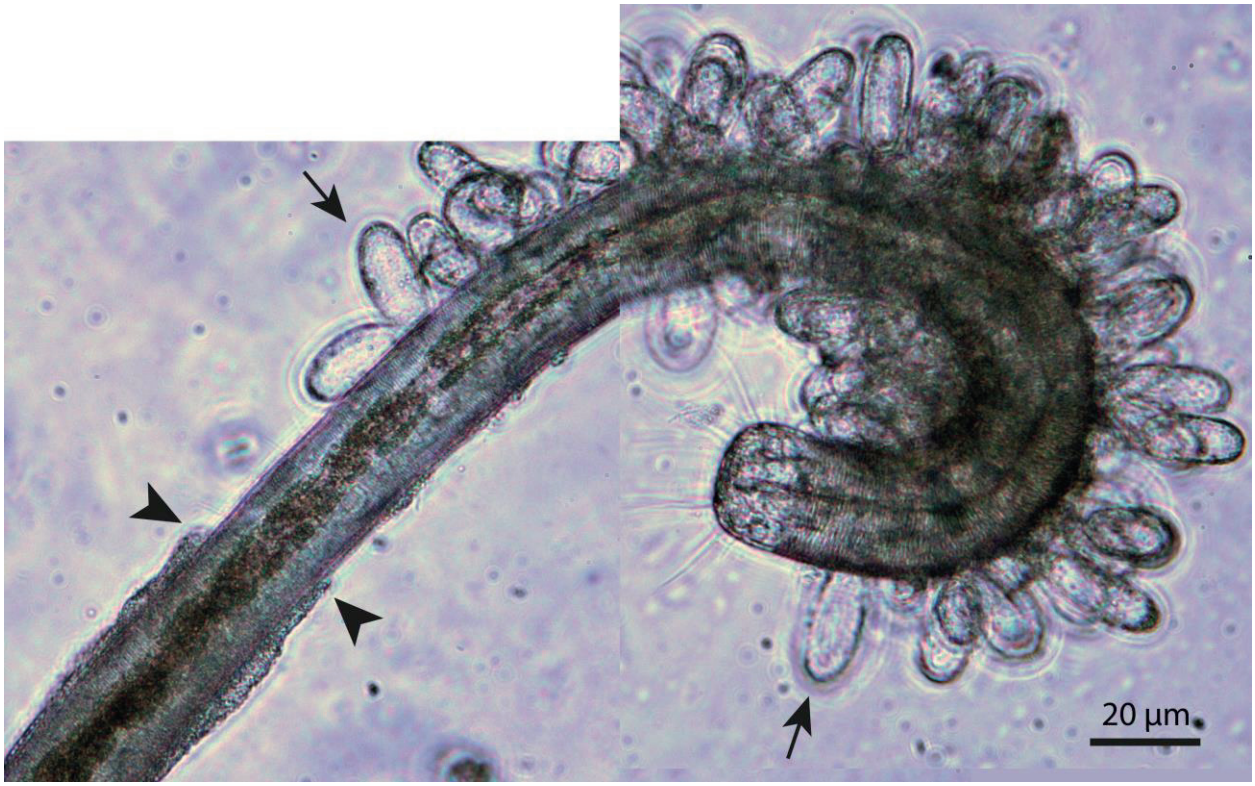

Fig. S2: *Leptonemella* sp. with numerous suctorians (Ciliophora) attached to the anterior end of the cuticle. Arrows point towards single suctorians, arrow heads point towards the beginning of the symbiont coat.

Chapter VII: General discussion and perspectives

This thesis contributes substantially to our current state of knowledge in the fields of Molecular Ecology and Symbiosis by shedding new light onto the diversity, specificity and evolutionary history of three chemosynthetic symbioses: gutless vestimentiferan tubeworm endosymbioses, gutless phallodriline oligochaete endosymbioses, and the main study object of this thesis, the stilbonematine nematode ectosymbioses (Chapter II - IV). Furthermore, it provides novel insights into the function of stilbonematine sulfur-oxidizing symbionts (Chapter V - VI).

7.1 The 18S rRNA gene as phylogenetic marker for stilbonematine nematodes

Before I started this thesis, the use of the 18S rRNA gene as a phylogenetic marker gene for stilbonematine nematodes had been questioned, because some species with similar morphological characters were placed in different clades by the 18S rRNA gene (Bayer *et al.* 2009). During this PhD thesis I was able to resolve this disagreement in collaboration with Prof. Dr. Jörg Ott (University of Vienna) and others. We found that in the previous study by Bayer *et al.*, (2009) the phylogeny and morphological descriptions did not match each other, because of a sample mix-up in the laboratory before sequencing (Appendix). We confirmed the value of the 18S rRNA by sequencing five additional stilbonematine nematode species and the 18S rRNA gene divergence always conformed to the morphological species and genus description (Appendix). This was an important achievement in the course of this PhD thesis and the basis for Chapter III and IV, because it strengthened the reliability of morphological characters.

Furthermore, it is an important finding for studying stilbonematines in the future, because the 18S rRNA gene has proven powerful to resolve both stilbonematine genera and closely related species (Chapter III, IV and Appendix). The power of the 18S rRNA gene as a reliable genetic marker was further strengthened by the fact that new species and even genera have been discovered with the help of 18S rRNA genes, which now await morphological description by nematode taxonomists (Chapter III and IV).

For molecular ecologists, morphological species and even genus identifications of stilbonematines can be very tedious and often impossible in the field, due to fine morphological characters that can sometimes only be seen under the SEM (pers. comm. J. Ott). This is not only true for stilbonematines, but nematodes in general are considered among the most difficult animals to identify (Powers 2004). Barcoding approaches using molecular marker genes are therefore widely used in this field (e.g. Powers 2004; Bhadury *et al.* 2006; Meldal *et al.* 2007). The work done in this thesis paves the way for large-scale biogeographical studies of stilbonematine nematodes. For example, batches of stilbonematines could be sampled and characterized without previous morphological identification from different locations around the globe and 18S rRNA-tag sequencing could be applied for estimating the genus and species diversities in these samples. Judging from this study, where various new species haven been identified by 18S rRNA sequencing (Chapter III and IV), such a study would most likely uncover a tremendous “hidden diversity” of stilbonematines and help to understand their distribution patterns.

For investigating the evolutionary history of stilbonematines, multigene phylogenies, including mitochondrial genes, would offer even more information than the 18S rRNA gene alone. Phylogenetic relationships between different genera cannot always be resolved in a single-gene analysis, as shown in Chapter III. The rapid development of new, faster and cost-effective sequencing technologies in the last years opens up many new possibilities in the field of molecular ecology (Ekblom & Galindo 2011; Koboldt *et al.* 2013; van Dijk *et al.* 2014). For example, our preliminary data from sequencing the metagenome of individual stilbonematine nematodes show that with approximately 300 - 400 Euro per sample, reconstruction of the complete host mitochondrial genomes alongside the symbiont bacterial genomes is possible (H. Gruber-Vodicka, unpublished results). Extraction of multiple genes from these metagenomes and construction of multigene phylogenies, including mitochondrial and ribosomal genes and preferentially nuclear genes of some representative species of each stilbonematine genus would likely result in a more robust phylogenetic backbone for stilbonematine nematodes. Ideally, genomes from each single specimen should be obtained, but in case of cost limitations, high-throughput 18S rRNA-tag sequencing to cover the large species diversity and resolve phylogenetic relationships within genera, combined with the phylogenetic backbone to resolve phylogenetic relationships among genera would be a good approach for future studies on diversity, ecology and evolution of stilbonematine nematodes.

7.2 Unexpected stability of ectosymbionts and flexibility of endosymbionts

Prior to this thesis, our understanding of the specificity and evolutionary stability of stilbonematine nematode ectosymbioses was clearly limited. A great body of literature existed on their distribution in sulfidic sediments, with ten different genera and numerous species described morphologically (reviewed by Tchesunov 2013). However, only a couple of studies investigated the specificity of the nematodes with their *Candidatus* Thiosymbion ectosymbionts (Polz et al. 1994; Bayer et al. 2009; Bulgheresi et al. 2011).

In Chapter III and IV of this thesis, I considerably increased the taxonomic sampling of stilbonematines for molecular phylogenetics compared to previous studies, and found that closely related stilbonematine species of one genus were consistently associated with species-specific and closely related *Candidatus* Thiosymbion ectosymbionts, independent of their geographic location. Looking at the global scale, most host and symbiont phylogenies were congruent within different host and symbiont clades, suggesting a tightly coupled evolution of hosts and ectosymbionts (Chapter III). This result was greatly surprising due to the following reasons: (1) stilbonematine nematodes had been believed prior to this thesis, to acquire their symbionts horizontally, which commonly results in incongruent host and symbiont phylogenies due to a higher chance in host switching (Ott et al. 2004; Bright & Bulgheresi 2010), and (2) stilbonematine nematodes molt their cuticle, to which the symbionts are attached to, four times in one life cycle (Ott et al. 1991, 2004), which provides several opportunities for host switches or uptake of symbionts from the environment.

This is the first example of such widely geographically distributed and diverse ectosymbiotic associations that show such clear patterns of evolutionary stability. The only other known ectosymbiosis that shows such a high evolutionary stability are *Bacteroidales* ectosymbionts on devescovinid flagellates in termite guts (Desai *et al.* 2010). However, in the case of flagellate ectosymbionts, codivergence seems easier to explain, because flagellates reproduce by simply performing cell division, leading to strict vertical transmission of their ectosymbionts. Thus, this PhD study should be of wide interest for the field of Symbiosis and Molecular Ecology, because it shows how an apparently non-intimate symbiotic couple can be one of the most successful and stable symbiosis. I therefore hypothesized that the stilbonematine nematode ectosymbionts are most likely vertically transmitted via a smear

infection and maintained until adulthood by subsequent inoculations of symbionts from the old to the new cuticle (Chapter III and IV).

In Chapter III, I could show in collaboration with Cecilia Wentrup (MPI Bremen) and others that cophylogenetic analyses of a largely increased dataset for gutless phallodrilines and their *Cand.* Thiosymbion endosymbionts revealed mainly incongruent host and symbiont phylogenies (Chapter III). Instead, endosymbiont phylogeny was strongly influenced by geography, i.e. distantly related hosts that were sampled in a similar ocean region commonly harbored closely related symbionts. This was highly surprising, because the hypothesis prior to our study was that *Cand.* Thiosymbion endosymbionts are vertically transmitted in gutless phallodrilines (Section 1.6.3) (Nussbaumer *et al.* 2004). I therefore expected a high degree of congruence between gutless phallodrilines and their endosymbionts. As discussed in Chapter III it is highly common that vertically transmitted symbioses occasionally take up a novel symbionts from the environment or co-occurring hosts (Ebert 2013). However, the degree of geographical influence compared to the host was striking. Our study therefore indicates that vertical transmission in gutless phallodriline endosymbioses must be rather leaky.

The clear genus-specific symbiont clustering pattern for stilbonematines and the clear geography-specific clustering pattern for gutless phallodrilines suggests that recognition mechanisms between stilbonematines and their ectosymbionts seem to be much more specific, enabling such highly stable and specific ectosymbioses over time. One such recognition mechanism has already been characterized for stilbonematines: host lectins that recognize specific sugars on the bacterial membrane (Nussbaumer *et al.* 2004; Bulgheresi *et al.* 2006, 2011). To understand differences in evolutionary stability between the two symbiotic systems, comparative transcriptomic analyses that investigate recognition and communication mechanisms between stilbonematines and gutless phallodrilines hosts and symbionts would a good starting point. Especially for the many co-occurring *Leptonemella* species from Sylt, which I described in Chapter IV, and which all have species-specific symbionts, looking into sequence variability of lectins could be a promising future project.

One question that remained open during the analyses of the *Cand.* Thiosymbion clade was the direction of the host switches between stilbonematine nematodes and gutless phallodrilines. The phylogenetic analysis of the 16S rRNA genes of *Cand.* Thiosymbion

species revealed a total of seven highly supported clades that contained both gutless oligochaete endo- and stilbonematine ectosymbionts, but could not resolve ancestral relationships clearly, which would indicate the direction of a host switch. The statistical codivergence analysis was similarly inconclusive (Chapter III). However, as discussed above, stilbonematine nematode ectosymbioses were highly stable over evolutionary time, whereas geography played a large role in the evolution of gutless phallodrilines. Arguably, this makes host switching events much more likely to have occurred from stilbonematine nematodes to gutless phallodrilines.

To investigate this hypothesis in future studies, the resolution of both host phylogenies and the phylogeny of the *Cand.* Thiosymbion clade have to be improved. Phylogenetic relationships of the hosts could be improved by using multiple genes for the phylogenetic reconstruction, which could be obtained by metagenomics or metatranscriptomics of single stilbonematines and gutless phallodrilines, respectively. The draft genomes of the *Cand.* Thiosymbion species could be obtained from the same metagenomes and phylogenomic symbiont trees could substantially improve the symbiont phylogeny. In addition, a larger sampling effort of many more *Cand.* Thiosymbion species from different ocean regions could eventually help to understand the evolutionary history and to clarify the direction of the host switches between both animal phyla.

7.3 The need to investigate the transmission mode of stilbonematine nematodes

To understand how stilbonematine nematode ectosymbioses are maintained over time, one future research project should be to investigate the transmission mode of stilbonematine ectosymbionts to the next generation. Therefore, the life cycle has to be studied first because we do not know when and how often stilbonematine nematodes reproduce. It is also not clear yet, whether fertilized eggs will be deposited in the sediment, such as known for gutless phallodrilines (Krieger, 2000; M. Schimak, unpublished results). There are some indications that stilbonematine nematodes could keep their eggs close to the mother until the juvenile hatches (S. Bulgheresi, pers. communication). This would be the perfect way to transmit the symbionts to the offspring but the hatching process has not been investigated *in vivo*. One possibility that cannot be excluded is that fertilized eggs may already contain ectosymbionts, which would make the transmission process even simpler. To collect fertilized females and

investigate the fixed eggs using symbiont-specific *in situ* hybridizations combined with transmission electron microscopy (TEM) would therefore be a good way to start this project. To understand how the symbionts are maintained over the different juvenile life stages, i.e. via inoculation of the new cuticle with symbionts from the old cuticle, or via uptake from the environment every life stage anew, it would be necessary to cultivate stilbonematine nematodes in the laboratory to facilitate ectosymbiont characterization at each of the life stages throughout the life cycle of individual stilbonematines.

The only symbiotic system with sulfur-oxidizing symbionts that has been successfully cultivated to date is the giant ciliate *Zoothamnium niveum* (Rinke *et al.* 2007; Bright *et al.* 2014). *Z. niveum* can be maintained in a flow-through respirometer system under stable hydrogen sulfide and oxygen conditions, without the need to generate a sulfide gradient (Rinke *et al.* 2007). A similar cultivation system would facilitate the study of the transmission mode considerably, because single individuals could be tracked easier throughout their life cycle. In contrast to *Z. niveum* that lives attached to solid substrates in the open water, stilbonematine nematodes live in the sediment. Thus, the system would have to be slightlly modified, i.e. sediment or glass beads to mimick the sand grains could be introduced to provide more natural conditions for the ectosymbioses.

Specific steps to approach the transmission mode would be to:

(1) Rearing of males and females in the aquaria.
(2) Collection of fertilized females, of which a symbiont subsample is characterized with molecular methods before continuing the life cycle investigation in the aquarium.
(3) Molecular characterization of an ectosymbiont subsample from each of the juvenile stages until adulthood.

7.4 Free-living members of *Candidatus* Thiosymbion?

If stilbonematine nematode ectosymbionts are predominantly vertically transmitted, as suggested in Chapter III and IV of this thesis, they would not have a free-living life stage in the sediment. In Chapter VI of this thesis I have compared the genomes of the *Leptonemella* ectosymbionts to other free-living, horizontally transmitted and vertically transmitted symbionts. I found that *Leptonemella* genomes encoded only few chemotaxis genes and that they also lacked the complete gene set for a flagellum (Chapter VI, Table 1). In contrast,

known facultative symbionts, such as *Cand.* Endoriftia persephone and *Vibrio fischeri* that are known to have free-living life-stages outside of their hosts, and free-living bacteria such as *Allochromatium vinosum* and *Pseudomonas aeruginosa,* encoded around ten times more chemotaxis genes and also a flagellum. Chemotaxis genes are commonly involved in responding to chemical gradients, such as nutrients (Sourjik & Wingreen 2012) while flagella are used for bacterial motility and swimming (reviewed by Terashima *et al.* 2008). In *Cand.* E. persephone, the endosymbiont of the hydrothermal vent tubeworm *Riftia pachyptila*, chemotaxis in combination with flagellar movement has been suggested to aid the free-living symbionts to move towards suitable substrates in a highly fluctuating environment (Robidart *et al.* 2008). Additionally, flagella were suggested to be used during horizontal transmission of the *Cand.* E. persephone symbionts, to escape the parental host tissue and to find new hosts (Harmer *et al.* 2008). Chemotactic signals by the host are known to trigger initial host colonization in the squid symbiosis by environmentally acquired *V. fischeri* that also possess flagella for motility (Ruby & Asato 1993; Mandel *et al.* 2012). In contrast, vertically transmitted endosymbionts of the deep-sea clam *Calyptogena* and pea aphids (*Buchnera aphidicola*), do not encode genes for flagella nor a single gene involved in chemotaxis (Chapter VI, Table 1). This indicates that these structures may be redundant in vertically transmitted symbionts that do not need to find their host but may be commonly used by horizontally transmitted symbionts to actively seek juvenile symbiont-free hosts. In fact, flagella and chemotaxis transcripts have also been reported from the endosymbionts of deep-sea *Bathymodiolus azoricus* mussel and the genomes of lucinid clam endosymbionts encoded flagella too (Egas *et al.* 2012, Kemper, 2015), and both of these symbionts are known to be horizontally transmitted (Gros *et al.* 1996, 1998; Won *et al.* 2003; Wentrup *et al.* 2015). *Cand.* Thiosymbion algarvensis, the endosymbionts of the gutless phallodriline *Olavius algarvensis* neither contains chemotaxis genes nor the complete gene set for flagella. This indicates that members of the *Cand.* Thiosymbion clade may not have a free-living life stage, which would also support the vertical transmission of the clade.

7.5 Mechanisms that could maintain a highly clonal and stable symbiont coat

In contrast to endosymbiotic bacteria that live protected within host cells or the host tissue layer, *Leptonemella* ectosymbionts are constantly exposed to the environment and thus

potential competitors or predators. Nevertheless, as shown in Chapter IV of this thesis, the symbiont population per *Leptonemella* individual essentially clonal. This indicates that the symbiosis has developed efficient mechanisms to protect itself from invasion by competing bacteria or cheaters. In fact, one feature that I found in the genomes of the *Leptonemella* ectosymbionts, that is not commonly found in chemosynthetic or obligate endosymbionts is the Type VI secretion system (T6SS) (Chapter VI). It is a bacteriophage-like cell-puncturing device present in many pathogenic gram-negative bacteria and known to inject effector proteins into target cells (Coulthurst 2013). The type VI secretion system (T6SS) is both known to efficiently target competitor cells by injection of antibacterial toxins, but has also been shown to be involved in symbiotic interactions (Records 2011; Coulthurst 2013; Russell *et al.* 2014). For example, in the root nodule-forming symbiont *Rhizobium leguminosarium,* T6SS is involved in host specificity while in the human pathogen *Salmonella enterica* it may limit acute virulence, and thereby contribute to long-term colonization of the host (Parsons & Heffron 2005). One of the subunits of the T6SS is the valine-glycine repeat protein G (VgrG) that forms the “cell puncturing” tip. The closest relative to the *VgrG* of *Leptonemella* symbionts was found in the purple sulfur bacterium *Thiocystis violascens* (57% aa similarity) while *VgrG* in the human pathogen *P. aeruginosa* was 51% identical. The T6SS in the latter is well characterized and known to secrete three toxins that target either eukaryotic or other prokaryotic cells (Hood et al., 2010). Secretion of one of these proteins led to a major growth advantage for *P. aeruginosa* strains, relative to those lacking immunity. The presence of T6SS in *Leptonemella* symbionts may thus be involved in defense against different competitors, non-relatives, cheaters or invaders and thus in sustaining the clonality of the symbiont coat, and therefore also the specificity of the ectosymbiotic association.

Scanning electron microscopy analyses of *Leptonemella* individuals from Sylt show clearly that the cells are embedded in a matrix or mucus layer, that seems to hold the cells together (Fig. 13A - B). It has been suggested that stilbonematines secrete mucus via the glandular sensory organs (GSOs) that are present below the cuticle of the worms and that this mucus is responsible for the adhesiveness of the symbiont coat (Nebelsick *et al.* 1992; Bauer-Nebelsick *et al.* 1995). However, in Chapter VI, I suggested that also the symbionts may be actively involved in the process of adhesion to the hosts surface and other cells, as shown by genes encoding type IV pili and genes potentially involved in biofilm matrix production.

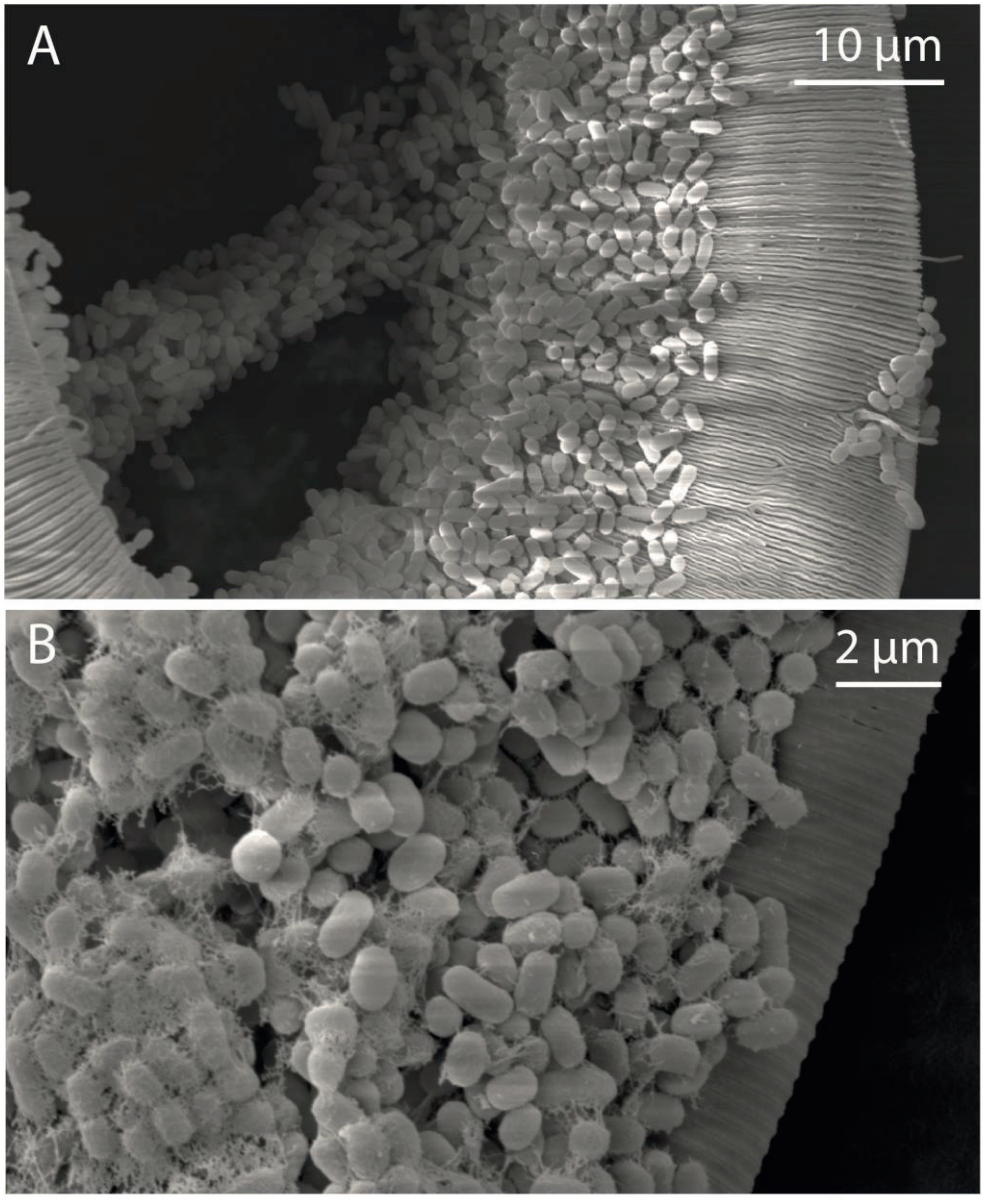

Fig. 13: Scanning electron microscopy images of the stilbonematine nematode *Leptonemella vicina* covered with coccoid ectosymbiotic bacteria that are embedded in a matrix. The large symbiont-free areas on the cuticle are an artifact of sample preparation (image courtesy of N. Leisch).

Further mechanisms that could help to maintain the stability and specificity of the symbiont coat and which are potentially of economic interest are antimicrobial peptides or secondary metabolites that were encoded in the genomes of the ectosymbionts (Chapter VI). Preliminary secondary metabolite analyses with antiSMASH v.3.0.0 (http://antismash.secondarymetabolites.org/, Weber *et al.* 2015) which suggested that each of the *Leptonemella* ectosymbionts encoded 12 – 19 secondary metabolites in their genomes, confirming the annotations by the RAST server (http://rast.nmpdr.org/, Overbeek *et al.* 2013) (preliminary results). These secondary metabolites could potentially yield novel

chemotherapeutics or antibiotics. A directed approach to test the antimicrobial properties of these metabolites would be to amplify and express the genes coding for the secondary metabolite of interest in a suitable expression vector, purify them and test their harmful properties against bacteria of interest.

Bacterial biofilm formation is a major problem on biomedical devices, such as catheters introduced into the human body, which can lead to highly resistant and untreatable biofilms, and chronic infections which often cause death (Francolini & Donelli 2010; Bjarnsholt 2013; Mulcahy *et al.* 2013). The medical sector has a major interest in preventing such biofilm formations. Understanding the exact mechanisms or substances of how stable biofilms, such as the ectosymbiotic coat, are established and maintained could help to counteract them. A first approach to identify possible metabolites involved in the stability of the coat could be identified with gas chromatographical (GC) or mass spectrometrical (MS) methods.

7.6 ”Hidden diversity” and general implications

Throughout this PhD thesis I have realized the tremendous possibilities next generation sequencing is providing us with in terms of studying diversity. In the beginning of my PhD thesis, clone libraries were one of the most reliable tools to distinguish between closely related strains within a single individual, due to limitations of 16S rRNA read lengths and a rather high error rate of next generation sequencing technologies (van Dijk *et al.* 2014). Today, Illumina platforms provide us with high quality reads and Pacific Biosciences (Pacbio) technologies with over 10 kB read lengths (Quail *et al.* 2012; Landolin *et al.* 2014). Metagenomics, tag sequencing and single cell genomics are replacing the old tools. Along with this sequencing revolution, our understanding of biological diversity has changed considerably (e.g. Kashtan *et al.* 2014).

The rapid change in sequencing technologies and the new understanding of diversity is directly reflected in my PhD thesis, where both clone libraries and metagenomics have proven powerful tools to uncover “hidden diversity” (Chapter II and IV). In Chapter II of this thesis, I was able to successfully answer my initial question of whether *Lamellibrachia* tubeworms from Mediterranean hydrothermal vents harbor multiple distinct intracellular symbiont types by using 16S rRNA clone libraries combined with symbiont-specific fluorescence *in situ* hybridizazion (FISH) probes. At the time of sequencing, these were still

widely used tools to investigate symbiont diversity and the published results have shed new light onto the evolution of vestimentiferan tubeworms that were previously assumed to only harbor a single symbiont (Zimmermann *et al.,* 2014).

In Chapter IV of this thesis, I have analyzed the ectosymbiont diversity of individual *Leptonemella* nematodes from the North Sea into more depth by using a combination of 16S rRNA-ITS clone library sequencing and Illumina HiSeq paired-end reads. I could clearly show that even though commonly used marker genes, such as the 16S-ITS only showed slight differences, ectosymbiont genomes varied considerably among different individuals of one host species (Chapter IV). Such a high symbiont-specificity, with each individual nematode of a host species harboring its own symbiont strain, has not yet been reported from any other chemosynthetic symbiosis. This novel finding is likely due to a very limited number of studies that analyzed symbiont genomes from multiple individuals of a single species, as discussed in detail in Chapter IV.

The importance of symbiont diversity within a species and for the population as a whole has already gained wide interest in the field of symbiosis (Hughes *et al.* 2008; Johnson *et al.* 2012; Parkinson & Baums 2014). Several studies that investigated the effect of symbiont diversity on the host found that different symbiont strains directly affect the fitness of their hosts, suggesting the importance of genetic diversity for evolution and adaptation, also with regard to climate change (Johnson *et al.* 2012; Parkinson & Baums 2014). For example, clonal carrots were inoculated with arbuscular mycorrhizal fungi, which resulted in variable root growth depending on the fungal strain (Koch *et al.* 2006). Another example are pea aphid hosts where pathogen resistance varied depending on which strain of facultative bacterial symbiont they harbored (Łukasik *et al.* 2013).

The next step for our study system should be to investigate, whether these individual differences between *Leptonemella* symbiont populations are of functional relevance for their hosts. One approach to do so would be to look at differential gene expression, differential protein or metabolic profiles of individual worms. The biggest challenge here will be most likely of a technical nature, such as sensitivity. Stilbonematine nematodes are rather small (3 - 10 mm in length) and currently it is not yet possible to get a metabolic profile, nor a proteome from single individuals (pers. comm. M. Liebeke and M. Kleiner). However, on the long run, these methods could provide valuable insights into functional differences between

individuals within a species and between species and consequently, help us to better understand the functional differences between them and ultimately the forces that shape their evolution.

Individual-specificity is not only important for understanding ecology, but is also of immediate interest to the health sector. Novel studies on the human gut microbiome showed that microbial strains are more similar between family members than between unrelated individuals, which is similar to what we see in *Leptonemella* individuals (Faith *et al.* 2013). In contrast to the *Leptonemella* ectosymbiosis, where only one type of bacterium is stably associated with the worm, the human gut microbiome is known to vary considerably in composition over time. Yet, individual-specific communities and strains are also found in humans (Schloissnig *et al.* 2013) and we already know that differences in the composition of our microbiomes can have a large impact on human health (Clemente *et al.* 2012). This is particularly taken into consideration in the model of “personalized medicine“ that proposes the customization of healthcare to the individual patient (Nicholson *et al.* 2005; ElRakaiby *et al.* 2014). Understanding the evolutionary forces that lead to such high intra-specific diversity and the functional implications of specificity for the individual host are therefore of general interest.

Bibliography

Achbergerová L, Nahálka J (2011) Polyphosphate - an ancient energy source and active metabolic regulator. *Microbial Cell Factories*, **10**, 14170–14175.

Ackert LTJ (2006) The role of microbes in agriculture: Sergei Vinogradskii's discovery and investigation of chemosynthesis, 1880–1910. *Journal of the History of Biology*, **39**, 373–406.

Acosta H, Dubourdieu M, Quiñones W *et al.* (2004) Pyruvate phosphate dikinase and pyrophosphate metabolism in the glycosome of *Trypanosoma cruzi* epimastigotes. *Comparative Biochemistry and Physiology Part B: Biochemistry and Molecular Biology*, **138**, 347–356.

Almassy RJ, Janson CA, Hamlin R, Xuong N-H, Eisenberg D (1986) Novel subunit—subunit interactions in the structure of glutamine synthetase. *Nature*, **323**, 304–309.

Altschul S, Madden T, Schaffer A *et al.* (1997) Gapped BLAST and PSI-BLAST: a new generation of protein database search programs., **25**, 3389–3402.

Anderson AJ, Dawes EA (1990) Occurrence, metabolism, metabolic role, and industrial uses of bacterial polyhydroxyalkanoates. *Microbiological Reviews*, **54**, 450–472.

Aravindraja C, Viszwapriya D, Karutha Pandian S (2013) Ultradeep 16S rRNA sequencing analysis of geographically similar but diverse unexplored marine samples reveal varied bacterial community composition. *PLoS ONE*, **8**, e76724.

Armenteros M, Rojas-Corzo A, Ruiz-Abierno A *et al.* (2014a) Systematics and DNA barcoding of free-living marine nematodes with emphasis on tropical desmodorids using nuclear SSU rDNA and mitochondrial COI sequences. *Nematology*, **16**, 979–989.

Armenteros M, Ruiz-Abierno A, Decraemer W (2014b) Taxonomy of Stilbonematinae (Nematoda: Desmodoridae): description of two new and three known species and phylogenetic relationships within the family. *Zoological Journal of the Linnean Society*, **171**, 1–21.

Asmus R (1982) Field measurements on seasonal variation of the activity of primary producers on a sandy tidal flat in the northern Wadden sea. *Netherlands Journal of Sea Research*, **16**, 389–402.

Aziz RK, Bartels D, Best AA *et al.* (2008) The RAST server: rapid annotations using subsystems technology. *BMC Genomics*, **9**, 75.

Bagarinao T (1992) Sulfide as an environmental factor and toxicant: tolerance and adaptations in aquatic organisms. *Aquatic Toxicology*, **24**, 21–62.

Baker AC (2003) Flexibility and specificity in coral-algal symbiosis: diversity, ecology, and biogeography of Symbiodinium. *Annual Review of Ecology, Evolution, and Systematics*, **34**, 661–689.

De Bary A (1879) Die Erscheinung der Symbiose: Vortrag gehalten auf der Versammlung Deutscher Naturforscher und Aerzte zu Cassel. R. J. Trübner, Strassburg.

Bauermeister J, Ramette A, Dattagupta S (2012) Repeatedly evolved host-specific ectosymbioses between sulfur-oxidizing bacteria and amphipods living in a cave ecosystem. *PLoS ONE*, **7**, e50254.

Bauer-Nebelsick M, Blumer M, Urbancik W, Ott JA (1995) The glandular sensory organ of Desmodoridae (Nematoda)- ultrastructure and phylogenetic implications. *Invertebrate Biology*, **114**, 211–219.

Bayer C, Heindl NR, Rinke C *et al.* (2009) Molecular characterization of the symbionts associated with marine nematodes of the genus *Robbea*. *Environmental Microbiology Reports*, **1**, 136–144.

De Beer D, Wenzhöfer F, Ferdelman TG *et al.* (2005) Transport and mineralization rates in North Sea sandy intertidal sediments, Sylt-Rømø basin, Wadden Sea. *Limnology and Oceanography* **,50**, 113–127.

Bennett GM, Moran NA (2015) Heritable symbiosis: The advantages and perils of an evolutionary rabbit hole. *Proceedings of the National Academy of Sciences*, 201421388.

Berger E, Urbancik W, Ott JA (1996) *Eubostrichus topiarius* sp. n., a new free-living, marine species of Stilbonematinae (Nematoda: Desmodoridae) from a shallow subtidal sand bottom. *Nematologica*, **42**, 521–536.

Bergin, (2009) Phylogenetic diversity and metabolic versatility of the bacterial endosymbionts in marine gutless oligochaete worms. PhD thesis (University Bremen, Germany).

Bergquist DC, Williams FM, Fisher CR (2000) Longevity record for deep-sea invertebrate. *Nature*, **403**, 499–500.

Bhadury P, Austen MC, Bilton DT *et al.* (2006) Development and evaluation of a DNA-barcoding approach for the rapid identification of nematodes. *Marine Ecology Progress Series*, **320**, 1–9.

Bjarnsholt T (2013) The role of bacterial biofilms in chronic infections. *APMIS. Supplementum*, 1–51.

Blaxter ML, De Ley P, Garey JR *et al.* (1998) A molecular evolutionary framework for the phylum Nematoda. *Nature*, **392**, 71–75.

Blazejak A, Erséus C, Amann R, Dubilier N (2005) Coexistence of bacterial sulfide oxidizers, sulfate reducers, and spirochetes in a gutless worm (Oligochaeta) from the Peru margin. *Applied and Environmental Microbiology*, **71**, 1553–1561.

Blazejak A, Kuever J, Erseus C, Amann R, Dubilier N (2006) Phylogeny of 16S rRNA, ribulose 1,5-bisphosphate carboxylase/oxygenase, and adenosine 5'-phosphosulfate reductase genes from gamma- and alphaproteobacterial symbionts in gutless marine worms (Oligochaeta) from Bermuda and the Bahamas. *Applied and Environmental Microbiology*, **72**, 5527–5536.

Böer SI, Arnosti C, van Beusekom JEE, Boetius A (2009) Temporal variations in microbial activities and carbon turnover in subtidal sandy sediments. *Biogeosciences*, **6**, 1149–1165.

Bordenstein SR, Paraskevopoulos C, Hotopp JCD *et al.* (2009) Parasitism and mutualism in *Wolbachia*: What the phylogenomic trees can and cannot say. *Molecular Biology and Evolution*, **26**, 231–241.

Bosch C, Grassé P-P (1984) Cycle partiel des bactéries chimioautotrophes symbiotiques et leurs rapports avec les bactériocytes chez *Riftia pachyptila* Jones (Pogonophore Vestimentifère). II. L'évolution des bactéries symbiotiques et des bactériocytes, **299**, 413–419.

Bot ANM, Rehner SA, Boomsma JJ (2001) Partial incompatibility between ants and symbiotic fungi in two sympatric species of *Acromyrmex* leaf-cutting ants. *Evolution*, **55**, 1980–1991.

Boucher G (1975) Nématodes des sables fins infralittoraux de la Pierre Noire (Manche Occidentale). I. Desmodorida. *Bulletin de Muséum National d'Histoire Naturelle (3)*, **285**, 101–128.

Boucher G (1997) Structure and biodiversity of nematode assemblages in the SW lagoon of New Caledonia. *Coral Reefs*, **16**, 177–186.

Boufahja F, Hedfi A, Amorri J *et al.* (2011) An assessment of the impact of chromium-amended sediment on a marine nematode assemblage using microcosm bioassays. *Biological trace element research*, **142**, 242–255.

Bourbonnais A, Lehmann MF, Butterfield DA, Juniper SK (2012) Subseafloor nitrogen transformations in diffuse hydrothermal vent fluids of the Juan de Fuca Ridge evidenced by the isotopic composition of nitrate and ammonium. *Geochemistry, Geophysics, Geosystems*, **13**, Q02T01.

Bright M, Bulgheresi S (2010) A complex journey: transmission of microbial symbionts. *Nature Reviews Microbiology*, **8**, 218–230.

Bright M, Espada-Hinojosa S, Lagkouvardos I, Volland J-M (2014) The giant ciliate *Zoothamnium niveum* and its thiotrophic epibiont Candidatus *Thiobios zoothamnicoli*: a model system to study interspecies cooperation. *Microbial Symbioses*, **5**, 145.

Bright, M, Keckeis H, Fisher CR (2000) An autoradiographic examination of carbon fixation, transfer and utilization in the *Riftia pachyptila* symbiosis. *Marine Biology*, **136**, 621–632.

Bright M, Lallier FH (2010) The biology of vestimentiferan tubeworms. *Oceanography and Marine Biology Annual Reviews*, **48**, 213–266.

Brileya K, Reysenbach A-L (2014) The class Archaeoglobi. *The Prokaryotes: Other Major Lineages of Bacteria and The Archaea*, 15–23.

Brock J, Schulz-Vogt HN (2011) Sulfide induces phosphate release from polyphosphate in cultures of a marine *Beggiatoa* strain. *The ISME journal*, **5**, 497–506.

Brune A, Ohkuma M (2010) Role of the termite gut microbiota in symbiotic digestion. In: *Biology of termites: a modern synthesis* (eds Bignell DE, Roisin Y, Lo N), pp. 439–475. Springer Netherlands.

Bucklin A, Steinke D, Blanco-Bercial L (2011) DNA barcoding of marine metazoa. *Annual Review of Marine Science*, **3**, 471–508.

Bulgheresi S, Gruber-Vodicka HR, Heindl NR *et al.* (2011) Sequence variability of the pattern recognition receptor Mermaid mediates specificity of marine nematode symbioses. *The ISME Journal*, **5**, 986–998.

Bulgheresi S, Schabussova I, Chen T *et al.* (2006) A new C-type lectin similar to the human immunoreceptor DC-SIGN mediates symbiont acquisition by a marine nematode. *Applied and Environmental Microbiology*, **72**, 2950–2956.

Burriesci MS, Raab TK, Pringle JR (2012) Evidence that glucose is the major transferred metabolite in dinoflagellate–cnidarian symbiosis. *The Journal of Experimental Biology*, **215**, 3467–3477.

Camacho C, Coulouris G, Avagyan V *et al.* (2009) BLAST+: architecture and applications. *BMC Bioinformatics*, **10**, 421.

Carney RS (1994) Consideration of the oasis analogy for chemosynthetic communities at Gulf of Mexico hydrocarbon vents. *Geo-Marine Letters*, **14**, 149–159.

Casiraghi M, Bordenstein SR, Baldo L *et al.* (2005) Phylogeny of *Wolbachia pipientis* based on gltA, groEL and ftsZ gene sequences: clustering of arthropod and nematode symbionts in the F supergroup, and evidence for further diversity in the *Wolbachia* tree. *Microbiology*, **151**, 4015–4022.

Caspi R, Altman T, Billington R *et al.* (2014) The MetaCyc database of metabolic pathways and enzymes and the BioCyc collection of Pathway/Genome Databases. *Nucleic Acids Research*, **42**, D459–D471.

Cataldi de Flombaum MA, Cannata JJB, Cazzulo JJ, Segura EL (1977) CO_2-fixing enzymes in *Trypanosoma cruzi*. *Comparative Biochemistry and Physiology Part B: Comparative Biochemistry*, **58**, 67–69.

Cavanaugh CM, Gardiner S, Jones ML, Jannasch HW, Waterbury JB (1981) Prokaryotic cells in the hydrothermal vent tube worm *Riftia pachyptila* Jones: possible chemoautotrophic symbionts. *Science*, **213**, 340–342.

Cavanaugh C, McKiness Z, Newton I, Stewart F (2006) Marine chemosynthetic symbioses. In: *The Prokaryotes*, pp. 475–507.

Chao LS-L, Davis RE, Moyer CL (2007) Characterization of bacterial community structure in vestimentiferan tubeworm *Ridgeia piscesae* trophosomes. *Marine Ecology*, **28**, 72–85.

Childress JJ, Fisher CR (1992) The biology of hydrothermal vent animals: physiology, biochemistry, and autotrophic symbioses. *Oceanography and Marine Biology*, **30**, 337–441.

Childress JJ, Fisher CR, Favuzzi JA, Sanders NK (1991) Sulfide and carbon dioxide uptake by the hydrothermal vent clam, *Calyptogena magnifica*, and its chemoautotrophic symbionts. *Physiological Zoology*, **64**, 1444–1470.

Chitwood BG (1936) Some marine nematodes from North Carolina. *Proceedings of the Helminthological Society of Washington*, **3**, 1–16.

Cianciotto NP (2005) Type II secretion: a protein secretion system for all seasons. *Trends in Microbiology*, **13**, 581–588.

Clayton DH, Bush SE, Goates BM, Johnson KP (2003) Host defense reinforces host–parasite cospeciation. *Proceedings of the National Academy of Sciences*, **100**, 15694–15699.

Clemente JC, Ursell LK, Parfrey LW, Knight R (2012) The impact of the gut microbiota on human health: An integrative view. *Cell*, **148**, 1258–1270.

Cobb NA (1894) Tricoma and other new nematode genera. *Proceedings of the Linnean Society of New South Wales*, **8**, 389–421.

Cobb NA (1920) One hundred new nemas. *Contributions to a Science of Nematology*, **9**, 217–343.

Comandatore F, Sassera D, Montagna M *et al.* (2013) Phylogenomics and analysis of shared genes suggest a single transition to mutualism in *Wolbachia* of nematodes. *Genome Biology and Evolution*, **5**, 1668–1674.

Conord C, Despres L, Vallier A *et al.* (2008) Long-term evolutionary stability of bacterial endosymbiosis in Curculionoidea: additional evidence of symbiont replacement in the dryophthoridae family. *Molecular Biology and Evolution*, **25**, 859–868.

Conow C, Fielder D, Ovadia Y, Libeskind-Hadas R (2010) Jane: a new tool for the cophylogeny reconstruction problem. *Algorithms for Molecular Biology*, **5**, 16.

Cordes EE, Bergquist DC, Fisher CR (2009) Macro-Ecology of Gulf of Mexico cold seeps. *Annual Review of Marine Science*, **1**, 143–168.

Corliss JB, Dymond J, Gordon LI *et al.* (1979) Submarine thermal springs on the Galapagos rift. *Science;(United States)*, **203,** 1073–1083.

Coull BC (1970) Shallow water meiobenthos of the Bermuda platform. *Oecologia*, **4**, 325–357.

Coulthurst SJ (2013) The Type VI secretion system–a widespread and versatile cell targeting system. *Research in microbiology*, **164**, 640–654.

Criscuolo A, Gribaldo S (2011) Large-scale phylogenomic analyses indicate a deep origin of primary plastids within cyanobacteria. *Molecular Biology and Evolution*, **28**, 3019–3032.

Currie CR, Scott JA, Summerbell RC, Malloch D (1999) Fungus-growing ants use antibiotic-producing bacteria to control garden parasites. *Nature*, **398**, 701–704.

Dagan T, Roettger M, Stucken K *et al.* (2013) Genomes of stigonematalean cyanobacteria (subsection V) and the evolution of oxygenic photosynthesis from prokaryotes to plastids. *Genome Biology and Evolution*, **5**, 31–44.

Dahl C (2008) Inorganic sulfur compounds as electron donors in purple sulfur bacteria. In: *Sulfur metabolism in phototrophic organisms*, pp. 289–317. Springer.

Dahl C, Prange A (2006) Bacterial sulfur globules: occurrence, structure and metabolism. In: *Inclusions in Prokaryotes,* pp. 21–51. Springer Berlin Heidelberg.

Dando PR, Jensen P, O'Hara SCM *et al.* (1994) The effects of methane seepage at an intertidal/shallow subtidal site on the shore of the Kattegat, Vendsyssel, Denmark. *Bulletin of the Geological Society of Denmark*, **41**, 65–79.

Dando PR, Southward AF, Southward EC *et al.* (1992) Shipwrecked tube worms*, Nature,* **356**, 667.

Darriba D, Taboada GL, Doallo R, Posada D (2012) jModelTest 2: more models, new heuristics and parallel computing. *Nature Methods*, **9**, 772–772.

Darwin C (1859) On the origins of species by means of natural selection. *London: Murray*.

Darwin C (1979) Fertilization of orchids by insects. *EM Coleman Enterprises*.

Dattagupta S, Schaperdoth I, Montanari A *et al.* (2009) A novel symbiosis between chemoautotrophic bacteria and a freshwater cave amphipod. *The ISME Journal*, **3**, 935–943.

Davis D (1985) The Oligochaeta of Georges Bank (NW Atlantic), with descriptions of four new species. *Proceedings of the Biological Society of Washington*, **98**, 158–176.

Decker C, Olu K, Arnaud-Haond S, Duperron S (2013a) Physical proximity may promote lateral acquisition of bacterial symbionts in vesicomyid clams. *PloS one*, **8**, e64830.

Desai MS, Strassert JFH, Meuser K *et al.* (2010) Strict cospeciation of devescovinid flagellates and Bacteroidales ectosymbionts in the gut of dry-wood termites (Kalotermitidae). *Environmental Microbiology*, **12**, 2120–2132.

Deudero S, Vincx M (2000) Sublittoral meiobenthic assemblages from disturbed and non-disturbed sediments in the Balearics. *Instituto de Ciencias del Mar*, **64**, 285–293.

Diepenbroek M, Grobe H, Reinke M *et al.* (2002) PANGAEA—an information system for environmental sciences. *Computers & Geosciences*, **28**, 1201–1210.

Van Dijk EL, Auger H, Jaszczyszyn Y, Thermes C (2014) Ten years of next-generation sequencing technology. *Trends in Genetics*, **30**, 418–426.

Distel DL, Lane DJ, Olsen GJ *et al.* (1988) Sulfur-oxidizing bacterial endosymbionts: analysis of phylogeny and specificity by 16S rRNA sequences. *Journal of Bacteriology*, **170**, 2506–2510.

Dmytrenko O, Russell SL, Loo WT *et al.* (2014) The genome of the intracellular bacterium of the coastal bivalve, *Solemya velum*: a blueprint for thriving in and out of symbiosis. *BMC Genomics*, **15**, 924.

Douglas AE (1994) *Symbiotic Interactions*. Oxford: Oxford University Press.

Douglas AE (2010) *The Symbiotic Habit*. Princeton University Press.

Van Dover CL (2000) *The ecology of deep-sea hydrothermal vents*. Princeton University Press, Princeton, NJ.

Dubilier N, Amann R, Erseus C *et al.* (1999) Phylogenetic diversity of bacterial endosymbionts in the gutless marine oligochete *Olavius loisae* (Annelida). *Marine Ecology Progress Series*, **178**, 271–280.

Dubilier N, Bergin C, Lott C (2008) Symbiotic diversity in marine animals: the art of harnessing chemosynthesis. *Nature Reviews Microbiology*, **6**, 725–740.

Dubilier N, Blazejak A, Rühland C (2006) Symbioses between bacteria and gutless marine oligochaetes. In: *Molecular Basis of Symbiosis* Progress in Molecular and Subcellular Biology. (ed Overmann PDJ), pp. 251–275. Springer Berlin Heidelberg.

Dubilier N, Giere O, Distel DL, Cavanaugh CM (1995) Characterization of chemoautotrophic bacterial symbionts in a gutless marine worm Oligochaeta, Annelida) by phylogenetic 16S rRNA sequence analysis and in situ hybridization. *Applied and Environmental Microbiology*, **61**, 2346–2350.

Dubilier N, Mulders C, Ferdelman T *et al.* (2001) Endosymbiotic sulphate-reducing and sulphide-oxidizing bacteria in an oligochaete worm. *Nature*, **411**, 298–302.

Dubos R, Kessler A (1963) Integrative and disintegrative factors in symbiotic associations. *Symposium of the Society for General Microbiology*, **13**, 1–11.

Duperron S, De Beer D, Zbinden M *et al.* (2009) Molecular characterization of bacteria associated with the trophosome and the tube of *Lamellibrachia* sp., a siboglinid annelid from cold seeps in the eastern Mediterranean. *FEMS Microbiology Ecology*, **69**, 395–409.

Duperron S, Bergin C, Zielinski F *et al.* (2006) A dual symbiosis shared by two mussel species, *Bathymodiolus azoricus* and *Bathymodiolus puteoserpentis* (*Bivalvia: Mytilidae*), from hydrothermal vents along the northern Mid-Atlantic Ridge. *Environmental Microbiology*, **8**, 1441–1447.

Durand É, Bernadac A, Ball G *et al.* (2003) Type II protein secretion in *Pseudomonas aeruginosa*: the pseudopilus is a multifibrillar and adhesive structure. *Journal of Bacteriology*, **185**, 2749–2758.

Durand L, Zbinden M, Cueff-Gauchard V *et al.* (2010) Microbial diversity associated with the hydrothermal shrimp *Rimicaris exoculata* gut and occurrence of a resident microbial community. *FEMS Microbiology Ecology*, **71**, 291–303.

Ebert D (2013) The epidemiology and evolution of symbionts with mixed-mode transmission. *Annual Review of Ecology, Evolution, and Systematics*, **44**, 623–643.

Egas C, Pinheiro M, Gomes P, Barroso C, Bettencourt R (2012) The transcriptome of *Bathymodiolus azoricus* gill reveals expression of genes from endosymbionts and free-living deep-sea bacteria. *Marine Drugs*, **10**, 1765–1783.

Ekblom R, Galindo J (2011) Applications of next generation sequencing in molecular ecology of non-model organisms. *Heredity*, **107**, 1–15.

ElRakaiby M, Dutilh BE, Rizkallah MR *et al.* (2014) Pharmacomicrobiomics: The Impact of Human Microbiome Variations on Systems Pharmacology and Personalized Therapeutics. *OMICS: A Journal of Integrative Biology*, **18**, 402–414.

Elsaied H, Kimura H, Naganuma T (2002) Molecular characterization and endosymbiotic localization of the gene encoding D-ribulose 1,5-bisphosphate carboxylase-oxygenase (RuBisCO) form II in the deep-sea vestimentiferan trophosome. *Microbiology*, **148**, 1947–1957.

Erséus C (1979) *Inanidrilus bulbosus* gen. et sp. n., a marine Tubificid (Oligochaeta) from Florida, USA. *Zoologica Scripta*, **8**, 209–210.

Erséus C (1984) Taxonomy and phylogeny of the gutless Phallodrilinae (Oligochaeta, Tubificidae), with descriptions of one new genus and twenty-two new species*. *Zoologica Scripta*, **13**, 239–272.

Erseus C (1991) Two new deep-water species of the gutless genus *Olavius* (Oligochaeta : Tubificidae) from sides of North America. *Proceedings of the Biological Society of Washington*, **104**, 627–630.

Erséus C (1992) A generic revision of the Phallodrilinae (Oligochaeta, Tubificidae). *Zoologica Scripta*, **21**, 5–48.

Erséus C (2003) The gutless Tubificidae (Annelida: Oligochaeta) of the Bahamas. *Meiofauna Marina*, **12**, 59–84.

Erséus C, Källersjö M, Ekman M, Hovmöller R (2002) 18S rDNA phylogeny of the Tubificidae (Clitellata) and its constituent taxa: Dismissal of the Naididae. *Molecular Phylogenetics and Evolution*, **22**, 414–422.

Erséus C, Prestegaard T, Källersjö M (2000) Phylogenetic analysis of Tubificidae (Annelida, Clitellata) based on 18S rDNA sequences. *Molecular Phylogenetics and Evolution*, **15**, 381–389.

Erséus C, Wetzel MJ, Gustavsson L (2008) ICZN rules–a farewell to Tubificidae (Annelida, Clitellata). *Zootaxa*, **1744**, 66–68.

Faith JJ, Guruge JL, Charbonneau M *et al.* (2013) The long-term stability of the human gut microbiota. *Science*, **341**, 1237439.

Francolini I, Donelli G (2010) Prevention and control of biofilm-based medical-device-related infections. *FEMS Immunology & Medical Microbiology*, **59**, 227–238.

Falcón LI, Magallón S, Castillo A (2010) Dating the cyanobacterial ancestor of the chloroplast. *The ISME Journal*, **4**, 777–783.

Felbeck H (1981) Chemoautotrophic potential of the hydrothermal vent tube worm, *Riftia pachyptila* Jones (Vestimentifera). *Science*, **213**, 336–338.

Felbeck H (1983) Sulfide oxidation and carbon fixation by the gutless clam *Solemya reidi*: an animal-bacteria symbiosis. *Journal of Comparative Physiology*, **152**, 3–11.

Felbeck H, Jarchow J (1998) Carbon release from purified chemoautotrophic bacterial symbionts of the hydrothermal vent tubeworm *Riftia pachyptila*. *Physiological and Biochemical Zoology*, **71**, 294–302.

Felbeck H, Liebezeit G, Dawson R, Giere O (1983) CO_2 fixation in tissues of marine oligochaetes (*Phallodrilus leukodermatus* and *P. planus*) containing symbiotic, chemoautotrophic bacteria. *Marine Biology*, **75**, 187–191.

Feldman RA, Black MB, Cary CS, Lutz RA, Vrijenhoek RC (1997) Molecular phylogenetics of bacterial endosymbionts and their vestimentiferan hosts. *Molecular Marine Biology and Biotechnology*, **6**, 268–277.

Fenchel T, Finlay BJ (1989) *horos*: a mouthless ciliate with a symbiotic kitchen garden. *Ophelia*, **30**, 75–93.

Ferraguti M, Erséus C, Kaygorodova I, Martin P (1999) New sperm types in *Naididae* and *Lumbriculidae* (Annelida: Oligochaeta) and their possible phylogenetic implications. *Hydrobiologia*, **406**, 213–222.

Fisher R (2003) Spatial and temporal variations in nematode assemblages in tropical seagrass sediments. *Hydrobiologia*, **493**, 43–63.

Fisher CR, Childress JJ (1986) Translocation of fixed carbon from symbiotic bacteria to host tissues in the gutless bivalve *Solemya reidi*. *Marine Biology*, **93**, 59–68.

Fisher CR, Childress JJ, Minnich E (1989) Autotrophic carbon fixation by the chemoautotrophic symbionts of *Riftia pachyptila*. *The Biological Bulletin*, **177**, 372–385.

Fisher CR, Kennicutt MC, Brooks JM (1990) Stable carbon isotopic evidence for carbon limitation in hydrothermal vent vestimentiferans. *Science*, **247**, 1094–1096.

Fisher R, Sheaves MJ (2003) Community structure and spatial variability of marine nematodes in tropical Australian pioneer seagrass meadows. *Hydrobiologia*, **495**, 143–158.

Fisher CR, Urcuyo IA, Simpkins MA, NIx E (1997) Life in the slow lane: growth and longevity of cold-seep vestimentiferans. *Marine Ecology*, **18**, 83–94.

Flemming H-C, Wingender J (2010) The biofilm matrix. *Nature Reviews Microbiology*, **8**, 623–633.

Folmer O, Black M, Hoeh W, Lutz R, Vrijenhoek R (1994) DNA primers for amplification of mitochondrial cytochrome c oxidase subunit I from diverse metazoan invertebrates. *Molecular Marine Biology and Biotechnology*, **3**, 294–299.

Lim-Fong GE, Regali LA, Haygood MG (2008) Evolutionary relationships of "*Candidatus Endobugula*" bacterial symbionts and their bugula bryozoan hosts. *Applied and Environmental Microbiology*, **74**, 3605–3609.

Da Fonsêca-Genevois V, Somerfield PJ, Neves MHB, Coutinho R, Moens T (2006) Colonization and early succession on artificial hard substrata by meiofauna. *Marine Biology*, **148**, 1039–1050.

Fontanez KM, Cavanaugh CM (2014) Evidence for horizontal transmission from multilocus phylogeny of deep-sea mussel (Mytilidae) symbionts. *Environmental Microbiology*, 3608–3621.

Forst S, Clarke D (2002) Bacteria–Nematode Symbiosis. *Entomopathogenic nematology*, 57.

Foster RA, Sztejrenszus S, Kuypers MMM (2013) Measuring carbon and N2 fixation in field populations of colonial and free-living unicellular cyanobacteria using nanometer-scale secondary ion mass spectrometry1. *Journal of Phycology*, **49**, 502–516.

Fourment M, Gibbs MJ (2006) PATRISTIC: a program for calculating patristic distances and graphically comparing the components of genetic change. *BMC Evolutionary Biology*, **6**, 1.

Frean MR, Abraham ER (2004) Adaptation and enslavement in endosymbiont-host associations. *Physical Review E*, **69**, 051913.

Freytag JK, Girguis PR, Bergquist DC *et al.* (2001) A paradox resolved: sulfide acquisition by roots of seep tubeworms sustains net chemoautotrophy. *Proceedings of the National Academy of Sciences of the United States of America*, **98**, 13408 –13413.

Friedrich CG, Rother D, Bardischewsky F, Quentmeier A, Fischer J (2001) Oxidation of reduced inorganic sulfur compounds by bacteria: emergence of a common mechanism? *Applied and Environmental Microbiology*, **67**, 2873–2882.

Frigaard N-U, Dahl C (2008) Sulfur metabolism in phototrophic sulfur bacteria. *Advances in microbial physiology*, **54**, 103–200.

Ftnogenova N (1986) Six new species of marine Tubificidae (Oligochaeta) from the continental shelf off Peru. *Zoologica Scripta*, **15**, 45–51.

Fu L, Niu B, Zhu Z, Wu S, Li W (2012) CD-HIT: accelerated for clustering the next-generation sequencing data. *Bioinformatics*, **28**, 3150–3152.

Van Gaever S, Vanreusel A, Hughes JA, Bett BJ, Kiriakoulakis K (2004) The macro-and micro-scale patchiness of meiobenthos associated with the Darwin Mounds (north-east Atlantic). *Journal of the Marine Biological Association of the UK*, **84**, 547–556.

Gambi MC, Schulze A, Amato E (2011) Record of *Lamellibrachia* sp. (Annelida: Siboglinidae: Vestimentifera) from a deep shipwreck in the western Mediterranean Sea (Italy). *Marine Biodiversity Records*, **4**, 1–6.

Garcia JR, Gerardo NM (2014) The symbiont side of symbiosis: do microbes really benefit? *Frontiers in Microbiology*, **5**.

Gardebrecht A, Markert S, Sievert SM *et al.* (2011) Physiological homogeneity among the endosymbionts of *Riftia pachyptila* and *Tevnia jerichonana* revealed by proteogenomics. *The ISME Journal*, **6**, 766–776.

Geng H, Belas R (2010) Molecular mechanisms underlying roseobacter–phytoplankton symbioses. *Current Opinion in Biotechnology*, **21**, 332–338.

Georgiadou M, Pelicic V, Barocchi MA, Telford JL, others (2014) Type IV pili: functions and biogenesis. *Bacterial Pili: Structure, Synthesis and Role in Disease*, **27**, 71–82.

Gerardo NM, Parker BJ (2014) Mechanisms of symbiont-conferred protection against natural enemies: an ecological and evolutionary framework. *Current Opinion in Insect Science*, **4**, 8–14.

Gerlach SA (1950) Über einige Nematoden aus der Familie der Desmodoriden. *N. Erg. Probl. Zool.(Klatt-Festschrift)*, 178–198.

Gerlach SA (1956) Die Nematodenbesiedlung des tropischen Brandungsstrandes von Pernambuco. *Kieler Meeresforschung*, **12**, 202–218.

Gerlach SA (1963) Freilebende Meeresnematoden von den Malediven II. *Kieler Meeresforschung*, **19**, 67–103.

Gerlach SA (1964) Freilebende Nematoden aus dem Roten Meer. *Kieler Meeresforschung*, **20**, 18–34.

Gerlach SA (1978) Food-chain relationships in subtidal silty sand marine sediments and the role of meiofauna in stimulating bacterial productivity. *Oecologia*, **33**, 55–69.

Giere O The gutless marine oligochaete *Phallodrilus leukodermatus* (1981) Structural studies on an aberrant tubificid associated with bacteria. *Maine Ecology Progress Series*, **5**, 353–357.

Giere O, Conway NM, Gastrock G, Schmidt C (1991) "Regulation" of gutless annelid ecology by endosymbiotic bacteria. *Marine Ecology Progress Series. Oldendorf*, **68**, 287–299.

Giere O, Erséus C (2002) Taxonomy and new bacterial symbioses of gutless marine Tubificidae (Annelida, Oligochaeta) from the Island of Elba (Italy). *Organisms Diversity & Evolution*, **2**, 289–297.

Giere O, Langheld C (1987) Structural organisation, transfer and biological fate of endosymbiotic bacteria in gutless oligochaetes. *Marine Biology*, **93**, 641–650.

Giere O, Liebezeit G, Dawson R (1982) Habitat conditions and distribution pattern of the gutless oligochaete *Phallodrilus leukodermatus*. *Marine Ecology Progress Series. Oldendorf*, **8**, 291–299.

Giere O, Windoffer R, Southward EC (1995) The bacterial endosymbiosis of the gutless nematode, *Astomonema southwardorum*: Ultrastructural aspects. *Journal of the Marine Biological Association of the United Kingdom*, **75**, 153–164.

Giere O, Wirsen CO, Schmidt C, Jannasch HW (1988) Contrasting effects of sulfide and thiosulfate on symbiotic CO_2-assimilation of *Phallodrilus leukodermatus* (Annelida). *Marine Biology*, **97**, 413–419.

Gilbert SF, Sapp J, Tauber AI (2012) A symbiotic view of life: we have never been individuals. *The Quarterly Review of Biology*, **87**, 325–341.

Gingold R, Mundo-Ocampo M, Holovachov O, Rocha-Olivares A (2010) The role of habitat heterogeneity in structuring the community of intertidal free-living marine nematodes. *Marine biology*, **157**, 1741–1753.

Girguis PR, Childress JJ (2006) Metabolite uptake, stoichiometry and chemoautotrophic function of the hydrothermal vent tubeworm *Riftia pachyptila*: responses to environmental variations in substrate concentrations and temperature. *Journal of Experimental Biology*, **209**, 3516–3528.

Goffredi SK (2010) Indigenous ectosymbiotic bacteria associated with diverse hydrothermal vent invertebrates. *Environmental Microbiology Reports*, **2**, 479–488.

Goffredi SK, Gregory A, Jones WJ, Morella NM, Sakamoto RI (2014) Ontogenetic variation in epibiont community structure in the deep-sea yeti crab, *Kiwa puravida*: convergence among crustaceans. *Molecular Ecology*, **23**, 1457–1472.

Goffredi SK, Jones WJ, Erhlich H, Springer A, Vrijenhoek RC (2008) Epibiotic bacteria associated with the recently discovered *Yeti crab*, *Kiwa hirsuta*. *Environmental Microbiology*, **10**, 2623–2634.

Gommers PJF, Kuenen JG (1988) Thiobacillus strain Q, a chemolithoheterotrophic sulphur bacterium. *Archives of Microbiology*, **150**, 117–125.

Gordon J, Knowlton N, Relman DA, Rohwer F, Youle M (2010) Superorganisms and holobionts. *Issues*.

Greeff R (1869) *Untersuchungen über einige merkwürdige Thiergruppen des Arthropoden-und Wurm-Typus: Mit 4 Tafeln*. Nicolai.

Green AM, Mueller UG, Adams RMM (2002) Extensive exchange of fungal cultivars between sympatric species of fungus-growing ants. *Molecular Ecology*, **11**, 191–195.

Grieshaber MK, Hardewig I, Kreutzer U, Pörtner H-O (1994) Physiological and metabolic responses to hypoxia in invertebrates. In: *Reviews of Physiology, Biochemistry and Pharmacology, Volume 125*, pp. 43–147. Springer.

Gros O, Darrasse A, Durand P, Frenkiel L, Mouëza M (1996) Environmental transmission of a sulfur-oxidizing bacterial gill endosymbiont in the tropical lucinid bivalve *Codakia orbicularis*. *Applied and Environmental Microbiology*, **62**, 2324–2330.

Gros O, Frenkiel L, Mouëza M (1998) Gill filament differentiation and experimental colonization by symbiotic bacteria in aposymbiotic juveniles of *Codakia orbicularis* (Bivalvia: Lucinidae). *Invertebrate Reproduction & Development*, **34**, 219–231.

Gruber-Vodicka HR, Dirks U, Leisch N *et al.* (2011) *Paracatenula*, an ancient symbiosis between thiotrophic Alphaproteobacteria and catenulid flatworms. *Proceedings of the National Academy of Sciences*, **108**, 12078–12083.

Guindon S, Gascuel O (2003) A simple, fast, and accurate algorithm to estimate large phylogenies by maximum likelihood. *Systematic Biology*, **52**, 696–704.

Halanych KM, Janosik AM (2006) A review of molecular markers used for Annelid phylogenetics. *Integrative and Comparative Biology*, **46**, 533–543.

Hammen CS, Osborne PJ (1959) Carbon dioxide fixation in marine invertebrates: a survey of major phyla. *Science*, **130**, 1409–1410.

Hammen CS, Wilbur KM (1959) Carbon dioxide fixation in marine invertebrates I. The main pathway in the oyster. *Journal of Biological Chemistry*, **234**, 1268–1271.

Hand SC (1987) Trophosome ultrastructure and the characterization of isolated bacteriocytes from invertebrate-sulfur bacteria symbioses. *The Biological Bulletin*, **173**, 260–276.

Harada M, Yoshida T, Kuwahara H *et al.* (2009) Expression of genes for sulfur oxidation in the intracellular chemoautotrophic symbiont of the deep-sea bivalve *Calyptogena okutanii*. *Extremophiles*, **13**, 895–903.

Harmer TL, Rotjan RD, Nussbaumer AD *et al.* (2008) Free-living tube worm endosymbionts found at deep-sea vents. *Applied and Environmental Microbiology*, **74**, 3895–3898.

Heath BD, Butcher RDJ, Whitfield WGF, Hubbard SF (1999) Horizontal transfer of *Wolbachia* between phylogenetically distant insect species by a naturally occurring mechanism. *Current Biology*, **9**, 313–316.

Heindl NR, Gruber-Vodicka HR, Bayer C *et al.* (2011) First detection of thiotrophic symbiont phylotypes in the pelagic marine environment. *FEMS Microbiology Ecology*, **77**, 223–227.

Van Hellemond JJ, Van Der Klei A, van Weelden SH, Tielens AG (2003) Biochemical and evolutionary aspects of anaerobically functioning mitochondria. *Philosophical Transactions of the Royal Society B: Biological Sciences*, **358**, 205–215.

Hentschel U, Berger EC, Bright M, Felbeck H, Ott JA (1999) Metabolism of nitrogen and sulfur in ectosymbiotic bacteria of marine nematodes (Nematoda, Stilbonematinae). *Marine Ecology Progress Series*, **183**, 149–158.

Hentschel U, Felbeck H (1993) Nitrate respiration in the hydrothermal vent tubeworm *Riftia pachyptila*. *Nature*, **366**, 338–340.

Herry A, Diouris M, Pennec ML (1989) Chemoautotrophic symbionts and translocation of fixed carbon from bacteria to host tissues in the littoral bivalve *Loripes lucinalis* (Lucinidae). *Marine Biology*, **101**, 305–312.

Himmel D, Maurin LC, Gros O, Mansot J-L (2009) Raman microspectrometry sulfur detection and characterization in the marine ectosymbiotic nematode *Eubostrichus dianae* (Desmodoridae, Stilbonematidae). *Biology of the Cell / Under the Auspices of the European Cell Biology Organization*, **101**, 43–54.

Hopper BE, Cefalu RC (1973) Free-living marine nematodes from Biscayne Bay, Florida V. Stilbonematinae: contributions to the taxonomy and morphology of the genus *Eubostrichus* Greeff and related genera. *Transactions of the American Microscopical Society*, **92**, 578–591.

Hoschitz M, Bright M, Ott JA (2001) Ultrastructure and reconstruction of the pharynx of *Leptonemella juliae* (Nematoda, Adenophorea). *Zoomorphology*, **121**, 95–107.

Hoschitz M, Buchholz TG, Ott JA (1999) *Leptonemella juliae* sp. n. and *Leptonemella* vestari sp. n.(Stilbonematinae), two new free-living marine nematodes from a subtidal sand bottom. *Annalen des Naturhistorischen Museums in Wien. Serie B für Botanik und Zoologie*, 423–435.

Hourston M, Warwick RM (2010) New species of free-living aquatic nematodes from south-western Australia (Nematoda: Axonolaimidae and Desmodoridae). *Records of the Western Australian Museum*, **42**, 26.

Huber T, Faulkner G, Hugenholtz P (2004) Bellerophon: a program to detect chimeric sequences in multiple sequence alignments. *Bioinformatics*, **20**, 2317–2319.

Hughes DJ, Crawford M (2008) A new record of the vestimentiferan *Lamellibrachia* sp. (Polychaeta: Siboglinidae) from a deep shipwreck in the eastern Mediterranean. *Marine Biodiversity Records*, **1**, 1–3.

Huigens ME, Almeida RP de, Boons P a. H, Luck RF, Stouthamer R (2004) Natural interspecific and intraspecific horizontal transfer of parthenogenesis–inducing *Wolbachia* in *Trichogramma wasps*. *Proceedings of the Royal Society of London. Series B: Biological Sciences*, **271**, 509–515.

Hunter S, Apweiler R, Attwood TK *et al.* (2009) InterPro: the integrative protein signature database. *Nucleic Acids Research*, **37**, D211–D215.

Inglis WG (1968) Interstitial nematodes from St. Vincent's Bay, New Caledonia. *Expédition Française sur les récifs corallines de la Nouvelle-Calédonie. Singer-Polignac, Paris, Edit*, **2**, 29–74.

Jamieson BG, Tillier S, Tillier A *et al.* (2002) Phylogeny of the Megascolecidae and Crassiclitellata (Annelida, Oligochaeta): combined versus partitioned analysis using nuclear (28S) and mitochondrial (12S, 16S) rDNA. *Zoosystema Paris*, **24**, 707–734.

Jan C, Petersen JM, Werner J *et al.* (2014a) The gill chamber epibiosis of deep-sea shrimp *Rimicaris exoculata*: an in-depth metagenomic investigation and discovery of Zetaproteobacteria. *Environmental Microbiology*, **16**, 2723–2738.

Jan C, Petersen JM, Werner J *et al.* (2014b) The gill chamber epibiosis of deep-sea shrimp *Rimicaris exoculata*: an in-depth metagenomic investigation and discovery of Zetaproteobacteria. *Environmental Microbiology*, **16**, 2723–2738.

Jensen (1987) Feeding ecology of free-living aquatic nematodes. *Marine Ecology Progress Series*, **35**, 187–196.

Jensen P (1995) Life history of the nematode *Theristus anoxybioticus* from sublittoral muddy sediment at methane seepages in the northern Kattegat, Denmark. *Marine Biology*, **123**, 131–136.

De Jesús-Navarrete A (2003) Diversity of nematoda in a Caribbean atoll: Banco Chinchorro, Mexico. *Bulletin of Marine Science*, **73**, 47–56.

De Jesús-Navarrete A (2007a) Nematodos de los arrecifes de Isla Mujeres y Banco Chinchorro, Quintana Roo, México. *Revista de Biología Marina y Oceanografía*, **42**, 193–200.

De Jesús-Navarrete A (2007b) Littoral free living nematode fauna of Socorro Island, Colima, Mexico nematofauna de vida libre en el litoral de Isla Socorro, Colima, México. *Hidrobiologica*, **17**, 61–66.

Jiggins FM (2002) The rate of recombination in *Wolbachia* bacteria. *Molecular Biology and Evolution*, **19**, 1640–1643.

Johnson D, Martin F, Cairney JWG, Anderson IC (2012) The importance of individuals: intraspecific diversity of mycorrhizal plants and fungi in ecosystems. *New Phytologist*, **194**, 614–628.

Johnson TL, Fong JC, Rule C *et al.* (2014) The Type II secretion system delivers matrix proteins for biofilm formation by *Vibrio cholerae*. *Journal of Bacteriology*, **196**, 4245–4252.

Jousselin E, Desdevises Y, D'acier AC (2009) Fine-scale cospeciation between *Brachycaudus* and *Buchnera aphidicola*: bacterial genome helps define species and evolutionary relationships in aphids. *Proceedings of the Royal Society B: Biological Sciences*, **276**, 187–196.

Joye SB, Boetius A, Orcutt BN *et al.* (2004) The anaerobic oxidation of methane and sulfate reduction in sediments from Gulf of Mexico cold seeps. *Chemical Geology*, **205**, 219–238.

Julian D, Gaill F, Wood E, Arp A, Fisher C (1999) Roots as a site of hydrogen sulfide uptake in the hydrocarbon seep vestimentiferan *Lamellibrachia* sp. *Journal of Experimental Biology*, **202**, 2245–2257.

Källersjö M, Von Proschwitz T, Lundberg S, Eldenäs P, Erséus C (2005) Evaluation of ITS rDNA as a complement to mitochondrial gene sequences for phylogenetic studies in freshwater mussels: an example using Unionidae from north-western Europe. *Zoologica Scripta*, **34**, 415–424.

Kamenev GM, Fadeev VI, Selin NI, Tarasov VG, Malakhov VV (1993) Composition and distribution of macro- and meiobenthos around sublittoral hydrothermal vents in the Bay of Plenty, New Zealand. *New Zealand Journal of Marine and Freshwater Research*, **27**, 407–418.

Kampfer S, Sturmbauer C, Ott J (1998) Phylogenetic analysis of rDNA sequences from Adenophorean nematodes and implications for the Adenophorea-Secernentea controversy. *Invertebrate Biology*, **117**, 29–36.

Kanehisa M, Goto S, Sato Y *et al.* (2014) Data, information, knowledge and principle: back to metabolism in KEGG. *Nucleic Acids Research*, **42**, D199–D205.

Kashtan N, Roggensack SE, Rodrigue S *et al.* (2014) Single-cell genomics reveals hundreds of coexisting subpopulations in wild *Prochlorococcus*. *Science*, **344**, 416–420.

Katoh K, Kuma K, Toh H, Miyata T (2005) MAFFT version 5: improvement in accuracy of multiple sequence alignment. *Nucleic Acids Research*, **33**, 511–518.

Katoh K, Standley DM (2013) MAFFT Multiple sequence alignment software version 7: improvements in performance and usability. *Molecular Biology and Evolution*, **30**, 772–780.

Katoh K, Toh H (2008) Recent developments in the MAFFT multiple sequence alignment program. *Briefings in Bioinformatics*, **9**, 286–298.

Kearse M, Moir R, Wilson A *et al.* (2012) Geneious Basic: An integrated and extendable desktop software platform for the organization and analysis of sequence data. *Bioinformatics*, **28**, 1647–1649.

Kimura H, Higashide Y, Naganuma T (2003) Endosymbiotic microflora of the vestimentiferan tubeworm (*Lamellibrachia* sp.) from a bathyal cold seep. *Marine Biotechnology*, **5**, 593–603.

Kleiner M, Petersen JM, Dubilier N (2012a) Convergent and divergent evolution of metabolism in sulfur-oxidizing symbionts and the role of horizontal gene transfer. *Current Opinion in Microbiology*, **15**, 621–631.

Kleiner M, Wentrup C, Lott C *et al.* (2012b) Metaproteomics of a gutless marine worm and its symbiotic microbial community reveal unusual pathways for carbon and energy use. *Proceedings of the National Academy of Sciences*, **109**, E1173–E1182.

Kleiner M, Young JC, Shah M, VerBerkmoes NC, Dubilier N (2013) Metaproteomics reveals abundant transposase expression in mutualistic endosymbionts. *mBio*, **4**, e00223–13.

Kneip C, Lockhart P, Voß C, Maier U-G (2007) Nitrogen fixation in eukaryotes – New models for symbiosis. *BMC Evolutionary Biology*, **7**, 55.

Koboldt DC, Steinberg KM, Larson DE, Wilson RK, Mardis ER (2013) The next-generation sequencing revolution and Its impact on genomics. *Cell*, **155**, 27–38.

Koch AM, Croll D, Sanders IR (2006) Genetic variability in a population of arbuscular mycorrhizal fungi causes variation in plant growth. *Ecology Letters*, **9**, 103–110.

Koga R, Bennett GM, Cryan JR, Moran NA (2013) Evolutionary replacement of obligate symbionts in an ancient and diverse insect lineage. *Environmental Microbiology*, **15**, 2073–2081.

Kogel K-H, Franken P, Hückelhoven R (2006) Endophyte or parasite – what decides? *Current Opinion in Plant Biology*, **9**, 358–363.

Kojima S, Ohta S, Yamamoto T *et al.* (2002) Molecular taxonomy of vestimentiferans of the western Pacific and their phylogenetic relationship to species of the eastern Pacific. *Marine Biology*, **141**, 57–64.

Kojima S, Watanabe H, TsuchidaO S *et al.* (2006) Phylogenetic relationships of a tube worm (*Lamellibrachia juni*) from three hydrothermal vent fields in the South Pacific. *Journal of the Marine Biological Association UK*, **86**, 1357–1361.

Kornberg A (1995) Inorganic polyphosphate: toward making a forgotten polymer unforgettable. *Journal of Bacteriology*, **177**, 491–496.

Kornberg HL, Madsen NB (1957) Synthesis of C4-dicarboxylic acids from acetate by a "glyoxylate bypass" of the tricarboxylic acid cycle. *Biochimica et Biophysica Acta*, **24**, 651–653.

Kutschera U, Niklas KJ (2005) Endosymbiosis, cell evolution, and speciation. *Theory in Biosciences*, **124**, 1–24.

Laubier L (1993) The emphemeral oases of the depths- end of a paradigm. *Recherche*, **24**, 855–862.

Landolin J, Chin J, Kim K *et al.* (2014) Initial de novo assemblies of the *D. melanogaster* genome using long-read PacBio sequencing.

Leduc D (2013) One new genus and two new deep-sea nematode species (Desmodoridae, Stilbonematinae) from phosphorite nodule deposits on Chatham Rise, Southwest Pacific Ocean. *Marine Biodiversity*, **43**, 421–428.

Lee SY (1996) Bacterial polyhydroxyalkanoates. *Biotechnology and Bioengineering*, **49**, 1–14.

Lee K-H, Ruby EG (1994) Effect of the squid host on the abundance and distribution of symbiotic *Vibrio fischeri* in nature. *Applied and Environmental Microbiology*, **60**, 1565–1571.

Lefèvre C, Charles H, Vallier A *et al.* (2004) Endosymbiont phylogenesis in the Dryophthoridae weevils: evidence for bacterial replacement. *Molecular Biology and Evolution*, **21**, 965–973.

Legendre P, Desdevises Y, Bazin E (2002) A statistical test for host–parasite coevolution. *Systematic Biology*, **51**, 217–234.

Leisch N, Verheul J, Heindl NR *et al.* (2012) Growth in width and FtsZ ring longitudinal positioning in a gammaproteobacterial symbiont. *Current Biology*, **22**, R831–R832.

Liao L, Wankel SD, Wu M, Cavanaugh CM, Girguis PR (2014) Characterizing the plasticity of nitrogen metabolism by the host and symbionts of the hydrothermal vent chemoautotrophic symbioses *Ridgeia piscesae*. *Molecular Ecology*, **23**, 1544–1557.

Li W, Godzik A (2006) Cd-hit: a fast program for clustering and comparing large sets of protein or nucleotide sequences. *Bioinformatics*, **22**, 1658–1659.

Li B, Lopes JS, Foster PG, Embley TM, Cox CJ (2014) Compositional biases among synonymous substitutions cause conflict between gene and protein trees for plastid origins. *Molecular Biology and Evolution*, msu105.

Lisa TA, Garrido MN, Domenech CE (1983) Induction of acid phosphatase and cholinesterase activities in *Pseudomonas aeruginosa* and their in-vitro control by choline, acetylcholine and betaine. *Molecular and Cellular Biochemistry*, **50**, 149–155.

Lisec J, Schauer N, Kopka J, Willmitzer L, Fernie AR (2006) Gas chromatography mass spectrometry-based metabolite profiling in plants : Article : Nature Protocols. *Nat. Protocols*, **1**, 387–396.

Lonsdale P (1977) Clustering of suspension-feeding macrobenthos near abyssal hydrothermal vents at oceanic spreading centers. *Deep Sea Research*, **24**, 857–863.

Lösekann T, Robador A, Niemann H *et al.* (2008) Endosymbioses between bacteria and deep-sea siboglinid tubeworms from an Arctic cold seep (Haakon Mosby mud volcano, Barents Sea). *Environmental Microbiology*, **10**, 3237–3254.

Luc M, De Coninck LAP (1959) Nématodes libres marins de la région de Roscoff.

Ludwig W, Strunk O, Westram R *et al.* (2004) ARB: a software environment for sequence data. *Nucleic Acids Research*, **32**, 1363–1371.

Łukasik P, Guo H, van Asch M, Ferrari J, Godfray HCJ (2013) Protection against a fungal pathogen conferred by the aphid facultative endosymbionts *Rickettsia* and *Spiroplasma* is expressed in multiple host genotypes and species and is not influenced by co-infection with another symbiont. *Journal of Evolutionary Biology*, **26**, 2654–2661.

Luque-Almagro VM, Gates AJ, Moreno-Vivián C *et al.* (2011) Bacterial nitrate assimilation: gene distribution and regulation. *Biochemical Society Transactions*, **39**, 1838–1843.

MacGregor BJ, Amann R (2006) Single-stranded conformational polymorphism for separation of mixed rRNAS (rRNA-SSCP), a new method for profiling microbial communities. *Systematic and Applied Microbiology*, **29**, 661–670.

Mandel MJ, Schaefer AL, Brennan CA *et al.* (2012) Squid-derived chitin oligosaccharides are a chemotactic signal during colonization by *Vibrio fischeri. Applied and Environmental Microbiology*, **78**, 4620–4626.

Manz W, Amann R, Ludwig W, Wagner M, Schleifer K-H (1992) Phylogenetic oligodeoxynucleotide probes for the major subclasses of proteobacteria : problems and solutions. *Systematic and Applied Microbiology*, **15**, 593–600.

Margulis L, Fester R (1991) *Symbiosis as a source of evolutionary innovation: speciation and morphogenesis*. MIT Press.

Markert S, Arndt C, Felbeck H *et al.* (2007) Physiological proteomics of the uncultured endosymbiont of *Riftia pachyptila*. *Science*, **315**, 247–250.

Markert S, Gardebrecht A, Felbeck H *et al.* (2011) Status quo in physiological proteomics of the uncultured *Riftia pachyptila* endosymbiont. *Proteomics*, **11**, 3106–3117.

Martin BD, Schwab E (2012) Current usage of symbiosis and associated terminology. *International Journal of Biology*, **5**, p32.

Mattick JS (2002) Type IV pili and twitching motility. *Annual Review of Microbiology*, **56**, 289–314.

Matz C, Webb JS, Schupp PJ *et al.* (2008) Marine biofilm bacteria evade eukaryotic predation by targeted chemical defense. *PLoS ONE*, **3**, e2744.

Maurin LC, Himmel D, Mansot J-L, Gros O (2010) Raman microspectrometry as a powerful tool for a quick screening of thiotrophy: An application on mangrove swamp meiofauna of Guadeloupe (FWI). *Marine environmental research*, **69**, 382–389.

McCutcheon JP, Moran NA (2011) Extreme genome reduction in symbiotic bacteria. *Nature Reviews Microbiology*, **10**, 13–26.

McFall-Ngai M (2008) Are biologists in “future shock”? Symbiosis integrates biology across domains. *Nature Reviews Microbiology*, **6**, 789–792.

McFall-Ngai M, Hadfield MG, Bosch TCG *et al.* (2013) Animals in a bacterial world, a new imperative for the life sciences. *Proceedings of the National Academy of Sciences*, **110**, 3229–3236.

McMullin E, Hourdez S, Schaeffer SW, Fisher CR (2003) Phylogeny and biogeography of deep sea vestimentiferan tubeworms and their bacterial symbionts. *Symbiosis*, **34**, 1–41.

Meldal BHM, Debenham NJ, De Ley P *et al.* (2007) An improved molecular phylogeny of the Nematoda with special emphasis on marine taxa. *Molecular Phylogenetics and Evolution*, **42**, 622–636.

Di Meo CA, Wilbur AE, Holben WE *et al.* (2000) Genetic variation among endosymbionts of widely distributed vestimentiferan tubeworms. *Applied and Environmental Microbiology*, **66**, 651–658.

Migné A, Spilmont N, Davoult D (2004) In situ measurements of benthic primary production during emersion: seasonal variations and annual production in the Bay of Somme (eastern English Channel, France). *Continental Shelf Research*, **24**, 1437–1449.

Minet AD, Gaster M (2010) Pyruvate carboxylase is expressed in human skeletal muscle. *Biochemical and Biophysical Research Communications*, **402**, 196–197.

Mira A, Moran NA (2002) Estimating population size and transmission bottlenecks in maternally transmitted endosymbiotic bacteria. *Microbial Ecology*, **44**, 137–143.

Mizrahi I (2013) Rumen Symbioses. In: *The Prokaryotes* (eds Rosenberg E, DeLong EF, Lory S, Stackebrandt E, Thompson F), pp. 533–544. Springer Berlin Heidelberg.

Moran NA (1996) Accelerated evolution and Muller’s rachet in endosymbiotic bacteria. *Proceedings of the National Academy of Sciences*, **93**, 2873–2878.

Moran NA (2006) Symbiosis. *Current Biology*, **16**, R866–R871.

Moran NA, McCutcheon JP, Nakabachi A (2008) Genomics and evolution of heritable bacterial symbionts. *Annual Review of Genetics*, **42**, 165–190.

Moya A, Peretó J, Gil R, Latorre A (2008) Learning how to live together: genomic insights into prokaryote–animal symbioses. *Nature Reviews Genetics*, **9**, 218–229.

Mulcahy LR, Isabella VM, Lewis K (2013) *Pseudomonas aeruginosa* biofilms in disease. *Microbial Ecology*, **68**, 1–12.

Muller F, Brissac T, Le Bris N, Felbeck H, Gros O (2010) First description of giant Archaea (Thaumarchaeota) associated with putative bacterial ectosymbionts in a sulfidic marine habitat. *Environmental Microbiology*, **12**, 2371–2383.

Musat N, Giere O, Gieseke A *et al.* (2007) Molecular and morphological characterization of the association between bacterial endosymbionts and the marine nematode *Astomonema* sp. from the Bahamas. *Environmental Microbiology*, **9**, 1345–1353.

Musat N, Werner U, Knittel K *et al.* (2006) Microbial community structure of sandy intertidal sediments in the North Sea, Sylt-Rømø Basin, Wadden Sea. *Systematic and Applied Microbiology*, **29**, 333–348.

Muscatine L (1990) The role of symbiotic algae in carbon and energy flux in reef corals. *Ecosystems of the world*, **25**, 75–87.

Muthumbi A, Verschelde D, Vincx M (1995) New Desmodoridae (Nematoda: Desmodoroidea): three new species from Ceriops mangrove sediments (Kenya) and one related new species from the North Sea. *Cahiers de biologie marine*, **36**, 181–195.

Muyzer G, Teske A, Wirsen C, Jannasch H (1995) Phylogenetic relationships of *Thiomicrospira* species and their identification in deep-sea hydrothermal vent samples by denaturing gradient gel electrophoresis of 16S rDNA fragments. *Archives of Microbiology*, **164**, 165–172.

Muyzer G, de Waal EC, Uitterlinden AG (1993) Profiling of complex microbial populations by denaturing gradient gel electrophoresis analysis of polymerase chain reaction-amplified genes coding for 16S rRNA. *Applied and Environmental Microbiology*, **59**, 695–700.

Myshrall KL, Mobberley JM, Green SJ *et al.* (2010) Biogeochemical cycling and microbial diversity in the thrombolitic microbialites of Highborne Cay, Bahamas. *Geobiology*, **8**, 337–354.

Naganuma T, Elsaied H, Hoshii D, Kimura H (2005) Bacterial endosymbioses of gutless tube-dwelling worms in nonhydrothermal vent habitats. *Marine Biotechnology*, **7**, 416–428.

Naganuma T, Kato C, Hirayama H *et al.* (1997) Intracellular occurrence of e-proteobacterial 16S rDNA sequences in the vestimentiferan trophosome. *Journal of Oceanography*, **53**, 193–197.

Nakagawa S, Shimamura S, Takaki Y *et al.* (2014) Allying with armored snails: the complete genome of gammaproteobacterial endosymbiont. *The ISME journal*, **8**, 40–51.

Nebelsick M, Blumer M, Novak R, Ott J (1992) A new glandular sensory organ in *Catanema* sp. (Nematoda, Stilbonematinae). *Zoomorphology*, **112**, 17–26.

Nelson K, Fisher CR (2000) Absence of cospeciation in deep-sea vestimentiferan tube worms and their bacterial endosymbionts. *Symbiosis*, **28**, 1–15.

Newton ILG, Woyke T, Auchtung TA *et al.* (2007) The *Calyptogena magnifica* chemoautotrophic symbiont genome. *Science*, **315**, 998–1000.

Nicholson JK, Holmes E, Wilson ID (2005) Gut microorganisms, mammalian metabolism and personalized health care. *Nature Reviews Microbiology*, **3**, 431–438.

Nishijima M, Lindsay DJ, Hata J *et al.* (2010) Association of thioautotrophic bacteria with deep-sea sponges. *Marine Biotechnology*, **12**, 253–260.

Nunoura T, Sako Y, Wakagi T, Uchida A (2003) Regulation of the aerobic respiratory chain in the facultatively aerobic and hyperthermophilic archaeon *Pyrobaculum oguniense*. *Microbiology*, **149**, 673–688.

Nussbaumer AD, Bright M, Baranyi C, Beisser CJ, Ott JA (2004) Attachment mechanism in a highly specific association between ectosymbiotic bacteria and marine nematodes. *Aquatic Microbial Ecology*, **34**, 239–246.

Nussbaumer AD, Fisher CR, Bright M (2006) Horizontal endosymbiont transmission in hydrothermal vent tubeworms. *Nature*, **441**, 345–348.

Nyholm SV, McFall-Ngai M (2004) The winnowing: establishing the squid–*Vibrio* symbiosis. *Nature Reviews Microbiology*, **2**, 632–642.

Nylander JAA, Erséus C, Källersjö M (1999) A test of monophyly of the gutless Phallodrilinae (Oligochaeta, Tubificidae) and the use of a 573-bp region of the mitochondrial cytochrome oxidase I gene in analysis of annelid phylogeny. *Zoologica Scripta*, **28**, 305–313.

O'Connor RM, Fung JM, Sharp KH *et al.* (2014) Gill bacteria enable a novel digestive strategy in a wood-feeding mollusk. *Proceedings of the National Academy of Sciences*, **111**, E5096–E5104.

Olafsson E (1995) Meiobenthos in mangrove areas in eastern Africa with emphasis on assemblage structure of free-living marine nematodes. *Hydrobiologia*, **312**, 47–57.

Oliver KM, Russell JA, Moran NA, Hunter MS (2003) Facultative bacterial symbionts in aphids confer resistance to parasitic wasps. *Proceedings of the National Academy of Sciences*, **100**, 1803–1807.

Ott JA (1997) A new symbiotic marine nematode, *Adelphos rolandi* gen. n. sp. n.(Stilbonematinae), from the Caribbean Sea. *Annalen des Naturhistorischen Museums in Wien. Serie B für Botanik und Zoologie*, 417–422.

Ott JA, Bauer-Nebelsick M, Novotny V (1995) The genus *Laxus* Cobb, 1894 (Stilbonematinae: Nematoda): Description of two new species with ectosymbiotic, chemoautotrophic bacteria. *Proc. Biol. Soc. Wash.*, **108**, 508–527.

Ott J, Bright M, Bulgheresi S (2004) Symbioses between marine nematodes and sulfur-oxidizing chemoautotrophic bacteria. *Symbiosis*, **36**, 103–126.

Ott JA, Gruber-Vodicka HR, Leisch N, Zimmermann J (2014a) Phylogenetic confirmation of the genus *Robbea* (Nematoda: Desmodoridae, Stilbonematinae) with the description of three new species. *Systematics and Biodiversity*, **12**, 434–455.

Ott JA, Leisch N, Gruber-Vodicka HR (2014b) *Eubostrichus fertilis* sp. n., a new marine nematode (Desmodoridae: Stilbonematinae) with an extraordinary reproductive potential from Belize, Central America. *Nematology*, **16**, 777–787.

Ott JA, Novak R (1989) Living at an interface: Meiofauna at the oxygen/sulfide boundary of marine sediments, 415 – 422.

Ott JA, Novak R, Schiemer F *et al.* (1991) Tackling the sulfide gradient: a novel strategy Involving marine nematodes and chemoautotrophic ectosymbionts. *Marine Ecology*, **12**, 261–279.

Ott J, Rieger G, Rieger R, Enderes F (1982) New mouthless interstitial worms from the sulfide system: Symbiosis with prokaryotes. *Marine Ecology*, **3**, 313–333.

Overbeek R, Olson R, Pusch GD *et al.* (2013) The SEED and the Rapid Annotation of microbial genomes using Subsystems Technology (RAST). *Nucleic Acids Research*, gkt1226.

Palumbi S, Martin A, Romano S *et al*. (1991) *The simple fool's guide to PCR, version 2*. University of Hawaii Zoology Department, Honolulu.

Parkinson JE, Baums IB (2014) The extended phenotypes of marine symbioses: ecological and evolutionary consequences of intraspecific genetic diversity in coral-algal associations. *Frontiers in Microbiology*, **5**.

Parsons DA, Heffron F (2005) sciS, an icmF homolog in *Salmonella enteric*a serovar *Typhimurium*, limits intracellular replication and decreases virulence. *Infection and immunity*, **73**, 4338–4345.

Quail MA, Smith M, Coupland P *et al.* (2012) A tale of three next generation sequencing platforms: comparison of Ion Torrent, Pacific Biosciences and Illumina MiSeq sequencers. *BMC Genomics*, **13**, 341.

Peek AS, Feldman RA, Lutz RA, Vrijenhoek RC (1998) Cospeciation of chemoautotrophic bacteria and deep sea clams. *Proceedings of the National Academy of Sciences*, **95**, 9962–9966.

Pende N, Leisch N, Gruber-Vodicka HR *et al.* (2014) Size-independent symmetric division in extraordinarily long cells. *Nature Communications*, **5**.

Perner M, Gonnella G, Kurtz S, LaRoche J (2014) Handling temperature bursts reaching 464°c: different microbial strategies in the sisters peak hydrothermal chimney. *Applied and Environmental Microbiology*, **80**, 4585–4598.

Petersen JM, Dubilier N (2009) Methanotrophic symbioses in marine invertebrates. *Environmental Microbiology Reports*, **1**, 319–335.

Petersen JM, Wentrup C, Verna C, Knittel K, Dubilier N (2012) Origins and evolutionary flexibility of chemosynthetic symbionts from deep-Sea animals. *The Biological Bulletin*, **223**, 123–137.

Petersen JM, Zielinski FU, Pape T *et al.* (2011) Hydrogen is an energy source for hydrothermal vent symbioses. *Nature*, **476**, 176–180.

Platt HM, Zhang ZN (1982) New species of marine nematodes from Loch Ewe, Scotland. *Bulletin of the British Museum of Natural History (Zoology)*, **42**, 227–246.

Polerecky L, Volkenborn N, Stief P (2006) High temporal resolution oxygen imaging in bioirrigated sediments. *Environ. Sci. Technol.*, **40**, 5763–5769.

Polz MF, Distel DL, Zarda B *et al.* (1994) Phylogenetic analysis of a highly specific association between ectosymbiotic, sulfur-oxidizing bacteria and a marine nematode. *Applied and Environmental Microbiology,* **60**, 4461–4467.

Polz MF, Felbeck H, Novak R, Nebelsick M, Ott JA (1992) Chemoautotrophic, sulfur-oxidizing symbiotic bacteria on marine nematodes: morphological and biochemical characterization. *Microbial Ecology*, **24**, 313–329.

Polz MF, Harbison C, Cavanaugh CM (1999) Diversity and heterogeneity of epibiotic bacterial communities on the marine nematode *Eubostrichus dianae*. *Applied and Environmental Microbiology*, **65**, 4271–4275.

Polz MF, Ott JA, Bregut M, Cavanaugh CM (2000) When bacteria hitch a ride- associations between sulfur-oxidizing bacteria and eukaryotes represent spectacular adaptations to environmental gradients. *ASM News-American Society for Microbiology*, **66**, 531–539.

Ponsard J, Cambon-Bonavita M-A, Zbinden M *et al.* (2012) Inorganic carbon fixation by chemosynthetic ectosymbionts and nutritional transfers to the hydrothermal vent host-shrimp *Rimicaris exoculata*. *The ISME Journal*, **7**, 96–109.

Postma PW, Lengeler JW (1985) Phosphoenolpyruvate:carbohydrate phosphotransferase system of bacteria. *Microbiological Reviews*, **49**, 232–269.

Potrikus CJ, Breznak JA (1981) Gut bacteria recycle uric acid nitrogen in termites: a strategy for nutrient conservation. *Proceedings of the National Academy of Sciences*, **78**, 4601–4605.

Powell EN, Crenshaw MA, Rieger RM (1979) Adaptations to sulfide in sulfide-system I. ^{35}S-sulfide accumulation and the presence of a sulfide detoxification system. *J Exp Mar Biol Ecol*, **37**, 57–76.

Powell MA, Somero GN (1986) Adaptations to sulfide by hydrothermal vent animals: sites and mechanisms of detoxification and metabolism. *The Biological Bulletin*, **171**, 274–290.

Powers T (2004) Nematode molecular diagnostics: from bands to barcodes. *Annual Review of Phytopathology*, **42**, 367–383.

Pradillon F, Schmidt A, Peplies J, Dubilier N (2007) Species identification of marine invertebrate early stages by whole-larvae in situ hybridisation of 18S ribosomal RNA. *Marine Ecology Progress Series*, **333**, 103–116.

Prange A, Engelhardt H, Trüper HG, Dahl C (2004) The role of the sulfur globule proteins of *Allochromatium vinosum*: mutagenesis of the sulfur globule protein genes and expression studies by real-time RT-PCR. *Archives of Microbiology*, **182**, 165–174.

Raes M, De Troch M, Ndaro SGM *et al.* (2007) The structuring role of microhabitat type in coral degradation zones: a case study with marine nematodes from Kenya and Zanzibar. *Coral Reefs*, **26**, 113–126.

Raverdy S, Foster JM, Roopenian E, Carlow CK (2008) The *Wolbachia* endosymbiont of *Brugia malayi* has an active pyruvate phosphate dikinase. *Molecular and biochemical parasitology*, **160**, 163–166.

Records AR (2011) The type VI secretion system: a multipurpose delivery system with a phage-like machinery. *Molecular Plant-Microbe Interactions*, **24**, 751–757.

Redman RS, Dunigan DD, Rodriguez RJ (2001) Fungal symbiosis from mutualism to parasitism: who controls the outcome, host or invader? *New Phytologist*, **151**, 705–716.

Riemann F, Thiermann F, Bock L (2003) *Leptonemella* species (Desmodoridae, Stilbonematinae), benthic marine nematodes with ectosymbiotic bacteria, from littoral sand of the North Sea island of Sylt: taxonomy and ecological aspects. *Helgoland Marine Research*, **57**, 118–131.

Riera R, Núñez J, del Carmen Brito M (2013) Temporal dynamics of shallow subtidal meiobenthos from a beach in Tenerife (Canary Islands, northeast Atlantic Ocean). *Acta Oceanologica Sinica*, **32**, 44–54.

Rinke C, Lee R, Katz S, Bright M (2007) The effects of sulphide on growth and behaviour of the thiotrophic Zoothamnium niveum symbiosis. *Proceedings of the Royal Society of London B: Biological Sciences*, **274**, 2259–2269.

Robidart JC, Bench SR, Feldman RA *et al.* (2008) Metabolic versatility of the *Riftia pachyptila* endosymbiont revealed through metagenomics. *Environmental Microbiology*, **10**, 727–737.

Rodríguez-Ezpeleta N, Embley TM (2012) The SAR11 group of Alpha-proteobacteria Is not related to the origin of mitochondria. *PLoS ONE*, **7**, e30520.

Ronquist F, Huelsenbeck JP (2003) MrBayes 3: Bayesian phylogenetic inference under mixed models. *Bioinformatics*, **19**, 1572–1574.

Ruby EG, Asato LM (1993) Growth and flagellation of *Vibrio fischeri* during initiation of the sepiolid squid light organ symbiosis. *Archives of Microbiology*, **159**, 160–167.

Ruehland C, Blazejak A, Lott C *et al.* (2008) Multiple bacterial symbionts in two species of co-occurring gutless oligochaete worms from Mediterranean sea grass sediments. *Environmental Microbiology*, **10**, 3404–3416.

Russell JA, Latorre A, Sabater-Muñoz B, Moya A, Moran NA (2003) Side-stepping secondary symbionts: widespread horizontal transfer across and beyond the Aphidoidea. *Molecular Ecology*, **12**, 1061–1075.

Russell JA, Moran NA (2006) Costs and benefits of symbiont infection in aphids: variation among symbionts and across temperatures. *Proceedings of the Royal Society of London B: Biological Sciences*, **273**, 603–610.

Russell AB, Peterson SB, Mougous JD (2014) Type VI secretion system effectors: poisons with a purpose. *Nature Reviews Microbiology*, **12**, 137–148.

Sandkvist M (2001) Type II secretion and pathogenesis. *Infection and Immunity*, **69**, 3523–3535.

Sandulli R, De Leonardis C, Vanaverbeke J (2010) Meiobenthic communities in the shallow subtidal of three Italian Marine Protected Areas. *Italian Journal of Zoology*, **77**, 186–196.

Santegoeds CM, Ferdelman TG, Muyzer G, de Beer D (1998) Structural and functional dynamics of sulfate-reducing populations in bacterial biofilms. *Applied and Environmental Microbiology*, **64**, 3731–3739.

Satchell KJF (2011) Structure and function of MARTX toxins and other large repetitive RTX proteins. *Annual Review of Microbiology*, **65**, 71–90.

Schiemer F, Novak R, Ott J (1990) Metabolic studies on thiobiotic free-living nematodes and their symbiotic microorganisms. *Marine Biology*, **106**, 129–137.

Schimak MP, Toenshoff ER, Bright M (2012) Simultaneous 16S and 18S rRNA fluorescence in situ hybridization (FISH) on LR White sections demonstrated in Vestimentifera (Siboglinidae) tubeworms. *Acta Histochemica*, **114**, 122–130.

Schizas NV, Street GT, Coull BC, Chandler GT, Quattro JM (1997) An efficient DNA extraction method for small metazoans. *Molecular marine biology and biotechnology*, **6**, 381–383.

Schloissnig S, Arumugam M, Sunagawa S *et al.* (2013) Genomic variation landscape of the human gut microbiome. *Nature*, **493**, 45–50.

Schmitt S, Angermeier H, Schiller R, Lindquist N, Hentschel U (2008) Molecular microbial diversity survey of sponge reproductive stages and mechanistic insights into vertical transmission of microbial symbionts. *Applied and Environmental Microbiology*, **74**, 7694–7708.

Semprucci F, Balsamo M (2014) New records and distribution of marine free-living nematodes in the Maldivian Archipelago. *Proceedings of the Biological Society of Washington*, **127**, 35–46.

Semprucci F, Colantoni P, Baldelli G *et al.* (2013) Meiofauna associated with coral sediments in the Maldivian subtidal habitats (Indian Ocean). *Marine Biodiversity*, **43**, 189–198.

Semprucci F, Colantoni P, Baldelli G, Rocchi M, Balsamo M (2010) The distribution of meiofauna on back-reef sandy platforms in the Maldives (Indian Ocean). *Marine Ecology*, **31**, 592–607.

Seymour JR, Ahmed T, Durham WM, Stocker R (2010) Chemotactic response of marine bacteria to the extracellular products of *Synechococcus* and *Prochlorococcus*. *Aquatic Microbial Ecology*, **59**, 161–168.

Shrout JD, Tolker-Nielsen T, Givskov M, Parsek MR (2011) The contribution of cell-cell signaling and motility to bacterial biofilm formation. *MRS Bulletin / Materials Research Society*, **36**, 367–373.

Sibuet M, Olu-Le Roy K (2003) Cold seep communities on continental margins: structure and quantitative distribution relative to geological and fluid venting patterns. In: *Ocean margin systems*, pp. 235–251. Wefer, G.; Billett, D. et al. (Ed.).

Singh Y, Ahmad J, Musarrat J, Ehtesham NZ, Hasnain SE (2013) Emerging importance of holobionts in evolution and in probiotics. *Gut pathogens*, **5**, 1–8.

Sjölin E, Erséus C, Källersjö M (2005) Phylogeny of Tubificidae (Annelida, Clitellata) based on mitochondrial and nuclear sequence data. *Molecular Phylogenetics and Evolution*, **35**, 431–441.

Smith DC (1979) From extracellular to intracellular: The establishment of a symbiosis. *Proceedings of the Royal Society of London. Series B, Biological Sciences*, **204**, 115–130.

Smith LT, Pocard JA, Bernard T, Le Rudulier D (1988) Osmotic control of glycine betaine biosynthesis and degradation in *Rhizobium meliloti*. *Journal of Bacteriology*, **170**, 3142–3149.

Smith SE, Read DJ (2010) *Mycorrhizal Symbiosis*. Academic Press.

Soetaert K, Vincx M, Heip C (1995) Nematode community structure along a mediterranean shelf-slope gradient. *Marine Ecology*, **16**, 189–206.

Somerfield PJ, Dashfield SL, Warwick RM (2007) Three-dimensional spatial structure: nematodes in a sandy tidal flat. *Marine Ecology Progress Series*, **336**, 177–186.

Sourjik V, Wingreen NS (2012) Responding to chemical gradients: bacterial chemotaxis. *Current Opinion in Cell Biology*, **24**, 262–268.

Stamatakis A, Hoover P, Rougemont J (2008) A rapid bootstrap algorithm for the RAxML web servers. *Systematic Biology*, **57**, 758–771.

Starr MP (1975) A generalized scheme for classifying organismic associations. In: *Symposia of the Society for Experimental Biology*, p. 1.

Steedman HF (1957) Polyester wax: a new ribboning embedding medium for histology. *Nature*, **179**, 1345.

Stewart FJ, Baik AHY, Cavanaugh CM (2009a) Genetic subdivision of chemosynthetic endosymbionts of *Solemya velum* along the southern New England coast. *Applied and Environmental Microbiology*, **75**, 6005–6007.

Stewart FJ, Cavanaugh CM (2006) Symbiosis of thioautotrophic bacteria with *Riftia pachyptila*. In: *Molecular Basis of Symbiosis* Progress in Molecular and Subcellular Biology., pp. 197–225. Springer, Berlin Heidelberg.

Stewart FJ, Newton ILG, Cavanaugh CM (2005) Chemosynthetic endosymbioses: adaptations to oxic-anoxic interfaces. *Trends in Microbiology*, **13**, 439–448.

Stewart FJ, Young CR, Cavanaugh CM (2008) Lateral symbiont acquisition in a maternally transmitted chemosynthetic clam endosymbiosis. *Molecular Biology and Evolution*, **25**, 673–687.

Stewart FJ, Young CR, Cavanaugh CM (2009b) Evidence for homologous recombination in intracellular chemosynthetic clam symbionts. *Molecular Biology and Evolution*, **26**, 1391–1404.

Streams ME, Fisher CR, Fiala-Médioni A (1997) Methanotrophic symbiont location and fate of carbon incorporated from methane in a hydrocarbon seep mussel. *Marine Biology*, **129**, 465–476.

Sunagawa S, Woodley CM, Medina M (2010) Threatened corals provide underexplored microbial habitats. *PLoS One*, **5**, e9554.

Tanaka A, Christensen MJ, Takemoto D, Park P, Scott B (2006) Reactive oxygen species play a role in regulating a fungus–perennial ryegrass mutualistic interaction. *The Plant Cell Online*, **18**, 1052–1066.

Tang K-H, Feng X, Tang YJ, Blankenship RE (2009) Carbohydrate metabolism and carbon fixation in *Roseobacter denitrificans* OCh114. *PLoS ONE*, **4**. e7233.

Tchesunov AV (2013) Marine free-living nematodes of the subfamily Stilbonematinae (Nematoda, Desmodoridae): taxonomic review with descriptions of a few species from the Nha Trang Bay, Central Vietnam. *Meiofauna Marina*, **20**, 71–94.

Tchesunov AV, Ingels J, Popova EV (2012) Marine free-living nematodes associated with symbiotic bacteria in deep-sea canyons of north-east Atlantic Ocean. *Journal of the Marine Biological Association of the United Kingdom*, **92**, 1257–1271.

Terashima H, Kojima S, Homma M (2008) Flagellar motility in bacteria: structure and function of flagellar motor. In: *International Review of Cell and Molecular Biology* (ed Jeon KW), pp. 39–85. Academic Press.

Thauer RK, Jungermann K, Decker K (1977) Energy conservation in chemotrophic anaerobic bacteria. *Bacteriological Reviews*, **41**, 100–180.

Thiermann F, Akoumianaki I, Hughes JA, Giere O (1997) Benthic fauna of a shallow-water gaseohydrothermal vent area in the Aegean Sea (Milos, Greece). *Marine Biology*, **128**, 149–159.

Thiermann F, Vismann B, Giere O (2000) Sulphide tolerance of the marine nematode *Oncholaimus campylocercoides*-a result of internal sulphur formation? *Marine Ecology Progress Series*, **193**, 251–259.

Thompson JN (2005) *The Geographic Mosaic of Coevolution*. University of Chicago Press.

Thrash JC, Boyd A, Huggett MJ *et al.* (2011) Phylogenomic evidence for a common ancestor of mitochondria and the SAR11 clade. *Scientific reports*, **1**.

Toft C, Andersson SGE (2010) Evolutionary microbial genomics: insights into bacterial host adaptation. *Nature Reviews Genetics*, **11**, 465–475.

Trench RK (1993) Microalgal-invertebrate symbioses-a review. *Endocytobiosis and Cell Research*, **9**, 135–175.

Vanaverbeke J, Gheskiere T, Steyaert M, Vincx M (2002) Nematode assemblages from subtidal sandbanks in the Southern Bight of the North Sea: effect of small sedimentological differences. *Journal of Sea Research*, **48**, 197–207.

De Vienne DM, Refrégier G, López-Villavicencio M *et al.* (2013) Cospeciation vs host-shift speciation: methods for testing, evidence from natural associations and relation to coevolution. *New Phytologist*, **198**, 347–385.

Vismann B (1991) Sulfide tolerance: Physiological mechanisms and ecological implications. *Ophelia*, **34**, 1–27.

Vrijenhoek RC (2010) Genetics and evolution of deep-sea chemosynthetic bacteria and their invertebrate hosts. In: *The Vent and Seep Biota* Topics in Geobiology. (ed Kiel S), pp. 15–49. Springer Netherlands.

Wallner G, Amann R, Beisker W (1993) Optimizing fluorescent in situ hybridization with rRNA-targeted oligonucleotide probes for flow cytometric identification of microorganisms. *Cytometry*, **14**, 136–143.

Walsh K, Koshland DE (1984) Determination of flux through the branch point of two metabolic cycles. The tricarboxylic acid cycle and the glyoxylate shunt. *The Journal of Biological Chemistry*, **259**, 9646–9654.

Warwick RM, Coles JW (1977) The marine flora and fauna of the Isles of Scilly: free-living Nematoda. *Journal of Natural History*, **11**, 393–407.

Watsuji T, Yamamoto A, Motoki K *et al.* (2014) Molecular evidence of digestion and absorption of epibiotic bacterial community by deep-sea crab *Shinkaia crosnieri*. *The ISME Journal*.

Weber T, Blin K, Duddela S *et al.* (2015) antiSMASH 3.0—a comprehensive resource for the genome mining of biosynthetic gene clusters. *Nucleic Acids Research*, gkv437.

Weinert LA, Werren JH, Aebi A, Stone GN, Jiggins FM (2009) Evolution and diversity of *Rickettsia* bacteria. *BMC Biology*, **7**, 6.

Wentrup C, Wendeberg A, Schimak M, Borowski C, Dubilier N (2015) Forever competent: deep-sea bivalves are colonized by their chemosynthetic symbionts throughout their lifetime. *Environmental Microbiology*, **12**, 3699-713

Werner U, Billerbeck M, Polerecky L *et al.* (2006) Spatial and temporal patterns of mineralization rates and oxygen distribution in a permeable intertidal sand flat (Sylt, Germany). *Limnology and Oceanography*, **51**, 2549–2563.

Westphalen D (1993) Stromatolitoid microbial nodules from Bermuda —a special micro habitat for meiofauna. *Marine Biology*, **117**, 145–157.

White TJ, Bruns T, Lee S, Taylor JW, others (1990) Amplification and direct sequencing of fungal ribosomal RNA genes for phylogenetics. *PCR protocols: a guide to methods and applications*, **18**, 315–322.

Wieser W (1959) Eine ungewöhnliche Assoziation zwischen Blaualgen und freilebenden marinen Nematoden. *Plant Systematics and Evolution*, **106**, 81–87.

Wieser W, others (1960) Benthic studies in Buzzards Bay. II. The meiofauna. *Limnology and Oceanography*, **5**, 121–137.

Willems KA, Sharma Y, Heip C, Sandee AJJ (1984) Long-term evolution of the meiofauna at a sandy station in lake Grevelingen, The Netherlands. *Netherlands journal of sea research*, **18**, 418–433.

Willems KA, Vincx M, Claeys D, Vanosmael C, Heip C (1982) Meiobenthos of a sublittoral sandbank in the Southern Bight of the North Sea. *Journal of the marine biological Association of the United Kingdom*, **62**, 535–548.

Winnepenninckx B, Backeljau T, Wachter RD (1995) Phylogeny of protostome worms derived from 18S rRNA sequences. *Molecular Biology and Evolution*, **12**, 641–649.

Won Y-J, Hallam SJ, O'Mullan GD *et al.* (2003) Environmental acquisition of thiotrophic endosymbionts by deep-sea mussels of the genus *Bathymodiolus*. *Applied and Environmental Microbiology*, **69**, 6785–6792.

Woyke T, Teeling H, Ivanova NN *et al.* (2006) Symbiosis insights through metagenomic analysis of a microbial consortium. *Nature*, **443**, 950–955.

Yancey PH (2005) Organic osmolytes as compatible, metabolic and counteracting cytoprotectants in high osmolarity and other stresses. *Journal of Experimental Biology*, **208**, 2819–2830.

Yellowlees D, Rees TAV, Leggat W (2008) Metabolic interactions between algal symbionts and invertebrate hosts. *Plant, Cell & Environment*, **31**, 679–694.

Yu Z, Mohn WW (2001) Bacterial diversity and community structure in an aerated lagoon revealed by ribosomal intergenic spacer analyses and 16S ribosomal DNA sequencing. *Applied and Environmental Microbiology*, **67**, 1565–1574.

Zientz E, Dandekar T, Gross R (2004) Metabolic interdependence of obligate intracellular bacteria and their insect hosts. *Microbiology and Molecular Biology Reviews*, **68**, 745–770.

Zilber-Rosenberg I, Rosenberg E (2008) Role of microorganisms in the evolution of animals and plants: the hologenome theory of evolution. *FEMS Microbiology Reviews*, **32**, 723–735.

Zimmermann J, Lott C, Weber M *et al.* (2014) Dual symbiosis with co-occurring sulfur-oxidizing symbionts in vestimentiferan tubeworms from a Mediterranean hydrothermal vent. *Environmental Microbiology*, **16**, 3638–3656.

Acknowledgements

I am very grateful to:

Prof. Dr. Nicole Dubilier, for accepting me in your group and being a great advisor and mentor over these years. Thank you for teaching me scientific writing and to express myself clearly. Your critical and constructive feedback, and your support were invaluable to me. I'll be armed for many challenges in life.

Prof. Dr. Thomas Hoffmeister, for graciously accepting to review my thesis and therefore facilitating my graduation.

Prof. Dr. Michael Friedrich, for graciously serving as member of my defense committee and for your interest in my work. I appreciate it very much.

Prof. Dr. Jörg Ott, for being a great mentor and collaborator over these years. Thank you so much for providing me with valuable skills in nematode sampling, preparation and identification, for many scientific discussions, but also, to enjoy the good things in life. More field trips are hopefully waiting!

Dr. Jillian Petersen, for being an excellent supervisor and friend over these years. For many fruitful scientific discussions, and "wild and crazy ideas", sharing your knowledge, teaching me how to write articles logically, for always being super friendly and professional, being there whenever I needed advice, and for always finding the right words. All the best for Wien- you deserve it!

Dr. Harald Gruber-Vodicka, for being a great advisor, always having an open ear and willingness to discuss scientific ideas and projects, for your talent to explain things in a simple way, and of course, your friendship.

Dr. Manuel Kleiner, for many scientific discussions, the very detailed and critical input, for proof reading parts of this thesis, lots of help with planning the Bermuda trip and your friendship.

Dr. Cecilia Wentrup for many scientific discussions, your moral support and your friendship.

Dr. Niculina Musat for initial teaching about nematodes and giving me a kick-start in this project, **Lubos Polerecky** for your expertise with optode measurements, **Rachel Foster, Gaute Lavik and Tim Ferdelman** for sharing your knowledge and ideas.

Andreas Ellrott for sharing your expertise and how to work with the CLSM, and **Sten Littmann** for teaching me how to use the NanoSIMS

Bernd Stickfort for providing me with non-findable manuscript within a few hours, **Christiane Glöckner** for administrative and moral support with anything related to PhD life and especially graduation, **Ralf Schwenke** for being super organized and fast with PhD

contracts, **Manfred Schlösser** for lots of help regarding shipping dangerous goods or sampling permit organization.

Kay Simmack for being my lab-hero and friend. Thanks for all your valuable help with PCRs and your excellent lab book organization.

Brandon, for being the most structured and clear-thinking person, for reviewing large parts of this thesis, many scientific discussions and your friendship.

Silke, for being a lab angel and friend- always willing to help in emergency situations, and making my life as PhD student much easier! Am also endlessly thankful for your help in organizing the Bermuda trip.

Adrien and **Mario** for being extremely funny and making life in the department enjoyable, for cheering me up during many phases of "I think I quit my PhD...". Adrien, thanks for sharing your Illustrator skills & many motivational sketches!

Miriam, Oliver, and Manuel L. for their excitement about research and your friendships. Special thanks to Miriam for awesome Sylt excursions, Manuel & Oliver for reviewing parts of this thesis.

Karina, Zwiebel, Stefan D., Amandine, Rahel, for being wonderful and motivating office mates during all these years. Zwiebel, the Chili is still alive!

All the other **Symbionts** and **Mollies**- for being a great team to work with!

Meine Mädels, **Jase, Tanja, Anja** und **Barbara**, dafür, dass ich mich immer auf euch verlassen kann. Ihr seid die Besten!

Betty, Saar, Dani, Linn, Michael, Mirja, Jimena, Johanna, Julian, Erik, Shungu, Laura, Antonio, Yoli, Jeff, Alexei und **Natali** for countless moments of happiness and for your friendship. You guys are irrreplacable and made life in Bremen super enjoyable!

Liz, I am not even sure where to start…Thanks so much for millions of scientific and non scientific discussions, making me re-think, enduring all of my emotional ups and downs, support in every situation, countless moments of laughter - my bioinformatic hero and dear friend.

I am especially grateful to **Rodrigo**, for being my biggest supporter and emotional holdfast. Thanks for all your care and love and for providing me with coffees and food even though you were writing the thesis at the same time. You are my biggest treasure and joy.

Ich widme diese Arbeit **meiner Familie**, die mich immer und überall unterstützt hat. **Simon, Sven, Frank** und **Mareike,** dafür dass ich immer auf euch zählen kann. Ganz besonderer Dank meinen **Eltern Fritz und Angela,** die mir mit ihren Lebensweisheiten "Interesse und Hingabe sind der Weg zum Erfolg" und "Wenn einmal ein Weg nicht weiterführt findet sich ganz gewiss ein anderer" den Grundstein für diese Arbeit gelegt haben.

Appendix

Published manuscript with authors' contribution

Phylogenetic confirmation of the genus Robbea (Nematoda: Desmodoridae, Stilbonematinae) with the description of three new species

Authors: Jörg A. Ott, Harald R. Gruber-Vodicka, Nikolaus Leisch, and Judith Zimmermann.

Published in *Systematics and Biodiversity* (2014), 12(4): 434-455

J.A.O.: developed the concept, sampling, morphological species descriptions including measurements and drawings, conceived and wrote the manuscript; H.R.G.: performed the phylogenetic analysis, helped to develop the concept with J.A.O, conceived, and helped to write the manuscript; N.L.: performed the electron microscopy analyses and re-drawing, edited the manuscript; J.Z.: performed the 18S rRNA sequencing, constructed Fig. 1, helped to write the manuscript.

Systematics and Biodiversity (2014), 1–22

Taylor & Francis
Taylor & Francis Group

Research Article

Phylogenetic confirmation of the genus *Robbea* (Nematoda: Desmodoridae, Stilbonematinae) with the description of three new species

JÖRG A. OTT[1], HARALD R. GRUBER-VODICKA[2], NIKOLAUS LEISCH[3] & JUDITH ZIMMERMANN[2]

[1]Department of Limnology and Biooceanography, University of Vienna, Althanstr. 14, A-1090 Vienna, Austria
[2]Department of Symbiosis, Max Planck Institute for Marine Microbiology, Celsiusstr. 1, D-28359 Bremen, Germany
[3]Department of Ecogenomics and System Biology, University of Vienna, Althanstr. 14, A-1090 Vienna, Austria

(Received 13 February 2014; accepted 12 June 2014)

The Stilbonematinae are a monophyletic group of marine nematodes that are characterized by a coat of thiotrophic bacterial symbionts. Among the ten known genera of the Stilbonematinae, the genus *Robbea* Gerlach 1956 had a problematic taxonomic history of synonymizations and indications of polyphyletic origin. Here we describe three new species of the genus, *R. hypermnestra* sp. nov., *R. ruetzleri* sp. nov. and *R. agricola* sp. nov., using conventional light microscopy, interference contrast microscopy and SEM. We provide 18S rRNA gene sequences of all three species, together with new sequences for the genera *Catanema* and *Leptonemella*. Both our morphological analyses as well as our phylogenetic reconstructions corroborate the genus *Robbea*. In our phylogenetic analysis the three species of the genus *Robbea* form a distinct clade in the Stilbonematinae radiation and are clearly separated from the clade of the genus *Catanema*, which has previously been synonymized with *Robbea*. Surprisingly, in *R. hypermnestra* sp. nov. all females are intersexes exhibiting male sexual characters. Our extended dataset of Stilbonematinae 18S rRNA genes for the first time allows the identification of the different genera, e.g. in a barcoding approach.

http://zoobank.org/urn:lsid:zoobank.org:pub:D37C3F5A-CF2B-40E6-8B09-3C72EEED60B0

Key words: Belize Barrier Reef, Caribbean Sea, chemosynthetic symbiosis, marine nematodes, molecular phylogeny, SSU rRNA, ectosymbionts, systematics, taxonomy

Introduction

Stilbonematinae are a marine subfamily within the nematode family Desmodoridae (order Desmodorida) and occur worldwide in sulphidic sediments (reviewed in Tchesunov, 2013). They are characterized by an ectosymbiosis with sulphur-oxidizing bacteria that covers their cuticle in a genus- and sometimes even species-characteristic manner (Polz *et al.*, 1992, 1994; Ott *et al.*, 2004). Although the family Desmodoridae is probably polyphyletic (van Megen *et al.*, 2009), molecular data (Kampfer *et al.*, 1998; van Megen *et al.*, 2009) suggest a monophyly of the subfamily Stilbonematinae. A distinct morphological synapomorphy of the subfamily is the complex glandular sense organ (GSO) described by Nebelsick *et al.* (1992) and Bauer-Nebelsick *et al.* (1995), that has so far only been found in members of the Stilbonematinae. This organ produces a special set of lectins (sugar-binding proteins) that seem to be involved in sustaining the specificity of the symbiosis (Bulgheresi *et al.*, 2006, 2011). Otherwise very few common features unite the group, such as the lack of a buccal armature and the weak development of the pharynx (Ott *et al.*, 2004). Some characters appear to have developed independently more than once. For example, there is a tendency towards the development of an enlarged muscular portion of the anterior part of the pharynx (corpus), which is conspicuous in all species of the genera *Robbea* and *Catanema*, and has been described for the single species of *Parabostrichus* (Tchesunov *et al.*, 2012), whereas in other genera (*Laxus*, *Leptonemella*, *Eubostrichus*) it is present only in a few species. Other examples are the reduction of the amphidial fovea or the presence of a stiff corpus gelatum protruding from the amphidial fovea (*Stilbonema*, *Catanema, Leptonemella* partim) (Tchesunov, 2013). This complicates the

Correspondence to: Jörg A. Ott. Email: joerg.ott@univie.ac.at

ISSN 1477-2000 print / 1478-0933 online

http://dx.doi.org/10.1080/14772000.2014.941038

assessment of the relationships between the various genera described until now.

In addition, the type species of several genera are either inadequately described or have features which are the exception rather than the rule in the subsequently described members of the genus. Liberal synonymization has added further confusion.

The genus *Robbea*, introduced by Gerlach (1956), is characterized by the clear separation of a muscular anterior corpus from a mostly glandular isthmus and posterior bulbus which make up the remaining portion of the pharynx. In some species the males have peculiar papillae in the ventromedian line of the cervical and post-cervical region, which resemble suction cups and have a stout conical setae in its centre. These appear to be unique for the genus *Robbea* and have not been described from other stilbonematine genera.

The aim of this study was to reinvestigate morphological characters that are shared by all species of the genus *Robbea* but clearly distinguish those from other stilbonematine nematode genera. We describe three new species of *Robbea* from shallow subtidal sands around the island Carrie Bow Cay on the Belize Barrier Reef (Caribbean Sea). We combine morphological and molecular analyses to clarify the status of the genus and support our findings by providing additional phylogenetic information on previously under-sampled genera.

Materials and methods

Sediment samples containing *Robbea* species were collected in the vicinity of the island of Carrie Bow Cay, Belize from shallow subtidal sand patches and from turtle grass (*Thalassia testudinum*) beds using buckets or cores. Samples for sequencing were obtained at the following coordinates: *R. hypermnestra*: 16° 48′ 47″N, 88° 04′ 58″W; *R. agricola:* 16° 52′ 58″N, 88° 07′ 11″W; *R. ruetzleri:* 16° 47′ 19″N, 88° 04′ 48″W (Fig. 1). Subtidal sediment containing *Catanema* sp. was collected in the bay off Capo di Sant' Andrea, Elba, Italy (42° 48′ 26″N, 10° 08′ 28″E) from sand patches surrounding sea grass beds of *Posidonia oceanica* in 4−8 m water depth (Fig. 1). *Leptonemella vicina* was collected off the island of Sylt,

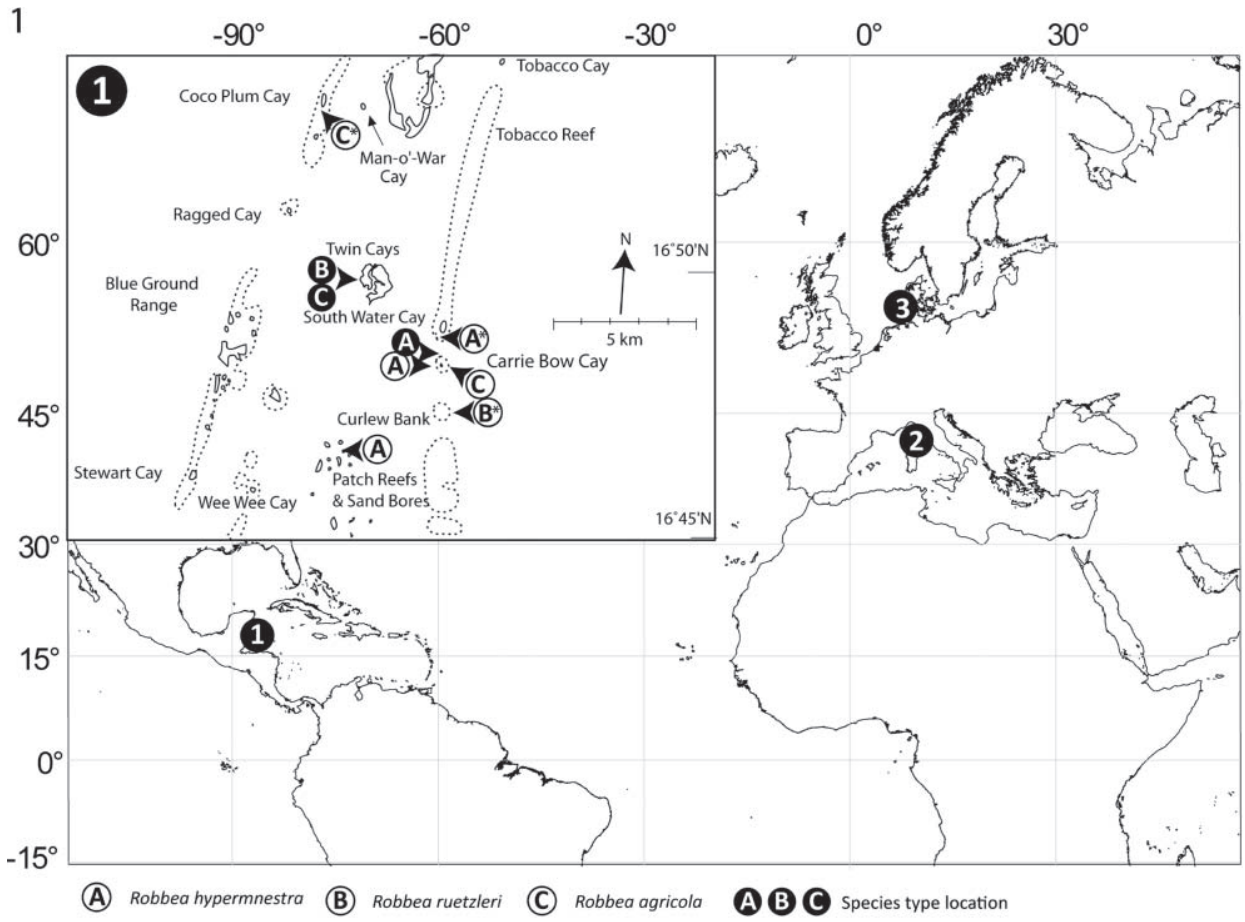

Fig. 1. Map showing sampling locations for the nematodes used in this study. 1, Carrie Bow Cay, Belize; 2, Elba, Italy; and 3, Sylt, Germany. Insert shows detailed locations in the vicinity of Carrie Bow Cay where the three new *Robbea* species were found. Asterisks mark the sampling locations of the individuals that were used for sequencing.

Germany (55° 00′ 54″N, 08° 26′ 16″E) with sediment cores from an intertidal sand flat (Fig. 1). Worms were extracted from the sand after anaesthesia with $MgCl_2$, shaking and decanting or simply shaking and decanting through a 32 μm mesh sieve. The live animals were sorted using a dissecting microscope and immediately fixed in 4% formaldehyde (for taxonomic preparations) or 2.5% glutaraldehyde in 0.1 sodium cacodylate buffer and post-fixed in 2% OsO_4 (for SEM and semi-thin sections). For light microscopy the worms were placed into glycerol: water 1:9, slowly evaporated and finally mounted in pure glycerol; for SEM specimens were critical point-dried and coated with gold. Specimens for sequencing of the 18S rRNA gene were preserved in 70% ethanol or methanol.

Drawings were done using a *camera lucida* on a Reichert Diavar or a Leitz Ortholux. Nomarsky interference contrast photos were taken on a Reichert Polyvar; SEM on a JEOL JSM-35 CF and a Phillips XL20; semi-thin sections were cut on a Reichert Ultracut and photographed in a Reichert Polyvar.

DNA extraction, PCR amplification and sequencing of the 18S rRNA gene

DNA for all sampled species was extracted and purified from single nematode specimens as described before (Schizas *et al.*, 1997). The partial 18S rRNA gene (~1800 bp) was amplified by PCR with the general eukaryotic primers 1F (5′-GGTTGATYCTGCCAGT-3′) (modified from Winnepenninckx *et al.*, 1995) and 2023R (5′-GGTTCACCTACGRAAA-3′) (modified from Pradillon *et al.*, 2007) using the Phusion® DNA polymerase (Finnzymes, Finland). Cycling conditions were as follows: initial denaturation at 96 °C for 5 min, followed by 35 cycles of 96 °C for 1 min, 55 °C for 1.5 min, 72 °C for 2 min and final elongation at 72 °C for 10 min. The purified PCR products (PCR Purification Kit; Qiagen, Hilden, Germany) were sequenced bidirectionally with the PCR primers and an internal reverse primer (5′-CAGACAAATCGCTCC-3′) 1272 nucleotides downstream of the 1F primer. All sequencing reactions were performed with an ABI PRISM 3100 genetic analyser (Applied Biosystems, Foster City, CA, USA).

The generated 18S rRNA gene sequences and all sequences from the Stilbonematinae available in GenBank, as well as four Draconematinae sequences as outgroup were aligned using MAFFT Q-INS-I, which considers the predicted secondary structure of the RNA for the alignment (Katoh *et al.*, 2005). Alignments were manually inspected and 5′ and 3′ end-trimmed using Geneious software version 6 (Drummond *et al.*, 2011). The optimal substitution model was assessed using the Akaike information criterion as implemented in MEGA 5.3 (Tamura *et al.*, 2011) and the GTR+G+I model was chosen. Phylogenetic trees were reconstructed using maximum likelihood- (RAxML) (Stamatakis, 2006) and Bayesian inference-based (MrBayes) (Ronquist & Huelsenbeck, 2003) methods. The dataset was screened for chimeric sequences by calculating maximum likelihood-based trees on three partitions of the alignments (0−600 bp, 601−1200 bp and 1201−1799 bp). The Stilbonematinae sequences Y16915 (designated *Eubostrichus dianae*) and Y16921 (designated *Robbea hypermnestra*) had statistically supported positions in 2 (Y16915) and 3 (Y16921) different genus level clades across all three partitions and were excluded from the final analysis. MrBayes was run for four Mio generations using four chains. Convergence was evaluated by plotting the generations versus logL and the burn-in was set to 1 Mio generations. Node stability was evaluated using posterior probabilities (pp, Bayesian inference) and bootstrap support (200 RAxML rapid bootstrap runs, maximum likelihood) (Stamatakis *et al.*, 2008) with values above .80 considered significant.

Nucleotide sequence accession numbers

The 18S rRNA sequences from this study were submitted to GenBank under accession numbers KJ414464 (*Robbea agricola*), KJ414465 (*Robbea ruetzleri*), KJ414466-7 (*Robbea hypermnestra*), KJ414468 (*Leptonemella vicina*) and KJ414469 (*Catanema* sp.).

Results

Class Chromadorea Inglis, 1983
Subclass Chromadoria Pearse, 1942
Order Desmodorida De Coninck, 1965
Suborder Desmodorina De Coninck, 1965
Superfamily Desmodoroidea Filipjev, 1922
Family Desmodoridae Filipjev, 1922
Subfamily Stilbonematinae Chitwood, 1936
Robbea Gerlach 1956

Diagnosis. (Modified from Tchesunov, 2013): Stilbonematinae. Cuticle transversely striated, except for the head region and the tip of the tail. Cephalic capsule when present with a block-layer; cephalic setae as long or longer than the subcephalic setae, usually directed straight forward. Amphidial fovea well developed, spirally coiled or loop-shaped. Pharynx distinctly tripartite, corpus muscular and clearly set off from the narrow isthmus. Pharynx bulbus largely glandular. Gubernaculum variable in shape, with or without dorso-caudal apophysis. The males of *R. tenax* Gerlach 1963 and the three new species have cup-shaped ventral papillae in the post-pharyngeal region. These species share also a stout body with *a* not exceeding 100. The species *R. gerlachi* Boucher 1975 from which

only a female has been described may also belong to this group. Symbiotic bacteria rod shaped, corn-kernel shaped or coccoid, usually covering the body as a monolayer.

Robbea hypermnestra sp. nov.
urn:lsid:zoobank.org:act:505DEA0B-614A-4086-A52F-62BA8A68F474

Synonymy. *Robbea* sp. in: Ott & Novak (1989), Schiemer *et al*. (1990), Ott *et al*. (1991), Polz *et al*. (1992), Bauer-Nebelsick *et al*. (1995), Urbancik *et al*. (1996a, 1996b), Polz *et al*. (2000); *Robbea* sp. 3 in: Bayer *et al*. (2009), Heindl *et al*. (2011); *Robbea hypermnestra* nomen nudum in: Kampfer *et al*. (1998), Polz *et al*. (2000).

Type material. Holotype (male), 4 paratypes (male), 4 paratypes (female /intersex).

Measurements. See Table 1.

Additional material. Several specimens in the author's collection and those used for SEM.

The sequences of the 18S rRNA gene are available from GenBank and have the accession numbers KJ414466-7.

Type locality. Subtidal sand bar in 10–50 cm depth at the north end of Carrie Bow Cay, Belize in coarse, poorly sorted calcareous sand with rubble (Fig. 1).

Distribution. This robust species is extremely common in the above sand bar (compare Ott & Novak, 1989) and a similar sand bar at the south end of neighbouring South Water Cay. Other localities are open sand patches between *Thalassia testudinum* beds and patch reefs to the west and north of Carrie Bow Cay in up to 1.5 m depth and medium, poorly sorted sand at the base of 'sand bores' south of Carrie Bow Cay in 5–6 m depth (Fig. 1).

Etymology. Named after Hypermnestra, the only one of the 50 daughters of the king of Argos, Danaos, who did not kill her husband in the wedding night as requested by her father although she was armed with a dagger. This refers to the presence of a spiculum in females (intersexes).

Table 1. Morphometric data for *Robbea hypermnestra* sp. nov. Ranges are given for the male and female paratypes. All measurements are in μm.

	Holotype	Paratypes (male) n = 4	Paratypes (female intersexes) n = 4
Length	3125	2765–3535	3020–3985
a	44.5	41.4–58.9	44.4–64.3
b	30.6	23.6–37.2	27.5–36.2
c	17.9	17.4–23.6	23.0–26.9
maximum width	70	55–65	65–82
pharynx length	102	92–100	90–117
tail length	174	140–162	120–150
nerve ring (% pharynx length)	50	48–54	46–58
corresponding body diameter (cbd)	45	45–52	48–55
bulbus length /width	25 /32	20–28 /29–30	25–38 /32–45
bulbus cbd	48	47–50	48–55
V	n.a.	n.a.	41–45
vulva cbd	n.a.	n.a.	65–82
anal (cloacal) body diameter	68	55–65	50–60
tail length:anal diameter	2.6	2.3–2.9	2.3–2.5
spiculae length arc /chord	105 /88	98–102 /80–85	62–70 /53–60
gubernaculum length /apophysis length	20 /25	20–30 /25–34	10–15 /10–15
amphid width	15	16–20	9–12
cephalic setae number /length	4 /38	4 /32–40	4 /30–38
subcephalic setae 1 number /length	8 /37	8 /30–38	8 /28–32
subcephalic setae 2 number /length	8 /30	8 /28–32	8 /28–32
Sucker-like papillae, number	17	16–18	n.a.
Position of first /last papilla	85 /501	65–95 /440–480	n.a.

n.a. = not applicable.

Description

Body cylindrical (Figs 2, 3), head diameter at level of cephalic setae 20−23 μm, diameter at level of posterior margin of amphidial fovea 40−54 μm in males, 33−42 μm in females, at end of pharynx 47−55 μm, maximum body diameter 55−82 μm, anal diameter 55−68 μm in males, 50−60 μm in females. Tail conical, 140−174 μm long in males and 120−150 μm in females (Figs 7, 8).

Cuticle finely transversely striated except for the first 28−36 μm of the head (Figs 5−8, 14) and the last 35−50 μm of the tail (Fig. 15), annules 0.45 to 0.55 μm wide (18−22 annuli/10 μm); non-striated head cuticle reinforced (cephalic capsule). The anteriormost circle of head sensillae (inner labial sensillae) is represented by 6 finger-like papillae, 2 μm long in lateral, subventral and subdorsal position surrounding the mouth opening (Fig. 19). The second circle consists of 6 short outer labial sensillae, 3−6 μm long, on the margin of the membranous buccal field; 4 cephalic setae flanking the anterior margin of the amphidial fovea, 32−38 μm long; 3 circles of 8 subcephalic setae each, 28−38 μm long, on the non-striated part of the head region, the posteriormost at the level of the posterior margin of the amphidial fovea (Figs 11, 17); 8 rows of somatic setae along the whole length of the body, 20−35 μm long somatic setae alternating with only 5−12 μm long bristles (Fig. 4). In males, there is a distinct field of about 7−10 stout, conical setae, 5 μm long on the ventral side in front of the cloacal opening (Figs 8, 25, 26). Non-striated part of the tail in females with 2 pairs of stout setae, the first pair 7 μm long, shortly behind the end of the annulation; the second pair of 3−4 μm long, close to the tip of the tail (Fig. 15); in males with a small velum ventrally (Fig. 23). Three caudal glands with separate openings at the tail tip (Fig. 16). Males have a 380−450 μm long row of 16−19 (mean 17.2, n = 16) conspicuous cuticular papillae along the mid-ventral line beginning at a distance of 65−95 μm from the anterior end at the level of the posterior bulbus of the pharynx (Figs 4, 20). Papillae cup-shaped, with a diameter of 11−15 μm, on short annulated stalks, bearing a conical seta in its centre (Figs 21, 22). Amphidial foveas situated at the anterior end bordering the buccal field, showing a distinct sexual dimorphism: small, slightly oval spirals with 1.25 turns in females, 13−18 μm long and 9−12 μm wide; in males much larger, elongated loops, 28−38 μm long and 16−20 μm wide (Figs 5, 6, 12, 18, 28, 29).

Pharynx (Figs 4, 27) 90−117 μm long, with a minute tubular buccal cavity, 7−12 μm long and 4 μm in diameter, leading into a conspicuous pyriform muscular corpus, 34−40 μm long and 18−25 μm wide, which is clearly set off from the following 32−40 μm long isthmus. Posterior bulbus subspherical, 20−38 μm long, 30−45 μm wide, largely glandular, containing only weak muscles. No cardia.

Nerve ring 50−65 μm from anterior end; no secretory-excretory pore or ventral gland seen; 8 rows of glandular sense organs (two in each lateral and each median line) connect to the small somatic setae.

Males monorchic, testis on the left side of the intestine, beginning at about 35% of body length; sperm spherical, 10 μm in diameter; spicula (Figs 8, 10, 31) strong, arcuate, slightly cephalate proximally, with blunt tips (Fig. 24), 80−88 μm (chord) or 98−105 μm (arc) long; gubernaculum massive, corpus embracing spicules, 20−30 μm long, with strong dorsocaudal apophysis, 28−34 μm long).

Females didelphic, ovaries reflexed, long uteri leading to a strongly cuticularized vagina; vulva (Fig. 13) at 41−45% of body length. Large eggs (190 × 50 μm) are often present in one or both uteri, which also contain usually many sperm cells of the same shape and size as seen in males. All females are intersexes, having spicula and a gubernaculum in the anal region (Figs 7, 9, 30). Spicula and gubernaculum much smaller and of simpler construction than in males: length of the female spicula, 53−60 μm (chord) or 62−70 μm (arc); gubernaculum, 10−15 μm long with a similar sized apophysis. No traces of other parts of a male genital apparatus were found. A weakly cuticularized vulva primordium but no other female or male characteristic features could be seen in 7 of 11 large (probably 4th stage) juveniles.

The bacteria covering the cuticle of the worms (Fig. 14) are distributed over the whole body, leaving only the tip of the tail and the cephalic capsule uncovered. On the ventral side the bacteria rarely reach the basis of the cephalic capsule. The bacteria are rod shaped and are usually attached with their longitudinal axis perpendicular to the cuticle surface. In a few cases, however, bacteria were seen lying parallel to the cuticular annuli of the worm (Fig. 14). The thiotrophic bacterial ectosymbionts have been previously characterized (Bayer *et al.*, 2009) and belong to the MONTS clade of Gammaproteobacteria (Heindl *et al.,* 2011) that also contains the symbionts of the mouthless nematode genus Astomonema and of gutless oligochaetes. The GenBank accession number for their 16S rRNA gene is EU711428.

Diagnosis. Species with a distinct cephalic capsule with block-layer; 16−19 cup-shaped stalked ventral papillae in the post pharyngeal region; pharynx almost equally divided into corpus, isthmus and bulbus; all females are intersexes; spicula weakly cephalate, gubernaculum with dorsocaudal apophysis, pronounced sexual dimorphism of the amphidial fovea. Symbiotic bacteria rod-shaped.

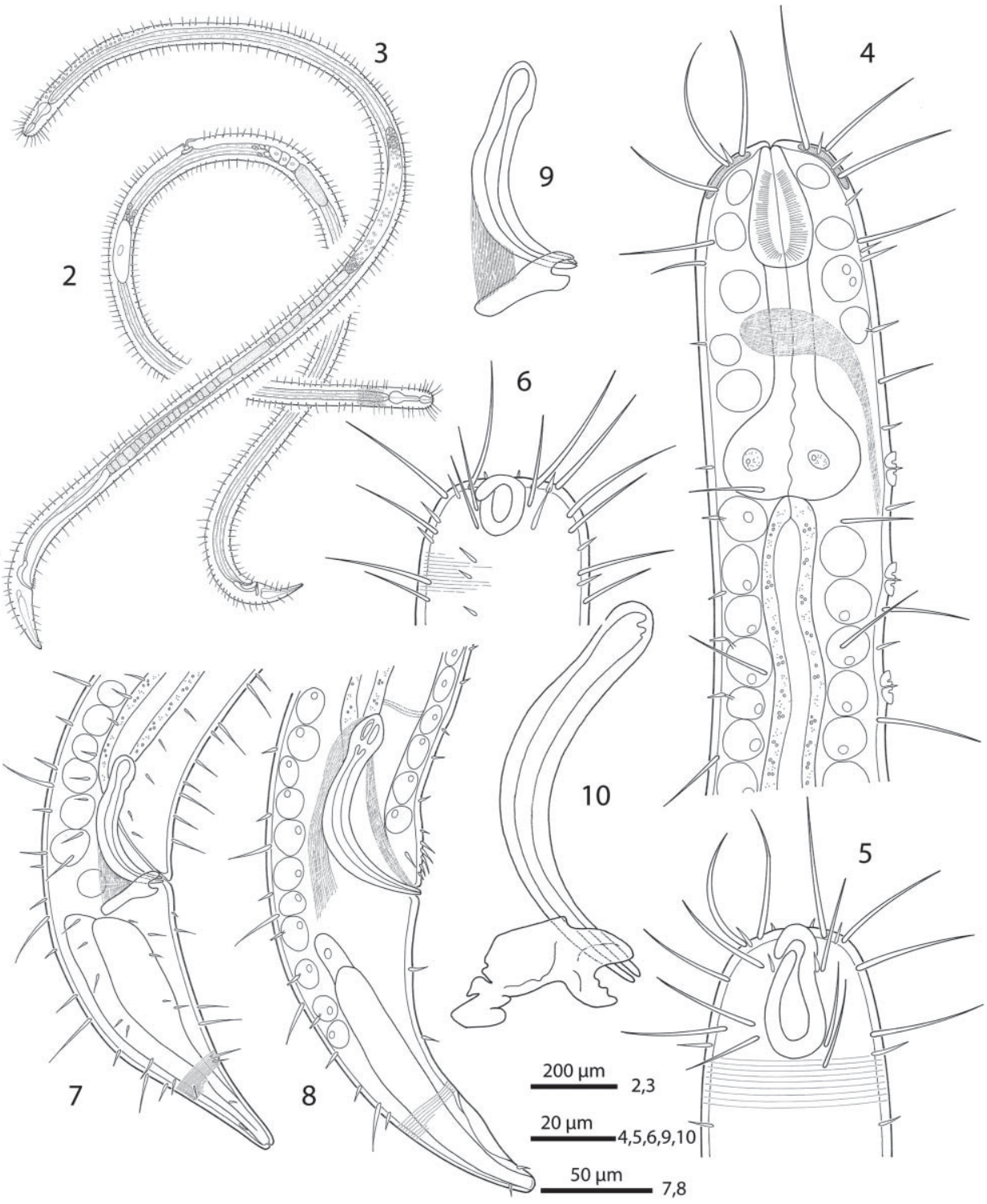

Figs. 2–**10.** *Robbea hypermnestra* sp. nov. **2**. Female, whole; **3**. Male, whole; **4**. Male, anterior body region; **5**. Male, head, surface view; **6**. Female, head, surface view; **7**. Female, tail; **8**. Male, tail (gubernaculum not drawn); **9**. Female, spiculum; **10**. Male, spiculum.

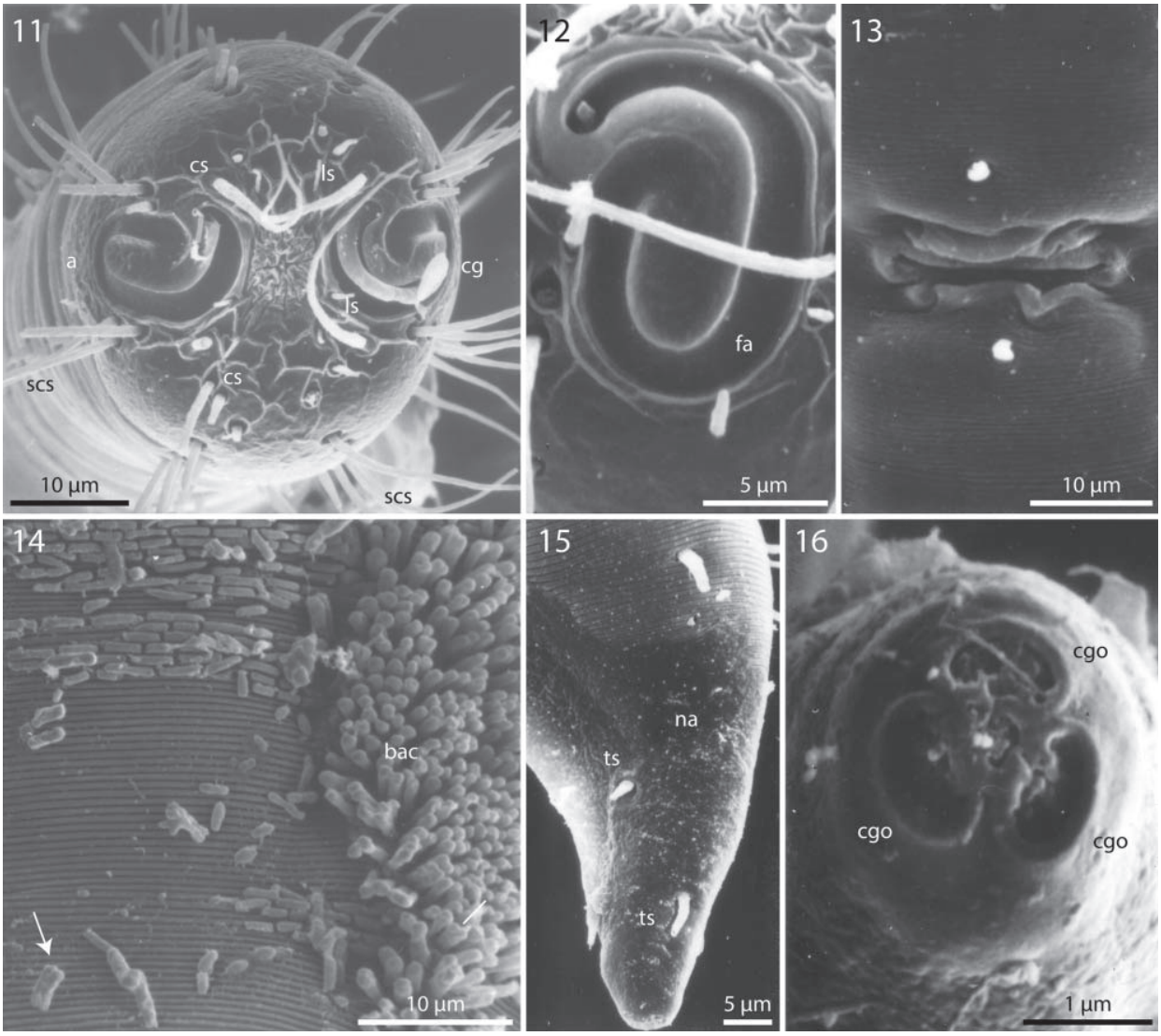

Figs. 11–16. *Robbea hypermnestra* sp. nov. Female. **11**. Head, in face view; **12**. Amphidial fovea; **13**. Vulva; **14**. Annulation and bacterial coat in midbody region; **15**. Tip of tail, non-striated portion; **16**. Openings of the caudal glands. SEM.

Robbea ruetzleri sp. nov.
urn:lsid:zoobank.org:act:92A7E898-62D0-452D-A6A3-9A622CBD4599

Type material. Holotype (male), 3 paratypes (male), 3 paratypes (female).

Measurements. See Table 2.

Additional material. Several specimens in the authors' collection and those used for SEM.

The sequence of the 18S rRNA gene is available from GenBank and has the accession number KJ414465.

Type locality. West side of Twin Cayes, Belize; shallow fine sand among *Rhizophora mangle* stilt roots and *Thalassia testudinum* beds (Fig. 1).

Distribution. Rare, in fine to medium subtidal sand samples (Fig. 1).

Etymology. Named in honour of Klaus Ruetzler, CCRE programme director, friend and generous host on Carrie Bow Cay.

Description

Body slender, cylindrical (Fig. 32), head diameter at level of cephalic setae 20–25 μm, diameter at level of posterior margin of amphidial fovea 25–30 μm at end of pharynx 33–39 μm, maximum body diameter 40–60 μm, anal diameter 32–45 μm. Tail conical, 60–88 μm long (Figs 35, 36).

Cuticle finely transversely striated except for the first 32–44 μm of the head and the last 30–42 μm of the tail,

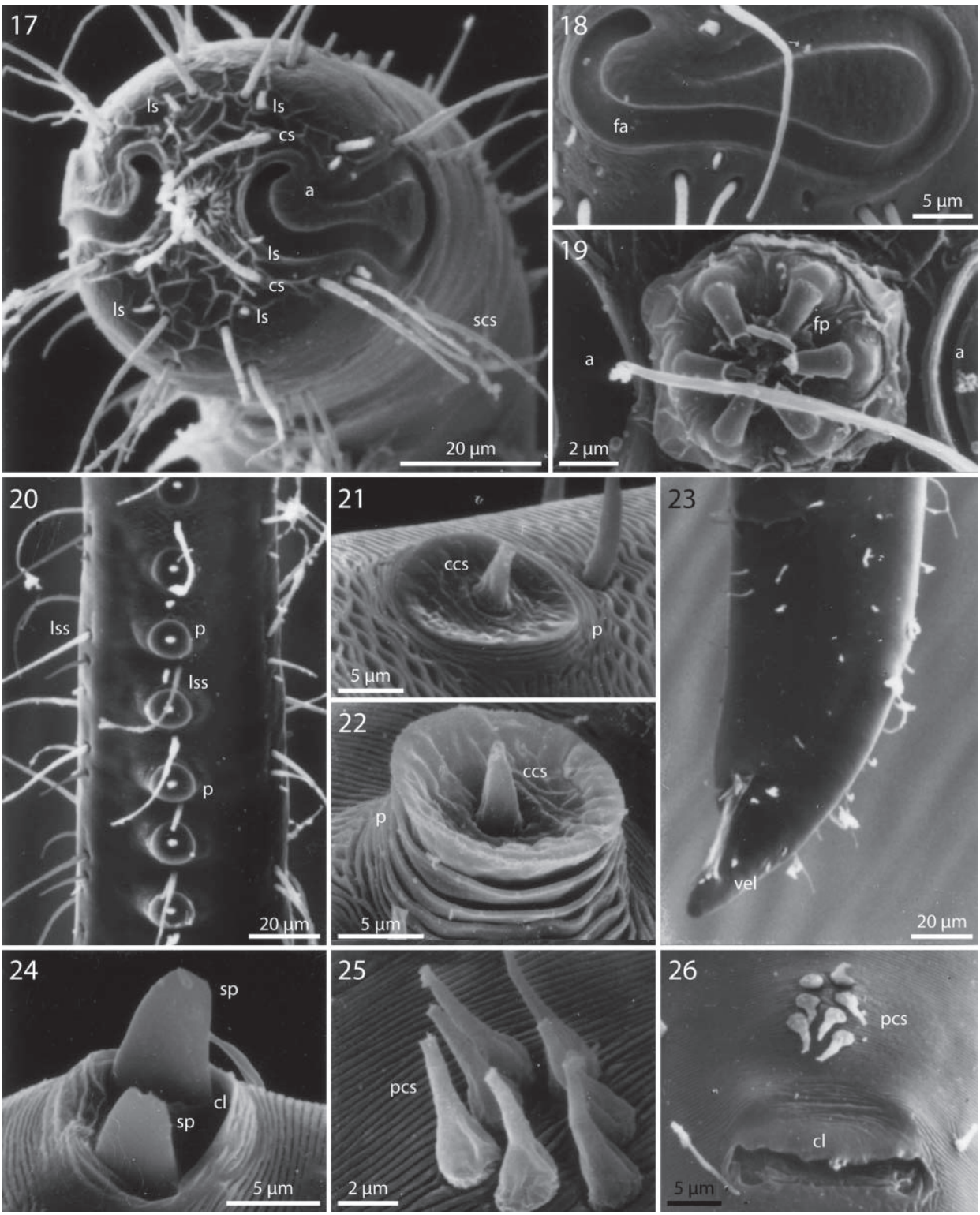

Figs. 17–26. *Robbea hypermnestra* sp. nov. Male. **17**. Head, in face view; **18**. Amphidial fovea; **19**. Mouth opening with fingerlike papillae; **20**. Row of ventral sucker-shaped papillae; **21**. Papilla withdrawn; **22**. Papilla extended; **23**. Tail; **24**. Tips of spicule protruding from cloaca; **25**. Group of precloacal setae; **26**. Cloaca and precloacal setae. SEM.

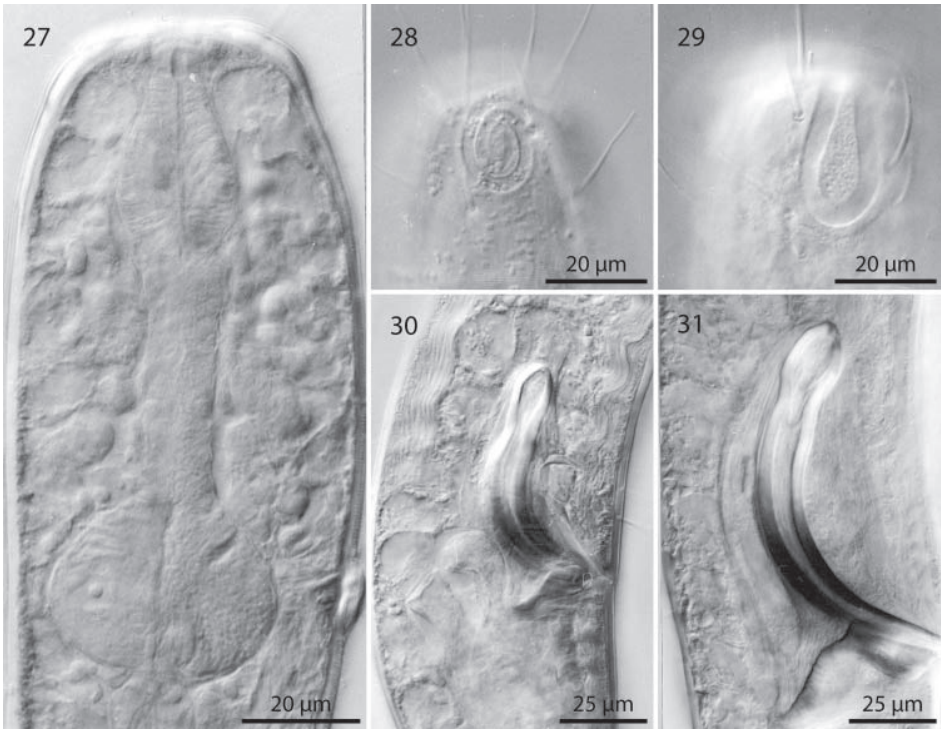

Figs. 27–31. *Robbea hypermnestra* sp. nov. **27**. Pharyngeal region, optical section; **28**. Female, amphidial fovea; **29**. Male, amphidial fovea; **30**. Female, spiculum; **31**. Male, spiculum. LM Interference contrast.

annules 0.5–0.65 μm wide (15–20 annuli/10 μm) (Figs 39, 42); head with a circle of 6 finger-like inner labial papillae surrounding the mouth opening (Fig. 38); 6 short outer labial sensillae, 2.5–4 μm long, at the margin of the membranous buccal field; 4 cephalic setae, flanking the anterior margin of the amphidial fovea, 21–27 μm long (Figs 33, 34, 37); a first circle of 8 subcephalic setae at the level of the amphidial fovea, a second circle approximately in the middle, a third circle at the posterior margin of the cephalic capsule; subcephalic setae, 18–27 μm long, 8 rows of somatic setae along the whole length of the body. Somatic setae of males in the region of the row of ventral papillae stout, 12–17 μm long, the following body setae thinner and shorter (8–13 μm). There is a transverse row of precloacal setae a short distance anterior to the cloacal opening (Figs 36, 42, 43). Somatic setae of females in cervical region 12–15 μm long, the following body setae 17–20 μm long. Males with a 250–320 μm long row of 15–17 conspicuous mid-ventral cuticularized papillae (Figs 34, 40), first papilla situated a short distance posterior to the end of the pharynx. Papillae with short annulated stalks, bearing central conical setae (Fig. 41). The non-striated part of the tail bears no terminal setae, in males there is a velum present (Figs 42, 44). Loop-shaped amphidial foveas (7–12 μm long, 10–12 μm wide), situated at the anterior end bordering the buccal field, with only slight sexual dimorphism.

Pharynx 72–90 μm long; minute tubular buccal cavity, 10–15 μm long and 2–4 μm in diameter, leading into a conspicuous pyriform muscular corpus, 22–30 μm long and 16–18 μm wide, clearly set off from the following 24–41 μm long isthmus. Spherical bulb, 12–18 μm long and 17–20 μm wide, mainly glandular and containing only weak muscles. No cardia (Figs 33, 34, 45).

Nerve ring 42–60 μm from anterior end; no secretory-excretory pore or ventral gland seen; there are 8 rows of glandular sense organs (two in each lateral and each median line) connecting to the small somatic setae.

Males monorchic, testis on the left side of the intestine, beginning at about 35% of body length; spicula strong, arcuate, distinctly cephalate proximally, 60–66 μm (chord) or 72–85 μm (arc) long, without velum; gubernaculum simple, embracing the distal part of the spicula laterally, with dorsally directed apophysis (35–37 μm long) (Figs 36, 47). Females didelphic, ovaries reflexed, long uteri leading to the vagina; vulva at 52–54 of body length.

A dense monolayer of rod-shaped symbiotic bacteria (Fig. 39) covers almost the whole body, beginning at the level of the pharyngeal terminal bulb or at the level of the posterior region of the cup-shaped cervical papillae (Fig. 46) and terminating with the cuticle striation at the tail tip or already at the level of the cloacal opening.

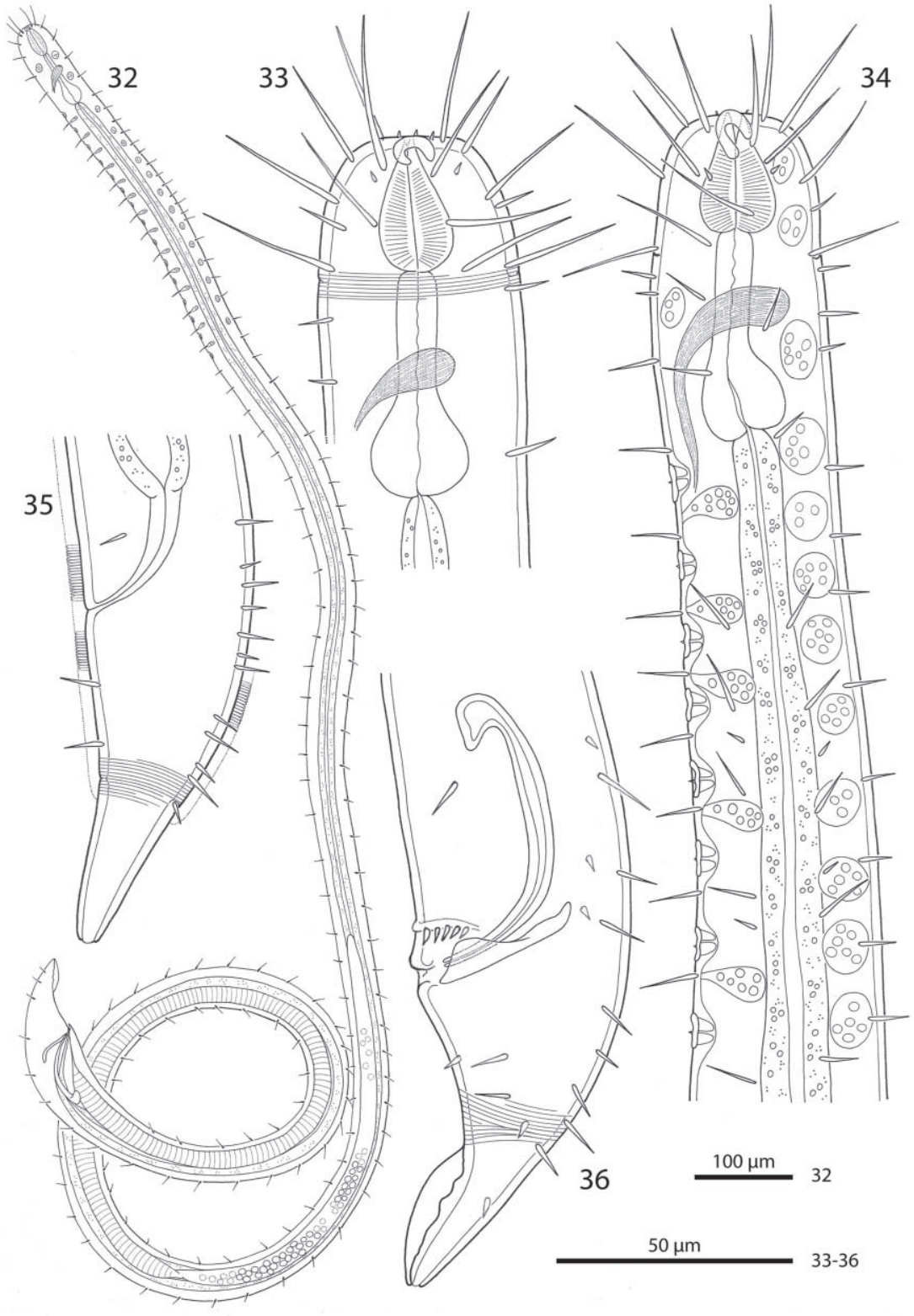

Figs. 32–**36.** *Robbea ruetzleri* sp. nov. **32**. Male, whole; **33**. Female, anterior body region; **34**. Male, anterior body region; **35**. Female, tail; **36**. Male, tail and spicular apparatus.

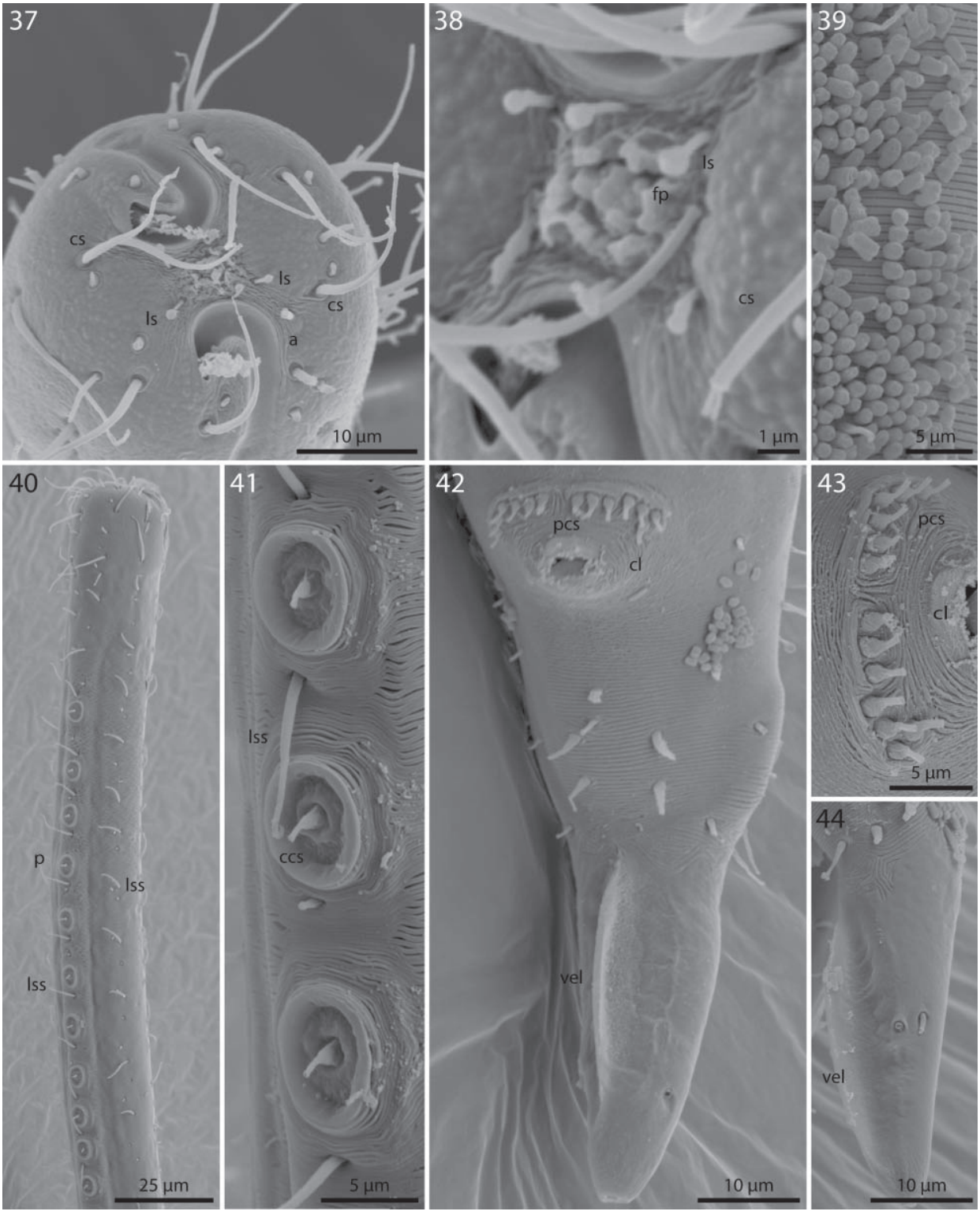

Figs. 37–44. *Robbea ruetzleri* sp. nov. **37**. Male, head in face view; **38**. Mouth opening with fingerlike papillae and circle of outer labial sensillae; **39**. Annulation and bacterial coat in midbody region; **40**. Male, anterior body region with row of sucker-shaped papillae; **41**. Male, detail of papillae; **42**. Male, tail, cloaca and precloacal setae; **43**. Precloacal setae; **44**. Male, Tip of tail with velum. SEM.

Table 2. Morphometric data for *Robbea ruetzleri* sp. nov. Ranges are given for the male and female paratypes. All measurements are in μm.

	Holotype	Paratypes (male) n = 3	Paratypes (female) n = 3
Length	2320	2280–3150	2750–3790
a	58.0	57.0–78.8	54.6–70.2
b	30.9	27.8–31.5	33.5–45.1
c	18.9	23.8–47.0	37.2–40.8
maximum width	40	40–45	50–60
pharynx length	75	72–90	72–78
tail length	72	70–88	69–75
nerve ring (% pharynx length)	53	55–60	55–58
corresponding body diameter (cbd)	38	35–40	38–42
bulbus length /width	12 /17	15–17 /19–20	12–18 /18–20
bulbus cbd	35	34–39	33 –39
V	n.a.	n.a.	52–54
vulva cbd	n.a.	n.a.	50–60
anal (cloacal) body diameter	40	40–45	32–40
tail length:anal diameter	1.8	1.8–2.0	1.7–2.2
spiculae length arc /chord	75 /60	72–85 /60–66	n.a.
gubernaculum length	35	36–39	n.a.
amphid width	10	10–12	10–12
cephalic setae number /length	4 /23	4 /21–27	4 /22–27
subcephalic setae 1 number /length	8 /26	8 /25–26	8 /23–27
subcephalic setae 2 number /length	8 /23	8 /20–22	8 /18–22
Sucker-like papillae, number	15	15–17	n.a.
Position of first /last papilla	72 /315	80–105 /305–415	n.a.

n.a. = not applicable.

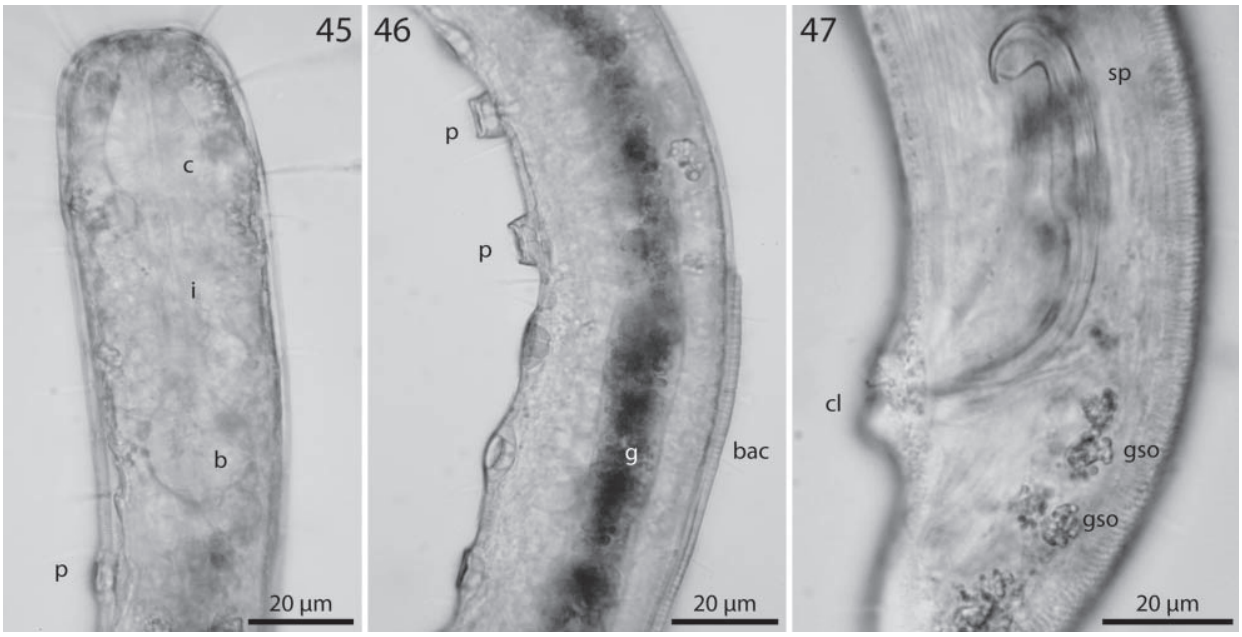

Figs. 45–47. *Robbea ruetzleri* sp. nov. **45**. Pharyngeal region, optical section; **46**. Male, sucker-shaped papillae and begin of bacterial coat; **47**. Male, spiculum. LM of live animals.

Rows or plaques of smaller cocci stretch forward up to the anterior bulbus of the pharynx, but not up to the non-striated part of the head.

Diagnosis. Species with indistinct cephalic capsule; 14−17 cup-shaped stalked ventral papillae in the post pharyngeal region; pharynx almost equally divided into corpus, isthmus and bulbus; spicula strongly cephalate, gubernaculums without apophysis; amphidial fovea in both sexes open loop-shaped. Symbiotic bacteria rod shaped.

Robbea agricola sp. nov.
urn:lsid:zoobank.org:act:97995BAA-7914-4578-A4DE-64ED0DEF761B

Type material. Holotype (male), 3 paratypes (male), 3 paratypes (female).

Additional material. Several specimens in the authors' collection and those used for SEM.

Measurements. See Table 3.
The sequence of the 18S rRNA gene is available from GenBank and has the accession number KJ414464.

Type locality. West side of Twin Cayes, Belize; shallow fine sand among *Rhizophora mangle* stilt roots and *Thalassia testudinum* beds (Fig. 1).

Distribution. Regularly in fine sand samples at several locations in the vicinity of the CBC laboratory (Fig. 1).

Etymology. Agricola (lat.) = farmer (German 'Bauer'), named after Monika Bright (then Monika Bauer) who provided the first specimens.

Description

Body slender, cylindrical (Figs 48, 49), tapering only slightly towards anterior end, head diameter at level of cephalic setae 18−25 μm, diameter at level of posterior margin of amphidial fovea 20−29 μm, at end of pharynx 25−33 μm, maximum body diameter 33−42 μm, anal diameter 24−35 μm. Tail conical, 70−105 μm long; non-striated tail tip 17−19 μm long in males and 23−30 μm in females (Figs 52, 53, 62).

Cuticle finely transversely striated except 24−28 μm of the anterior part of the head (cephalic capsule) and the tail tip, annules 0.6 to 0.7 μm wide (14−17 annuli/10 μm) (Fig. 57). Mouth opening surrounded by 6 finger-like inner labial papillae in lateral, subventral and subdorsal position (Fig. 56) followed by a circle of 6 short labial sensillae, 3−4 μm long, surrounding the membranous buccal field; a circle of 4 cephalic setae flanking the anterior margin of the amphidial fovea, 20−22 μm long; closely followed by a circle of 8 subcephalic setae, 16−26 μm long, a second circle near the end of the cephalic capsule (Figs 50, 51, 55); 8 rows of somatic setae along the whole length of the body, 5−8 μm long; a pair of 6−8 μm long setae at the begin of the non-striated part of the tail. No special precloacal setae. Mid-ventral line of males with a 150−170 μm long row of 8−9 conspicuous cup-shaped papillae (diameter 7 μm) positioned on short stalks. Papillae with central setae (1.5 μm long) (Figs 51, 59, 60). The first of these papillae is situated at a distance of 70−110 μm from the anterior end at the level of the pharyngeal terminal bulb. Amphidial foveas spiral with 2.5 turns, slight sexual dimorphism: in females oval, 12−13 μm long and 8−12 μm wide, situated directly at the anterior end bordering the buccal field; in males larger, somewhat elongated, 15−16 μm long, 12−14 μm wide, 1−4 μm from the anterior end (Figs 50, 51, 64).

A minute tubular buccal cavity, 7−10 μm long and 2−3 μm in diameter, leading into a tripartite, 60−95 μm long pharynx consisting of an anterior pyriform muscular corpus (19−30 μm long, 12−18 μm wide), the following isthmus (30−50 μm long) and the terminal bulb (12−18 μm long, 17−20 μm wide). Terminal bulb largely glandular, containing only weak muscles. No cardia (Figs 50, 51, 63, 69).

Nerve ring 44−67 μm from anterior end; no secretory-excretory pore or ventral gland seen; 8 rows of glandular sense organs (two in each lateral and each median line) connecting to the small somatic setae.

Males monorchic, testis on the left side of the intestine, beginning at about 35% of body length; spicula strong, arcuate, slightly cephalate proximally, 35−45 μm (chord) or 55−58 μm (arc) long, with a velum; gubernaculum with a strong dorso-caudal directed apophysis (13−15μm long) ending in a spherical swelling (Figs 53, 54, 65).

Females didelphic, ovaries reflexed, long uteri leading to the vagina, ventral gso enlarged in the region of the uteri; vulva at 52−55% of body length.

Epigrowth of symbiotic bacteria starting at a defined line at a distance from the anterior end (Figs 66, 67) showing a sexual dimorphism: in males the bacterial coat begins at 220−340 μm (2.7−3.5 pharynx length), in females at 155−195 μm (2−2.3 pharynx length). A monolayer of corn-kernel shaped bacteria (1.5 × 0.8 μm) (Figs 57, 58) covers the remaining body except the non-striated tip of the tail. At the start of the coat the body diameter abruptly becomes smaller to accommodate the thickness of the bacterial layer without increasing the consortium's diameter (Fig. 67). In some specimens patches of bacteria occur around the cup-shaped papillae; here rods lie parallel to the cuticle surface (Fig. 61). Occasionally larger coccoid bacteria are found on the normally symbiont-free anterior body part (Fig. 68). The role of these bacteria is unknown.

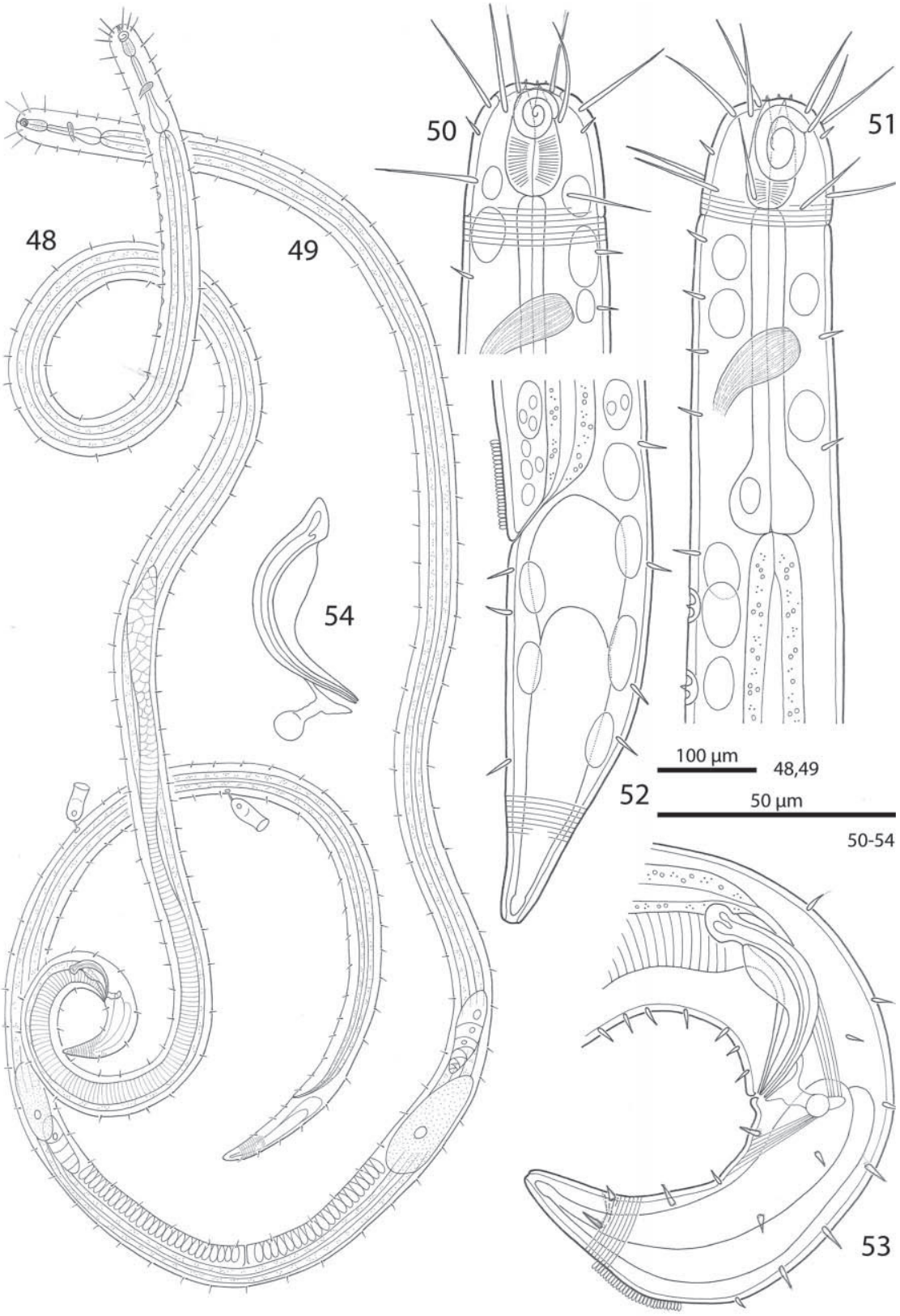

Figs. 48–**54.** *Robbea agricola* sp. nov. **48**. Male, total; **49**. Female, total; **50**. Female, head region; **51**. Male, anterior body region; **52**. Female, tail; **53**. Male, tail; **54**. Spicular apparatus.

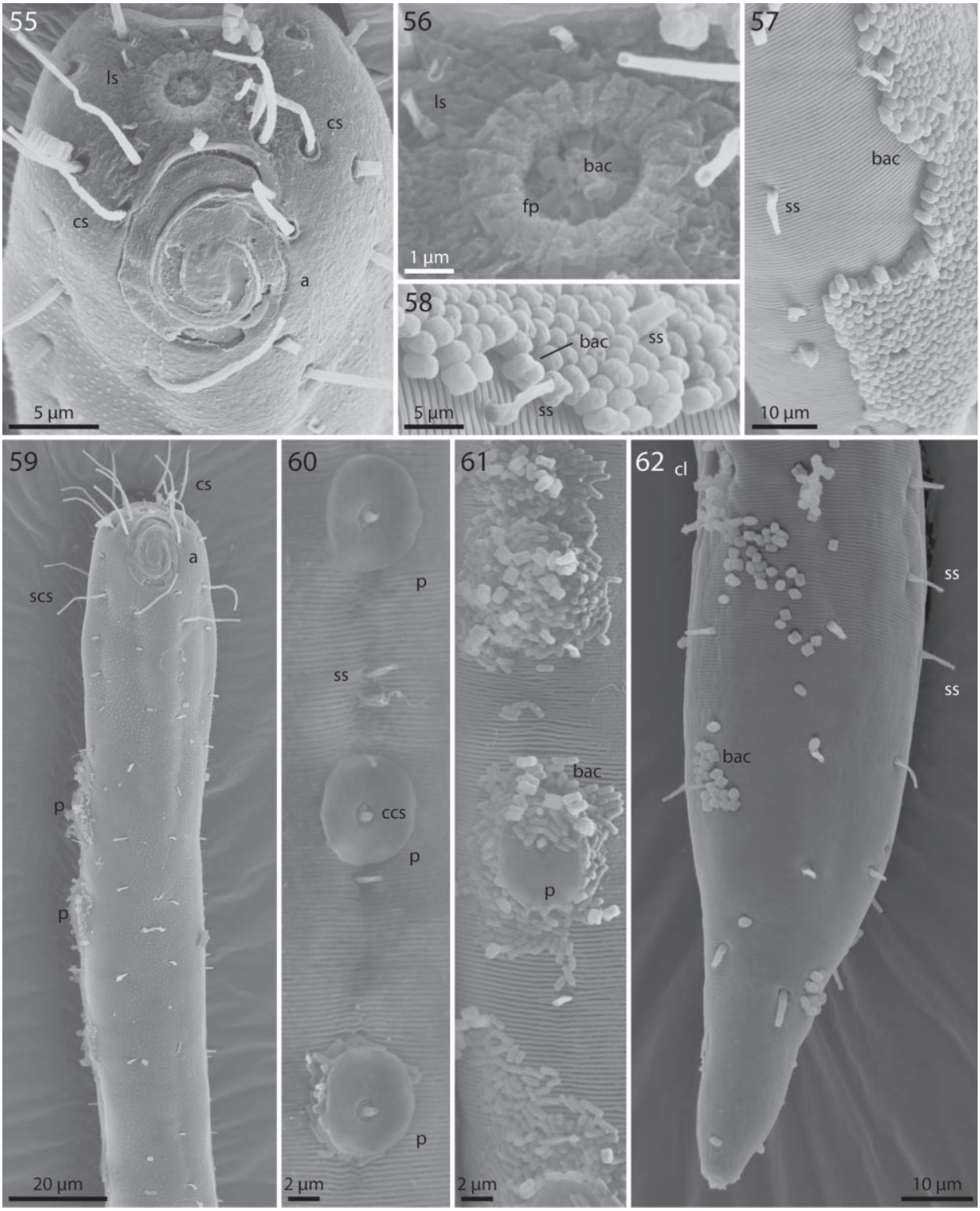

Figs. 55–62. *Robbea agricola* sp. nov. **55**. Male, head in face view; **56**. Mouth opening with fingerlike papillae; **57**. Annulation and bacterial coat in midbody region; **58**. Coat of corn-kernel shaped bacteria; **59**. Male, anterior body region with the first part of the row of sucker-shaped papillae; **60**. Papillae; **61**. Papillae surrounded by bacterial growth; **62**. Female, tail. SEM.

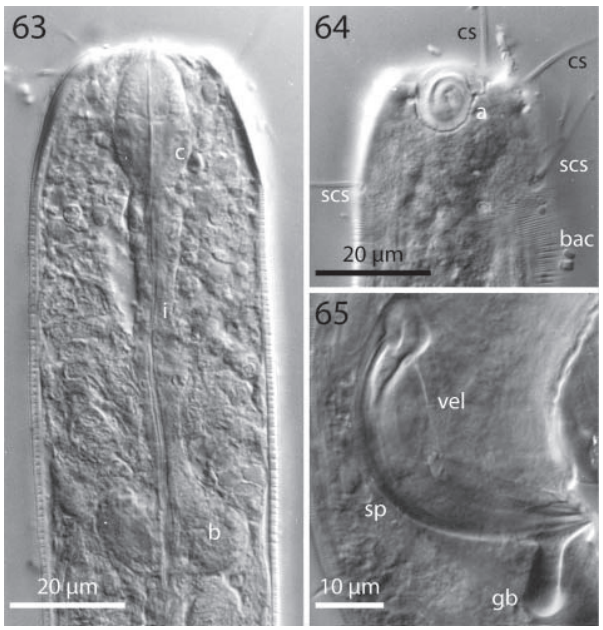

Figs. 63–65. *Robbea agricola* sp. nov. 63. Pharyngeal region, optical section; **64**. Male, amphidial fovea; **65**. Male, spiculum. LM Interference contrast.

Suctorians are frequently attached to the cuticle in the posterior body region (Fig. 49).

Diagnosis. Species with indistinct cephalic capsule; 8–9 cup-shaped ventral papillae in post-pharyngeal region; isthmus occupies more than 50% of pharynx length; spicula cephalate with velum, gubernaculums with dorso-caudal apophysis ending in a spherical swelling; amphidial fovea spiral in both sexes, larger in males. Symbiotic bacteria corn-kernel shaped, bacterial coat starting at a defined line 2 to 3.5 pharynx lengths from the anterior end.

Discussion

Systematics

Gerlach (1956) erected the genus *Robbea* for a male animal collected on the coast of Brazil, which he named *Robbea caelestis*. A second species was subsequently described from the Maldive Islands by the same author, *Robbea tenax* Gerlach (1963). The material consisted of one female and three males, the latter showing conspicuous cervical papillae. Both *Robbea* species were later placed into the genus *Catanema* Cobb, 1920 by Platt & Zhang (1982). Recently Tchesunov (2013) proposed diagnoses for both *Robbea* and *Catanema* in which the major distinguishing character is the shape of the amphidial fovea, which is distinct in *Robbea* but is reduced to a small apical opening in *Catanema*. Other characters such as the degree to which the pharyngeal corpus is set off from the isthmus, 'clearly' in *Robbea*, 'distinctly' in *Catanema* (see Fig. 70 for the situation in *Robbea hypermnestra*), and the presence (*Robbea*) or absence (*Catanema*) of a cephalic capsule are less clear and not all descriptions published so far contain explicit statements regarding these characters. According to Tchesunov's criteria, the

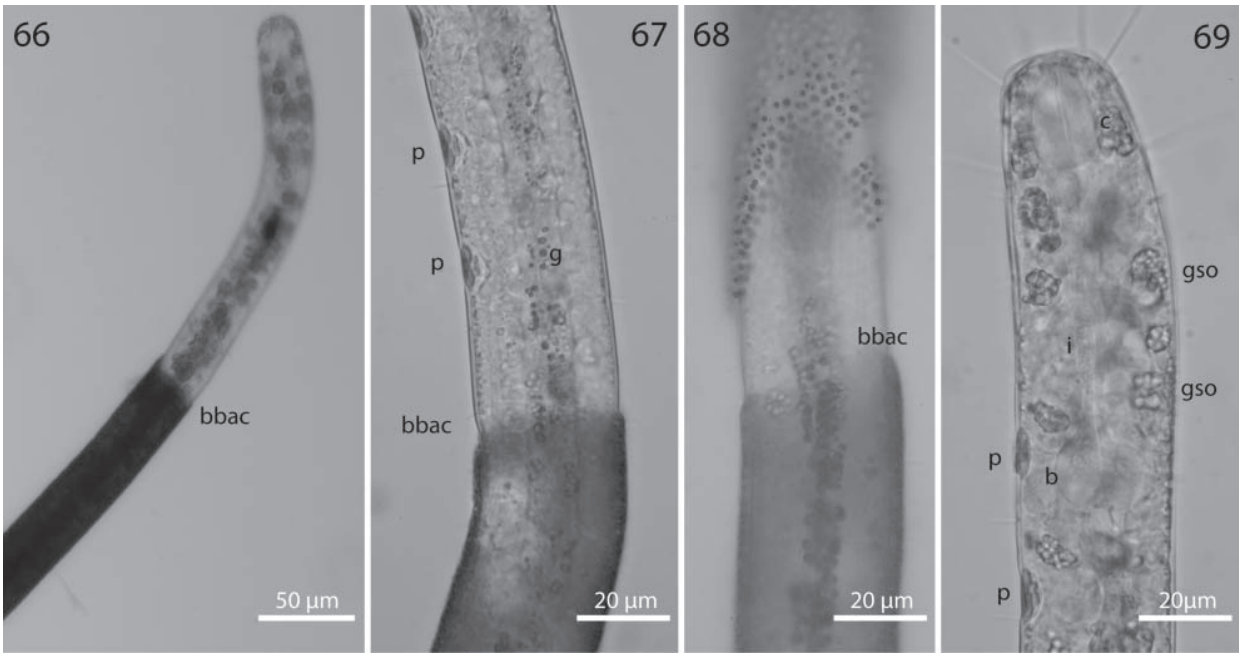

Figs. 66–69. *Robbea agricola* sp. nov. **66**. Anterior body region and beginning of bacterial coat; **67**. Beginning of bacterial coat, detail; **68**. Large cocci on anterior body region; **69**. Glandular sensory organs. LM of live animals.

Table 3. Morphometric data for *Robbea agricola* sp. n. Ranges are given for the male and female paratypes. All measurements are in μm.

	Holotype	Paratypes (male) n = 3	Paratypes (female) n = 3
Length	1880	1780–2550	2280–2550
a	47.0	40.0–54.3	57.0–68.2
b	19.8	19.6–28.7	28.0–37.4
c	22.1	18.8–21.3	27.3–29.6
maximum width	40	33–38	35–42
pharynx length	95	60–75	80–90
tail length	85	78–105	70–85
nerve ring (% pharynx length)	57	53–60	53–62
corresponding body diameter (cbd)	30	28–35	30–32
bulbus length /width	15 /20	12–15 /17–18	12–15 /18–20
bulbus cbd	30	25–32	28–33
V	n.a.	n.a.	52–55
vulva cbd	n.a.	n.a.	35–42
anal (cloacal) body diameter	30	30–35	24–30
tail length:anal diameter	2.8	2.6–3.3	2.3–3.5
spiculae length arc /chord	55 /40	45–58 /35–45	n.a.
gubernaculum length /apophysis length	15 /15	10–12 /10–13	n.a.
amphid width	16	12–14	8–12
cephalic setae number /length	4 /21	4 /20–21	4 /21–22
subcephalic setae 1 number /length	8 /20	8 /16 –20	8 /20–26
subcephalic setae 2 number /length	8 /16–18	8 /13–16	8 /18–22
Sucker-like papillae, number	9	9	n.a.
Position of first /last papilla	90 /260	70–98 /225–268	n.a.

n.a. = not applicable.

following species belong to the genus *Robbea*: *R. caelestis* Gerlach 1956, *R. tenax* Gerlach 1963, *R. gallica* Vitiello 1974, R. (*Catanema*) *porosum* Hopper & Cefalu 1973, *R.* (*Catanema*) *macintyrei* Platt & Zhang 1982, *R.* (*Catanema*) *smo* Platt & Zhang 1982, furthermore the animal that Hopper & Cefalu (1973) described as *R. tenax* from Florida and the three new species described herein. *R. gerlachi* Boucher 1975 has only been described from a female, but according to the shape of its amphidial fovea it should be placed into the genus *Robbea.* One additional species of *Robbea* has been suggested by Tchesunov (2013), but due to the lack of male specimens the species has not been described in detail yet.

In the genus *Catanema* only two formally described species remain, the type species *C. exile* Cobb 1920 and *C. dambayensis* Tchesunov 2013. *Catanema cobbi* Inglis 1967 has been placed into the genus *Laxus* by Ott *et al.* (1995), *Catanema gerlachi sensu* Hopper & Cefalu 1973 most probably belongs to *Laxus cosmopolitus* (Ott *et al.*, 1995).

To consolidate the taxonomic descriptions of the three newly described *Robbea* species on a molecular level we used phylogenetic 18S rRNA analyses. The tree shows a clear separation between the clade containing the three new *Robbea* species and the other Stilbonematinae (Fig. 71). We also provide additional 18S rRNA gene sequences for the genera *Catanema* and *Leptonemella* that only had a single 18S rRNA gene deposited prior to this study. The morphological characters of the three yet undescribed *Catanema* species included in the phylogenetic analyses conform to the diagnosis given by Tchesunov (2013). Our data confirm that both *Robbea* and *Catanema*, as well as all other genera of Stilbonematinae with available sequence data are represented by statistically supported genus level clades in 18S rRNA gene based phylogenetic analyses. This high resolution of the 18S rRNA gene finally allows to assign or to re-evaluate the correct taxonomic affiliation at the genus level for new or already deposited sequences.

For the moment this ends the confusion around these two genera to which we have added by assigning two stilbonematine species to the genus *Robbea* (namely *Robbea* sp. 1 and 2) in Bayer *et al.* (2009). We have reinvestigated the nematode material used in that paper where possible. In the case of *Robbea* sp. 1 from Calvi (Corse), there obviously had been a mix-up during the sample sorting, and

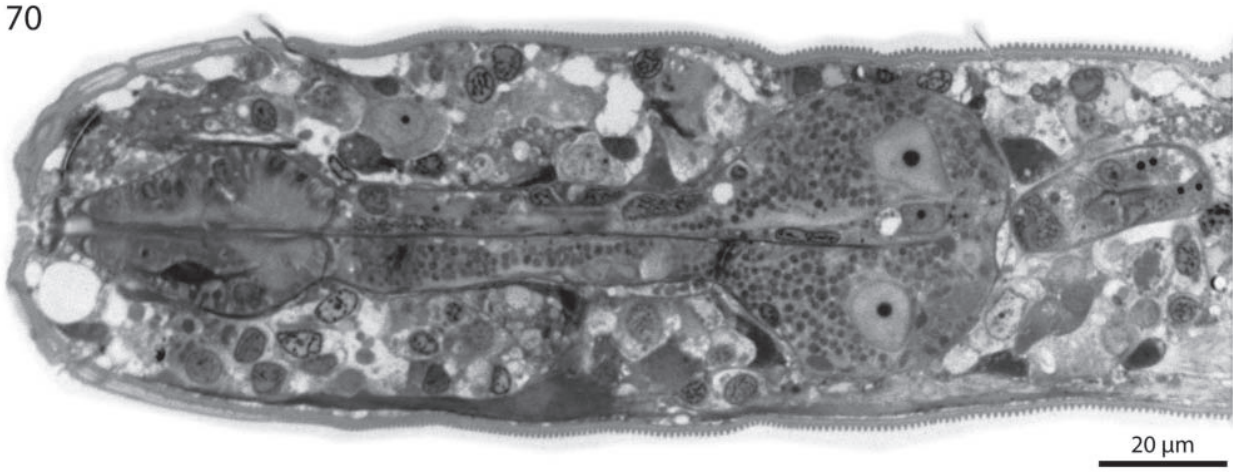

Fig. 70. *Robbea hypermnestra* sp. nov. Semi-thin longitudinal section through pharynx showing separation of corpus from isthmus and glandular bulbus.

two different nematode species were present in the sample analysed: a *Laxus* sp. that is morphologically indistinguishable from *Laxus cosmopolitus* described from the Adriatic (Ott *et al*., 1995) and a yet undescribed *Catanema* species. Judging from the phylogenetic position of the deposited 18S rRNA gene, a specimen of the former species was probably sequenced. *Robbea* sp. 2 from the Cayman Islands is a member of the *Catanema* clade (Fig. 71). *Robbea* sp. 3 is morphologically and phylogenetically identical to the newly sequenced *Robbea hypermnestra* sp. nov. specimens (Fig. 71). The 18S sequences for *Robbea hypermnestra* sensu Kampfer 1998 (*nomen nudum*) that were formerly deposited under Y19621 were identified as chimeric but the last 600 bp are identical to the correct *Robbea hypermnestra* sp. nov. sequences from this study as well as to the *Robbea* sp. 3 sequence published by Bayer *et al*. (2009). The sequences in the Kampfer *et al*. (1998) paper were generated from pools of up to 50 nematodes that likely were contaminated by other nematode species. Thus, the chimeric nature of the published sequences could likely be attributed to different priming bias in the forward and reverse primers used. In contrast, all sequences generated in the present work come from single nematode specimens. This has been made possible with high-yield DNA extraction methods based on GeneReleaser (Bioventures) (Schizas *et al*., 1997) or the Blood and Tissue kit (Qiagen) combined with highly sensitive and efficient polymerases such as the Phusion® DNA polymerase (Finnzymes). Successful PCR based sequencing of multiple genes from the DNA of a single meiofauna individual has been performed without amplification using specimens as small as 500 μm long microturbellarians (Gruber-Vodicka *et al*., 2011). We thus emphasize that, wherever possible, single individuals should be used for PCR-based gene assays.

While the diagnoses given by Tchesunov (2013) currently hold true for the genera *Robbea* and *Catanema*, they are based on characters such as the reduction of the amphidial foveas. However, these characters are also present in some species of other genera, such as *Stilbonema* and *Leptonemella* (e.g. in the type species *L. cincta* COBB 1920). Findings of new species may make emendation of diagnoses that were based on morphology alone necessary. Our results clearly indicate the necessity to provide molecular data to confirm the morphological identification and that larger taxon sampling is an important factor to be able to validate sequencing results and enable for example barcoding approaches.

Intersexes

Cases of intersexuality have been described from various terrestrial, parasitic or marine nematodes (e.g. Zhuo *et al*., 2009; Moura *et al*., 2014). In the latter, intersexes are most commonly reported as females with a functional reproductive system and rudimentary male sexual characters (e.g. Gourbault & Vincx, 1990; Riemann *et al*., 2003; Zhuo *et al*., 2009; Miljutina *et al*., 2013; Moura *et al*., 2014), just as observed in our newly described *R. hypermnestra*. However, only few intersex individuals are usually found within nematode populations (Gourbault & Vincx, 1990). As driving factor for intersexuality in nematodes, unfavourable environmental conditions (Davide & Triantaphyllou, 1968), hybridization between closely related species (Steiner, 1923; Krall, 1972) or genetic or chromosomal disorder (Roy & Gupta, 1975; Jairajpuri *et al*., 1977) have been hypothesized. Considering the clean and stable environment around Carrie Bow Cay and the fact that all females of *R. hypermnestra* are intersexes, environmental sex determination appears unlikely. We cannot exclude

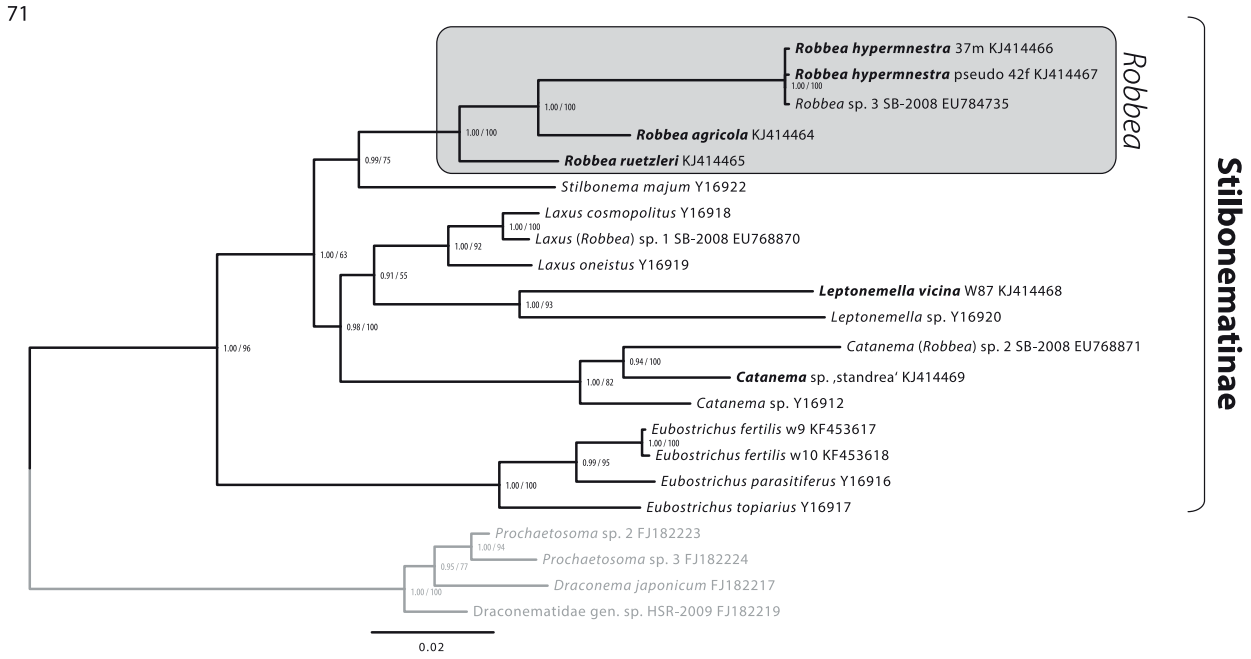

Fig. 71. Phylogenetic relationships of the genera of the Stilbonematinae based on the 18S rRNA gene. The tree shown was calculated using maximum likelihood (RAxML) and node support is given as aLRT as well as Bayesian posterior probabilities. The scale bar indicates 0.02 nucleotide substitutions per site.

hybridization events with closely related species in the past. It is difficult to assign any specific function to the spicula observed in *R. hypermnestra* intersexes and the *R. hypermnestra* chromosome set has not been determined, thus our hypotheses will remain rather speculative. The spicula could be remnants from a previously hermaphroditic lifestyle, but since no hermaphroditic lifestyle is known from stilbonematine nematodes, the interpretations that *R. hypermnestra* females are in a transition to a hermaphroditic stage, is more likely. In fact, individuals of the well-studied terrestrial nematodes *C. elegans* and *C. briggsae* are either male or hermaphrodites where the hermaphrodites are descendants from male or female ancestors and mutations in two independent pathways were sufficient for *C. elegans* to develop self-fertile hermaphrodites (Baldi *et al.*, 2009). This indicates a high plasticity and flexibility in the expression of sexual phenotypes in nematodes in general. Hermaphroditism could be favourable at low effective population densities to ensure reproduction in the absence of a mating partner (Pires-DaSilva, 2007). To test whether this is the case, the distribution patterns and gender ratios of the *R. hypermnestra* populations need to be monitored systematically.

Ecological notes

The shallow subtidal sands around Carrie Bow Cay harbour a diverse interstitial meiofauna. Among these are representatives of several taxa known to harbour bacterial symbionts. These include the ciliate genus *Kentrophoros*, the mouthless nematode genus *Astomonema* (authors' unpublished observation), several species of the mouthless catenulid flatworm genus *Paracatenula* (Dirks *et al.*, 2011; Gruber-Vodicka *et al.*, 2011) and the gutless marine oligochaete genera *Inanidrilus* and *Olavius* (Erséus, 1990). So far, stilbonematid nematode species of several genera have been described from shallow water habitats around Carrie Bow Cay. These include *Laxus oneistus*, *Stilbonema majum*, *Adelphus rolandi*, *Eubostrichus dianae*, *E.parasitiferus* and *E. fertilis* (Ott *et al.*, 1995, 2014; Ott, 1997; Kampfer *et al.*, 1998; Polz *et al.*, 1999). We add to this diversity with our description of three new *Robbea* species that live in vicinity of Carrie Bow Cay (Fig. 1). Available physiological and molecular evidence shows that all (*Paracatenula*, Stilbonematinae) or the majority of bacterial symbionts (oligochaetes) are sulphur-oxidizing chemoautotrophs (SOBs) (Dubilier *et al.*, 2006; Bayer *et al.*, 2009; Gruber-Vodicka *et al.*, 2011). Associations of SOBs with motile hosts appear to be beneficial when oxygen-containing surface layers are spatially separated from sulphidic deeper layers and vertical migration by the host can alternately supply the symbiotic bacteria with sulphide and oxygen (Giere *et al.*, 1991; Ott *et al.*, 1991).

Shallow sandbars in the immediate back reef area of Carrie Bow Cay consist of coarse to medium, unsorted carbonate sand of local origin that has been deposited under sheltered conditions and has a spacious interstitium with reduced, sulphidic conditions in layers several

centimetres below the sediment surface (Ott & Novak, 1989). Here large species of Stilbonematinae (*Laxus oneistus*, *Stilbonema majum*) and also *R. hypermnestra* are found in high densities (Ott & Novak, 1989). In contrast, a diverse assemblage of smaller Stilbonematinae species such as *E. dianae*, *E. fertilis*, *R. agricola* and *R. ruetzleri* inhabit the fine sands in the vicinity of lagunal mangrove islands and *Thalassia testudinum* seagrass beds (Ott *et al.*, 2014). Additionally to the described species, several undescribed species and possibly genera of stilbonematine nematodes can be found in the shallow water habitats in the vicinity of Carrie Bow Cay (authors' pers. observation).

Acknowledgements

We thank Werner Urbancik, Veronica Novotny and Monika Bright for providing several micrographs and Sigrid Neulinger for executing the ink drawings. We gratefully acknowledge the generous help of Klaus Ruetzler and the staff of the Carrie Bow Cay Laboratory. We are grateful to the Core Facility Cell Imaging and Ultrastructure Research of the University of Vienna for technical support and the Max Planck Society for funding. This is contribution # 962 from the Carrie Bow Cay Laboratory (CCRE Program of the National Museum of Natural History, Washington, DC). N.L. was supported by an Austrian Science Fund (FWF) grant P22470-B17 (S. Bulgheresi, PI) and H.R. G.-V. by a Marie-Curie Intra-European Fellowship PIEF-GA-2011-301027 CARISYM.

References

Baldi, C., Cho, S. & Ellis, R.E. 2009. Mutations in two independent pathways are sufficient to create hermaphroditic nematodes. *Science* **326**, 1002–1005.

Bauer-nebelsick, M., Blumer, M., Urbancik, W. & Ott, J.A. 1995. The glandular sensory organ of Desmodoridae (Nematoda) – ultrastructure and phylogenetic implications. *Invertebrate Biology* **114**, 211–219.

Bayer, C., Heindl, N.R., Rinke, C., Lücker, S., Ott, J.A. & Bulgheresi, S. 2009. Molecular characterization of the symbionts associated with marine nematodes of the genus *Robbea*. *Environmental Microbiology Reports* **1**, 136–144.

Boucher, G. 1975. Nématodes des sables fins infralittoraux de la Pierre Noire (Manche occidentale). I. Desmodorida. *Bulletin du Muséum National d'Histoire Naturelle, Paris 3e série* **285**, 101–128.

Bulgheresi, S., Schabussova, I., Chen, T., Mullin, N.P., Maizels, R.M. & Ott, J.A. 2006. A new C-type lectin similar to the human immunoreceptor DC-SIGN mediates symbiont acquisition by a marine nematode. *Applied and Environmental Microbiology* **72**, 2950–2956.

Bulgheresi, S., Gruber-vodicka, H.R., Heindl, N.R., Dirks, U., Kostadinova, M., Breiteneder, H. & Ott, J.A. 2011. Sequence variability of the pattern recognition receptor Mermaid mediates specificity of marine nematode symbioses. *International Society of Microbial Ecology Journal* **5**, 986–998.

Cobb, N. 1920. One hundred new nemas (type species of 100 new genera). *Contributions to a Science of Nematology* **9**.

Davide, R. & Triantaphyllou, A. 1968. Influence of the environment on development and sex differentiation of root-knot nematodes. *Nematologica* **14**, 37–46.

Dirks, U., Gruber-vodicka, H.R., Leisch, N., Sterrer, W. & Ott, J.A. 2011. A new species of symbiotic flatworms, *Paracatenula galateia* sp. nov. (Platyhelminthes: Catenulida: Retronectidae) from Belize (Central America). *Marine Biology Research* **7**, 769–777.

Drummond, A., Ashton, B., Buxton, S., Cheung, M., Cooper, A., Duran, C., Field, M., Heled, J., Kearse, M., Markowitz, S., Moir, R., Stones-havas, S., Sturrock, S., Thierer, T. & Wilson, A. 2011. *Geneious* v5.5. http://www.geneious.com/ (accessed 18 June 2014).

Dubilier, N., Blazejak, A. & Rühland, C. 2006. Symbioses between bacteria and gutless marine Oligochaetes. In: Overmann, J., Ed., *Molecular Basis of Symbiosis*. Springer Berlin, Heidelberg, Germany, pp. 251–275.

Erséus, C. 1990. The marine Tubificidae (Oligochaeta) of the barrier reef ecosystems at Carrie Bow Cay, Belize, and other parts of the Caribbean Sea, with descriptions of twenty-seven new species and revision of Heterodrilus, Thalassodrilides and Smithsonidrilus. *Zoologica Scripta* **19**, 243–303.

Gerlach, S.A. 1956. Die Nematodenbesiedlung des tropischen Brandungsstrandes von Pernambuco. Brasilianische Meeres-Nematoden II, *Kieler Meeresforschungen* **12**, 202–218.

Gerlach, S.A. 1963. *Robbea tenax* sp. n., ein merkwürdiger mariner Nematode von den Malediven. *Internationale Revue der gesamten Hydrobiologie und Hydrographie* 48, 153–158.

Giere, O., Conway, N., Gastrock, G. & Schmidt, C. 1991. "Regulation" of gutless annelid ecology by endosymbiotic bacteria. *Marine Ecology Progress Series* **68**, 287–299.

Gourbault, N. & Vincx, M. 1990. Chromadorida (Nematoda) from Guadeloupe and Polynesia with evidence of intersexuality. *Zoologica Scripta* **19**, 31–37.

Gruber-vodicka, H.R., Dirks, U., Leisch, N., Baranyi, C., Stoecker, K., Bulgheresi, S., Heindl, N.R., Horn, M., Lott, C., Loy, A., Wagner, M. & Ott, J. 2011. *Paracatenula*, an ancient symbiosis between thiotrophic Alphaproteobacteria and catenulid flatworms. *Proceedings of the National Academy of Sciences USA* **108**, 12078–12083.

Heindl, N.R., Gruber-vodicka, H.R., Bayer, C., Lücker, S., Ott, J.A. & Bulgheresi, S. 2011. First detection of thiotrophic symbiont phylotypes in the pelagic marine environment. *Federation of European Microbiological Society Microbiology Ecology* **77**, 223–227.

Hopper, B.E. & Cefalu, R.C. 1973. Free-living marine nematodes from Biscayne Bay, Florida V. Stilbonematinae: contributions to the taxonomy and morphology of the genus *Eubostrichus* Greeff and related genera. *Transactions of the American Microscopical Society* **92**, 578–591.

Inglis, W. 1967. Interstitial nematodes from St Vincent's Bay New Caledonia. *Editions de la Fondation Singer-Polignac, Paris, France*, 29–74.

Jairajpuri, M., Ahmad, I. & Ahmad, M. 1977. Record of an intersex of *Aquatides thornei* with remarks on the phenomenon of intersexuality in nematodes. *Indian Journal of Nematology* **7**, 177–181.

Kampfer, S., Sturmbauer, C. & Ott, J.A. 1998. Phylogenetic analysis of rDNA sequences from Adenophorean nematodes and implications for the Adenophorea-Secernentea controversy. *Invertebrate Biology* **117**, 29–36.

Katoh, K., Kuma, K.-I., Toh, H. & Miyata, T. 2005. MAFFT version 5: improvement in accuracy of multiple sequence alignment. *Nucleic Acids Research* **33**, 511–518.

Krall, E. 1972. On the biological background of the intersexuality in the genus *Aphelenchoides* (Nematoda: Tylenchida). *Indian Journal of Nematology* **2**, 206–207.

Miljutina, M.A., Miljutin, D.M. & Tchesunov, A.V. 2013. Seven *Acantholaimus* (Chromadoridae: Nematoda) species from one deep-sea sediment sample (Angola Basin, south-east Atlantic). *Journal of the Marine Biological Association of the United Kingdom* **93**, 935–953.

Moura, J.D.R., da Silva, M.C. & Esteves, A.M. 2014. Four new species of Desmodora (Nematoda) from the deep south-east Atlantic, and a case of intersexuality in Desmodoridae. *Journal of the Marine Biological Association of the United Kingdom* **94**, 85–104.

Nebelsick, M., Blumer, M., Novak, R. & Ott, J.A. 1992. A new glandular sensory organ in *Catanema* sp. (Nematoda, Stilbonematinae). *Zoomorphology* **112**, 17–26.

Ott, J. 1997. A new symbiotic marine nematode, *Adelphos rolandi* gen. n. sp. n.(Stilbonematinae), from the Caribbean Sea. *Annalen des Naturhistorischen Museums in Wien Serie B Botanik und Zoologie* **99**, 417–422.

Ott, J.A. & Novak, R. 1989. Living at an interface: meiofauna at the oxygen/sulfide boundary of marine sediments. In: Ryland, J.S. & Tyler, P.A., Eds., *23rd European Marine Biology Symposium*. Olsen & Olsen, Fredensborg, Denmark, pp. 415–422.

Ott, J.A., Novak, R., Schiemer, F., Hentschel, U., Nebelsick, M. & Polz, M. 1991. Tackling the sulfide gradient: a novel strategy involving marine nematodes and chemoautotrophic ectosymbionts. *Pubblicazioni Stazione Zoologica Napoli I: Marine Ecology* **12**, 261–279.

Ott, J.A., Bauer-nebelsick, M. & Novotny, V. 1995. The genus *Laxus* Cobb, 1894 (Stilbonematinae: Nematoda): description of the two species with ectosymbiotic chemoautotrophic bacteria. *Proceedings of the Biological Society of Washington* **108**, 508–527.

Ott, J.A., Bright, M. & Bulgheresi, S. 2004. Symbioses between marine nematodes and sulfur-oxidizing chemoautotrophic bacteria. *Symbiosis* **36**, 103–126.

Ott, J., Leisch, N. & Gruber-vodicka, H.R. 2014. *Eubostrichus fertilis* sp. n., a new marine nematode (Desmodoridae: Stilbonematinae) with an extraordinary reproductive potential from Belize, Central America. *Nematology*, in press.

Pires-dasilva, A. 2007. Evolution of the control of sexual identity in nematodes. *Seminars in Cell and Developmental Biology* **18**, 362–370.

Platt, H.M. & Zhang, Z.N. 1982. New species of marine nematodes from Loch Ewe, Scotland. *Bulletin of the British Museum (Natural History)/Zoology Series* **42**, 227–246.

Polz, M.F., Felbeck, H., Novak, R., Nebelsick, M. & Ott, J.A. 1992. Chemoautotrophic, sulfur-oxidizing symbiotic bacteria on marine nematodes: morphological and biochemical characterization. *Microbial Ecology* (*Historical Archive*) **24**, 313–329.

Polz, M.F., Distel, D.L., Zarda, B., Amann, R., Felbeck, H., Ott, J.A. & Cavanaugh, C.M. 1994. Phylogenetic analysis of a highly specific association between ectosymbiotic, sulfur-oxidizing bacteria and a marine nematode. *Applied and Environmental Microbiology* **60**, 4461–4467.

Polz, M.F., Harbison, C. & Cavanaugh, C.M. 1999. Diversity and heterogeneity of epibiotic bacterial communities on the marine nematode *Eubostrichus dianae*. *Applied Environmental Microbiology* **65**, 4271–4275.

Polz, M., Ott, J.A., Bright, M. & Cavanaugh, C. 2000. When bacteria hitch a ride. *American Malacological Society News* **66**, 531–539.

Pradillon, F., Schmidt, A., Peplies, J. & Dubilier, N. 2007. Species identification of marine invertebrate early stages by whole-larvae in situ hybridisation of 18S ribosomal RNA. *Marine Ecology Progress Series* **333**, 103–116.

Riemann, F., Thiermann, F. & Bock, L. 2003. *Leptonemella* species (Desmodoridae, Stilbonematinae), benthic marine nematodes with ectosymbiotic bacteria, from littoral sand of the North Sea island of Sylt: taxonomy and ecological aspects. *Helgoland Marine Research* **57**, 118–131.

Ronquist, F. & Huelsenbeck, J.P. 2003. MrBayes 3: Bayesian phylogenetic inference under mixed models. *Bioinformatics* **19**, 1572–1574.

Roy, T. & Gupta, A. 1975. Intersex or sex reversal amongst plant parasitic nematodes. *Acta Morphologica Neerlando–Scandinavica* **13**, 213–218.

Schiemer, F., Novak, R. & Ott, J.A. 1990. Metabolic studies on thiobiotic free-living nematodes and their symbiotic microorganisms. *Marine Biology* (*Berlin*) **106**, 129–137.

Schizas, N.V., Street, G.T., Coull, B.C., Chandler, G.T. & Quattro, J.M. 1997. An efficient DNA extraction method for small metazoans. *Molecular Marine Biology and Biotechnology* **6**, 381–383.

Stamatakis, A. 2006. RAxML-VI-HPC: maximum likelihood-based phylogenetic analyses with thousands of taxa and mixed models. *Bioinformatics* **22**, 2688–2690.

Stamatakis, A., Hoover, P. & Rougemont, J. 2008. A rapid bootstrap algorithm for the RAxML Web servers. *Systematic Biology* **57**, 758–771.

Steiner, G. 1923. Intersexes in Nematodes. *Journal of Heredity* **14**, 147–158.

Tamura, K., Peterson, D., Peterson, N., Stecher, G., Nei, M. & Kumar, S. 2011. MEGA5: Molecular Evolutionary Genetics Analysis using maximum likelihood, evolutionary distance, and maximum parsimony methods. *Molecular Biology and Evolution* **28**, 2731–2739.

Tchesunov, A. V., Ingels, J., Popova, E. V. 2012. Marine free-living nematodes associated with symbiotic bacteria in deep-sea canyons of north-east Atlantic Ocean. Journal of the Marine Biological Association of the United Kingdom **92**, 1257–1271.

Tchesunov, A.V. 2013. Marine free-living nematodes of the subfamily Stilbonematinae (Nematoda, Desmodoridae): taxonomic review with descriptions of a few species from the Nha Trang Bay, Central Vietnam. *Meiofauna Marina* **20**, 71–94.

Urbancik, W., Bauer-nebelsick, M. & Ott, J.A. 1996a. The ultrastructure of the cuticle of Nematoda. *Zoomorphology* **116**, 51–64.

Urbancik, W., Novotny, V. & Ott, J.A. 1996b. The ultrastructure of the cuticle of Nematoda. II. The cephalic cuticle of Stilbonematinae (Adenophorea, Desmodoridae). *Zoomorphology* **116**, 65–75.

van Megen, H., van Den Elsen, S., Holterman, M., Karssen, G., Mooyman, P., Bongers, T., Holovachov, O., Bakker, J. & Helder, J. 2009. A phylogenetic tree of nematodes based on about 1200 full-length small subunit ribosomal DNA sequences. *Nematology* **11**, 927–950.

Vitiello, P. 1974. Nouvelles espèces de Desmodorida (Nematoda) des côtes de Provence. *Tethys* **5**, 137–146.

Winnepenninckx, B., Backeljau, T. & De wachter, R. 1995. Phylogeny of protostome worms derived from 18S rRNA sequences. *Molecular Biology and Evolution* **12**, 641–649.

Zhuo, K., Liao, J., Cui, R. & Li, Y. 2009. First record of female intersex in *Hirschmanniella shamimi* Ahmad, 1972 (Nematoda: Pratylenchidae), with a checklist of intersexes in plant nematodes. *Zootaxa* **1973**, 61–68.

List of abbreviations in figures

a = amphidial fovea
b = pharyngeal bulbus
bac = bacteria
c = pharyngeal corpus
ccs = central conical setae
cg = corpus gelatum
cgo = caudal gland opening
cl = cloaca
cs = cephalic seta
fa = amphidial fovea fovea
fp = finger-like papillae
g = gut
gso = glandular sensory organ
i = pharyngeal isthmus
ls = labial sensillae
lss = long somatic setae
na = non-striated tail tip
p = sucker shaped papillae
pcs = precloacal setae
ss = somatic setae
scs = subcephalic seta
sp = spiculum
ss = somatic setae
ts = terminal seta
vel = velum

Associate Editor: Adrian Glover

Table S1: Stilbonematine nematode distribution: Table combining so far reported findings of stilbonematine nematodes, including taxonomic descriptions, reports and own observations.

Stilbonematine nematode genus	Sampling location	Latitude	Longitude	Reference	remarks
***Catanema* species**					
C. sp.	Elba, Italy	42.80722	10.14111	(Ott *et al.* 2014a)	
Catanema exile	Jamaica	17.940522	-76.817122	(Cobb 1920)	
Catanema	Canary islands	28.164018	-16.429368	(Riera *et al.* 2013)	
Catanema dambayensis	Tre island, Vietnam	12.222757	109.245787	(Tchesunov 2013)	
Catanema	Farol Beach, Brazil	-22.999225	-42.006514	(Da Fonsêca-Genevois *et al.* 2006)	
C. australis	Penguin island, West, Australia	-32.306944	115.691667	(Hourston & Warwick 2010)	
Catanema	Bermuda	32.349385	-64.725177	(Coull 1970)	
Catanema	Baja California, Mexico	31.550000	-114.28333	(Gingold *et al.* 2010)	
Catanema	Magnetic Island, Australia	-19.169404	146.814871	(Fisher 2003; Fisher & Sheaves 2003)	
C. sp.	Punta Francés Reef, Cuba,	21.608244	-83.176222	(Armenteros *et al.*, 2014)	
C. "belize 1", C. "schleife"	CBC, Belize	16.82861	-88.10955	(Zimmermann *et al.,* Chapter III; own observation)	
Catanema sp. (*Robbea* sp. 2)	Cayman Islands	19.70222	-79.96278	(Bayer *et al.*, 2009; Ott *et aL.*, 2014)	
C. sp.	Darwin mounds, 1000m	59.814833	-7.375167	(Van Gaever *et al.* 2004)	
Catanema cobbi	New Caledonia	-21.954191	166.1273	(Inglis 1968; Boucher 1997)	
Catanema porosum	Florida, US	25.497827	-80.307541	(Hopper & Cefalu 1973)	
***Eubostrichus* species**					
E. filiformis	North Sea, Belgium	51.191394	2.776337	(Greeff 1869)	
E. africanus	Intertidal mangroves, Kenya	-4.37345	39.834707	(Muthumbi *et al.* 1995)	
Eubostrichus sp.	Kenya	-4.234932	39.608115	(Raes *et al.* 2007)	
Eubostrichus sp.	Zanzibar	-6.466667	39.533333	(Raes *et al.* 2007)	
E. parasitiferus	Biscayne, Florida Key	25.497827	-80.307541	(Hopper & Cefalu 1973)	renamed Chitwood from *E. dianae*, renamed Muthumbi from *E. hopperi*
E. longosetosus	North Sea	51.191394	2.776337	(Muthumbi *et al.* 1995)	
E. parasitiferus	North Carolina, US	34.686863	-76.642799	(Chitwood 1936)	
E. phalacrus	Canary islands			(Greeff 1869)	

E. topiarius	Adriatic Sea	45.035556	13.683611	(Berger *et al.* 1996)	
Eubostrichus sp.	Corsica	42.58028	8.72417	(Bayer *et al.* 2009; Ott *et al.* 2014a)	
Eubostrichus sp.	Calvi, Corsica 160m depth	42.621667	8.671667	(Soetaert *et al.* 1995)	
E. cf. *topiarius*	Elba, Italy	42.80722	10.14111	(Zimmermann *et al.,* Chapter III)	
Eubostrichus sp.	Calais, France	50.99695N	1.98212E	own observation	
E. africanus	Nha Trang Bay, estuary of Be River (Cua Be), Vietnam	12.202938	109.181374	(Tchesunov 2013)	
Eubostrichus sp.	Porto Cesare, Italy	40.233963	17.819708	(Sandulli *et al.* 2010)	
Eubostrichus sp.	Isles of Scilly, UK	49.956994,	-6.290683	(Somerfield *et al.* 2007)	
	Bermuda	32.326887	-64.698515		
E. hortulanus	Chatham rise, Southwest Pacific, 350m	-43.331	178.288	(Leduc 2013)	
E. dianae	Heron island, Australia	-23.43487	151.94495	own observation	
E. dianae	Guadeloupe	16.277999	-61.557654	(Maurin *et al.* 2010)	
Eubostrichus sp.	Darwin mounds, 1000m	59.814833	-7.375167	(Van Gaever *et al.* 2004)	
Eubostrichus sp.	Mallorca, Balearic islands	39.262774	3.051712	(Deudero & Vincx 2000)	
Eubostrichus sp..	Cabrera, Balearic islands	39.143509	2.929275	(Deudero & Vincx 2000)	
E. dianae	Bermuda	32.349385	-64.725177	(Coull 1970)	
E. porosum, hopperi	Banco Chinchorro, Mexico	18.619190	-87.364538	(De Jesús-Navarrete 2003, 2007a)	
E. dianae, parasitiferus	Bermuda	32.348832	-64.661824	(Westphalen 1993)	
E. dianae, parasitiferus	Bermuda	32.349389	-64.725167	(Westphalen 1993)	
E. parasitiferus	Isla Socorro, Mexico	18.712004	-110.96253	(De Jesús-Navarrete 2007b)	
E. porosum,	Isla Mujeres, Mexico	21.266667	-86.775000	(De Jesús-Navarrete 2007a)	
E. porosum	Isla Mujeres, Mexico	21.266667	-86.750000	(De Jesús-Navarrete 2007a)	
E. otti	Penguin point, West Australia	-32.028611	115,7475	(Hourston & Warwick 2010)	
E. dianae, fertilis	CBC, Belize	16.82861	-88.10955	(Ott *et al.* 2014b; Pende *et al.* 2014)	
E. hopperi	Cuba	21.608244	-83.176222	(Armenteros *et al.* 2014b)	
E. exilis	Red Sea	28.520719	34.568557	(Gerlach 1964)	renamed Tchesunov from *Laxus gerlachi*
E. gerlachi	Red Sea	28.520719	34.568557	(Gerlach 1964)	renamed Chitwood from *E. parasitiferus*

E. exilis, parasitiferus	Maledives	4.007036	72.810085	(Gerlach 1963; Semprucci *et al.* 2010, 2013; Semprucci & Balsamo 2014)	renamed Tchesunov from *Laxus gerlachi* and Ott from *E. gerlachi*
***Laxus* species**					
Laxus longus	New South Wales, Australia	-33.027088	151.739502	(Cobb 1894)	
Laxus sp.	Maledives	4.007036	72.810085	(Semprucci *et al.* 2013; Semprucci & Balsamo 2014)	
Laxus cobbi	New Caledonia	-21.954191	166.1273	(Inglis 1968)	
Laxus sp.	Adriatic	45.035556	13.683611	(Ott *et al.* 1995)	
L. cf. cosmopolitus	Elba	42.80722	10.14111	(Zimmermann *et al.,* Chapter III)	
Laxus contortus	Bay of Naples, Italy	40.808612	14.117203	(Cobb 1894)	
Laxus oneistus, cosmopolitus	CBC, Belize	16.82861	-88.10955	(Ott *et al.* 1995)	
Laxus sp.	Nha Trang Bay, Hon Mun Island, Vietnam	12.169233	109.296427	(Tchesunov 2013)	
Laxus parvum	Punta Francés Reef, Cuba	21.608244	-83.176222	(Armenteros *et al.* 2014b)	questionable
Laxus heron 1 heron2	Heron island	-23.43487	151.94495	(Zimmermann *et al.,* Chapter III)	
***Leptonemella* species**					
L. cincta	Florida, US	25.497827	-80.307541	(Cobb 1920)	
L. aphanothecae, pellita, cincta	Cape Cod, US	41.522001	-70.776498	(Wieser 1959; Wieser, others 1960)	
Leptonemella sp.	Mallorca, Balearic islands	39.262774	3.051712	(Deudero & Vincx 2000)	
Leptonemella sp	Cabrera, Balearic islands	39.143509	2.929275	(Deudero & Vincx 2000)	
L. aphanothecae	Isles of Scilly, UK	49.956994,	-6.290683	(Warwick & Coles 1977; Somerfield *et al.* 2007)	
L. aphanothecae	Belgian coast	51.271394	2.776337	(Willems *et al.* 1982; Vanaverbeke *et al.* 2002)	
L. aphanothecae	Holland coast	51.734683	3.979683	(Willems *et al.* 1984)	
L. aphanothecae, gorgo	Kiel, Germany	54.4397	10.367889	(Gerlach 1950)	
L. aphanothecae	Tunisia	37.283620,	9.881075	(Boufahja *et al.* 2011)	
Leptonemella sp.	Zanzibar, Africa	-6.150000	39.200000	(Olafsson 1995)	
Leptonemella sp	Zanzibar, Africa	-6.200000	39.200000	(Olafsson 1995)	
Leptonemella sp	Zanzibar, Africa	-6.183333	39.416667	(Olafsson 1995)	
Leptonemella sp	Zanzibar, Africa	-5.916667	39.233333	(Olafsson 1995)	
L. granulosa, sp.	Banco Chinchorro, Mexico	18.619190	-87.364538	(De Jesús-Navarrete 2003)	
L. aphanothecae, gorgo, vicina	Sylt, Germany	55.01467	8.43752	(Riemann *et al.* 2003)	
L. aphanothecae	White Sea, North Russia	64.821367	38.688671	(Tchesunov 2013)	
L. granulosa	Western English Channel	48.643798	-3.882408	(Boucher 1975)	
L. cf. *juliae, L.* cf. *vestari*	Elba, Italy	42.80722	10.14111	(Zimmermann *et al.,* Chapter III)	

L. juliae, vestari	Adriatic Sea	45.035556	13.683611	(Hoschitz *et al.* 1999)	
L. cincta	Red Sea	28.520719	34.568557	(Gerlach 1963)	
	Coast of Kenya	-4.37345	39.834707	(Raes *et al.* 2007)	
Leptonemella sp	Sardinia, Italy	40.566667	8.216667	(Sandulli *et al.* 2010)	
Leptonemella sp	Bermuda	32.349385	-64.725177	(Coull 1970)	
Leptonemella sp	France	48.730509	-3.999369	(Luc & De Coninck 1959)	
L. sigma	Maledives	4.007036	72.810085	(Gerlach 1963; Semprucci *et al.* 2010)	renamed Tchesunov from *Laxus sigma*
L. brevipharynx	Punta Francés Reef, Cuba	21.608244	-83.176222	(Armenteros *et al.* 2014b)	
Leptonemella sp.	CBC, Belize	16.80306	-88.08194	own observation	
Leptonemella sp	Darwin mounds, 1000m	59.814833	-7.375167	(Van Gaever *et al.* 2004)	
L. aphanothecae	Denmark, Gas seeps	57.403235	10.523764	(Jensen 1995)	
L. peronensis	West Australia	-32.268889	115.692778	(Hourston & Warwick 2010)	
***Robbea* species**					
R. calaestis	Pernambuco, Brazil	-8.260948	-34.943524	(Gerlach 1956)	
R. gallica	Gulf of Marseilles, 82m, France	43.322991	5.316648		
R. gerlachi	Western English Channel, France	48.643798	-3.882408	(Boucher 1975)	
R. macintyrei, smo	Scotland	57.833603	-5.677586	(Platt & Zhang 1982)	
R. tenax	Maledives	4.007036	72.810085	(Gerlach 1963; Semprucci *et al.* 2010, 2013; Semprucci & Balsamo 2014)	
Robbea sp.	Nha Trang Bay, Tre island, Dam bay, Vietnam	12.189172	109.290227	(Tchesunov 2013)	
R. hypermnestra, *agricola, ruetzleri*	CBC, Belize	16.80306	-88.08194	(Ott *et al.* 2014a)	
R. porosum	Cuba	21.608244	-83.176222	(Armenteros *et al.* 2014b)	questionable
***Stilbonema* species**					
S. brevicolle, *majum*	Kingston Harbour, Jamaica	17.940522	-76.817122	(Cobb 1920)	
S. brevicolle	Bermuda	32.349385	-64.725177	(Coull 1970)	
S. annulatum	Maledives	4.007036	72.810085	(Gerlach 1963; Semprucci *et al.* 2010, 2013; Semprucci & Balsamo 2014)	
S. smurovi	Nha Trang Bay, Hon Mun island, Vietnam	12.169233	109.296427	(Tchesunov 2013)	
S. majum	Bahamas	24.716667	-76.816667	(Myshrall *et al.* 2010)	
S. majum	CBC, Belize	16.82861	-88.10955	own observation	
S. “st andrea”	Elba	42.80722	10.14111	(Zimmermann *et al.*, Chapter III)	

S. “heron 1”,“heron 2”	Heron Island	-23.43487	151.94495	(Zimmermann *et al.,* Chapter III)	
Stilbonema sp.	France, Calais	5.099695	198.212	own observation	
S. brevicolle	Cuba	21.608244	-83.176222	(Armenteros *et al.* 2014b)	questionable
Other genera					
Centonema	Chatham rise, Southwest Pacific, 350m	-43.331	178.288	(Leduc 2013)	
unknown genus	Bay of Plenty, New Zealand	-37.651667	177.111667	(Kamenev *et al.* 1993)	
unknown genus	Paleohori Bay, Milos, Greece	36.674522	24.517171	(Thiermann *et al.* 1997)	
unknown genus	Scotland	56.161697	-2.770599	Blaxter, partial seq	
Adelphos	CBC, Belize	16.80306	-88.08194	(Ott 1997)	
Squanema articulatum, annulatum	Maledives	4.007036	72.810085	(Gerlach 1963; Semprucci *et al.* 2013; Semprucci & Balsamo 2014)	
Squanema sp.	CBC, Belize	16.80306	-88.08194	own observation	
Parabostrichus bathyalis	Slope canyons, Northeast Atlantic, 700-1000m	50.73	-11.258333	(Tchesunov *et al.* 2012)	
undescribed genus A „Paralaxus“	Heron island, Australia	-23.43487	151.94495	(Zimmermann *et al.,* Chapter III)	
undescribed genus A „Paralaxus“	CBC, Belize	16.82861	-88.10955	(Zimmermann *et al.,* Chapter III)	
undescribed genus B „Culleus“	CBC, Belize	16.82861	-88.10955	(Zimmermann *et al.,* Chapter III)	

CBC: Carrie Bow Cay

References

Armenteros M, Ruiz-Abierno A, Decraemer W (2014) Taxonomy of Stilbonematinae (Nematoda: Desmodoridae): description of two new and three known species and phylogenetic relationships within the family. *Zoological Journal of the Linnean Society*, **171**, 1–21.

Bayer C, Heindl NR, Rinke C *et al.* (2009) Molecular characterization of the symbionts associated with marine nematodes of the genus *Robbea*. *Environmental Microbiology Reports*, **1**, 136–144.

Berger E, Urbancik W, Ott JA (1996) *Eubostrichus topiarius* sp. n., a new free-living, marine species of Stilbonematinae (Nematoda: Desmodoridae) from a shallow subtidal sand bottom. *Nematologica*, **42**, 521–536.

Boucher G (1975) Nématodes des sables fins infralittoraux de la Pierre Noire (Manche Occidentale). I. Desmodorida. *Bulletin de Muséum National d'Histoire Naturelle (3)*, **285**, 101–128.

Boucher G (1997) Structure and biodiversity of nematode assemblages in the SW lagoon of New Caledonia. *Coral Reefs*, **16**, 177–186.

Boufahja F, Hedfi A, Amorri J *et al.* (2011) An assessment of the impact of chromium-amended sediment on a marine nematode assemblage using microcosm bioassays. *Biological trace element research*, **142**, 242–255.

Chitwood BG (1936) Some marine nematodes from North Carolina. *Proceedings of the Helminthological Society of Washington*, **3**, 1–16.

Cobb NA (1894) *Tricoma* and other new nematode genera. *Proceedings of the Linnean Society of New South Wales*, **8**, 389–421.

Cobb NA (1920) One hundred new nemas. *Contributions to a Science of Nematology*, **9**, 217–343.

Coull BC (1970) Shallow water meiobenthos of the Bermuda platform. *Oecologia*, **4**, 325–357.

Deudero S, Vincx M (2000) Sublittoral meiobenthic assemblages from disturbed and non-disturbed sediments in the Balearics. *Scientia Marina*, **64**, 285–293.

Fisher R (2003) Spatial and temporal variations in nematode assemblages in tropical seagrass sediments. *Hydrobiologia*, **493**, 43–63.

Fisher R, Sheaves MJ (2003) Community structure and spatial variability of marine nematodes in tropical Australian pioneer seagrass meadows. *Hydrobiologia*, **495**, 143–158.

Da Fonsêca-Genevois V, Somerfield PJ, Neves MHB, Coutinho R, Moens T (2006) Colonization and early succession on artificial hard substrata by meiofauna. *Marine Biology*, **148**, 1039–1050.

Van Gaever S, Vanreusel A, Hughes JA, Bett BJ, Kiriakoulakis K (2004) The macro-and micro-scale patchiness of meiobenthos associated with the Darwin Mounds (north-east Atlantic). *Journal of the Marine Biological Association of the UK*, **84**, 547–556.

Gerlach SA (1950) Über einige Nematoden aus der Familie der Desmodoriden. *Zoologischer Anzeiger* **145**, 178–198.

Gerlach SA (1956) Die Nematodenbesiedlung des tropischen Brandungsstrandes von Pernambuco. *Kieler Meeresforschung*, **12**, 202–218.

Gerlach SA (1963) Freilebende Meeresnematoden von den Malediven II. *Kieler Meeresforschung*, **19**, 67–103.

Gerlach SA (1964) Freilebende Nematoden aus dem Roten Meer. *Kieler Meeresforschung*, **20**, 18–34.

Gingold R, Mundo-Ocampo M, Holovachov O, Rocha-Olivares A (2010) The role of habitat heterogeneity in structuring the community of intertidal free-living marine nematodes. *Marine Biology*, **157**, 1741–1753.

Greeff R (1869) *Untersuchungen über einige merkwürdige Thiergruppen des Arthropoden-und Wurm-Typus: Mit 4 Tafeln*. Nicolai.

Hopper BE, Cefalu RC (1973) Free-living marine nematodes from Biscayne Bay, Florida V. Stilbonematinae: contributions to the taxonomy and morphology of the genus *Eubostrichus* Greeff and related genera. *Transactions of the American Microscopical Society*, **92**, 578–591.

Hoschitz M, Buchholz TG, Ott JA (1999) *Leptonemella juliae* sp. n. and *Leptonemella vestari* sp. n. (Stilbonematinae), two new free-living marine nematodes from a subtidal sand bottom. *Annalen des Naturhistorischen Museums in Wien. Serie B für Botanik und Zoologie*, 423–435.

Hourston M, Warwick RM (2010) New species of free-living aquatic nematodes from south-western Australia (Nematoda: Axonolaimidae and Desmodoridae). *Records of the Western Australian Museum*, **42**, 26.

Inglis WG (1968) Interstitial nematodes from St. Vincent's Bay, New Caledonia. *Expédition Française sur les récifs corallines de la Nouvelle-Calédonie. Singer-Polignac, Paris, Edit*, **2**, 29–74.

Jensen P (1995) Life history of the nematode *Theristus anoxybioticus* from sublittoral muddy sediment at methane seepages in the northern Kattegat, Denmark. *Marine Biology*, **123**, 131–136.

De Jesús-Navarrete A (2003) Diversity of nematoda in a Caribbean atoll: Banco Chinchorro, Mexico. *Bulletin of Marine Science*, **73**, 47–56.

De Jesús-Navarrete A (2007a) Nematodos de los arrecifes de Isla Mujeres y Banco Chinchorro, Quintana Roo, México. *Revista de Biología Marina y Oceanografía*, **42**, 193–200.

De Jesús-Navarrete A (2007b) Littoral free living nematode fauna of Socorro Island, Colima, Mexico Nematofauna de vida libre en el litoral de Isla Socorro, Colima, México. *Hidrobiologica*, **17**, 61–66.

Kamenev GM, Fadeev VI, Selin NI, Tarasov VG, Malakhov VV (1993) Composition and distribution of macro- and meiobenthos around sublittoral hydrothermal vents in the Bay of Plenty, New Zealand. *New Zealand Journal of Marine and Freshwater Research*, **27**, 407–418.

Leduc D (2013) One new genus and two new deep-sea nematode species (Desmodoridae, Stilbonematinae) from phosphorite nodule deposits on Chatham Rise, Southwest Pacific Ocean. *Marine Biodiversity*, **43**, 421–428.

Luc M, De Coninck LAP (1959) Némátodes libres marins de la région de Roscoff.

Maurin LC, Himmel D, Mansot J-L, Gros O (2010) Raman microspectrometry as a powerful tool for a quick screening of thiotrophy: An application on mangrove swamp meiofauna of Guadeloupe (FWI). *Marine Environmental Research*, **69**, 382–389.

Muthumbi A, Verschelde D, Vincx M (1995) New Desmodoridae (Nematoda: Desmodoroidea): three new species from Ceriops mangrove sediments (Kenya) and one related new species from the North Sea. *Cahiers de biologie marine*, **36**, 181–195.

Myshrall KL, Mobberley JM, Green SJ *et al.* (2010) Biogeochemical cycling and microbial diversity in the thrombolitic microbialites of Highborne Cay, Bahamas. *Geobiology*, **8**, 337–354.

Olafsson E (1995) Meiobenthos in mangrove areas in eastern Africa with emphasis on assemblage structure of free-living marine nematodes. *Hydrobiologia*, **312**, 47–57.

Ott JA (1997) A new symbiotic marine nematode, *Adelphos rolandi* gen. n. sp. n.(Stilbonematinae), from the Caribbean Sea. *Annalen des Naturhistorischen Museums in Wien. Serie B für Botanik und Zoologie*, 417–422.

Ott JA, Bauer-Nebelsick M, Novotny V (1995) The genus *Laxus* Cobb, 1894 (Stilbonematinae: Nematoda): Description of two new species with ectosymbiotic, chemoautotrophic bacteria. *Proceedings of the Biological Society of Washington*, **108**, 508–527.

Ott JA, Gruber-Vodicka HR, Leisch N, Zimmermann J (2014a) Phylogenetic confirmation of the genus *Robbea* (Nematoda: Desmodoridae, Stilbonematinae) with the description of three new species. *Systematics and Biodiversity*, **12**, 434–455.

Ott JA, Leisch N, Gruber-Vodicka HR (2014b) *Eubostrichus fertilis* sp. n., a new marine nematode (Desmodoridae: Stilbonematinae) with an extraordinary reproductive potential from Belize, Central America. *Nematology*, **16**, 777–787.

Pende N, Leisch N, Gruber-Vodicka HR *et al.* (2014) Size-independent symmetric division in extraordinarily long cells. *Nature Communications*, **5**.

Platt HM, Zhang ZN (1982) New species of marine nematodes from Loch Ewe, Scotland. *Bulletin of the British Museum of Natural History (Zoology)*, **42**, 227–246.

Raes M, De Troch M, Ndaro SGM *et al.* (2007) The structuring role of microhabitat type in coral degradation zones: a case study with marine nematodes from Kenya and Zanzibar. *Coral Reefs*, **26**, 113–126.

Riemann F, Thiermann F, Bock L (2003) *Leptonemella* species (Desmodoridae, Stilbonematinae), benthic marine nematodes with ectosymbiotic bacteria, from littoral sand of the North Sea island of Sylt: taxonomy and ecological aspects. *Helgoland Marine Research*, **57**, 118–131.

Riera R, Núñez J, del Carmen Brito M (2013) Temporal dynamics of shallow subtidal meiobenthos from a beach in Tenerife (Canary Islands, northeast Atlantic Ocean). *Acta Oceanologica Sinica*, **32**, 44–54.

Sandulli R, De Leonardis C, Vanaverbeke J (2010) Meiobenthic communities in the shallow subtidal of three Italian Marine Protected Areas. *Italian Journal of Zoology*, **77**, 186–196.

Semprucci F, Balsamo M (2014) New records and distribution of marine free-living nematodes in the Maldivian Archipelago. *Proceedings of the Biological Society of Washington*, **127**, 35–46.

Semprucci F, Colantoni P, Baldelli G *et al.* (2013) Meiofauna associated with coral sediments in the Maldivian subtidal habitats (Indian Ocean). *Marine Biodiversity*, **43**, 189–198.

Semprucci F, Colantoni P, Baldelli G, Rocchi M, Balsamo M (2010) The distribution of meiofauna on back-reef sandy platforms in the Maldives (Indian Ocean). *Marine Ecology*, **31**, 592–607.

Soetaert K, Vincx M, Heip C (1995) Nematode community structure along a mediterranean shelf-slope gradient. *Marine Ecology*, **16**, 189–206.

Somerfield PJ, Dashfield SL, Warwick RM (2007) Three-dimensional spatial structure: nematodes in a sandy tidal flat. *Marine Ecology Progress Series*, **336**, 177–186.

Tchesunov AV (2013) Marine free-living nematodes of the subfamily Stilbonematinae (Nematoda, Desmodoridae): taxonomic review with descriptions of a few species from the Nha Trang Bay, Central Vietnam. *Meiofauna Marina* , **20**, 71–94.

Tchesunov AV, Ingels J, Popova EV (2012) Marine free-living nematodes associated with symbiotic bacteria in deep-sea canyons of north-east Atlantic Ocean. *Journal of the Marine Biological Association of the United Kingdom*, **92**, 1257–1271.

Thiermann F, Akoumianaki I, Hughes JA, Giere O (1997) Benthic fauna of a shallow-water gaseohydrothermal vent area in the Aegean Sea (Milos, Greece). *Marine Biology*, **128**, 149–159.

Vanaverbeke J, Gheskiere T, Steyaert M, Vincx M (2002) Nematode assemblages from subtidal sandbanks in the Southern Bight of the North Sea: effect of small sedimentological differences. *Journal of Sea Research*, **48**, 197–207.

Warwick RM, Coles JW (1977) The marine flora and fauna of the Isles of Scilly: free-living Nematoda. *Journal of Natural History*, **11**, 393–407.

Westphalen D (1993) Stromatolitoid microbial nodules from Bermuda —a special micro habitat for meiofauna. *Marine Biology*, **117**, 145–157.

Wieser W (1959) Eine ungewöhnliche Assoziation zwischen Blaualgen und freilebenden marinen Nematoden. *Plant Systematics and Evolution*, **106**, 81–87.

Wieser W, others (1960) Benthic studies in Buzzards Bay. II. The meiofauna. *Limnology and Oceanography*, **5**, 121–137.

Willems KA, Sharma Y, Heip C, Sandee AJJ (1984) Long-term evolution of the meiofauna at a sandy station in lake Grevelingen, The Netherlands. *Netherlands Journal of Sea Research*, **18**, 418–433.

Willems KA, Vincx M, Claeys D, Vanosmael C, Heip C (1982) Meiobenthos of a sublittoral sandbank in the Southern Bight of the North Sea. *Journal of the Marine Biological Association of the United Kingdom*, **62**, 535–548.